The Mechanisms of Right Ventricular Dysfunction Following Lung Resection

Dr Adam William Glass
MB, BCH, BAO, FRCA

Submitted in fulfilment of the requirements for the Degree of Doctor of Medicine

School of Medicine, Veterinary and Life Sciences
University of Glasgow

January 2021

Dedication

To Fionnuala, Francesca and Theo,
Thank you for all your continual patience, support and encouragement throughout.

To my parents and Amy,
Thank you for literally everything.

Abstract

Lung cancer is the leading cause of cancer death in the UK and whilst lung resection, in appropriate cases, offers the best chance of cure it is associated with significant post-operative morbidity and mortality. Post-operative right ventricular dysfunction, secondary to an increase in afterload, has long been hypothesised to contribute to this morbidity although this has not been well demonstrated. Previous studies have used echocardiography and volumetric pulmonary artery catheters to assess changes in right ventricular function and afterload. These studies, however, are undermined by the reliability of the methods utilised and by their incomplete assessment of afterload. To better evaluate this our research group has undertaken a cardiac magnetic resonance study and demonstrated right ventricular dysfunction following lung resection. This thesis details investigation of right ventricular strain and afterload as potential mechanisms of this dysfunction.

The introduction (Chapter 1) reviews the management of lung resection and the right ventricle, detailing its anatomy and physiology, with a particular focus on the pathophysiology and assessment of right ventricular failure secondary to increases in afterload. In Chapter 2, a literature review of studies investigating changes in right ventricular function and afterload following lung resection is presented. These studies have failed to demonstrate a significant change in afterload quantified by measurement of pulmonary artery pressure and/or pulmonary vascular resistance. These indices, however, only assess global impedance to steady flow and overlook impedance to pulsatile flow.

Chapter 3 details the aims and the investigations performed in this thesis. The rationale, design, methodology and generic results of the first sequential cardiac magnetic resonance study to investigate right ventricular dysfunction are presented in Chapter 4. Additionally, the previous results from this study (reported prior to this thesis) are presented, the main finding of which is a post-operative reduction in right ventricular ejection fraction. All subsequent investigations presented in this thesis are performed on the cardiac magnetic resonance images collected within this study.

The first investigation (Chapter 5) utilises CMR right ventricular strain analysis to assess changes in right ventricular function following lung resection. A review of strain analysis, measurement and changes in states of increased right ventricular afterload is presented followed by a review of three prior, but contradictory echocardiographic strain investigations in patients undergoing lung resection. This investigation demonstrates that there is no immediate change, but a delayed reduction in global and free wall right ventricular longitudinal strain evident at 2-months following lung resection.

Chapters 6 and 7 investigate changes in right ventricular afterload, focusing on assessment of the pulsatile components of afterload. As lung resection is a unilateral insult to the pulmonary vasculature, indices that allow assessment of unilateral changes of afterload are described. Assessment is therefore performed in the main pulmonary artery and the branch (right or left) supplying the resected lung (termed the operative pulmonary artery) and the non-resected lung (non-operative pulmonary artery).

Chapter 6 assesses pulmonary artery flow, acceleration time and distensibility following lung resection. It demonstrates, for the first time, an increase in right ventricular pulsatile afterload following lung resection. Post-operatively, pulsatile afterload is increased along with an altered distribution of cardiac output away from the operative pulmonary artery. On post-operative day two, indices of afterload in the non-operative pulmonary artery are associated with a reduction in right ventricular ejection fraction.

The first use of wave intensity analysis in a lung resection cohort is presented in Chapter 7. Wave intensity analysis combines flow and area measurements in the time domain to calculate wave intensity, a measure of the rate of transport of wave energy, and assesses pulsatile afterload by calculation of wave reflection index. This investigation again demonstrates a post-operative increase in pulsatile afterload and the presence of early wave reflection in the operative pulmonary artery.

Finally, Chapter 8 investigates the relationship between changes in right ventricular function (ejection fraction and strain) and changes observed in pulsatile afterload. This is the first evidence linking a reduction in right ventricular

function to an increase in afterload following lung resection. At 2-months postoperatively, increased wave reflection is strongly associated with a reduction in right ventricular free wall strain. The increase in pulsatile afterload observed in the operative pulmonary artery is associated with an increase in the percentage of cardiac output travelling in the non-operative pulmonary artery which, in turn, is associated with the reduction in both right ventricular ejection fraction and strain at 2-months.

The investigations presented in this thesis demonstrate, for the first time, the widely hypothesised increase in right ventricular afterload occurring following lung resection and its association with a decrease in right ventricular function. The thesis concludes with a discussion of future work describing the design and successful funding of two studies building on the results from this thesis; a pilot study investigating the right ventricular response to exercise following lung resection and a cardiac magnetic resonance investigation of right ventricular inflammation following lung resection.

Table of Contents

List of Tables

List of Figures

List of Equations

Acknowledgement

I would like to acknowledge the advice, help and expertise offered by the following people. Completion of this thesis would not have been possible without them.

- My supervisor Dr Ben Shelley, Consultant Anaesthetist at the Golden Jubilee National Hospital and Honorary Clinical Associate Professor. It has been a long journey since I first visited the Golden Jubilee to discuss applying for a research fellowship, thank you for the continual enthusiastic support, advice, guidance and reassurance.
- My supervisor Dr Philip McCall, Consultant Anaesthetist at the Golden Jubilee National Hospital. Thank you for undertaking such a complex study and sharing it with myself.
- Professor John Kinsella, now retired head of the Academic Unit of Anaesthesia, Pain and Critical Care at the University of Glasgow. Thank you for giving me the opportunity to undertake this work and for your continual enthusiastic support.
- Dr Isma Quasim and colleagues in the Golden Jubilee anaesthetic/ICU department for support in my clinical work during my research fellowship and for supporting me in the pursuit of my academic goals.
- Dr Alex Arthur for recruitment and follow-up of participants in the study and for dual reporting all of the pulmonary artery CMR scans.
- Dr Kenneth Mangion for providing training on QStrain and assisting with analysis of CMR strain.
- Dr Martin Shaw for providing training in R and for support in wave intensity modelling.
- The team at the Golden Jubilee for supporting the study.
    - Mr. Alan Kirk for supporting a complex study in patients under his care
    - Dr John Payne, Dr Des Alcorn and Vanessa Richards for ensuring safe and timely CMR scanning for all participants
    - Christine Groundwater, Rachel Small and Christine Aitken for their support as research nurses

- The entire, theatre, recovery, high dependency and ward staff for supporting the study.
- The Association of Cardiothoracic Anaesthetists and Critical Care for providing funding for the study on which this thesis is performed and for funding the studies detailed in the future work section (along with the National Institute of Academic Anaesthesia).

Finally, I would like to that the patients that participated in this study. Though undergoing life changing cancer surgery their willingness to support research was remarkable.

Author's Declaration

I declare that, except where reference is made to the contribution of others, this thesis is a result of my own work. As detailed in the thesis, the investigations are performed on CMR data previously collected although I have performed all of the scan reporting (except for where dual reported), data cleaning, mathematical modelling, statistical analysis and interpretation. This thesis and the design of the studies detailed in the future work section are entirely written by the author. I confirm that the thesis has not been submitted for any other degree at the University of Glasgow or any other institution.

Dr Adam William Glass (MB, BCH, BAO, FRCA)

Word count: 78,227

Definitions/Abbreviations

ANCOVA	Analysis of covariance
ANOVA	Analysis of variance
AUROCC	Area under receiver operating characteristics curve
BCW	Backward compression wave
BEW	Backward expansion wave
BMI	Body mass index
BNP	Brain natriuretic peptide
C	Compliance
CMR	Cardiac magnetic resonance
CMR-FT	CMR feature tracking strain analysis
CMR-Tag	CMR tagging strain analysis
CO	Cardiac output
COPD	Chronic obstructive pulmonary disease
CTEPH	Chronic thromboembolic pulmonary hypertension
CV	Coefficient of variation
CVP	Central venous pressure
EDA	End diastolic area
EDV	End diastolic volume
ESA	End systolic area
ESV	End systolic volume
FCW	Forward compression wave
FEV_1	Forced expiratory volume in one second
FEW	Forward expansion wave
FW	Free wall
GCS	Global circumferential strain
GLS	Global longitudinal strain
GRS	Global radial strain
HDU	High dependency unit
HR	Heart rate
hsTnT	High sensitivity Troponin T
ICC	Intra-class co-efficient
LV	Left ventricle/ventricular
LVLA	Left ventricular long axis
LVSA	Left ventricular short axis
LVEF	Left ventricular ejection fraction
MPA / LPA / RPA	Main / left / right pulmonary artery
MPAP	Mean pulmonary artery pressure
OLV	One lung ventilation

PA	Pulmonary artery
PAAT	Pulmonary artery acceleration time
PAAT/ET	Pulmonary artery acceleration time / ejection time (corrected for heart rate)
PAC	Pulmonary artery catheter
PAP	Pulmonary artery pressure
Percentage.CO	Percentage of total cardiac output
PH/PAH	Pulmonary hypertension / pulmonary arterial hypertension
POD	Post-operative day
PRSW	Preload recruitable stroke work
PVR	Pulmonary vascular resistance
PVreserve	Pulmonary vascular reserve
QA loop	Flow-area loop
R	Resistance
RV	Right ventricle/ventricular
RVEDP	Right ventricular end diastolic pressure
RVEDV(I)	Right ventricular end diastolic volume (index)
RVEF	Right ventricular ejection fraction
RVESV(I)	Right ventricular end systolic volume (index)
RVF	Right ventricular failure
RVLA	Right ventricular long axis
RVPO	Right ventricular pressure overload
RVCreserve	Right ventricular reserve
RVSA	Right ventricular short axis
RVSP	Right ventricular systolic pressure
SOS	Sum of squares
SPAP	Systolic pulmonary artery pressure
STE	Speckle tracked echocardiography
TAPSE	Tricuspid annular plane systolic excursion
TDI	Tissue Doppler imaging
TTE	Transthoracic echocardiography
VATS	Video-assisted thoracic surgery
VPAC	Volumetric pulmonary artery catheter
WIA	Wave intensity analysis
WRI	Wave reflection index

Chapter 1 Introduction

This chapter will provide an overview of the surgical management of lung cancer, specifically highlighting the significant cardiopulmonary morbidity faced by patients even after a "successful" lung resection. It will focus on the hypothesised role of right ventricular (RV) dysfunction and highlight potential pathophysiological mechanisms.

1.1 Lung cancer

1.1.1 Incidence and mortality of lung cancer

It is easy to understand the burden that lung cancer places on the health of the United Kingdom and in particular Scotland by looking at local and national statistics provided by Cancer Research UK. Whilst lung cancer is the third most common cancer in the UK, it is the leading cause of cancer deaths (22% of all cancer deaths)[1]. This burden is even greater in Scotland and in particular Glasgow. European age-standardised rates (incidence per 100,000 person-years at risk) reveal that, compared to England, Scotland has a higher incidence of lung cancer 106.7 vs 76.6, this increases to 143.6 within Greater Glasgow and Clyde, Figure 1-1. Unsurprisingly Glasgow also has the highest lung cancer mortality rate in Scotland[1].

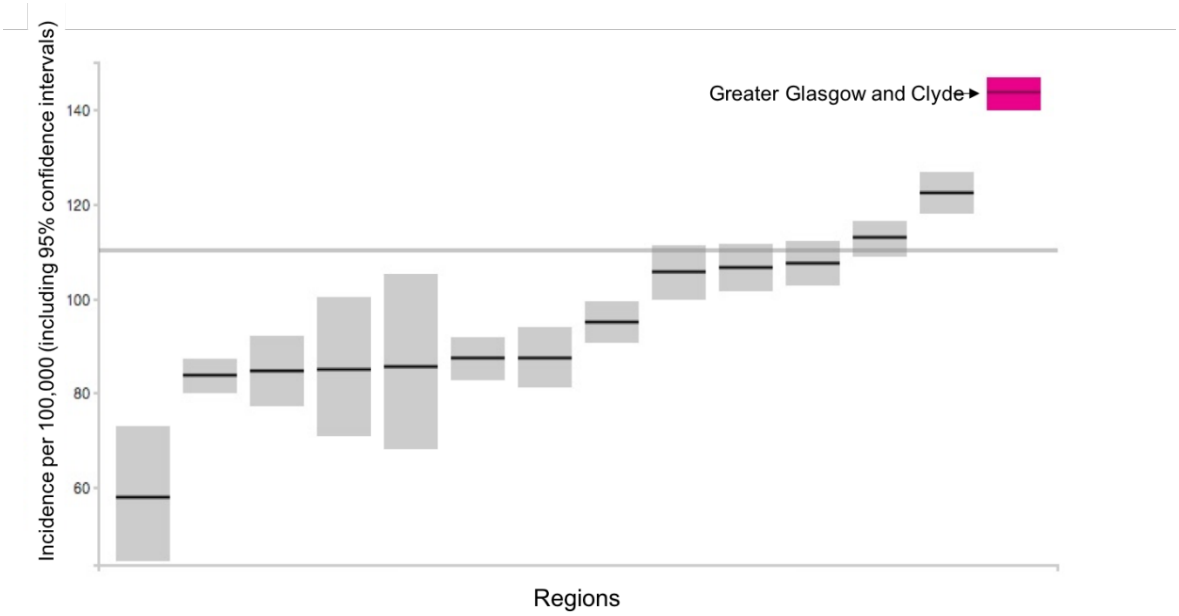

Figure 1-1 Lung cancer incidence in Scottish regions
Each box represents the ranked incidence and 95% confidence intervals of lung cancer in a Scottish region. Greater Glasgow and Clyde highlighted in top right demonstrating the markedly increased lung cancer incidence of the population. Image from Cancer Research UK[1].

Public health campaigns have sought to decrease smoking habits since the link between cigarette smoking and lung cancer was demonstrated in the 1950's[2, 3]. Rates of cigarette smoking have decreased in both sexes, with a greater relative decrease in males, subsequently lung cancer rates in males have decreased but increased in females[1]. This has resulted in largely static lung cancer incidence over the last 20 years. One year survival (32.1% in 2011) has consistently improved since the 1970's however there has only been modest improvements in five (9.5% in 2011) and ten year (4.9% in 2011) survival[1], Figure 1-2. In comparison, the five year survival for bowel cancer survival has improved from 20% to 50% since 1970[4].

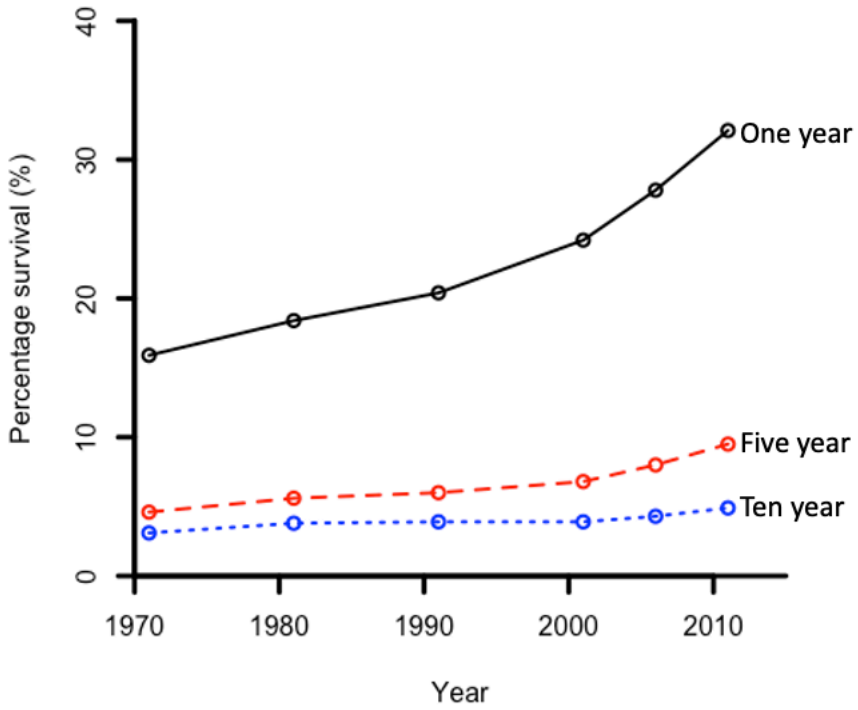

Figure 1-2 Trend in lung cancer survival rates
Trend in percentage survival over time for lung cancer. Note significant increase in one-year survival (black solid line) and gradual improvement in five-year (red dashed line) and ten-year (blue dotted line) survival. Plot constructed with data from Cancer Research UK[1].

1.1.2 Management of lung cancer

National Institute for Health and Care Excellence guidelines recommend surgical resection, where appropriate, as the first-choice treatment for lung cancer with chemotherapy and radiotherapy as additional or alternative treatments[5]. In 2011 Coleman et al. highlighted that the UK had lower one and five-year survival than Denmark, Norway, Sweden, Canada or Australia (data from 1995-2007)[6]. Historically, the UK rates of surgical resection have lagged behind other comparative countries. A British Medical Journal editorial titled 'Thoracic surgery in crisis' summarised the troubling 2001 report of a joint Working Group of The British Thoracic Society and The Society of Cardiothoracic Surgeons of Great Britain and Ireland. With only 40 purely thoracic surgeons operating in the UK, resection rates were less than 10% compared to 25% in the USA[7, 8]. Since this time rates have rapidly increased, Figure 1-3, particularly in elderly patients, Figure 1-4, resulting in patients who previously would have been ineligible for surgery due to increased age and/or comorbidities now being offering lung resection.

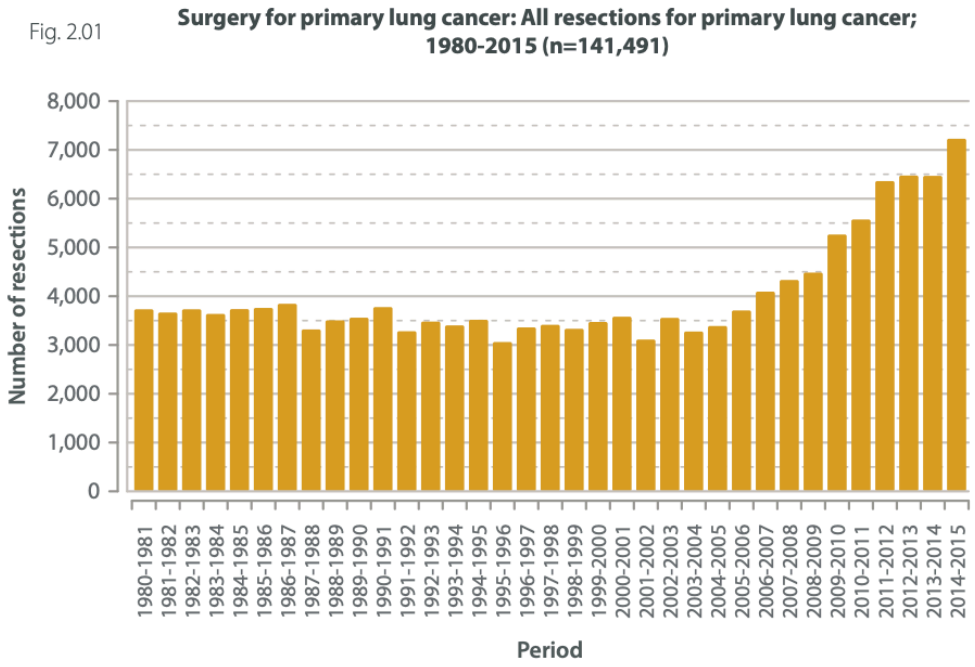

Figure 1-3 Lung cancer resection rates, 1980-2015
Resection numbers have doubled from the 1980-2005 plateau to 2015.
Image from the Society for Cardiothoracic Surgery in Great Britain & Ireland 'Blue Book' 2018[9].

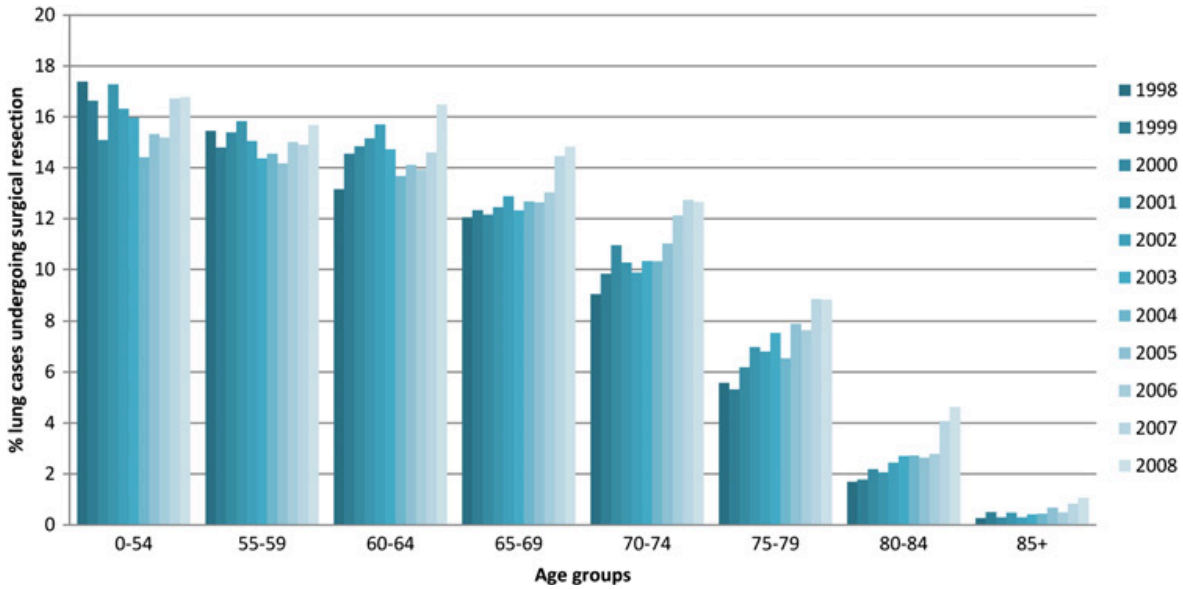

Figure 1-4 Lung cancer resection rates per age group, 1998-2008
Data from England, 1998-2008, Resection rates are increasing over time predominantly in the older groups. Image from Riaz et al[10].

Analysis of geographical variation across the UK demonstrates significant inequality in rates of resection. This variation was demonstrated in studies covering 1998-2008[11-13], prior to the increases demonstrated in Figure 1-3. Analysis of 2010-2013 English lung cancer registers show that geographical variation persists with resection rates ranging from 9.3% to 17.2%, with similar variation for rates of chemotherapy and radiotherapy. Comparison of the quintile of highest

resection rates of treatment to the lowest gives an adjusted (age, sex and cancer stage) hazard ratio for survival of 0.80 [95% CI 0.75-0.84][14].

An increase in the rate of surgical resection has consistently been shown to be associated with reduced mortality[11-14] highlighting the potential for improvement in UK practice. A caveat to this argument is that there is limited randomised control trial evidence that specifically investigate which patients actually benefit from surgery[4]. Drives to increase resection rates must be balanced by appropriate evidence driven patient selection.

1.1.2.1 Methods of lung resection

Lung resection has developed in line with other surgical specialties towards a minimal size of resection by a minimally invasive approach. This equates to preferentially performing lobar resection in favour to pneumonectomy and utilising video-assisted thoracic surgery (VATS). Nationally pneumonectomy rates have fallen from 40% in 1980 to 5% in 2015 having been superseded by lobectomy and wedge/segmentectomy resection[a] [9]. The 2015 European Society of Thoracic Surgeons Database Annual Report demonstrated that the UK now lead the way within Europe in both minimal resection and minimally invasive approach to lung resection; 84.9% of UK lung resection by lobectomy vs 71.2% average with 55.3% of cases performed by VATS vs an average of 22%[15]. Interestingly the increase in lung resections described in section 1.1.2, is predominantly due to an increase in the number of VATS lobectomies[9].

1.1.2.2 Mortality following lung resection

In-hospital mortality rate following lung resection is relatively low given the degree of surgical insult in a population with multiple comorbidities[16, 17]. Crude mortality data for all lung resections from the European Society of Thoracic Surgeons reported a 30-day mortality following lung resection of 2% between 2011-

[a] As surgical practice continues the shift from pneumonectomy to lobectomy the generalisability of any research performed in a pneumonectomy population diminishes. As less than 5% of resections are pneumonectomies all further evidence presented in this thesis will relate to predominately lobectomy populations unless explicitly stated. Intuitively (and as demonstrated later in this thesis) any insult caused by lobectomy is generally lesser than pneumonectomy. In order to ensure that the work within the thesis remains relevant to current practice the focus of investigation is lobectomy populations.

2014[15]. This is in a population who are invariably current or ex-smokers with high levels of cardio-pulmonary co-morbidities[16-18]. Long-term survival is poor in contrast and is influenced by grade of tumour at time of resection[19], Figure 1-5.

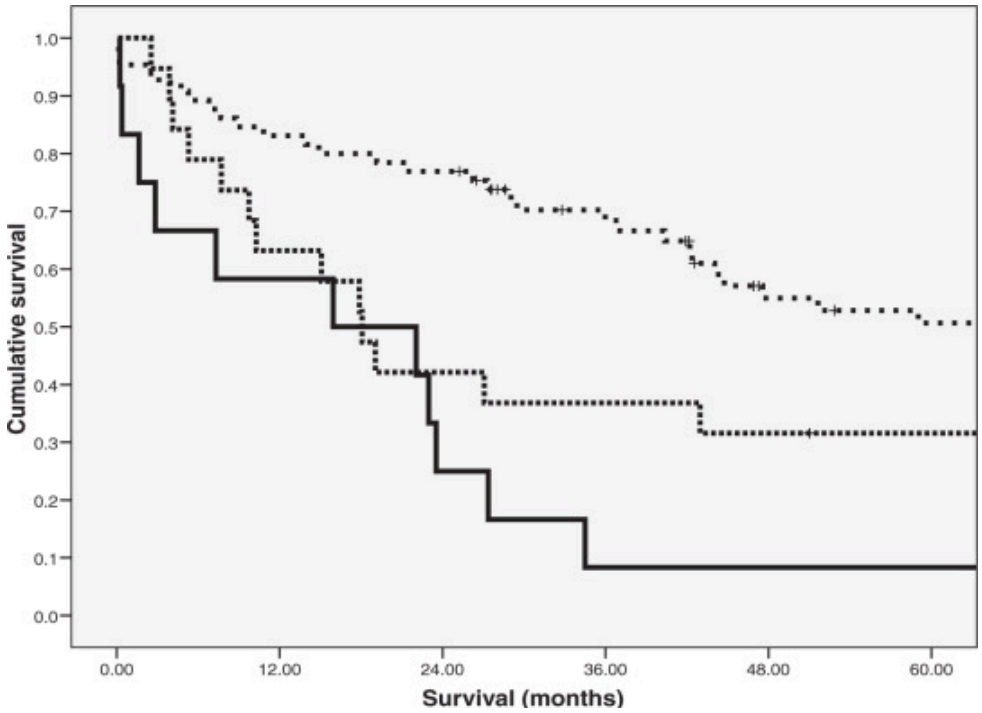

Figure 1-5 Cancer specific survival following lung resection by cancer stage
Note worsening survival with increasing stage of cancer (I, II and III from top to bottom), median follow up 28 months. Image from O'Dowd et al.[19].

Surgery specific mortality rates can be seen in the 2015 Thoracic Surgery Registry Brief Report produced by the Society for Cardiothoracic Surgery in Great Britain and Ireland[9]. They demonstrated a greater survival to discharge with VATS lobectomy (mortality 1%, 57/5838 patients) compared to open lobectomy (2.1%, 356/16984), VATS pneumonectomy (2.9%, 1/34) and open pneumonectomy (5.3%, 107/2034). Whilst these results follow the increasing surgical and physiological insults of VATS vs open and lobectomy vs pneumonectomy, they do not detail conversions from VATS to open or the cause of death. Any VATS procedure with intra-operative complications or increased difficulty may be converted to open, this may hide a true mortality difference in terms of planned approach. With regards to VATS pneumonectomy, the numbers are too low for any robust analysis to be performed. Additionally, there are obvious implications from patient selection for procedures; surgical approach will be determined by size, spread and location of tumour(s) and therefore more advanced cancers will require more extensive surgery. As such crude mortality rates may only represent the difference in patient baseline risk.

The evidence base supporting the rapid shift in practice from open to VATS lung resection is divided. There is consistent evidence of reduced complications and peri-operative morbidity following VATS lobectomy. It is associated with reduced arrhythmias, re-intubations, blood loss, blood transfusions, chest drain insertion, post-operative pain/analgesia and length of hospital stay compared to an open approach[20, 21].

Retrospective database cohort studies have not demonstrated a mortality difference between open and VATS lobectomies[20, 22, 23]. Paul et al. found no difference in mortality with two large database reviews, both including over 6000 patients. Investigation of in-hospital mortality (2010)[20] and long-term survival (2014) (median follow-up of 40 months) found no difference between VATS and open lobectomy[24]. More recently, Falcoz et al. (2016) demonstrated a lower mortality rate with VATS lobectomy vs open in a propensity matched analysis of 5442 patients[22]. Their matching however did not include pathological cancer stage resulting in the VATS group having more stage 1 cancers than the open group, potentially limiting the validity of the result.

Further investigation of post-operative physical function, safety and cost-effectiveness is underway in the 500-patient study, Video Assisted Thoracoscopic Lobectomy Versus Conventional Open LobEcTomy for Lung Cancer (VIOLET). The primary outcome in this RCT is to determine a difference in self-reported physical function five weeks following surgery in open and VATS lobectomy groups. A secondary outcome of the study is survival to one year, whilst this study is not powered to detect survival differences it represents the largest VATS vs open RCT to date[25]. Without robust large RCTs specifically powered to detect mortality difference between surgical approaches it is impossible to definitively state whether this change in practice will convey a mortality benefit.

1.1.2.3 Morbidity following lung resection

The relatively low post-operative mortality rate is balanced against significant early and late post-operative morbidity. Early post-operative morbidity leads to increased in-hospital[26] and long-term mortality[27-29].

1.1.2.3.1 Early post-operative morbidity

The incidence of early post-operative morbidity following lung resection ranges from 18.4%-47%[27, 28]. This variation is, at least in part, due to differing definitions of post-operative complications used in these studies. In 2015 The Society of Thoracic Surgeons (United Kingdom) and the European Society of Thoracic Surgeons produced a joint standardisation of variable definitions and terminology that defined cardiopulmonary complications[b] following lung resection, Table 1-1.

Major cardiopulmonary complications	
Respiratory	Acute respiratory distress syndrome/acute lung injury Respiratory failure Need for reintubation Prolonged mechanical ventilation >24 h Pneumonia Atelectasis requiring bronchoscopy Pulmonary oedema Pulmonary embolism
Cardiovascular	Arrhythmia requiring treatment Acute myocardial ischemia Acute cardiac failure Stroke/transient ischaemic attacks
Renal	Acute kidney injury

Table 1-1 Major cardiopulmonary complications following lung resection
Definitions by The Society of Thoracic Surgeons and the European Society of Thoracic Surgeons general thoracic surgery databases: joint standardisation of variable definitions and terminology[30].

Major complications are increased in pneumonectomy vs lobectomy, open vs VATS approach, >75 vs <75 years, with vs without cardiac comorbidities and predicted post-operative forced expiratory volume in 1 second <70% vs >70%[17]. A meta-analysis of 20,755 patients by Pucher et al. demonstrated reduced overall survival after post-operative infectious complication (HR 1.92 [95% CI 1.50, 2.35]) and after any post-operative complication (HR 1.28, [95% CI 1.21, 1.34])[27]. Lugg et al. showed, even after excluding early post-operative deaths, patients who specifically develop post-operative pulmonary complications have decreased survival (median survival 40 months vs 45.8 months)[28], Figure 1-6.

[b] Whilst complications directly related to the operation itself (haemorrhage, haemo-/pneumo-thorax, air leak, empyema, bronchopleural fistula, infection, etc) have significant impact on immediate post-operative morbidity and mortality, discussion will focus on non-surgical complications as they more closely relate to the underlying hypothesis of this thesis.

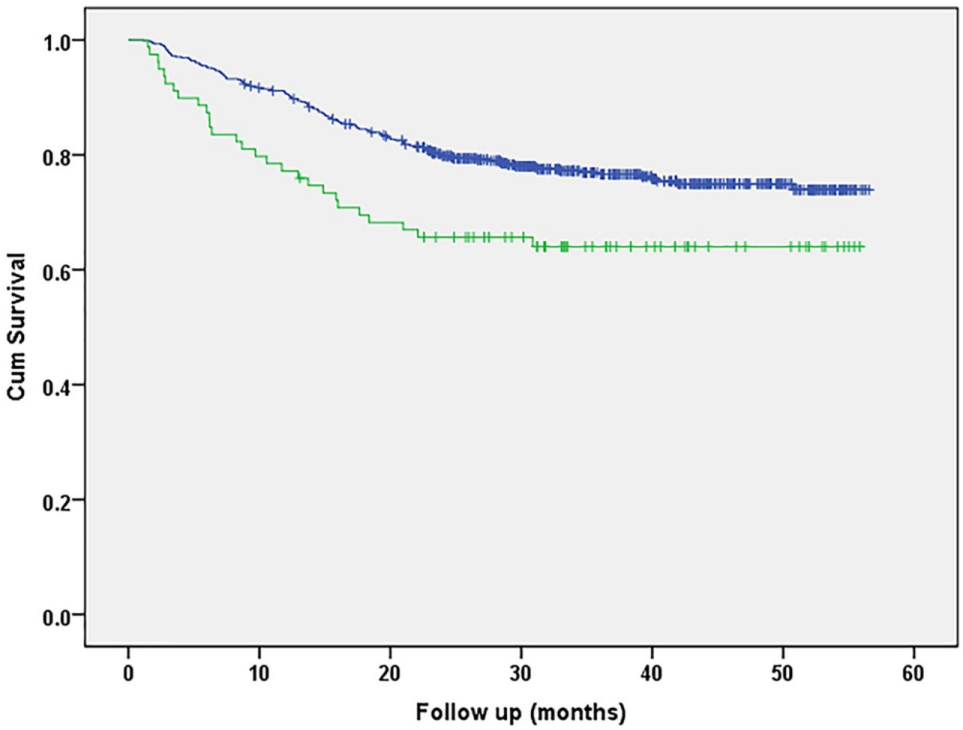

Figure 1-6 Survival of patients with and without a post-operative pulmonary complication
Kaplan-Meyer plot of survival of patients who develop a post-operative pulmonary complication(bottom line) vs patients without a complication (top line), median survival 40 months, [95% CI 34.1, 43.8] vs 45.8 months [95% CI 44.3, 47.3], p=0.006. Early post-operative deaths excluded. Mean follow-up 40 months. Image from Lugg et al.[28].

Our research group has completed the largest cohort study (253 patients) of unplanned admission to the intensive care unit (ICU) following lung resection published to date[31]. We demonstrated an unplanned ICU admission rate of 2.3% with an ICU mortality of 29.0% [95% CI 23.2, 35.3%] vs a mortality of 0.03% [95% CI 0.01, 0.10%] in patients not admitted to ICU ($p < 0.001$). The majority of patients were admitted with respiratory failure (68.1%) of which the main causes were; infection (27.3%), sputum retention (15.4%), persistent air leak/surgical emphysema (6.7%) and acute lung injury (6.3%). Alternative reasons for ICU admission were; bleeding (6.4%), airway compromise (6.0%), acute kidney injury (5.2%), cardiac arrest (4.8%) and sepsis (2.8%). Subsequent analysis of the patients admitted to ICU demonstrated that the requirement for both mechanical ventilation with renal replacement therapy (OR 2.04, [95% CI 1.07, 3.90]) and RV dysfunction (OR 3.93, 95% CI 1.71, 9.03) were predictive of ICU mortality, data unpublished at time of writing.

1.1.2.3.2 Late post-operative morbidity

Patients face significant long-term morbidity following lung resection with reduced pulmonary function[32-36], impaired quality of life (QOL)[37-40] and reduced

exercise tolerance[34, 36, 41-46]. Two-thirds of patients of who survive 5 years or more following lung resection report at least one pulmonary symptom with a third reporting dyspnoea[47].

Lung resection is associated with a post-operative reduction in physical components of quality of life (QOL) scoring[c] [37-40]. Möller and Sartipy demonstrated the relationship between pre-operative and 6-month post-operative QOL and survival with the Short Form-36 (SF-36) questionnaire; a reduction in pre-operative and the post-operative change in the physical component of SF-36 summary scores, was associated with reduced survival (HR 0.932 [95% CI 0.932, 0.985] and 0.82 [95% CI 0.692, 0.985]). Of note, a reduction in physical function had the strongest association with reduced survival (HR 0.72 [95% CI 0.606, 0.855]).

Multiple studies have investigated changes in exercise tolerance from pre-operative baseline following lung resection with 6MWT[41], stair climbs[36], cardiopulmonary exercise testing (CPET)[34, 41-45] and volumetric flow catheters[46, 48, 49]. Exercise capacity measured by maximal consumption of oxygen (VO_2 max) has universally been shown to decrease following pneumonectomy by a range of 16.1-28%[42, 46, 50-54] however the changes following lobectomy are less clear with studies demonstrating no significant change in VO_2 max[42, 46, 55] with others demonstrating a significant fall of 13-20.8%[34, 44, 50, 52].

The two largest studies to assess exercise capacity give conflicting results for patients undergoing lobectomy. Brunelli et al. used stair climbing to predict VO_2 max in 200 patients[36] and Win et al. performed shuttle walk testing measuring distance completed in 110 patients[56]. Brunelli et al. investigated exercise capacity pre-operatively, at discharge, 1 and 3 months post-operatively, they found a persistent decrease in VO_2 max in the patients that had undergone pneumonectomy (11–17.6%) but only a transient reduction at discharge in patients who had undergone lobectomy (12%)[36]. Win et al. showed a similar pattern of a greater reduction in pneumonectomy but the 3 and 6-month lobectomy follow-up

[c] Poghosyan et al.s' systematic review demonstrate a post-operative improvement in mental health QOL. This may purely represent the difference in mental health QOL scoring prior to major cancer surgery against post-operative testing in survivors.

had persistent reduction in distance covered (reduction of 75m (17%) and 68m respectively (16%))[56].

1.1.2.3.3 Factors affecting late post-operative morbidity

There is a clear difference in post-operative exercise capacity between pneumonectomy and lobectomy although the relationship between the change in lung function and exercise capacity is relatively poor. A decrease in forced expiratory volume in one second (FEV_1) only partially accounts for the decrease in exercise capacity (R^2=30%)[51] and a decrease in VO_2 Max (R^2=18%)[50]. This suggests that it may not be solely a decrease in respiratory function that causes a reduction in exercise capacity.

Cardiovascular limitation may limit exercise capacity following lung resection[34, 56]. Nezu et al. performed CPET of 82 patients (62 lobectomy) and demonstrated a post-operative reduction in exercise capacity. Patients only demonstrated a reduction of cardiac function on exercise (reduction in maximal heart rate (HR) and O_2 pulse (VO_2 max/HR)) without any reduction in respiratory function[34]. The hypothesis of cardiovascular limitation following lung resection is discussed later in this chapter and throughout the thesis.

1.1.2.4 Summary of management of lung cancer

Whilst surgical management has progressed towards a minimally invasive approach, there is no definitive evidence of a mortality benefit compared to an open approach, there is however evidence favouring VATS in terms of morbidity, as detailed above. Lobectomy (vs pneumonectomy) has reduced post-operative morbidity and a smaller reduction in post-operative exercise capacity, if present at all.

It is apparent that the increasing rates of resection and ages of patients undergoing resection will present the thoracic anaesthetist with older, sicker, higher risk and ultimately more challenging patients. Whilst surgical advances have limited peri-operative complications, the anaesthetist must also endeavour to advance their peri-operative management of such patients. To do so they must understand the challenges lung resection poses to a patient, particularly in reference to the debilitating post-operative dyspnoea (“pulmonary disability”). Of

note, 2013 guidelines for the assessment of patient suitability for lung resection concluded that:

"Ultimately though, the factors that contribute to long-term pulmonary disability, either individually or in concert, remain largely unknown. This makes predicting who exactly will suffer long-term pulmonary disability following lobectomy or pneumonectomy largely speculative."

Alessandro Brunelli (2013)[57]

1.1.3 The hypothesis of right ventricular dysfunction following lung resection

It seems intuitive that removal of lung parenchyma alone could result in pulmonary complications and a reduction in exercise capacity but there is evidence that the pathophysiological mechanism is multifactorial with cardiovascular limitation widely hypothesised to contribute. Previous work has focused on the role of RV dysfunction following lung resection[48, 49, 58-77]. Early work by Reed et al. and Okada et al. hypothesised that RV dysfunction occurred and that it was caused by an increase in RV afterload[48, 49, 58-60]. Although their results are questioned based on the design of the studies and the validity of the methods of assessment of RV function used, the hypothesis remains widely accepted without definitive evidence[78, 79]. This hypothesis is the basis of this thesis and the evidence base will be explored in detail in Chapter 2.

It is the hypothesis of our research team that RV dysfunction contributes to this "pulmonary disability". Before describing the conflicting evidence to date and the work our research group has undertaken to demonstrate RV dysfunction following lung resection, it is imperative to understand the normal structure, physiology and complex interaction(s) of the RV and pulmonary vasculature.

1.2 The right ventricular pulmonary vasculature unit

The RV has long been overlooked and under-investigated. An early description of the RV from 1628 highlights the persisting view that it purely acts as a conduit of peripheral blood to the lungs:

"... And I ask, as the lungs are so close at hand, and in continual motion, and the vessel that supplies them is of such dimensions, what is the use or meaning of this pulse of the right ventricle? And why was nature reduced to the necessity of adding another ventricle for the sole purpose of nourishing the lungs?"

Sir William Harvey, 1628[80]

In the almost 400 years since this description there has been slow improvement in the understanding of the importance of the RV. In 2006 the National Heart, Lung, and Blood Institute Working Group on Cellular and Molecular Mechanisms of Right Heart Failure produced the first of a series of reviews of the RV to be published in Circulation[81]. It was their conclusion that:

"The consensus of the working group is that the role of the right ventricle in a spectrum of cardiovascular diseases has been relatively neglected proportionate to its central importance."

Voelkel et al.[81]

Additionally, they highlighted the need for RV "awareness" and for research to focus on the RV.

A further review titled "Assessment of Right Ventricular Function in the Research Setting: Knowledge Gaps and Pathways Forward" was published in 2018 by a group of twenty experts convened by the American Thoracic Society. Whilst it highlights the progress made in understanding of the RV there are clear gaps in basic knowledge regarding RV function and failure, in particular the method of assessing RV function and the specific mechanisms of RV failure[82].

Historically research has focused on the LV and to a lesser extent the pulmonary circulation. Much of the previous knowledge of the RV had been based on simple

translation of the LV literature[83, 84]. As this section will outline, the RV is very different to the LV[d].

1.2.1 Anatomy

In understanding the structure and then physiology of the RV, it is again important to stress its differences and therefore its vulnerabilities compared to the LV. The two ventricles can be thought of as two pumps connected in series in a closed system. Both pumps must have the same (cardiac) output for the system to work. As both ventricles contract at the same (heart) rate they therefore must pump the same (stroke) volume. The differences between the work required of each pump is dictated by the structure of each circulation (pulmonary and systemic). The RV is only required to pump blood to the adjacent lungs whereas the LV must pump blood around the entire body. To achieve this the RV only needs to generate a small pressure compared to the LV. The nature of the pumps (muscular mass and ability to generate pressure) and of the vessels (structure, pressure and resistance) that form the circulations are matched to this requirement. A summary of the differences between the two ventricles and their circulations is included after further discussion, Table 1-2.

1.2.1.1 Anatomy of the right ventricle

The RV is the most anterior chamber of the heart and receives deoxygenated blood from the venous circulation via the right atrium (RA). The anatomy of the RV is again subsidiary to the LV as it wraps around the conical LV, Figure 1-7. This results in a triangular crescent shape curled around the LV with a shared interventricular septum between the two ventricular insertion points of the RV free wall. Additionally, there are encircling epicardial fibres linking the two ventricles[81]. The RV can be divided into three regions: inlet/sinus (tricuspid valve, chordae tendineae and papillary muscles), apex (trabeculated myocardium) and outlet/infundibulum (smooth muscle outflow tract to pulmonary valve)[83].

[d] This section will provide an overview of RV function and afterload. In subsequent chapters, there will be further in-depth review of RV function and afterload specific to the topic of each investigation.

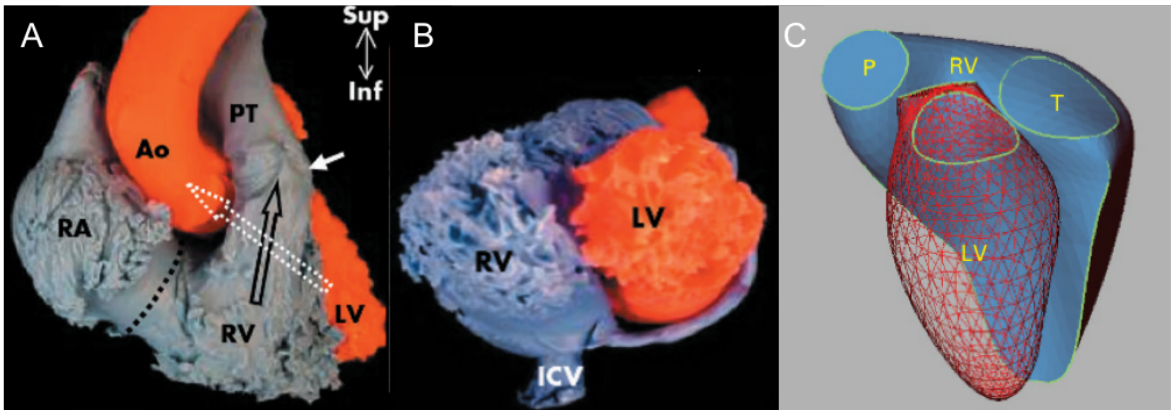

Figure 1-7 Structure of right ventricle and its relationship to the left ventricle
Images formed from endocast of a normal heart. Right ventricle (RV) in blue/grey, left ventricle (LV) in red. A (view from anterior) RV blood flow travels from right atrium (RA) through the tricuspid valve (black dotted line) and out the RV outflow tract (black arrow) to pulmonary trunk (PT). Ao= aorta.
B (view from apex) and C (3D model) RV wraps around the concentric LV. ICV= inferior vena cava. P= pulmonary valve. T= tricuspid valve. Images from Ho et al.[85] and Sheehan et al.[86]

As the pulmonary circulation is at a lower pressure than the systemic circulation the RV only performs 25% of the stroke work of the LV, this results in the RV having a thin musculature wall of 3-5mm in thickness (compared with 7-11mm in the LV)[81] and a lower overall muscle mass[87]. Within the RV myocardium, myofibres are predominately arranged longitudinally with some helical fibres that give torsion. The LV has an additional middle layer of circumferential myofibres that contract to decrease the cross-sectional diameter of the LV[86]. The musculature of the interventricular septum is predominantly LV fibres although there are some longitudinal RV[83, 88].

Contraction of the RV is by sequential contraction of the inlet, trabeculated myocardium and finally outlet[88]. The resultant contraction is formed through three movements; RV free wall toward septum (bellow movement), shortening (longitudinal fibres) and traction of RV free wall (from LV via insertion points)[83]. Due to the motion of the interventricular septum, ventricular insertion points and myofibre continuity between ventricles, LV contraction will lead to a degree of "passive" RV contraction. This is part of ventricular interdependence; the function of one ventricle is influenced by the other[89]. This dependence may be of particular importance in the lung resection population as isolated RV dysfunction may lead to LV dysfunction.

The blood supply to the RV is mainly by the right coronary artery in right-dominant coronary artery systems (80% of the population), with the anterior wall supplied by the left anterior descending artery[88]. Unlike the higher pressure LV the RV myocardium receives blood during systole and diastole although this is reduced in RV hypertrophy and/or pressure overload[90].

1.2.1.2 Anatomy of the pulmonary circulation

The pulmonary circulation is described as a low pressure low resistance system in contrast to the high pressure high resistance systemic circulation[91]. The pulmonary vasculature is a series of bifurcations rapidly originating from the curved main pulmonary artery (PA), Figure 1-8. After bifurcating to right and left PA each subsequent division follows the corresponding conducting airways to the alveolar capillary beds[92, 93]. The majority of the surface area of the pulmonary vasculature is in the capillaries, 50-70m^2 compared to 1.4m^2 in the arteries and arterioles combined[69, 93]. The pulmonary arteries are elastic in nature with less smooth muscle than the systemic circulation. Whilst this ensures the vessels are compliant the low pulmonary artery pressure and resistance also limits its ability to control regional blood flow[94, 95].

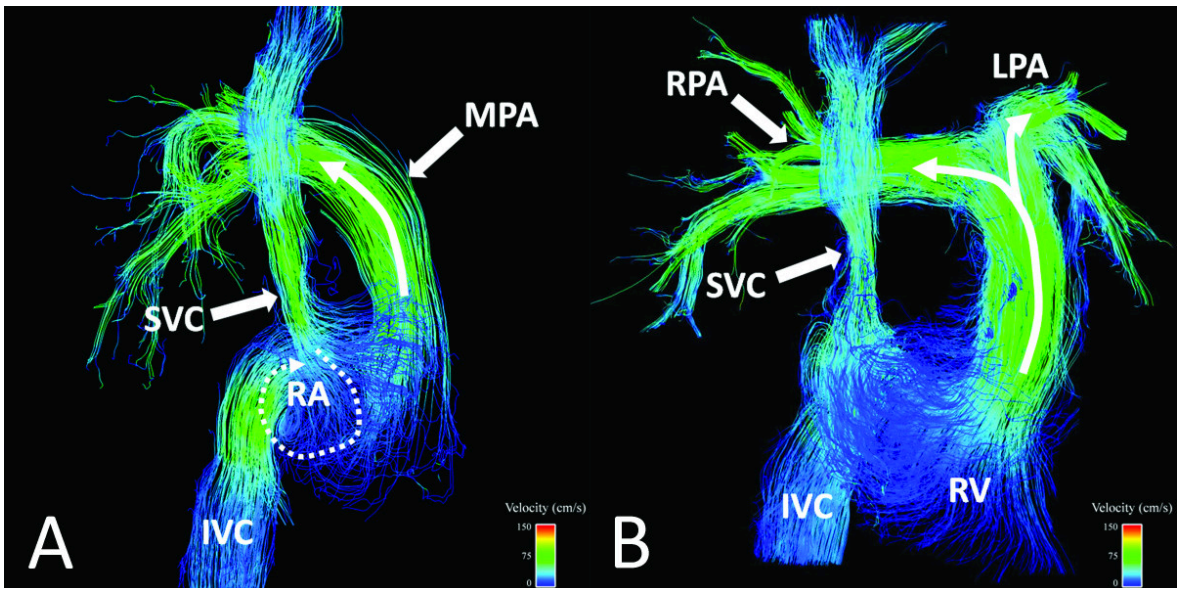

Figure 1-8 Blood flow in pulmonary arteries
4D cardiac magnetic resonance imaging of systolic flow in a healthy volunteer's pulmonary arteries. A, venous blood returns to the right atrium (RA) from the inferior (IVC) and superior vena cava (SVC) but is blocked from entering the right ventricle (RV) by closed tricuspid valve. RV removed from image for clarity.
B, RV propels blood through main pulmonary artery (MPA) to the bifurcation of into right (RPA) and left pulmonary arteries (LPA). Note the very short distance blood has to travel to the lungs.
Image from Francois et al.[96].

	Right ventricle	Left ventricle
Shape	Side: triangular Cross section: crescentic	Elliptic
Mass, g/m2	26±5 (17–34)	87±12 (64–109)
Thickness of ventricular wall (mm)	2-5	7-11
Ventricular pressures, (mmHg)	25/4 [(15–30)/(1–7)]	130/8 [(90–140)/(5–12)]
Vascular resistance (dyne.s.cm^{-5})	70 (20–130)	1100 (700–1600)

Table 1-2 Summary of right and left ventricle characteristics
Data from Haddad et al.[83]

1.2.2 Physiology

The function of the RV is determined by its ability to eject blood by contraction and the loading conditions of the circulation it sits within, i.e. contractility, preload and afterload[83].

1.2.2.1 Contractility

Contractility[e] is:

> *"the innate ability of the muscle to generate force."*
>
> Carabello 2002[97]

Contraction of the RV results in the pressure and flow changes demonstrated in Figure 1-9. There is a rapid increase in RV pressure (RVP) which will open the pulmonary valve once it exceeds pulmonary artery pressure (PAP) and lead to forward flow of blood in the MPA. Flow and pressure in the PA rapidly peak and fall with the pulmonary valve closing as the RV relaxes in diastole[88, 98]. Diastolic relaxation is caused by the energy dependent process of calcium re-uptake into the sarcoplasmic reticulum within the myocyte. The ability of the ventricle to relax in termed lusitropy[99].

[e] Contractility will be explored in greater detail in Chapter 5

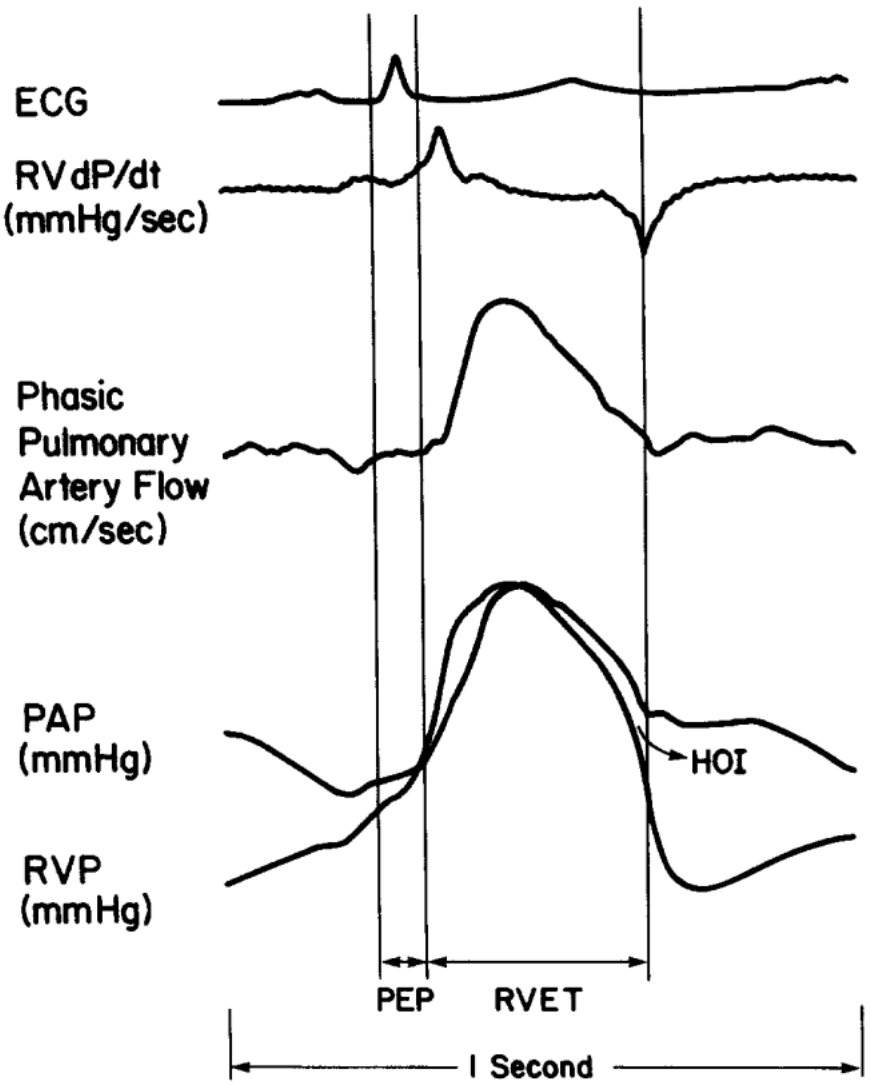

Figure 1-9 Simultaneous right ventricle and pulmonary artery cardiac cycle
Electrical stimulation of the right ventricle (RV) stimulates RV contraction following isovolumetric contraction/pre-ejection period (PEP). After the pulmonary valve opens a rapid increase in RV pressure (RVP) leads to increased pulmonary artery pressure (PAP) and flow. This coincides with peak rate of RV pressure development (RV dP/dt). Hangout interval (HOI) occurs when forward flow of blood in PA continues in spite of a negative pressure gradient between PA and RV. Image from Dell'Italia[88].

The period of RV contraction with a closed tricuspid valve prior to pulmonary valve opening is termed isovolumetric contraction (referred to as PEP in Figure 1-9). As the RV has a lower arterial pressure to overcome it has a shorter isovolumetric contraction time compared to the LV. At low pulmonary pressures there may be no isovolumetric contraction period with tricuspid closure and pulmonary valve opening simultaneously[88]. Timing of the closure of the pulmonary valve is more complex. Some authors argue that, under certain conditions, there is a "hangout interval" when PAP is greater than RVP, but the pulmonary valve remains open and there is still forward flow of blood, seemingly against a pressure gradient. It is thought this may be due to the momentum of blood through the outflow tract[88].

Interestingly the hangout interval shortens with increasing pulmonary artery pressure suggesting this phenomena is reduced with an increase in afterload[86, 98]. The complex relationship between afterload and pulmonary blood flow will be discussed in detail in Chapter 7.

1.2.2.2 Preload

Preload is:

> *"the load present before contraction"*
>
> Haddad 2008[83]

Preload is dependent on intravascular volume status, passive/active RV filling, RV relaxation/compliance and factors external to the RV (pressures resultant of LV filling, respiration and pericardial constraint)[100]. Dell'Italia demonstrated the presence of RV Frank Starling mechanisms that link preload and contraction by measuring stroke volume following extrasystolic beats. The prolonged RV filling following an extrasystolic beat resulted in increased RV end-diastolic volume (RVEDV) and pressure (RVEDP), stroke volume (SV) and ejection fraction (RVEF) without a change in end-systolic volume or pressure, i.e. the RV increases its contractility in the presence of increased preload[101]. Excessive RV preload can impair cardiac output by overstretching of myocytes and impairment of LV filling by flattening the interventricular septum, an example of ventricular interdependence[102]. Additionally, volume overload of the RV can lead to tricuspid annular dilatation and tricuspid regurgitation reducing forward flow of blood to the lungs[88]. Classically the compliant RV is said to be tolerant of preload.

1.2.2.3 Afterload

Afterload[f] is most accurately described as:

> *"the load that the RV has to overcome during ejection."*
>
> Haddad 2008[83]

[f] Afterload will be discussed in detail later in this chapter and in Chapters 6 and 7.

It is easy to assume afterload is simply the opposing pressure in the pulmonary artery that the RV must exceed, i.e. to open the pulmonary valve and generate forward flow of blood, but this interpretation is overly simplistic. This can be seen in the hangout interval where forward flow of blood continues against a pressure gradient. In describing the hang-out interval Dell'Italia comments on the complexity of afterload:

"The observation of continued forward flow in the presence of not only a declining pressure but also a negative pressure gradient emphasizes the inability of pressure measurements alone to define the mechanisms of right ventricular-pulmonary artery coupling because total right ventricular afterload comprises resistive, capacitative, inertial, and pulse wave reflection properties of the pulmonary vasculature."

Dell'Italia 1991[88]

Afterload can therefore be considered to comprise of resistive (resistance to steady flow and inertia of blood) and pulsatile (absorption/storage and reflection of each pulse wave) components[103]. Given the highly compliant low resistance nature of the pulmonary vasculature it is unsurprising that the RV is intolerant to increases in afterload[91]. As the load resisting RV ejection increases the thin walled RV struggles to maintain its stroke volume and output[102], Figure 1-10.

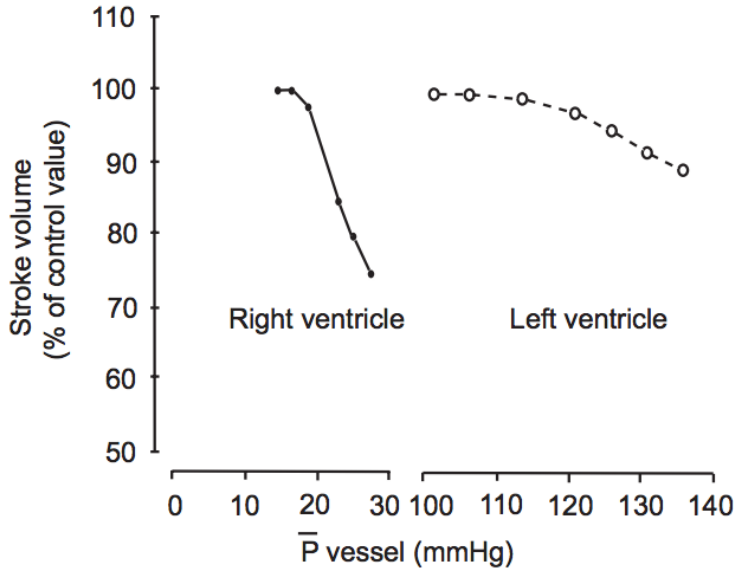

Figure 1-10 Right and left ventricular response to increase in afterload
Compared to the left, the right ventricle is unable to maintain its stroke volume in the face of small increases in afterload/pressure (P). Image from Chin et al.[102]

1.2.2.4 Relationship between contractility, preload and afterload

Myocardial function can be pictured as a single myocyte contracting against a given load, Figure 1-11. On initial stimulation the myocyte will contract until it generates a tension greater than the opposing force (a-b in Figure 1-11), only at this point will myocyte shortening occur (b-c). Similarly, the myocyte maintains tension as it reverts to its original length (point c). The maximal velocity of shortening can be plotted as the maximal gradient of shortening after point b[104].

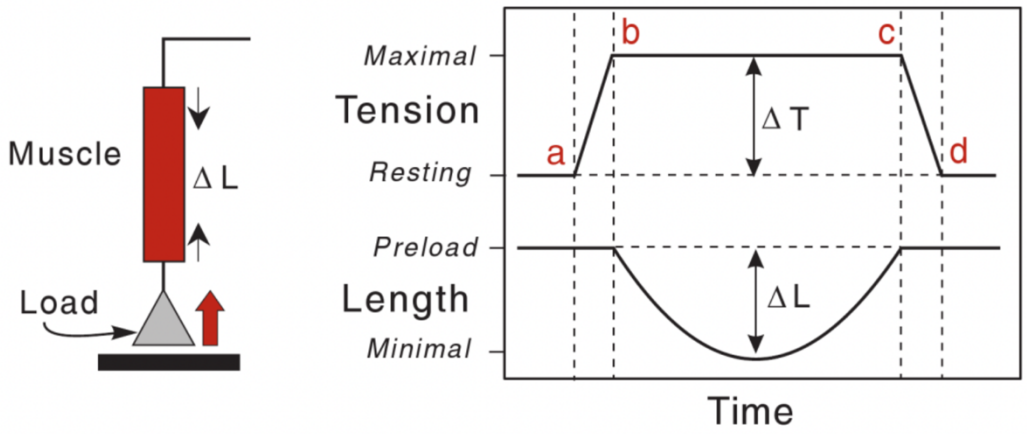

Figure 1-11 Isolated myocardium contraction
Myocyte contraction against a given load generates an increase in tension (ΔT, top plot) and shortening (ΔL, bottom plot). Images from Cardiovascular Physiology Concepts by Klabunde[104].

As the load against which the myocyte contracts (*afterload*) increases a greater tension (ΔT) is required prior to shortening resulting in a reduction in myocyte shortening (ΔL) and the velocity at which the shortening occurs[105], discussed later in section 5.2.3.1 page 150. Experimentation in skeletal[106] and cardiac[105] muscle has demonstrated that there is an inverse relationship between the force opposing myocyte contraction (*afterload*) and the velocity of myocardial shortening. This relationship is described as the *force-velocity relationship*, demonstrated by the red curves in Figure 1-12[104].

An increase in *afterload* decreases the velocity of shortening until the maximal force that the myocyte can generate (Fmax) is insufficient to overcome the opposing load and shortening does not occur. Conversely, as afterload decreases the velocity of shortening increases until a theoretical maximal velocity (Vmax), this cannot be directly measured as the myocyte cannot contract against no load, Figure 1-12[104].

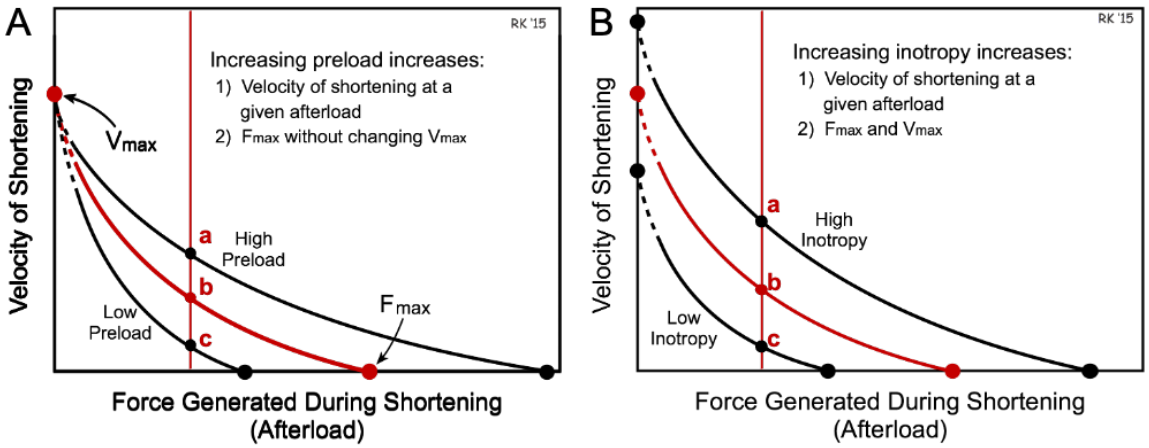

Figure 1-12 Change in force-velocity relationship with preload and inotropy
Force-velocity relationship alteration with preload (A) and inotropy (B). Note inverse force-velocity relationship throughout and the change in maximal velocity (Vmax, y intercept) and force (Fmax, x intercept) with changes in preload and inotropy. Increased preload and inotropy will increase the velocity of shortening for the same afterload (increase in velocity at points c -> b -> a). Image annotated from Cardiovascular Physiology Concepts by Klabunde[104].

The force-velocity relationship of the myocyte is altered by preload and inotropy. As described by the length-tension relationship, an increase in preload will increase the starting tension of the myocyte allowing it to generate a greater tension (increase in Fmax) and a greater velocity of shortening for the same load, however, it will not change Vmax, left plot in Figure 1-12[104]. An increase in inotropy/contractility will lead to a right shift of the force-velocity relationship with an increase in Vmax and Fmax. As such the velocity of myocardial shortening is influenced by contractility, preload and afterload therefore an increase in afterload can be compensated by an increase in preload and/or contractility.

1.2.2.5 Pressure volume loops

The interaction between RV contractility, preload and afterload can also be demonstrated by pressure-volume loops[103], Figure 1-13. Simultaneous measurement of intra-ventricular pressure and volume allow the calculation of elastance (the change in pressure for a given change in volume)[107]. Whilst this approach is predominately performed in animals as a research tool it gives a complete picture of RV physiology[103, 108, 109].

1.2.2.5.1 Baseline function and definitions

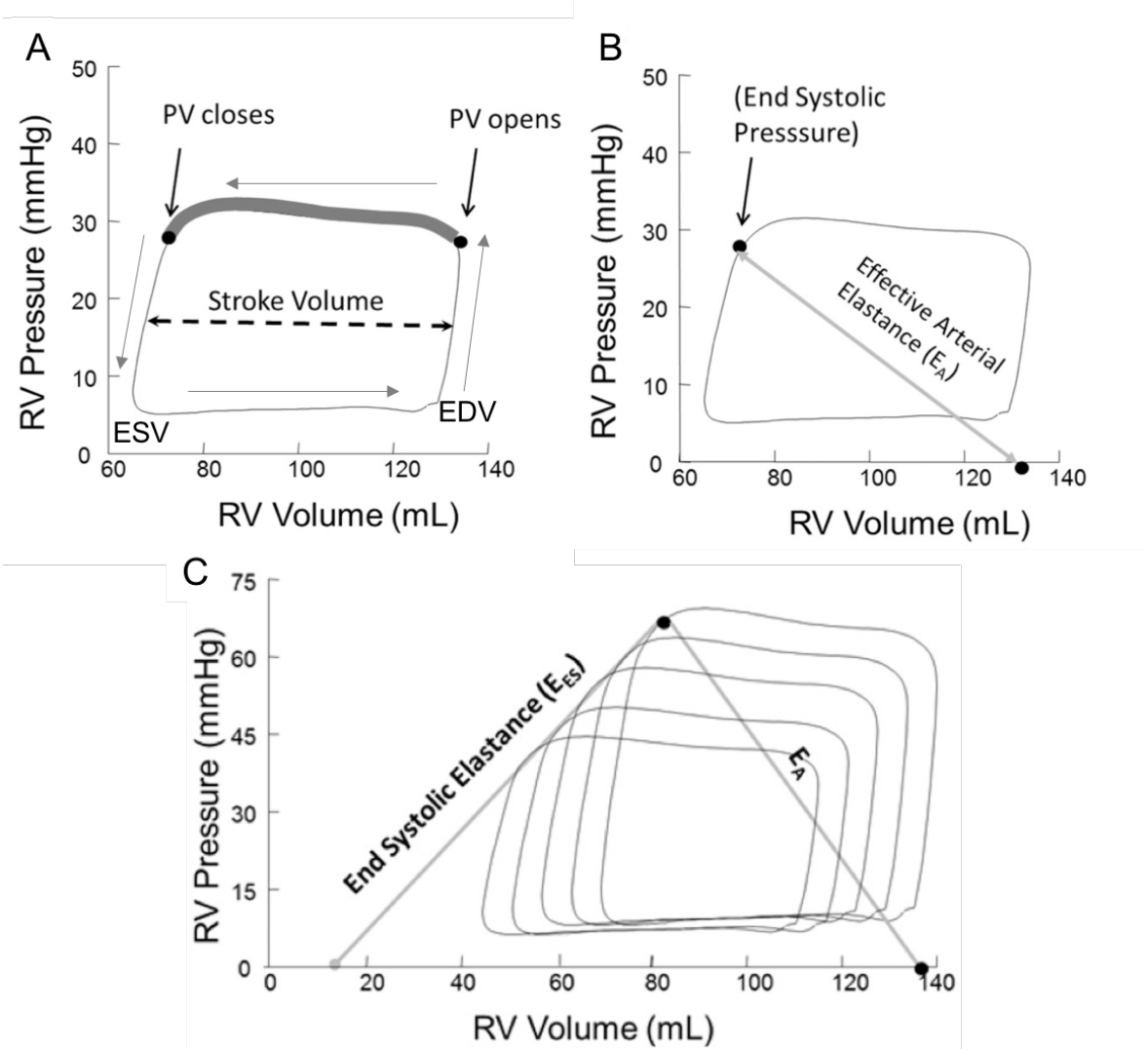

Figure 1-13 Right ventricular pressure volume loops
Illustrative plots of simultaneous measurement of RV pressure and volume.
A, RV volume increases from end systolic volume (ESV) without increase in pressure. At end diastolic volume (EDV) isovolumetric contraction occurs until the pulmonary valve (PV) opens. Ejection of the RV stroke volume occurs until the PV closes, followed by isovolumetric relaxation.
B, Effective arterial elastance (E_A) calculated from point joining (ESV, ESP) to (EDV, 0).
C, End systolic elastance (E_{ES}) calculated as gradient to ESP of pressure volume loops of varying load. Images from Tedford[103].

Effective arterial elastance (E_A) is described by Tedford as a "lumped measure of afterload" that accounts for resistive and pulsatile components[103, 110]. It is calculated from the gradient of a line joining end systolic pressure/volume to end diastolic volume[111], see Figure 1-13C. A surrogate measurement of E_A, calculated as mean PAP (MPAP) divided by SV, is markedly increased in pulmonary hypertension[110, 112].

End systolic or maximal elastance (E_{ES} or E_{max}) are load independent measures of contractility, they are often, somewhat inappropriately, used

interchangeably[110, 113, 114]. E_{ES} is calculated from the gradient of the end systolic pressure-volume relationship (ESPVR) of incrementally varied loading conditions, whilst E_{max} is calculated from the gradient of the line joining the points of maximal elastance of synchronised beats of varying load[115], Figure 1-14. Often the two measures will give the same value although with the varying preloads used for calculation, subsequent changes in afterload can alter the time taken to reach maximal end-systole, i.e. it doesn't occur at the corner of the pressure-volume loop. Frequently authors calculate E_{ES} but use the notation of E_{max}.

In the RV, E_{max} has been demonstrated to be representative of changes in inotropy over a wide range of loading conditions and it may be superior to E_{ES} due to lack of isovolumetric relaxation period. Compared to the LV, RV pressure-volume loops tend to have a trapezoid shape due to the lack of a straight line of increasing/decreasing pressure at static volumes during isovolumetric contraction/relaxation. Measuring E_{ES} from the point of end-systolic point therefore may be inaccurate[86].

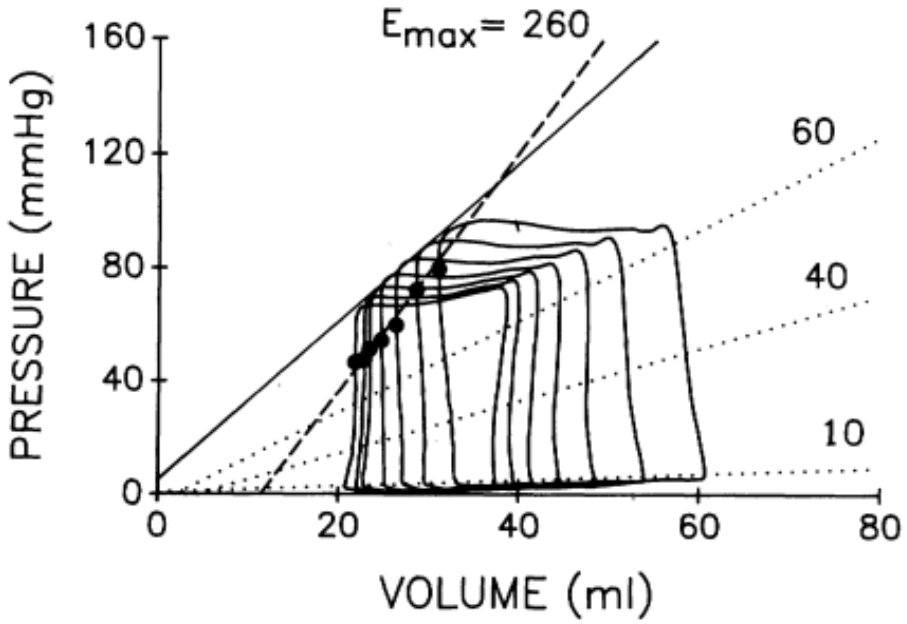

Figure 1-14 Comparison of end systolic and maximal elastance
Demonstration of difference between end systolic elastance (E_{ES}) and maximal elastance (E_{max}), data from the left ventricle of a closed chest dog measured by conductance catheter. E_{ES} (solid line) joins the end-systolic pressure volume relationship (ESPVR) of varying load whereas E_{max} (dashed line) joins the points of maximal elastance for each loop (260ms in this example). Dotted lines represent E_{max} at 10, 40 and 60ms. Note steeper E_{max} than E_{ES}. Image from Kass and Maughan[115].

Coupling (E_{max}/E_a) is the ratio between ventricular and arterial elastance, i.e. the balance between contractility and afterload[111]. RV coupling varies on the method

used to calculate it and both E_{max}/E_a and E_a/E_{max} are used in literature[103, 110-112, 116], for consistency coupling will be calculated as E_{max}/E_a in this thesis. In a perfectly balanced system coupling would be assumed to equal 1, however a range of 1.5-2 is seen in normal human physiology[109, 110].

1.2.2.5.2 Right ventricular adaption

The ventricular response to afterload demonstrates the adaption required to maintain coupling between the ventricle and the circulation. Leeuwenburgh et al. demonstrated the RV and LV response to increased RV afterload in lambs[117], Figure 1-15 and Figure 1-16. Five lambs were subjected to pulmonary artery banding and, after 8 weeks, conductance catheters were placed into the RV and LV. Preload reduction by gradual inferior vena cava compression allowed calculation of E_{max}. This was compared to five age matched control lambs. Additionally, a dobutamine infusion was administered to assess the ability of the ventricles to increase contractility, Figure 1-16.

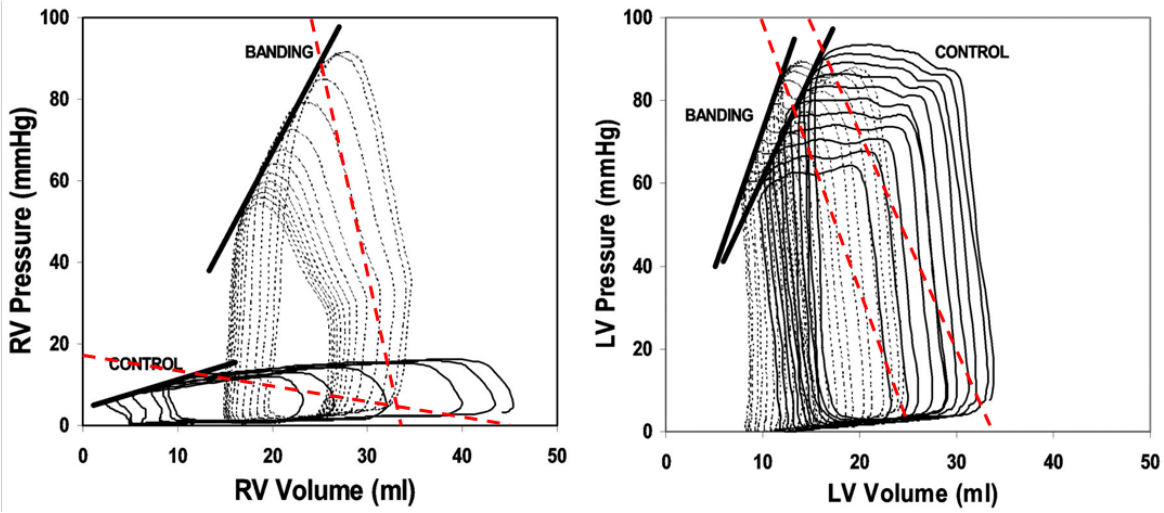

Figure 1-15 Right and left ventricular pressure volume loop in simulated pulmonary hypertension
Lamb pressure-volume loops of the RV (left) and LV (right). Solids lines represent control lambs, dashed lines represent pulmonary artery banding lambs. Red lines depict E_a for the loop at maximal preload, i.e. baseline. Thick solid gradient line represents end-systolic elastance. Note increased RV pressure and volume in the banding group. Image annotated from Leeuwenburgh et al.s' originals[117].

The adaption of the RV to chronic increase in afterload is apparent in the left pane Figure 1-15. To maintain the stroke volume and therefore cardiac output the RV must generate a far greater pressure, the increase in the height of the loop. This will increase the pressure at which the PV closes and so the angle of E_a (red dashed line). To achieve this increase in pressure generation the RV has to increase its

contractility (E_{max}) and its work (the area within the loop). In the experiment RV wall thickness increased in the banding group, this led to a reduced RVEDV potentially due to a decrease in compliance and therefore filling of the ventricle.

The subsequent effect of the PA banding on the LV is shown in the right pane of Figure 1-15. The RV afterload increase reduces blood flow through the pulmonary vasculature (reduced stroke volume) and the higher pressure in the RV can compress the interventricular septum (reduced LVEDV and LVESV) leading to an underfilled LV, demonstrated by the dashed banding loops at a lower volume. As the systemic circulation is unchanged there is no change in E_a (afterload), no change in the LV maximal pressure and minimal change in E_{max} (contractility).

A dobutamine infusion predominately increases inotropy[g] and therefore contractility for the ventricles[119]. The banding group had a lower cardiac output both at rest and with dobutamine compared to the control group. The degree of increase in RV contractility in response to exercise is termed RV contractile reserve[120] (RVCreserve, discussed further in 1.2.6.2). Under normal conditions the RV should be able to increase its contractility to meet increased demands, as seen in the control group response to dobutamine in the RV pane in Figure 1-16. The banding group has increased its contractility at rest to meet the demands and so has a lower relative increase its contractility with dobutamine, i.e. it has reduced contractile reserve. The relatively unaffected LV has reduced volume in the banding group but has a similar contractility at baseline and in response to dobutamine.

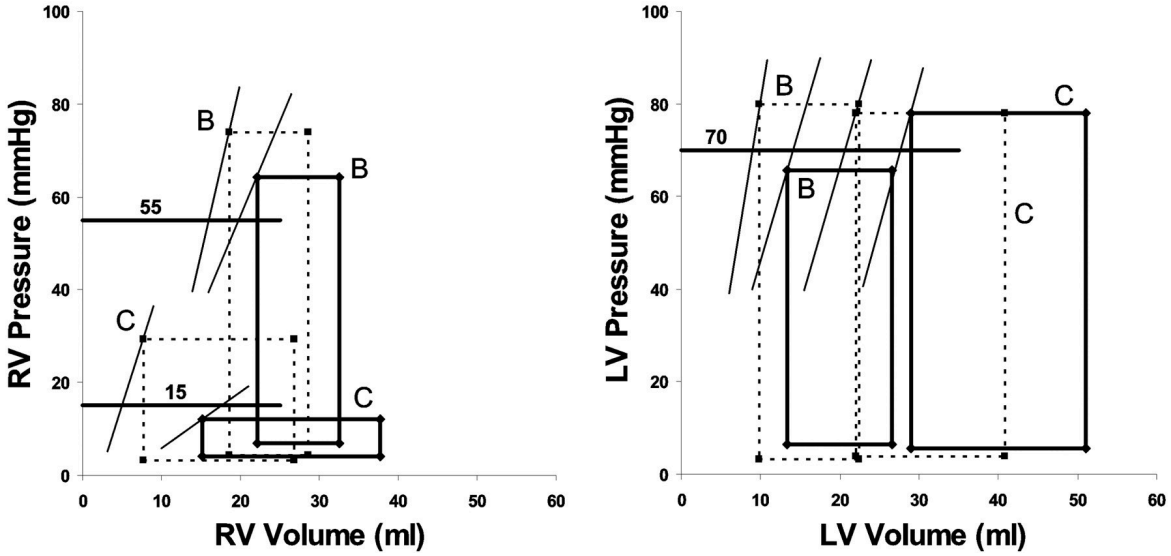

Figure 1-16 Right and left ventricular response to dobutamine
Illustrative pressure-volume loops of the right ventricle (RV) (left) and left ventricle (LV) (right). Solids lines represent baseline measures, dashed lines represent dobutamine infusion. Loop B= pulmonary artery banding lambs, C= control lambs. Images from Leeuwenburgh et al.[117]

1.2.3 Right ventricular failure

This section will review the mechanisms of RV failure (RVF) with particular focus on pulmonary arterial hypertension (PAH), chronic thromboembolic pulmonary hypertension (CTEPH) and pulmonary embolism (PE). Not only are these some of the most common mechanisms of RVF but they are also analogous to the

[g] Dobutamine may also cause dilation of the pulmonary vasculature and reduced pulmonary vascular resistance at doses below 10mcg/kg/min but can increase PVR at higher doses [118]. In Leeuwenburgh et al.s' study the infusion was 2mcg/kg/min therefore there may be a slight degree of dobutamine induced reduction in PVR.

mechanism(s) of RVF following lung resection, discussed below. The specific methods of investigating RV function following lung resection will be explored later in 0, page 61.

The hypothesised mechanism of RV failure following lung resection is secondary to an increase in afterload which may be; an acute intra-operative increase, a chronic post-operative increase, or a combination of the two. There is potentially an acute intra-operative increase in afterload secondary to one lung ventilation (OLV). Intra-operatively the patient is in the lateral position with the operative (non-dependent) lung raised. Institution of OLV leads to collapse of the non-dependent lung and hypoxic pulmonary vasoconstriction (HPV) with the majority of blood flow diverted to the dependent lung[121]. The effect of HPV continues for hours into the post-operative period[122] and there is multifactorial lung injury to the remaining operative lung and the non-operative lung[123]. These acute insults may increase RV afterload and are potentially analogous to the changes seen in a PE which may cause a complete occlusion[h] of the RPA/LPA or a lobar PA branch (similar to the arterial clamping in a pneumonectomy or lobectomy). Following lung resection there may be a chronic increase in afterload secondary to reduced lung volume. It is possible that both these mechanisms contribute to RV failure. Examination of the subtle distinctions between the response to acute and chronic afterload, may demonstrate the mechanisms of RV dysfunction following lung resection.

1.2.3.1 Definition of right ventricular failure

In 2018 two reviews were published on RVF. Ten experts in the field wrote a "state-of-the-art" paper for publication in Intensive Care Medicine[124] and a multidisciplinary working group published an American Thoracic Society (ATS) Research Statement[82]. Prior to these publications there was no consensus definition of RVF. In the ATS review, "Assessment of Right Ventricular Function in the Research Setting: Knowledge Gaps and Pathways Forward" they defined RVF as,

[h] Animal models of PE often use PA clamping to simulate an occlusive PE, a process almost identical to the anatomical change in lung resection.

"a complex clinical syndrome characterized by insufficient delivery of blood from the RV in the setting of elevated systemic venous pressure at rest or exercise."

Lahm et al.[82]

Prior to the ATS definition, Haddad et al. had, separately to RVF, defined *RV dysfunction* as abnormalities of RV filling or contraction without signs of fluid retention, decreased systolic reserve and/or arrhythmia[84]. The ATS definition lowered the threshold for RVF and incorporated "dysfunction" into their definition of failure[i]. The authors stress that early recognition and early intervention may prevent the progression of the previously termed "RV dysfunction" to symptomatic RVF and that acute deterioration may occur at any stage[82]. Ultimately, RV dysfunction can be thought of as asymptomatic RVF under the definitions of both the ATS and Haddad et al.

The RVF definition also covers multiple RVF phenotypes. The primary differentiation is between acute and chronic RVF, both have differing mechanisms of disease and likely different mechanisms of response. There is, however, considerable overlap between acute and chronic RVF and there is potential of acute deterioration in both[82].

1.2.3.2 Classification of right ventricular failure

The American College of Cardiology Foundation/American Heart Association Task Force classify chronic RVF into four stages, A-D. Stages range from at risk of PAH and/or RVF (Stage A) to requiring circulatory support (Stage D), Figure 1-17. Whilst patients often progress through the stages, clinical deterioration may be prevented or even reversed with appropriate identification and management[82]. Acute deterioration may occur at any stage of RVF, often precipitated by infection, PE or disease progression. This may result in a cycle of reduced RV function leading to hypotension, impaired myocardial oxygen supply due to reduced coronary prefusion gradient (especially if increased RV pressures) and

[i] As detailed in Chapter 2 the existing evidence base of RV response to lung resection is contested and predates this change in definition. Whilst it is the hypothesis of our research group that RV failure, as per the ATS definition, occurs following lung resection, the publication of our work and the bulk of this thesis predate this change. As such RV dysfunction will be used in this thesis to describe a reduction in RV function.

arrhythmias. In patients with PAH that require hospitalisation with RVF there is a 14% in hospital and 35% 1 year mortality[125].

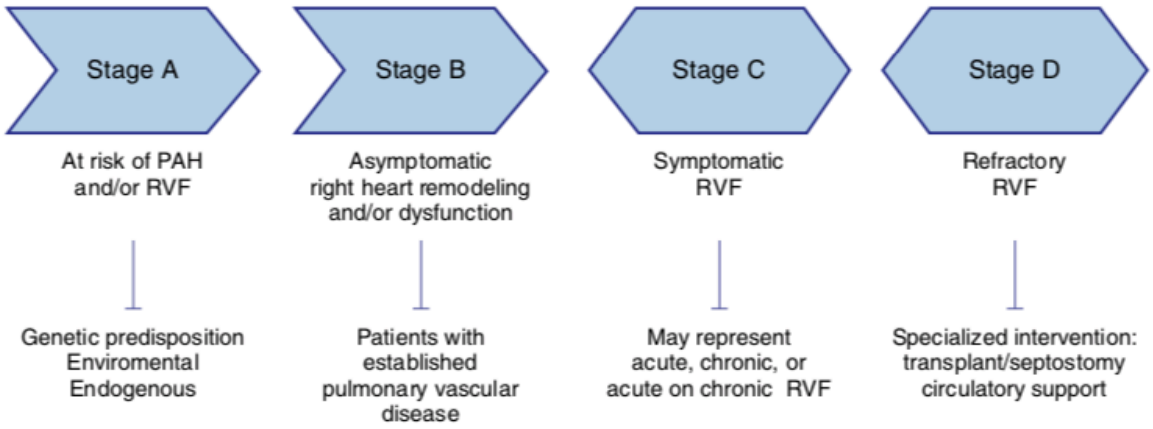

Figure 1-17 Classification of right ventricular failure
Note the low threshold for Stage A and patients are asymptomatic until stage C. PAH= pulmonary artery hypertension. RVF= right ventricular failure. Image from Lahm et al.[82].

1.2.3.3 Mechanism of right ventricular failure in chronic pressure overload

As the RV is subjected to chronic pressure overload (RVPO) it will maintain coupling by *increasing* contractility in parallel with the *increase* in afterload (E_{es} and E_a in Figure 1-18). Similarly, a *reduction* in E_a will cause a *reduction* in E_{es} (highlighting the therapeutic potential of afterload reduction). As disease progresses, the coupled state is initially maintained with a gradual increase in RV volume and decrease in stroke volume. Uncoupling occurs when the RV is no longer able to maintain increased contractility, leading to reduced E_{es}/E_a with further decreases in stroke volume and further dilation of the RV[82, 126].
Uncoupling is not *necessarily* triggered by an increase in afterload. The process of ventricular adaption to afterload leads to detrimental ventricular interactions and increased oxygen demand with impaired supply, discussed below, exhaustion of these processes results in uncoupling[126].

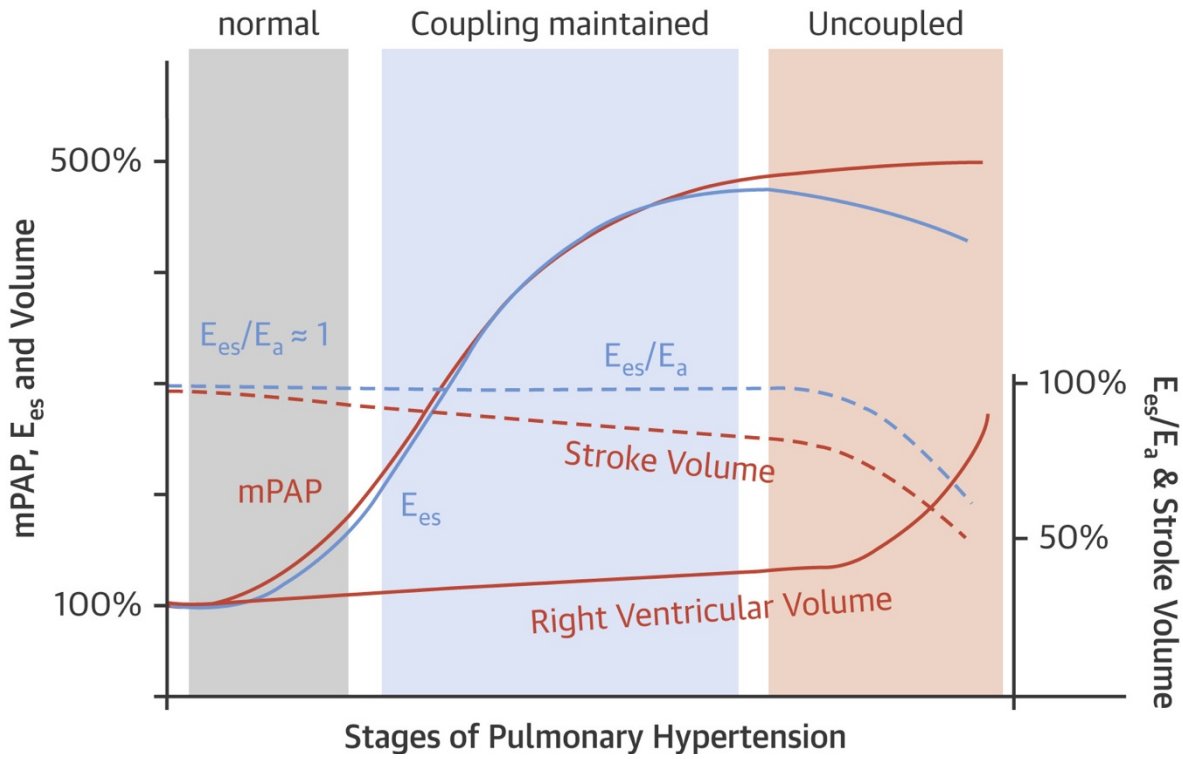

Figure 1-18 Right ventricular adaption in pulmonary hypertension
E_a= arterial elastance (afterload). E_{es}= end-systolic elastance (contractility). E_{es}/E_a= coupling. Contractility initially increases with afterload to maintain coupling until uncoupling at which point the RV dilates and stroke volume is reduced. mPAP= mean pulmonary artery pressure. Image from Vonk-Noordegraff et al.[126]

The concept of impaired coronary blood flow to the RV in pulmonary arterial hypertension (PAH) has been elegantly demonstrated by van Wolferen et al. through comparing left and right coronary blood flow between patients with PAH and controls[127]. Under normal loading conditions the RV receives blood flow throughout systole and diastole (an even systolic/diastolic ratio) whilst the LV predominately receives flow during diastole due to the differences between wall tension and aortic pressure (a low systolic/diastolic ratio)[83]. As RV mass and pressure increase there is an inverse, proportional, reduction in systolic/diastolic ratio, leading to RV supply matching the pattern of the LV[127]. RV oxygen consumption also increases secondary to increased muscle mass, workload and decreased diastolic filling time (increased heart rate with reduced stroke volume). These factors ultimately result in an oxygen supply/demand imbalance[126].

As discussed in 1.2.1.1, the anatomical features of the RV and LV invariably leads ventricular interdependence. Interaction can either be thought of as in "series," when reduced RV stroke volume leads to reduced LV preload or in "parallel" when geometric distortions of the RV and septum impairs filling of the LV[128]. Bowing of the interventricular septum into the LV can be caused by pressure and/or volume

overload of the RV[89] and dyssynchrony in contraction/relaxation between the ventricles[129], Figure 1-19. Increased RV afterload results in prolongation of the duration of RV contraction and asynchrony between contraction of the RV and the LV limiting LV early diastolic filling[129].

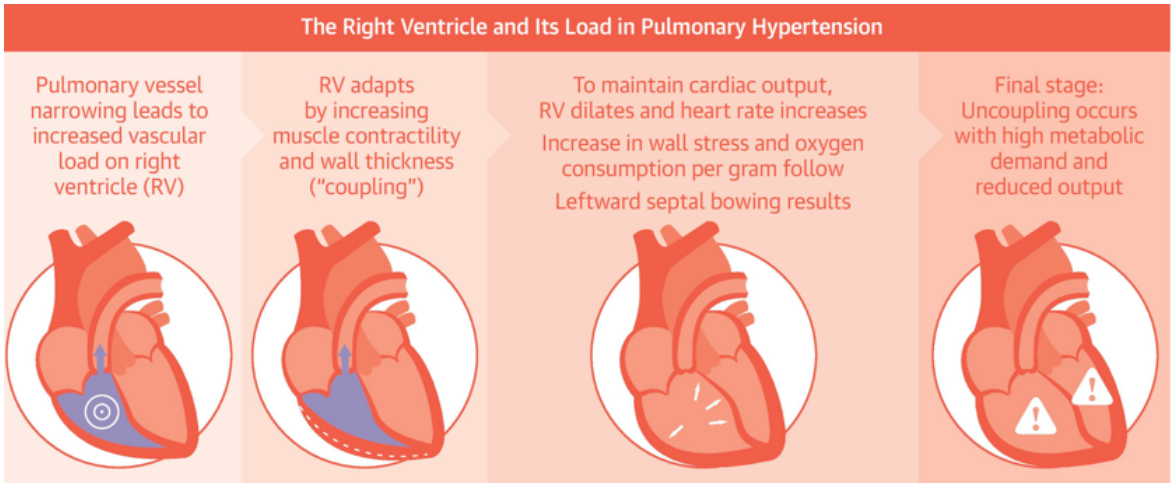

Figure 1-19 Right ventricular response to chronic increase in afterload
Initial response of the right ventricle (RV) is to increase contractility and therefore muscle mass (coupling). Once this mechanism is exhausted, the RV dilates to maintain stoke volume causing bowing of septum into the LV. Finally, uncoupling occurs as the RV is unable to maintain cardiac output. Image from Vonk-Noordegraaf et al.[126].

The ATS review of RVF details that the molecular and pathogenic mechanisms responsible for RVF are poorly understood[82]. Angiogenesis occurs secondary to oxygen supply/demand imbalance and increased muscle mass with ventricular hypertrophy, an insufficient upregulation of these proangiogenic pathways may contribute to RV decompensation[130]. Additionally, altered contractile signalling and calcium handling has been demonstrated in chronic RVPO and is linked to myocyte stiffness and diastolic dysfunction[131]. Interestingly, this has been demonstrated following lung resection in pigs[132]. Understanding the multifactorial mechanisms responsible, would not only lead to better understanding of the development of RVF, but may provide targets for therapeutic interventions.

1.2.3.4 Mechanism of right ventricular failure in acute pressure overload

Whilst there is significant overlap in the acute and chronic response to RVPO, there are important distinctions. In contrast to global hypertrophy seen in response to chronic RVPO, a purely acute insult will result in thinning and scarring of the RV[82, 133], Figure 1-20. A PE causes an acute occlusion of a pulmonary artery (analogous to lung resection) with a sudden increase in afterload which causes a

rapid increase in RV wall stress and exhaustion of myocyte energy resources. Within hours, a cascade of inflammatory chemokines, cytokines, cell infiltration and oxidative/nitrosative stress occurs that can lead to myocyte death within days[82, 133]. In rats, a simulated PE has been shown to cause acute RV myocardial inflammation (neutrophil infiltration) leading to myocardial fibrosis (macrophage infiltration) by 6 weeks following initial insult[134, 135].

There are regional differences in RV response to acute and chronic RVPO. Watts et al. demonstrated inflammation and scarring at the RV base and outflow tract following acute RVPO[133-135]. In chronic RVPO global hypertrophy occurs, CMR has demonstrated fibrosis in the area where the RV joins the septum[j] (RV insertion points)[136] and that ischaemia predominately occurs in the RV free wall[137].

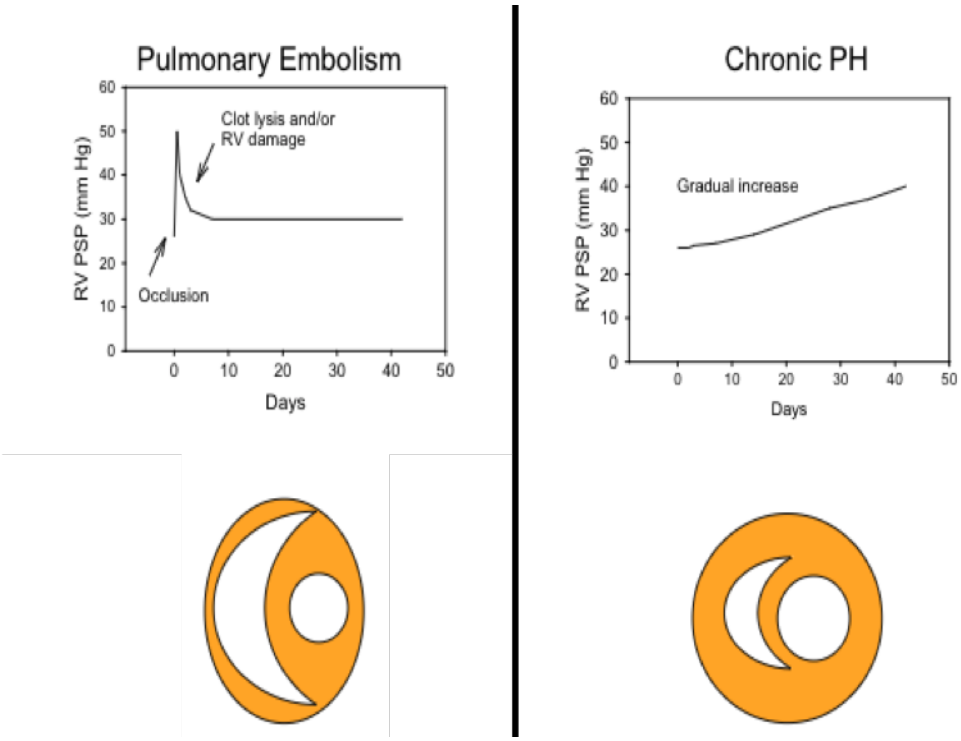

Figure 1-20 Comparison of right ventricular response to acute and chronic increases in afterload
Left pane, an acute increase of afterload secondary to pulmonary embolism causes a rapid increase in right ventricular peak systolic pressure (RVPSP) (top) leading to thinning and scarring of the right ventricle (RV) (bottom).
Right pane, in chronic pulmonary hypertension (PH) a gradual increase in RSPVP (top) leads to global RV hypertrophy of (bottom).
Image from Watts et al.[133].

[j] The inflammatory changes following PE demonstrated by Watts et al. are the basis for a subsequent study detailed in the future work section, 9.3.2 page 332 and Appendix 3.

1.2.4 Measures of right ventricular function

As discussed in 1.2.3.1, a consensus definition of RVF was only established in 2018[82]. Of note, there is no agreed measure by which to define the term *"insufficient delivery of blood from the RV"* for this definition. The numerous methods and indices of quantifying RV function highlight the lack of a single ideal parameter.

1.2.4.1 Contractility

According to Carabello[97], an ideal measure of contractility must be:

- Sensitive to changes in inotropy
- Independent of load
- Independent of heart size and mass
- Easy and safe to apply
- Proven to be useful in the clinical setting

Indices of contractility covered in this thesis[k] are summarised in Table 1-3.

Ventricular elastance (E_{max}) is the most complete measure of RV contractility[138], it is load independent and highly sensitive to changes in inotropy[88, 139]. It can be calculated from pressure volume loops as demonstrated above in 1.2.2.4 and Figure 1-13. The main limitations preventing widespread use is that conductance catheters are invasive, time consuming and expensive[83]. There are only a few studies of ventricular elastance in humans[109, 140].

Right ventricular ejection fraction (RVEF) and RV fractional area change (RVFAC) are the most widely used indices of RV function but both are dependent on loading conditions[83]. RVFAC is used as an estimate of RVEF in 2D imaging of the RV, although this can be inaccurate due to the complex 3D shape of the RV. They are however easily interpreted and are sensitive to changes in inotropy[97].

[k] Assessment of RV function within this thesis is performed predominately by CMR therefore indices that are measured by CMR are mainly discussed.

Tricuspid annular plane systolic excursion (TAPSE) is an echocardiographic measure of the distance the tricuspid valve annulus moves towards the apex during systole and **S' wave** velocity is the velocity of this movement[83]. It is a single measure of longitudinal function taken from a 4-chamber view of the heart although it is influenced by loading conditions[141].

Strain[l] is a measure of myocardial shortening and measures deformation (change in shape of an object due to regional differences in velocities). It calculates the percentage reduction of the length of a region of the RV wall between systole and diastole[142].

Strain rate is the temporal derivative of strain and measures the rate of myocardial shortening. Both strain and strain rate correlate with RVEF/RVFAC[143] and contractility function as measured by sonomicrometry (insertion of piezoelectric crystals into pig myocardium)[144]. Impaired strain is predictive of adverse outcomes in pulmonary hypertension[145].

Functional parameters	Load dependence	Clinical utility
Maximal RV elastance (mmHg/mL)	+	Most reliable index of contractility
RVEF (%)	+ + +	Clinical validation, wide acceptance.
RVFAC (%)	+ + +	Good correlation with RVEF
Strain (%)	+ + +	Correlates with stroke volume
Strain rate (s^{-1})	+ +	Correlates with contractility

Table 1-3 Indices of right ventricular contractility
RV= right ventricle. RVEF= RV ejection fraction. RVFAC= RV fractional area change. Interpretation from Haddad et al.[83]

1.2.4.2 Afterload

A complete understanding of RV function requires assessment of its loading conditions. There are numerous definitions and indices of right ventricular (RV) afterload but Haddad et al. state that it is most concisely described as:

> *"the load that the RV has to overcome during ejection."*
>
> Haddad 2008[83]

[l] Strain analysis is described in detail and performed in Chapter 5.

If afterload is imagined in a single myofibre, the load it has to *"overcome during ejection"* can be pictured as a weight to be lifted. The force required to lift this is distributed over the cross-sectional area of the myofibre and can be measured as wall stress (force applied per unit area). With this definition, afterload can be depicted as the RV wall stress that occurs during ejection by LaPlace's law, Equation 1-1. This definition is derived from the calculation of wall tension in a thin-walled sphere although as the RV is not spherical, this is only an *estimate* of stress and as the RV has a small radius and thin walls, RV wall stress is predominately influenced by RV pressure.

$$Wall\ stress\ \propto \frac{P_{EJ}\ x\ R_{EJ}}{H_{EJ}}$$

Equation 1-1 Right ventricular wall stress
P_{EJ}= pressure during ejection. R_{EJ}= radius of ventricle. H_{EJ}= wall thickness. Equation form Tedford [103].

An ideal measure of afterload must assess the factors that determine RV pressure during ejection. Whilst numerous authors describe the factors that influence afterload[83, 88], the most concise description is offered in Tedford's review titled the "Determinants of right ventricular afterload"[103] which states that afterload is determined by the sum of;

- resistance to steady flow
- compliance of the vessels
- inertia of the blood
- arterial wave reflections

It can be argued that there is no single ideal/complete measure of afterload, there are however distinct approaches to its assessment. As detailed below and throughout this thesis there are numerous different methods of assessing *afterload* and each method only assesses a specific component of afterload[103]. Additionally, there is interdependence between these different components[146]. Throughout this thesis discussion of a change in afterload relates to the specific component(s) of afterload assessed by the measure discussed.

An important distinction between measures of afterload is if they assess resistance to steady flow (steady afterload) and/or impedance to pulsatile flow (pulsatile afterload)[147]. Conventional measures of afterload tend to rely on single measurements of flow or pressure, or a combination of such measurements and therefore they tend to only assess individual aspects. For example, pulmonary vascular resistance (PVR) only assesses resistance to steady flow as it is calculated from the means of PA pressure and flow (cardiac output over a minute), therefore it only accounts for *steady* afterload and fails to account for *pulsatile* afterload[103, 148], Equation 1-2. PVR is however, the mainstay of assessment of pulmonary artery hypertension and is predictive of both cardiac function and survival[149, 150].

$$PVR = \frac{MPAP - LAP}{CO}$$

Equation 1-2 Pulmonary vascular resistance
PVR= pulmonary vascular resistance. MPAP= mean pulmonary artery pressure. LAP= left atrial pressure. CO= cardiac output.

Afterload can also be assessed by combined interpretation of the changes in pressure and flow throughout the cardiac cycle by impedance analysis or wave intensity analysis (WIA). A comparison of the properties of the main methods of assessment of afterload is shown in Table 1-4, impedance analysis is discussed below and WIA is discussed in detail (and performed) in Chapter 7.

	PVR & MPAP	Impedance analysis	WIA
Widely used in clinical practice	Yes	No	No
Easy to measure	Yes	No	No
Describes the steady state afterload	Yes	Yes	Not directly
Describes the pulsatile afterload	No	Yes	Yes
Provides information about the ventricle	No	No	Yes
Describes travelling waves	No	Yes	Yes
Wave separation possible	--	Yes	Yes
Allows decompression waves	--	No	Yes
Results presented in domain	--	Frequency	Time
Depiction of waves	--	Sinusoidal	Wavefronts

Table 1-4 Overview of methods of afterload analysis
PVR= pulmonary vascular resistance. MPAP= mean pulmonary artery pressure. WIA= wave intensity analysis. Table adapted from Su et al.[151]

1.2.4.3 Preload

RV end-diastolic volume (RVEDV) and pressure (RVEDP) can be used as surrogate measures for preload although both measures have limitations. RVEDP requires an invasive pulmonary artery catheter (PAC) for accurate measurement. RVEDV is challenging to measure as estimation of RV volumes is complicated by its shape, discussed below. Additionally, RVEDP and RVEDV do not have a linear relationship and therefore they cannot be used interchangeably[83].

1.2.5 Assessment modalities of right ventricular function

Jiang et al. describe the challenges contributing to RV imaging due to the RV's[152]:

- complex geometry
- heavily trabeculated myocardium
- retrosternal position
- marked load dependence

Assessment of the RV can be performed invasively by catheterisation (conductance or PAC) or non-invasively by imaging (echocardiography, CT or CMR). Invasive modalities are superior at assessing pressure measurements, as they are measured directly and only are estimated by non-invasive imaging, whereas non-invasive modalities are superior at assessing structure, Table 1-5. Each approach has advantages/disadvantages but a truly complete assessment of RV function is only possible by a combination of invasive and non-invasive measures[153, 154] .

Region	Parameter	Cardiac MRI	Echo (including 3D imaging)	Pulmonary artery catheter
RV	Volumes	+++	++	+
	Ejection fraction	+++	++	+
	Strain	+++	++	−
	Pressure	−/+	++	+++
	Stroke volume	+++	+	+++
	Mass	++	−/+	−
	Remodelling	+++	++	−
RA	Assessment	++	+	−
	Pressure	−	−	+++
PA	Dimensions	+++	+	+
	Distensibility	+++	+	−/+
	Haemodynamics	−/+	+	+++
	Quantitative lung flow	+++	−	−

Table 1-5 Comparison of common assessment modalities of the right ventricle
−= not useful; += may be useful; ++= useful; +++= extremely useful
Note CMR superior in all measures except for pressure assessment. PAC stroke volume calculated form cardiac output divided by heart rate. Conductance catheters not included due to limited clinical use. RV= right ventricle. RA= right atrium. PA= pulmonary artery. Interpretation from Benza et al.[155].

The investigations carried out within this thesis will examine specific measures of RV/pulmonary vascular function. Each investigation will discuss measures and methods of assessing RV function in depth, so only a brief overview of assessment will be detailed in this section[m].

1.2.5.1 Non-invasive assessment of right ventricular function

Echocardiography assessment of the RV is challenging due to its retrosternal position, complex geometry and difficulty in determining the endocardial border of the trabeculated myocardium[141]. Complete assessment requires imaging of the RV from numerous planes and isolated measures of RV function need cautious interpretation[85, 141].

Contractility can be estimated by numerous measures including; RVFAC, RVEF, TAPSE and strain imaging, section 1.2.4. Compared to CMR RVEF measurement, 2D estimation of RVEF had a strong association in healthy volunteers ($r=0.8$, $p<0.001$)[157] whereas TAPSE had poor correlation with CMR RVEF in a lung resection population ($r=0.34$, $p<0.01$)[156]. Continuous wave Doppler assessment of the tricuspid regurgitant jet can estimate pulmonary artery pressures. This method has been shown to underestimate SPAP, with almost half of patients having a difference of >10mmHg with direct PAC measurement (the gold standard in pressure measurement)[158].

Cardiac magnetic resonance (CMR) imaging is the gold standard in assessment of RV volumes[80]. Imaging of the ventricles will construct a series of cine images (a video of the full cardiac cycle divided into frames) of short axis sections from the apex of the heart to the valves. Tracing of the endocardium will allow calculation of end-systolic and end-diastolic ventricular volumes and therefore ejection fraction[159]. With post-processing using feature tracking analysis, strain and strain rate can be measured for both ventricles from short and long axis images[160, 161].

[m] A comprehensive comparison of echocardiographic and cardiac magnetic resonance imaging of the RV in a lung resection population has been published by a supervisor of this thesis, Dr McCall [156]. This paper is from the same study that the analysis in this thesis is based upon. It is not discussed in this section, except where values differ greatly from previously published literature, in order to demonstrate why the study was required based on previous literature.

Imaging of the pulmonary arteries allows measurement of blood flow/velocity and assessment of the cross sectional area of the pulmonary arteries[162].

There are disadvantages to CMR; it has limited availability, is expensive, generates numerous artefacts and requires specialist interpretation. Additionally, it requires patients to lie in the long, narrow and noisy bore of the scanner for up to an hour. Only certain patients are suitable as any ferromagnetic objects can become projectiles or overheat in the magnetic field therefore patients with certain pacemakers or metallic foreign bodies are excluded[159, 163]. The disadvantages limit its use in the clinical setting, except in specialist centres, but the advantages make it an ideal research tool. In PAH trials, the lower variability of CMR RV analysis and therefore smaller required sample size for study design has shown that CMR is a more cost effective research tool than echocardiography[164].

1.2.5.2 Invasive assessment of right ventricular function

Central vein cannulation allows passage of catheters into the right side of the heart and the pulmonary artery. These catheters can directly measure pressure throughout the insertion allowing direct measurement of central venous, right atrial, RV, pulmonary arterial and pulmonary capillary wedge pressures[165]. Flow and therefore cardiac output can be estimated by thermodilution[166]. Additional measurements can be made by conductance and volumetric catheters. Whilst the technique is safe, compared to non-invasive assessment there remains a slight morbidity and mortality risk. In a review by Hoeper et al. of 7218 catheterisations, 2 patients died directly from catheter related complication (PA rupture and a another deemed related but cause of death unexplained at autopsy) while 76 patients had serious adverse events (haematoma, pneumothoraces, arrhythmia, vasovagal events and hypotension)[167].

Conductance catheters are equipped with a micromanometer channel and multiple electrodes at regular intervals from the coiled tip[80, 168], Figure 1-22. When placed in the RV, they measure pressure directly from a continual fluid column and estimate volume from the electrical conductance of blood[168, 169]. Electrodes are positioned between the apex and base of the ventricle and a current is generated between the two ends. The electrodes within the RV then measure the

conductance and derive the volume of each "slice" (level of the heart at which they sit) and the ventricular volume is calculated as the sum of the slices[170].

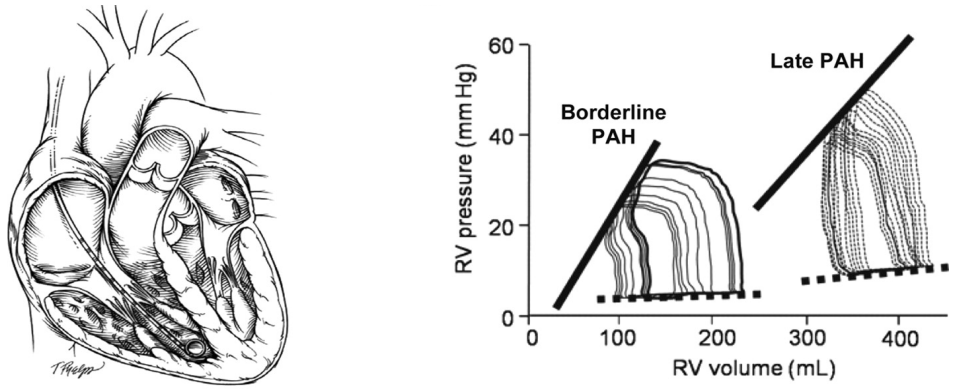

Figure 1-21 Right ventricular conductance catheterisation
Left pane, position of conductance catheter. Note electrodes along the end.
Right pane, pressure-volume loops are generated allowing complete assessment of right ventricular function. Note higher peak pressure and lower end-systolic elastance (thick black line) in late pulmonary artery hypertension (PAH). Image from Champion et al.[80]

Whilst this expensive technique has been predominantly used in animals[109] it has recently been utilised in a lung resection population to investigate the effect of thoracic epidural anaesthesia on RV function[140]. Either balloon insufflation (usually within the inferior vena cava) or Valsalva manoeuvres can be performed to generate pressure volume loops over varying loads[80], Figure 1-21 and section 1.2.2.4.

Volumetric pulmonary artery catheters (VPAC) use thermodilution to derive RVEDV and ejection fraction[168]. The difference from conventional pulmonary artery catheters is the presence of a rapid response thermistor, a specialised RV injection port and two intra-cardiac electrodes for ECG measurement[171]. Ejection fraction, cardiac output and RVEDV are calculated using the decay constant of temperature changes of blood within the RV measured by the VPAC's thermal component[172-174], Equation 1-3. Modern VPACs utilise a heating element in the RV to induce temperature change[168] but the method of injecting ice-cold saline, as originally described by Dhainaut[174], is depicted in Figure 1-22.

$$RVEDV = \frac{CO}{HR\ x\ RVEF}$$

Equation 1-3 Calculation of right ventricular end-diastolic volume (RVEDV)
RVEDV= right ventricular end-diastolic volume. CO= cardiac output. HR= heart rate. RVEF= right ventricular ejection fraction.

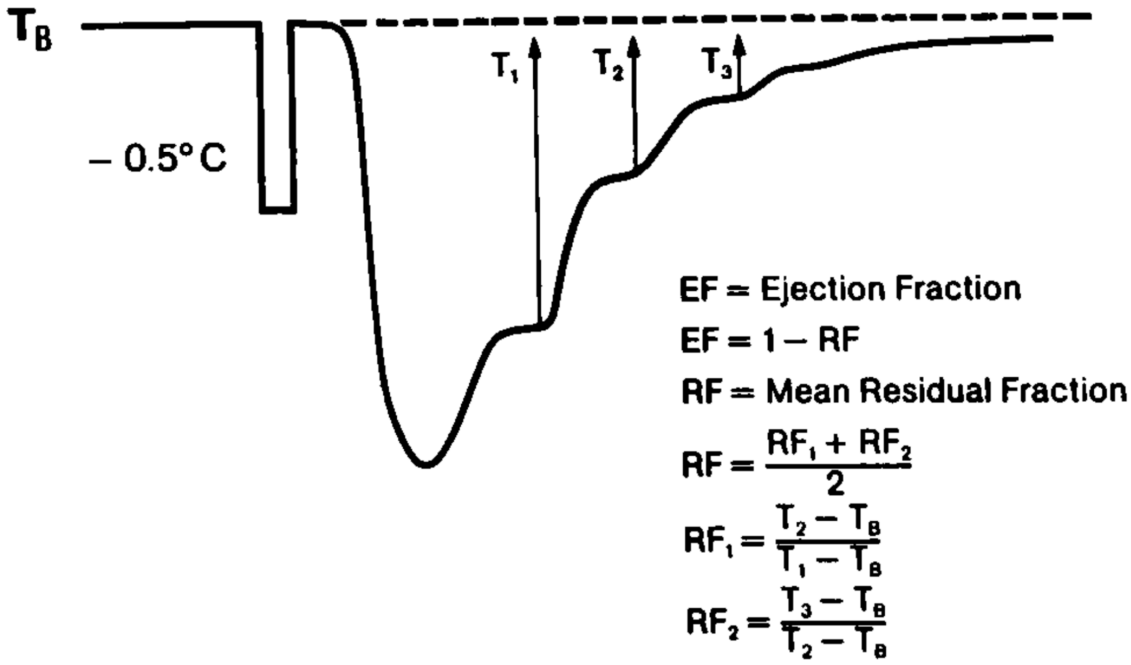

Figure 1-22 Calculation of ejection fraction from thermodilution curve
Ice cold saline injected, the temperature (T) difference with each beat from baseline (T_B) is used to calculate the residual fraction (RF) and therefore ejection fraction (EF). Image from Dhainaut et al.[174].

In spite of the once established research use of VPACs, there is little evidence of accuracy in the derived measurements[171]. Particular concern has been raised over the RVEDV measurement, calculated as per Equation 1-3, as it has been shown to be a poor predictor of preload and fluid responsiveness[175, 176]. Two studies have compared VPACs with the gold standard measurements of RV volume in patients with pulmonary artery hypertension[173] and induced RV ischaemia[168], raising concerns that VPACs may be inaccurate in these conditions.

Hoeper et al. performed CMR and VPAC assessment in 16 patients with PAH and 6 healthy controls[173]. The differences in RVEDV, RVESV and RVEF were marked in terms of difference in value but also the large standard deviation within the VPAC measures. Against CMR, VPAC overestimated RVEDV (180±35 vs 412±168mL) and RVESV (120±32 vs 372±178mL) and underestimated RVEF (34±10% vs 12±8 %). The differences between the measures increased with the degree of tricuspid regurgitation. CMR measurements in 119 patients by van de Veerdonk[177] et al. demonstrated RVEDV, RVESV and RVEF values in keeping with the CMR results from the study by Hoeper et al.[173]

Hein et al. performed an animal study in 7 pigs comparing VPAC with conductance catheters[168] with induced RV ischaemia (temporary ligation of the RCA). Similar to the CMR studies, VPAC overestimated RVEDV and underestimated RVEF when compared to the conductance catheter, Figure 1-23. The mean difference in RVEF (REF in figure) showed a VPAC bias of -9.9% and a proportional bias of increasing underestimation at higher RVEF whilst RVEDV showed a bias of 31mL with systematic overestimation by VPAC. The VPAC RVEF and RVEDV had low sensitivity (57% and 43% respectively) and specificity (71% and 86% respectively) for detection of RV ischaemia compared to the conductance catheter. The area under receiver operating characteristics curve (AUROCC) for the VPAC did not reach statistical significance for detection of RV ischaemia.

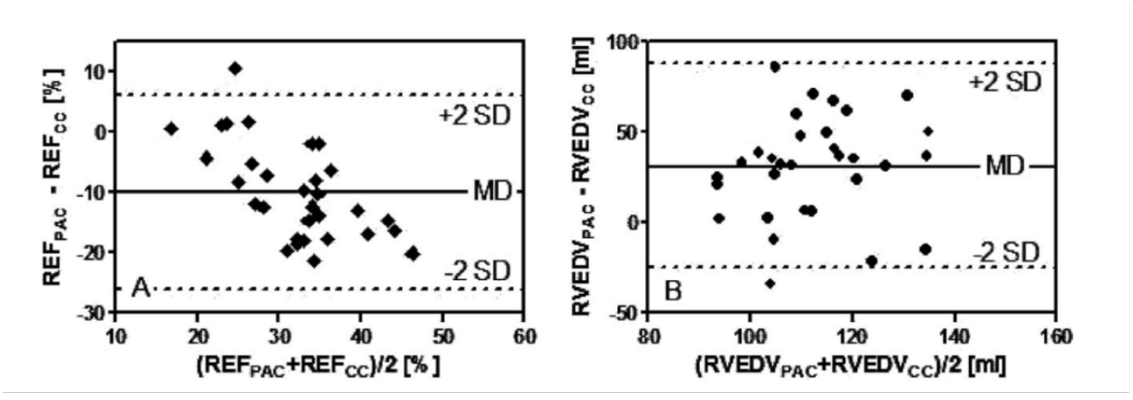

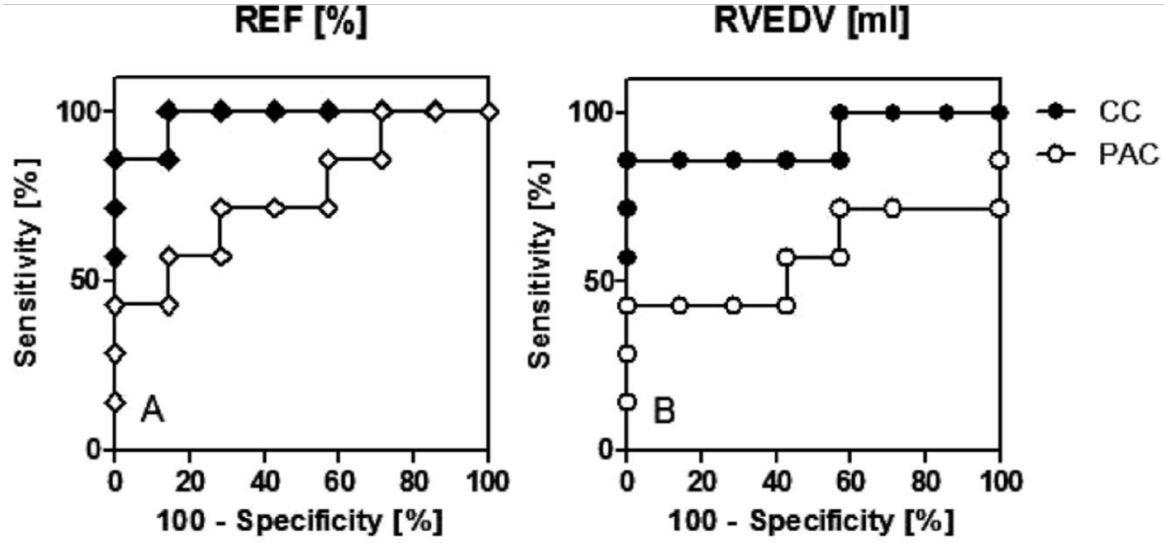

	AUC	p	p_{AUC}	Threshold	Sensitivity	Specificity
REF_{CC}	0.98	<0.001	0.04	< 40%	100%	86%
REF_{PAC}	0.76	0.06		< 25%	57%	71%
$RVEDV_{CC}$	0.92	<0.001	0.02	> 94 mL	86%	100%
$RVEDV_{PAC}$	0.57	0.65		> 113 mL	43%	86%

Figure 1-23 Comparison of volumetric pulmonary artery catheter and conductance catheters in measuring right ventricular function parameters
Top row, Bland-Altman plots for volumetric pulmonary artery catheter (PAC in figure) and conductance catheter (CC) measurement of right ventricular ejection fraction (REF in figure, on left) and right ventricular end-diastolic volume (RVEDV, on right).
Middle row, receiver operator curves for REF (REF in figure, on left) and RVEDV (on right).
Bottom table, area under receiver operating characteristic (AUROCC) curves, sensitivity and specificity analysis.
Note superior performance by conductance catheter in middle and bottom rows. Images from Hein et al.[168]

The studies of Hoeper et al.[173] and Hein et al.[168] question the validity of VPAC assessment of RV dysfunction. Given that these studies demonstrate that the VPACs are inaccurate in both PAH and RV ischaemia the validity of VPAC is particularly questionable following lung resection as these are potential mechanisms of the RV dysfunction, as discussed in Section 1.2.3, page 50. The study of Hein et al. had an accompanying editorial, the name of which conveys the evidence for their use:

"Pulmonary artery catheter determined right ventricular ejection fraction and right ventricular end-diastolic volume: Another case of "The Emperor Has No Clothes"

Leibowitz 2009[178]

1.2.5.3 Biomarker assessment of right ventricular function

In clinical practice natriuretic peptides (brain natriuretic peptide (BNP) or its pre-cursor NT-pro-BNP) and troponins are used to detect or monitor for ventricular dysfunction. Release of neither BNP nor troponin are specific to the RV, although in the absence of LV dysfunction they may indicate RV dysfunction.

Brain natriuretic peptide (and its precursor NT-proBNP) are released in response to myocardial stretch[179] and enlarged cardiac chambers[180]. In a meta-analysis of studies investigating adverse outcome following PE, an elevated BNP was associated with RV dysfunction and 30-day mortality[181]. It has been shown as an effective screening tool for RV dysfunction in patients with PAH[182]. In lung resection cohorts, elevated pre-operative BNP has also been shown to be predictive of post-operative atrial fibrillation [183-185].

Troponin (I or T) are contractile proteins released secondary to myocardial injury. They are primarily used in the diagnosis of myocardial infarction, although non-specific troponin release occurs in numerous cardiac diseases and following non-cardiac surgery[180].

1.2.5.4 Assessment of right ventricular function following lung resection

In the ATS review, described above in section 1.2.3.1 page 51, the authors detail the challenges faced in assessing RV function in a research setting. According to Lahm et al.[82] an ideal measure of RV function would be:

- Sensitive enough to capture subtle cardiac structural changes
- Reliable
- Reproducible
- Inexpensive
- Easily obtained

In clinical practice, trans-thoracic echocardiography (TTE) is the main method of assessing RV function but is inferior to CMR for almost all parameters presented in Table 1-5. The low cost, widespread availability and relative ease of interpretation however mean echocardiography is predominantly used in clinical practice[83]. CMR has greater sensitivity and reproducibility than echocardiography[82] therefore in a clinical trial the ability of CMR to accurately detect a small change in RVEF could allow a reduced study sample size and negate the additional costs of CMR[164].

In a study investigating RV volume changes following lung resection, VPAC may be of limited value. They have questionable accuracy in patients with raised pulmonary pressures[173] and RV ischaemia[168], both potential mechanisms of RV dysfunction following lung resection[78]. Additionally, serial assessment by VPAC or conductance catheters subjects the patient to the risk of complications with each insertion[167]. Whilst CMR and conductance catheters are both deemed "gold standard" in individual aspects of RV assessment, CMR has the advantages of being non-invasive, more readily available and established in clinical practice[168].

1.2.6 Assessment of right ventricular afterload

This chapter, along with Chapter 2, will describe how PVR's inability to measure the pulsatile components of afterload may result in underestimation of the changes in afterload following lung resection. Studies that have previously assessed the change in RV afterload following lung resection, described later in Chapter 2, have exclusively assessed the change in steady state afterload by measuring PVR and PAP. Lung resection results in a unilateral ligation and occlusion of a proximal PA. As detailed below and in Chapters 6 and 7, this may alter the distribution of cardiac output between the lungs and lead to a marked increase in pulsatile afterload with little or no change in PVR and PAP. Ultimately, these studies may have missed the hypothesised changes in afterload following lung resection by only assessing the steady afterload.

1.2.6.1 Pulmonary vascular resistance

Pulmonary vascular resistance is the most commonly used index of afterload but there have been longstanding concerns regarding its widespread use. Of note, the

topic has received two editorials in the leading intensive care journal, Intensive Care Medicine, both titled, “Pulmonary vascular resistance. A meaningless variable” published in 1984 by Versprille[186] and in 2003 by Naeije[187]. In the years between these publications, 7,158 papers were published reporting PVR calculations[187], highlighting its enduring use. Naeije details that PVR is dependent on flow and vasomotor tone of the pulmonary vasculature at the time of measurement and therefore a single measurement can be influenced by either of these factors. He concludes that PVR is best defined at multiple points of flow and pressure, this can be achieved by pharmacological intervention (i.e. a dobutamine infusion, Figure 1-16 page 50) or with exercise[187].

1.2.6.2 Assessment of pulmonary vascular reserve

The ability of the pulmonary vasculature to accommodate an increase in cardiac output (CO) has been termed pulmonary vascular reserve (PVreserve). It has been demonstrated in a combined CMR and PAC investigation of patients with CTEPH, before and after pulmonary endarterectomy (PEA), and healthy subjects by Claessen et al.[120, 188], Figure 1-24. PVreserve is measured by the gradient of the linear increase in MPAP with CO, an increase in the gradient of the MPAP-CO relationship is interpreted as a decrease in PVreserve. Following PEA, patients have a lower resting indices of afterload (MPAP and PVR) than the patients with CTEPH although exercise testing reveals a similar rate of increase in MPAP with CO on exercise, i.e. there is a persistent reduction in PVreserve. Additionally, the post-PEA have decreased RVCreserve as they are unable to increase RVEF on exercise (discussed in 1.2.2.5.2). Of note, PVR did not change on exercise in any of the three groups[120]. Exercise testing therefore can reveal an underlying pulmonary vascular disease and increase in afterload that is not apparent at rest and that may contribute to impaired RV function.

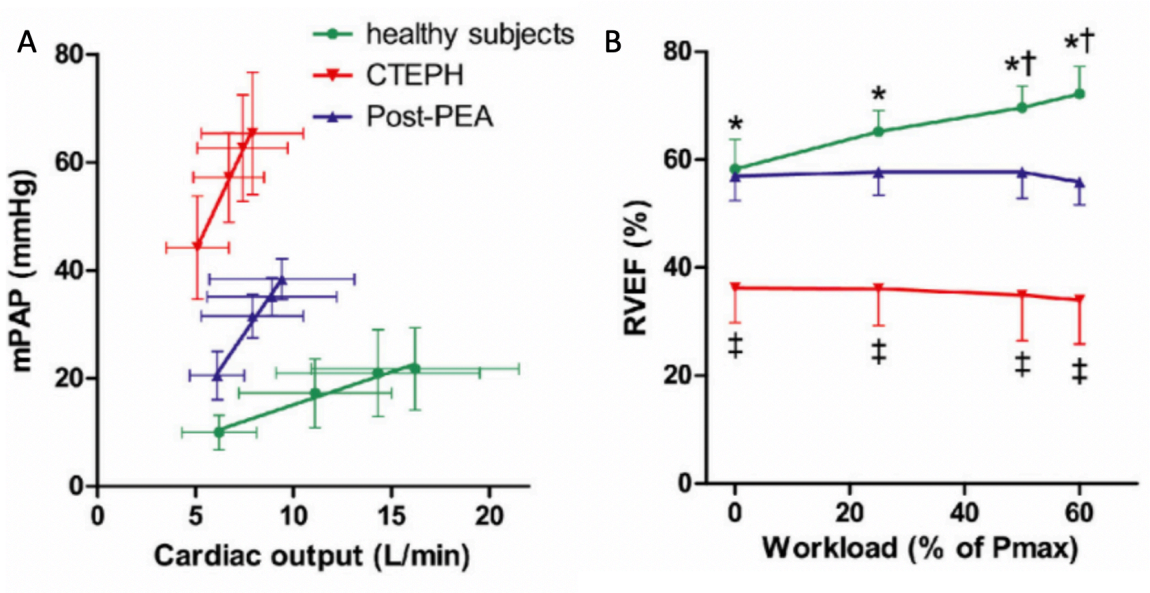

Figure 1-24 Pulmonary vascular and right ventricular contractile reserve
Normal pulmonary vascular (PVreserve, gradual increase in mean pulmonary artery pressure (MPAP) on exercise) and right ventricular contractile reserve (RVCreserve, increase in right ventricular ejection fraction (RVEF) on exercise) demonstrated in the healthy subjects (green line). Patients with chronic thromboembolic pulmonary hypertension (CTEPH) have markedly increased MPAP and reduced RVEF at rest. Exercise testing reveals reduced PVreserve (increased gradient of MPAP-cardiac output relationship) and reduced RVCreserve (lack of increase in RVEF on exercise). Patient post-pulmonary endarterectomy (PEA) however have resting MPAP and RVEF similar to healthy controls although exercise reveals a similar reduction in PVreserve and RVCreserve to the patients with CTEPH. Images from Claessen et al[120].

1.2.6.3 Impedance analysis

Impedance analysis has been described as the most comprehensive description of RV afterload[103, 189]. Impedance analysis is complex to perform and interpret, although it assesses the four components of afterload described by Tedford[103], 1.2.4.2. The main distinction (and complexity) of impedance analysis from other methods of afterload analysis is that it is performed and interpreted in the frequency domain. Flow and pressure profiles are measured simultaneously at the same point in the pulmonary artery. The profiles are decomposed by Fourier analysis into a collection of sinusoidal waves of increasing frequencies (f) that when combined form the original wave. f represents the number of complete sinusoidal waves in the decomposition of a single heartbeat, as f increases the amplitude of the sinusoidal wave decreases. f=0 is the mean (0 sinusoidal waves) of pressure/flow, whilst f=1 has the greatest amplitude and therefore represents the greatest contribution to pressure/flow of any of the frequencies[190]. The impedance spectra, example shown in Figure 1-25, is formed by the modulus of pressure and flow for each harmonic/frequency, Equation 1-4.

$$Z_n = \frac{P_n}{Q_n}$$

Equation 1-4 Impedance calculation
Z= impedance. P= pressure. Q= flow. n=harmonic number.

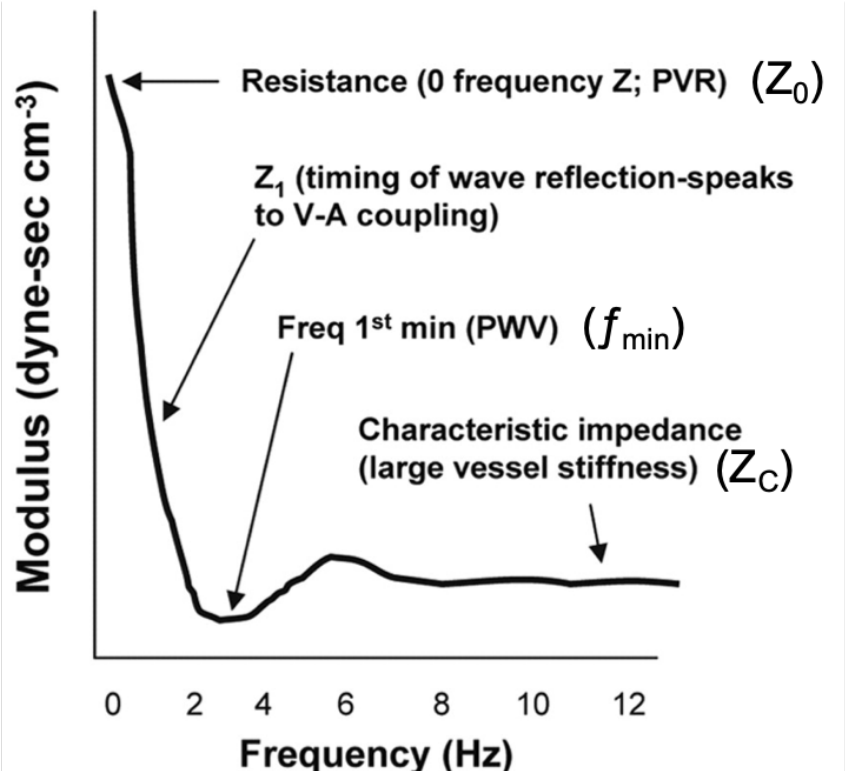

Figure 1-25 Pulmonary artery impedance spectra
Schematic example of impedance spectra plotted as impedance modulus against frequency. Z_0 is impedance measured at 0Hz, i.e. steady flow and therefore measures pulmonary vascular resistance. Z_1= impedance at first harmonic, largely influenced by wave reflection in proximal vessels. Z_C= characteristic impedance, represents "stiffness" and resistance in large proximal vessels to steady flow. f_{min}=frequency at first impedance minimum and relates to wave speed and timing of wave reflections. Image from Champion et al.[80]

1.2.6.3.1 Interpretation of impedance analysis

Interpretation of impedance analysis is performed from the graphical display generated, Figure 1-25. There are 2 main sections of the spectra to analyse, the zero harmonic (Z_0) and the harmonic numbers. Each give information on separate components of the pulmonary vascular tree[190]. Z_0 is the modulus of flow and pressure at a frequency of 0Hz. The resultant modulus is the mean flow divided by the mean pressure, it is therefore equivalent to PVR and representative of the resistance of distal vessels. The harmonic numbers are representative of the contribution of the first 5 divisions of the proximal pulmonary vasculature to overall afterload[191]. The harmonics can be split into the lower order harmonics (Z_1

and Z_2) and the higher order "reflectionless" harmonics (Z_C). The impedance at a frequency of 1Hz (Z_1) is influenced primarily by wave reflection of the proximal vessel; significant wave reflections will result in an increased impedance at Z_1. Z_C is the sum of the impedance at higher frequencies; it measures the ratio of blood mass inertia to proximal vessel compliance and equates to the impedance of proximal vessels to steady flow[103, 189, 190]. f_{min} is the frequency of the first minimum of impedance, measured as the minimum point of impedance following the initial rapid decrease (Figure 1-25). It allows calculation of the pulse wave velocity (c) and distance to reflection site(s)[103].

1.2.6.3.2 Performing impedance analysis

Impedance analysis was first performed in man by Milnor et al. in 1969[192], but has never been adopted into clinical practice and therefore there remain a limited number of studies reporting its use. It requires simultaneous pressure and flow measurement in the PA; pressure measurement is performed invasively with a pulmonary artery catheter (PAC), high fidelity data requires a sensor at the tip of the PAC whilst lower fidelity data can be acquired with a standard PAC[189]. Accurate measurement of flow has been the main limiting factor; flow can be estimated from velocity measurement[192], measured with a specialised sensor on a PAC[193-196] or measured non-invasively by echocardiography of the PA[197-202]. As described in 1.2.5.2, the insertion of an invasive PAC has an associated morbidity and mortality risk. Following lung resection there is also a theoretical risk of disruption of the newly ligated branch of the PA.

In Milnor et al.s' original study, flow measurements were computed from pressure differences, although the author recognised this as a fundamental limitation of the study[192]. The first time an impedance study was performed with a specialised multi-tip PAC was in 1984 by Murgo and Westerhof [193] and subsequently in further studies[194-196]. The flow tipped catheter approach has largely been superseded by combined PAC pressure measurement and echocardiography flow measurement.

Impedance analysis is challenging to perform accurately. This has been investigated by a paediatric research team in Colorado who have performed validation studies of a PAC pressure measurement and Doppler flow analysis method of assessing impedance[199-201]. Errors in pulsed wave Doppler assessment

of flow creates large uncertainty in impedance analysis at higher harmonics. They caution the use of impedance analysis without specific investigation of and correction for such errors[200].

1.2.6.4 Windkessel models

Development of "lumped parameter" models such as the 2- element or 3-element Windkessel[n] models may overcome some of the limitations of impedance analysis[204]. First described by Westerhof et al. in 1971, the 3-element Windkessel, models the pulmonary vasculature as an electrical circuit with a proximal resistor of characteristic impedance (Z_C) with a capacitor (compliance (C)) and resistor (resistance (R)) arranged in parallel. Investigation of this method still predominately relies on invasive monitoring to obtain flow and pressure measurements for calculation of each the individual parameters. The 2-element Windkessel does not include the Z_C component and has been described to provide more "accurate data" than the 3-element model[205].

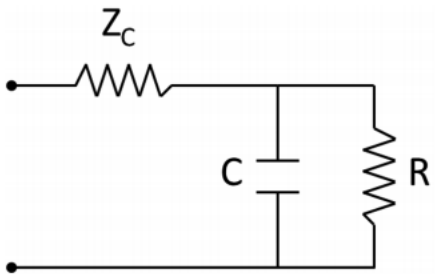

Figure 1-26 Three element Windkessel model
The 3-element Windkessel model is an electrical circuit analogous to the pulmonary circulation. Z_C= characteristic impedance, C= compliance. R= resistor. Image from Tedford[103].

1.2.6.4.1 Resistance - compliance time constant

Numerous different mathematical approaches to calculate C have been suggested (Z_C and R can be calculated from impedance analysis)[204, 206, 207]. The simplest method of estimating C (stroke volume/pulse pressure) and R (PVR) have been validated in 2 studies by Lankhaar et al.[147, 148]. These and multiple further investigations have shown that there is an inverse hyperbolic relationship between R and C, with the product of R and C constant, described as the RC time constant, Figure 1-27. Whilst the position on the hyperbolic curve changes with compliance

[n] The Windkessel analogy was originally described by Frank as a two-element Windkessel in 1899[203] Other variations on this include a four and five element Windkessel model.

(pulsatile afterload) and resistance (steady afterload), the nature of the relationship is unchanged in the presence of PAH, interstitial lung disease, age or with treatment of PAH[147, 148 208, 209].

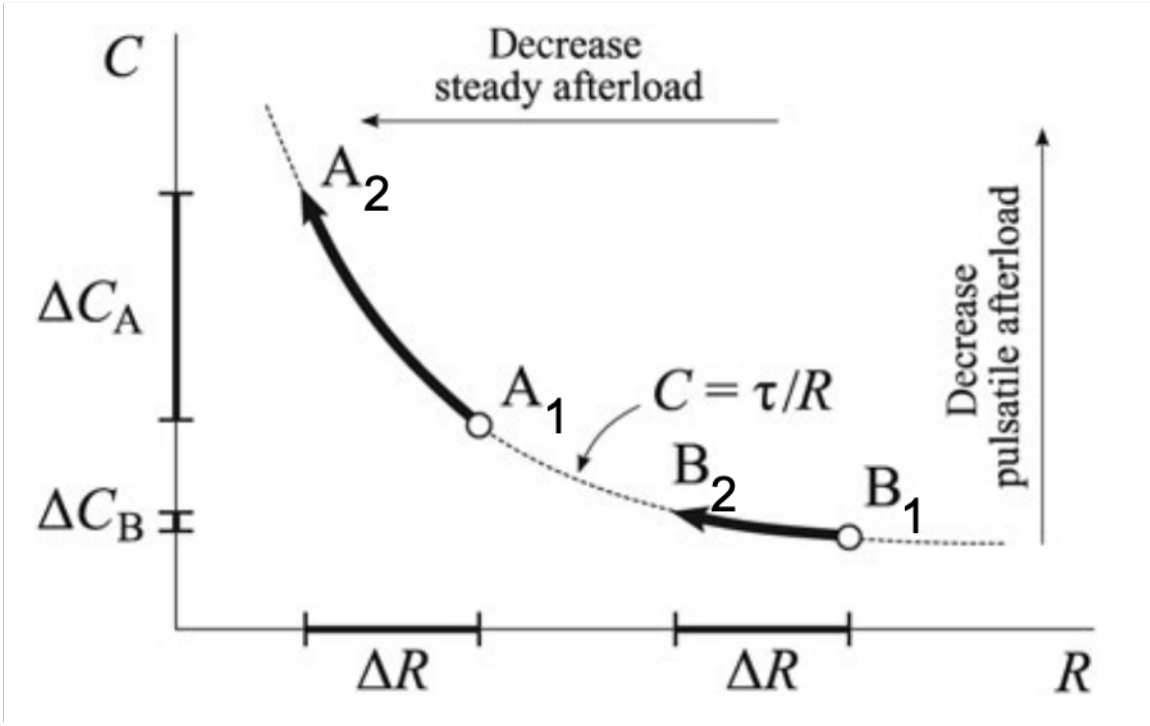

Figure 1-27 Resistance-compliance relationship
Plot demonstrating the relationship between resistance (R), compliance (C) and the time constant (τ). Patient A has mild pulmonary artery hypertension (PAH) at baseline (A_1) and patient B has severe PAH at baseline (B_1). An equivalent decrease in R (ΔR) in both patients results in a small increase in compliance (ΔC) for patient B (B_2) but a large increase in compliance for patient A (A_2). Patient A will have a substantial improvement in C (pulsatile afterload) and R (steady afterload) whereas patient B will only have a substantial improvement in R. This relationship is similar in reverse for an increase in R. Image form Lankhaar et al. [147]

The relationship between an increase in "steady afterload" (PVR, R) and the change in "pulsatile afterload" (compliance, C) for patients with mild and severe PAH are demonstrated in Figure 1-27. As the RC relationship is constant, the changes demonstrated with a therapeutic decrease in R therefore are also true in reverse, i.e. in an increase in afterload. If the patient starts at A_2 with low pulsatile (C) and steady (R) afterload then PVR increases by ΔR to A_1 there is a large increase in pulsatile afterload (ΔC_A) relative to ΔR. If the patient starts at a point of high pulsatile and steady afterload (B_2) then the resultant increase in pulsatile afterload is relatively small (ΔC_B) from an identical increase in steady afterload by ΔR to point B_1. As such the increase in pulsatile afterload in the setting of normal PVR, may be a more sensitive marker of RV afterload than PVR. This relationship has been demonstrated in patients with mild PAH, a small

increase in PVR is associated with a far greater relative decrease in compliance and the change in compliance is a better predictor of survival than PVR[147, 210].

1.2.6.4.2 Resistance – compliance time constant in individual lungs

The RC time constant can be applied to each individual lung. Saouti et al. performed an informative study in 23 patients, 19 with CTEPH and 4 with chronic pulmonary embolisms, but without pulmonary hypertension[146]. They combined CMR flow and area measurements (MPA, RPA and LPA) with PAC pressure measurements in the MPA to form a 2-element Windkessel model. Of note, PA pressure was assumed equal in the MPA, RPA and LPA. From this they calculated PVR and compliance ((systolic–diastolic area)/pulse pressure) for each vessel, Figure 1-28. The distribution of cardiac output (CO) was influenced by the distribution of clots (and therefore afterload) between the RPA and LPA, they were termed low flow (higher afterload) or high flow (lower afterload) dependent on percentage of total CO. The low flow lung had higher PVR and lower compliance compared to the high flow lung. To combine the parameters from each lung, they added the compliances while the resistances were combined as resistors in parallel ($1/R_{total=} 1/R_{low.flow} + 1/R_{high.flow}$). The finding that the combined values for R and C in the high and low flow PAs were equal to the calculated values in the MPA and the RC time constant was similar in all vessels suggests that the RC time constant is universal in the pulmonary vasculature.

The authors interpret the finding of a similar RC time constant as evidence that the relationship between resistance and compliance is an “intrinsic property of each lung”, irrespective of the magnitude of flow or resistance. This means that unilateral resistance and compliance are independent of the other lung although the governing relationship (RC time constant) is similar in both lungs. They speculate that both resistance and compliance therefore originate from the same area of the pulmonary vasculature, namely the distal circulation. Through reinterpretation of CMR studies that have previously investigated PA compliance[211-213], Saouti et al. demonstrated that the proximal PAs account for only a fifth of overall compliance with the remainder originating in the distal vasculature[146]. Vessel occlusion (or lung resection) may lead to an increase in resistance and a decrease in compliance secondary to reduction in the distal vasculature leading to a reduced blood flow in that lung (akin to the low flow lung

in Figure 1-28) whereas the contralateral lung is unable to compensate for the increase in flow as its relationship between resistance and compliance is constant.

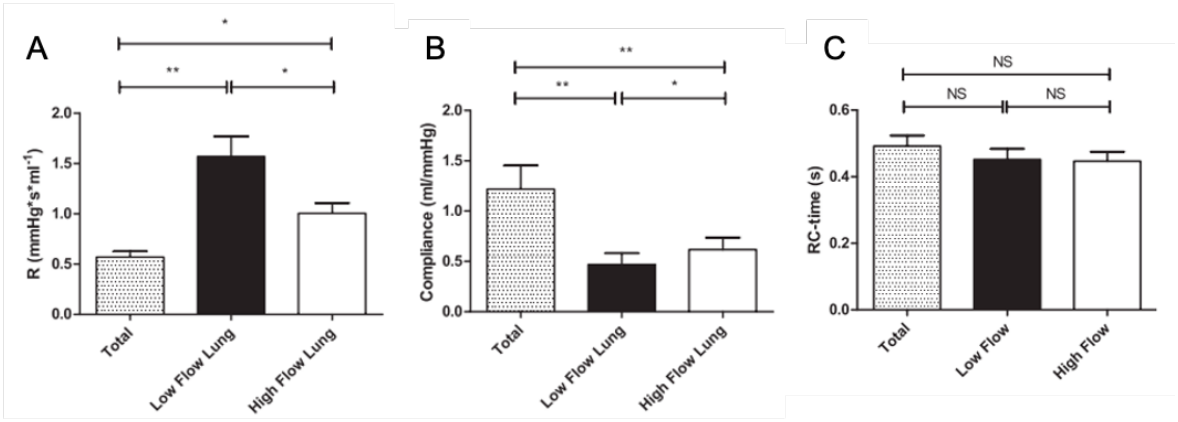

Figure 1-28 Resistance-compliance relationship in the main, right and left pulmonary arteries
A and B, resistance (R) and compliance (C) in the main pulmonary artery (PA) (Total) and the right or left PA termed low or high flow lung. R calculated as mean PA pressure (measured in main PA, assumed constant between vessels) divided by mean flow in that vessel. Compliance calculated as systolic–diastolic area (in that vessel) divided by pulse pressure (in the main PA).
C, RC time constant is equal in each individual lung and is equal to the total value.
Images from Saouti et al.[146].

1.2.6.4.3 Resistance – compliance time constant in pulmonary artery occlusion

The constant RC relationship may not apply in the case of proximal pulmonary artery occlusion (similar to following lung resection). Pagnamenta et al.[207] calculated RC relationship in dogs with two levels of simulated proximal PA occlusion (by ensnarement) compared to distal PA occlusion (glass microbeads injected into the right atrium). They demonstrated a reduction of the RC time constant in the proximal occlusion group, Figure 1-29, signified by a left shift of RC curve. This reduction results in reduced compliance for the same PVR following occlusion, the alteration of the proximal pulmonary vasculature (occlusion) therefore fundamentally changed the relationship between steady and pulsatile afterload whereas distal alteration (PE) did not. Of note, they caution against the use of Doppler derived echocardiographic estimation of MPAP in the setting of proximal PA occlusion as the normal correlation between SPAP and MPAP is altered by the reduction in compliance and RC time constant and therefore the derived estimation of MPAP may be inaccurate[207], discussed further in Chapter 2.

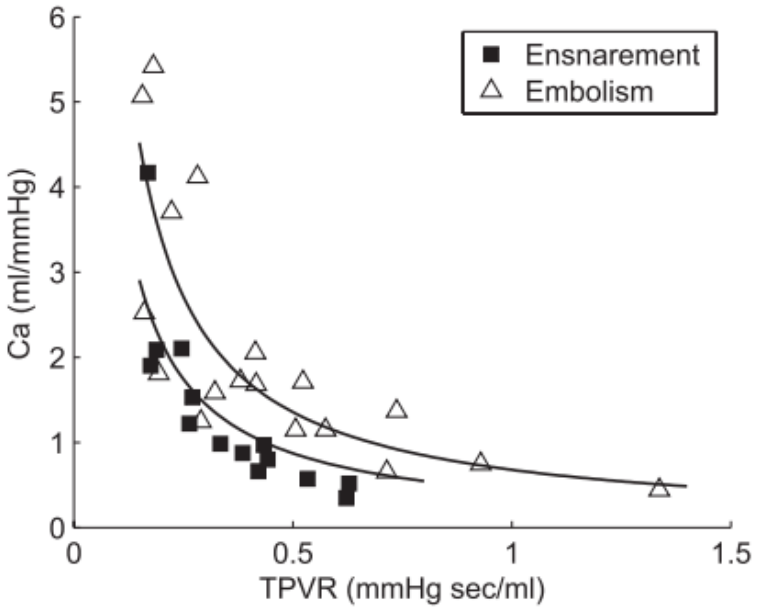

Figure 1-29 Resistance-compliance relationship in disease
Compliance (Ca, stroke volume/pulse pressure) against total pulmonary vascular resistance (TPVR, mean pulmonary pressure/cardiac output) following PA occlusion (ensnarement, black squares) and emoblisation (white triangles). Black line represent resistance compliance (RC) relationship for each group. PA occlusion leads to a left shift in the RC relationship from the embolism group. Note reduction in Ca for given TPRV in ensnarement group. Image from Pagnamenta et al. [207].

Pagnamenta et al. also performed impedance analysis in this study, Figure 1-30. At a low level of proximal occlusion Z_0 was unchanged (no change in PVR, representative of afterload contributed by distal vasculature) whilst Z_1 and Z_c increased (increased pulsatile and steady afterload contribution from proximal vasculature). Greater proximal PA occlusion subsequently led to an increase in Z_0 and further increase in Z_1 and Z_c. Embolization showed the opposite pattern, no change in Z_C or Z_1 but an increase in Z_0 at low and high levels of embolization[207].

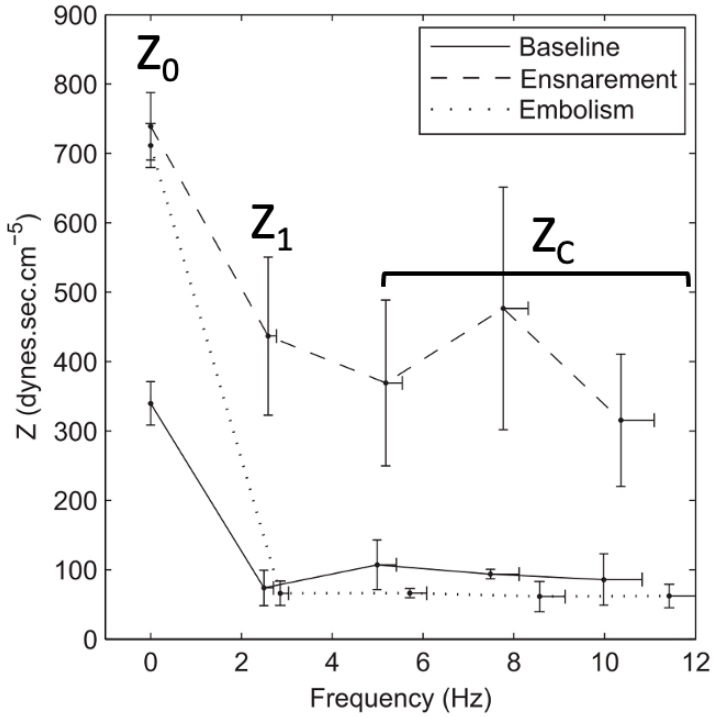

Figure 1-30 Impedance analysis in proximal and distal pulmonary artery occlusion
Impedance (Z) against frequency for healthy (baseline, solid line), pulmonary artery (PA) embolism (distal occlusion, dotted line) and proximal PA occlusion (ensnarement, dashed line). Note increase in steady afterload (Z_0) only in embolism group whereas Z_0, wave reflection (Z_1) and proximal vessel resistance to steady flow (Z_C) are all increased in PA occlusion/ensnarement group. Image from Pagnamenta et al.[207].

The results of Pagnamenta et al are similar to an impedance swine study of pneumonectomy by Heerdt et al.[214]. In 4 pigs, they demonstrated that, following pneumonectomy, there was a modest increase in MPAP and PVR, indicating minimal change in impedance from the distal vasculature. There was however a marked increase in Zc suggesting an increase in impedance from the proximal vasculature[214]. This supports the suggestion that PVR and MPAP may be unable to detect changes in afterload following lung resection.

	CO (L/min)	RVEF (%)	MPAP (mmHg)	PVR (dyn.s.cm-5)	Zc (dyn.s.cm-5)
Control (n=3)	3.5 (0.2)	49 (2)	26 (2)	254 (16)	41 (4)
POD3 (n=4)	3.4 (0.3)	41 (3)	30 (2)	295 (22)	64 (6)
Percentage change (%)	↓3%	↓16%	↑15%	↑16%	↑56%

Table 1-6 Changes in right ventricular function and afterload following pneumonectomy
Impedance analysis before (control) and on post-operative day 3 (POD3) following pneumonectomy in pigs. Note reduction in right ventricular ejection fraction (RVEF). There is only a small increase in distal vessel impedance, pulmonary vascular resistance (PVR) and mean pulmonary artery pressure (MPAP), but a marked increase proximal vessel impedance highlighted by the 56% increase in characteristic impedance (Zc). CO= cardiac output. Data from Heerdt et al.[214].

1.2.6.5 Assessment of right ventricular afterload following lung resection

Whilst PVR and MPAP are most commonly used to assess changes in afterload they only assess changes in steady afterload. The studies by Pagnamenta et al.[207] and Heerdt et al.[214] demonstrate that a proximal PA occlusion may lead to a marked increase in pulsatile afterload, not detected by isolated assessment of PVR and MPAP. If the RC time constant is unchanged and the baseline PVR is low then a marked increase in pulsatile afterload may result in only a modest increase in PVR (Figure 1-27) although if the RC time constant is altered by the proximal occlusion (as in Pagnamenta et al.[207], Figure 1-29) then the increase in pulsatile afterload may occur without any change in PVR.

Assessment of pulsatile afterload can be performed invasively by specialised PACS and impedance analysis or by CMR and assessment of measures of pulsatile afterload (discussed later in Chapter 6) or WIA (discussed later in Chapter 7). Similar to the assessment of RV function following lung resection, 1.2.5.4, CMR has the advantage of being non-invasive and can perform assessment of both RV function and RV afterload although it cannot measure PAP. Whilst a conductance catheter would allow simultaneous assessment of RV function and afterload peri-operatively it would require repeated invasive catheter placement to assess post-operative changes adding a significant burden to any participant involved in the study and an, albeit slight, risk of morbidity and mortality.

1.3 Conclusion

Lung cancer is the leading cause of cancer death and although lung resection offers the best chance of cure, it is associated with significant post-operative morbidity. RV dysfunction, secondary to an increase in RV afterload, has been widely hypothesised as a potential contributory factor to this morbidity. As detailed above, assessment of RV function and afterload are challenging due to the irregular RV shape, load dependency, difficulty in imaging and complexity of RV afterload. Whilst each modality of assessment has limitations, CMR is the optimum modality for assessment of the changes in RV function and afterload following lung resection.

Chapter 2 Right ventricular response to lung resection - literature review

2.1 Introduction

This thesis builds upon a study undertaken by its supervisors investigating "The Right Ventricular Response to Lung Resection". The aim of the study was to investigate the established hypothesis that RV function deteriorates following lung resection. This was the first study of lung resection patients to utilise CMR, the gold standard method of investigating RV volumes[168, 215], to analyse cardiac function pre- and post-operatively. The study was required due to the lack of consistent evidence for the hypothesis. In a 2009 review of RV function following lung resection, Pedoto and Amar stated:

"Currently, it remains controversial whether routine lung resection leads to clinically significant changes in right heart function."

Pedoto 2009[78]

The evidence base on which this conclusion was made is flawed due to the potentially inaccurate methods in which RV function was assessed, namely volumetric pulmonary artery catheters (VPACs) or echocardiography. This chapter will discuss the major studies, highlighting their insights and limitations. It will summarise the evidence to date for the existence of RV dysfunction following lung resection, whilst focusing on specific papers that investigate its potential mechanisms, the remit of this thesis.

2.2 Method

A database search of the Ovid Medline (R) Database, 1946 until search date, was performed in September 2017 and updated in November 2020[o]. The following search terms and results were generated;

[o] Publications arising from "The Right Ventricular Response to Lung Resection" are excluded from discussion in this section.

1. exp Ventricular Function, right/ (6575)
2. exp Ventricular Function/ (65272)
3. exp ventricular dysfunction, right/ (5970)
4. exp ventricular dysfunction/ (37908)
5. cardiac function.mp. (29110)
6. heart function.mp. (17425)
7. ejection fraction.mp. (58176)
8. ('pulmonary artery' adj2 pressure).mp. (11896)
9. afterload.mp. (6633)
10. pulmonary vascular resistance.mp. (8765)
11. (lobectomy adj4 lung).mp. (1665)
12. (lung adj2 resection).mp. (5412)
13. exp Pneumonectomy/ (26594)
14. 11 or 12 or 13 (29733)
15. 1 or 2 or 3 or 4 or 5 or 6 or 7 or 8 or 9 or 10 (179107)
16. 14 and 15 (331)
17. limit 16 to English language (215)
18. limit 17 to human (179)

The results were screened for studies investigating RV function and/or pulmonary afterload following lung resection, with investigations performed pre-operatively and post-operatively. Studies were only included if the extent of surgery was lobectomy or greater[p]. Review articles and case reports were excluded, although their references were screened for additional studies. In total, 179 studies were screened with 42 selected for full text analysis and 21 of these studies were included in the review below. Five further studies identified from a review of references were included.

The methods used in the studies vary, although they can be broadly grouped by the modality of assessment namely; volumetric pulmonary artery catheters[48, 49, 58-66], non-volumetric pulmonary artery catheters [67-69] and echocardiography[70-77]. These studies are summarised in Table 2-1, Table 2-2 and Table 2-3. Of note, 2

[p] Sublobar resections may result in minimal change cardiopulmonary function. AS such they were not included in the literature review of the overall study, see section 4.3.5.1 page 117.

studies investigated RV function utilising echocardiographic strain analysis, they are discussed separately in Chapter 5.

2.3 Pulmonary artery catheter studies

2.3.1 Volumetric pulmonary artery catheter studies

In the 1990's two main groups, those of Reed et al. and Okada et al., investigated RV dysfunction following lung resection[48, 49, 58-60]. In combination, they investigated not only changes in RV function at rest and on exercise but also RV preload, afterload and contractility. Whilst the studies were innovative and gave a thorough investigation of RV function following lung resection, they are undermined by use of the VPAC[178]. Although the derived values (RVEF and RVEDV) are potentially unreliable, the studies remain informative, particularly in terms of possible mechanisms of RV dysfunction. The directly measured pulmonary artery pressures (PAP), along with the derived measures of cardiac output and therefore PVR[q] are more readily accepted and remain in clinical use.

2.3.1.1 Investigations by Reed et al.

In the USA during the early 1990's Carolyn Reed and colleagues undertook three studies assessing RV function[60] and the mechanisms of RV dysfunction following pulmonary resection including the role of contractility[58, 59]. Their hypothesis and study of RV dysfunction following lung resection is based on observational experience with translation of RV assessment methods from sepsis, shock and cardiac surgery populations.

2.3.1.1.1 Effect of Pulmonary Vascular Resection on Right Ventricular Function, 1992.

A VPAC was placed prior to induction of anaesthesia in 15 patients undergoing open lung resection (13 lobectomies, 2 pneumonectomies)[60]. Direct measurement of PA pressures and derived measurements of cardiac output, PVR, RVEF and RVEDV were preformed pre-induction, on opening of the chest, on partial and on

[q]The VPAC studies measure *afterload* by PVR. As detailed in the introduction and later in the afterload chapters, PVR is an incomplete measure of afterload. For ease of interpretation and consistency with the authors interpretation of the following papers, PVR will be discussed as afterload in this section.

complete PA branch clamping, at the end of resection and on closure of the chest. Repeated measurements were performed 4-6 hours, 1 and 2 days post-operatively.

Intra-operatively RVEF and RVEDV were unchanged. Post-operatively RVEF was decreased from baseline (4-6 hours and lowest at POD2) and RVEDV was increased (POD 1 and 2). PVR and SPAP increased on occlusion of the branch of the PA (dependent on side and extent of surgery) although PVR was lower than baseline in the initial post-operative period.

The authors' conclusions are not a true representation of their results and potentially highlight the persistent hypothesis of RV dysfunction due to increased afterload. They conclude that RV dysfunction was present post-operatively and that afterload was not the "sole determinant," in spite of only detecting a transient intra-operative increase in afterload temporally unrelated to the main POD2 drop in RVEF. They focus on the increase in RVEDV as "significant RV dilatation" although it is similar to the preoperative fasted state, a low RVEDV can be used as a marker of hypovolaemia[216]. Impaired contractility is suggested as an additional potential mechanism and their subsequent study is designed to investigate this.

2.3.1.1.2 Assessment of right ventricular contractile performance after pulmonary resection, 1993

In an attempt to remove the influence of RV loading conditions on contractility measurement, Reed et al. tested a mechanism of assessing the preload recruitable stroke work (PRSW)[59]. PRSW is proposed as a load independent measure of RV contractility generated when RV stroke work (RVSW, ((MPAP - CVP) x RVSV)) is plotted against RVEDV over varying load conditions. Given that the value for stroke volume is this calculation is derived from the VPAC, PRSW is subject to the same inaccuracies as VPAC RVEF calculation. Pre-operatively patients are given rapid fluid boluses in increments up to a total 1000ml with RVSW and RVEDV calculated. This is essentially a pilot study trialling the technique in a lung resection population of 10 patients.

In this small study, they again find a reduced PVR and increased RVEDV following lung resection. Of note, SPAP was increased post-operatively, this may be

secondary to increased cardiac filling caused by a 1000ml preload challenge given pre-operatively as part of the study.

2.3.1.1.3 Mechanisms of right ventricular dysfunction after pulmonary resection, 1996

This two-part study was designed to investigate changes in RVEF after lung resection and the effect of pulmonary vasodilation on any such changes in a subgroup of patients[58].

Part one, 35 patients undergoing open lung resection (lobectomy and pneumonectomy) repeat the 1993 study protocol. RVEF reduced on POD2 with increased RVEDV but without any change in MPAP, SPAP or PVR. A subset of 6 patients repeated the PRSW fluid loading on POD2. Post-operative RV PRSW (a surrogate marker of contractility) was unchanged, although post-operative fluid loading resulted in a marked increase in RVEDV. Unfortunately, the authors do not provide matched analysis of the difference in response to fluid challenge in the 6 patients pre- and post-operatively.

Part two, in 6 additional patients a prostaglandin E1 (PGE1) infusion was commenced intra-operatively and continued until POD2. PGE1 was given to reduce afterload with the hypothesis that this would prevent the reduction in RVEF. A reduction in PVR was maintained until POD2, although the reduction in RVEF was again present. Interestingly there was no difference in post-operative RVEF when the PGE1 group was compared to the control, i.e. reducing peri-operative afterload did not have an effect on RVEF.

2.3.1.1.4 Summary of Reed at al studies

This trio of studies demonstrates, with caution given VPAC controversies, a decrease in RVEF and increase in RVEDV without an increase in afterload or decrease in contractility.

As the VPACs are kept in situ from insertion, the duration of the studies is limited. Therefore, they are peri-operative studies focusing on mechanisms of RV dysfunction with the latest assessments occurring on POD2 and no longer-term investigation of RV function. In the discussions, the drop in RVEF at POD2 is

repeatedly claimed by the authors to be a "peak", without any measurements after this time point. We can see the pathophysiological argument, that RV dysfunction must be caused by an increase in afterload, is well established even in these early studies. In spite of the first two studies demonstrating reduced post-operative PVR, the design of the third study investigates if RV dysfunction is prevented by reducing afterload.

In conclusion to the third study the author states:

". . . RV dysfunction after pulmonary resection is not caused by primary alterations in contractility or immediate changes in afterload."

Reed 1996[58]

There are subtle signs of RV and pulmonary circulation dysfunction in the post-operative response to fluid loading in the 1996 study. Direct comparison is not provided between pre- and post-operative response to fluid; yet there is a reduction in RVEF and an increase in RVEDV, RVSWI, SPAP and heart rate compared to the pre-operative response to fluid loading. This suggests that when the RV and pulmonary vasculature are challenged post-operatively there is an increase in afterload (increased PAP), RV dilatation (increased RVEDV) and an increase in contractility to maintain output (decreased RVEF and increased HR, increased RVSWI).

2.3.1.2 Investigations by Okada et al.

In Japan, Okada et al. contemporaneously investigated RV function following lung resection in a similar approach to Reed et al., although they also *stressed* the RV. They assessed RV function on exercise pre-operatively potentially as method of identifying patients at risk of RV dysfunction[48] and post-operatively as a method of detecting RV dysfunction[49]. Additionally, both studies had a longer post-operative follow-up period of 3 weeks.

2.3.1.2.1 Right ventricular dysfunction after major pulmonary resection, 1994

The aim of the study was to "confirm the existence of RV dysfunction" and to determine its causes[49]. VPACs were inserted into 20 patients undergoing open lung resection, 3 pneumonectomies and 17 lobectomies, with assessment of RV

function pre-operatively then 1 hour, 6 hours, 1 day, 2 days and 3 weeks post-operatively. The final 10 patients underwent assessment of RV function during a single stage submaximal exercise protocol pre-operatively and 3 weeks post-operatively.

The resting results are similar to Reed et al.; decreased RVEF at all post-operative time points, with the nadir at day 2. There was no change in PVR or PAP. Interestingly the results show increased RVEDV on day 2, also observed by Reed et al., but the longer follow-up period shows that it returns to pre-operative levels by three weeks.

Exercise results, for the first time, convincingly demonstrate the hypothesised post-operative RV dysfunction with increased afterload. Pre-operative exercise does not result in changed RVEF or PVR whereas on post-operative exercise RVEF decreased whilst MPAP, SPAP, PVR and HR all had a greater relative increase from rest than pre-operatively. Absolute values of RVEDVI and RVESVI were increased but there was no relative increase from rest.

2.3.1.2.2 Right ventricular ejection fraction in the preoperative risk evaluation of candidates for pulmonary resection, 1996

This study investigated potential predictors of post-operative morbidity, measured by complications and hospital length of stay[48]. Pre-operative and predicted post-operative lung function values were able to predict post-operative complications but failed to discriminate between patients who had increased length of stay and those that did not. Baseline RVEF did not predict complications or length of stay. When patients were divided into groups based on whether their RVEF increased or decreased on pre-operative exercise, the decreased RVEF group had increased complications and nearly double the hospital length of stay. At 3 weeks post-operatively, both groups had unchanged PAP, CO and HR but the decreased RVEF group had a lower RVEF than pre-operative testing.

2.3.1.2.3 Summary of Okada et al. studies

Okada et al. (and their patients) performed a challenging protocol including exercise testing at 3 weeks post-operatively. The 3-week follow-up testing added additional patient burden and risk given the (presumed) second central venous

access and catheter placement, this is not detailed in the paper. Their second study is not designed or powered as a true pre-operative screening tool but does highlight a potential method of identifying “at risk” patients.

The design of the studies allows retrospective determination of the reserve of the pulmonary vasculature and RV, i.e. their ability to cope with increased demand on exercise (increased cardiac output). The gradient of the linear relationship between MPAP and cardiac index/output is a measure of pulmonary vascular reserve (PVreserve)[120]. An increase in the gradient, a greater increase in MPAP per unit increase cardiac index, is a sign of reduced PVreserve. Okada et al.s’ studies can be reinterpreted to assess PVreserve from the results presented in their studies. An example is shown in Figure 2-1, the light grey lines depict each individual patients PVreserve before (dashed line) and after (solid line) lung resection. The longer darker lines depict the averaged results for the study and show an increased gradient (decreased PVreserve) following lung resection. This may be due to an inability of the reduced volume of pulmonary vasculature to accommodate the increased CO, meaning afterload rapidly increases.

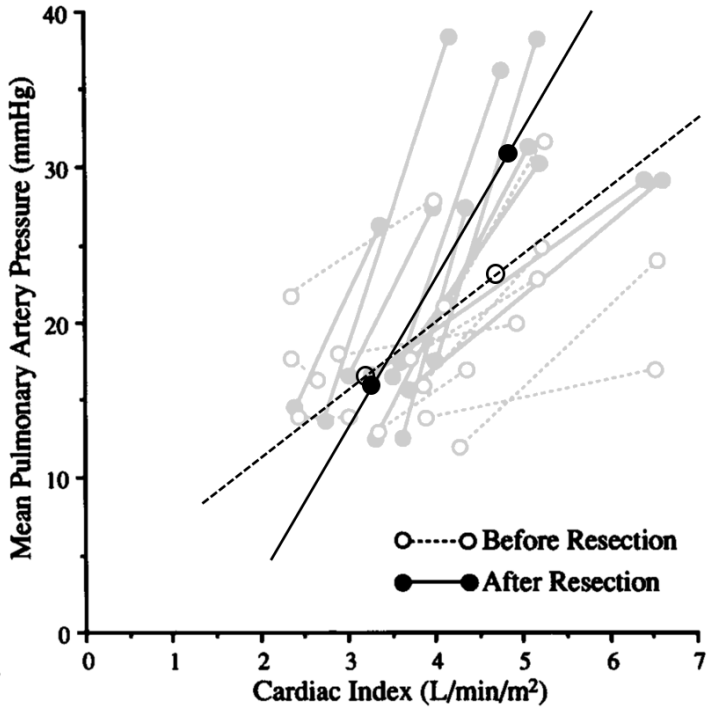

Figure 2-1 Pulmonary vascular reserve following lung resection, Okada et al.
Relationship between mean pulmonary artery pressure and cardiac index before (dotted lines) and after (solid lines) lung resection. Light grey lines are individual patients from original Okada et al. paper. The long black lines are the mean values for each group. Note the steep gradient after resection in all of the subjects (lightly shaded solid lines). Image from Okada et al. 1994[49] with superimposed PVreserve before and after lung resection (long black lines).

In their second study, the difference in PVreserve between the increased RVEF and decreased RVEF groups can be determined on initial exercise testing. The decreased RVEF group have a greater increase in mPAP on exercise than the increased RVEF group suggesting reduced PVreserve[48]. This may indicate that patients with reduced PVreserve are at increased risk of post-operative complications.

Right ventricular reserve (RVCreserve) is measured by the gradient of RVEF plotted against cardiac index. In health, RVEF increases on exercise, whilst in patients with pulmonary vascular disease (demonstrated in patients with chronic thromboembolic pulmonary hypertension), RVEF decreases (reduced RVCreserve)[120]. In the 1996 study by Okada et al. the patients with normal RVCreserve (increase RVEF on exercise group) had fewer complications, a shorter length of stay and no post-operative RVEF decrease[48]. In the 1994 study there is evidence of reduced RVCreserve following resection, pre-operatively RVEF is unchanged on exercise however at three weeks post-op RVEF decreases on exercise[49].

This approach of challenging the RV (with exercise) demonstrated, for the first time, increased afterload with a decrease in RVEF following lung resection. It is arguably more important to understand what happens to the RV when it is challenged in order to explain and potentially limit morbidity following lung resection.

2.3.1.3 Investigation by Elrakhawy et al.

The largest patient population investigation RV dysfunction is the recently published retrospective study of 178 patients (142 lobectomies and 36 pneumonectomies) by Elrakhawy et al.[62]. Of note, a VATS approach was an exclusion criteria for inclusion in the study. Standard practice for lung resections (lobectomy and pneumonectomy) in their Egyptian institution included insertion of a VPAC post-induction, remaining in situ until at least 48 hours post-operatively. Any patient with pre-operative evidence of RV dysfunction or pulmonary hypertension was excluded from the study, the number excluded is not stated in the paper.

Pneumonectomy and lobectomy groups had reduced RVEF with increased RVEDVI, MPAP and PVR at all post-operative time points (3 to 48 hours). These changes were greater in the pneumonectomy group compared with the lobectomy group, Figure 2-2.

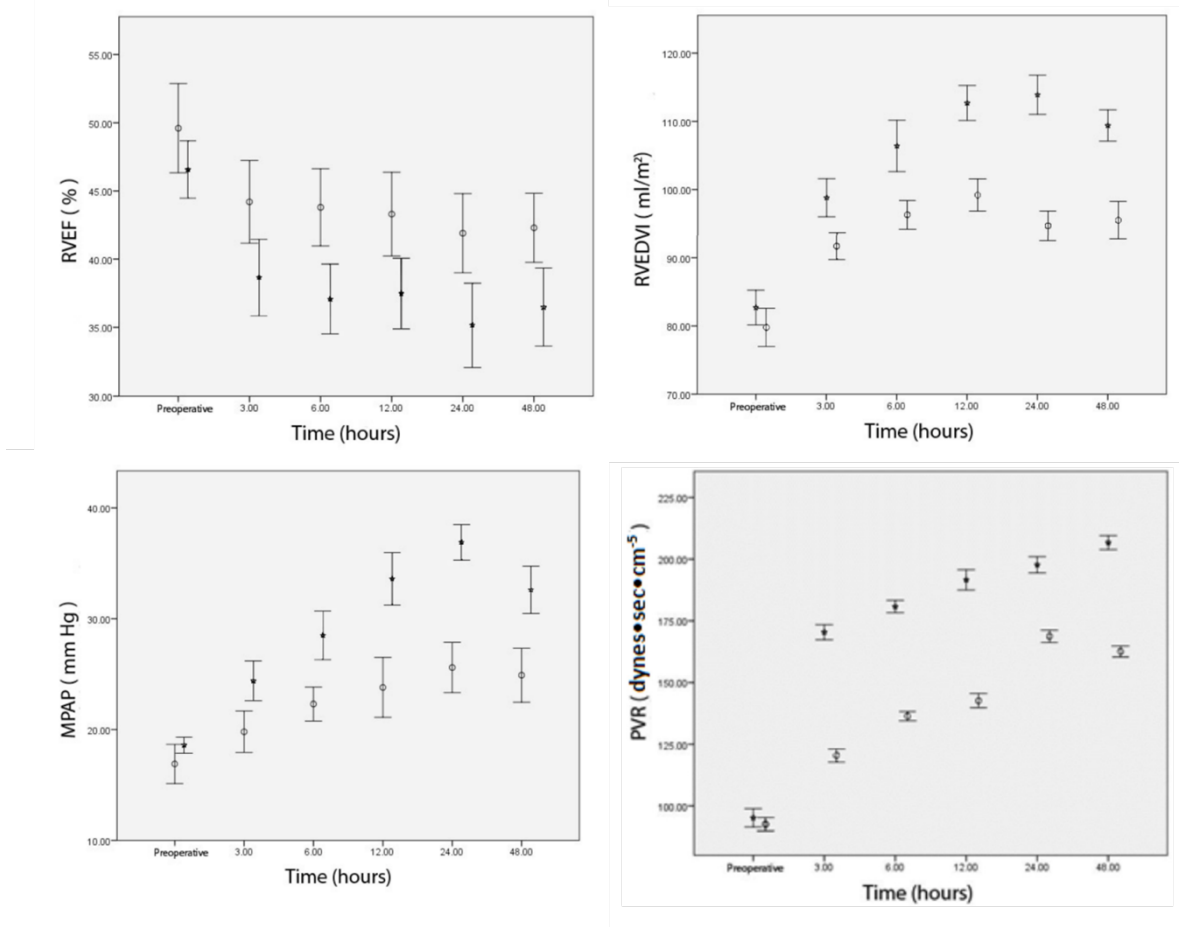

Figure 2-2 Post-operative haemodynamic changes to lung resection
Changes in right ventricular (RV) and pulmonary function following lobectomy (open circles) and pneumonectomy (closed stars), all values mean and 95% confidence intervals. Note the similar trends but differing degree of the reduction in RV ejection fraction (RVEF) and increase in RV end-diastolic volume index (EDVI), mean pulmonary artery pressure (MPAP) and pulmonary vascular resistance (PVR) between pneumonectomy and lobectomy. Images from Elrakhawy et al.[62].

The results of this study vary significantly from the prospective studies in terms of PVR. This is the only study to find a persistent and meaningful post-operative rise in PVR in the immediate post-operative period whereas all others showed either no difference[48, 49, 65] or a decrease[58-60]. The practice of VPAC insertion for all patients until 48 hours post-operatively is out of keeping with current practice[217] and raises the question of what other aspects of care are different. Due to the retrospective nature of Elrakhawy et al.s' study, there was no control over fluid management and no standardised approach to VPAC measurements.

2.3.1.4 Additional studies

Lewis et al. investigated intra-operative changes in a high-risk population of 20 patients undergoing pneumonectomy with moderately severe COPD with 77% of patients having pulmonary arterial hypertension (PAH) secondary to COPD at baseline[63]. Intra-operatively, RVEF decreased and PVR increased on PA clamping. RVP/RVESVI (described as a "reflector of contractility") was unchanged suggesting that the increase in afterload was responsible for the RVEF deterioration however there was no association between RVEF and PVR. Of note, the response to PA clamping in the patients with PAH showed two distinct responses. Seven patients had a drop in PAP (8mmHg) whilst the other 6 patients had a rise in PAP (12mmHg). This may represent differing disease processes in the pulmonary vasculature and may explain why there was no *overall* change in PAP or PVR on clamping.

Boldt et al. randomised patients into two different anaesthetic and extubation strategy groups without determining any post-operative difference between the groups[61]. Remarkably, this is one of the few remaining unretracted papers from the discredited German researcher[218]. Its results are mentioned for completeness, they are in line with the previous studies and will not be included in any further discussion. The ten pneumonectomy patients had RV dysfunction (reduced RVEF and increased RVEDV) and increased SPAP intra- and post-operatively.

Bäcklund et al. performed a randomised controlled trial investigating the impact of the duration (1-day vs 3 days) of supplemental oxygen (O_2) therapy on RV function and afterload in the post-operative period[65]. There were no consistent differences in RVEF, PVR or atrial fibrillation (AF) occurrence between the two O_2 therapy groups although raised PVR was associated with development of post-operative AF. Interestingly, in the 1-day group RVEF decreased and PVR increased following cessation of O_2 therapy. The authors argue that the cessation of O_2 led to hypoxic pulmonary vasoconstriction resulting in an increase in afterload, PVR and reduced RVEF. They also attempted echocardiographic assessment of RVEF in all patients but, *"reliable measurements of RVEF could not be obtained"*.

Mikami et al. compared post-operative changes between open lobectomy (10 patients) and VATS lobectomy (13 patients) groups[66]. Neither group showed a change in RVEF from pre-operative values although the authors, somewhat

tenuously, comment that there was a trend to reduction in RVEF in the open group at six hours post-op (p=0.08). At this point RVEF was lower (relative to pre-op) in the open group compared to the VATS group. Similar to Reed at al[58-60], total PVR actually decreased post-operatively in both groups.

Mageed et al. investigated peri-operative changes in RV function, loading and gas exchange in 30 patients undergoing open/VATS lobectomy[64]. Measurements were taken pre-induction, 15 minutes post-induction and 2 hours post-operatively. Given that the patients had VPAC monitoring in situ for the duration of surgery, they unfortunately did not assess changes in RV function and loading before during and after institution of one lung ventilation (OLV) or PA clamping. They do not explicitly state whether the "15 minutes post-induction" time point is on OLV or not. There was no change in any parameter post-induction although RVEF and stroke volume index were reduced at 2 hours post-op. As the latest point of investigation was at 2 hours post-op, they do not investigate any potential recovery in RVEF following this time point.

2.3.2 Non-volumetric pulmonary artery catheter studies

Three further studies have investigated changes in afterload before and after lung resection using a conventional (non-volumetric) pulmonary artery catheter (PAC), Table 2-2, page 102. These studies investigate afterload changes peri-operatively[69], at 6 months[67] and at 4 years[68] following lung resection. The two studies with post-operative follow-up also assess the response to exercise (Nishimura et al.[67] and Miyazawa et al.[68]) and support the reduced pulmonary vascular reserve reinterpretation of the work by Okada et al.s[48, 49].

The two exercise studies assess the change in the haemodynamic response to supine bicycle exercise. They were performed in the same Japanese centre[67, 68]. Nishimura et al. (1993) assessed 9 patients pre-operatively and 6 months post-operatively and Miyazawa et al. (1999) assessed 8 patients using the same protocol as Nishimura et al. with an additional follow-up at 4 years[r]. Both were in mixed lobectomy and bilobectomy patients, the results are similar between the studies and are presented together.

Compared to pre-op testing, resting MPAP was unchanged at 6 months but there was a modest increase at 4 years (17.8±3.9 vs 14.4±1.7mmHg pre-op, $p<0.05$, paired t-test). As there were no control subjects in this study the increase may result from other factors, such as aging[219]. On exercise, MPAP was increased at both post-op time points compared to the pre-op exercise values. Of note not all patients were able to complete the 50W exercise post-operatively. Similar to the reinterpretation of the work by Okada et al. presented in section 2.3.1.2.3 page 88, PVreserve can be plotted for both Nishimura et al. and Miyazawa et al., Figure 2-3. When the gradient (PVreserve) is plotted for each complete time-point there is a clear progressive increase in the gradient, i.e. there is a progressive reduction in PVreserve at 6 months post-operatively and a further reduction by 4 year post-operatively.

[r] It is difficult to determine whether Miyazawa et al.s' study include any of the patients from Nishimura et al.s' study. The pre-op and 6 months results are very similar but not identical although the loss of one patient may explain. Contrary to this both authors provide baseline details(age, surgery and pack years) about the patients in each study. Only 5 of the 8 patients in Miyazawa et al. correspond to Nishimura et al. assuming that the ages provided are age at follow-up in Miyazawa et al.

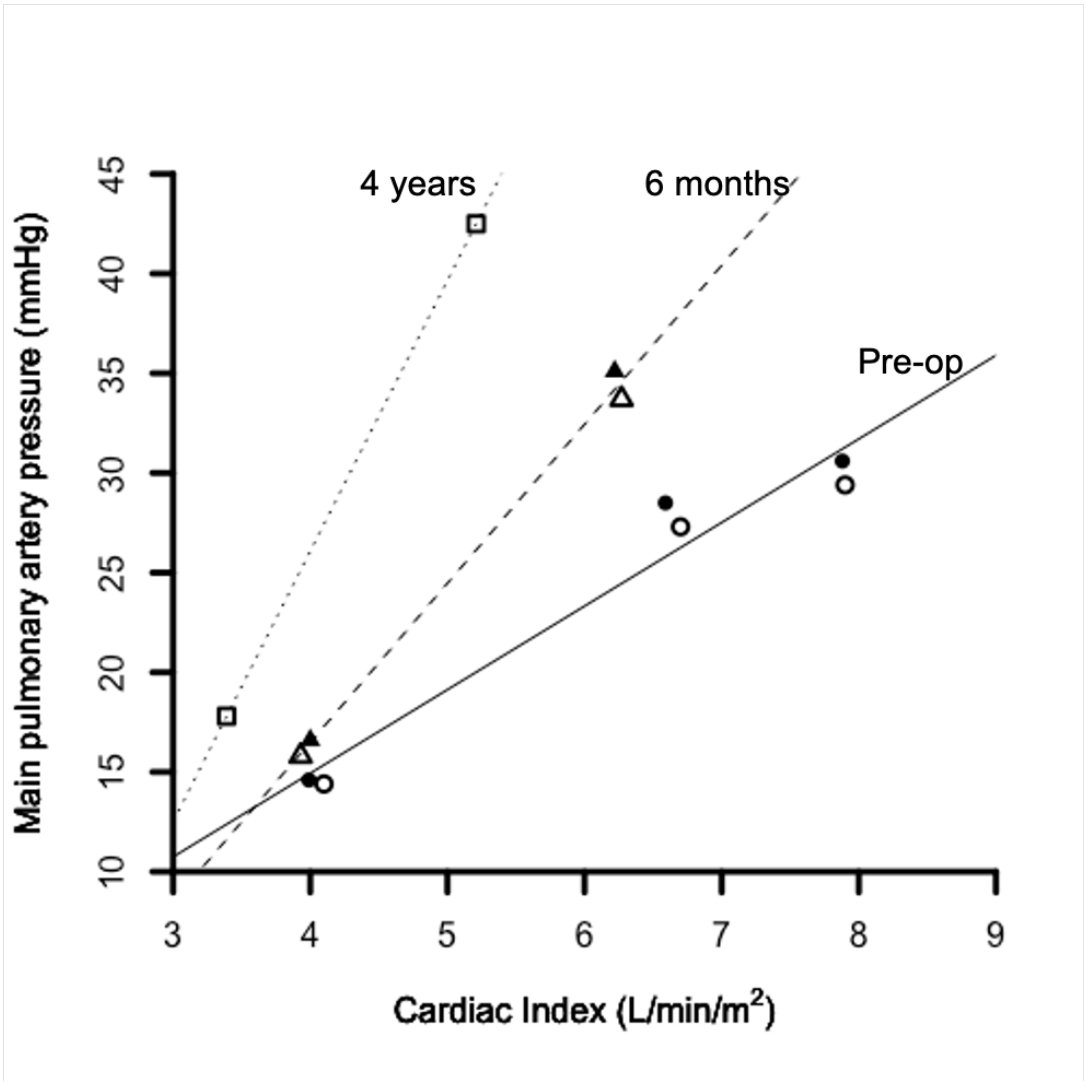

Figure 2-3 Pulmonary vascular reserve following lung resection, Nishimura et al. and Miyazawa et al.
Relationship between mean pulmonary artery pressure and cardiac index pre-operatively (circles and solid lines), 6 months (triangles and dashed lines) and 4 years (squares and dotted line) following lung resection. Closed shapes are Nishimura et al.[67] open shapes are Miyazawa et al.[68] Values are taken at rest, 25W and 50W pre-operatively. As not all subjects were able to complete 50W exercise post-operatively values presented are rest and 25W exercise. Note, the progressively increasing gradient after resection. Note very similar results at pre-op and 6 months between studies as there is likely at least some shared patients between the trials.

Pulmonary vascular resistance, indexed to body surface area (PVRI), was increased, compared to pre-op, at 6 months[67] and 4 years[68]. Similar to MPAP, PVRI increased on exercise compared to corresponding pre-operative exercise values. Of note, pulmonary capillary wedge pressure, representative of left atrial pressure and therefore LV filling, was unchanged at all time-points suggesting that the increase in afterload was not secondary to back pressure from the LV. Whilst RV function was not assessed in these studies, there is a clear increase in afterload on exercise following resection and no evidence that LV dysfunction contributes to this.

Finally, Waller et al. investigated the peri-operative changes in PVR and MPAP in patients undergoing open lobectomy (11 patients) or open pneumonectomy (10 patients)[69]. There was only a modest increase in MPAP (26.5mmHg [18-45] from 19.5mmHg [16-27]) on PA clamping and an increase in PVR at the end of the surgery and 2 hours post-op. At 18 hours post-op there was no change in either parameter. Interestingly, they demonstrated an inverse relationship (r=-0.68, p=0.02) between the pre-operative MPAP and the peri-operative increase in MPAP, i.e. the patients with higher MPAP had a lesser peri-operative increase in MPAP. They suggest that this may be explained as the patients with pre-existing pulmonary '*reactive vasoconstriction*' in the lung containing the cancer may have little subsequent change in blood flow and therefore pressure.

2.3.3 Summary of pulmonary artery catheter studies

It is unfortunate that a large proportion of this series of studies (those utilising the VPAC) is based on a flawed method of assessment. The main findings (decreased RVEF, increased RVEDV and unchanged RV contractility (RVSWI)) cannot be accepted given the lack of association between VPACs and the gold standards of RV assessment[168, 173]. These findings are however remarkably consistent between the studies with a relative decrease in RVEF at POD1/2 of 10-20% (22% in pneumonectomy alone[62]), as seen in Table 2-1.

The risk of complication of PACs limits the duration of the majority of these studies[220], with only Okada et al. assessing RV function after 48 hours. Whilst they did not show any improvement in RVEF at 3 weeks, this is insufficient to definitively state that there is persistent RV dysfunction following lung resection. These studies may only demonstrate a transient peri-operative insult that may have limited clinical significance, as concluded from the echocardiography evidence, detailed below, by Pedoto and Amar[78].

VPACs tend to overestimate RVEDV and underestimate RVEF, the same changes seen following lung resection, but the design of all the studies ensures any comparison is between the same patient pre-, intra- and post-operatively. This *within-subject* analysis may mitigate for any bias in the measurement, as long as it is consistent and in the same direction. It is not possible to conclude that RV

dysfunction occurs following lung resection based on this evidence but clearly it warrants further investigation.

There are, however, inferences that can be taken from the VPAC (and PAC) work if we look at the data which they can reliably measure, i.e. PAP, CO and (by calculation) PVR, Table 2-1 and Table 2-2. Intra-operatively, Reed et al. found that PVR and MPAP increased on PA clamping[60]. Post-operatively, PVR was shown to increase in the immediate post-operative period in two prospective studies[65, 69] and reduce in three other studies[59, 60, 66]. In the longer post-operative follow-up of Nishimura et al.[67] and Miyazawa et al.[68] increased PVR developed by 6 months and a modest increase in MPAP was only present at 4 years months post-operatively.

Nishimura et al.[67], Miyazawa et al. [68] and Okada et al.[49] demonstrated that MPAP and PVR increase on exercise post-operatively. In Okada's words:

"exercise-loading pushes the RV to its limitations, unmasking a clear elevation in afterload."

Okada 1994[49]

Table 2-1 Summary of right ventricular changes following lung resection assessed by volumetric pulmonary artery catheter

Study	Patients (pneumo)		Comparisons	RVEF (%change)		RVEDV	RVSWI	PVR	SPAP	MPAP	Comment
Reed et al. 1992[60]	15 (2)		Pre- vs intra-op (PA occlusion)	↔		↔	-	↑	↑	↔	RV dysfunction only present post-op. Afterload increased intra-op but decreased post-op
			Pre- vs post-op (4hrs, POD1+2)	↓	(10)	↔	-	↓	↔	↔	
Reed et al. 1993[59]	10 (0)		Pre- vs post-op (1, 4-6, 24hrs)	↔		↑	↔	↓	↑	↔	No post-op difference in RVEF and mixed changes in afterload
Reed et al. 1996[58]	35 (?)	Part 1	Pre- vs post-op (POD1+2)	↓	(14)	↑	↔	↔	↔	↔	RV dysfunction with no post-op difference in afterload. RV dysfunction similar in prostaglandin E_1 group and control despite reduction in afterload
	10 (0)	Part 2	Pre- vs post-op (POD2)	↓	(19)	↑	-	↓	-	-	
			POD2 $pPGE_1$ vs control	↔		↔	-	↓PGE_1	-	-	

Study	Patients (pneumo)		Comparisons	RVEF (% change)	RVEDV	RVSWI	PVR	SPAP	MPAP	Comment
Okada et al. 1994[49]	20 (3)	Rest	Pre- vs post-op (1, 6hrs, POD1+2, 3weeks)	↓ (20)	↑ (only POD2)	-	↔	↔	↔	RV dysfunction with no difference in afterload Decrease of RVEF on exercise with marked increase in afterload on exercise
	10 (?)	Exercise	Exercise, pre-op vs 3weeks post-op	↓ (17.5)	↑	-	↑	↑	↑	
Okada et al. 1996[48]	18 (3)		Increase vs decrease RVEF on pre-op exercise	↓ in decrease	-	-	-	-	↔	Decrease in RVEF on exercise pre-op developed decreased RVEF at rest post-op
Lewis et al. 1994[63]	20 (20)		Pre vs intra-op (PA clamping)	↓ (16)	↔	-	↔	↔	↔	Deterioration of RV function and coupling on PA clamping without increase in PVR.
Boldt et al. 1996[61]	40	Lobectomy	Pre vs intra-op (30min OLV) A/B	↔/↓ (2)	↔/↔	-	-	↑/↑	-	Lobectomy were split into two groups based on anaesthesia and post-op ventilation. Only post-op ventilation group had RV dysfunction intra-op Pneumonectomy group had RV dysfunction and increase SPAP intra- and post-op
			Pre- vs post-op (Surgery end, 2hrs, POD1) A/B	↔/↔	↔/↔	-	-	↔/↔	-	
	10	Pneumo-	Pre vs intra-op (30min OLV)	↓ (22)	↑	-	-	↑	-	
			Pre- vs post-op (end of Surgery, 2hrs, POD1)	↓	↑	-	-	↑	-	

Study	Patients (pneumo)		Comparisons	RVEF (%change)	RVEDV	RVSWI	PVR	SPAP	MPAP	Comment
Bäcklund et al. 1998[65]	24 (2)	Oxygen therapy	Prolonged (P) vs short (S) O2 group	↔	↔	↔	↔	-	↔	No difference between groups in O2 therapy. Decreased RVEF and increased PVR from baseline in S group
	10 (?)		Pre vs post-op (P/S)	↔/↓ (16)	↔/↔	↔/↔	↔/↑	-	↔/↔	
Mikami et al. 2001 [66]	23 (0)		Pre- vs post-op (6, 12, 24, 48 hours)	↔	-	↔	↓	-	-	Comparisons of haemodynamic effects of VATS vs open surgery. RVEF lower in open that VATS at 24hours only. No change from baseline.
			Open (10) vs VATS (13)	↓ (in open at 24 hrs)	-	↔	↔	-	-	
Mageed et al. 2005 [64]	30 (0)		Pre- vs intra-op	↔	↔	↔	↔	-	↔	Peri-operative study demonstrating reduced RVEF at 2 hours post-op only. Intra-op time point not defined if OLV or not. No follow-up after 2 hours.
			Pre- vs post-op (2 hours)	↓ (27)	↔	↔	↔	-	↔	

Study	Patients (pneumo)		Comparisons	RVEF (% change)	RVEDV	RVSWI	PVR	SPAP	MPAP	Comment
Elrakhawy et al. 2017[62]	178 (36)	Pneumo-	Pre- vs post-op (3, 6, 12, 24, 48 hours)	↓ (24)	↓	-	↑	-	↑	Largest retrospective review of patients undergoing lung resection. Only study to show increase in PVR and MPAP in lobectomy group. As retrospective the study highlights the markedly different routine management of lung resection in Egypt compared to UK.
		Lobectomy	Prost-op (3, 6, 12, 24, 48 hours)	↓ (5)	↓	-	↑	-	↑	
		Pneumo- vs lobectomy	Post-op (3, 6, 12, 24, 48 hours)	↓ (in pneumo)	↓	-	↑	-	↑	

Pneumo= pneumonectomy. RV= right ventricle. RVEF= RV ejection fraction. RVEDV= RV end-diastolic volume. RVSWI= RV stroke work index. PVR= pulmonary vascular resistance. SPAP= systolic pulmonary artery pressure. MPAP= mean pulmonary artery pressure. VATS= video assisted thoracoscopic surgery. POD= post-operative day. PA= pulmonary artery. OLV= one lung ventilation.

Table 2-2 Summary of changes in afterload following lung resection assessed by pulmonary artery catheter

Study	Patients (pneumo)		Comparisons	PVR	SPAP	MPAP	Comment
Nishimura et al. 1993[67]	9 (0)	At rest	Pre- vs post-op (4-6 months)	↑	↔	↔	Increased MPAP at rest post-operatively with increased MPAP and SPAP on exercise post-op. Also reduced stroke volume index on post-operative exercise.
		On exercise	Pre- vs post-op (4-6 months)	↑	↔	↑	
Waller et al., 1996[69]	21 (10)	Pneumo	Pre- vs intra-op	↔	-	↑	Transient increases in PVR and MPAP in pneumonectomy group only. No changes in lobectomy group. Longest follow-up 18 hours with no changes at this time point.
			Pre- vs post-op (end + 2hrs)	↑	-	↔	
		Lobectomy	Pre- vs intra-op	↔	-	↔	
			Pre- vs post-op (end + 2hr)	↔	-	↔	
Miyazawa et al.1999[68]	8 (0)	At rest	Pre- vs post-op (4-6 months)	↑	↔	↔	Repeat of Nishimura et al. study with longer follow-up in same centre. PVR increased at rest by 42-48 months. Similar increase in MPAP on exercise post-operatively. Likely includes patients from Nishimura et al.[67].
			Pre- vs post-op (42-48 months)	↑↑	↔	↑	
		On exercise	Pre- vs post-op (4-6 months)	↑	↔	↑	
			Pre- vs post-op (42-48 months)	↑	↔	↑	

Pneumo= pneumonectomy. RV= right ventricle PVR= pulmonary vascular resistance. SPAP= systolic pulmonary artery pressure. MPAP= mean pulmonary artery pressure. Echo= echocardiography. PAC= pulmonary artery catheter.

2.4 Echocardiography studies

The echocardiographic studies can be broadly grouped into studies that focused on assessing RV loading conditions or assessing RV contractile function. Loading conditions were assessed my surrogate markers of RV dilation (RV volume or RV diameter) and estimated SPAP or RV systolic pressure[s] (RVSP) whilst a variety of methods to assess contractile function were used. As previously described, the hypothesis was that increased afterload and impaired contractility resulted in RV dysfunction.

2.4.1 Studies investigating right ventricular loading conditions

Amar et al. performed a series of studies utilising TTE to investigating RV function and its relationship with dysrhythmias in patients undergoing lung resection, published between 1995-7[70, 71, 221]. They investigated RVSP by measuring the tricuspid regurgitant jet (TRJ) velocity and calculation by a modified Bernoulli formula, Equation 2-1.

$$\text{Right ventricular systolic pressure (mmHg)} = 4(peak\ TRJ\ velocity)^4 + RA$$

Equation 2-1 Pulmonary artery systolic pressure
TRJ= tricuspid regurgitant jet. RAP= right atrial pressure.

The first paper, 1994, showed that patients who developed dysrhythmias had a higher TRJ velocity (a surrogate of SPAP interpreted as increased afterload)[71]. Only peri-operative blood loss of >1000ml and a TRJ velocity of ≥2.7 m/s were identified as independent predictors of dysrhythmia in a stepwise logistic regression. There was no evidence of RV enlargement in the group with dysrhythmia.

The second paper, 1996, in the series specifically investigated changes in RV loading conditions[70]. In the 86 patients (47 lobectomy and 39 pneumonectomy) TTE examination was performed pre-operatively, on POD1 and once between POD2 to POD6 (usually POD3). Technically adequate studies of the lobectomy group were achieved in 79% pre-operatively, 87% on POD1 and 77% on POD2-6.

[s] RVSP is assumed equal to SPAP unless RV outflow obstruction is present[73].

Similar percentages of studies were adequate following pneumonectomy except on POD1 when only 59% were adequate. Neither group showed a change in RVSP or TRJ velocity at any time point, the POD2-6 RVSP and TRJ velocity were greater in the pneumonectomy group. RV enlargement was said to have occurred in 5 pneumonectomy and 2 lobectomy patients although there was no definition, timing or degree of enlargement documented in the text. The 1997 paper investigated the use of prophylactic administration of diltiazem or digoxin to prevent dysrhythmias, there was no significant changes in RV function or RVSP in either group[221].

The authors argue that their results show increased afterload (RVSP) in pneumonectomy compared to lobectomy in the post-operative period following resection, but that there is no difference from baseline or impact on RV function. They however claim that this is in line with the results of Reed at als' 1992 and 1993 studies that show "mild elevations in pulmonary vascular resistance". As detailed above, this is the opposite of their actual results and PAP/RVSP are not equitable with PVR or afterload. Additionally, they claim to demonstrate a lack of a "significant incidence of right ventricular systolic dysfunction" despite not discussing their methods of echocardiographically assessing RV function.

Foroulis et al., 2004, performed a similar study to Amar et al.s' 1996 TTE paper but extended the post-operative follow-up until 6 months[73]. By 6 months, SPAP had increased following pneumonectomy and, to a lesser extent, lobectomy. Interestingly there was a stepwise reduction in SPAP from right pneumonectomy to left pneumonectomy and then (bi)lobectomy suggesting SPAP change is related to volume of lung resection[t]. A similar pattern is observed with a progressive increase in SPAP with increasing dyspnoea, significant for pneumonectomy (ANOVA, p=0.016, 35 patients) but non-significant for lobectomy. Post-operative RV dilation occurred in 60% of pneumonectomies and 23% of lobectomies, with the degree of RV dilatation associated with increasing SPAP.

[t] In the relevant part of the table within the paper, right and left pneumonectomy are incorrectly labelled but the result is detailed in the text. As such the results detailed here are different to those stated in paper.

Venuta et al., 2007, further extended follow-up echocardiography until 4 years post-operatively[74]. In the pneumonectomy group, RV diameter and SPAP progressively increased with time, but there were no changes seen in the lobectomy group. There was a smaller increase in SPAP than Foroulis et al. (31.8mmHg vs 40.5mmHg) although this may be explained by the higher proportion of right sided pneumonectomy and larger resected lung volume in Foroulis et al.

2.4.2 Studies investigating contractile function

Kowalewski et al., 1999, performed detailed TTE assessment of the RV pre-operatively and on POD2 in 31 patients undergoing open resection (22 pneumonectomies, 9 lobectomies) [72]. The aim of the study was to confirm the presence of RV dysfunction and investigate its relationship with dysrhythmia but contrary to Amar et al. their focus of investigation was RV function and not pulmonary vascular pressures. RV volume were calculated by subtraction of LV volume from the volume of both ventricles in systole and diastole with RVEF then calculated.

The results are similar to VPAC studies; post-operatively the pneumonectomy group had decreased RVEF (19% relative reduction) and increased RV volume (RVEDV and RVESV), with no significant changes in the lobectomy group. Within the pneumonectomy group, the patients who developed post-operative arrhythmias had lower RVEF and higher RVEDVI than those who did not develop arrhythmia, however, the rate of arrhythmias was far greater in this study than previously reported; 64% of pneumonectomy patients in this cohort developed arrhythmia (10/14 atrial fibrillation, 4/14 supraventricular tachycardia) compared to 10-22% in previous studies[60, 71, 222]. All cases of arrhythmia occurred after the POD2 TTE imaging and they concluded that RV dysfunction leads to the arrhythmia.

An explanation for the high rate of arrhythmias is not given in the paper although they discuss a subsequent change in practice to give prophylactic digoxin in the presence of post-operative RV dilatation. They report this results in reduced arrhythmias although this work has not been published. Separately, Amar et al. have demonstrated that diltiazem reduces the incidence of arrhythmias in high-risk groups following lung resection[221, 223].

Andaluz-Ojeda et al., 2011, attempted to overcome the limitations of 2D TTE estimation of RVEF by measuring tricuspid annular systolic plane excursion (TAPSE), a measure of the longitudinal contraction of the RV[75]. TAPSE (mm) was only slightly reduced (22.98±3.71 to 21.18±3.27) on POD3 in the 38-patient mixed pneumonectomy/lobectomy population. There was no change in LV function.

Potaris et al., 2014, assessed 69 patients who underwent pneumonectomy with echocardiographic and functional assessment by New York Heart Association (NYHA) classification[77]. Patients were followed up for 12-months. During this time there was a progressive increase in SPAP and decrease in functional status. Increased SPAP at any time point was predictive of '*suboptimal clinical outcome*', defined as reduction in functional status or death.

Mandal et al., 2017, performed the most extensive TTE investigations to date in this population[76]. Twenty-six patients (5 pneumonectomies and 21 lobectomies) had detailed TTE examinations pre-operatively, POD2, POD3, POD7 and POD30. Unfortunately, this work has been negated by the statistical analysis of the results. A repeated measures analysis of variance has been performed only determining if there was a change over all time points. No subsequent analysis between pre-operative and any post-operative time-points was performed. It is impossible to determine if the POD30 values are significantly different to pre-operative values. There however appears to be a trend of reduced RV function (TAPSE, RV strain and RV fractional area change) and increased RVSP at POD2 with recovery by POD7.

2.4.3 Summary of echocardiographic studies

TTE cannot directly assess pressure and so they have estimated RSVP/SPAP from the tricuspid regurgitant jet[70, 73, 74, 76, 224]. This technique has been demonstrated to have an accuracy of only 56% in a lung transplant population[85], have a sensitivity of 60% and specificity of 74% for diagnosing PAH in an emphysematous population[225] and so may be inaccurate in a lung resection population[78]. Additionally, as described in 1.2.6.4.3 page 78, proximal PA occlusion may alter the RC time constant of the pulmonary vasculature therefore the derived estimations of SPAP and MPAP from the TRJ may be inaccurate following lung

resection[207]. VPACs are superior in assessing pressure and therefore the afterload data from the VPACs studies are more reliable than the TTE studies.

Measurement of RV volume is complicated by its shape and so accurately measuring RV volume by TTE is difficult[85]. RV diameter and volume are consistently shown to increase in the echocardiography studies however their measurement by TTE only show, at best, moderate association with CMR assessment[156, 226]. Only Kowalewski et al. estimate RVEF although their approach of subtracting LV volume from total ventricular volume has been shown to underestimate RVEF[78].

The reliability of the echocardiography studies must be questioned given the difficulties in obtaining echographic images following lung resection and the difference to the PAC results. The increase in SPAP demonstrated by echocardiography is directly contradicted by the PAC studies. The majority of studies suggest an increase in RVEDV which neither echocardiography nor VPAC can accurately measure.

Table 2-3 Summary of right ventricular changes following lung resection assessed by echocardiography

Study	Patients	Group	Comparisons	RVFAC/ RVEF	RVEDV/ RVEDD	SPAP/RVSP	Comment
Amar '96[70]	47	Lobectomy	Pre- vs post-op (POD1-6)	-	-	↔	No evidence of RV dysfunction except for higher RVSP in pneumonectomy
	39	Pneumo	Pre- vs post-op (POD1-6)	-	-	↔	
		Lobectomy vs Pneumo	Post-op lobectomy vs pneumonectomy	-	-	↑ in pneumo	
Kowalewski '99[72]	9	Lobectomy	Pre- vs post-op (POD2)		↔	-	RV dysfunction following pneumonectomy with increased incidence of arrhythmia.
	22	Pneumo	Pre- vs post-op (POD2)	↓	↑	-	
Foroulis '04[73]	17	Lobectomy	Pre- vs post-op (6 months)	-	↑	↑	Increased SPAP and RV dilatation, lobectomy > pneumonectomy.
	35	Pneumo	Pre- vs post-op (6 months)	-	↑↑	↑↑	
		Lobectomy vs Pneumo	Post-op lobectomy vs pneumonectomy	-	↑ in pneumo	↑ in pneumo	
Venuta '07[74]	36	Lobectomy	Pre- vs post-op (1 week, 3, 6, 12-months)	-	↔	↔	Increase in SPAP and RVEDD in pneumonectomy only progressively over 4 years of follow-up.
	15	Pneumo	Pre- vs post-op (1 week, 3, 6, 12-months)	-	↑	↑	

Study	Patients	Group	Comparisons	RVFAC/ RVEF	RVEDV/ RVEDD	SPAP/ RVSP	Comment
Andaluz-Ojeda et al., 2011[75]	47	Lobectomy	Pre- vs post-op (POD1-6)	-	-	↔	No evidence of RV dysfunction except for higher RVSP in pneumonectomy
	39	Pneumo	Pre- vs post-op (POD1-6)	-	-	↔	
		Lobectomy vs Pneumo	Post-op lobectomy vs pneumonectomy	-	-	↑ in pneumo	
Potaris et al. 2014[77]	69 (69)	Pneumo	Pre- vs post-op (1, 6, 12-months)	-	-	↑	Progressive increase in SPAP. Increased SPAP predictive of "suboptimal clinical outcome" at each timepoint, including pre-op.
Mandal et al., 2017[76]	17	Lobectomy	Pre- vs post-op (6 months)	-	↑	↑	Increased SPAP and RV dilatation, lobectomy > pneumonectomy.
	35	Pneumo	Pre- vs post-op (6 months)	-	↑↑	↑↑	
		Lobectomy vs Pneumo	Post-op lobectomy vs pneumonectomy	-	↑ in pneumo	↑ in pneumo	

Pneumo= pneumonectomy. RV= right ventricle. RVEF= RV ejection fraction. RVFAC= RV fractional area change. RVEDV= RV end-diastolic volume. RVEDD= RV end-diastolic diameter. RVSP= RV systolic pressure. SPAP= systolic pulmonary artery pressure. POD= post-operative day.

2.5 Cardiac magnetic resonance study

Smulders et al. performed the only CMR study in this population prior to the RV Response to Lung Resection Study[227]. They imaged 15 pneumonectomy patients over 5 years after their surgery and compared the results to population reference values. Patients had a higher HR and lower SV than healthy controls, with a lower LVEF and LV mass. RVEDV was reduced, the only study to show this, whilst there was no evidence of RV hypertrophy and RV mass was within normal limits. Unfortunately, RVEF was not calculated and the authors do not comment on it. There was marked rotation of the heart following left sided pneumonectomy, Figure 2-4.

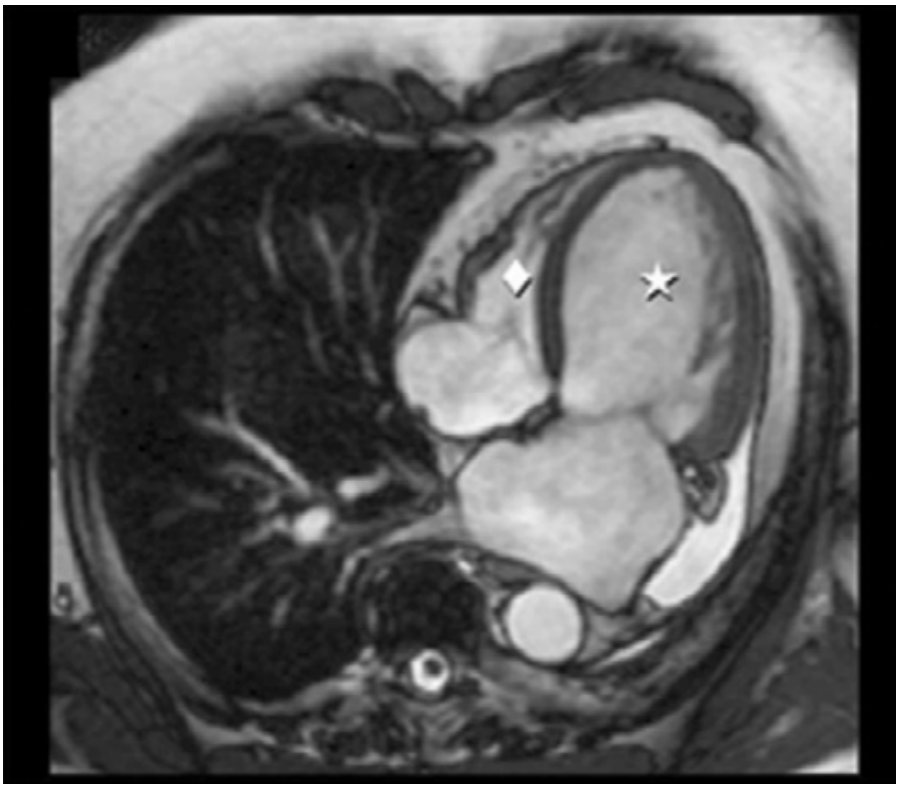

Figure 2-4 Four chamber view of heart following left sided pneumonectomy
Heart shifted from normal mediastinal position towards left. Note clear outline of right ventricle (diamond) wrapped around left ventricle (star). Image from Smulders et al.[227]

Although this study is the first use of CMR in this population, it is limited by the design. The patient population imaged likely do not represent an average lung resection population; they did not have pulmonary or cardiac disease pre-operatively and they were selected from a group of survivors. This is not the normal lung cancer population who frequently have COPD[16] and have a 5 year survival following pneumonectomy of 30%[228, 229]. As patients were only scanned post-operatively a healthy control group from another study were used a

comparator. Little information is given regarding the group other than a substantial difference in age between the participants (64±10 years) and controls (43±14 years). Such a marked difference limits the conclusions that can be drawn from this study.

2.5.1 Conclusion

In conclusion the PA catheters and echocardiographic studies contradict each other. They each show a change in the measure that they are inaccurate in, i.e. VPAC shows a reduction in RVEF whereas echocardiography shows an increase in PA pressure. The converse is also true, (V)PAC show no change in PA pressure whereas echocardiography shows no change in RV function. Given the methodological concerns with all of the above studies, the hypothesised reduction in RV function following lung resection is unproven.

Chapter 3 Thesis aims and hypotheses

As detailed in Chapter 2, there is insufficient prior evidence to confirm the widely hypothesised presence of RV dysfunction secondary to an increase in afterload following lung resection. To investigate this the "RV Response to Lung Resection Study" (RV study) was designed and undertaken by this research group[u230]. The study, detailed in Chapter 4, demonstrates the presence of RV dysfunction following lung resection and was designed to investigate the potential mechanisms that contribute to this dysfunction. This thesis will detail and perform the investigations into the hypothesised mechanisms of RV dysfunction following lung resection, as described below.

3.1 Chapter 4, Generic methods and results

This section will detail the design of the "RV study" and present the results that have been described elsewhere by McCall et al.[156, 231-234]. All the investigations in this thesis are performed on the cardiac magnetic resonance images from this study, as such this chapter describes the patient population for these investigations.

3.2 Chapter 5, Right ventricular strain analysis

Hypothesis 1: RV contractility decreases following lung resection.

McCall et al. have shown that RVEF decreases following lung resection[230], however RVEF is significantly impacted by loading conditions. Strain and strain rate analysis are considered to be less load dependent than RVEF and therefore may offer a more complete assessment of RV contractility and allow assessment of regional changes in RV function. Although speckle tracked echocardiography strain analysis did not demonstrate RV dysfunction[233] in this study group, CMR strain analysis is the gold standard and can be performed post-hoc on the CMR images. Chapter 5 details CMR strain analysis methodology and investigation.

[u] The investigations are performed on CMR scans of the patients from the "Right ventricular response to lung resection" study[230]

3.3 Right ventricular afterload analysis

Hypothesis 2: RV afterload increases following lung resection.

As detailed in the Chapter 2, the hypothesis that afterload increases following lung resection is well established. The previous studies have however focused on incomplete measures of afterload and so they have been unable to demonstrate this. Chapter 1 justifies that the measures used in these studies (PVR and PA pressure) are insufficient to assess changes in afterload, particularly following lung resection. Such measures predominately assess the resistance to the steady flow of blood and therefore overlook the pulsatile components of afterload.

Two separate methods of assessing pulsatile afterload will be presented. Both methods are derived from flow and cross-sectional area plots of the pulmonary arteries. The data which investigation Chapter 6 and Chapter 7 utilise are the pre-operative, POD2 and 2-months post-operative CMR scans of the 27 patients described in Chapter 4. At each time-point velocity encoded flow sequences of the PAs (main, left and right) were performed. This allows both comparison over time within each vessel and comparison between left and right PA dependent on which side the resection was performed.

3.3.1 Chapter 6, Pulmonary artery blood flow, acceleration time and distensibility

Chapter 6 will assess conventional CMR measures of afterload taken directly from area and flow plots to test hypothesis 2. Additionally, it will describe changes in the distribution of blood flow in the pulmonary vasculature following lung resection.

3.3.2 Chapter 7, Pulmonary artery wave intensity analysis

Chapter 7 will combine the area and flow profiles to generate wave intensity and allow assessment of afterload in a time-domain based approach. This is the first use of wave intensity analysis in this population.

3.4 Chapter 8, Mechanisms of right ventricular dysfunction following lung resection

Chapter 8 will combine the changes in afterload, and RV function (assessed by strain and RVEF) to explore potential mechanisms linking RV function and afterload.

Chapter 4 Generic methods and results

4.1 Introduction

This chapter details the design, methods and initial results of the "RV Response to Lung Resection" study. As described in Chapter 2, a cardiac magnetic resonance study was required to investigate the hypothesised RV dysfunction following lung resection. Whilst the primary outcome of the study, post-operative change in RVEF, has been reported by McCall et al.[230], the study was designed to perform an extensive investigation of the mechanisms of RV dysfunction following lung resection. All investigations undertaken within this thesis are performed on the data collected from this study. As such, this chapter will summarise the design, methods and patient characteristics of the study and briefly summarise the relevant[v] results reported separately to the analysis performed within this thesis[156, 230, 233-236].

4.2 Study design

Prospective observational cohort study of patients presenting for lung resection of primary lung cancer.

4.2.1 Primary outcome

4.2.1.1 Primary outcome measure

Change in CMR determined RVEF, at 2 days following lung resection compared to pre-operative values.

4.2.1.2 Rationale for primary outcome

To overcome the methodological issues of the previous studies, see Chapter 2, this study was designed to be the first sequential study of RV dysfunction utilising cardiac magnetic resonance (CMR) imaging, the gold standard in assessing RV function [80, 168]. The hypothesis that RV dysfunction occurs following lung resection

[v] There are other investigations performed as part of this study and they have been detailed elsewhere. Only the general study population and the aspects of the study that are relevant to the investigations within this thesis are described.

is well established but poorly investigated. As previously discussed, multiple previous studies have investigated both the presence and the mechanism of RV dysfunction following lung resection but there remains uncertainty over the true RV response to lung resection. These studies utilised echocardiography and volumetric pulmonary artery catheters (VPAC), both of which are potentially flawed in this population[48, 49, 58-77]. Although the accuracy of VPAC ability to measure RVEF is questioned[237] these studies consistently demonstrated a post-operative (absolute) reduction in RVEF of 6-9% on POD2 [49, 58, 60].

Pre-operative, POD2 and 2-month imaging allowed assessment of the acute and longer-term RV response to lung resection. Whilst RVEF is load dependent and is influenced by changes in contractility and afterload, Table 1-3 page 58, it is the most commonly used measure of RV function[83].

4.2.2 Secondary outcomes

4.2.2.1 Secondary outcomes measures

- Association of changes in RVEF with CMR and echocardiographically derived indices of contractility and loading
- Change in RVEF (ΔRVEF) compared to changes in left ventricular ejection fraction (ΔLVEF) over the same period
- Association between biomarkers of myocardial and endothelial dysfunction and ΔRVEF

4.2.2.2 Rationale for secondary outcomes

- Association of ΔRVEF with CMR and echocardiographically derived indices of contractility and loading[w].

Complete interpretation of RV function following lung resection requires assessment of RV function within its loading conditions. CMR allows assessment of RV preload (initial volume), contractility (strain), coupling and afterload

[w] Echocardiographic assessment of RV function and indices of contraction and loading were investigated by Dr Philip McCall. Changes in CMR derived loading conditions and contractility and its relationship to RVEF are the basis of this thesis therefore discussion will focus on CMR investigations.

(pulmonary artery diameter and flow analysis). The measures of CMR loading conditions defined a-priori within the study protocol are detailed below. All echocardiographic investigations, CMR coupling and preload investigations were performed Dr Philip McCall, results detailed below, whilst the CMR investigations of contractility and afterload are the basis of the investigations in this thesis and are explored in greater detail in the corresponding investigations.

Preload, RV end-diastolic volume determined by manual planimetry of a "stack" of short axis images of the RV.

Afterload, measured by pulmonary artery distensibility and flow analysis[212]. Afterload was also assessed by echocardiographic estimation of systolic pulmonary artery pressure (SPAP) (derived from the tricuspid regurgitant jet via the Bernoulli equation[70]) and measuring pulmonary artery acceleration time (PAAT) form pulsed wave Doppler interrogation of the RV outflow tract[80]. CMR based afterload assessment is performed in Chapter 6 and Chapter 7.

Ventriculo-arterial coupling, matching between contractility and afterload (E_{max}/E_a)[110].

Diastolic dysfunction, E/A ratio determines the ratio of ventricular filling from passive early diastolic filling rate (E) and peak filling rate due to atrial contraction (A), discussed further in 5.2.3.2 page 151.

Contractility, strain analysis was performed by echocardiography and CMR. Echocardiographic strain assessment was performed by speckle tracking echocardiography (STE). Strain is a dimensionless number that measures myocardial shortening, the ratio between the length of a myocardial segment after contraction to its initial length[238]. Speckle tracking utilises artefacts from echocardiographic images to track the shortening of myocardial segments throughout the cardiac cycle[239], results below. CMR strain investigation performed in Chapter 5.

- ΔRVEF compared to changes in left ventricular ejection fraction (ΔLVEF) over the same period.

Right ventricular function must be assessed with LV function. A decrease in RV function could be due to impaired global cardiac function or lead to a decrease in LV function due to ventricular interdependence[89].

- Association between biomarkers of myocardial and endothelial dysfunction and ΔRVEF.

RV myocardial dysfunction, brain natriuretic peptide (BNP) and high sensitivity Troponin-T (hsTnT) were used as markers of myocardial stress and dysfunction [240].

4.3 Generic methods

4.3.1 Ethical approval

Ethical approval was gained from the West of Scotland Research Ethics Committee (REC Ref: 134/WS/0055, Approval Date 16th April 2013).

4.3.2 Study setting

The study was performed at the Golden Jubilee National Hospital (GJNH), West of Scotland heart and Lung Centre, Clydebank.

4.3.3 Patient population

Patients scheduled for the Wednesday elective lung resection list were screened by the lead surgeon (Mr Kirk). Patients meeting the inclusion criteria were approached at pre-operative assessment the Friday prior to surgery. Providing no exclusion criteria were met, they were issued with information leaflets about the study. The patients had the opportunity to read the information prior to admission the day before surgery (Tuesday). If willing to participate in the study, informed consent was obtained by a member of the study team.

4.3.4 Power analysis

The study was powered to investigate the primary outcome detailed in 4.2.1.1. The VPAC studies by Reed et al.[60 58] and Okada et al.[49] demonstrated an absolute reduction in RVEF of 6-9% with a standard deviation of up to 7%, therefore an absolute reduction in RVEF of at least 6% on POD2 was used for power calculation.

This was carried out in consultation with the Robertson Centre for Biostatistics (University of Glasgow). A study of 19 patients would have 80% power to detect a deterioration in RVEF of 6%, based on a 2-sided, paired t-test with a significance level of 5%. Allowing a margin of 30% for withdrawals, 28 patients were planned to be recruited.

4.3.5 Inclusion and exclusion criteria

Inclusion criteria defined as;

- provision of informed consent
- age >16 years
- planned elective lobectomy by thoracotomy

Exclusion criteria were;

- pregnancy
- on-going participation in any investigational research which could undermine the scientific basis of the study
- contraindications to magnetic resonance imaging
    a. cardiac pacemaker, artificial heart valve, neurostimulator, cochlear implant
    b. aneurysm clips
    c. metal injuries to the eye
    d. loose metal in any part of the body
- wedge/segmental/sub-lobar lung resection
- pneumonectomy
- isolated middle lobectomy
- video assisted thoracoscopic surgery (VATS)/minimal access lung resection.

4.3.5.1 Justification of inclusion/exclusion criteria

The rate of pneumonectomy has fallen over recent years representing only 5% of total resections[9], although pneumonectomy has a greater physiological disruption, the reduced numbers of resections performed would limit the generalisability of any results. Selection of solely pneumonectomy patients would also greatly reduce

the population of patients to recruit from. Conversely, wedge/segmental/sub-lobar resections may lead to less physiological disruption, thus potentially increasing the sample size required for detection of RV dysfunction.

VATS resections were excluded as, at time of study design, they accounted for only 30% of lung resections in our institution[241]. Additionally, VATS are associated with reduced inflammatory response compared to an open approach[242]. As such the decision was taken to exclude any patients undergoing VATS resection from this study. Pregnancy and contraindications to CMR were excluded on the basis of patient safety.

4.3.6 Peri-operative management

The peri-operative management protocols of the study were designed with the intention to support standardised patient care.

4.3.6.1 Surgical management

Surgical management reflected the standard practice of the operating surgeon; postero-lateral muscle sparing thoracotomy with anatomically appropriate lymph node clearance.

4.3.6.2 Anaesthetic protocol

In order to prevent variation in patient care during the study period, an anaesthetic protocol based on the practice of the lead anaesthetist (Dr Mark Steven) was developed.

Thoracic epidural was placed prior to induction of anaesthesia, was "loaded" intra-operatively and maintained post-operatively with continuous infusion. If insertion failed, paravertebral catheters were placed intra-operatively by the surgeon and a patient controlled analgesic morphine pump used post-operatively. Anaesthesia was commenced by intra-venous (IV) induction and maintained with volatile anaesthetic. Lung isolation was performed with double lumen endo-tracheal tube. A lung protective ventilation strategy of tidal volume <8ml/kg, positive end-expiratory pressure of 0-5cmH_20, maximal airway pressure <30cmH_20, inspired oxygen to maintain saturations maintained at 92-98% and a permissive

approach to hypercapnia was used. All patients had arterial and central lines placed. Fluid administration was by a generally restrictive approach with a target of <1000ml unless exceptional losses.

4.3.7 Data collection

During the hospital stay and at the 2-month follow-up appointment data collection was perform by Dr McCall and research nursing staff. Postal questionnaires were distributed one year following surgery and data input was performed by the author and Dr McCall. Data was anonymised and stored on a password protected database (Microsoft Access® 2007, Microsoft, Washington, USA). Data collection timetable demonstrated in Table 4-1.

	Pre-op	Post-op/ recovery	POD1	POD2	2-months
Signed consent form (stored in site file)					
Baseline demographics					
CMR					
ECHO					
Biomarkers					

Table 4-1 Timetable for data collection
Data collection timetable. CRF – case report form. CMR= cardiac magnetic resonance imaging. ECHO= echocardiography. POD= post-operative day. Amended table from study protocol.

4.3.7.1 Baseline demographic data

Routine patient demographics were collected once the patient consented to participate in the study. Data collected included baseline demographics, smoking status, past medical history and medications. The results of routinely performed pulmonary function tests and pre-operative bloods were also collected.

4.3.7.2 Imaging

Cardiac magnetic resonance imaging and trans-thoracic echocardiography (TTE) were performed pre-operatively, on POD2 and at 2-months post op. Further details of the CMR and TTE protocols are described in 4.4.

4.3.7.3 Laboratory sampling

Markers of cardiac dysfunction, BNP and hsTnT were testing pre-operatively, immediately post-operatively (in recovery), on POD1 and POD2, and 2-months post-op.

Where possible all blood samples (including pre-operative) were taken from an arterial cannula that is routinely placed prior to induction of anaesthesia for lung resection. If the arterial cannula had been removed as it was no longer required for clinical reasons venepuncture was performed. At each time point 20 millilitres of blood was taken, BNP and hsTnT were tested as described below.

4.3.7.3.1 Brain Natriuretic Peptide

Brain Natriuretic Peptide was measured by a point-of-care fluorescence-based immunoassay, Alere Triage® system (Alere, Stockport, UK). All research team members received device training prior to use.

4.3.7.3.2 High sensitivity Troponin-T

High sensitivity Troponin-T was processed in the biochemistry laboratory in GJNH by enhanced immunoturbidimetric assay run on a Roche Cobas 6000e analyser (Roche, Basel, Switzerland) under the supervision of Dr Frank Findlay (consultant clinical scientist, biochemistry).

4.3.7.4 Clinical data

4.3.7.4.1 Intra-operative

The duration of one lung ventilation (OLV) and duration of surgery were calculated from the electronic anaesthetic record, 'RECALL Anaesthetic Intra-operative Management System' (Informatics Clinical Information Systems Limited, Glasgow). OLV was either recorded by the anaesthetist in charge of the case or calculated from the anaesthetic record. When not recorded, the change in airway pressure and tidal volume observed when switching between ventilating two lungs to one lung and vice versa was used as a marker for the start and end of OLV. The duration of surgery was calculated as the duration of an end-tidal carbon dioxide trace (only recorded in an intubated patient).

4.3.7.4.2 Post-operative

At the time the study was conducted, patients in the GJNH were routinely cared for in the high dependency unit (HDU) following lung resection. An electronic record of patient observations was generated throughout the HDU stay by the electronic clinical information system (Centricity CIS; GE Healthcare©, Buckinghamshire, UK). Haemodynamic and respiratory parameters were recorded at two-minute intervals. Fluid administration and urine output were recorded in the system by nursing staff and overall fluid balance is calculated from 08:00am to 07:59am the following morning. Additionally, the requirement for vasopressors and the presence of arrhythmia were recorded.

Duration of HDU stay was determined as the duration of continual oxygen saturation monitoring. Frequently patients are deemed 'ward ready' but remain in HDU awaiting transfer to the ward for a variety of reasons, e.g. lack of available ward bed, time of day, etc. Transition from continual to intermittent monitoring was taken as a pragmatic definition of the end of HDU (level 2) care. Similarly, hospital length of stay was defined as the *post-operative* length of stay due to the variation in time admitted prior to surgery. Numerous factors can increase the pre-operative length of stay and so this time was excluded from the hospital length of stay. For instance, patients at the GJNH travel from a wide geographical area, often necessitating arrival to hospital early on the day before surgery.

4.3.8 Data synthesis and statistics[x]

Parametric data are presented as mean (standard deviation) if normally distributed/parametric, or median (inter-quartile range) if non-parametric. Normality was assessed using visual inspection and with use of the Shapiro-Wilk test (normal distribution confirmed if $p>0.05$).

Testing for changes over time in parametric data were performed by one-way repeated measures analysis of variance (ANOVA) or Friedman's test for non-parametric data, significance accepted if $p<0.05$. Sphericity (a condition where

[x] Statistical advice was sought throughout the thesis from supervisors Ben Shelley and Phil McCall. Further advice and technical support were provided by Dr Martin Shaw for performing the statistical analysis in R.

the variance of the differences between all related groups are equal) was tested with Mauchly's test and assumed if $p>0.05$, if sphericity is not met the results are interpreted with Greenhouse-Geisser correction. Post-hoc comparisons were performed with paired t-test (parametric) or Wilcoxon rank sum test (non-parametric). Comparisons between results for unpaired comparisons was performed by unpaired t-test (parametric) or Wilcoxon signed rank test (non-parametric).

Association testing between two continuous variables was performed by visual inspection of a plot and with either Pearson's or Spearman's correlation coefficient testing performed and interpreted as per Landis and Koch[243], Table 4-2.

Correlation coefficient	Interpretation
0-0.19	Very weak
0.20-0.39	Weak
0.40-0.59	Moderate
0.60-0.79	Strong
0.80-1	Very strong

Table 4-2 Interpretation of correlation coefficient
Strength of association interpretation as per Landis and Koch[243]

Given the design of the study, patients were tested at multiple time points. Pooled analysis of such studies is widely reported although, as Bland and Altman describe, this "could be highly misleading"[244]. Regression analysis assumes independence of observations, repeated measures violates this assumption[245]. An alternative to this is offered by Bland and Altman by performing analysis of covariance (ANCVOA) with the patient as the factor with the two variables of which the association is being tested used as the dependent and covariate variables (interchangeably)[244]. This assesses the association between the two continual variables controlling for the categorical variable, i.e. the patient.

Analysis at individual time points assess between-subject associations whereas ANCOVA analysis measures within-subject association[245]. An 'R' package "Rmcorr" (repeated measures correlation) was used to perform the analysis described above for association testing with repeated measures[245]. An example of this is shown in Figure 4-1.

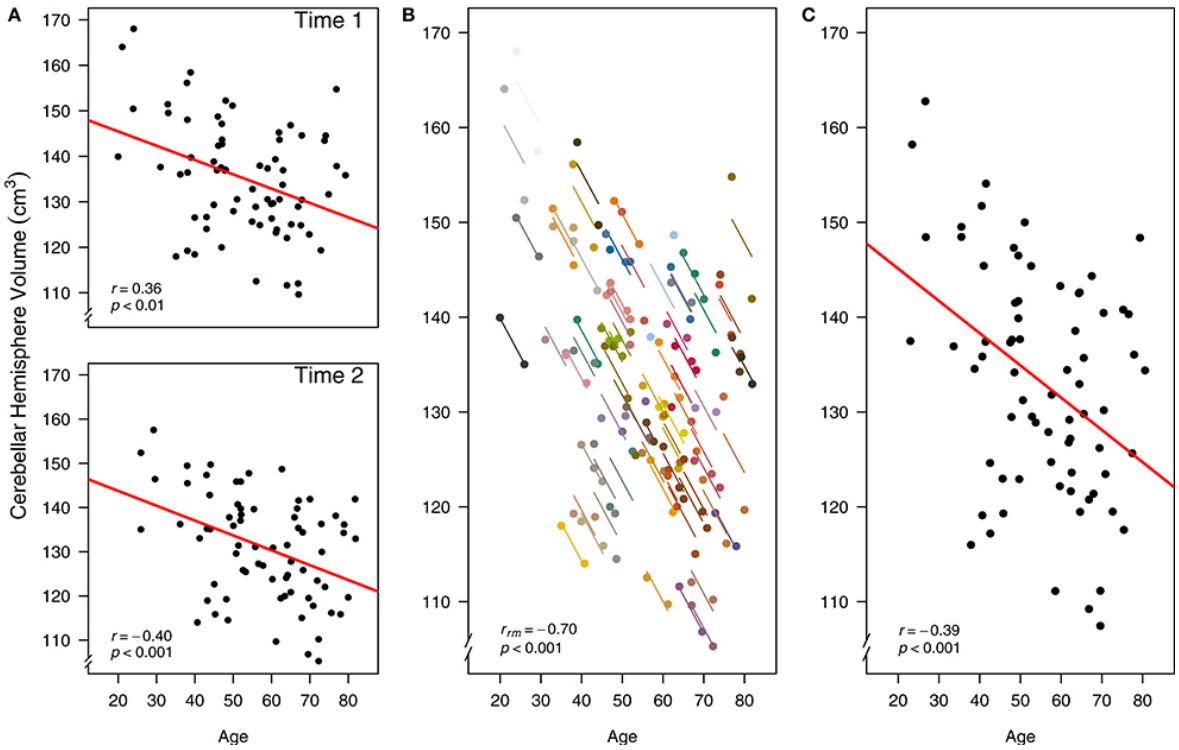

Figure 4-1 Example of analysis of covariance controlling for repeated measures
Measures of cerebellar hemisphere volume at two points analysed separately (plots in A), by combining both time points (plot C) and by analysis of covariance (plot B). In plot B the paired coloured dots and line represent the 2 time points and a regression line for that patient, the regression line is parallel to the overall line of fit and is plotted between the two values on the x-axis and at the mid-point between the two measures in the y-axis. Note that there is a strong correlation within-subject association although only weak/moderate associations at individual time points and pooled analysis. Example from Bakdash et al.[245].

4.3.8.1 Reliability testing

Reliability is defined as

> *"the extent to which measurements can be replicated"*
>
> Koo et al.[246]

A test of reliability must assess both agreement and correlation between measurements. Intraclass correlation coefficient (ICC) is an index that can assess both components or reliability[246]. Agreement between separate observers (interobserver) and repeated assessment by the same observer (intraobserver) were performed to determine variability. Two-way mixed effect models testing for absolute agreement were performed and interpreted as per Koo et al.[244], Table 4-3.

Coefficient of variation (CV) was calculated, Equation 4-1, to assess the degree of variability within measurements. CV is a standardisation of the standard

deviation, it removes the influence of the magnitude of the value being measured and expresses variation as a percentage[247].

$$Coefficient\ of\ variation\ (\%) = \frac{Standard\ deviation}{Mean} x\ 100$$

Equation 4-1 Coefficient of variation

Coefficient of variation (%)	Intraclass correlation coefficient (ICC)	Interpretation of reliability
>15	<0.5	Poor
10-15	0.5-0.75	Moderate/acceptable
<10	0.75-0.9	Good
	>0.9	Excellent

Table 4-3 Definitions of reliability and variability
Interpretation from Koo et al. and Holm et al.[246, 248].

Data handling, interpretation and statistical analysis of the results presented in this thesis was performed in R Studio (Version 1.1.463 – © 2009-2018). A p-value <0.05 was considered statistically significant. Exact p values are reported to 3 decimal places down to <0.001.

4.4 Imaging

4.4.1 Cardiac magnetic resonance

Patients underwent CMR pre-operatively, on POD2 and at 2-month follow up. Pre-operative scanning was performed either the day before surgery or, if this was not possible, on the morning of surgery. POD2 scanning was performed in the afternoon of the second day following surgery and 2-month scanning arranged to coincide with their routine follow-up clinic appointment.

CMR imaging was performed using a 1.5 Tesla Siemens Avanto (Siemens, Germany) whole body scanner. A standardised protocol was completed by band 7 Health and Care Professionals Council (HCPC) accredited advanced practitioner radiographers.

4.4.1.1 Safety checks

Patients were asked to complete a CMR safety questionnaire prior to recruitment and consent, to ensure that there were no contra-indications to CMR. A departmental safety questionnaire was completed prior to entering the CMR scanning room. Patients were dressed in either pyjamas or a hospital gown. Continuous 3-lead echocardiographic and oxygen saturation monitoring were applied with the patient lying on the examination table but outside the bore to the scanner. Ear defenders and an emergency buzzer were provided for patient safety. The ability to communicate with the patient was maintained throughout the scan with a microphone and headphones.

Additional precautions were required for POD2 scanning. All patients were escorted throughout the scan by a member of the research team and a consultant thoracic surgeon was available for management of potential complications.

Thoracotomy and lung resection introduce surgical clips and staples to the thorax. A detailed record of all implanted medical equipment was reviewed by a consultant radiologist (Dr Alcorn) prior to scanning. CMR safety of all equipment was confirmed with the manufacturer generating a list of "confirmed MR safe" equipment. 2-month scanning did not require any additional checks unless the patient had undergone subsequent procedures following the POD2 scan.

At POD2 patients may have chest drains in situ and medication infusions ongoing. Chest drains are routinely sited following lung resection to drain air and fluid from the thoracic cavity. In the GJNH chest drains are routinely attached to an electronic system, Thopaz (Mendela, Switzerland), which is not MR safe thus the chest drain was switched to an MR safe underwater seal system for the duration of the scan. Where feasible, infusions were disconnected for the duration of the scan or transferred to MR safe infusion pumps. Epidural infusions were disconnected for the duration of the scan and re-established following completion.

4.4.1.2 Image acquisition

ECG-gated fast imaging steady state free precision cines (TrueFISP, Siemens) were utilised throughout. For functional assessment slices of 6mm thickness with a 4mm gap between and voxel size 1.5 x 1.3 x 6mm were measured. Following localisation

scans, short axis stacks of the ventricles were performed from the atrioventricular valve plane to the cardiac apex, this was perfumed during breath holds.

Flow analysis was performed in the aorta and pulmonary arteries (main, left and right). The parameters for flow imaging were: field of view 320-360mm, slice thickness 5mm, base resolution 256, phase resolution 100%, echo time 2.7ms, repetition time 29.2ms, velocity encoding as appropriate (150cm.s^{-1} for normal flow). Effective temporal resolution was one thirtieth of the duration of the cardiac cycle. Reporting of the flow analysis is described in Chapter 6.

Completed scans were stored locally on the hard drive of the scanner with copies on the hospital imaging network. On completion of the study the scans were randomised and anonymised by a member of the radiography staff (Miss Vanessa Orchard) with a random number sequence generated by the 'RAND' function in Microsoft Excel® 2007 (Microsoft, Washington, USA).Two copies of the allocation were stored at the GNJH, one in the radiography office and one in a locked drawer in the research office. The completed images were stored on CDs (10 studies per disc) and analysed as detailed below.

4.4.1.3 Analysis

Safety reporting of all anonymised scans was performed by Dr John Payne (consultant cardiologist and lead for cardiac imaging at GJNH) with a report generated that entered the patients' clinical notes.

All analysis was performed in proprietary software (Argus, Siemens, Erlangen, Germany). Randomised images were dual reported. Functional images were reported by Dr Philip McCall (PM) and Dr Alex Arthur (AA) (both clinical research fellows in cardiothoracic anaesthesia at time of reporting). Dr David Corcoran (Clinical Research Fellow in CMR imaging with level 3 European Association of Cardiovascular Imaging certification in CMR imaging) provided initial training in assessment and assisted with scan analysis. He gave an expert deciding opinion in cases of disagreement in reporting between Drs Arthur and McCall. Interpretation was performed as per guidelines produced by the Society for Cardiovascular Magnetic Resonance (SCMR) Board of Trustees Task Force on Standardized Post Processing[249].

4.4.1.3.1 CMR reporting

For functional assessment the 'short axis stacks' for each individual anonymised scan was loaded into Argus from the CD file. The images were reviewed for duplication of slices, this can occur if there was concern over image quality or artefact at time of scanning. For any duplicated slices the poorer image was removed.

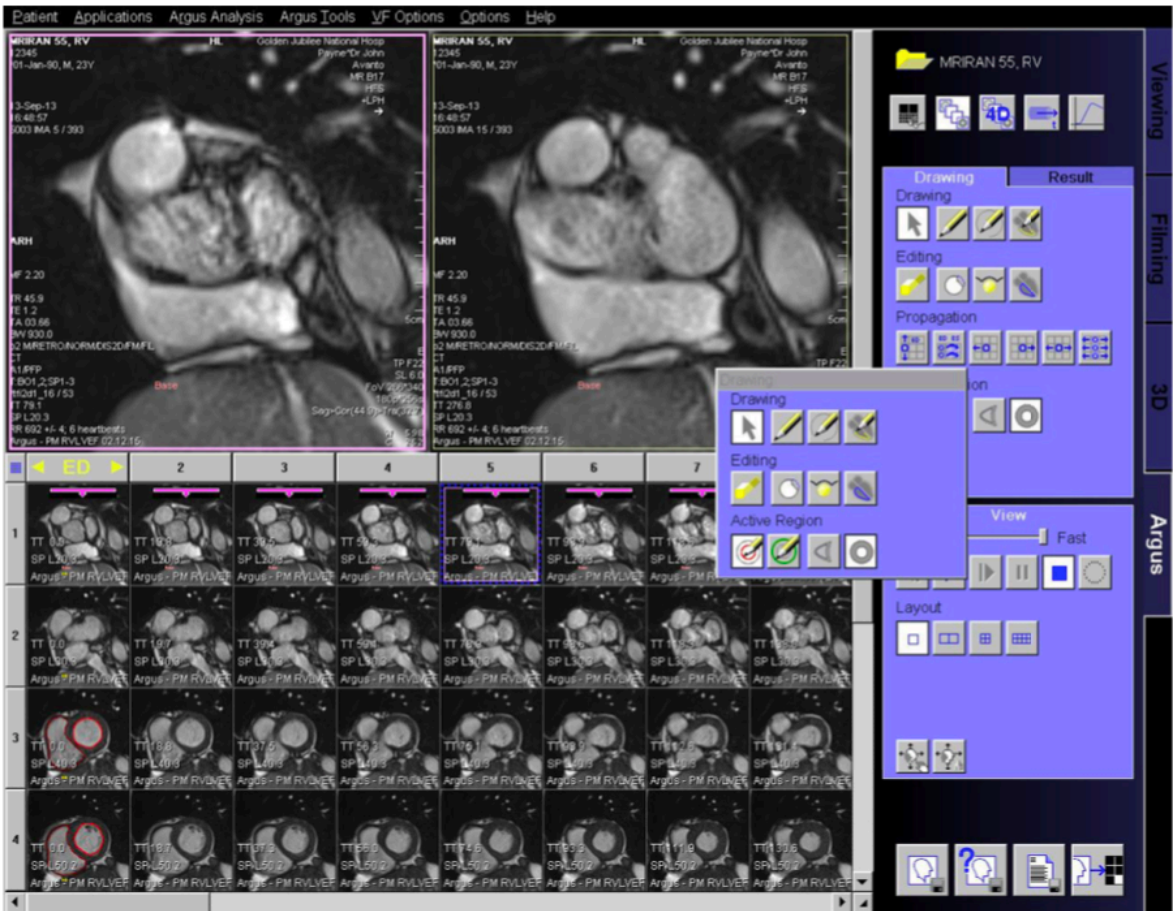

Figure 4-2 Short axis stack interpretation
Bottom section, each row represents a cine loop of short axis stack of the heart. One loop represents an entire cardiac cycle start from end-diastole (ED). Top row represents the base of the heart with consecutive slices represented by each row until the apex of the heart, not demonstrated in image.
Top panels display image selected from bottom row and column. Manual planimetry preformed on the top panels. Image from analysis of study patient.

The cardiac cycle is represented by a cine loop of the heart with the cardiac cycle divided into 35 frames (irrespective of duration of cardiac cycle) starting at end-diastole (matched to the R wave of the ECG). End-systole was manually determined by visual assessment of the frame with the smallest LV blood volume. The same frame was used for RV and LV end-systole. The endocardial borders of the ventricles were traced at end-diastole and end-systole, Figure 4-3. The

selection of the basal RV slice was initially performed on the short axis stack and then cross referenced with the long axis view to ensure that the right atrium had not been mistakenly included. Incorrect selection of the basal slice can lead to large errors in ventricular volumes by inappropriately including/excluding a large volume. The RV outflow tract (up to the pulmonary valve) was included in the RV volumes where visualised. A smooth RV border was drawn and trabeculations of the RV were ignored, this standard technique increases reproducibility[249].

Left ventricular (LV) volumes were determined by a similar approach to the RV. The basal slice was determined as the most basal slice surrounded by greater than 50% of ventricular myocardium. Papillary muscles were included in the blood pool.

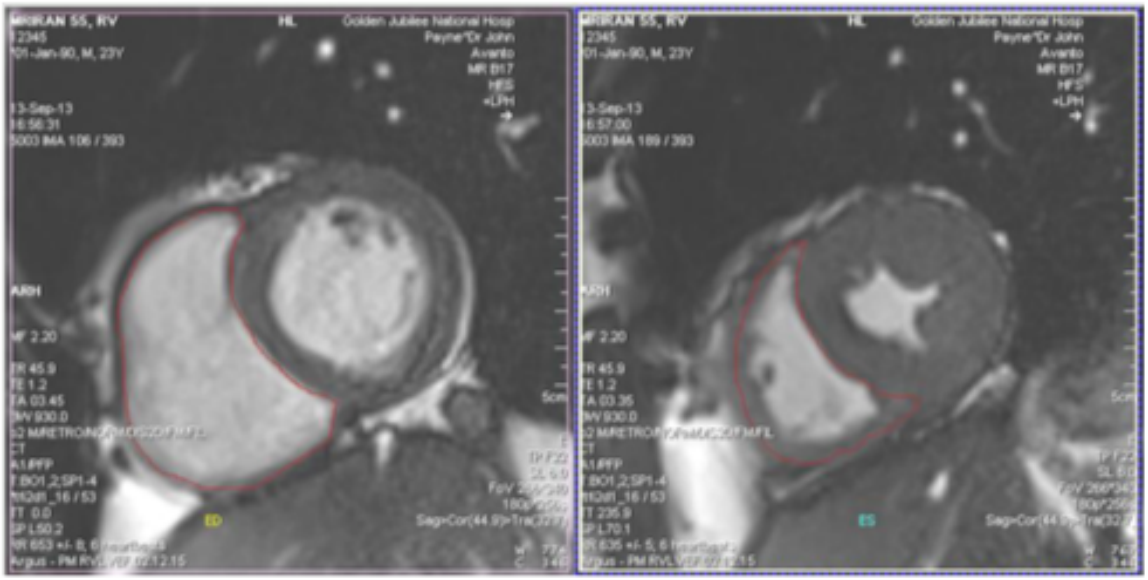

Figure 4-3 Defining ventricular borders
The endocardial border of the ventricle is manually traced (red line) and Argus calculates the ventricular volume. Volumes determined at end-diastole (left) and end-systole (right). Image from study patient.

Argus automatically calculates the volume of each mapped slice of the ventricle and therefore the total volume of the ventricle giving end-diastolic volume (EDV) and end-systolic volume (ESV). The difference between EDV and ESV is the stroke volume (SV) of the ventricle, Equation 4-2. Ejection fraction (EF) is calculated as the SV divided by the EDV, Equation 4-3.

$$Stroke\ volume\ (ml) = End\ Diastolic\ Volume\ (ml) - \ End\ Systolic\ Volume\ (ml)$$

Equation 4-2 Stroke volume

$$Ejection\ Fraction\ (\%) = \left(\frac{Stroke\ Volume\ (ml)}{End\ Diastolic\ Volume\ (ml)}\right) x\ 100$$

Equation 4-3 Ejection fraction

A CMR derived surrogate of RV-PA coupling was calculated from the RV volumes as per Sanz et al.[110].

$$Coupling = \frac{E_{max}}{E_a} \cong \frac{Stroke\ Volume\ (ml)}{End\ Systolic\ Volume\ (ml)}$$

Equation 4-4 Right ventricular coupling
E_{max}= maximal elastance. E_a= arterial elastance.

4.4.2 Echocardiography

Whilst CMR is the gold standard of RV assessment, echocardiography is the most commonly utilised assessment in clinical practice. As described in 1.2.5.1 page 63, echocardiography is particularly challenging following lung resection. Comprehensive echocardiographic analysis of RV function was performed and published by PM[156], only the afterload and strain echocardiographic analysis is discussed in this thesis.

4.4.2.1 Image acquisition

Contemporaneous trans-thoracic echocardiography (TTE) was performed with CMR imaging (pre-op, POD2 and 2-months). Where possible, TTE was performed on the same transfer to/from the CMR scanner. All imaging was performed according to a standardised protocol by band 7 British Society of Echocardiography (BSE) accredited cardiac physiologists on the Vivid E9 cardiovascular ultrasound system (GE Healthcare, Chicago, Illinois, USA) using a M5Sc-D transducer with a frequency of 1.5 to 4.6 MHz. Imaging was performed in the lateral decubitus position, except on POD2 in patients who were unable to tolerate this position due to surgical wounds and chest drains. The standardised protocol utilised parasternal, apical 4-chamber (A4C) and subcostal views.

4.4.2.2 Afterload assessment

Pulmonary artery systolic pressure (SPAP) was calculated from the pressure gradient across the tricuspid valve was estimated from the tricuspid regurgitant jet (TRJ) velocity with the simplified Bernoulli equation. The TRJ was imaged with continuous wave Doppler in each view of the RV and the measurement with the greatest velocity was used. RV systolic pressure (RVSP) was then estimated with the addition of right atrial pressure (estimated by inferior vena cava diameter), Equation 2-1 page 103. RVSP is assumed equal to pulmonary artery systolic pressure (SPAP) if there is no RV outflow tract or pulmonary valve obstruction.

Pulmonary artery acceleration time (PAAT), was measured as the time to peak flow from a pulsed wave Doppler analysis of flow in the main pulmonary artery[250].

4.4.2.3 Two-dimensional speckle tracked echocardiography

Speckle tracked echocardiography (STE) is angle independent measure of contractility. Contrary to tissue doppler imaging, STE is not dependent on the angle of incidence of ultrasound and has the ability to obtain an image along the true axis of RV wall movement [251]. It tracks artefacts on 2D echo images of the myocardium (speckles; generated from reflections, refractions and scattering of echo beams) during the cardiac cycle. The position of these speckles and their movement relative to each other allows calculation of strain parameters[252].

4.4.2.3.1 Image analysis

Apical four chamber views at a frame rate of 60-80 frames per second were obtained for four consecutive cardiac cycles during the echocardiography protocol. Anonymised and randomised A4C views were uploaded into proprietary analysis software (EchoPAC, GE Healthcare, Chicago, United States). Analysis was performed by PM with support from Dr Piotr Sonecki (Consultant cardiologist with a special interest in imaging). Semi-automated tracking of the RV endocardial border was performed of the RV free wall and septum. The software divides the RV into six segments and calculates RV global peak longitudinal strain (RV-GPLS) by averaging strain in each segment and RV free wall peak longitudinal strain (RV-FWLS) by averaging the three free wall segments.

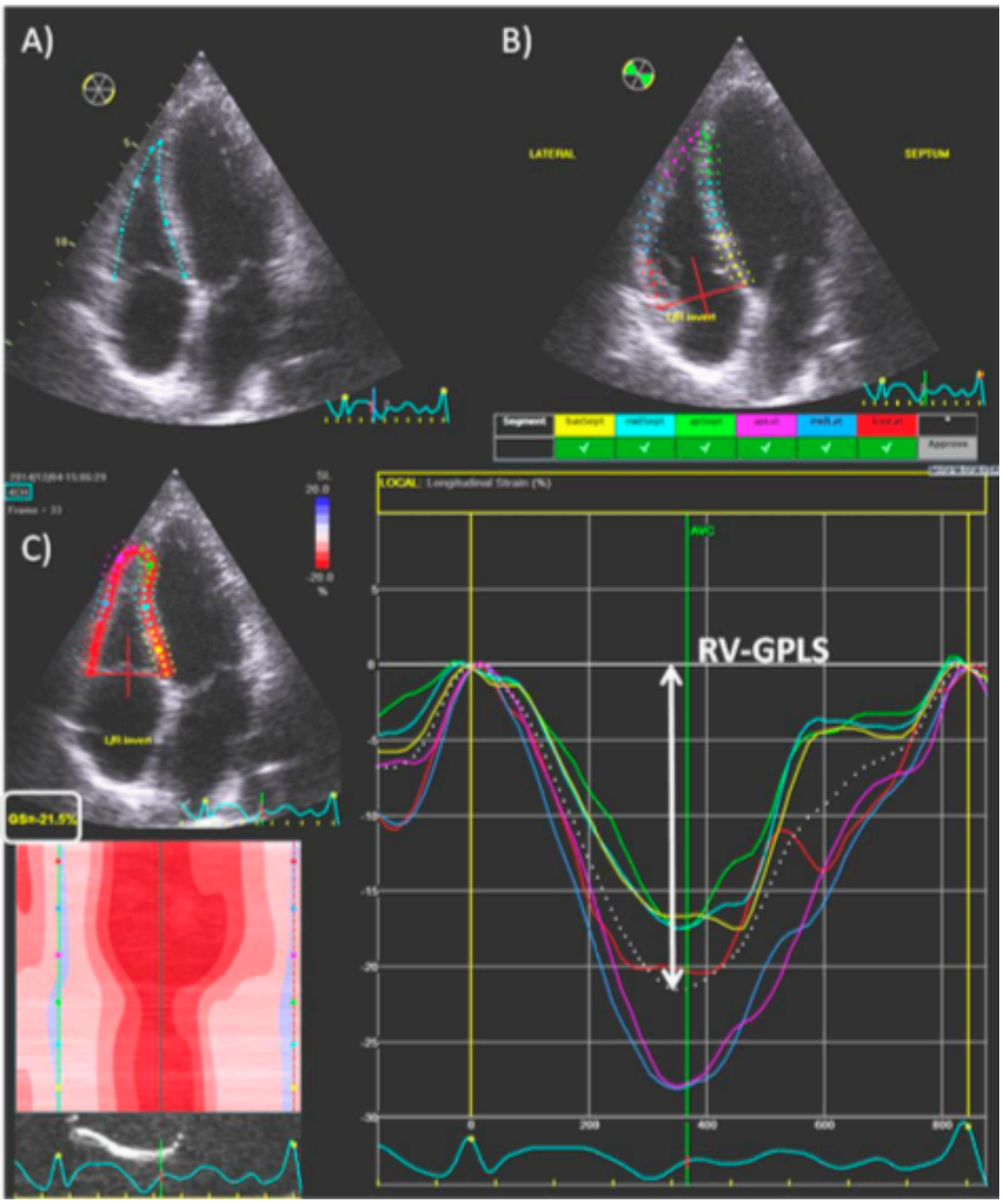

Figure 4-4 Speckle tracked echocardiography strain calculation
Contouring of the right ventricular endocardial border at end diastole (A) and end systole (B). Strain calculated by tracking each segment of the RV (C) generating right ventricular global peak longitudinal strain (RV-GPLS), dashed line in graph. Image from McCall et al.[253].

4.5 Results

This section will detail the patient cohort used in the investigations Chapters 5, 6, 7 and 8, with an overview of the results of the study as described by previous authors.

4.5.1 Generic results

4.5.1.1 Patient recruitment and imaging

Recruitment took place from September 2013 to September 2014. In total, 28 patients were recruited from 44 patients that were approached, Figure 4-5. Patient recruitment was performed by PM and AA. Twelve patients approached refused to participate in the study. Of the 28 recruited, one patient was excluded due to discovery of a contra-indication to CMR on pre-operative scanning. During scanning it was discovered that there was a ferromagnetic object in the patient's chest wall. Whilst there were no clinical sequelae from this it prevented imaging of the heart and so this patient was removed from the study and had no further follow-up.

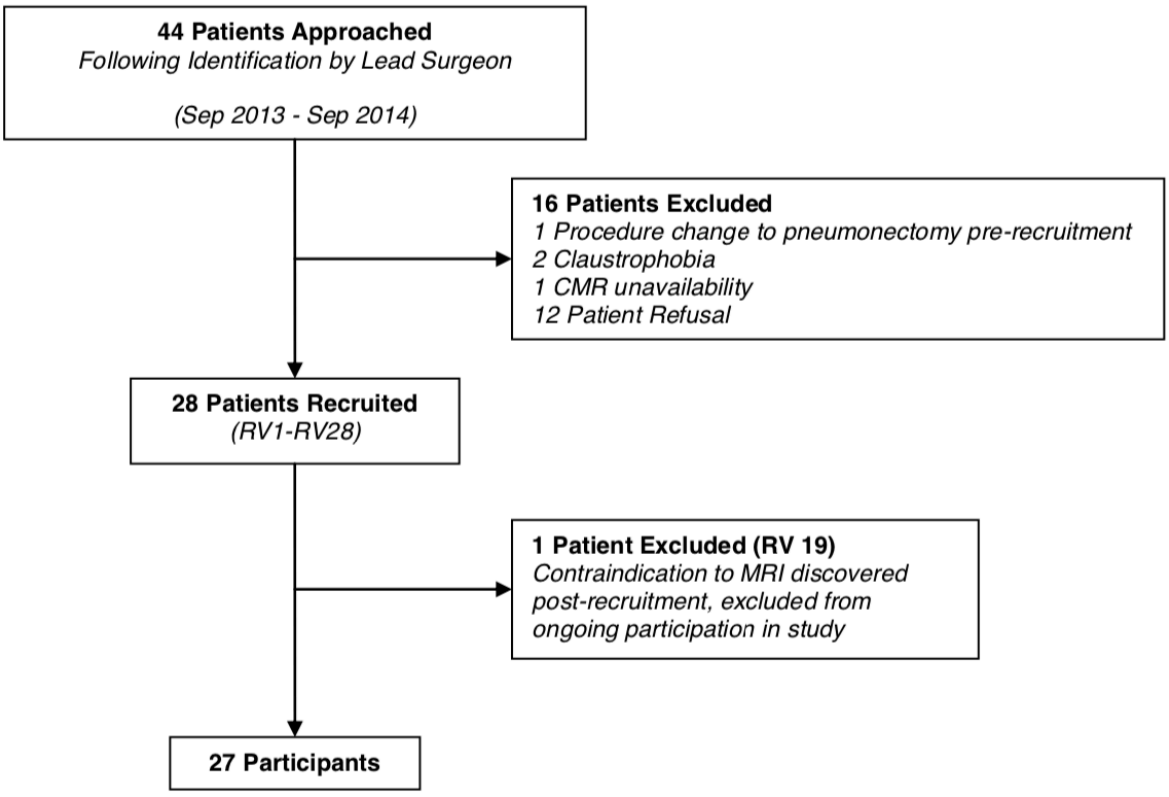

Figure 4-5 Consort diagram of study recruitment
RV1-RV28 notation used as anonymised patient study numbers. CMR= cardiac magnetic resonance. MRI= magnetic resonance imaging.

Pre-operative CMR imaging was performed in 27 patients, however one patient had incomplete imaging performed due to an administrative error that omitted the short axis stack of the heart. As such, pre-operative ventricular volumes and function could be calculated for 26 patients. Twenty-two patients (81.5%) completed POD2 imaging: three patients declined imaging, one had a persistent air leak preventing CMR transfer and one had an epidural catheter that was deemed incompatible with CMR[254]. Twenty-four patients (88.9%) completed 2-month imaging; one patient declined, one had undergone cataract surgery since their lung resection (CMR contraindicated within 6 weeks of cataract surgery) and one was an inpatient in another hospital with a broncho-pleural fistula. Ultimately, complete pre-operative, POD2 and 2-month scans were available for 20 patients. Patient demographics and results are presented for the 27 patients form the study and the 20 patients with complete imaging. CMR strain analysis, described in investigation Chapter 5, was performed on the patients with complete imaging (Strain cohort) and thus their characteristics are described separately below[y].

4.5.1.2 Patient demographics and operative characteristics

Baseline, intra-operative and post-operative details are described for the patients in Table 4-4, Table 4-5 and Table 4-6 respectively. The strain cohort were similar to the overall cohort in all parameters.

[y] As described in Chapter 5, strain analysis was performed on patients with complete sets.

Patient Demographics	All patients		Strain patients	
	n	Descriptive statistics	n	Descriptive statistics
Age (years)	27	67.0 (59.0, 74.0)	20	65 (58.8, 74.5)
Female sex	27	17 (62.9%)	20	12 (60%)
Height (cm)	27	163.3 (9.0)	20	163 (9.1)
Weight (kg)	27	69.9 (13.4)	20	69 (13.9)
BMI (kgm^{-2})	27	26.1 (3.9)	20	26 (3.9)
Smoking status	27		20	
Current smoker		13 (46.4%)		12 (60%)
Ex-smoker		12 (42.9%)		6 (30%)
Never smoked		2 (7.1%)		2 (10%)
Pack years	25	38.2 (21.7)	18	34 (22.3)
Pre-operative pulmonary function				
SaO_2 on air (%)	27	96.4 (1.7)	20	97 (1.7)
FEV_1 (L)	27	1.9 (1.6, 2.4)	20	2.0 (1.6, 2.5)
% Predicted FEV_1 (FEV_1%)	26	87.5 (25.1)	19	89 (28.4)
FEV_1/FVC (%)	27	64.1 (14.8)	20	63 (15.1)
TLCO (ml/kPa/min)	27	5.2 (1.7)	20	5.0 (1.9)
% Predicted TLCO (TLCO%)	27	66.6 (15.2)	20	65 (16.7)
Co-morbidities and risk score				
History of Cancer	27	7 (25.9%)	20	7 (35%)
COPD	27	6 (22.2%)	20	4 (20%)
Hypertension	27	9 (33.3%)	20	4 (20%)
IHD	27	6 (22.2%)	20	4 (20%)
Diabetes Mellitus	27	0	20	0
PVD	27	5 (18.5%)	20	2 (10%)
Obesity	27	2 (7.4%)	20	1 (5%)
Alcoholism	27	0	20	0
Thoracoscore (%)	27	0.7 (0.5, 0.8)	20	1 (0.6, 0.8)
ASA score	27		20	
1		0		0
2		2 (7.4%)		1 (5%)
3		25 (92.6%)		19 (95%)
4		0		0
5		0		0

Table 4-4 Baseline demographic data
Thoracoscore is a validated multivariate model that predicts in-hospital mortality (as a percentage) in patients undergoing general thoracic surgery [255]. Values are number (%), mean (SD) or median (IQR). n=number of patients for each parameter. BMI= body mass index. SaO_2= oxygen saturations. FEV1= forced expiratory volume in 1 second. FVC= forced vital capacity. TLCO= transfer factor for carbon monoxide. COPD= chronic obstructive pulmonary disease. IHD= ischaemic heart disease. PVD= peripheral vascular disease. ASA= American Society of Anaesthesiologists.

Patient Demographics		All patients		Strain patients	
		n	Descriptive statistics	n	Descriptive statistics
Resection type		27		20	
Pneumonectomy[z]			1 (3.7%)		1 (5%)
Lobectomy			22 (81.5%)		17 (85%)
Bilobectomy			4 (14.8%)		2 (10%)
Right Sided Procedure			17 (63%)		12 (60%)
Segments Resected			5 (3, 5)		5 (3, 5)
Predicted post-operative lung function					
ppoFEV1 %		26	67.66 (20.8)	20	68.85 (23.4)
ppoTLCO%		27	51.2 (11.6)	20	49.54 (12.7)
Pathology		27		20	
Primary Lung Cancer			24 (88.9%)		17(85%)
Other Malignant			1 (3.7%)		1 (5%)
Benign Disease			2 (7.4%)		2 (10%)
Lung Cancer Staging					
Stage	TNM subset	27		20	
1A	T1a N0		5 (18.5%)		4 (20%)
	T1b N0		4 (14.8%)		2 (10%)
1B	T2a N0		9 (33.3%)		6 (30%)
2A	T2b N0		2 (7.4%)		2 (10%)
2B	T2b N1		1 (3.7%)		1 (5%)
	T2a N2		1 (3.7%)		1 (5%)
3A	T3 N2		1 (3.7%)		1 (5%)
	T4 N0		1 (3.7%)		0 (0%)
Missing			3 (11.1%)		3 (15%)
Volatile anaesthetic agent		27		20	
Desflurane			1 (3.7%)		1 (5%)
Isoflurane			3 (11.1%)		2 (10%)
Sevoflurane			23 (85.2%)		17 (85%)
Duration					
Surgery (mins)		27	146 (116, 169)	20	128 (114, 154)
One lung ventilation (mins)		27	56 (48, 84)	20	53 (46, 64)

Table 4-5 Operative data
Values are number (%), mean (SD) or median (IQR). n=number of patients for each parameter. ppoFEV1= predicted post-operative forced expiratory volume in 1 second. ppoTLCO= predicted post-operative transfer factor for carbon monoxide.

[z] The planned surgery for all recruited patients was a lobectomy or bilobectomy (incorporating the right middle lobe). One patient had an intra-operative conversion to pneumonectomy. They are included in all results and sensitivity analysis was performed in this section. They are discussed further in the afterload analysis, Chapter 6, as this requires comparison of post-operative blood flow in the right and left pulmonary arteries pulmonary which is impossible following pneumonectomy.

Patient Demographics	All patients		Strain patients	
	n	Descriptive statistics	n	Descriptive statistics
Fluid administration (L)				
Intra-op	27	0.9 (0.4)	20	0.94 (0.43)
Op day to 07:59 POD1	27	1.7 (1.4, 2.2)	20	1.6 (1.3, 2.2)
to 07:59 POD2	17	2.3 (2.0, 2.5)	12	2.3 (2.1, 2.5)
to 07:59 POD3	6	1.9 (1.4, 2.7)	2	2.9 (2.7, 3.2)
HDU Fluid Balance (L)				
Op day to 07:59 POD1	27	1.0 (0.6, 1.4)	20	1.1 (0.8, 1.4)
to 07:59 POD2	17	0.1 (-0.5, 0.7)	12	0.1 (-0.4, 0.6)
to 07:59 POD 3	6	-0.6 (-1.2, 0.3)	2	-1.3 (-1.3, -1.4)
Vasoconstrictor required during HDU admission				
Noradrenaline		9 (33.3%)		6 (30%)
Nil		18 (66.7%)		14 (70%)
Arrhythmia				
Atrial Fibrillation		2 (7.4%)		2 (10%)
Length of stay				
HDU (Hours)	27	47.2 (29.2, 53.5)	20	47 (29.2, 51.3)
Hospital (Days)	27	8 (7, 11)	20	8 (7, 10.5)

Table 4-6 Fluid administration and post-operative clinical data
Values are number (%), mean (SD) or median (IQR). n=number of patients for each parameter. Op= operation. POD= post-operative day. HDU= high dependency unit.

4.5.2 Imaging results

4.5.2.1 Cardiac magnetic resonance

In total 72 CMR scans were completed and interpreted (26 pre-operatively, 22 on POD2 and 24 at 2-months). Inter-observer variation was good/excellent for RVEDV, RVESV, LVEDV and LVESV (ICC >0.84) whilst RVEF and LVEF were acceptable (ICC 0.53 and 0.71 respectively). Intra-observer variation was good/excellent for all RV and LV volume and ejection fractions (ICC >0.85).

Haemodynamic and ventricular results are detailed in Table 4-6. Heart rate and cardiac output were increased from baseline at POD2 but by 2-months had returned to baseline.

	Pre-op	POD2	2-months	p value
	n=26	n=22	n=24	
HR (bpm)	64.4 (13.0)	77.0 (11.0) #	69.4 (10.3)¥	***0.002 ****
CO (l/min)	6.6 (1.7)	8.0 (1.6) #	6.5 (1.7)¥	***0.004 ****
Right ventricle				
RVEF (%)	50.5 (6.9)	45.6 (4.5) #	44.9 (7.7) #	***0.003 ****
RVEDV (ml)	119.1 (25.4)	125.9 (22.5)	109.4 (31.6) #¥	***0.019 ****
RVESV (ml)	59.8 (17.1)	68.6 (14.5) #	59.8 (17.6)¥	***0.040 ****
RVSV (ml)	59.3 (12.0)	57.3 (10.7)	49.6 (16.5) #	***0.002 ****
Left ventricle				
LVEF (%)	58.4 (7.1)	57.4 (7.3)	59.7 (9.3)	0.621 *
LVEDV (ml)	109.2 (19.5)	106.3 (19.2)	93.6 (28.2) #¥	***0.001 ****
LVESV (ml)	46.0 (13.2)	46.0 (14.2)	37.7 (13.1) #¥	***0.019 ****
LVSV (ml)	63.2 (11.7)	60.3 (9.0)	55.9 (18.0) #	***0.004 ****

Table 4-7 Right and left ventricular changes following lung resection
Results displayed for the complete cohort. Data are mean (SD). *= One-way repeated measures ANOVA. #= Significant difference from Pre-op. ¥= Significant difference from POD2. POD= post-operative day. HR= heart rate. Bpm= beats per minute. CO= cardiac output. RV= right ventricle. LV= left ventricle. EF= ejection fraction. EDV= end diastolic volume. ESV= end systolic volume. SV= stroke volume. Data from McCall[231].

RVEF was decreased at POD2 and 2-months from pre-operative ($p<0.001$ and $p=0.002$, paired t-tests), Figure 4-6. The mean POD2 drop was 4.84%. There was a clear outlier for RVEF at 2-months (16.9%), sensitivity analysis revealed that there was no difference in the result when this patient was excluded[aa]. RVESV was higher on POD2 ($p=0.003$, paired t-test) and RVEDV was lower than pre-op and POD2 at 2-months ($p>0.017$, paired t-test). RVSV was reduced at 2-months ($p=0.0005$, paired t-test). There was no change in LVEF throughout the study. At 2-months LVEDV, LVESV and LVSV were all lower than pre-operative.

[aa] This patient was an outlier in numerous measures at 2-months post-op in the study. On cardiology follow-up it was deemed that they had suffered a myocardial infarction between POD2 and 2-month follow-up.

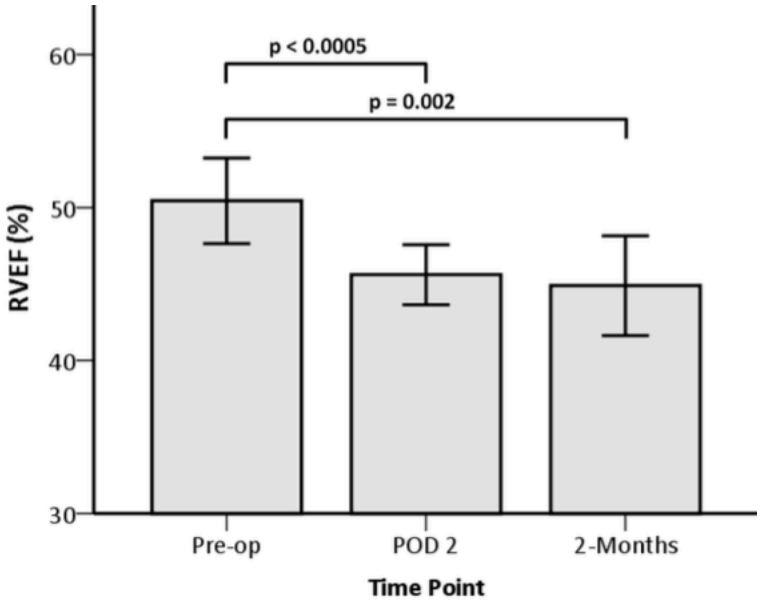

Figure 4-6 Right ventricular ejection fraction following lung resection
Box plots representing median and interquartile ranges of right ventricular ejection fraction. Note reduction at post-operative day 2 (POD2) and 2-months. Image from McCall et al.[231]

Right ventricular coupling was reduced at POD2 and at 2-months, Table 4-8 and Figure 4-7.

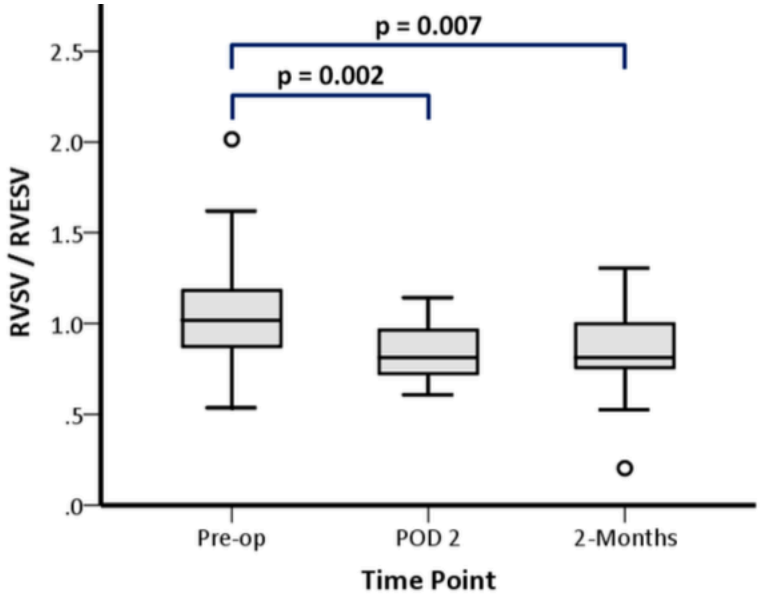

Figure 4-7 Right ventricular coupling following lung resection
Box plots representing median and interquartile ranges of right ventricular (RV) "coupling" calculated by RV stroke volume (RVSV) divided by RV end systolic volume (RVESV). Note deterioration in coupling at post-operative day 2 (POD2) and 2-months. Image from McCall et al.[231]

	Pre-op	POD2	2-months	p value
	n=26	n=22	n=24	
RVSV/RVESV	1.0 (0.9, 1.2)	0.8 (0.7, 1.0) #	0.8 (0.8, 1.0) #	0.011 §

Table 4-8 Right ventricular coupling following lung resection
Right ventricular (RV) coupling calculated by RV stroke volume (RVSV) divided by RV end systolic volume (RVESV). Data are median (IQR). §= Friedman's test. #= Significant difference from Pre-op. POD= post-operative day. Data from McCall et al. [230]

4.5.2.2 Echocardiographic results

In total 77 transthoracic echocardiography scans were completed, 27 patents pre-operatively, 26 patients on POD2 and 24 patients at 2-months. All scans were dual reported by PM and echocardiography technicians (ET).

4.5.2.2.1 Afterload

Pulmonary artery systolic pressure was only obtained by PM and ET in 12 patients pre-operatively (44.5), 14 patients on POD2 (53.8%) and 6 patients at 2-months (25.0%). PAAT was obtained in 26 patients pre-operatively (96.3), 23 patients on POD2 (88.5%) and 23 patients at 2-months (95.8%). There were acceptable limits of agreement and minimal bias between observers. There was a trend to change in SPAP (p=0.074, Friedman's) but no change in PAAT (p=0.350, ANOVA), Table 4-9.

	Pre-op	POD2	2-months	**p value**
SPAP (mmHg)	30.8 (29.2, 39.8) n=12	42.9 (34.9, 54.0) n=10	37.1 (30.8, 46.0) n=5	0.074 §
PAAT (ms)	86.4 (24.9) n=26	72.0 (16.9) n=23	81.0 (22.8) n=23	0.350 *

Table 4-9 Echocardiographic measures of afterload following lung resection
Values are median (IQR) or mean (SD) . §= Friedman's test. *= One-way repeated measures ANOVA. POD= post-operative day. SPAP= systolic pulmonary artery pressure. PAAT= pulmonary artery acceleration time.

4.5.2.2.2 Speckle tracked echocardiography

Strain calculation was available in 27 patients pre-operatively (100% of completed scans), 22 patients on POD2 (84.6%) and 24 patients at 2-months (100%). Inter- and intra-observer variability was excellent (ICC >0.91). There were no changes

in RV-GLPS or FWPLS over time (p>0.229, Friedman's test), Table 4-10. Pooled analysis demonstrated moderate association between RV-GLPS or FWPLS and RVEF (r=-0.412, p=0.001 and r=-0.477, p<0.001, both Pearson's). At each individual time-points there was moderate association between RV-GLPS or FWPLS and RVEF (r>-0.409, p<0.038, all Pearson's), Figure 4-8.

	Pre-op	POD2	2-months	p value
	n=27	n=22	n=24	
RV-GPLS (%)	-17.7 (-20.1, -13.6)	-17.5 (-21.8, -14.1)	-17.8 (-18.8, -12.2)	0.387
RV-FWPLS (%)	-22.1 (-27.2, -16.0)	-20.4 (-26.5, -13.3)	-22.7 (-26.1, -18.6)	0.229

Table 4-10 Speckle tracked strain changes following lung resection
Values are median (IQR). Both Friedman's test. POD= post-operative day. RV-GLPS= right ventricular global peak longitudinal strain. RV-FWPLS= right ventricular free wall peak longitudinal strain.

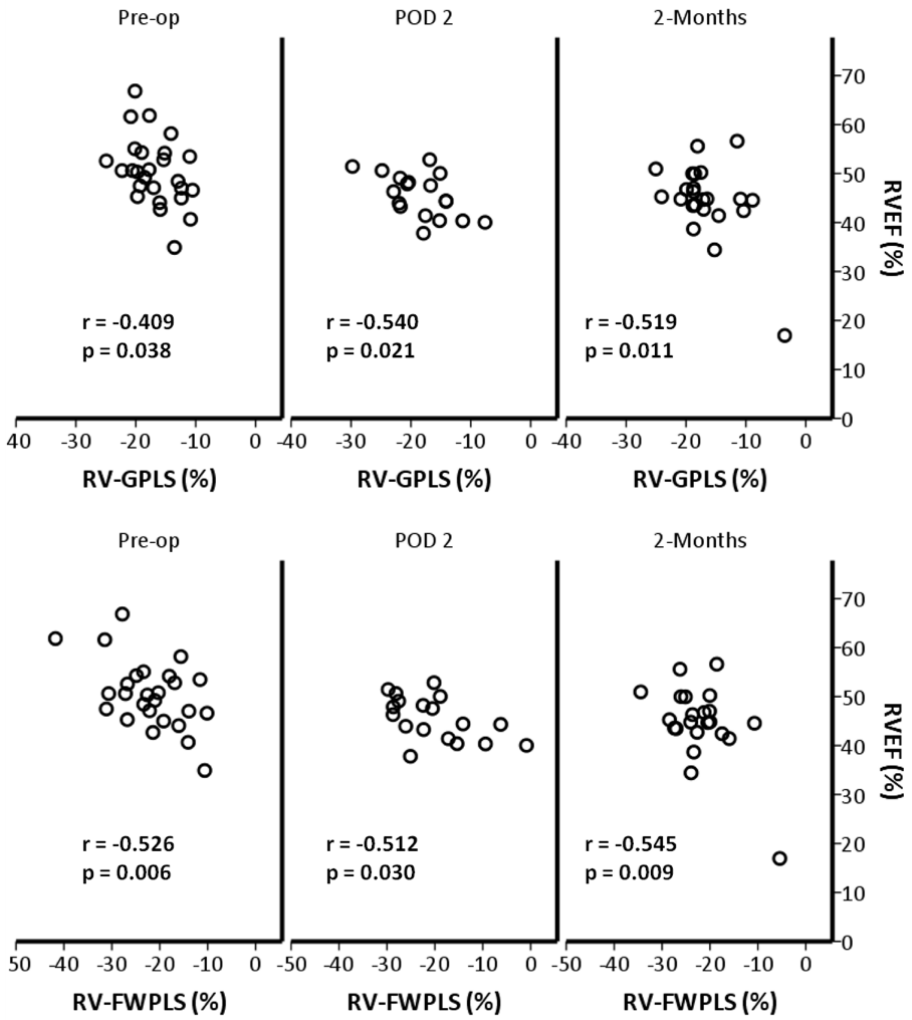

Figure 4-8 Association between right ventricular speckle tracked strain and ejection fraction
Note moderate association between right ventricular global longitudinal peak strain (RV-GLPS) and free wall peak longitudinal strain (RV-FWPLS) with right ventricular ejection fraction (RVEF) measured by cardiac magnetic resonance at all time points. All Pearson's correlation coefficient. Pre-op= pre-operative. POD= post-operative day. Image from McCall [253].

4.5.3 Plasma biomarkers of myocardial dysfunction

Brain natriuretic peptide and hsTnT both changed over the duration of the study, Table 4-11. BNP raised post-operatively and, within the time points tested, peaked at POD2. At this point, increased BNP was associated with the fall in RVEF from pre-op (r=0.490, p=0.021, Spearman's), there were no other significant associations. hsTnT increased post-operatively and peaked at POD1 although it was not associated with any change in RVEF. At 2-months a small, not clinically significant, hsTnT increase remained whilst BNP had returned to baseline.

	Pre-op	Post-op	POD1	POD2	2-months	p-value
BNP (pg/ml)	n =27	n=27	n=27	n=27	n=24	
	28.0 (5.0, 160.0)	32.0 (6.0, 170)	71.0 (5.0, 381.0) #¥	93.0 (5.0, 304.0) #¥	28.5 (5.0, 199.0) § ll	< 0.001
hsTnT (pg/ml)	n=26	n=26	n=26	n=26	n=22	
	6.8 (3.0, 27.2)	6.9 (3.0, 23.2)	12.3 (3.7, 21.9) #¥	9.5 (3, 20.7) #¥	9.0 (3.9, 24.9) #¥	< 0.001

Table 4-11 Plasma biomarkers of myocardial dysfunction following lung resection
Data are presented as median (IQR). Both Friedman's test. BNP= Brain Natriuretic Peptide. hsTnT= Highly sensitive Troponin-T. POD= post-operative day. #= Significant difference from Pre-op. ¥= Significant difference from Immediate Post-op. §= Significant difference from POD1. ll= Significant difference from POD2. Data from McCall et al.[230]

4.6 Discussion

In total, 27 patients were recruited into the study. In spite of the significant extra investigations required to participate in the study patients tolerated the study well with only three patients refusing scanning at POD2 and only one patient refusing at 2-months. All other scans that were not completed were due to medical contraindications. The recruited patients were similar to the overall cohort at GJNH and in published literature; an older population with multiple co-morbidities and the vast majority either current or ex-smokers[16-18, 256]. There were no significant differences between the cohort analysed as part of the "strain group" and the overall group.

The primary outcome of the study was confirmed, RVEF is reduced on POD2 following lung resection. Interestingly this reduction remained at 2-months and occurred without any reduction in LVEF. The mean absolute reduction of RVEF at POD2 of 4.9% is comparable to the 6-9% reduction seen in VPAC studies[49, 58-60].

As discussed in Chapter 1 and 2, the cause of impaired RV function following lung resection is widely hypothesised to be an increase in afterload. The impaired coupling, determined by CMR, on POD2 and 2-months suggest either an increase in afterload, a decrease in contractility or a combination of both. Contractility and afterload were only assessed by TTE in this part of the analysis. Accurate interpretation of the changes in coupling and RVEF requires assessment of RV loading conditions and contractility.

The ability of echocardiography to determine changes in contractility and afterload was poor. It was not possible to obtain the required apical four chamber view required for STE strain in four patients (15.4%) on POD2, a further 22.1% of all scans required "expert review" due to discrepancies between reporters. Although RV-GPLS and RV-FWPLS were consistently associated with RVEF at each time point they were unable to demonstrate the post-operative reduction in RVEF. There was however some evidence of a relationship between RV-FWPLS and RVEF. Trend analysis showed that the change in RV-FWPLS and the change in RVEF had a moderate association on POD2 ($r=-0.317$, $p=0.019$) and a RV-FWPLS of <-18.0% on POD2 was predictive of RVEF <45% (AUROCC= 0.76, [95% CI 0.65, 0.88]).

Systolic pulmonary artery pressure could only be estimated in 32 out of 77 attempted scans although there was a trend to increased SPAP at POD2 ($p=0.09$, Wilcoxon Signed Rank Test). PAAT could be measured in 72 out of 77 scans. It was associated with RVEF in pooled and *within-subject* analysis but it did not change over the study period. There was however a moderate association between the change in PAAT and the change in RVEF from pre-op to POD2 ($r=0.596$, $p=0.009$, Pearson's correlation coefficient) suggesting that afterload increase is associated with RV dysfunction in the early post-operative period.

4.6.1 Strengths and limitations

The main strength of the study is in the design. This is the first sequential use of the gold standard method of assessing the RV (CMR) in a lung resection population. This overcomes the methodological concerns expressed in Chapters 1 and 2. As patients were imaged pre-op, on POD2 and at 2-months the acute post-operative and longer term post-operative function of each patient can be tracked. The post-

operative completion rate of CMR and TTE are encouraging given the labour-intensive investigations required from each patient.

The main limitation of the design of the study is that RV loading conditions are not directly measured. As CMR and echocardiography are non-invasive, direct pressure measurements cannot be performed. Although echocardiography analysis showed some associations of increased afterload and decreased contractility on POD2 with RVEF this interpretation is undermined by the lack of consistency and the lack of a change in contractility or afterload over time. Whilst there were difficulties in obtaining echocardiographic estimation of strain and afterload measures there is a growing evidence base of validated methods of assessing contractility and afterload from CMR. Flow analysis of the pulmonary arteries and RV strain imaging could overcome these issues.

4.7 Conclusion

The main finding of the investigation is that RVEF is decreased following lung resection with a decrease in RV coupling. TTE was unable to detect the reduced RVEF demonstrated by CMR. Although impaired contractility and/or increased afterload are suggested by decreased coupling, TTE did not demonstrate consistent post-operative changes in measures of contractility or afterload. Further investigation of RV loading conditions and contractility are required to explore the mechanisms of the demonstrated RV dysfunction following lung resection.

Chapter 5 Cardiac magnetic resonance strain measurement

5.1 Introduction

This investigation will examine changes in myocardial strain following lung resection. It is the first use of cardiac magnetic resonance (CMR) strain analysis in a lung resection population.

5.2 Right ventricular strain

A general overview of RV function is in provided in Chapter 1. Compared to conventional measures of RV function, strain analysis has a number of potential benefits. It allows regional assessment of the RV[257-260], assessment of diastolic function and ventricular relaxation[257, 259-262], it may detect early RV dysfunction[263, 264] and it is predictive of morbidity and mortality in numerous conditions[265-269]. Analysis of changes in regional RV strain from pre-operatively to the acute post-operative and longer-term follow-up has the potential to help understand the mechanisms of RV dysfunction following lung resection.

5.2.1 Strain definitions

Strain is a measure of myocardial shortening[238]. It is calculated as the difference between length of a defined section of the myocardium after contraction (L) and the initial length (Lo) relative to its initial length (Lagrangian strain)[238], Equation 5-1 and Figure 5-1A.

$$Strain\ (\%) = \frac{(L - Lo)}{Lo} \times\ 100$$

Equation 5-1 Strain calculation
Lo= initial length. L= contracted length.

Strain rate is the rate of myocardial shortening. It can be calculated as the temporal derivative of strain or by the difference in velocity measured at two points divided by the distance between them[270], Equation 5-2 and Figure 5-1B.

$$Strain\ rate\ (s^{-1}) = \frac{V1 - V2}{d} = \frac{\partial(Strain)}{\partial t}$$

Equation 5-2 Strain rate calculation
V_1= velocity at point 1. V_2= velocity at point 2. d= distance between points. ∂(Strain)= derivative of strain. ∂t= temporal derivative.

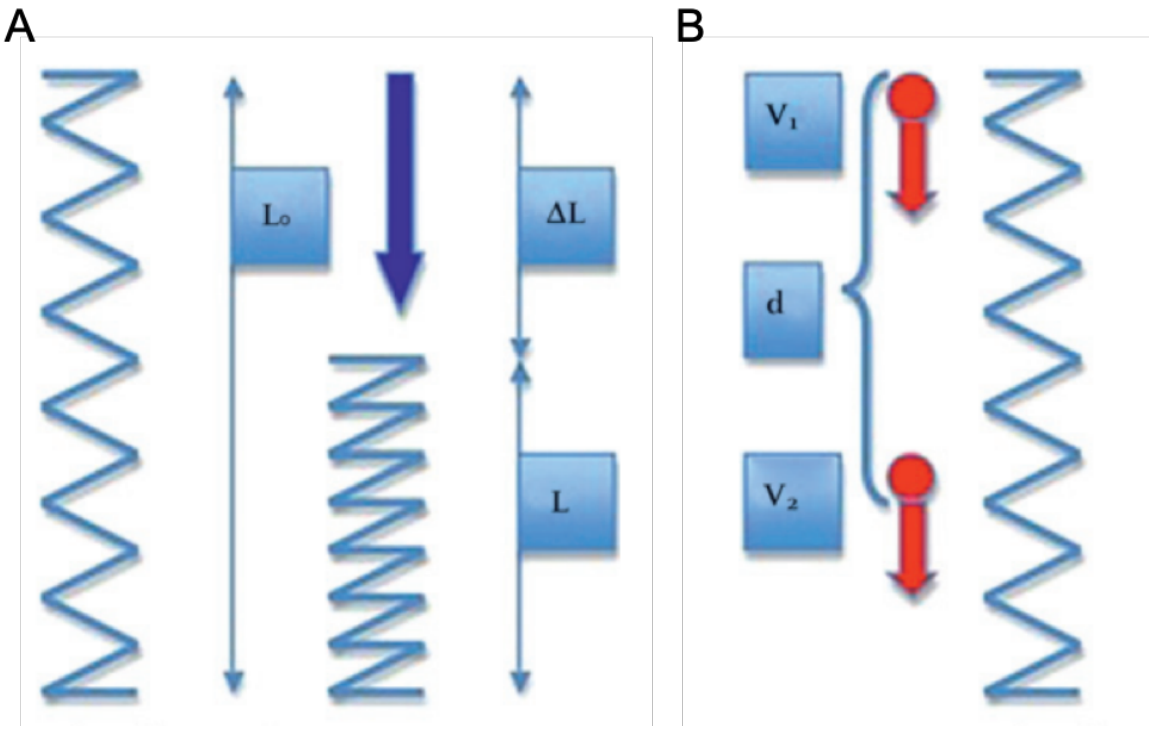

Figure 5-1 Strain and strain rate derivation
A, Strain derived by difference in length (ΔL) divided by initial length (Lo).
B, Strain rate is the difference in relative velocity at two points (V_1 and V_2) divided by the distance (d) between them. Images from Blessberger and Binder[270].

The distinction between displacement and deformation is important in the understanding and calculation of strain. Displacement is the change in position of an object, whereas deformation is the change in shape of an object due to regional differences in velocities. Displacement of the RV may occur without contraction and therefore without deformation, i.e. passive movement of an akinetic RV secondary to contraction of the LV. Deformation (measured by strain) will measure the relative movement of a specific region of the ventricle[257]. Strain therefore is able to differentiate between active and passive movement of the RV and determine regional variations in the extent and rate of deformation[238, 257].

Maximal RV volume and therefore maximal RV myocyte length occurs at end-diastole, this is the initial length for strain calculation. Contraction causes shortening of the RV and therefore a negative strain value, Figure 5-2. Peak systolic strain occurs at maximal shortening of the RV. Strain rate is negative

during shortening of the RV (contraction/emptying) but positive during lengthening (relaxation/filling). During diastole there are two strain rate peaks; the early (E) diastolic peak is caused by passive relaxation and filling of the RV and the late diastolic peak is caused by atrial contraction (A) leading to RV filling[261].

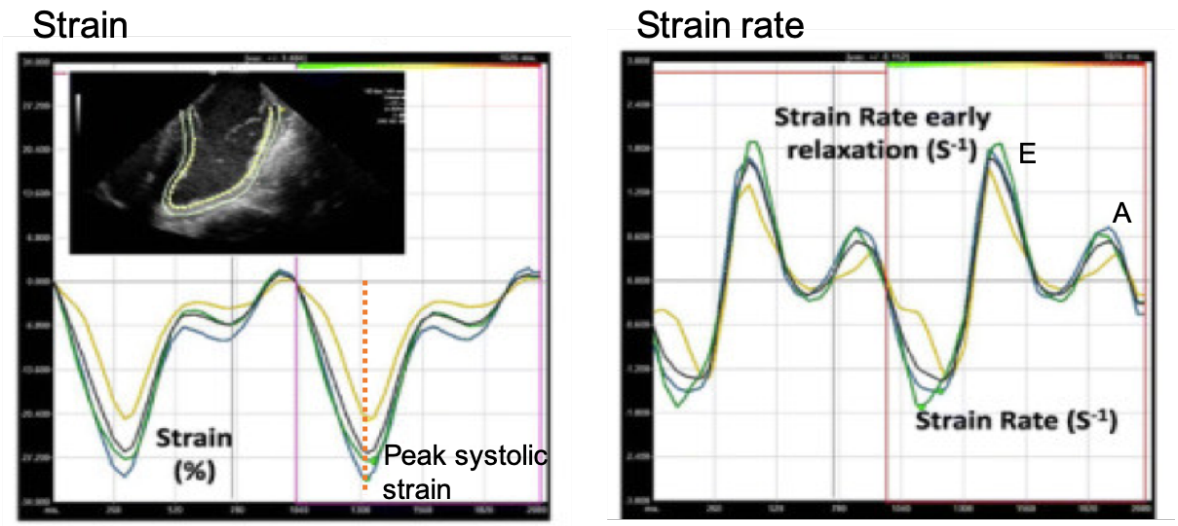

Figure 5-2 Right ventricular strain and strain rate curves
Right ventricular (RV) longitudinal free wall strain (left panel) and strain rate (right panel) over two cardiac cycles. Note strain rate is temporal derivative of strain, i.e. at turning points of strain, strain rate is 0. Strain is always negative and strain rate is negative until peak contraction then it is positive during relaxation of the RV. Peak systolic strain highlighted by dashed red line in left panel. Diastolic strain rate peaks highlighted in right panel, early (E) diastolic and atrial (A) peaks. Images from Orde et al.[262].

5.2.2 Strain classifications

The majority of research into myocardial strain has focused on LV strain. The LV contracts in 3 planes (longitudinal, circumferential and radial)[270], Figure 5-3. In contrast to the LV, RV muscle fibres are predominately arranged in superficial and deep muscle layers that will cause longitudinal and circumferential contraction without significant radial contraction[271], it is estimated that 80% of RV contraction occurs in the longitudinal plane[272, 273].

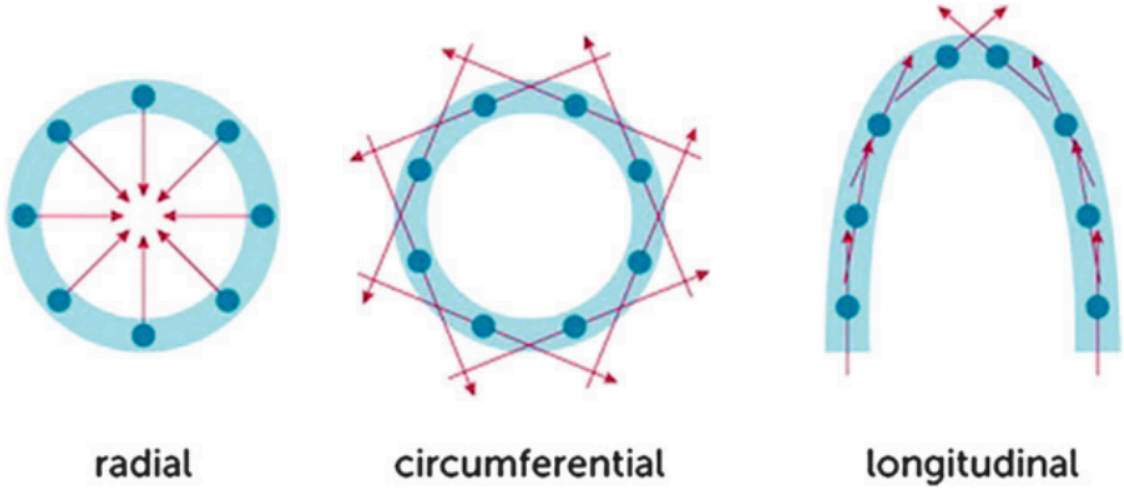

Figure 5-3 Diagrammatic representation of left ventricular strain analysis
Strain can be measured in three vectors; radial, circumferential and longitudinal. Image from Blessberger and Binder[270].

Regional division of the RV is demonstrated in Figure 5-4. RV strain measures global longitudinal strain (RVGLS) in a long axis view along the free wall (RVGLS.FW) and septum (RVGLS.S), this can further be divided into apical, mid-ventricular and basal segments[bb]. RV global circumferential strain (RVGCS) can be measured in a short axis view at basal, mid-ventricular and apical[274]. The majority of studies that perform RV strain measure RVGLS and, to a lesser extent, RVGCS[160, 224]. Whist global radial strain (GRS) measurement is utilised in LV assessment it is not commonly measured in the RV due to its limited contribution to RV function and difficulty in measurement in the thin-walled RV[271, 275].

[bb] The notation RVGLS.FW and RVGLS.S are used as per Lee et al.[271]. This is primarily used for the CMR results presented below as, for example, RVGLS.FW are free wall segments of the original RVGLS imaging and not a separate analysis of isolated RV free wall strain.

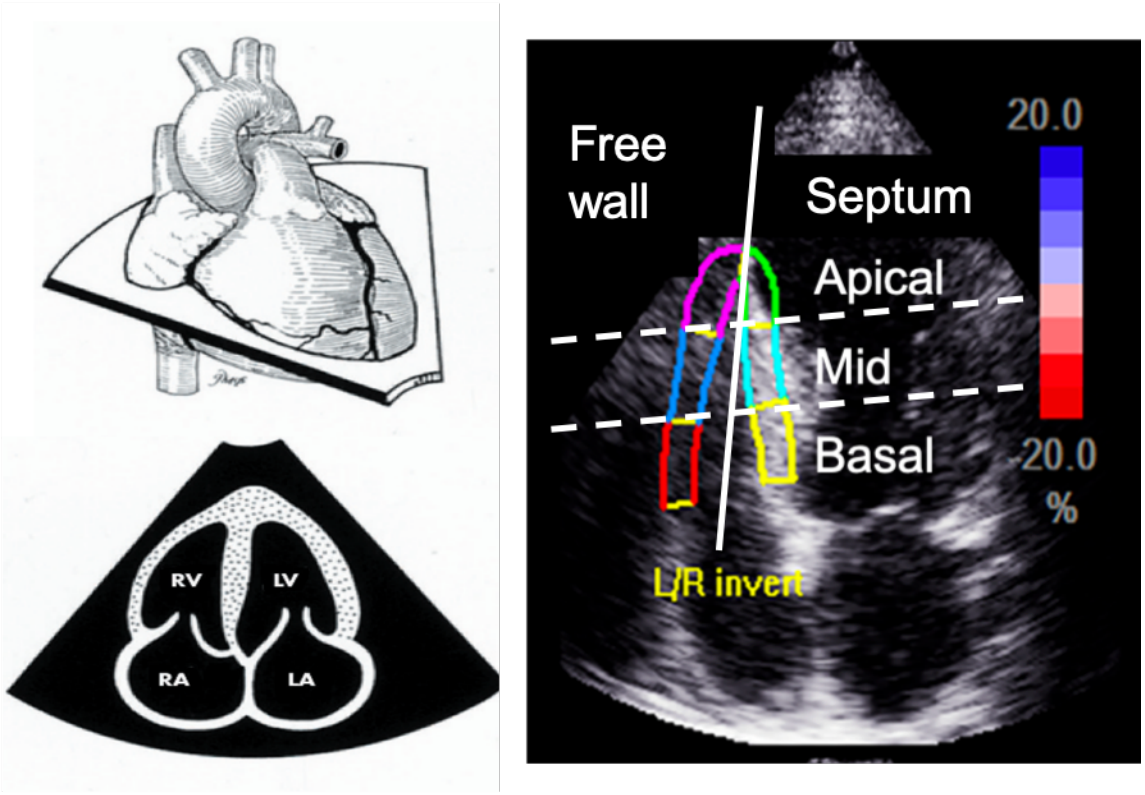

Figure 5-4 Long axis view of right ventricular regional strain
Left panel demonstrates the echocardiographic plane and image of an apical four-chamber view of the heart with right (R) and left (L) ventricles (V) and atria (A) all visible. Right panel depicts the regional definitions of RV strain from a corresponding echocardiographic image. Solid white line divides long axis into free wall and septum. Dashed white line, division of the RV into basal mid and apical regions. Images annotated from Ho et al.[85] and Chang et al.[274].

5.2.3 Strain interpretation

5.2.3.1 Load dependence

Strain and strain rate have been described as "load-independent" measures of RV function, i.e. they are not dependent on preload and/or afterload[276]. In a 2010 review of RV strain, La Gerche et al. detail the changes in myocyte contraction with increased afterload, demonstrating that they are in fact load dependent[277], Figure 5-5. As detailed in 1.2.2.4 page 44, myocyte function can be described by the force generated, the degree of shortening (strain) and the velocity of myocardial fibre shortening (strain rate). Each strain parameter is affected by the loading conditions of the myocyte. Increased afterload will require a greater force (and pressure) to generate the forward flow of blood, there will also be a reduction in the shortening of the myocyte (strain) and the velocity at which this occurs (strain rate). Increased preload (starting length of myocyte) will result in increased shortening (strain) to reach minimum fibre length[277].

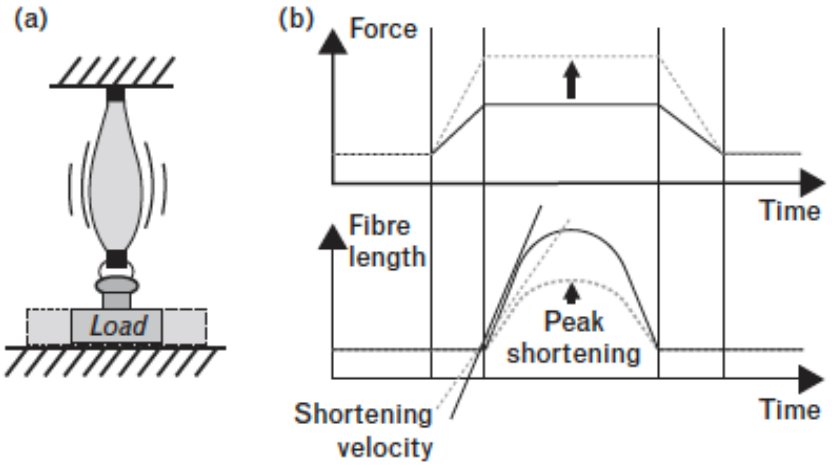

Figure 5-5 Change in myocyte contraction with loading
Myocyte contraction against a given load (a) will determine the force generated (b, top plot), the degree of shortening and the velocity of myocyte shortening (b, bottom plot). When loading (afterload) is increased (dashed line) a greater force (pressure) is required and there is a reduction in the degree (strain) and the velocity (strain rate) of myocardial shortening. Image from la Gerche et al.[277]

Further experimental data supports the argument that strain analysis is load dependent. In sheep, Missant et al. demonstrated that strain rate increases with contractility in states of increased inotropy, however in the setting of increased afterload, strain rate inappropriately decreased when contractility was unchanged[278]. Jamal et al. similarly demonstrated with sonomicrometry strain analysis that strain rate was less sensitive at detecting changes in contractility during altered loading conditions[144]. In patients with atrial septal defects (increased preload due to left to right shunt) Jategaonkar et al. demonstrated that RVGLS decreased with closure of the defect, i.e., the value of RVGLS was influenced by change in preload without any change in RV contractility[142]. Human and animal studies have consistently shown that strain is related to PA pressure and therefore loading[279-282].

5.2.3.2 Diastolic strain assessment

Over recent years there has been growing interest in the utility of strain analysis to evaluate diastolic relaxation of the RV[cc]. Hachulla et al. investigated the pattern of diastolic RV strain rate during passive RV filling (E) and filling secondary to atrial contraction (A), analogous to the echocardiographic labels given to Doppler assessment of flow across the atrioventricular valves[284]. They

[cc] Assessment of RV diastolic strain has been performed by Dr Emma Murphy[283] based on the work presented in this chapter.

demonstrated that in pulmonary hypertension there is a reduction in early diastolic strain rate, (E) with a secondary increase in late diastolic strain rate caused by atrial contraction (A), Figure 5-6. The authors theorised that this is a sign of RV hypertrophy with impaired lusitropy, therefore it has reduced passive early diastolic filling (E) and is more reliant on atrial filling (A)[261].

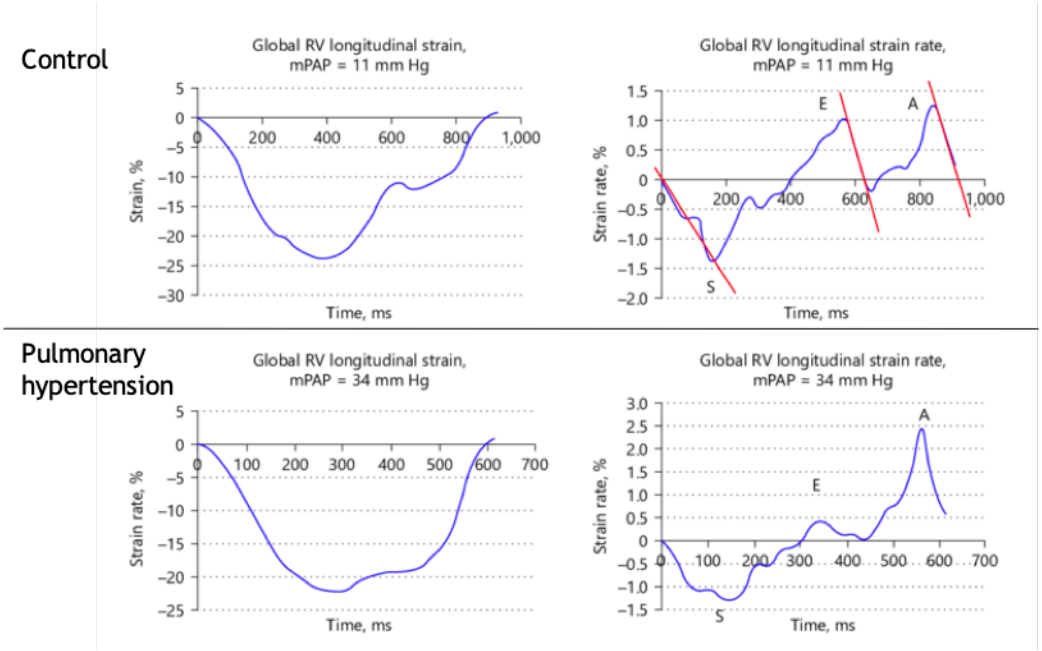

Figure 5-6 Right ventricular diastolic strain and strain rate
Strain and strain rate in control (top row) and a patient with pulmonary hypertension (bottom row). Note reduction in right ventricular (RV) early diastolic strain rate (E) with increased main pulmonary artery pressure (MPAP), red lines in top right highlight the systolic and diastolic strain rates. In pulmonary hypertension the RV is more dependent on atrial filling (A). Image from Hachulla et al.[261].

5.2.4 Modalities of strain measurement

The main methods of strain analysis are by echocardiography and CMR imaging, although it can also be assessed with computed tomography[dd 270, 285, 286]. Within echocardiography and CMR there are differing methods of strain analysis, the main distinction between methods is if it requires additional images/techniques during the scans or if it can be performed post-processing with the routinely collected images. The advantages and disadvantages of each method will be discussed below. As with the majority of RV literature, the techniques discussed were first

[dd] The discussion of RV strain will focus on echocardiographic and CMR measurement of strain. The previous evidence in lung resection is exclusively of echocardiographic strain and this chapter describes the first analysis of RV strain with CMR in a lung resection cohort.

devised, performed and validated on the LV although there is growing interest in the assessment of RV strain[287].

5.2.4.1 Echocardiographic strain measurement

Introduced in 1997, tissue Doppler imaging (TDI) was the first echocardiographic method of calculating strain[288]. TDI relies on real time Doppler imaging along the ventricular wall to assess the velocity of the myocardium. It can only assess the velocity towards or away from the transducer[252], Figure 5-7. This results in angle dependency, i.e. as the angle between the true vector of contraction and the ultrasound beam increases the angular error of strain measured also increases[251]. The technique has been validated against direct sonomicrometry strain assessment in animal models (r=0.92)[289] and CMR strain analysis (r>0.89)[290] and its use is well established in clinical practice[291].

Strain calculation can be performed from the velocity measurement. Whilst TDI measures the velocity of the myocardium relative to the stationary transducer, the velocity of myocardium can be calculated relative to adjacent myocardium and therefore strain rate can be determined. This can then be integrated to calculate strain[292]. This technique can lead to error with excessive signal noise[252, 292].

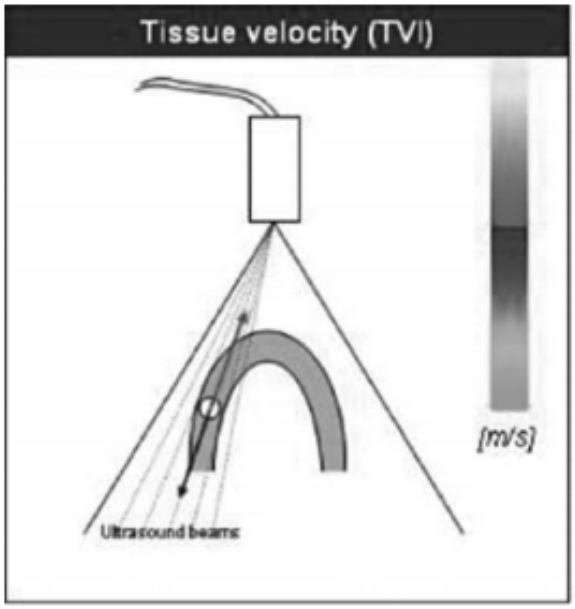

Figure 5-7 Echocardiographic strain assessment
Tissue velocity (Doppler) imaging (TVI). Velocity of myocardium measured in parallel to the ultrasound beam. Movement only measured in one dimension. Image from Sareen et al.[252].

Speckle tracked echocardiography (STE) was introduced in 2004 by Reisner et al.[239] and Leitman et al.[293]. This technique utilises artefacts within the echo image created by reflection, refraction and scattering of the ultrasound beams. These "speckles" will move relative to each other through the cardiac cycle and thus allow the calculation of the change in distance between these points throughout the cardiac cycle, i.e. two-dimensional Langrangian strain (2D-STE)[270], Figure 5-8. Interpretation requires tracking of the myocardium to define regions of interest (ROI), this can be performed post-processing on appropriate echocardiography images. Three-dimensional STE (3D-STE) can be performed on 3D echocardiographic images and is increasingly performed in research studies to assess the RV. It has been shown to provide accurate and reproducible assessment of RV volume, RVEF and strain[294, 295].

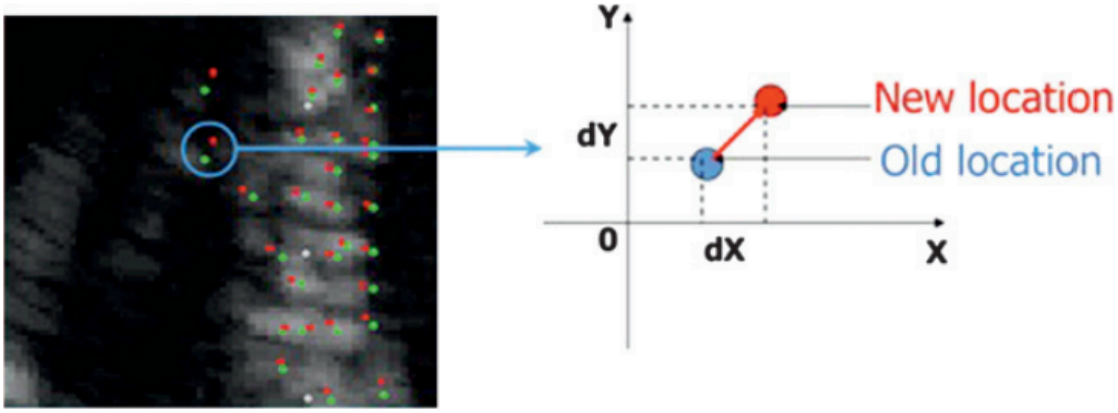

Figure 5-8 Speckle tracked echocardiography
Green dots represent initial position of speckle, red dots final position. Tracking of individual speckles allow measurement of deformation of the ventricle in two dimensions. Image from Blessberger and Binder [270].

In comparison to TDI, STE has potential advantages. It is angle independent, less sensitive to noise, has better reproducibility and can be performed post-processing, thus reducing scan duration. Additional, as demonstrated in Figure 5-7 and Figure 5-8, STE measures strain in two-dimensions whereas TDI measures strain in only one dimension (towards or away from transducer). TDI has greater temporal resolution (greater ability to detect short lived cardiac events and increased accuracy of temporal parameters) whereas STE has greater spatial resolution (greater ability to distinguish between two adjacent points in the myocardium)[252].

5.2.4.2 Cardiac magnetic resonance strain measurement

Cardiac magnetic resonance strain measurement can be performed with tissue tagging (CMR-Tag) or post-processing feature tracking (CMR-FT)[286].

The first description of CMR-Tag, 1988, predates echocardiographic TDI strain analysis[296]. Through pulsation of selective radiofrequency saturation planes a magnetised grid is imprinted onto the myocardium at the onset of systole, Figure 5-9D. As the heart contracts the grid is deformed thus allowing deformation calculation. The tags fade throughout the cardiac cycle resulting in poor assessment of regional relaxation and diastolic function[286, 297]. Additionally, the tagging at the onset of systole results in a temporal delay in strain assessment potentially underestimating strain, especially at higher heart rates as the true end-diastolic length is not imaged. Whilst CMR tagging is the most widely validated method of strain assessment, it remains predominately a research tool due to the additional time taken for imaging, specialist software required for analysis and numerous variations of the tissue tagging process[297]. CMR-Tag is more established in the thicker LV although authors have performed it in the RV where the thin RV wall further increases the technical difficulties[298].

Feature tracking software can be applied to standard cine sequences of the heart to calculate myocardial deformation post-processing, Figure 5-9C. The advantage of this technique is that it can be performed without dedicated additional imaging. As CMR images of the myocardium are relatively homogenous, CMR-FT is unable to determine strain by detection of intramyocardial features (as performed in speckle tracking). Strain calculation is instead performed by a “block matching” approach, i.e. it tracks anatomical features on regions of the myocardial boundaries[297].

5.2.4.3 Comparison between modalities of strain measurement

There are common causes of variations in strain measurement between modalities (inter-modality) and within modalities (intra-modality).

The images generated by echocardiography and CMR differ in terms of spatial and temporal resolution, Figure 5-9. High spatial and temporal resolution are required to ensure accurate strain analysis. Low spatial resolution will require

tracking of a larger area of the myocardium thus limiting the analysis of subsegments of the ventricular wall[297, 299]. Low temporal resolution can underestimate strain and prevent detection of short-lived events such as isovolumetric contraction (especially in the RV)[297, 299]. Speckle tracked echocardiography has excellent spatial resolution (2D-STE 0.2-0.3mm and 3D - STE 0.4-0.5mm) although it has low temporal resolution (2D-STE 40-60 frame.s^{-1} and 3D-STE 20-50 frame.s^{-1}) whereas TDI determined strain has excellent temporal resolution (>100 frame.s^{-1}) although this results in a lower spatial resolution than STE[257, 292, 297]. Comparatively, CMR techniques (tagging and FT) have lower spatial resolution (1-2mm) and temporal resolution (20-30 frames per heartbeat for tagging techniques and 25-35 frames per heartbeat for feature tracking)[297].

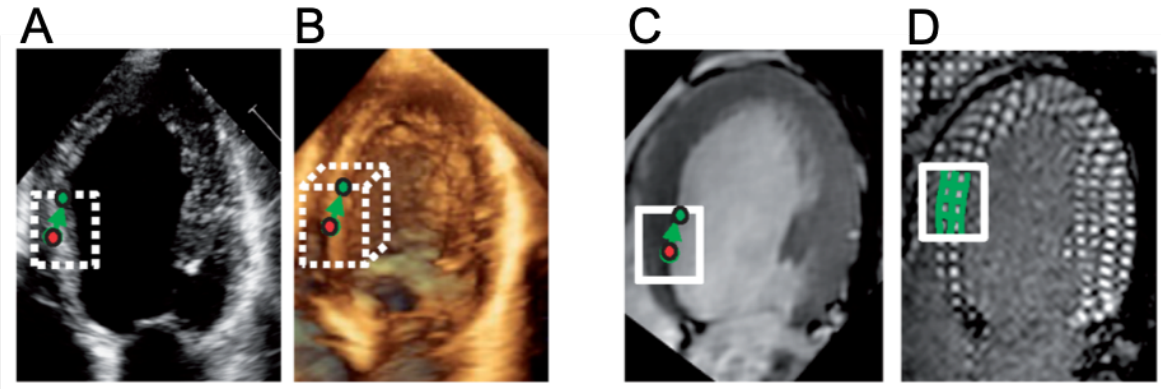

Figure 5-9 Modalities of tissue tracking strain analysis
Tissue tracking in two-dimensional echocardiography (A), three-dimensional echocardiography (B), feature tracking cardiac magnetic resonance (C) and tissue tagging cardiac magnetic resonance (D). Images from Amzulescu et al. [297].

The acquisition of the images will also affect the strain analysis. Echocardiography relies on acoustic windows and probe positioning to obtain true long and short axis images of the RV. 2D imaging planes that are not correctly orientated can result in foreshortening and the ROI determined at end-diastole may move out of the plane during systole[297]. This may be especially challenging for the imaging of the RV following lung resection[85, 156]. The mapping process of CMR should limit this variation, although this depends on the position of the heart remaining constant in the chest and therefore depends on the patient's ability to perform breath holds, again potentially limiting its utility following lung resection[300].

Speckle tracking echocardiography software requires smoothing of the temporal and spatial data collected to reduce noise. This can lead to loss of short-lived

events and localised motion abnormalities[301]. Differing smoothing parameters of localised areas of myocardium can result in variation between segments causing the reliability of regional strain to be lower than global strain[297].

The experience of the operator will also influence results. Manual tracing of the myocardium and determination of the level of the heart can result in marked differences between observers[297, 302]. Although both have excellent reliability, STE has better intra- and inter-observer variability than CMR-FT for LVGLS (intra-observer 0.94 vs 0.89 and inter-observer 0.91 vs 0.86)[303]. Automated detection of the myocardium, in STE, has been shown to have lower inter-observer variability although the majority of packages still rely on manual tracing[304].

Strain values are not directly comparable between differing modalities due to the subtle differences in how it is calculated[297, 305]. As demonstrated in Figure 5-10, there is marked variation in the value for LVGLS in healthy subjects between modalities[297].

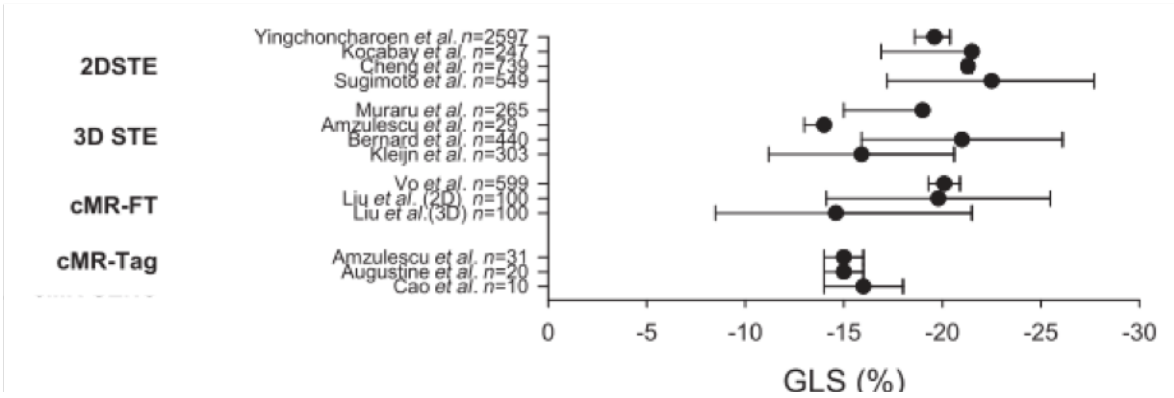

Figure 5-10 Reported normal left ventricular global longitudinal strain values
Mean and 95% confidence intervals for left ventricular global longitudinal strain (GLS) in healthy subjects. Note variation in mean value dependent on modality and low numbers in cardiac magnetic resonance tagging techniques (cMR-Tag) compared to two- and three- dimensional (2D and 3D) speckle tracking echocardiography (STE). cMR -FT, feature tracking cMR. Image from Amzulescu et al.[297]

Taha et al. performed the first direct comparison of STE and CMR-FT strain analysis in the RV[306]. They imaged 110 subjects; 34 with arrhythmogenic RV cardiomyopathy (ARVC, a condition of progressive loss of cardiac myocytes), 30 relatives (at-risk of ARVC or pre-clinical ARVC) and 46 controls. CMR-FT was successfully performed in 99% of RV segments versus 95% in STE. Whilst STE and CMR-FT were both able to detect reduced RVGLS in the ARVC patients, CMR-FT strain values were consistently greater than STE and there was “suboptimal” inter-

modality agreement. RVGLS had strong correlation (r=0.578) between STE and CMR-FT, whilst the agreement was poor in the apical region (r=-0.261), discussed later in 5.2.6.2.

5.2.5 Strain measurement in the right ventricle

As detailed above, each method of strain analysis has its advantages and disadvantages. The modalities were predominately developed, validated and subsequently compared in analysis of LV strain, there are additional challenges of assessment of RV strain, particularly in a lung resection population. CMR strain had not been performed in this population prior to this investigation. The work by McCall et highlight the difficulty in echocardiographic assessment following lung resection[156, 233].

5.2.5.1 Reliability of strain assessment in the right ventricle

Mirea et al. demonstrated, in 200 patients, that the reproducibility of 2D-STE measurement of RV strain is comparable to LV strain measurement. Intra- and inter-observer variabilities were excellent/good for RVGLS (ICC= 0.90 and 0.83 respectively) and moderate/good for RVGLS.FW of basal, mid-ventricular and apical subsegments (ICC 0.61 – 0.81). The images were interpreted for intra-observer variability by a single experienced observer with >2000 prior analyses and for inter-observer variability by a second observer of “average” experience, 100 analyses prior to study[307]. Chamberlain et al. have demonstrated a marked improvement in intra-observer variability with experience in 2D-STE, eventually reaching a plateau after 100 patients[302], Figure 5-11. In order to achieve their sample size of 200, Mirea et al. scanned 221 patients with 21 patients (9.5%) patients excluded due to poor image quality[307]. Whilst reliability of image *interpretation* is excellent, the issues of image *acquisition* quality may limit the utility of 2D-STE in a research setting, particularly in a lung resection study.

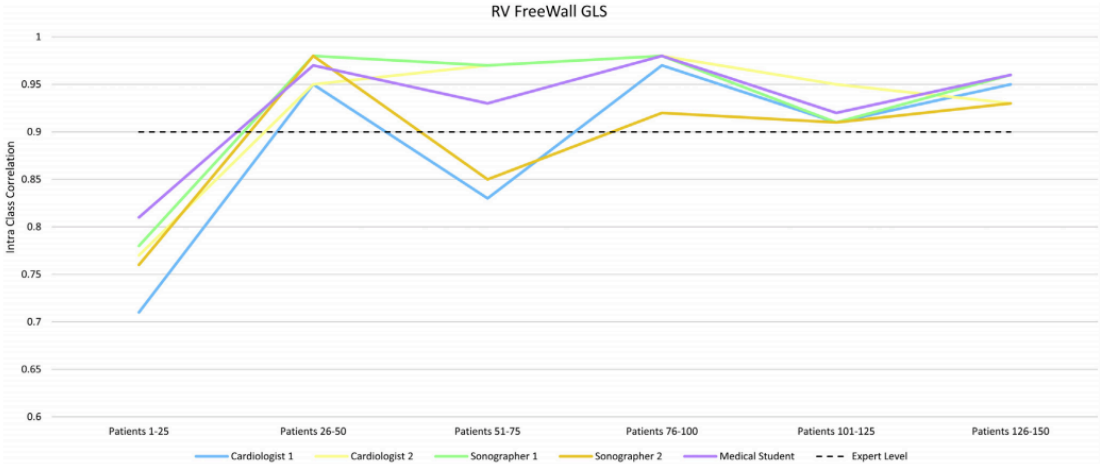

Figure 5-11 Right ventricular speckle tracked echocardiography learning curve
Right ventricular (RV) free wall global longitudinal strain (GLS) intra-class co-efficient (ICC) against groups of 25 scans reported. Note the rapid improvement in Intra-class coefficient after reporting of first 25 scans and plateau after 100 scans. Dashed horizontal line represents an ICC of >0.9 required for "expert level of competency". Image from Chamberlain et al.[302].

Cardiac magnetic resonance RVGLS is susceptible to inaccuracies in tracking and may also have a learning curve similar to STE[300]. Liu et al. performed an informative CMR-FT analysis of RV strain in 100 healthy individuals, 10 females and 10 males from each decade of life from 20-70 years who were in "optimal health". Intra- and inter-observer variability showed excellent/good reliability for RVGLS (ICC 0.92 and 0.80)[259].

5.2.5.2 Regional strain patterns

There are normal regional variations in strain; in healthy patients, RVGLS.FW is greater than RVGLS.S[259] although all regions contract together with the time to peak strain similar between all regions[264]. RVGLS (RVGLS.FW and RVGLS.S combined) and RVGLS.FW are both commonly reported in literature. RVGLS.S is influenced by LV function due to the shared interventricular septum. Impaired RVGLS.S may purely be secondary to LV dysfunction, however, this will still influence RV function[271, 308].

As detailed below, the regional response of the RV to increased afterload is dependent on the nature of the insult. Region specific reduction in strain has been shown to be diagnostic and predictive of mortality; reduced RVGLS.FW is predictive of mortality in sepsis[309], heart failure[310, 311], PE[265-268] and pulmonary hypertension[145, 269, 312, 313]. Regional impairment in RV strain also lead to RV dyssynchrony with a delay in time to peak strain between the RV regions[264]; in

PAH, RV dyssynchrony is increased in RV dysfunction[160, 314] and is predictive of reduced exercise capacity[315].

5.2.6 Right ventricular strain in disease

In a review of RV strain, La Gerche et al. detail the potential changes in strain related to changes in afterload and myocardial function [277]. In response to changes in RV afterload and/or contractility RV deformation (measured by strain) may be normal or reduced;

- normal deformation
  - normal afterload and contractility
  - or
  - *increased* afterload with *increased* contractility
- reduced deformation
  - *increased* afterload with normal/reduced contractility
  - or
  - normal afterload and *reduced* contractility

Reduced deformation (less negative strain) may therefore occur if RV contractility is reduced or if RV contractility does not increase to compensate for an increase in afterload. Differentiation between the groups may be based on the degree of impairment in strain[316], the response of the RV to exercise[317] (RV contractile reserve, discussed in 1.2.6.1 page 70) or evidence of myocardial injury[133, 135].

As discussed in 1.2.3 page 50, the RV has subtly different responses to acute and chronic increases in afterload. The global measure of RVEF is unable to determine the regions that contribute to any deterioration. Although there is significant overlap in the regions affected by acute and chronic insults, it may be possible to demonstrate a temporal difference between RV regions and insults. With an understanding of the temporal and regional responses to chronic pressure overload (PAH) and acute pressure overload (PE) it may be possible to determine whether the mechanism of RV dysfunction following lung resection results from an acute intra-operative insult, chronic increase in afterload or both.

5.2.6.1 Right ventricular strain in pulmonary hypertension

One of the largest studies investigating RVGLS in pulmonary hypertension (PH) is the work of Fine et al.[269]. RVGLS.FW was measured with 2D-STE in 575 patients referred for investigation of known or suspected PH along with extensive echocardiographic, clinical, functional and biochemical testing. The PH group (406 patients) had impaired (less negative) RVGLS.FW than the non-PH group, (−19.6±6.6% vs −25.0±5.2%), Figure 5-12 A. The greatest difference was in basal and mid free wall segments, there was no assessment of septal strain. Dividing the PAH patients into quartiles based on RVGLS.FW showed a progressive deterioration in all measured echocardiographic, functional and biochemical parameters in each quartile ($p<0.04$ for all). Patients were followed up until 18 months post-investigations and RVGLS.FW of >-15%[ee] had a sensitivity of 89% for predicting cardiopulmonary death[269], Figure 5-12B.

[ee] Cut-off values are only generalisable if the method of strain analysis is the same, i.e. the value of >-15% is applicable to RVGLS measured by 2D-STE with the software used in that study.

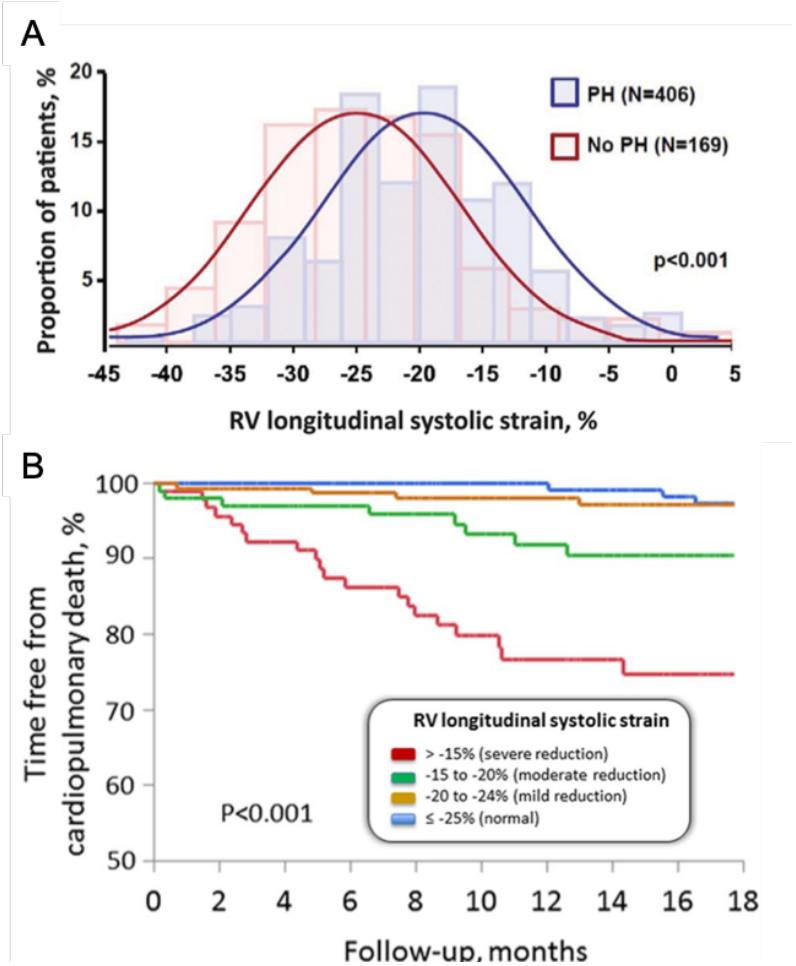

Figure 5-12 Right ventricular free wall strain in pulmonary hypertension
A. Right ventricular (RV) longitudinal strain (speckle tracking echocardiographic) distribution in patients with and without pulmonary hypertension (PH). Note significant overlap between populations.
B. Reduced strain predictive of all-cause mortality (406 patients). Note progressive increase in cardiopulmonary death with progressive reduction in strain. Images from Fine et al.[269].

Hardegree et al. investigated the effect of initiation of medical therapies (treatment determined by routine clinician preference) on RVGLS in patients with PAH. Prior to commencing medical therapy, 80 patients underwent 2D-STE with 50 patients undergoing repeat imaging 6 months following treatment with survival follow-up for 4 years. The remaining 30 patients were excluded due to no further imaging (12 patients), death prior to follow-up (10 patients) and inadequate imaging for strain analysis (8 patients, 10%). Therapeutic interventions did not reduce PAP or PVR, but RVGLS improved from -15±5% to -20±7% (p=0.0001). Failure to improve RVGLS by >5% (22/50 patients) and a follow-up RVGLS.FW of >-12.5% were both predictive of increased mortality[313].

In a combined conductance catheter and CMR strain study, Tello et al. confirmed that, RVGLS reduction is associated with RV-PA uncoupling in PAH. In chronic

pressure overload the initial adaptive increase in contractility with increased afterload/preload (maintaining coupling) becomes exhausted. Ultimately the RV uncouples with RV strain markedly reduced[282].

5.2.6.2 Right ventricular strain in pulmonary embolism

Regional reduction in RVGLS has also been demonstrated in patients with PE by Platz et al.[258], Figure 5-13. All echocardiography was performed within 72 hours of diagnosis of PE; when comparing patients with PE to healthy controls, the greatest reduction in RVGLS was seen in the basal and mid ventricular regions of the RV free wall with lesser reduction in the free wall apex, mid septum and basal septum. This pattern is similar to the free wall findings of Fine et al.[269]. Platz et al. also demonstrated a weak association between brain natriuretic peptide (BNP) and RVGLS ($r=0.39$, $p<0.05$)[258].

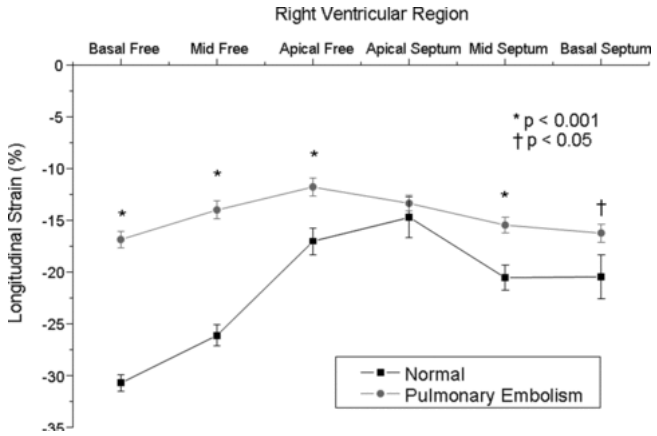

Figure 5-13 Regional right ventricular longitudinal strain in pulmonary embolism vs control
Regional right ventricular global longitudinal strain is reduced in patients with pulmonary embolism (n=75) compared to controls (n=30). Note greatest reduction is in the free wall. Image from Platz et al.[258].

Comparison of strain analysis with the classical echocardiography sign of PE (McConnell's sign, McCS) highlights the utility of regional strain analysis in distinguishing between displacement and deformation. The original description of McCS is an echocardiographic picture of *"akinesia of the mid-free wall ... but normal motion at the apex"*[318]. In Platz et al.s' study in patients with PE; comparison of patients *with* McCS (36/72 patients, 50%) to those *without* McCS demonstrated no difference in RVGLS.FW in the basal or mid segments, but a reduction in RVGLS.FW at the apex in those with McCS[258]. Similarly, Mediratta et al. investigated RV strain by STE in patients with McCS[319], they also demonstrated reduced apical strain in patients with McCS. This seemingly paradoxical reduced

strain but apparent normal motion of the apical RV free wall may be caused by the apical attachment of the RV to a hyperdynamic LV. Strain analysis reveals that the apparently “normal motion” of the RV free wall apex in McCS is actually passive, i.e. it is displacement not deformation.

Echocardiography within 72 hours of PE diagnosis has consistently demonstrated that acute reduction in RVGLS.FW is predictive of morbidiy and mortality[265-268]. Vitarelli et al. investigated wether there is resolution of RV dysfunction following PE. In 66 patients with confirmed PE, they repeated echocardiography at 30 days and 6 months following initial diagnosis and imaging. They showed that the acute reduction in RVGLS.FW seen following PE is transient and recovers by 30 days post-event, whilst RVEF and RV systolic pressure (RVSP) only partially recover by 6 months, Figure 5-14. The authors state that the acute pressure overload distorts the RV free wall reducing RVGLS.FW and that a rapid reduction of this pressure overload, by treatment of the PE, rapidly resolves this distortion and therefore resolves RVGLS.FW. The delayed and incomplete recovery in RVEF is secondary to the persistent increase in RVSP and PVR[320].

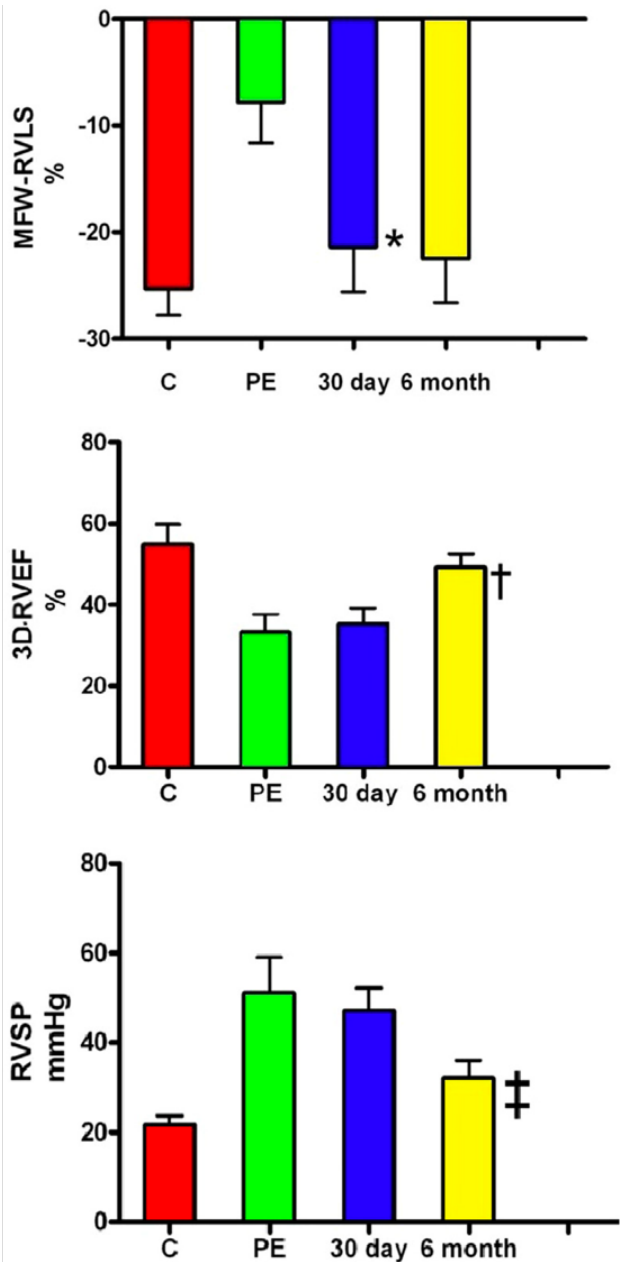

Figure 5-14 Resolution of right ventricular function following pulmonary embolism
Mid free wall right ventricular longitudinal strain (MFW-RVLS) (top pane), right ventricular ejection fraction (3D-RVEF) (middle pane) and right ventricular systolic pressure (RVSP) (bottom pane) following pulmonary embolism (PE) over time and against controls (C). Note RVLS and RVEF are acutely reduced against controls following PE, RVLS recovers by 30 days whilst RVEF remains reduced until 6 months. *= $p<0.001$ vs PE. † and ‡= $p<0.005$ vs PE. Image from Vitarelli et al.[320].

As discussed in 1.2.3.4 page 55, a rat model of PE reveals a similar pattern of RV damage as above. Watts et al. introduced microspheres into the pulmonary circulations of rats to simulate a PE. They demonstrated an inflammatory response within the RV free wall without any RV apical or LV changes. Longitudinal strips of the RV free wall were isolated and paced showing a reduction in contractile force, at 24 hours and at 6 weeks following PE, compared to rats that did not received the microspheres. Histological examination revealed an acute post-operative neutrophil and macrophage infiltration of the RV free wall, which results

in collagen deposition and scarring by 6 weeks[ff]. This process may contribute to prolonged reduction in RV free wall contractility[134, 135, 321].

5.2.6.3 Summary of right ventricular strain in disease

It is established that reduced RVGLS occurs with increased afterload. This predominately affects the RV free wall in both acute increases[258, 265-268] (PE) and chronic increases[145, 269, 313] (PAH). 2D-STE consistently demonstrates reduced RVGLS.FW within 72 hours following a PE[258, 265-268] although Vitarelli et al. showed that this recovers by 30 days[320]. In PAH, RVGLS.FW is a sensitive marker of disease serverity, marker of repsonse to treatment, and is predictive of morbidity and mortality[145, 269, 313].

5.2.7 Studies investigating right ventricular strain following lung resection

Three investigations of RV strain following lung resection have been performed to date[76, 224, 233]. All of the studies have been performed with 2D-STE and the results are inconsistent.

5.2.7.1 Study by Wang et al.

Thirty patients (10 pneumonectomies and 20 lobectomies) had pre-operative and one-week post-operative echocardiography studies[224]. They demonstrated marked reduction in all measures of RV and LV strain. Pneumonectomy patients had a greater post-operative reduction in RVGLS.FW than lobectomy (-30.86±5.88% to -11.77±4.14%, $p<0.05$ and -29.7±6.23% to -18.03±8.06%, $p<0.05$) and RVGLS.S (-17.51±7.11% to -10.1±5.92%, $p<0.05$ and -19.88±5.92% to -15.6±6.40%, $p<0.05$). Additionally, LV longitudinal strain reduced in both groups.

Comparison of their results to PH cohorts raises potential concerns regarding the levels of post-operative strain in the results. Vitarelli et al. demonstrated that a 2D-STE RVGLS.FW strain of <-18% had an 89% sensitivity and a 74% specificity for detection of RV failure[322]. Smith et al. demonstrated that 2D-STE values for RVGCS

[ff] The inflammatory response and scarring of the RV demonstrated in the Watts et al. rat studies is discussed further in the future work section, section 9.3.2 page 337, and is the physiological basis of one of the two future studies, detailed in Appendix 3.

<-9.9% and RVGLS <-16.1% had hazard ratios for mortality of 4.17 (1.93-12.97) and 7.63 (1.76-10.27) respectively[323]. Whilst the results of Wang et al. are in a post-operative setting, the reduction in RV strain values demonstrated are in keeping with a severe reduction in RV function[269].

The authors argue that speckle tracked echocardiography has been validated in other diseases, but that the changes in heart position may influence the image acquisition. Overall inter- and intra-observer variability were good (ICC >0.84) but they do not differentiate this between pre-operative and post-operative scans. Heart rate was elevated in both groups post-operatively which may influence strain results when measured by 2D-STE[317, 324] although this was included as a co-variate in the analysis.

5.2.7.2 Study by Bhat et al.

Twenty-six patients (5 pneumonectomies and 21 lobectomies) underwent echocardiographic assessment pre-operatively and on POD 2, 7 and 30[76]. RVGLS changed over the course of the study (p=0.045), whilst the lowest value was at POD2 (-15.1±3.7%) there was no post-hoc testing to determine if this was a significant difference from pre-operative (-19.2±4.5%).

5.2.7.3 Study by McCall et al.

Twenty-seven patients from the RV Response to Lung Resection study underwent speckled tracked echocardiography pre-operatively, POD2 and 2-months post-op[156, 233]. In pooled analysis RVGLS and RVGLS.FW were associated with CMR RVEF (r=-0.412 and r=-0.477) and were able to identify RV dysfunction (RVEF <45%), Figure 5-15. A RVGLS value of −17.7% had 76.0% sensitivity and 66.7% specificity for identifying RV dysfunction and a RVGLS.FW value of −20.0% had 62.5% sensitivity and 79.5% specificity for identifying RV dysfunction[156]. There was no change in RVGLS or RVGLS.FW over time.

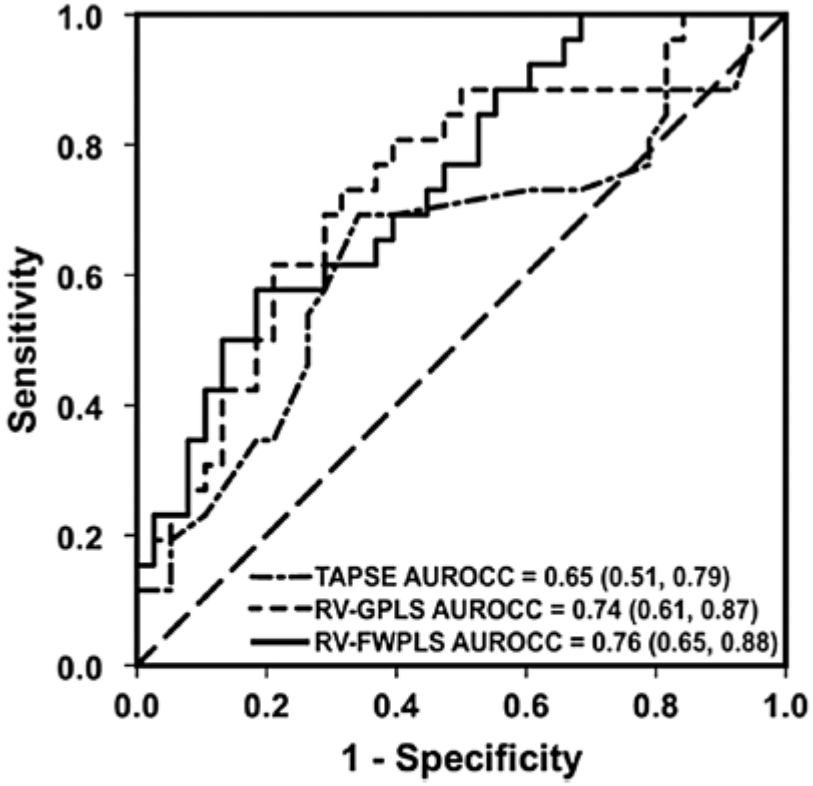

Figure 5-15 Receiver-operator curves for identification of right ventricular dysfunction
Area under receiver operator curve (AUROCC) for tricuspid annular plane systolic excursion (TAPSE, dashed-dotted line), right ventricular global longitudinal peak strain (RV-GPLS in image, dashed line) and right ventricular free wall longitudinal peak strain (RV-FWPLS in image, solid line). Diagonal dashed line is the line of no effect. Image from McCall et al.[156].

5.2.7.4 Summary of right ventricular strain following lung resection

There are differing results between the three studies; Wang et al. show a marked reduction in RVGLS and RVGCS[224] whilst Bhat et al. show only a transient small reduction[76] and McCall et al. show no change[233]. All three studies have similar patient numbers although differing numbers of pneumonectomy patients (ten in Wang et al., five in Bhat et al. and one in McCall et al.). This may explain the difference in RV strain results, the greater physiological insult may cause a greater reduction in strain. Contrary to this is the fact that the lobectomy patients in Wang et al. have reduced strain and there is no difference between the lobectomy and pneumonectomy strain results in Bhat et al.

5.3 Hypotheses

Hypotheses:

- RV contractility, measured by CMR-FT RVGLS and $RVGLS_{rate}$,

a. decreases following lung resection
b. predominately affects the RV free wall.

- The magnitude of a reduction in RVGLS/$RVGLS_{rate}$ will be associated with
  a. reduction in RVEF
  b. increase in BNP
  c. increase in afterload[gg]

5.4 Methods

Patients from the RV Response to Lung Resection Study with complete CMR scans at each time point were selected for strain analysis using commercially available software (QStrain, Version 2.1.12.2, Medis Medical Imaging, Leiden, The Netherlands). In total, pre-operative, POD2 and 2-months post-operative scans for 20 patients, 60 in total, were analysed.

The description of the generic methods, statistical analysis plan, patient population and previously described results are discussed in Chapter 4.

5.4.1 Strain analysis

5.4.1.1 Image interpretation

Anonymised and randomised cardiac magnetic resonance scans were uploaded into QStrain and interpreted as per Padervinskienė et al.[325]. Visual inspection of the four-chamber "cine" was performed to assess for artefact in both; RV and LV long axis motion.

LVGLS and LVGCS were calculated from two, three and four chamber views of the LV. QStrain constructs a 3D model of the LV from these views and calculates GLS, GCS and GRS. RVGLS, RVGLS.S and RVGLS.FW were calculated form the four chamber long axis views of the RV[hh], Figure 5-16. For both ventricles, the endocardial border was traced at end-diastole and then automatically interpolated across the cardiac cycle. Visual inspection of each of the 35

[gg] This will be explored in chapter 8.

[hh] QStrain does not calculate subsegmental strain regions of the RV free wall or septum. This prevents calculation of strain in the basal, mid-ventricular and apical segments of the RV free wall and septum.

sequential frames of the cardiac cycles was then performed with correction of the automated endocardial border where required. This was repeated for each of the views detailed above.

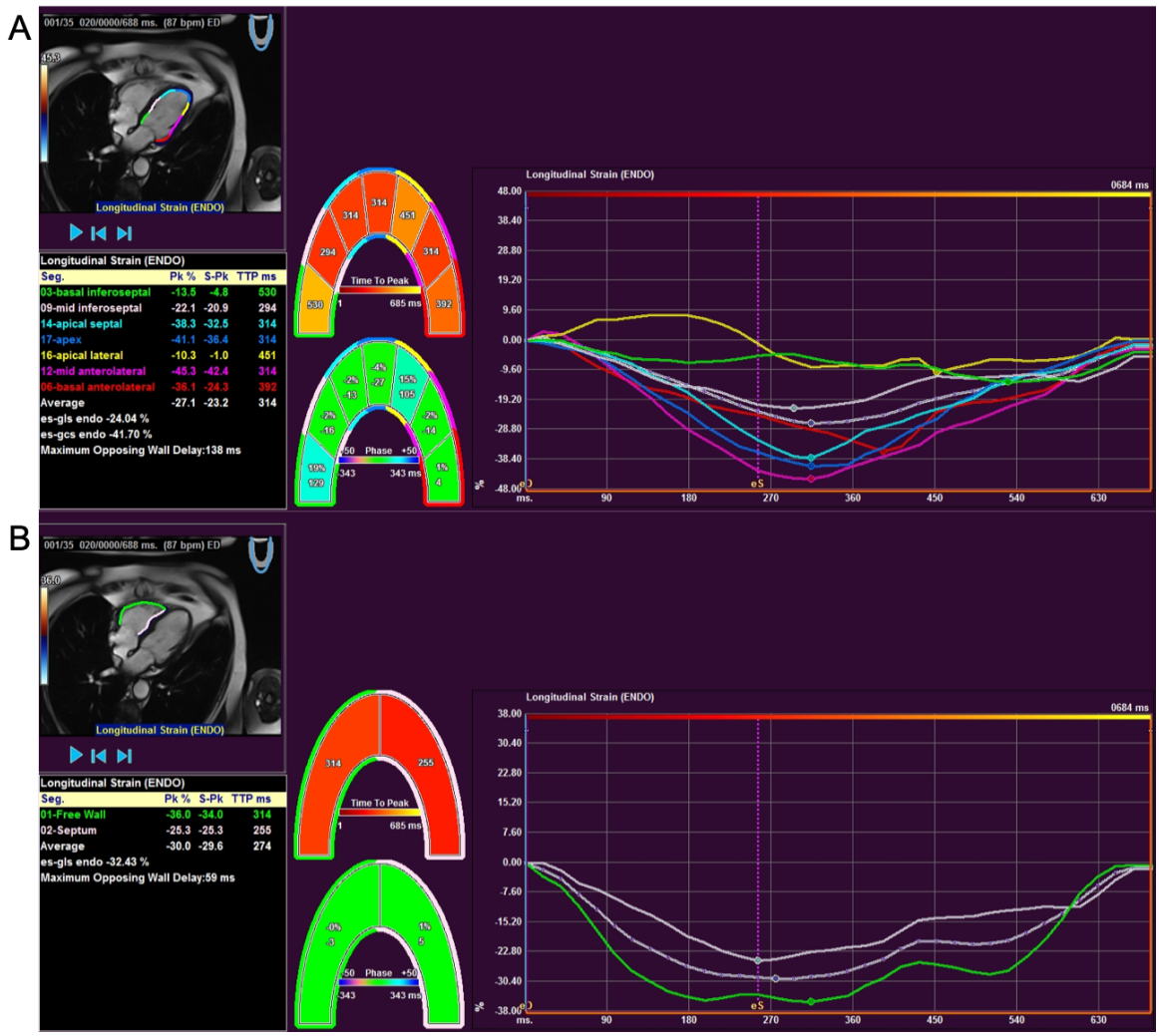

Figure 5-16 Generation of global longitudinal strain for left and right ventricles
Mapping of endocardial border of left ventricle (A) and right ventricle (B). QStrain, Medis, calculates regional and global longitudinal strain. Note free wall in green and septal strain in pink in image B. Indicative image from interpretation of scan MRIRAN 15 from this study.

All scans were reported by the author, with 15 scans randomly selected for repeat interpretation by the author to allow calculation of intra-observer variability, this was performed one week after completion of the original 60 scans. A further selection of 9 randomly selected scans were interpreted for inter-observer variability by Kenneth Mangion (KM), Cardiology Research Fellow, University of Glasgow. KM is an expert in CMR strain interpretation and provided training in QStrain.

5.4.1.2 Data processing

QStrain calculates strain and time to peak strain (TTPS) for each defined cardiac region. This output is in the form of single data results displayed on the console, bottom left in Figure 5-16. Additionally, a ".txt" file including values for strain, area/volume and time points for each of the images of the cine is generated. The data in the .txt file is required for calculation of strain rate and for more detailed assessment of the strain plots generated[ii]. Using R Studio (Microsoft, Version 1.1.463) an automated programme was written by the author to convert the ".txt" files to an excel ".csv" file. Once in ".csv" format the data was uploaded to R Studio for processing and analysis as detailed below. The process detailed below was completed for calculation of strain and strain rate from plots of RVGLS, RVGLS.FW, RVGLS.S, LVGLS, LVGCS and LVGRS.

In order to calculate strain rate, the strain data generated in the ".txt" must be filtered and the temporal differential calculated. QStrain uses a filter to smooth the measured strain values to predict peak strain and TTPS. Medis does not publish the filtering method used in QStrain. In order to replicate this, the data was smoothed with a second order, seven point Savitzky Golay filter [326] and then interpolated to 1 millisecond, this technique is discussed in greater detail in section 7.2.6.2 page 261. Visual inspection was performed to compare smoothed and original data for all plots generated, an example is demonstrated in Figure 5-17. Agreement was then tested between the smoothed strain results and the result generated by QStrain for RVGLS, RVGLS.FW, RVGLS.S, LVGLS, LVGCS and LVGRS.

An original R Studio programme was written to measure TTPS and strain values. These were automatically detected as the time to and value of the most negative strain value from the smoothed data. Plots for each scan were automatically generated, with the point at which these values were measured indicated upon it. Visual inspection of the generated plot profile was performed to assess for physiological plausibility. The points at which the automated programme

[ii] The results generated by QStrain for the RV limit analysis to the timing and magnitude of strain. Filtering and smoothing of the data not only allowed strain rate calculation, but also investigation of diastolic function, performed separately by Dr Emma Murphy.

measured values for TTPS and strain were assessed to ensure accuracy of the programme, an example is given in Figure 5-18.

Strain rate is not calculated for each region in QStrain and so the temporal differential of strain was calculated in R. Calculation of the derivative from the 35 time points of the original data exaggerates any small sudden change in the strain value measured whereas using the smoothed data minimises this effect, see Figure 5-17 (bottom panel). The differential of this smoothed data was interpreted with the same programme as strain, i.e. time to and value of most negative strain with visual inspection of plots again performed.

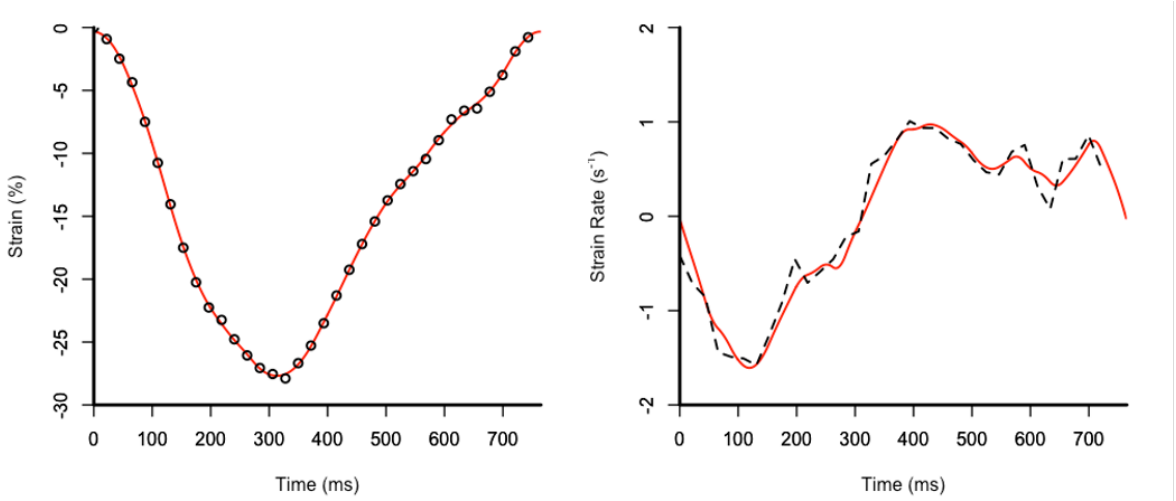

Figure 5-17 Strain and strain rate plots demonstrating effect of data filter
Strain (%) (left panel) and strain rate (s^{-1}) (right panel) plots from scan MRIRAN 32 in this study. Black circles represent measured data points of strain. Dashed black line (strain rate) represents differential of these points. Solid red line demonstrates these results following fitting of a smoothing filter (Savitzky Golay filter applied to measured vales of strain) and 1ms temporal interpolation. Note minimal divergence from measured value in strain plot but significant smoothing of differential in strain rate plot. The temporal relationship and the magnitude of peaks in strain and strain rate are maintained between measured and smoothed data.

5.5 Results

Strain analysis was completed at all time points for the 20 patients. Visual inspection was performed on the plots of all strain analysis parameters, an example of normal plots for strain and strain rate are given in Figure 5-18. There were no abnormal patterns found for any LV strain, RVGLS or RVGLS.S although RVGLS.FW had two abnormal plots at POD2, scans MRIRAN 29 and MRIRAN 44. MRIRAN 29 had a positive strain inflection in early systole and MRIRAN 44 had positive strain in early and late systole, neither of which were present in the RVSA

views or RVLA septum. Both scans were excluded from RVGLS.FW and $RVGLS_{rate}$.FW analysis and subsequent association testing.

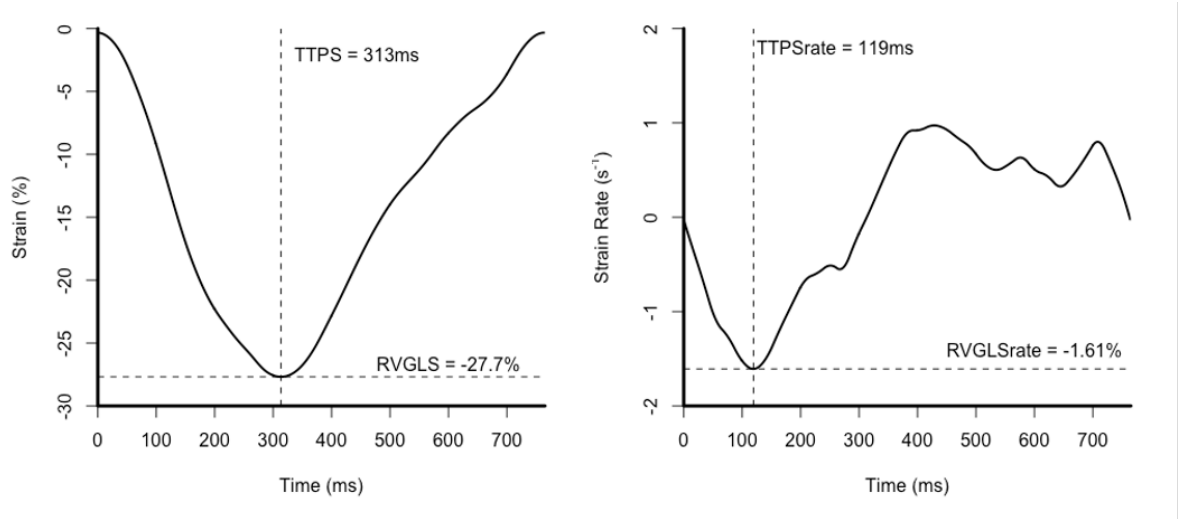

Figure 5-18 Normal strain and strain rate plot interpretation
Automated R programme detects the value at and timing of the point of lowest strain (left panel) and strain rate (right panel) then generates plots demonstrating these results for visual inspection and plausibility checking. TTPS=time to peak strain. RVGLS=right ventricular global longitudinal strain. ms=millisecond. Image of a right ventricular longitudinal strain interpretation of scan MRIRAN 32 from this study.

5.5.1 Reliability and variability of CMR measurements

A random selection of the 60 scans were selected for repeat reporting by the author (15 scans) and for reporting by KM.

5.5.1.1 Interobserver reliability and variability

Interobserver testing showed moderate agreement and low variability for RVGLS (ICC 0.50, CV 8.68%), Table 5-1 and Figure 5-19. Interpretation of LVLA scans showed moderate/good reliability and good variability (ICC >0.57, CV <9.81%). All ICCs had wide confidence intervals.

Ventricle	Measure	CV (%)	ICC (95% CI)	p value
RV	GLS(%)	8.68	0.50 (-0.12, 0.86)	0.077
LV	GLS (%)	7.36	0.85 (0.15, 0.97)	0.011
	GCS (%)	7.57	0.57 (-0.01, 0.88)	0.027
	GRS (%)	9.81	0.71 (-0.04, 0.94)	0.034

Table 5-1 Interobserver variability for right and left ventricular strain
Intraclass correlation coefficient (ICC) calculated as interobserver two-way mixed method absolute agreement. RV= right ventricle. LV= left ventricle. GLS= global longitudinal strain. GCS= global circumferential strain. GRS= global radial strain. CV= coefficient of variation. CI= confidence interval. Nine repeated scans.

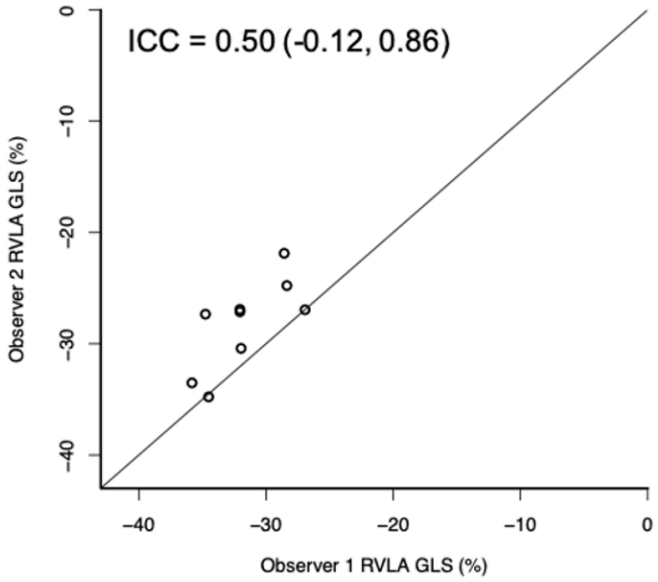

Figure 5-19 Interobserver reliability in strain measurement
Association between observer 1 and 2 in right ventricular long axis (RVLA) measurement of global longitudinal strain (GLS). Solid line is the line of association, i.e. no difference between measurements. Nine repeated scans. ICC= intra-class correlation co-efficient.

5.5.1.2 Intraobserver reliability and variability

Intraobserver testing showed moderate reliability and low variability in RVGLS (ICC 0.73, CV 8.48%), Table 5-2 and Figure 5-20. LVLA had good/excellent reliability and low variability (ICC >0.88, CV <4.55%) with narrower confidence intervals than the RV.

Ventricle	Measure	CV (%)	ICC (95% CI)	p value
RV	GLS(%)	8.48	0.73 (0.37, 0.90)	<0.001
LV	GLS (%)	4.55	0.88 (0.68, 0.96)	<0.001
	GCS (%)	4.21	0.94 (0.83, 0.98)	<0.001
	GRS (%)	3.44	0.96 (0.89, 0.98)	<0.001

Table 5-2 Intraobserver variability for right and left ventricular and strain
Intraclass correlation coefficient (ICC) calculated as intraobserver two-way mixed method absolute agreement. RV= right ventricle. LV= left ventricle. GLS= global longitudinal strain. GCS= global circumferential strain. GRS= global radial strain. CV= coefficient of variation. CI= confidence interval.

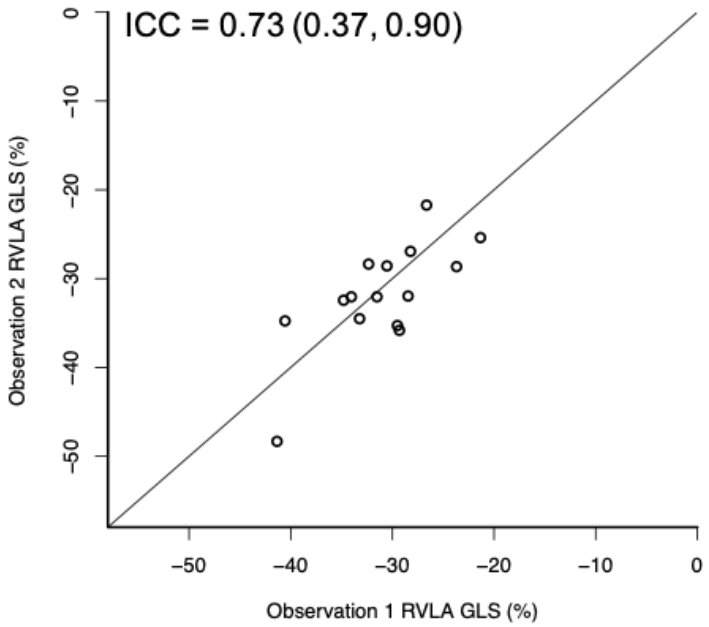

Figure 5-20 Intraobserver reliability in strain measurement
Association between observation 1 and 2 by author in right ventricular long axis (RVLA) measurement of global longitudinal strain (GLS). Solid line is the line of association, i.e. no difference between measurements. Fifteen repeated scans. ICC= intra-class correlation co-efficient.

5.5.1.3 Agreement between smoothed and original data

Visual inspection of the smoothed plots against the original data did not highlight any discrepancies between them. There was excellent agreement between the peak strain values calculated after smoothing of the data and the results generated in QStrain (ICC>0.98, two-way mixed method absolute agreement). Smoothed data was consistently more negative (greater strain) than the QStrain generated results although relative magnitude of the mean difference was not clinically significant, Table 5-3.

Ventricle	Measure	Mean difference	SD	CV (%)	ICC (95% CI)	p value
RV	GLS(%)	0.84	1.35	2.55	0.98 (0.93, 0.99)	<0.001
	GLS.FW (%)	0.06	0.08	0.15	1.00 (1.00,1.00)	<0.001
	GLS.S(%)	0.07	0.08	0.19	1.00 (1.00,1.00)	<0.001
LV	GLS (%)	0.44	0.80	1.41	0.98 (0.95, 0.99)	<0.001
	GCS (%)	0.53	1.01	1.78	0.99 (0.97, 0.99)	<0.001
	GRS (%)	-1.23	2.69	1.51	0.99 (0.97, 0.99)	<0.001

Table 5-3 Agreement between smoothed data and QStrain results
Mean difference (QStrain – smoothed) and standard deviation (SD) of smoothed data compared with QStrain generated results. Intraclass correlation coefficient (ICC) calculated as intraobserver two-way mixed method absolute agreement. RV= right ventricle. LV= left ventricle. GLS= global longitudinal strain. GCS= global circumferential strain. GRS= global radial strain. CV= coefficient of variation. CI= confidence interval.

5.5.2 Changes in strain and strain rate over time

5.5.2.1 Right ventricular strain and strain rate over time

The results for RVGLS, $RVGLS_{rate}$, RVGLS.FW, $RVGLS_{rate}$.FW, RVGLS.S and $RVGLS_{rate}$.S are shown in Table 5-4, Figure 5-21 and Figure 5-22. Data were a mixture of parametric and non-parametric, with ANOVA or Friedman's test used as indicated.

Region	Parameter	Pre-op	POD2	2-months	p-value
Global	RVGLS (%)	-32.73 (6.18)	-29.66 (6.85)	-28.06 (7.34) #	***0.049 ****
	$RVGLS_{rate}$ (s^{-1})	-1.42 (-1.61, -1.20)	-1.44 (-1.80, -1.17)	-1.31 (-1.62, -1.08)	0.387 §
Free wall	RVGLS.FW (%)	-37.31 (10.21)	-36.48 (9.13)	-32.47 (10.62) #	***0.025 ****
	$RVGLS_{rate}$.FW (s^{-1})	-2.06 (-2.38, -1.67)	-2.15 (-2.64, -1.67)	-1.82 (-2.24, -1.49) #	***0.016*** §
Septum	RVGLS.S (%)	-31.56 (9.10)	-26.00 (9.85) #	-27.27 (7.97)	***0.018 ****
	$RVGLS_{rate}$.S (s^{-1})	-1.47 (-1.77, -1.14)	-1.46 (-1.74, -1.04)	-1.35 (-1.88, -1.07)	0.247 §

Table 5-4 Right ventricular global longitudinal strain and strain rate results
Values are mean (SD) or median (IQR). RVGLS= right ventricular global longitudinal strain. RVGLS.FW= free wall RVGLS. RVGLS.S= septal RVGLS. *= one-way repeated measures ANOVA. §= Friedman's test. #= significant difference from pre-op. n=20 for each time-point. Significant results (p<0.05) highlighted ***bold italics.***

RVGLS showed a significant difference over time (p=0.049, ANOVA). Paired t-test showed that RVGLS was reduced at 2-months from pre-operatively (p=0.022) and at POD2 the reduction in RVGLS from pre-op approached significance (p=0.082, paired t-test), Figure 5-21. There was no change in $RVGLS_{rate}$ over this period.

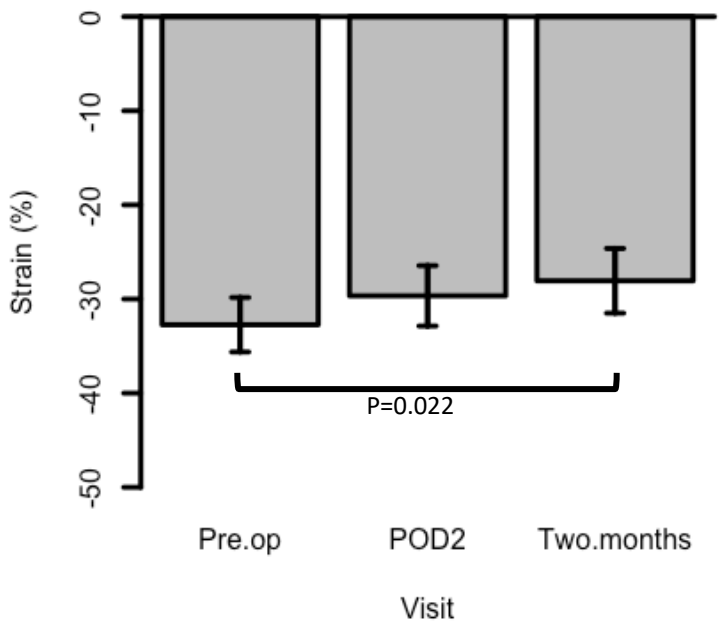

Figure 5-21 Right ventricular global longitudinal strain over time
Reduction in strain by 2-months post-op. Non-significant reduction at post-operative day 2 POD2 (p=0.082). Paired t-test for both comparisons. Bar plot represents mean and 95% CI.

There was a difference in RVGLS.S over the study period, with a significant reduction at POD2 from pre-operative (p=0.018, paired t-test) and trend to reduction at 2-months (p=0.061, paired t-test). RVGLS.FW showed a reduction from pre-operative levels to 2-months post-operative (p=0.023, paired t-test), Figure 5-22. Of the strain rate results, only $RVGLS_{rate}$.FW was reduced from baseline at 2-months (p=0.019, Wilcoxon).

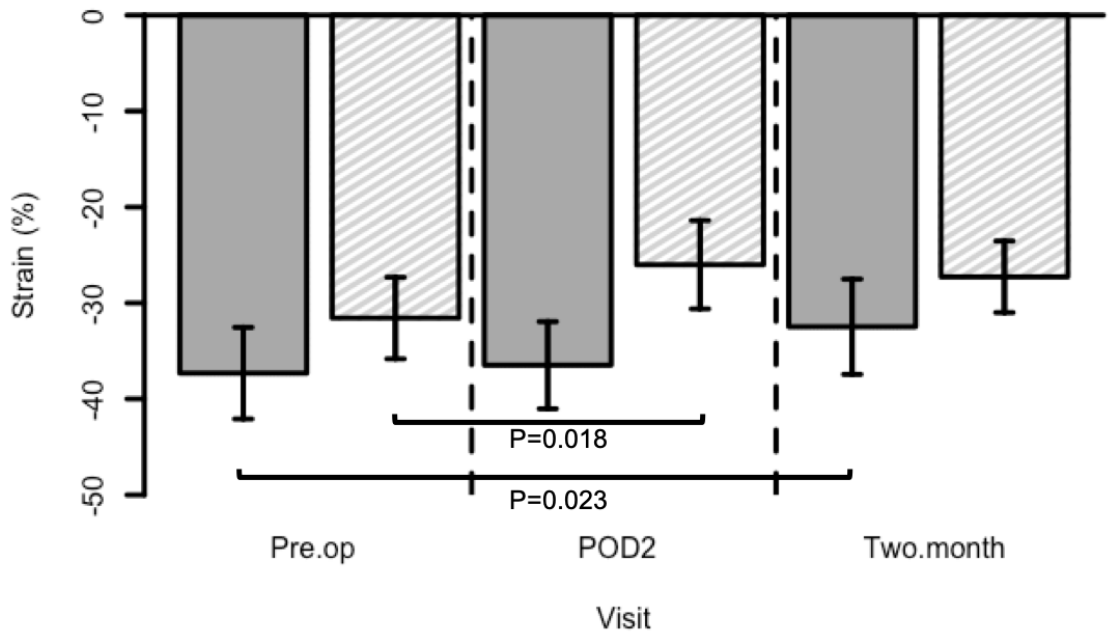

Figure 5-22 Right ventricular free wall and septal global longitudinal strain over time
Bar plot represents mean and 95% CI. Free wall right ventricular global longitudinal strain (RVGLS.FW) in dark grey and septal right ventricular global longitudinal strain (RVGLS.S) in striped light grey. RVGLS.S reduced at post-operative day 2 (POD2), RVGLS.FW reduced at 2-months. Both tests Paired t-test. Note stepwise reduction in RVGLS.S at POD2 followed by a reduction in RVGLS.FW at 2-months.

5.5.2.2 Left ventricular strain and strain rate over time

There were no changes in LVGLS, LVGCS or LVGRS over the duration of the study, Table 5-5. ANOVA demonstrated a change in both $LVGLS_{rate}$, $LVGCS_{rate}$ and $LVGRS_{rate}$ over the study period. On comparison between time points there was only POD2 (against pre-op) increases in $LVGLS_{rate}$ (p=0.007), $LVGCS_{rate}$ (p=0.005) and $LVGRS_{rate}$ (p=0.013), all paired t-tests.

Region	Parameter	Pre-op	POD2	2-months	p -value
Longitudinal	LVGLS (%)	-25.42 (5.02)	-26.18 (3.38)	-25.34 (4.39)	0.739 *
	$LVGLS_{rate}$ (s^{-1})	-1.12 (0.32)	-1.39 (0.32) #	-1.26 (0.27)	***0.013 ****
Circumferential	LVGCS (%)	-33.33 (6.54)	-34.70 (6.56)	-32.97 (7.66)	0.500 *
	$LVGCS_{rate}$ (s^{-1})	-1.62 (0.30)	-1.89 (0.35) #	-1.85 (0.41)	***0.021 ****
Radial	LVGRS (%)	70.65 (18.48)	73.97 (17.68)	69.17 (19.73)	0.524 *
	$LVGRS_{rate}$ (s^{-1})	3.11 (0.79)	3.89 (1.12) #	3.59 (1.21)	***0.049 ****

Table 5-5 Left ventricular global longitudinal and circumferential strain and strain rate results
Strain and strain rate changes in left ventricular global longitudinal strain (LVGLS), global circumferential strain (LVGCS) and global radial strain (LVGRS) changes over time. Values are mean (SD) or median (IQR). *= one-way repeated measures ANOVA. §= Friedman test. #= significant difference from pre-op. Significant results (p<0.05) highlighted ***bold italics.***

5.5.3 Association between right ventricular ejection fraction and longitudinal strain and strain rate

5.5.3.1 Right ventricular longitudinal strain

There were moderate negative *within-subject* associations between the change in RVGLS.S and the change in RVEF between pre-op and POD2 and between pre-op and 2-months, Table 5-6 and Figure 5-23, impaired RVGLS.S was associated with reduced RVEF. Individual time point associations reveal moderate negative associations between RVGLS.FW and RVEF on POD2 and at 2-months, Figure 5-24, impaired RVGLS.FW was associated with reduced RVEF.

Analysis of covariance, within-subject					
Change between pre-op and POD2					
			RVGLS	RVGLS.FW	RVGLS.S
RVEF		r	-0.365	-0.066	***-0.446***
		p	0.103	0.788	***0.043***
Change between pre-op and 2-months					
			RVGLS	RVGLS.FW	RVGLS.S
RVEF		r	-0.423	-0.282	***-0.463***
		p	0.062	0.229	***0.040***
Time point analysis					
			RVGLS	RVGLS.FW	RVGLS.S
RVEF	Pre-op	r	-0.393	-0.171	-0.279
		p	0.086 *	0.471 *	0.234 *
	POD2	r	-0.238	***-0.510***	0.104
		p	0.313 *	***0.031 ****	0.660 *
	2-months	r	-0.341	***-0.528***	0.398
		p	0.153 §	***0.020 ****	0.091 §

Table 5-6 Within-subject association between RVGLS and RVEF
RVGLS= right ventricular global longitudinal strain. RVGLS.FW= free wall RVGLS. RVGLS.S= septal RVGLS. RVEF= right ventricular ejection fraction. Analysis of covariance with patient as factor. *= Pearson's correlation co-efficient. §= Spearman's correlation co-efficient. Significant results ($p<0.05$) highlighted ***bold italics.***

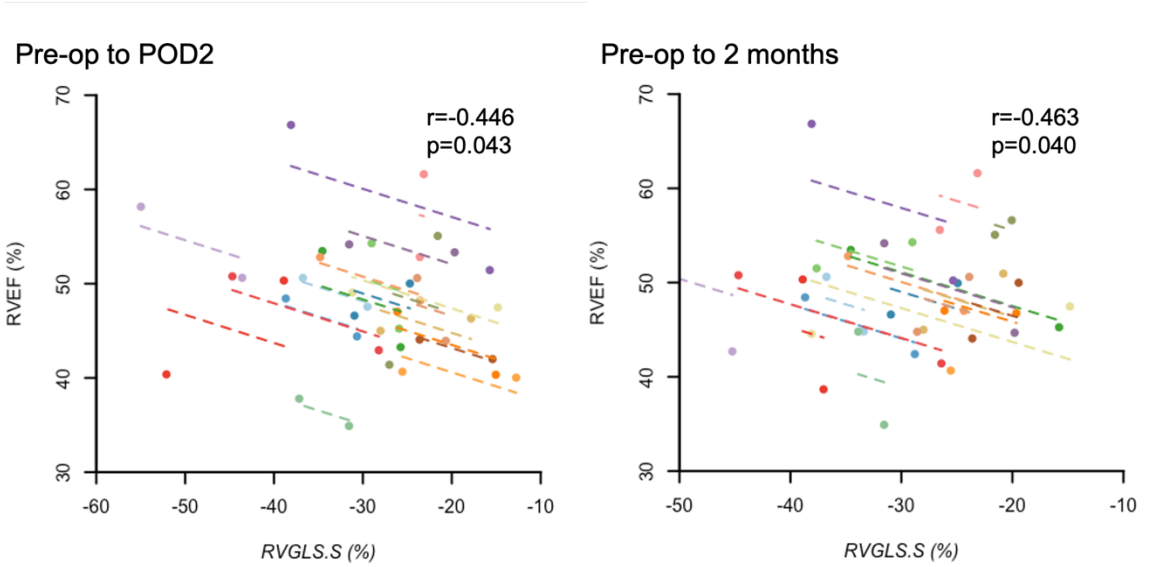

Figure 5-23 Within-subject association between RVGLS and RVEF
Within-subject associations between septal right ventricular global longitudinal strain (RVGLS.S) and right ventricular ejection fraction (RVEF) between pre-op and post-operative day 2 (left) and 2-months (right). Note reduction in RVGLS.S associated with reduction in RVEF. Analysis of covariance with patient as factor. Coloured dots represent each patient and lines depict parallel lines of association for each patient.

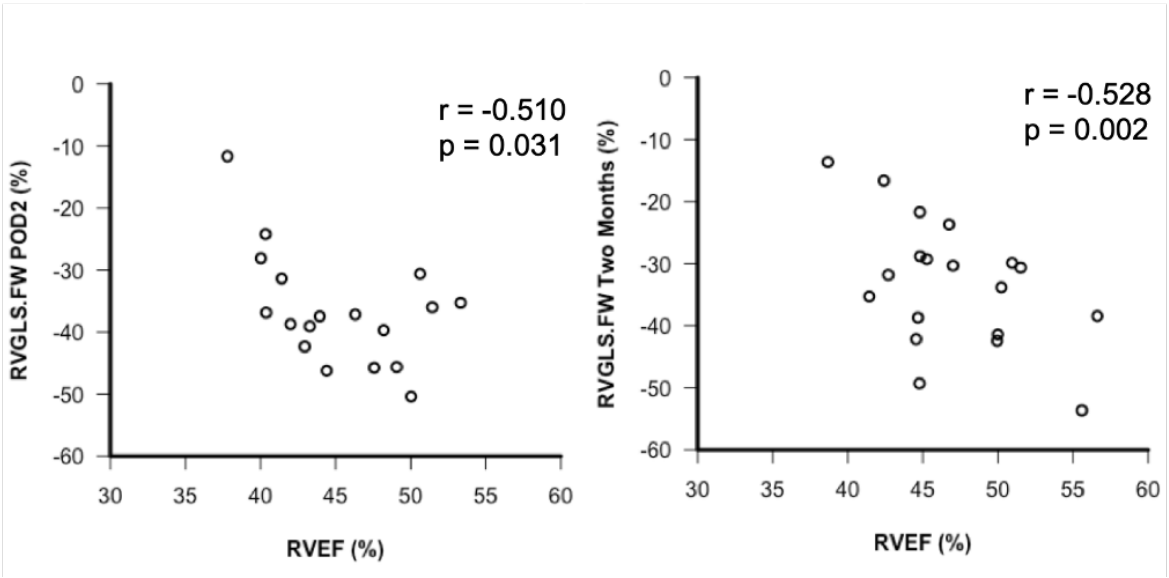

Figure 5-24 Association between RVGLS.FW and RVEF at post-operative day two and 2-months
Moderate negative associations between free wall right ventricular global longitudinal strain (RVGLS.FW) and right ventricular ejection fraction (RVEF) at post-operative day 2 (POD2) and two months, both Pearson's.

5.5.3.2 Right ventricular longitudinal strain rate

There were no associations on within-subject ANCOVA or individual time-points association testing between $RVGLS_{rate}$, $RVGLS_{rate}$.FW or $RVGLS_{rate}$.S and RVEF, Table 5-7.

Analysis of covariance, within-subject					
Change between pre-op and POD2					
			$RVGLS_{rate}$	$RVGLS_{rate}$.FW	$RVGLS_{rate}$.S
RVEF		r	-0.014	-0.092	-0064
		p	0.951	0.709	0.783
Change between pre-op and **2-month**s					
			$RVGLS_{rate}$	$RVGLS_{rate}$.FW	$RVGLS_{rate}$.S
RVEF		r	-0.335	-0.317	-0.309
		p	0.124	0.174	0.184
Time point analysis					
			$RVGLS_{rate}$	$RVGLS_{rate}$.FW	$RVGLS_{rate}$.S
RVEF	Pre-op	r	-0.260	-0.361	-0.279
		p	0.268 §	0.118 §	0.234 *
	POD2	r	-0.184	-0.225	0.114
		p	0.437 *	0.370 *	0.633 *
	2-months	r	-0.105	-0.264	0.326
		p	0.669 *	0.275 *	0.173 *

Table 5-7 Association between $RVGLS_{rate}$ and RVEF
$RVGLS_{rate}$= right ventricular global longitudinal strain rate. $RVGLS_{rate}$.FW= free wall $RVGLS_{rate}$. $RVGLS_{rate}$.S= septal $RVGLS_{rate}$. RVEF= right ventricular ejection fraction. Analysis of covariance with patient as factor. *= Pearson's correlation co-efficient. §= Spearman's correlation co-efficient.

5.5.4 Association between BNP and right ventricular strain and strain rate

5.5.4.1 Right ventricular longitudinal strain/strain rate

There were no within-subject associations between RVGLS/$RVGLS_{rate}$, RVGLS.FW/$RVGLS_{rate}$.FW or RVGLS.S/$RVGLS_{rate}$.S and BNP, ($p>0.292$). Association testing at each individual time-point is shown in Table 5-8. There were moderate and strong positive associations between BNP and RVGLS.S pre-operatively and 2-months post-operatively ($r=0.506$ and 0.666). $RVGLS_{rate}$.S had a strong positive association with BNP at 2-months. At POD2 RVGLS and $RVGLS_{rate}$ were moderately associated with BNP and RVGLS.FW approached significance ($p=0.052$). In each association increased BNP was associated with impaired (less negative) strain.

Individual time point analysis					
			RVGLS	RVGLS.FW	RVGLS.S
BNP	Pre-op	r	0.028	-0.062	***0.506***
		p	0.905§	0.796§	***0.023§***
	POD2	r	***0.497***	0.465	0.223
		p	***0.026****	0.052*	0.345*
	2-months	r	0.070	-0.125	***0.666***
		p	0.769§	0.600§	***0.001§***
			$RVGLS_{rate}$	$RVGLS_{rate}$.FW	$RVGLS_{rate}$.S
	Pre-op	r	-0.129	-0.312	0.344
		p	0.588§	0.181§	0.138§
	POD2	r	***0.490***	0.387	0.163
		p	***0.028****	0.113*	0.492*
	2-months	r	0.019	-0.218	***0.722***
		p	0.937§	0.357§	***<0.001§***

Table 5-8 Association between RVGLS/ $RVGLS_{rate}$ and BNP at individual time-points
RVGLS/ $RVGLS_{rate}$= right ventricular global longitudinal strain/ strain rate. RVGLS.FW/ $RVGLS_{rate}$.FW= free wall RVGLS/ $RVGLS_{rate}$. RVGLS.S/ $RVGLS_{rate}$.S= septal RVGLS/ $RVGLS_{rate}$.S. BNP= brain natriuretic peptide. *= Pearson's correlation co-efficient. §= Spearman's correlation co-efficient. Significant results ($p<0.05$) highlighted ***bold italics.***

5.5.5 Association between left ventricular strain with BNP

There were no within-subject associations between the change in LVGLS, LVGCS or LVGRS and the change in BNP between any time points ($p>0.178$). There were moderate within-subject associations between the change in $LVGLS_{rate}$ ($r=-0.595$, $p=0.006$) and $LVGRS_{rate}$ ($r=0.41$, $p=0.046$) and the change in BNP between pre-op to POD2. On individual time-point analysis only 2-month post-op $LVGCS_{rate}$ was associated with BNP ($r=0.590$, $p=0.006$, Spearman's). There were no other significant associations between LVGLS, $LVGLS_{rate}$, LVGCS or $LVGCS_{rate}$ and BNP on individual time-point analysis.

5.5.6 Summary of main results

Hypotheses:

- RV contractility, measured by CMR-FT RVGLS and $RVGLS_{rate}$,
    a. decreases following lung resection
    b. preferentially affects the RV free wall.

The main finding is that RVGLS changes over time, with reduction at 2-months following lung resection. The RV septum and the free wall that contribute to this reduction have differing temporal responses. RVGLS.S is reduced from baseline at POD2 with a trend to reduction at 2-months (p=0.061) whereas RVGLS.FW is unchanged at POD2 but reduced at 2-months, with a concurrent reduction in strain rate.

- The magnitude of reduction in RV strain/strain rate will be associated with
    a. reduction in RVEF
    b. increased BNP
    c. increased afterload[jj]

Within-subject analysis demonstrated a moderate association between the change in RVGLS.S and the post-operative change in RVEF. Post-operative (POD2 and 2-month) RVGLS.FW was moderately associated with RVEF. Whilst there were numerous individual time-point associations between strain and BNP, there were no within-subject associations between the change in RV strain and the change in BNP.

5.6 Discussion

5.6.1 Strengths and limitations

The main strength of this study is that it is the first utilisation of CMR strain in a lung resection population, allowing temporal tracking of the changes in RV strain following lobectomy. Whilst all patients (of the 27 patients in the study) completed the CMR protocol pre-operatively, five patients did not complete the POD2 scan. Three patients refused, one patient had a persistent air leak requiring intercostal drainage that could not safely be transferred and one patient had an epidural catheter in-situ that was not CMR compatible[254]. Patient refusal to return to the MRI scanner on POD2 (3/27, 11%) results in a similar non-completion rate to RV 2D-STE. 2D-STE RV analysis was not possible in 9.5% of patients in a comparable studies[307] and in 15.6% in patients from this study[254]. Echocardiography and CMR are both challenging for patients following lung

[jj] Investigation performed in Chapter 8.

resection. CMR can be a lengthy process for patients to undertake; it requires transfer to the scanner, lying flat for up to an hour, frequent breath holds and can be claustrophobic. Given this, it is perhaps encouraging that so many patients were willing to perform the follow-up scans.

The main limitation in the data collected is the reliability of the strain measurement. The intra- and inter-observer ICC were lower than published literature[143, 259, 303, 307, 327] and there is evidence of a systematic inter-observer bias.

Backhaus et al. argue that QStrain, Medis (the software used in this analysis) may have lower reproducibility with inexperienced operators, but greater reproducibility when used by an experienced operator, due to a large degree of manipulation required in tracing the RV border. Additionally, the four-chamber views required for RVGLS interpretation are greatly affected by the motion of breathing[300]. This may cause the greatest impact in the immediate post-operative period (POD2); secondary to altered breathing mechanics, acutely reduced lung volume, increased respiratory rate and pain. The two RVGLS.FW scans removed in the current analysis were both on POD2 and the causes of the factors limiting analysis, are potentially due to motion artefact secondary to breathing and/or incorrect tracing of the myocardium due to operator inexperience. Neither of the excluded scans were dual reported in the randomly selected intra- or inter-observer reliability tests. Given that RVGLS is calculated from RVGLS.FW and RVGLS.S, the abnormalities in the RVGLS.FW analysis may influence RVGLS. Sensitivity analysis with removal of the corresponding RVGLS scans on POD2 showed that the change in RVGLS over time retained significance ($p=0.006$ vs $p=0.049$ prior to removal, ANOVA) and the result of the comparison between pre-op and POD2 was also unaffected ($p=0.096$ vs $p=0.082$ prior to removal, paired t-test).

Schmidt et al. have performed an extensive reliability assessment of RV and LV CMR-FT strain analysis[327]. It includes 40 patient scans dual reported by 4 observers (320 interpretations) allowing interobserver and intraobserver ICC and CV calculation, comparison with the results of this study are shown in Table 5-9. When compared to Schmidt et al., there was lower interobserver and intraobserver

reliability throughout. Two potential explanations for this difference are; experience of observer and difference in the population investigated.

	Ventricle	Measure	Current study		Schmidt et al.	
			CV (%)	ICC	CV (%)	ICC
Inter-observer	**RV**	**GLS (%)**	8.68	0.50	18.7	0.75
	LV	**GLS (%)**	7.36	0.85	15.4	0.78
		GCS (%)	7.57	0.57	5.1	0.96
		GRS (%)	9.81	0.71	19.2	0.62
Intra-observer	**RV**	**GLS (%)**	8.48	0.73	7.1	0.96
	LV	**GLS (%)**	4.55	0.88	5.2	0.94
		GCS (%)	4.21	0.94	2.1	0.97
		GRS (%)	3.44	0.96	6.4	0.90

Table 5-9 Comparison of reliability and variability data with Schmidt et al.
Note lower Intraclass correlation coefficient (ICC) in majority of interobserver and intraobserver variability but lower CV data between the results of the current study and Schmidt et al.[327]. RV= right ventricle. LV= left ventricle. GLS= global longitudinal strain. GCS= global circumferential strain. GRS= global radial strain. CV= coefficient of variation.

As demonstrated by Chamberlain et al., there is learning curve for 2D-STE RVGLS analysis; this may also be present in CMR-FT[302], contrary to this, a study by Backhaus et al. suggest that training does not improve reliably with QStrain. In an investigation of the effect of training on the reproducibility of CMR-FT analysis they did not find any difference in RVGLS values before and after training. In QStrain they actually demonstrated a reduction in ICC (intra-observer ICC 0.89 to 0.76 and inter-observer ICC 0.70 to 0.58) and CV following training. Their ICCs after training are similar to the results presented here[300].

Inter-observer testing, detailed in 5.5.1.2, demonstrated that Observer 2 (KM) consistently reported a less negative RVGLS than Observer 1 (author) with a mean difference of 3.5±2.8%, Figure 5-25. There was a similar inter-observer bias between observers of equal experience in the QStrain results from the study of Backhaus et al. with a mean difference between RVGLS of 3.06±3.54% before training and 3.33±4.72% after training although this was not replicated in a similar study by Gertz et al.[328]. The bias was not present with either of the other two CMR-FT software investigated by Backhaus et al.[300] or in separate studies[327, 329]. To the best of our knowledge a comparison between experienced and inexperienced observer has not been performed in QStrain for RV strain although Feisst et al. have demonstrated that inexperienced observers tend to report lower (less negative) LVGCS strain than experience observers in CMR-FT[330].

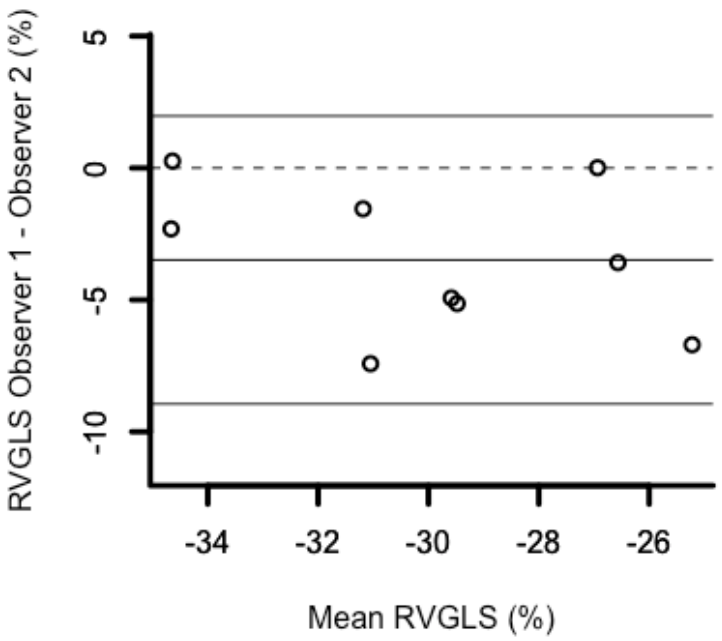

Figure 5-25 Bland-Altman plot for inter-observer strain analysis
Absolute difference in right ventricular global longitudinal strain (RVGLS, %) between Observer 1 and Observer 2 against mean RVGLS. Note consistent bias with Observer 1 reporting more negative RVGLS than Observer 2.

In order to minimise any potential inaccuracies in this investigation I undertook extensive training in CMR reporting. I completed Level 1 Society for Cardiac Magnetic Resonance training, Kings College London, prior to commencing the CMR analysis detailed in this thesis. Subsequently, I performed CMR analysis of patients from this study in Argus with supervision of CMR experienced anaesthetic research fellows (AA and PM) who have dual reported the RV volume analysis, discussed in Chapter 4, and the cardiology research fellow David Corcoran. Prior to undertaking the interpretation detailed above in QStrain, I had further training by the cardiology research fellow (KM) who performed the interobserver scans. This included direct supervision of reporting of training scans from this study, these reports were discarded prior to commencing the interpretation detailed above.

There are marked differences in the study populations in the study by Schmidt et al. and this study. The patients in the Schmidt et al study were either healthy controls or patients with myocarditis with a mean age of 36 and 37 respectively. This is very different to the older (mean age 64) and co-morbid population of our study who subsequently underwent lung resection, which has been shown to reduce CMR image quality. In reporting RVEF in the patients from this study,

McCall et al. demonstrated CV for RVEF increased post-operatively (12.9% pre-op to 16.8% on POD2 and 15.9% at 2-months)[231].

The inter-observer reliability is limited by the small number of repeated measures and therefore the wide 95% confidence intervals. Although all ICC lie between moderate to excellent reliability it is impossible to conclude where the true ICC absolute agreement lies within the confidence intervals. Additionally, it was not possible to investigate the impact of lung resection on reliability due to low numbers dual reported at each time point. Further investigation of inter-observer differences in RV strain analysis following lung resection should be incorporated into future work in this setting.

5.6.2 Strain results

5.6.2.1 Magnitude of changes in strain

The numerical value of strain measurement is determined by not only the method of analysis (TDI, STE, CMT-Tag or CMR-FT, section 5.2.4.3) but also the software used within each method. Bourfiss et al. demonstrated that repeated CMR-FT analysis of the same CMR images with different software results in a poor inter-vendor agreement, ICC= 0.373[331], with Gertz et al. showing RVGLS has the lowest inter-vendor agreement of any strain measurement[328]. To quantify the changes in strain reported in this study, a comparison must be made to CMR-FT studies that used QStrain for RV strain analysis. There are a limited number of such studies and they all focus on RVGLS, the results of these studies are detailed below.

In pulmonary hypertension Leng et al. demonstrated that RVGLS is reduced; -21±7% vs -29±4% in controls and progressively lower in patients at low risk (-25.4%), intermediate risk (-19.2%) and high risk (-13.0%) of clinical deterioration. It was also lower in patients who developed adverse events (-14.8% vs -22.5% no adverse event)[332]. In a study investigating patients with heart failure, RVGLS was -14.9% versus -26.2% in controls[328]. In patients with ARVC, Taha et al. demonstrated RVGLS of -27.9% in ARVC patients, -33.6% in ARVC relatives (an at risk or pre-clinical population) and -36.4% in controls[306]. Not only is there variation in RVGLS between diseases, but there is also marked variation in apparently similar control groups with RVGLS reported from -24.1% to -36.4%. The control

groups are younger and healthier than the pre-op patients in this current study, although the pre-op RVGLS of -32.73% seen in this study is in the middle of this range. Of note, volunteer STE studies have shown that RVGLS decreases with age and authors advise adjustment for age when comparing different groups[333, 334].

The post-operative reduction in RVGLS, -28.06% from -32.73% pre-op, is a modest reduction compared to patients with established PAH. Compared to the RVGLS values of Leng et al., 2-months post-operative RVGLS remains greater than RVGLS values seen in patients with PAH[332]. The patients in the study of Leng et al. had established PAH, therefore potentially have greater RV afterload than in this current study. As discussed in 5.2.3.1 and contrary to some author's interpretation, strain is a load dependent variable and in states of increased afterload, strain measurements can be reduced whilst contractility is actually unchanged[278]. To fully assess contractility, strain must be interpreted with the RV loading conditions. Leng et al. also found that reduced RVGLS (-25% cut-off) was had 69.9.% sensitivity and 86.3% specificity for detection of pulmonary hypertension (AUROC 0.838)[332]. At 2-months, six patients in the current study had RVGLS <-25% although there was no difference in either RVEF or the change in RVEF between those above or below this cut-off. The post-op RVGLS decrease is however similar to the difference between "at-risk" ARVC relatives and established ARVC patients demonstrated by Taha et al.[306].

Strain values for the LV seen in the current cohort are similar to the healthy patients in the studies by Gertz et al.[328], Backhaus et al.[300] and in a pulmonary hypertension study by collaborators from this current study[335]. The increase in LV strain rate and within-subject associations between the change in LV strain rate and the change in BNP between pre-op and POD2 may be explained by an increase in heart rate to meet increased cardiac output, although there is not a change in RV strain. Within-subject association testing revealed consistent associations between the change in heart rate and the change in LV strain rate, whereas there was no such association for RV strain rate, Table 5-10. The increase may be influenced by reduced filling (preload) secondary to RV dysfunction; although LV ejection fraction, stroke volume, end-diastolic and end-systolic volumes were all unchanged at this time point.

Analysis of covariance, within-subject					
		$RVGLS_{rate}$	$LVGLS_{rate}$	$LVGCS_{rate}$	$LVGRS_{rate}$
Heart rate	r	-0.062	***-0.497***	***-0.318***	***0.455***
	p	0.709	***0.001***	***0.049***	***0.004***

Table 5-10 Within-subject association between left ventricular strain rate and heart rate
$RVGLS_{rate}$= right ventricular global longitudinal strain rate. $LVGLS_{rate}$= left ventricular global longitudinal strain rate. $LVGCS_{rate}$= left ventricular global circumferential strain rate. $LVGRS_{rate}$= left ventricular radial strain rate. Analysis of covariance with patient as factor for all time points. Significant results ($p<0.05$) highlighted ***bold italics.***

5.6.2.2 Temporal and regional pattern of strain changes

As described in 5.2.6 page 160, a reduction in RV strain may be caused by an increase in afterload and/or a reduction in contractility (from myocardial injury and/or dysfunction). Furthermore, a reduction in strain with increased afterload may occur with or without a reduction in RV contractility[277]. The early post-operative reduction in RVGLS.S and late reduction in RVGLS.FW are therefore either secondary to afterload increase and/or myocardial injury, the reduced strain alone does not confirm the hypothesised reduced contractility following lung resection. Additionally, the reduction in RVGLS.S may be influenced by LV dysfunction, there were however no associations between the reduction in RVGLS.S and the change in LVGLS or LVGCS between any timepoints (ANCOVA, $p>0.184$).

As the mechanism of RV dysfunction following lung resection is widely hypothesised to result from increased afterload, RV strain analysis may be able to determine the temporal nature of an afterload increase, i.e. an acute increase, a chronic increase or both. Both predominately affect the RV free wall but with differing temporal responses. As demonstrated in Chapter 4, RVEF decreased at POD2 and remained decreased at 2-months in the study population. If the nature of the insult is truly analogous to a PE this would be expected to result in decreased RVGLS.FW in the immediate peri-operative period (imaging at POD2) that recovers by 2-months whilst RVEF may remain decreased, similar to the PE results by Vitarelli et al.[320], 5.2.6.2 and Figure 5-14 page 165. If solely due to a chronic increase in afterload, secondary to reduction in lung volume and pulmonary vasculature circulation, RVGLS.FW reductions would be expected to develop gradually over the 2-months post-operatively, both situations may occur concurrently.

The strain results observed, demonstrate no immediate post-operative change in RVGLS.FW, but a delayed reduction at 2-months. The development of impaired RVGLS.FW over the 2-month period is suggestive of a chronic increase in afterload. Previous studies, however, have failed to demonstrate increased afterload following lung resection. Pulmonary artery catheterisation studies demonstrate that PVR is either unchanged[48, 49, 63] or actually reduced in days to weeks following lung resection[58-60]. Through exercise testing post-operatively by Okada et al. [49], Nishimura et al.[67] and Miyazawa et al.[68] provided evidence of reduced pulmonary vascular reserve following lung resection, i.e. an increase in afterload due to an inability of the pulmonary vasculature to accommodate increased cardiac output. The sequalae of an afterload increase may not develop in the immediate post-operative period but develop gradually in the weeks to months after surgery, but this requires concurrent analysis of strain with afterload to confirm.

There is a consistent post-operative relationship between RVGLS.FW and RVEF, with reduced RVGLS.FW consistently occurring with reduced RVEF. There are moderate associations between these parameters both on POD2 ($r=-0.510$, $p=0.031$) and at 2-months ($r=-0.528$, $p=0.020$). Reduced RVGLS.FW appears to be at least contributory to the reduction in RVEF demonstrated.

5.6.2.3 Strain associations with BNP

An alternative mechanism of the reduction in strain is that it occurs secondary to an intrinsic reduction in contractility caused by myocardial dysfunction. Local inflammation and scarring secondary to the significant peri-operative stresses placed on the RV during lung resection (acute afterload increase with one lung ventilation and stress response to major surgery) could result in myocardial dysfunction and impaired contractility[336]. BNP is released secondary to myocardial stretch and is a non-specific marker of RV dysfunction[337], its release is associated with impaired RVGLS.FW following PE[258]. In this study group, the change in RVEF from pre-op to POD2 was associated with POD2 BNP, i.e. the patients with greatest drop in RVEF had the highest BNP[230]. Although there are positive associations between strain and BNP at individual time points (increased BNP associated with impaired strain), there are no consistent within-subject associations between the change in RV strain or strain rate and the change in BNP.

5.6.2.4 Comparison with previous studies

There are important distinctions between these results and the three previous studies[kk] that have investigated RV strain following lung resection[156, 224]. All three studies have investigated strain with 2D-STE, with similar patient numbers and study design, but all giving conflicting results, discussed in 5.2.7.

Wang et al.[224] demonstrated a marked universal reduction in all RV strain parameters (and LVGLS) following lobectomy (20 patients) and pneumonectomy (10 patients) at one week post-operatively. Comparison of RVGLS between the lobectomy group and the patients in this investigation (19 lobectomies and 1 pneumonectomy) reveals that whilst both show a reduction in RVGLS, the results of Wang et al. are strikingly different. It is not reliable to directly compare numerical strain values between different modalities, but the relative decrease in RVGLS seen by Wang et al. is far greater than in this investigation, Table 5-11. Additionally, we did not find any signal of the marked reduction in LV strain shown by Wang et al. No other studies investigating ventricular function following lung resection has shown any change in LV function, Chapter 2. In contrast Bhat et al. demonstrated results similar to this investigation although as they have not performed post-hoc testing to compare post-operative strain against pre-operative for each time point, the temporal nature of this decrease is unclear.

[kk] Study by McCall et al. is performed in the same patients as this study.

		Wang et al.		Glass at al	
		Strain (%) 2D-STE	Percentage change (%)	Strain (%) CMR	Percentage change (%)
RVGLS	Pre-op	-25.69 (4.71)		-32.73 (6.18)	
	POD2			-29.66 (6.85)	-9.4
	1 week	-17.07 (5.26)	-33.6		
	2-months			-28.06 (7.34)	-14.3
RVGLS.FW	Pre-op	-29.7 (6.23)		-37.31 (10.21)	
	POD2			-36.48 (9.13)	-2.2
	1 week	-18.03 (8.06)	-39.3		
	2-months			-32.47 (10.62)	-13.0
RVGLS.S	Pre-op	-19.88 (5.92)		-31.56 (9.10)	
	POD2			-26.00 (9.85)	-17.6
	1 week	-15.65 (6.40)	-21.3		
	2-months			27.27 (7.97)	-13.6

Table 5-11 Comparison of changes in RV strain with study by Wang et al.
Note difference between percentage change in Wang et al.[224] and results of this investigation. 2D-STE= two-dimensional speckle tacked echocardiography. CMR= cardiac magnetic resonance. RVGLS= right ventricular global longitudinal strain. RVGLS.FW= free wall RVGLS. RVGLS.S= septal RVGLS. POD2= post-operative day 2.

A potential explanation for a degree of the difference is that Wang et al. had healthier pre-operative patients; they were younger (57.0±11.4 years vs 65.2±10.8 years), had less comorbidities, lower BMI and significantly lower pre-op SPAP (20.3mmHg vs 30.8mmHg, estimated on echocardiography) than the patients included in this current study. Additionally, the 2D-STE strain results in this investigation's patient group (detailed in 4.5.2.2.2 page 141) had lower pre-operative RVGLS than in Wang et al.[156]. There is evidence that healthier patients have greater post-operative impairment following lung resection[63, 231, 338].

Any reduction in strain may also be influenced by heart rate. In healthy participants, an increased heart rate during exercise has been shown to increase RVGLS.FW when measured by TDI but decrease when measured by 2D-STE[317, 324]. In the study by Wang et al., one-week post-operative heart rate was 87.8±18.5 beats/min (lobectomy group) whilst POD2 heart rate was 77.0±11.0 beats/min in the current study. This may cause underestimation of strain with 2D-STE or it may be due to impaired myocardial function necessitating an increased heart rate to maintain cardiac output[224]. The timing of post-operative scanning is also different between the studies, although it is difficult to explain such a marked reduction in strain at one-week post-op when it is not present at POD2 or 2-months.

5.6.3 Conclusion

Strain analysis demonstrated that RVGLS is reduced at 2-months following lung resection. In the initial post-operative period, there is a reduction in RVGLS.S but by 2-months there is a reduction in RVGLS.FW and ultimately RVGLS. On individual time point analysis, reduced RVGLS.FW is associated with the previously demonstrated post-operative reduction in RVEF. The delayed reduction in RVGLS.FW is hypothesised by the author to be caused by a chronic increase in afterload. Further correlation between RV function, strain values and afterload are required.

Chapter 6 Pulmonary artery blood flow, acceleration time and distensibility

This chapter will describe the first of two investigations of pulsatile afterload following lung resection. Previous investigations of afterload following lung resection are discussed in Chapter 2. These investigations assessed pulmonary artery pressure (PAP) and pulmonary vascular resistance (PVR) however, as detailed in Chapter 1, these are incomplete measures of afterload and overlook potential changes in pulsatile afterload.

6.1 Cardiac magnetic resonance indices of afterload

The use of CMR in pulmonary arterial hypertension (PAH) is predominantly to assess RV function, however there is growing interest in CMR derived indices of afterload[149, 211-213, 339-344]. Its use in research is rapidly expanding and has numerous potential benefits, in summarising a review on this topic Bradlow et al. conclude that CMR,

"is a flexible research tool which has opened new avenues for understanding treatment effects, outcomes and pathogenesis."

Bradlow et al.[162]

6.1.1 Pulmonary artery distensibility

Multiple definitions are used in literature for the term *distensibility*[ll], see below. Within this thesis, distensibility will describe the percentage area change from minimum to maximum cross-sectional area of a vessel[149, 159, 345, 346], Equation 6-1. Other definitions for distensibility include; relative area change from maximal area[343, 347] and relative area change for change in pressure[211, 212] whilst others have used alternative terms to describe the area change; pulsatility[212], PA strain[342], relative area change[211] and elasticity[348].

[ll] The lack of agreed terminology in CMR research highlights the lack of an agreed approach that would be required for use in clinical practice. Of note, in papers just two years apart, Sanz et al. use different terms in each paper to describe Equation 6-1 (PA strain[342] and pulsatility[212]).

$$Distensibility\ (\%) = 100\ x\ \frac{Maximum - minimum\ PA\ area}{Minimum\ PA\ area}$$

Equation 6-1 Distensibility
PA= pulmonary artery

Distensibility and compliance are mathematically linked[212], Equation 6-1 and Equation 6-2. Whilst compliance requires measurement of PA pressure, distensibility does not, therefore it can be measured non-invasively. Swift et al. demonstrated a similar inverse relationship between distensibility and PVR, Figure 6-1, as demonstrated between compliance and PVR[340], Figure 1-27 page 76.

$$Compliance\ (mm^2/mmHg) = 100\ x\ \frac{Maximum - minimum\ PA\ area}{Systolic - diastolic\ PAP}$$

Equation 6-2 Compliance
PA= pulmonary artery. PAP= PA pressure

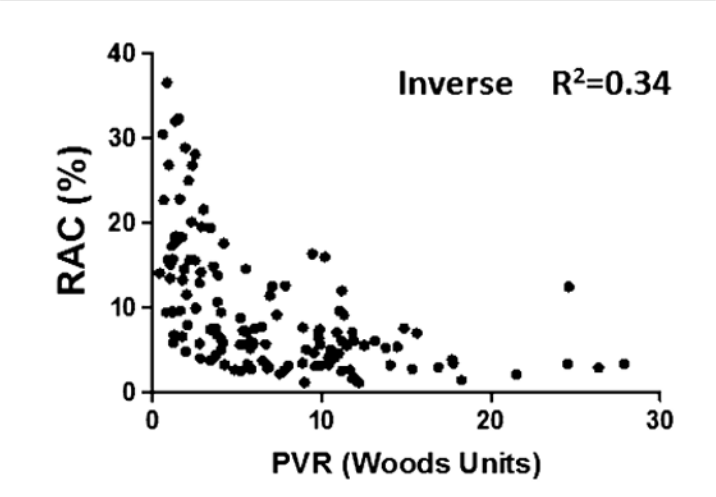

Figure 6-1 Relationship between distensibility and pulmonary vascular resistance
Distensibility (RAC in image) has an inverse relationship with pulmonary vascular resistance (PVR). Image from Swift et al.[340].

Numerous studies have demonstrated that distensibility (or any other term used to describe the product of Equation 6-1) is reduced in PAH[212, 213, 340-342, 349]. Ray et al. demonstrated that MPA distensibility is markedly reduced, even in mild PAH and therefore may be able to detect early PAH[350]. In this setting, it is also predictive of; poor outcome[340], reduced functional capacity[149], response to treatment[343] and survival[211, 340, 344]. Distensibility has also been shown to be a better predictor of survival than other methods of assessing afterload. Gan et al. found that distensibility of <16% (AUROC=0.78) is a stronger predictor of death

than PVR (AUROC=0.67) [211], Figure 6-2. Similarly, Swift et al. demonstrated that MPA distensibility <16% was predictive of reduced survival, whereas compliance and PVR were not[340].

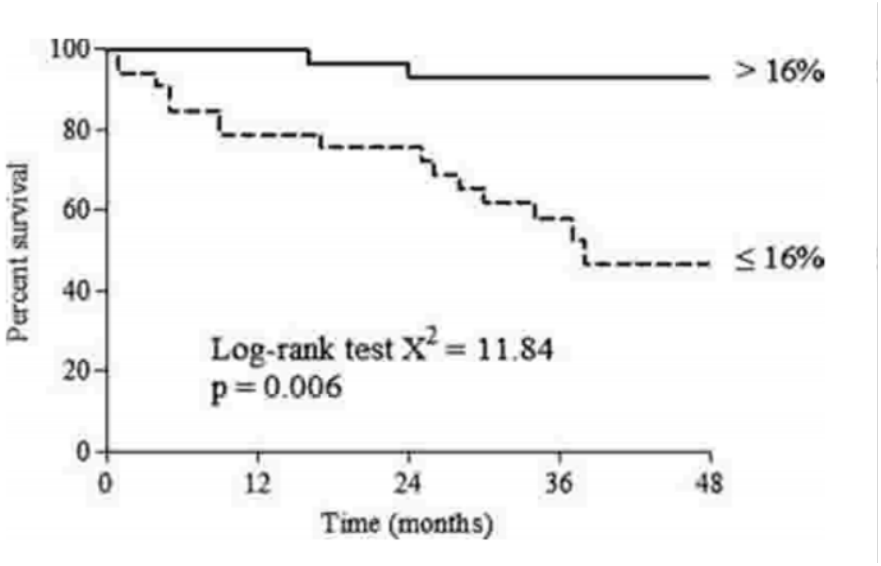

Figure 6-2 Distensibility Kaplan-Meier survival curve
Kaplan-Meier survival curve for distensibility above and below 16% in a pulmonary hypertension cohort. Image from Gan et al. [211].

The differences in vessel area and distensibility between main and left/right pulmonary arteries has been investigated sparingly. Some studies have negated this by using the left/right pulmonary artery for assessment, with the assumption of uniform disease between each lung[211, 351]. Given the predominately unilateral insult in lung resection it is clearly important to assess potential differences in the MPA and PA branches (LPA and RPA).

6.1.2 Flow measurements

An example of a flow profile generated from CMR and its interpretation is shown in Figure 6-3. Measurements of peak flow, time to peak flow (pulmonary artery acceleration time (PAAT)), ejection time (ET) and flow rate can all be made from simple interpretation of the flow profile[346]. Total blood flow can also be calculated as the area under the curve for the entire cardiac cycle. PAAT may be influenced by heart rate although PAAT/ET normalises the PAAT to the duration of cardiac ejection (systole)[342]. PAAT and PAAT/ET have been shown to be reduced in PAH and CTEPH[213, 342, 345, 346, 351-353].

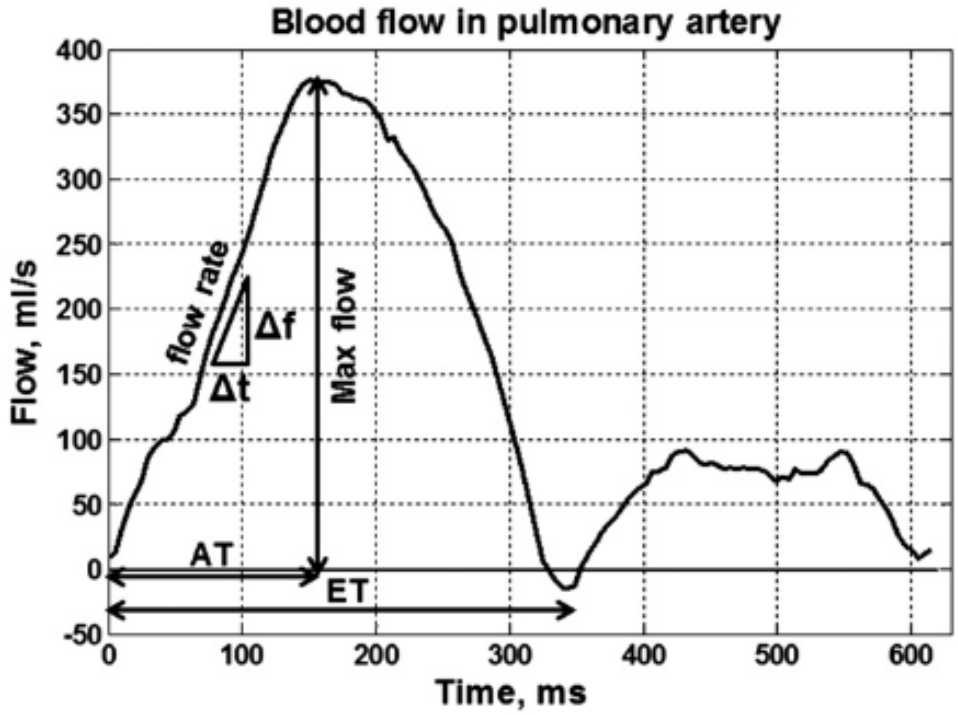

Figure 6-3 Assessment of pulmonary artery flow profile
Representative plot of flow against time in the pulmonary artery. Parameters derived from plot include max/peak flow, acceleration time (AT), ejection time (ET) and acceleration flow rate ($\Delta f/\Delta t$). Image from Ibrahim et al.[354]

In CTEPH, there is a characteristic 'notched' appearance to the flow profile[345, 346, 351, 353], Figure 6-4. This has been shown to be secondary to a proximal site of wave reflection, i.e. a proximal clot in CTEPH[351]. Wave reflection is the reflection of forward travelling blood flow from a change in vessel calibre or compliance, this is discussed in detail in 7.2.4.4 page 242. The notch disappears following removal of the clot by pulmonary endarterectomy (PEA), whilst elevated PAPs may persist due to distal changes in the pulmonary vasculature[346], Figure 6-4.

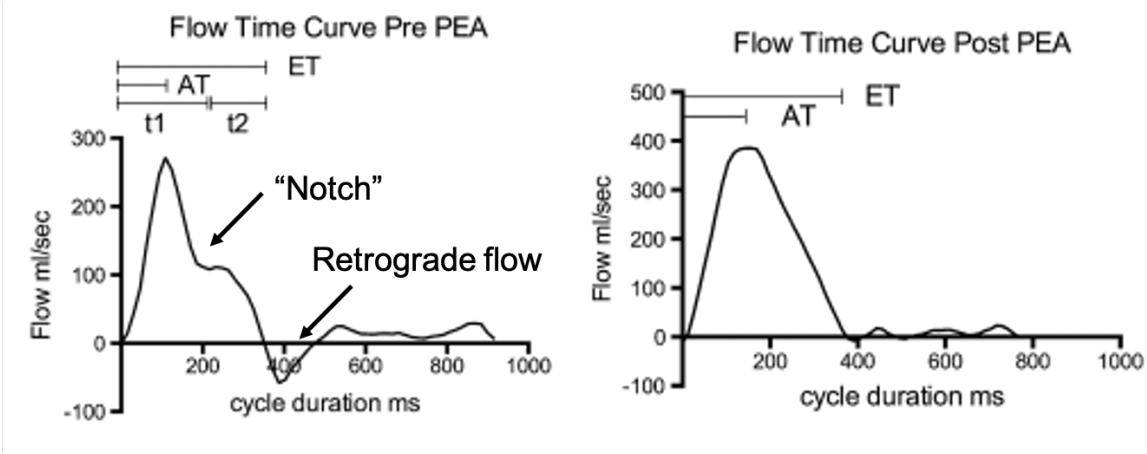

Figure 6-4 Flow profile with and without proximal clot
Plots of flow against time in patient with chronic thromboembolic pulmonary hypertension before pulmonary artery endarterectomy (PEA) (left) and after PEA (right). Note notching of flow profile and negative (retrograde) flow in pre-PEA patient, (marked on left plot). Images from Rolf et al.[346].

6.2 Hypotheses

As detailed in Chapter 3 and throughout this thesis the hypothesised change in pulsatile afterload following lung resection are:

- Pulsatile afterload, measured by PAAT, PAAT/ET and distensibility,
    a. increases following lung resection
    b. predominately affects operative PA.
- The magnitude of increase in pulsatile afterload rate will be associated with
    a. reduction in RVEF
    b. increased BNP
    c. impaired strain[mm]

6.3 Methods

The description of the generic methods, statistical analysis plan, patient population and previously described results are discussed in Chapter 4. Methodology specific to this investigation is explained below.

6.3.1 Analysis

6.3.1.1 Image interpretation

Anonymised and randomised cardiac magnetic resonance scans were uploaded into the proprietary CMR analysis software (Argus, Siemens, Erlangen, Germany) as per 4.4.1.3 page 128. Flow and area assessment was performed for the MPA, RPA and LPA as per Schulz-Menger et al.[249], detailed below.

Argus displayed a single perpendicular slice of the artery in phase[nn] and magnitude images of the 30 frames comprising a cine loop of the cardiac cycle, Figure 6-5. The border of the vessel was manually traced in the frame with the greatest intensity of flow then Argus extrapolated the border to each frame of the cardiac

[mm] This will be explored in Chapter 8.

[nn] Phase-contrast CMR quantifies blood velocity by measuring the change in phase (proportional to blood velocity) compared to stationary tissue. The brightness of the blood increases with increasing of blood velocity in the phase images, this results in greatest demarcation of the vessel outline during systole. Magnitude images best display the anatomical structures[355, 356].

cycle. Visual inspection and augmentation of the extrapolated border was performed for each frame. Flow, velocity and vessel area were plotted by Argus for each frame and displayed as plots against time. Visual inspection of the plots was performed prior to generating the final results. Results were generated as a ".txt" file. Similar to Chapter 5, an automated programme was written by the author to convert the ".txt" files to an excel ".csv" file in R Studio (Microsoft, Version 1.1.463). Once in ".csv" format the data was uploaded to R Studio for processing and analysis as detailed below.

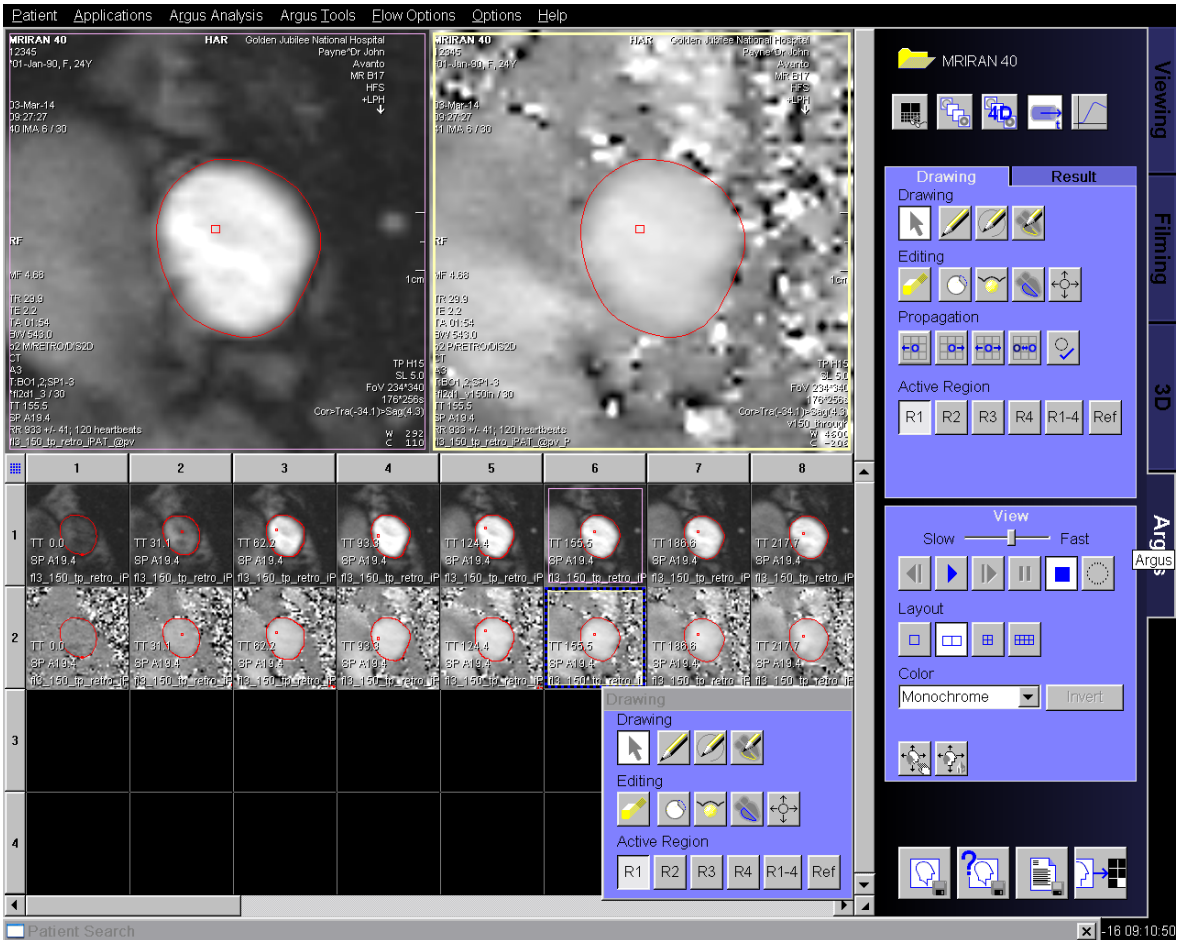

Figure 6-5 Main pulmonary artery interpretation
Top left panel of top row display the magnitude images of the main pulmonary artery. Top right panel and bottom row display the phase images of the same artery. Each column of the bottom panel represents a frame of the cine loop of the cardiac cycle. Endocardial border mapping displayed by red line in both magnitude and phase images and in each pane of the cardiac cycle in the corresponding rows. Image from study patient MRIRAN40.

All images and vessels were dual reported by Alex Arthur (clinical research fellow) and the author. Six weeks after initial reporting, a further 9 patients (27 vessels) were randomly selected for repeat interpretation by the author to calculated intra-observer variability.

6.3.1.2 Data processing

Data processing was performed in R Studio with an original R programme written by the author. The process described below was repeated for each individual vessel in each scan. In order to differentiate the changes in pulsatile afterload between the PA (RPA or LPA) supplying the operated lung and the PA supplying the non-operated they was termed “operative” or “non-operative” dependent on the side of lung resection. For example, in a patient who had a right sided lobectomy the RPA would be termed the operative PA for each time point whilst the LPA would be the non-operative PA.

The two “.csv” files for the interpreter’s report of an individual vessel were uploaded into R Studio. The averages were calculated for the measurements of flow, area and velocity at each individual time point between the two reports. Averaging of the measured data prior to interpretation was performed to reduce inaccuracies at individual time points in an attempt to minimise the artifactual changes in area and flow prior to interpretation. This is particularly important in the subsequent wave intensity analysis investigation, Chapter 7. The data was then interpolated to 1 millisecond temporal resolution by performing a spline fit without smoothing of the data, Figure 6-6.

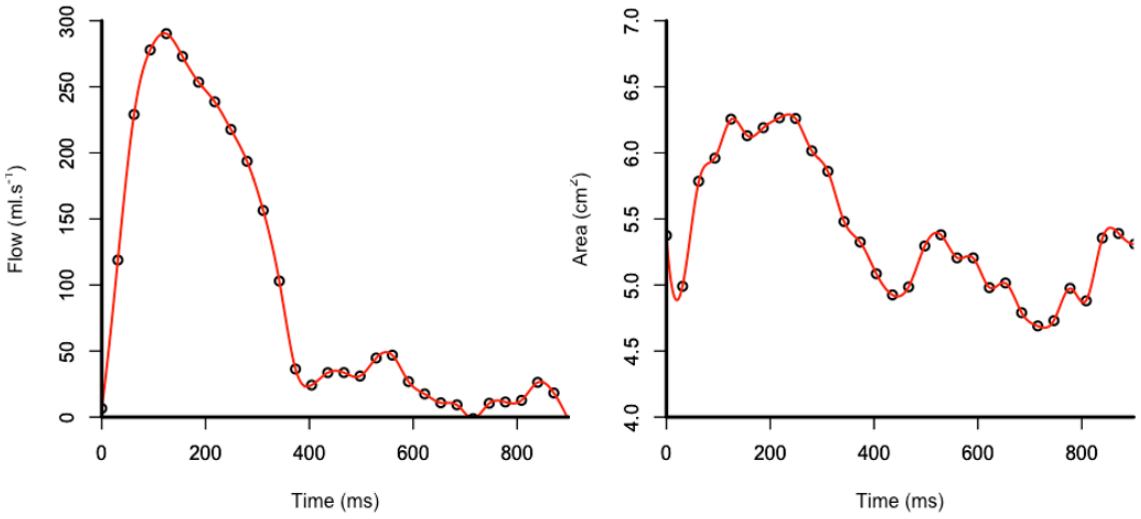

Figure 6-6 Flow and area plots demonstrating interpolation
Flow (left plot) and area (right plot) vs time plots from the main pulmonary artery of scan MRIRAN 40[oo] in this study. Black circles represent measured data points whilst the red line demonstrates these results following temporal interpolation. Note no divergence from measured values.

[oo] Results for MRIRAN 40 are used repeatedly for consistency between plots and images.

Peak flow was measured as the value of maximal flow and PAAT was measured as the time to peak flow. As PAAT is influenced by heart rate, PAAT was normalised to heart rate by calculating PAAT as a percentage of ejection time (ET). ET is defined as the time from onset of flow to the "horizontalization of flow", i.e. end systole[136], Figure 6-3.

Total flow was measured as the total blood flow per minute in that vessel. This was calculated by the area under the curve for the entire cardiac cycle multiplied by heart rate. For the MPA and the sum of the operative and non-operative PA, this equates to cardiac output. The percentage of the cardiac output (CO) in the operative PA and non-operative PA was calculated as the total flow in that vessel divided by the sum of the flow in the operative PA and non-operative PA combined, Equation 6-3. Of note the percentage.CO was only calculated if both vessels were imaged at that time point, the patient that had a pneumonectomy is therefore not included in this analysis.

$$Non.op\ PA\ percentage.\mathrm{CO}\ (\%) = 100\ x\ \frac{total\ non.op\ PA\ flow}{total\ op\ PA\ flow + total\ non.op\ PA\ flow}$$

Equation 6-3 Percentage of non-operative cardiac output
Non-op= non-operative. PA= pulmonary artery. Op= operative.

Pulmonary artery distensibility was calculated from the maximum and minimum area, as per Equation 6-1 page 195. In order to check accurate detection of PAAT and distensibility, minimum and maximum areas ".pdf" files were generated for the flow and area against time plots for each vessel with the point of measurement indicated. Visual inspection of all plots was performed to ensure accurate detection of results, Figure 6-7. This process was repeated for the 3 vessels in each of the scans.

To calculate inter- and intra-observer variability, the process detailed above was performed for the results generated by each interpreter's original analysis without averaging of values. Comparison was made on the results generated for peak flow, PAAT, total flow, maximum and minimum areas. The methodology and interpretation of reliability and variability assessment is discussed previously in 4.3.8.1 page 125.

6.4 Results

As described in Chapter 4, CMR scans were completed in 27 patients pre-operatively[pp], 22 on POD2 and 24 at 2-months. In three of these scans imaging was not completed in all three PAs. In the two post-operative scans of RV6 (the patient that had an on-table conversion to pneumonectomy) the LPA had been resected and so was not imaged. Due to a scanning oversight, neither the LPA nor RPA was visualised in the POD2 scan of RV14. All imaged vessels were included in the analysis. In total, 73 scans are included in the analysis with results available for 215 vessels (73 MPAs, 70 LPAs and 72 RPAs).

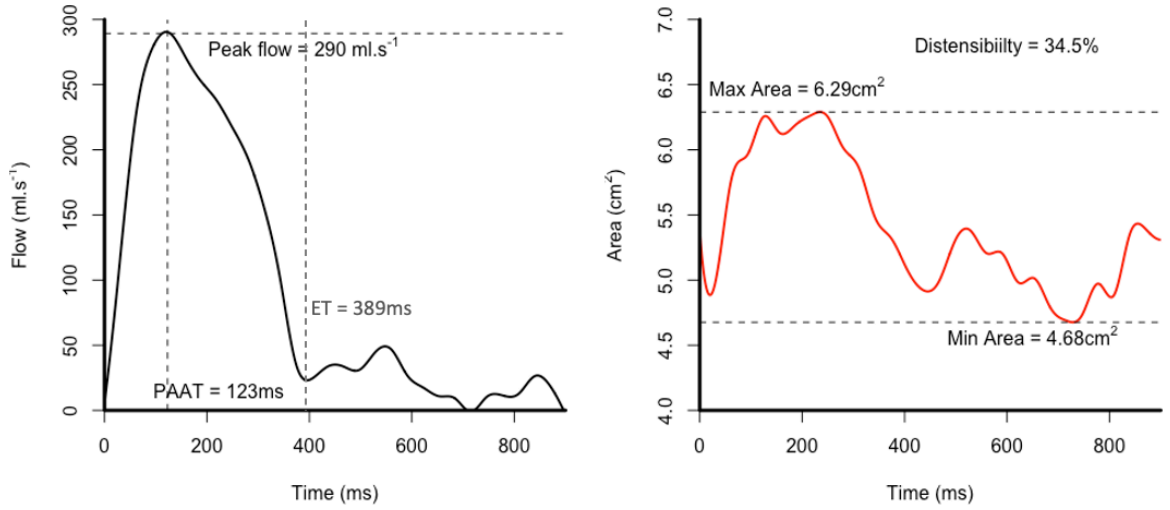

Figure 6-7 Normal flow and area plot interpretation
Example of interpretation of flow and area plots against time. For the flow plot (left panel) R was programmed to detect the peak flow, the time at which it occurs (pulmonary artery acceleration time (PAAT)) and the time to end of ejection (ET). For the area plot (right panel) R was programmed to detect the minimum and maximum area for distensibility calculation. The results generated were programmed to be displayed on the plots of flow and area for visual inspection. Images of the MPA of MRIRAN 40 from this study.

Visual inspection was performed for the plots of area and flow against time for all vessels, examples shown in, Figure 6-7. The were no abnormalities detected in flow profiles for any vessel. Whilst there were no obvious area plot abnormalities detected in the RPA or LPA, there were numerous abnormalities revealed in MPA scans. Non-physiological diastolic peaks in area were visualised in 14 MPA scans (8 pre-op, 2 POD2 and 4 at 2-months), an example is shown in Figure 6-8. Area and distensibility analyses are therefore only performed on the MPA scans without the

[pp] Of note the one patient that did not have a short axis stack of the ventricles performed at pre-operative scanning did have flow analysis performed and so is included in this analysis.

diastolic movement artefact, discussed further in 6.6.1. The flow profile was not affected by the artefact therefore all of the MPA flow results were included in analysis.

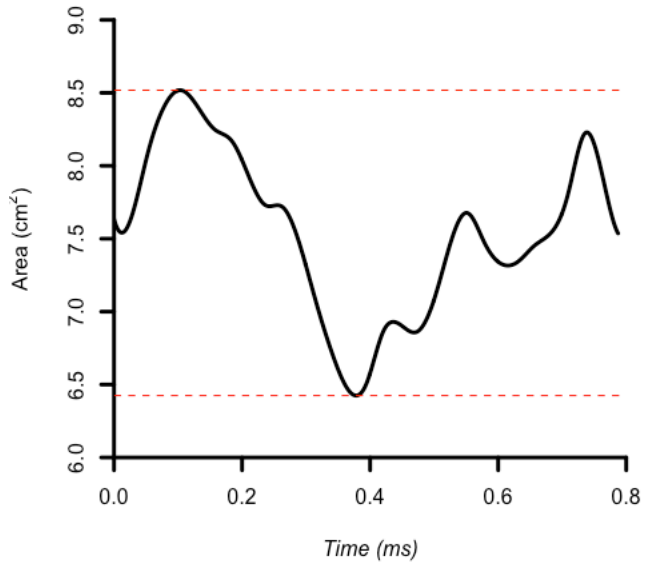

,

Figure 6-8 Example of main pulmonary artery plot with artifact
Area against time plot for main pulmonary artery (PA), red lines highlight minimum and maximum area. Note the minimum area occurs towards end-systole with a marked increase in area following this. There was no reciprocal change in flow to correspond to the increase in area or corresponding diastolic area changes in the operative or non-operative PAs (not shown). Image MPA of MRIRAN69 from study.

6.4.1 Reliability and variability of measurements

6.4.1.1 Interobserver reliability and variability

Interobserver testing showed good to excellent agreement and variance for all flow measurements, Table 6-1. Maximal and minimal areas showed good/excellent agreement for all vessels (ICC > 0.919 CV < 5.24% and ICC > 0.847 CV < 10.37%) with maximal area agreement and variance superior to minimum area in each comparison.

Measure	Vessels	Result	CV (%)	ICC (95% CI)	p value
Flow	All n=215	Peak flow (ml.s^{-1})	4.10	0.983 (0.977, 0.987)	<0.001
		PAAT (ms)	5.96	0.876 (0.839, 0.905)	<0.001
		Total flow (ml)	4.10	0.987 (0.983, 0.990)	<0.001
	LPA + RPA n=142	Peak flow (ml.s^{-1})	4.55	0.959 (0.942, 0.971)	<0.001
		PAAT (ms)	5.90	0.872 (0.824, 0.908)	<0.001
		Total flow (ml)	4.57	0.964 (0.949, 0.974)	<0.001
	MPA n=59	Peak flow (ml.s^{-1})	4.11	0.984 (0.979, 0.988)	<0.001
		PAAT (ms)	5.94	0.880 (0.842, 0.909)	<0.001
		Total flow (ml)	4.09	0.987 (0.982, 0.990)	<0.001
Area	All n=215	Maximum area (cm^2)	5.17	0.955 (0.941, 0.966)	<0.001
		Minimum area (cm^2)	9.16	0.935 (0.914, 0.950)	<0.001
	LPA + RPA n=142	Maximum area (cm^2)	5.24	0.917 (0.885, 0.940)	<0.001
		Minimum area (cm^2)	10.37	0.847 (0.778, 0.893)	<0.001
	MPA n=59	Maximum area (cm^2)	5.03	0.957 (0.943, 0.968)	<0.001
		Minimum area (cm^2)	9.20	0.937 (0.916, 0.953)	<0.001

Table 6-1 Interobserver variability for flow and area results
Intraclass correlation coefficient (ICC) calculated as interobserver two-way mixed method absolute agreement. PA= pulmonary artery. LPA= left PA. RPA= right PA. MPA= main PA. PAAT= pulmonary artery acceleration time. CV= coefficient of variation. CI= confidence interval. 73 dual reported scans.

6.4.1.2 Intraobserver reliability and variability

Intraobserver testing showed excellent reliability and variability for flow measurements (ICC>0.94, CV<4.94%), Table 5-2. Area plots had good reliability and good variability (ICC>0.859, CV<7.71%) for maximum and minimum areas.

Measure	Vessels	Result	CV (%)	ICC (95% CI)	p value
Flow	All n=27	Peak flow (ml.s^{-1})	2.24	0.998 (0.996, 0.999)	<0.001
		PAAT (ms)	3.90	0.960 (0.913, 0.982)	<0.001
		Total flow (ml)	1.82	0.998 (0.993, 0.999)	<0.001
	LPA + RPA n=18	Peak flow (ml.s^{-1})	2.83	0.997 (0.991, 0.999)	<0.001
		PAAT (ms)	3.35	0.970 (0.919, 0.989)	<0.001
		Total flow (ml)	2.31	0.991 (0.952, 0.997)	<0.001
	MPA n=9	Peak flow (ml.s^{-1})	1.12	0.997 (0.988, 0.999)	<0.001
		PAAT (ms)	4.94	0.941 (0.770, 0.986)	<0.001
		Total flow (ml)	0.90	0.999 (0.997, 1.000)	<0.001
Area	All n=27	Maximum area (cm^2)	3.44	0.982 (0.961, 0.992)	<0.001
		Minimum area (cm^2)	6.90	0.947 (0.886, 0.976)	<0.001
	LPA + RPA n=18	Maximum area (cm^2)	3.54	0.981 (0.946, 0.993)	<0.001
		Minimum area (cm^2)	7.71	0.910 (0.773, 0.966)	<0.001
	MPA n=9	Maximum area (cm^2)	3.23	0.971 (0.882, 0.993)	<0.001
		Minimum area (cm^2)	5.37	0.859 (0.522, 0.966)	<0.001

Table 6-2 Intraobserver variability for flow and area results
Intraclass correlation coefficient (ICC) calculated as intraobserver two-way mixed method absolute agreement. PA= pulmonary artery. LPA= left PA. RPA= right PA. MPA= main PA. PAAT= pulmonary artery acceleration time. CV= coefficient of variation. CI= confidence interval. 9 repeated scans.

6.4.2 Flow results

6.4.2.1 Changes in blood flow and distribution over time

Total blood flow, measured in the MPA, increased at POD2 before returning to pre-operative level of flow by 2-months, Table 6-3. Compared to pre-op, at POD2 and 2-months, both the value of total flow and the percentage of CO were reduced in the operative PA and increased in the non-operative PA ($p<0.001$, paired t-test for all). Pre-operatively, there was no difference between the percentage of CO travelling in the (what would be) operative PA and in the non-operative PA ($p=0.486$, unpaired t-test) although non-operative PA percentage of CO was greater than in the operative PA at POD2 and at 2-months (both $p<0.001$, unpaired t-test), Figure 6-9.

Vessel	Parameter	Pre-op	POD2	2-months	p-value
MPA	Total flow ($l.min^{-1}$)	6.57 (1.68)	8.00 (1.57) #	6.52 (1.65) ¥	***<0.001 ****
	Peak flow ($ml.s^{-1}$)	351.5 (332.8, 388.6)	389.8 (347.0, 434.4) #	339.2 (293.6, 388.2) #¥	***0.026 §***
	n	27	22	24	
Operative PA	Total flow ($l.min^{-1}$)	2.99 (0.82)	2.31 (0.74) #	2.33 (0.75) #	***<0.001 ****
	Percentage of CO (%)	51.92 (6.23)	33.69 (9.52) #	39.06 (11.41) #¥	***<0.001 ****
	Peak flow ($ml.s^{-1}$)	181.9 (52.4)	123.6 (42.1) #	117.8 (44.3) #¥	***<0.001 ****
	n	27	20	23	
Non-operative PA	Total flow ($l.min^{-1}$)	2.82 (0.96)	4.72 (1.43) #	3.84 (1.45) #¥	***<0.001 ****
	Percentage of CO (%)	48.08 (6.23)	66.31 (9.52) #	60.94 (11.41) #¥	***<0.001 ****
	Peak flow ($ml.s^{-1}$)	156.6 (136.7, 179.8)	247.8 (195.5, 284.8) #	197.5 (164.2, 260.0) #¥	***<0.001 §***
	n	27	21	24	

Table 6-3 Changes in flow in pulmonary arteries over time
Values are mean (SD) or median (IQR). PA=pulmonary artery. MPA=main PA. *= one-way repeated measures ANOVA. §= Friedman's test. #= significant difference from pre-op. ¥= significant difference from post-operative day 2 (POD2). Percentage of flow is calculated from sum of operative and non-operative vessel flow. Significant results ($p<0.05$) highlighted ***bold italics.***

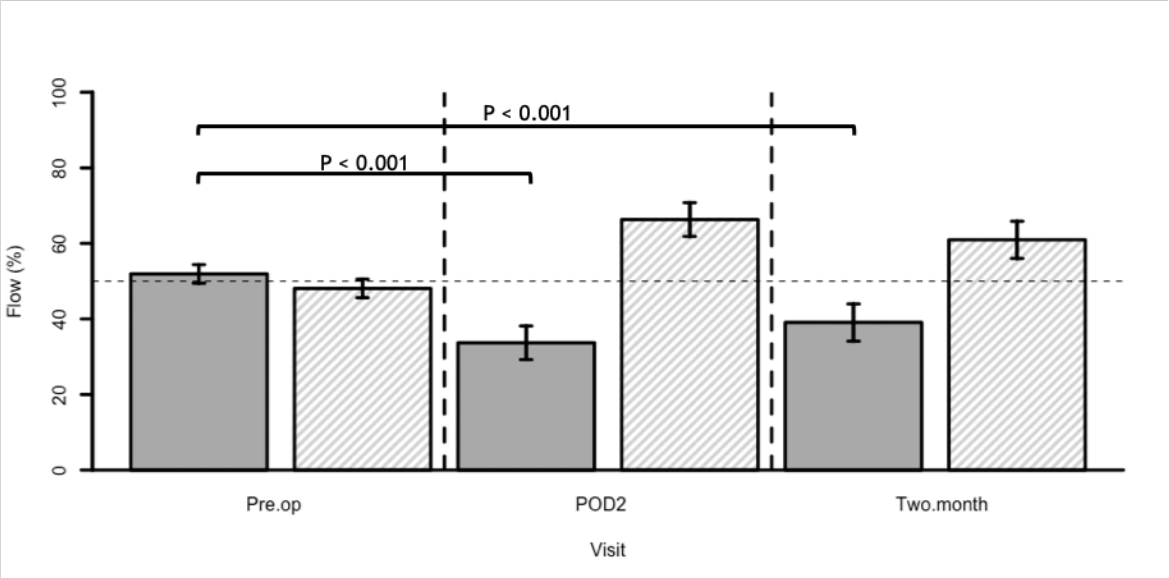

Figure 6-9 Changes in distribution of pulmonary artery blood flow over time
Percentage of blood flow through the operative pulmonary artery (PA) (dark grey boxes) and non-operative (light grey boxes). Note reduction in percentage of total blood flow on operative PA at post-operative day 2 (POD2) and 2-months compared to pre-operative, ($p<0.001$, paired t-test for both). Operative PA flow percentage lower than non-operative at POD2 and 2-months (unpaired t-test for both). Bar plot represents mean and 95% CI.

Compared to pre-operatively, on POD2 and at 2-months, peak flow was increased in the non-operative PA (both $p<0.001$, paired Wilcoxon signed rank test) and decreased in operative PA (both $p<0.001$, paired t-test). Operative PA and non-operative PA peak flow was similar pre.op ($p=0.256$, Wilcoxon rank sum test)

whereas operative PA peak flow was lower than non-operative PA at POD2 and 2-months ($p<0.001$, Wilcoxon rank sum test).

6.4.2.2 Pulmonary artery acceleration time

Pulmonary artery acceleration time was shorter at POD2 and 2-months in the MPA, Table 6-4 and Figure 6-10. PAAT was also shorter in the operative PA and non-operative PA at POD2, although by 2-months only operative PA remained shorter than pre-op, Figure 6-11. There was no difference between operative PAAT and non-operative PAAT pre-operatively ($p=0.588$, unpaired t-test) although operative PAAT was shorter than non-operative PAAT on POD2 and at 2-months ($p=0.008$ and $p=0.022$ respectively, both unpaired t-test). When corrected for heart rate, PAAT/ET, the POD2 reduction remained significant in all vessels whereas at 2-months only operative PAAT/ET was shorter than pre-operatively. Compared to the non-operative PA, operative PAAT/ET was shorter on POD2 and at 2-months ($p=0.007$ and $p=0.046$, unpaired t-tests).

Vessel	Parameter	Pre-op	POD2	2-months	p-value
MPA	PAAT (ms)	115.9 (20.7)	82.7 (18.9) #	104.0 (19.5) #¥	***<0.001 ****
	PAAT/ET (%)	30.0 (3.8)	24.0 (5.4) #	29.0 (5.9) ¥	***<0.001 ****
	n	27	22	24	
Operative PA	PAAT (ms)	124.7 (19.3)	82.1 (23.0) #	106.0 (23.9) #¥	***<0.001 ****
	PAAT/ET (%)	31.3 (4.5)	23.1 (5.3) #	28.2 (6.4) #¥	***<0.001 ****
	n	27	20	23	
Non-operative PA	PAAT (ms)	128.0 (24.8)	100.5 (18.8) #	121.4 (20.4) ¥	***<0.001 ****
	PAAT/ET (%)	31.9 (5.3)	27.1 (4.3) #	32.0 (4.7) ¥	***0.003 ****
	n	27	21	24	

Table 6-4 Pulmonary artery acceleration time results
Values are mean (SD). PA= pulmonary artery. MPA= main PA. PAAT= PA acceleration time. ET= ejection time. *= one-way repeated measures ANOVA. §= Friedman's test. #= significant difference from pre-op. ¥= significant difference from post-operative day 2 (POD2). Significant results ($p<0.05$) highlighted ***bold italics.***

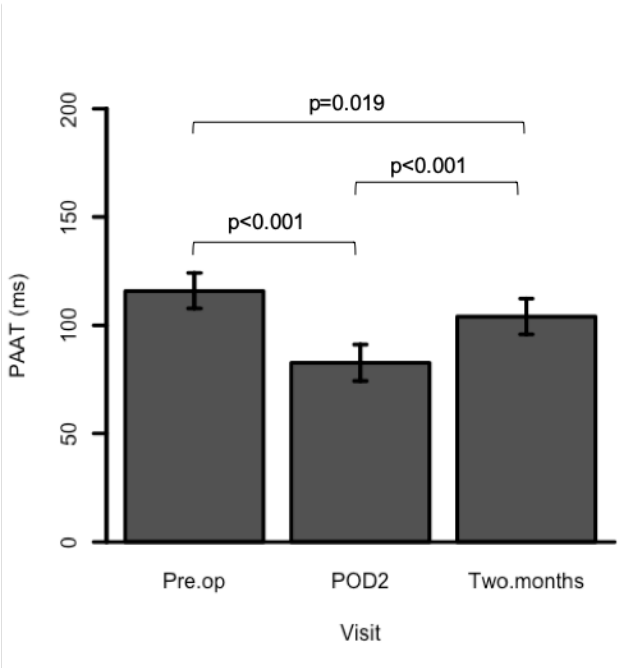

Figure 6-10 Main pulmonary artery acceleration time
Main pulmonary artery acceleration time (PAAT) was shorter at post-operative day 2 (POD2) and 2-months. All paired t-tests.

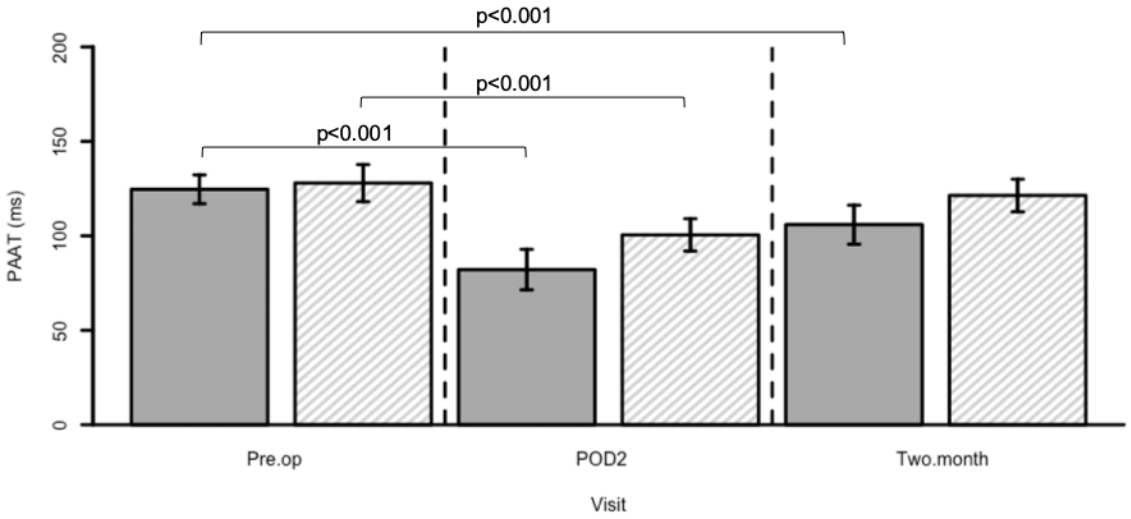

Figure 6-11 Operative and non-operative pulmonary artery acceleration time
Pulmonary artery acceleration time (PAAT) was shorter at post-operative day 2 (POD2) in operative pulmonary artery (PA) (dark grey boxes) and non-operative PA (light grey boxes) whilst only operative PA remains shortened at 2-months. All paired t-tests. Note operative PA PAAT lower than non-operative PA at POD2 and 2-months (p=0.008 and p=0.022 respectively, unpaired t-tests).

6.4.3 Pulmonary artery distensibility

There was no change in MPA distensibility over time, Table 6-5. Operative PA distensibility was decreased from pre.op on POD2 and at 2-months (p=0.020 and p=0.043, both paired t-test) and non-operative PA distensibility was increased at 2-months from POD2 (p=0.012, paired t-test). Non-operative PA and operative PA

distensibility were similar pre.op (p=0.644, unpaired t-test) and on POD2 (p=0.494, unpaired t-test) although operative PA distensibility was lower at 2-months (p=0.027, unpaired t-test), Figure 6-12.

Vessel	Parameter	Pre-op	POD2	2-months	p-value
MPA	Distensibility (%)	30.9 (23.6, 42.1)	31.3 (23.3, 38.6)	27.8 (25.0, 45.7)	***1.000 §***
	n	19	20	20	
Operative PA	Distensibility (%)	65.2 (25.5)	50.7 (16.9) #	51.8 (16.2) #	***0.037 ****
	n	27	20	23	
Non-operative PA	Distensibility (%)	62.6 (23.2)	54.4 (17.7)	67.4 (28.7) ¥	***0.029 ****
	n	27	21	24	

Table 6-5 Distensibility changes over time
Values are mean (SD) or median (IQR). OP= operative. NONOP= non-operative. PA= pulmonary artery. MPA= main PA. *= one-way repeated measures ANOVA. §= Friedman's test. #= significant difference from pre-op. ¥= significant difference from post-operative day 2 (POD2). Significant results (p<0.05) highlighted ***bold italics.***

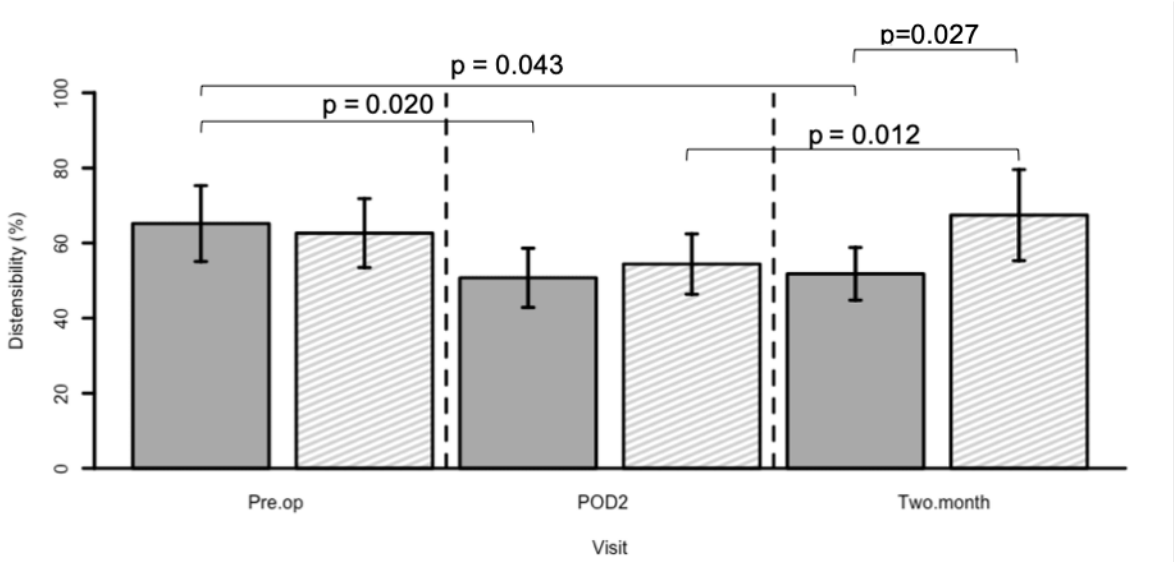

Figure 6-12 Operative and non-operative distensibility
Distensibility was reduced on post-operative day 2 (POD2) in the operative pulmonary artery (PA) (dark grey boxes) and at 2-months. Non-operative PA distensibility (light grey boxes) was increased at 2-months compared to POD2. All paired t-tests. Note operative PA distensibility lower than non-operative PA at 2-months, unpaired t-test.

6.4.4 Association between pulmonary artery acceleration time and distensibility

Within-subject association testing showed that there were weak to moderate positive associations between PAAT and PA distensibility in the operative PAs and between PAAT, PAAT/ET and PA distensibility in the non-operative PA, Table 6-6.

Analysis of covariance, within-subject				
Distensibility (%)				
		MPA	Operative PA	Non-operative PA
PAAT (ms)	r	-0.108	***0.377***	***0.571***
	p	0.551	***0.013***	***<0.001***
PAAT/ET (%)	r	-0.142	0.245	***0.410***
	p	0.430	0.114	***0.005***

Table 6-6 Associations between pulmonary artery acceleration time and distensibility
PAAT= pulmonary artery acceleration time. PAAT/ET= PAAT/ejection time, normalised for heart rate. PA= pulmonary artery. Analysis of covariance with patient as factor. Significant results ($p<0.05$) highlighted ***bold italics.***

6.4.5 Association between right ventricular ejection fraction and afterload results

6.4.5.1 Pulmonary artery acceleration time

Within-subject association testing between pre-op and POD2 revealed that there were moderate to strong positive within-subject associations between the change in RVEF and the change in PAAT in all vessels, Table 6-7, although when corrected for heart rate (PAAT/ET) only the association in the non-operative PA retained significance, Figure 6-13. The shortening in non-operative PAAT/ET (increase in pulsatile afterload) was associated with a decrease in RVEF. Looking at individual time points, PAAT and PAAT/ET had moderate positive associations with RVEF on POD2. Again, a shorter PAAT or PAAT/ET (increased afterload) was associated with reduced RVEF, Figure 6-14.

Analysis of covariance, within-subject								
Change between pre-op and POD2								
			PAAT (ms)			PAAT/ET (%)		
			MPA	Operative PA	Non-operative PA	MPA	Operative PA	Non-operative PA
RVEF		r	***0.571***	***0.519***	***0.613***	0.400	0.329	***0.482***
		p	***0.004***	***0.016***	***0.002***	0.059	0.146	***0.023***
Change between pre-op and 2-months								
			PAAT (ms)			PAAT/ET (%)		
			MPA	Operative PA	Non-operative PA	MPA	Operative PA	Non-operative PA
RVEF		r	-0.046	0.099	-0.042	-0.086	0.094	0.118
		p	0.836	0.662	0.848	0.697	0.676	0.592
Individual time point analysis								
			PAAT (ms)			PAAT/ET (%)		
			MPA	Operative PA	Non-operative PA	MPA	Operative PA	Non-operative PA
RVEF	Pre-op	r	-0.075	-0.210	-0.003	-0.076	-0.301	0.034
		p	0.716	0.304	0.989	0.712	0.135	0.870
	POD2	r	0.323	0.125	***0.464***	0.322	0.001	***0.459***
		p	0.143	0.598	***0.034***	0.144	*0.995*	***0.036***
	2-months	r	-0.307	-0.011	-0.173	-0.318	-0.184	-0.301
		p	0.155	0.962	0.429	0.0139	0.412	0.163

Table 6-7 Association between pulmonary artery acceleration time and RVEF
PA= pulmonary artery. MPA= main PA. RVEF= right ventricular ejection fraction. POD2= post-operative day 2. Analysis of covariance with patient as factor. All individual time point analysis Pearson's correlation co-efficient. Significant results ($p<0.05$) highlighted ***bold italics.***

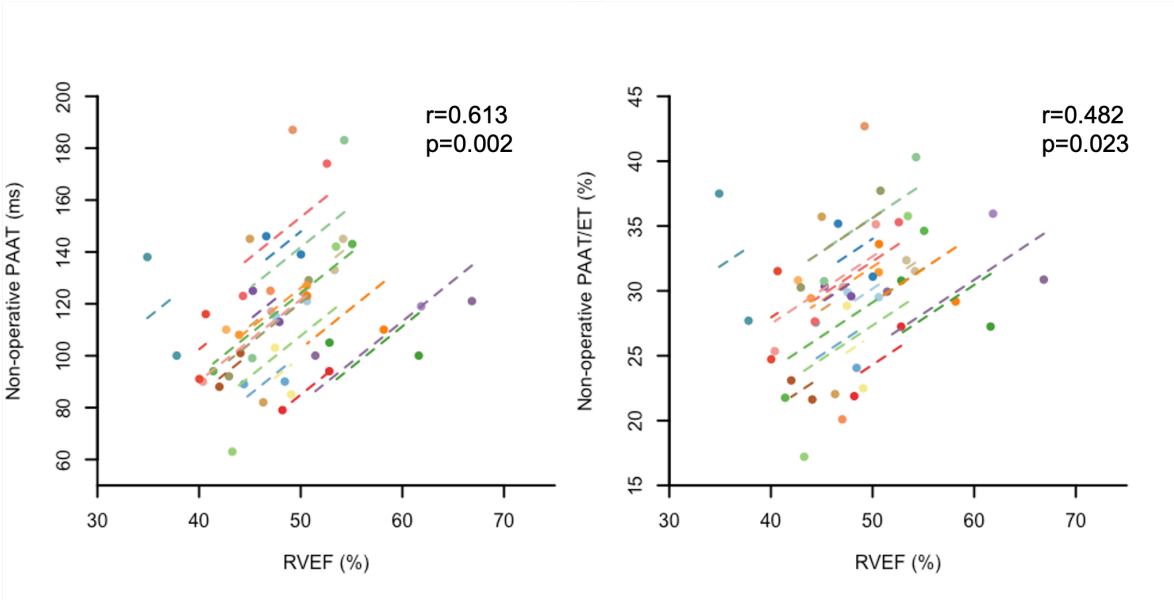

Figure 6-13 Within-subject association between non-operative pulmonary artery acceleration time and right ventricular ejection fraction
Pre-operative to post-operative day 2 within-subject analysis of covariance between non-operative pulmonary artery acceleration time (PAAT, left plot), PAAT/ejection time (PAAT/ET, right plot) and right ventricular ejection fraction (RVEF). Coloured dots represent each patient and lines depict parallel line of association for each patient. Note that a reduction in non-operative PAAT and PAAT/ET were associated with a decrease in RVEF.

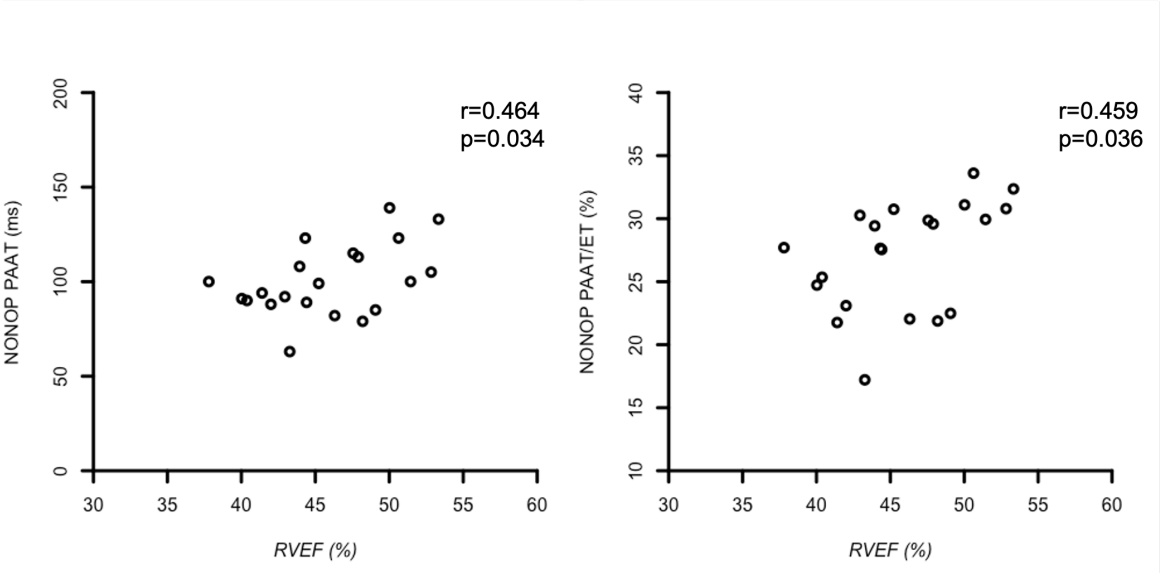

Figure 6-14 Association between PAAT and RVEF on POD2
Note association between non-operative (NONOP) pulmonary artery acceleration time (PAAT, left plot), PAAT/ejection time (PAAT/ET, right plot) and right ventricular ejection fraction (RVEF) at post-operative day 2 (POD2). Both Pearson's correlation co-efficient. ms= millisecond.

6.4.5.2 Distensibility

There were moderate positive within-subject associations in the operative and non-operative PAs between the change in RVEF and the change in PA distensibility between pre-op and POD2, Table 6-8 and Figure 6-15. Again, increased pulsatile

afterload was associated with reduced RVEF. There were no associations between RVEF and distensibility on individual time point analysis in any vessel.

Analysis of covariance, within-subject					
Distensibility (%)					
Change between pre-op and POD2					
			MPA	Operative PA	Non-operative PA
RVEF		r	0.010	***0.488***	***0.547***
		p	0.970	***0.025***	***0.037***
Change between pre-op and 2-months					
			MPA	Operative PA	Non-operative PA
RVEF		r	0.371	0.407	-0.181
		p	0.157	0.060	0.407
Individual time point analysis					
Distensibility (%)					
			MPA	Operative PA	Non-operative PA
RVEF	Pre-op	r	0.038	0.088	0.142
		p	0.880 §	0.667 *	0.488 *
	POD2	r	0.079	-0.131	0.322
		p	0.742 *	0.582 *	0.154 *
	2-months	r	0.209	-0.247	-0.181
		p	0.404 §	0.267 *	0.408 *

Table 6-8 Association between distensibility and RVEF
PA= pulmonary artery. MPA= main PA. RVEF= right ventricular ejection fraction. Analysis of covariance with patient as factor. *= Pearson's correlation co-efficient. §= Spearman's correlation co-efficient. Significant results ($p<0.05$) highlighted ***bold italics.***

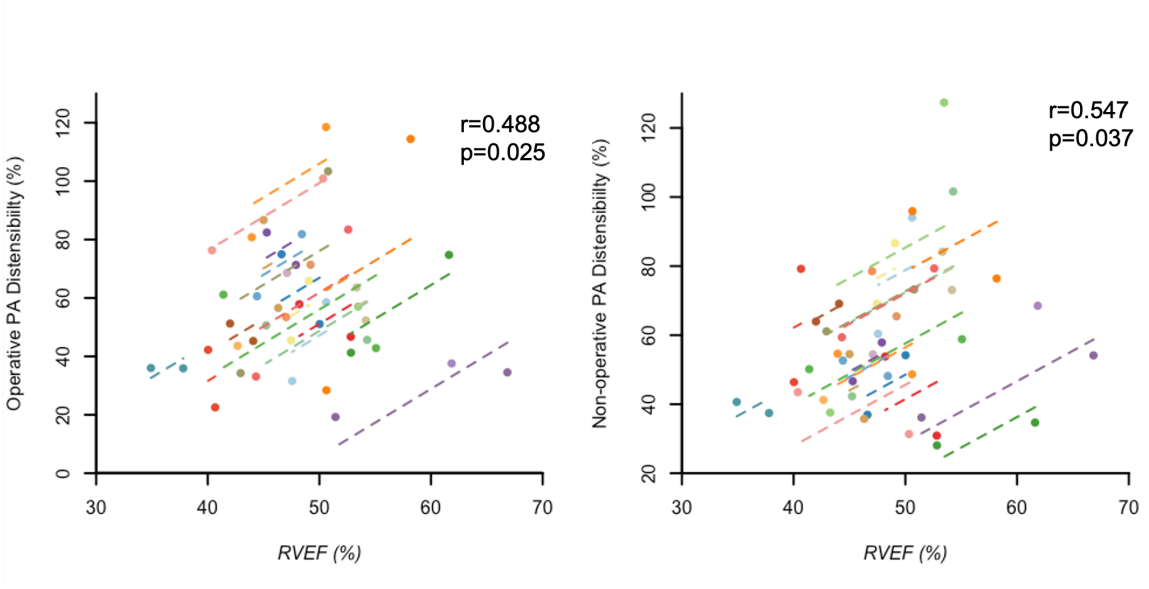

Figure 6-15 Within-subject association between operative pulmonary artery distensibility and right ventricular ejection fraction
Pre-operative to post-operative day 2 within-subject analysis of covariance between operative pulmonary artery (PA) distensibility (left), non-operative PA distensibility (right) and right ventricular ejection fraction (RVEF). Coloured dots represent each patient and lines depict parallel line of association for each patient. Note that a lower operative PA distensibility (increased afterload) was associated with lower RVEF.

6.4.6 Association between brain natriuretic peptide and afterload results

6.4.6.1 Pulmonary artery acceleration time

There were negative within-subject associations between the change in BNP and the change in PAAT in all vessels between pre-op and POD2 analysis, Table 6-9. The MPA and non-operative PA had moderate to strong within-subject associations between the change in PAAT/ET and the change in BNP between pre-op and POD2, Figure 6-16. The negative associations showed that an increase in afterload (shortened PAAT and PAAT/ET) at POD2 was associated with increased BNP release. There were no associations between PAAT or PAAT/ET and BNP at individual time points.

Analysis of covariance, within-subject								
Change between pre-op and POD2								
			PAAT (ms)			PAAT/ET (%)		
			MPA	Operative PA	Non-operative PA	MPA	Operative PA	Non-operative PA
BNP		r	***-0.584***	***-0.392***	***-0.799***	***-0.555***	-0.246	***-0.796***
		p	***0.003***	***0.079***	***<0.001***	***0.006***	0.283	***<0.001***
Change between pre-op and 2-months								
			PAAT (ms)			PAAT/ET (%)		
			MPA	Operative PA	Non-operative PA	MPA	Operative PA	Non-operative PA
BNP		r	0.270	0.240	-0.288	0.300	0.326	-0.250
		p	0.212	0.283	0.183	0.164	0.139	0.249
Individual time point analysis								
			PAAT (ms)			PAAT/ET (%)		
			MPA	Operative PA	Non-operative PA	MPA	Operative PA	Non-operative PA
BNP	Pre-op	r	-0.055	-0.056	-0.116	-0.268	-0.067	-0.232
		p	0.786 §	0.779 §	0.566 §	0.176 §	0.740 §	0.245 §
	POD2	r	-0.248	-0.104	-0.178	-0.359	0.107	-0.389
		p	0.266 *	0.664 *	0.305 *	0.101 *	0.654 *	0.082 *
	2-months	r	0.276	0.202	0.044	0.009	-0.093	-0.245
		p	0.213 §	0.380 §	0.848 §	0.968 §	0.689 §	0.271 §

Table 6-9 Association between pulmonary artery acceleration time and BNP
PA= pulmonary artery. MPA= main PA. BNP= brain natriuretic peptide. POD2= post-operative day 2. Analysis of covariance with patient as factor. All individual time point comparisons Pearson's correlation co-efficient. Significant results ($p<0.05$) highlighted ***bold italics.***

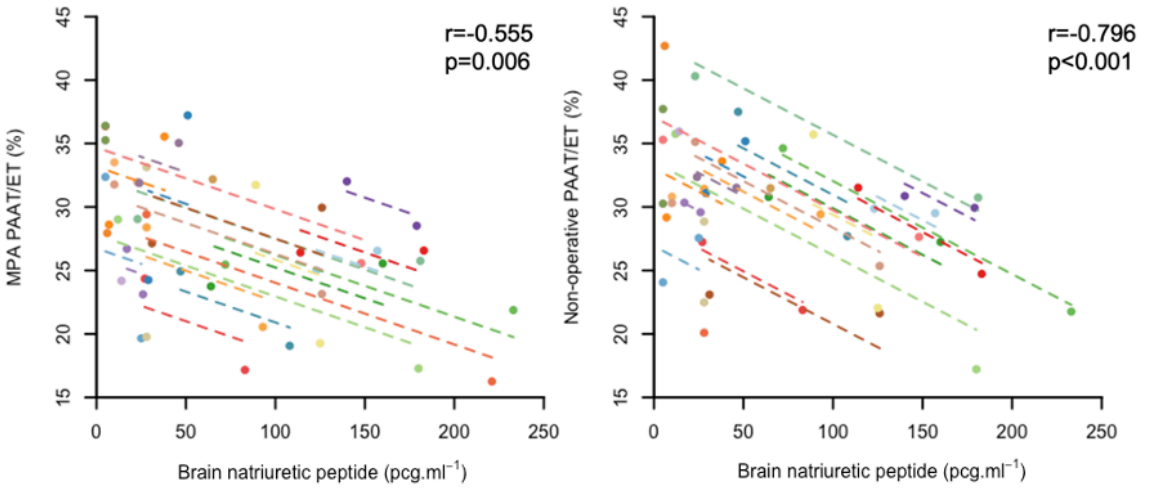

Figure 6-16 Within-subject association between PAAT/ET and brain natriuretic peptide
Pre-operative to post-operative day 2 within-subject analysis of covariance between pulmonary artery acceleration time normalised for heart rate (ejection time, PAAT/ET) in main (left) and non-operative pulmonary artery (right) against brain natriuretic peptide (BNP). Coloured dots represent each patient and lines depict parallel line of association for each patient. Note that shortened PAAT/ET (increased afterload) was associated with an increase in BNP at post-operative day 2.

6.4.6.2 Distensibility

There was a moderate negative within-subject association between the change in BNP and the change in non-operative PA distensibility between pre-op and POD2, Table 6-10. On individual time point analysis, operative PA distensibility had a weak association with BNP pre-operatively whilst MPA and non-operative PA distensibility had a moderate negative association with BNP at POD2, Figure 6-18. In each association an increased afterload is associated with an increase in BNP.

Analysis of covariance, within-subject					
Distensibility (%)					
Change between pre-op and POD2					
			MPA	Operative PA	Non-operative PA
BNP		r	-0.419	-0.143	***-0.535***
		p	0.106	0.535	***0.010***
Change between pre-op and 2-months					
			MPA	Operative PA	Non-operative PA
BNP		r	-0.388	0.004	-0.327
		p	0.137	0.985	0.128
Individual time point analysis					
Distensibility (%)					
			MPA	Operative PA	Non-operative PA
BNP	Pre-op	r	0.206	***-0.382***	-0.139
		p	0.398 ***§***	***0.049 §***	0.490 ***§***
	POD2	r	***-0.484***	-0.177	***-0.545***
		p	***0.031 ****	0.456 *	***0.011 ****
	2-months	r	-0.195	-0.316	-0.018
		p	0.453 ***§***	0.162 ***§***	0.936 ***§***

Table 6-10 Association between distensibility and BNP at individual time points
PA= pulmonary artery. MPA= main PA. BNP= brain natriuretic peptide. Analysis of covariance with patient as factor. *= Pearson's correlation co-efficient. *§*= Spearman's correlation co-efficient. Significant results (p<0.05) highlighted ***bold italics.***

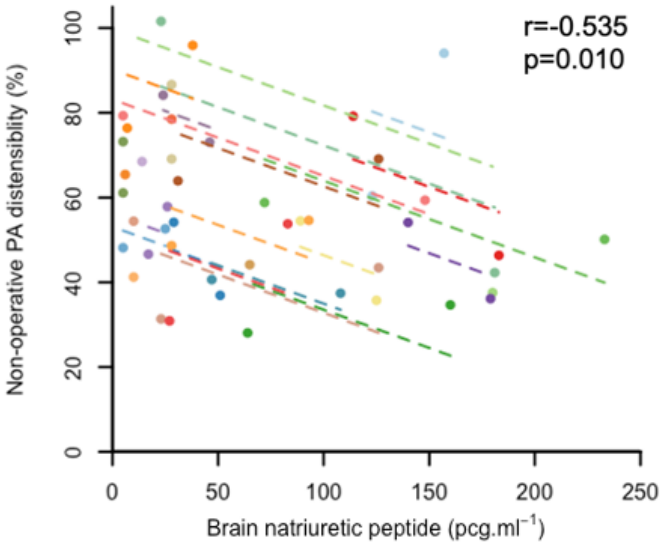

Figure 6-17 Within-subject association between non-operative pulmonary artery distensibility and brain natriuretic peptide
Pre-operative to post-operative day 2 within-subject analysis of covariance between pulmonary artery (PA) distensibility and brain natriuretic peptide (BNP). Coloured dots represent each patient and lines depict parallel line of association for each patient. Note that reduced non-operative distensibility (increased afterload) was associated with an increase in BNP at POD2.

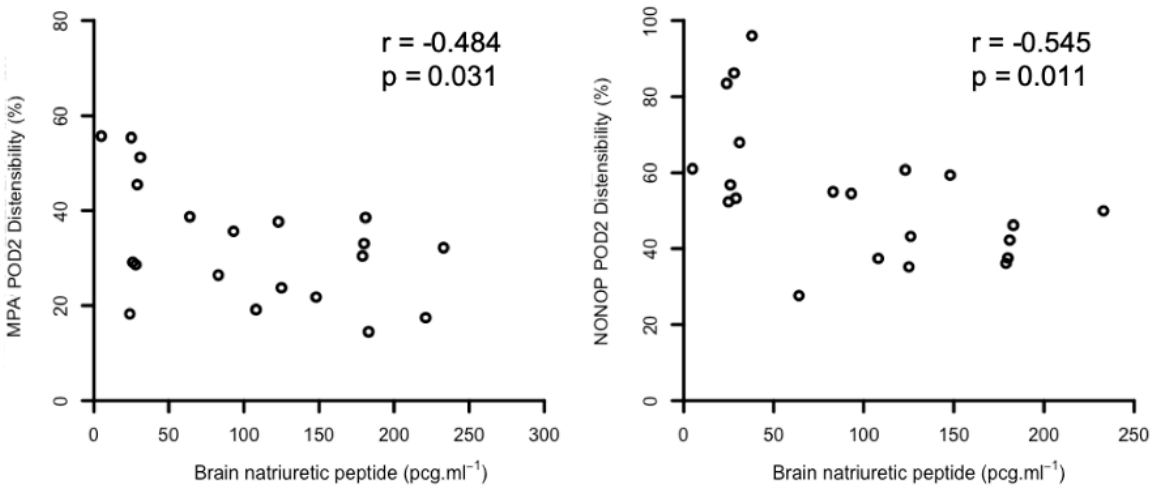

Figure 6-18 Association between main and non-operative pulmonary artery distensibility and BNP on POD2
Main pulmonary artery (MPA) and non-operative pulmonary artery (NONOP) distensibility is moderately associated with brain natriuretic peptide (BNP) at post-operative day 2 (POD2). The patients with the lower distensibility have higher BNP.

6.5 Summary of main results

The main findings of this investigation are summarised in Table 6-11 and Table 6-12. Following lung resection, the distribution of blood flow is uneven between the operative and non-operative PAs, the percentage of flow travelling in the non-operative PA is increased on POD2 (66%) and 2-months (61%). Indices of pulsatile afterload increased following lung resection, predominately in the operative PA. On POD2, PAAT was shortened in all vessels and remained shortened in the MPA and operative PA at 2-months. Distensibility was reduced at both post-operative time points in the operative PA alone, with no changes in the non-operative PA or MPA.

Parameter	Pulmonary artery	Pre-op	POD2	2-months
Percentage of total flow	Operative		↓↓	↓
	Non-operative		↑↑	↑
	Operative vs non-operative	=	↓	↓
PAAT	Main		↓↓	↓
	Operative		↓↓	↓
	Non-operative		↓	-
	Operative vs non-operative	=	↓	↓
PAAT/ET	Main		↓	-
	Operative		↓↓	↓
	Non-operative		↓	-
	Operative vs non-operative	=	↓	↓
Distensibility	Main		-	-
	Operative		↓	↓
	Non-operative		-	-
	Operative vs non-operative	=	=	↓

Table 6-11 Summary of changes in pulmonary artery blood flow, acceleration time and distensibility
PAAT= pulmonary artery acceleration time. PAAT/ET= PAAT normalised for ejection time (heart rate). POD2= post-operative day 2.
Comparisons are POD2 vs pre-op and 2-months vs pre-op. - = no change. ↓= less than pre-operatively. ↓↓= less than pre-op and 2-months. ↑= greater than pre-operatively. ↑↑= greater than pre-op and 2-months.
Operative vs non-operative, no difference between measures (=). ↓= operative less than non-operative. ↑= operative greater than non-operative.

Whilst the increases in indices of pulsatile afterload were predominately in the operative PA the strongest associations with impaired RV function (RVEF and BNP) were in the non-operative PA. A shortening of PAAT and PAAT/ET (increased afterload) in the non-operative PA had a strong negative association with an increase in BNP between pre-op and POD2, i.e. patients with the largest increase in non-operative pulsatile afterload on POD2 had the largest increase in BNP. Similarly, on POD2 a reduction in non-operative PA distensibility had a moderate negative association with BNP and a moderate positive association with RVEF (increased afterload was associated with decreased RVEF). The only consistent within-subject association in the operative PA was that reduced PA distensibility (increased afterload) was associated with a reduction in RVEF between pre-op and POD2. There were no within-subject associations between pre-op and 2-months.

Comparison	Parameter	Pulmonary artery	RVEF	BNP
Pre-op to POD2	PAAT	Main	+ +	- -
		Operative	+ +	-
		Non-operative	+ + +	- - -
	PAAT/ET	Main		- -
		Operative		
		Non-operative	+	- - -
	Distensibility	Main		
		Operative	+ +	
		Non-operative	+ +	- -

Table 6-12 Summary of association between indices of afterload, RVEF and BNP
+/+ +/+ + += weak/moderate/strong positive association. -/- -/- - - = weak/moderate/strong negative association. Blank= no association. RVEF= right ventricular ejection fraction. BNP= brain natriuretic peptide. POD2= post-operative day 2. PAAT= pulmonary artery acceleration time. PAAT/ET= PAAT normalised for ejection time (heart rate). Note associations predominately between pre-op and POD2 in the non-operative PA. NB there were no associations between any index of afterload and RVEF or BNP between pre-op and 2-months, not displayed.

6.6 Discussion

This is the first study to investigate the change in pulsatile afterload following lung resection, as such it is the first to describe a predominately unilateral increase in pulsatile afterload. The distribution of cardiac output is potentially altered by this unilateral increase in afterload. Interestingly, the associations with the measures of pulsatile afterload and RV function are strongest in the non-operative PA, suggesting an inability to accommodate the increased blood flow may result in impaired RV function.

6.6.1 Strengths and limitations

The main strength of this study is the detailed analysis of afterload pre- and post-operatively. Additionally, imaging of the MPA, LPA and RPA provide an overall measure of afterload for both lungs combined and comparison of afterload in the operative and non-operative. CMR provides detailed and reproducible data with inter- and intra-observer testing revealing good to excellent agreement for all measures of flow and area which is comparable to published CMR results[352, 357].

A limitation of the study is the diastolic area increases seen in some of the MPA scans. It is possible that this reflects a true increase in vessel area, however there was no reciprocal change in flow in that vessel and the corresponding operative and non-operative PA area plots do not show matching diastolic increases in area

that would be expected if this was a true reading. Additionally, PA area can be used as a surrogate for PA pressure and as such a diastolic increase to the extent seen in these images is not in keeping with normal physiology.

A potential explanation for the MPA diastolic increase in area is the motion of the PA during CMR imaging. Quail et al. described that when the RV contracts it pulls the PA inferiorly, bringing the narrower distal MPA into the imaging plane[351]. This motion could lead to an artificially early time to minimum area occurring during or just after peak RV contraction. This may explain why, for the MPA only, there is a diastolic increase in area as the larger proximal MPA moves back into the imaging plane. Additionally, the MPA is known to be affected by a "rocking" motion secondary to contraction of the RV which moves the MPA in and out of the defined imaging plane of the perpendicular cross section of the vessel[358]. This also could erroneously lead to measuring increased cross-sectional area in diastole. An alternative explanation is reporting error, on mapping the PA endocardial border the brightness of the enclosed blood is proportional to the rate of flow in that frame. During diastole there is minimal blood flow and vessel mapping is therefore more challenging.

Post hoc analysis demonstrated the time to minimum area was lower in the MPA scans with diastolic artefact compared to those without (442±81.8ms vs 612.4±169.2ms, $p<0.001$ unpaired t-test). The relationship between the time to minimum area and RV contraction can be demonstrated by the time difference between peak RV longitudinal contraction, measured by the time to peak RV global longitudinal strain (RVGLS), see Chapter 6, and the time to minimum area. In the MPA scans with diastolic artefact, the time difference between peak RVGLS and minimum area is lower than the time difference in MPA scans without diastolic artefact (115.7±109.3ms vs 300.7±140.1ms, $p<0.001$, unpaired t-test). As such, the diastolic artefacts are temporally related to MPA motion secondary to RV contraction. There is, however, likely a continuum between the MPA scans with marked motion artifact and the scans without any motion artifact, as such the accuracy of MPA area measurement must be considered.

The flow results are minimally affected by diastolic motion artefact as PAAT and PAAT/ET are measured during systole. Whilst cardiac output measurement may be marginally affected as it includes diastolic flow, the difference may not be

significant as diastolic blood flow is minimal and its measurement may not be significantly affected by either a change in the site of measurement within the MPA or a rotation from the true vessel cross-section.

6.6.2 Afterload results

Previous studies have repeatedly shown that afterload (measured by PA pressure and/or PVR) does not increase in the days to months following lung resection[49, 58-60, 63-68]. Whilst there are no directly comparable studies of PAAT and distensibility following lung resection the results can be interpreted in the context of published control groups and studies that investigated changes seen in PAH and CTEPH. Of note, such comparisons must account for the vessel imaged and the age of the subject. Distensibility decreases with age and tends to be higher in RPA than the LPA potentially secondary to the larger blood volume travelling in the RPA. Burman et al. demonstrated that in healthy volunteers aged 60-69 (similar to the patients in the study presented here) RPA distensibility is 7-11% greater than LPA distensibility[359].

In this study, MPA distensibility is similar to healthy age-matched controls[347, 359, 360] and greater than in patients with PAH[149, 212, 348] from other studies. In comparison to the RPA distensibility analysis performed by Gan et al., pre-operative RPA distensibility in the study presented here is greater than the control group of Gan et al. (72±23% versus 58±21%) and the post-operative reduction in operative PA distensibility on POD2 (50.7±16.9%) and at 2-months (51.8±16.2%) are modest compared to the marked reduction in patients with PAH in the study by Gan et al. and (20±10%)[211].

In the current study pre-operative and 2-month main PAAT and PAAT/ET are shorter than those described in patients with established PAH (PAAT; pre-op 115.9±20.7ms and 2-months 104 ±19.5ms vs 127.8±26ms in Sanz et al., PAAT/ET; pre-op 30.0±3.8% and 2-months 29.0±5.9% vs 34±8 % in Sanz et al.)[342]. Of note, Ertan et al. have demonstrated that PAAT is reduced in patients with mild COPD (98.1±32.3ms vs 139.7±24.4ms in healthy controls)[361], therefore the shortened PAAT may represent underlying pulmonary vascular disease in this cohort. Quail

et al.[qq] assessed PAAT in the RPA and LPA in controls and in patients with PAH. In the current study, pre-op operative PAAT and non-operative PAAT (124.7±19.3ms and 128.0±24.8ms) are similar to the PAAT in control group of Quail et al. (121±11ms). The reduction in operative PAAT on POD2 and at 2-months (82.1±23.0ms and 106.0±23.9ms) were modest compared to marked reduction[rr] seen in patients with PAH in Quail et al. (67±4ms). They also showed that in patients with CTEPH, PAAT <57.6ms was predictive of the presence of a proximal PA clot (area under the curve 0.84 (95% CI 0.70-0.90)), in no patient from the current study is operative PAAT below this value at 2-months[351].

6.6.2.1 Cardiac output distribution

Any change in afterload should be interpreted with the conditions in the pulmonary vasculature at that time, i.e. the cardiac output (CO). On POD2 CO is increased compared to pre-op and 2-months post-operatively. At this point, PAAT and PAAT/ET are shortened in all vessels and distensibility is reduced in the operative PA. The increased CO predominately travels down the non-operative PA (66.3%) and at 2-months although the CO has returned to baseline the distribution between the operative PA (39.1%) and NONPO.PA (60.9%) remains uneven. Operative PAAT, PAAT/ET and distensibility all remain shortened/reduced at 2-months when the total flow down the operative PA is essentially unchanged (2.31 $l.min^{-1}$ on POD2 and 2.33 $l.min^{-1}$ at 2-months). To our knowledge, this is the first description of the post-operative change in the distribution of blood flow between the operative PA and non-operative PA.

Pulmonary vascular reserve (PVreserve), classically measured by the gradient of the positive linear association between PAP and cardiac output, measures the ability of the pulmonary vasculature to accommodate an increase in cardiac output[120, 362], discussed further in 1.2.6.1 page 70. Pulmonary artery catheter studies have shown that there is not a significant increase in MPAP at rest following

[qq] This study was primarily designed to assess wave intensity analysis changes in PAH and is discussed further in Chapter 7.

[rr] PAAT in the study of Quail et al. is lower than other published studies whilst PAAT in the investigation presented in this chapter is lower than in patient with established PAH in the study by Sanz et al. This may be explained by an increased accuracy secondary to an increase in the temporal resolution of the CMR imaging between Quail et al. (10.5ms), this investigation (27.7ms) and Sanz et al. (75-105ms).

lung resection[48, 49, 58-61, 63, 65, 67-69], although PVreserve decreases as demonstrated by reinterpretation of the studies by Okada et al., Nishimura et al. and Miyazawa et al.[49, 67, 68], 2.3 page 84. A reduction in blood flow through the operative PA may be expected given the reduced quantity of lung that remains, although it may highlight a potential mechanism of the reduction in PVreserve following lung resection. Even with a reduced blood volume travelling through the operative PA on POD2 and at 2-months, there are signs of increased afterload compared to pre-op. This may be interpreted as reduced PVreserve in the operative PA. Whilst the non-operative PA anatomical architecture may be unchanged, it is required to accommodate a higher total blood flow for the same level of cardiac output therefore the 'starting point' on the PVreserve gradient is increased. A subsequent increase in cardiac output would results in a greater increase in MPAP than pre-operatively.

An illustrative example of this scenario using the operative and non-operative cardiac output at pre-operative and 2-months seen in the current study is presented in Figure 6-19. This illustration describes the theorised physiological basis of the reduction in the PVreserve seen following lung resection and trend in changes of MPAP/afterload. MPAP is assumed to be equal in both PAs and the non-operative lung is assumed not to compensate for changes in the operative lung, as per Saouti et al.[146], discussed in 1.2.6.4 page 75, and that there is a constant split in cardiac output between the PAs irrespective of cardiac output.

In the top- plot, the “normal” PVreserve MPAP-CO relationship (solid line) from the pre-operative results from Nishimura et al.[67] and Miyazawa et al.[68] is plotted and the pre-operative values of the operative and non-operative PA CO from this current investigation are plotted. If the cardiac output doubles, as may be seen with exercise, flow in both the operative and non-operative PAs is assumed to increase by the same amount (50:50 split in CO) and MPAP increases by ΔMPAP.

In the bottom plot, the CO from the non-operative PA at 2-months post-op (in this current study) is plotted on the normal PVreserve MPAP-CO relationship although at a higher ‘starting position’ with a modest increase in MPAP. The non-operative PVreserve is assumed to be unchanged as the non-operative pulmonary vasculature is anatomically unchanged. As the operative PA CO is reduced at 2-months, when it is plotted it must have a separate steeper PVreserve MPAP-CO relationship than the non-operative PA as MPAP is assumed to be equal in each PA. If CO doubles, flow in both vessels doubles, assuming the 60:40 split in CO demonstrated at 2-months in the current study is maintained. This results in a larger absolute increase in non-operative CO and a smaller absolute increase in operative CO than pre-operatively resulting in a greater overall increase in MPAP (ΔMPAP increases by a factor of 1.2 in this example). This may be an underestimation if the CO percentage in the non-operative PA further increases with cardiac output. In the current study, when CO was increased on POD2 the ratio of CO in the non-operative increased to 66:34 as the absolute value of CO in the operative PA is unchanged.

The above processes may explain the changes observed following lung resection demonstrated in previous studies. Differing PVreserve between the operative and non-operative PAs may account for the lack of significant increase in MPAP at reset and the rapid increase on exercise. Additionally, it highlights the requirement for the non-operative PA to accommodate increased blood flow, this may lead to an increase in pulsatile afterload in the non-operative PA.

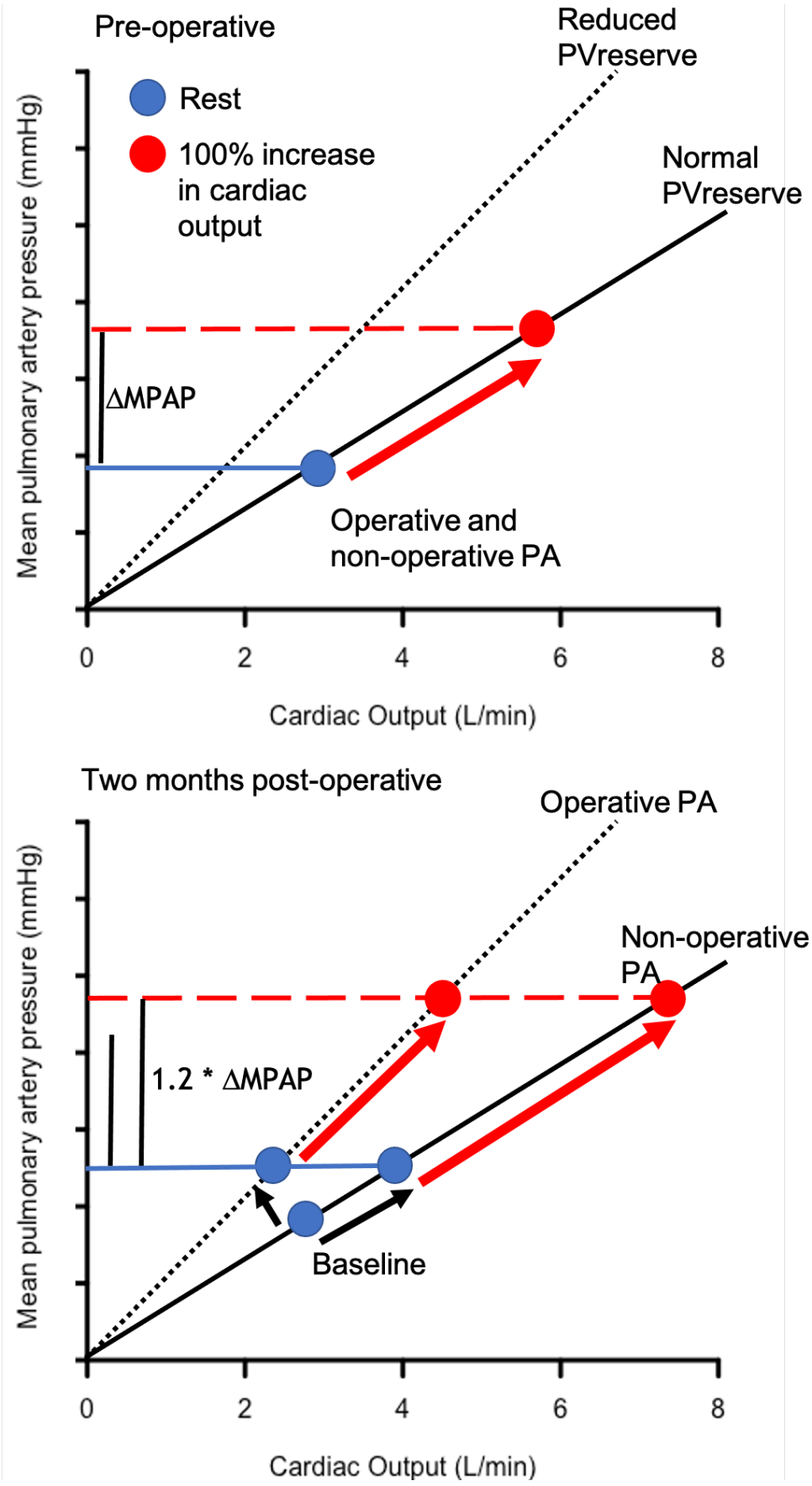

Figure 6-19 Pulmonary vasculature reserve before and after lung resection
Illustrative representation of theoretical change in pulmonary vascular reserve (PVreserve) following lung resection. Red lines depicts doubling of cardiac output on exercise. PA= pulmonary artery. Image constructed by author. NB mean pulmonary artery pressure units are removed as this is not intended as a literal interpretation of values but to illustrate a potential mechanism of a decrease in PVreserve following lung resection.

Evidence that the increased blood flow in the non-operative PA results in increased pulsatile afterload and may lead to RV impairment can be seen in the within-subject associations between RVEF, BNP and indices of afterload between pre-op and POD2. The POD2 shortening in non-operative PAAT/ET and reduction in distensibility have moderate to strong associations with the reduction in RVEF and increase in BNP, Figure 6-13 and Figure 6-16. This suggests that an inability of the non-operative PA to accommodate the increased flow may be a significant factor in the development of impaired RV function. This may be a purely peri-operative effect (as it resolves by 2-months) or it may be revealed by the increased cardiac output on POD2 and this relationship may persist post-operatively were the patient challenged by an increased CO.

6.6.3 Conclusion

This study demonstrates, for the first time, that there is an increase in the indices of pulsatile afterload in the operative PA following lung resection. As the changes are unilateral, they may be the cause of the increase in the percentage of cardiac output travelling in the non-operative PA. The combination of increased pulsatile afterload in the operative PA and increased blood flow in the non-operative PA is a potential mechanism of a reduction in PVreserve following lung resection. On POD2 it is the increase in pulsatile afterload in non-operative PA that is associated with impaired RV function and not the operative PA.

Chapter 7 Pulmonary artery wave intensity analysis

This chapter details the background to and the first use of wave intensity analysis (WIA) in a lung resection population. WIA combines the changes in flow and pressure (or area) throughout the cardiac cycle to model wave travel and assess pulsatile afterload. Similar to impedance analysis, 1.2.6.3 page 72, and the surrogate indices of pulsatile afterload investigated in Chapter 6, it may demonstrate increases in afterload following lung resection that previous studies may have missed.

7.1 Arterial wave mechanics

The main distinction between impedance and WIA is based on the mathematical approach of decomposition of the arterial waveform[ss] [363]. Impedance analysis is performed in the frequency domain whilst WIA is performed in the time domain. Each method has its own strengths and limitations. It is important to note that the method of interpretation does not imply any underlying characteristics of the waveform, as Parker states,

"No particular decomposition is inherently better than any other; their value depends solely on their utility."

Kim Parker (2009)[364]

7.1.1 Wave definition and decomposition

The term "wave" has a general broad usage in medicine and can be interpreted as the arterial waveform or as a sinusoidal "wavetrain"[364]. Hughes et al. define a wave as,

[ss] References in this section are predominately from a special issue of Medical & Biological Engineering & Computing, volume 47, Issue 2, February 2009. It is a complete and thorough review of the scientific background of wave intensity analysis and impedance. Detailed description of mathematical derivation of the approach can be found in Parker's two reviews[363, 364]

"a disturbance that is propagated through a medium with an exchange between kinetic and potential energy"

Hughes et al. [365].

In the arterial system, a wave causes a transmission of energy with a simultaneous change in pressure and flow. It is important to note that a wave can travel at a velocity greater than and separate to the bulk flow velocity of blood[365].

The two main methods by which arterial waveform can be interpreted, Fourier analysis and successive wavefronts, demonstrated in Figure 7-1. Impedance analysis by Fourier decomposition breaks the waveform into constituent sinusoidal waves (wavetrains) that sum to give the original waveform, impedance is therefore measured in the frequency domain. Successive wavefronts are formed by the decomposition of the waveform into successive wavelets. This equates to successive incremental changes in pressure over time and therefore wavefronts are assessed in the time domain. Each wavelet can be calculated as the change in pressure during the sampling period (Δt), Equation 7-1, and is demonstrated as 16 successive wavefronts in Figure 7-1. The accuracy of the wavefront model can be improved by reducing the sampling period[364].

$$dP = P(t + \Delta t) - P(t)$$

Equation 7-1 Wavelet decomposition
dP= change in pressure. P= pressure. t= time. ∆t= sampling period. P(t)= pressure at time t.

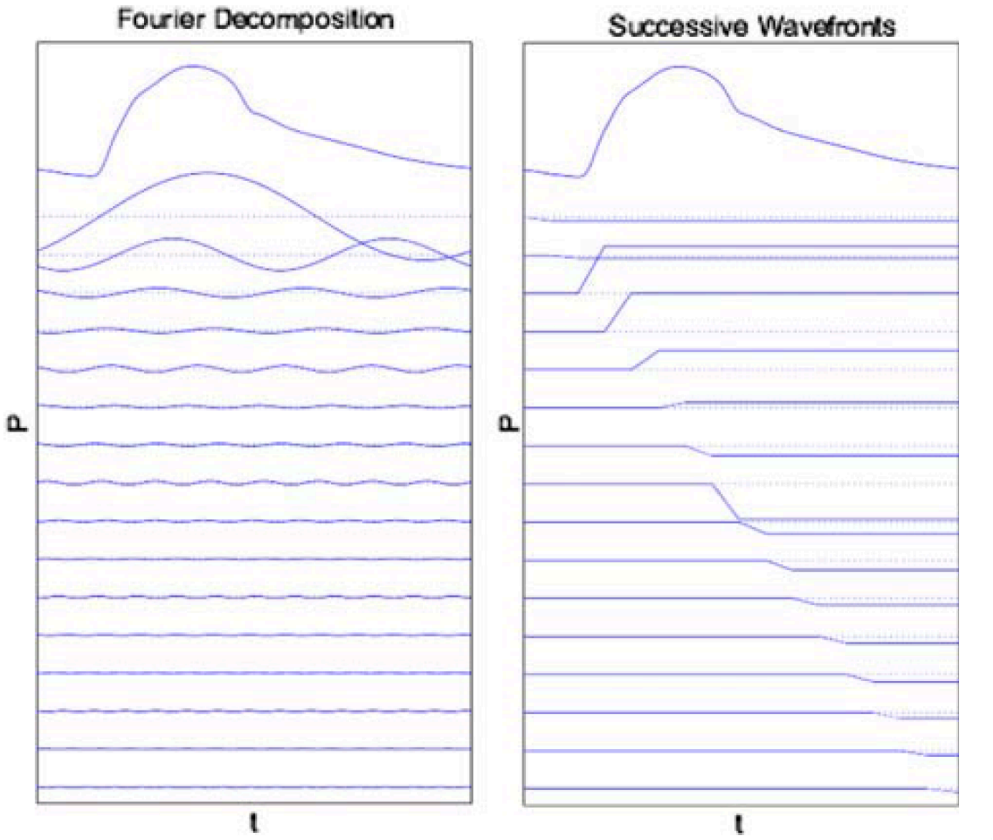

Figure 7-1 Decomposition of arterial waveform
The arterial waveform (top line) can be decomposed into sinusoidal wavetrain (left panel, Fourier decomposition) or successive wavefronts (right panel, wave intensity analysis). P= pressure. t= time. Image from Parker[364].

The fundamental difference between the two methods is whether an arterial pulse is an isolated event or part of a long series of pulses[366]. Fourier analysis presumes that the overall waveform is comprised of underlying sinusoidal waves and a heartbeat is not an isolated event. The cardiac system must therefore be deemed to be in steady-state oscillation. This view is established in literature and reinforced by observation; under normal physiology the heart has a regular "near-periodic" rhythm. Evidence against this can be seen following ectopic or missed heart beats, Figure 7-2. The rapid exponential decline in pressure without any further upward inflection following the missed beat demonstrates that the arterial system is over-damped, i.e. oscillations stop immediately following cessation of stimulus. Over-damped systems cannot oscillate by definition as there is no continuum between one heartbeat and the next, therefore it can be argued that the arterial system is not in steady-state oscillation and heart beats should be viewed as isolated events[364].

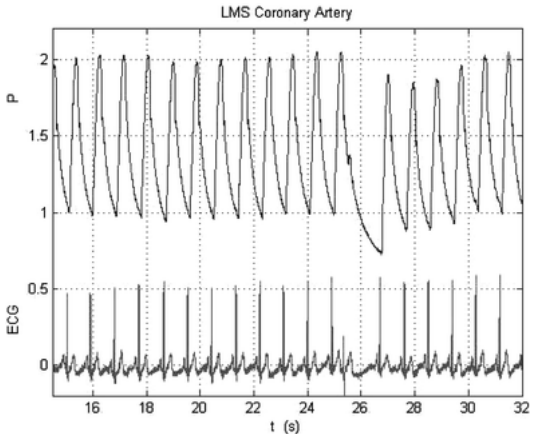

Figure 7-2 Pressure response following missed beat in coronary artery
Arterial pressure (P) waveform (top panel) shows rhythmic pulsation until missed beat, demonstrated on ECG (bottom panel). Following a missed beat the pressure trace rapidly decreases until the following beat occurs. The lack of any oscillation demonstrates that the cardiovascular system is over-damped. ECG= electrocardiogram. LMS= left main stem. t= time. Image from Parker[364].

Whilst the interpretation that a heartbeat is an isolated event is logical, it is based on a literal interpretation of Fourier analysis. When describing this interpretation Remington commented that, *''The most major assumption is that the harmonics obtained by a Fourier curve fitting actually exist as separate waves, traveling independently…''*[367]. It also assumes that, for each harmonic, there is a linear relationship between pressure and flow rate[368]. The most accurate interpretation of Fourier analysis is that it, as described by Avolio et al., "*predicts, based on assumed linearity, what single, separate harmonics would do*" and it does not imply that the sinusoidal wavetrains calculated at each harmonic exist in the artery[366]. As commented by Parker, both methods of wave decomposition are valid although wave intensity analysis does not require the assumption of steady state oscillation[364, 368].

7.2 Wave intensity analysis

Parker et al. published the basis of wave intensity analysis (WIA) in two papers in 1988[369] and 1990[368]. These papers detail the complex mathematical derivation on which the technique is based. In his 2009 review Kim Parker, who holds a PhD in aerospace and mechanical engineering, states that, "*the mathematics are not always accessible to those whose mathematical training does not extend to partial differential equations, eigenvalues and eigenvectors*". In the review, he attempts to provide a detailed mathematical and a non-mathematical overview.

A balanced description will be provided in this thesis as a non-mathematical description alone is sufficient to interpret the results generated[364].

7.2.1 Wave intensity definition

Hughes et al. defines wave energy as, *"the part of a fluid's total energy, that is associated with a wave"* and wave intensity[tt] (dI) as, *"the rate of transport of wave energy"*[365]. Wave energy and intensity therefore are only part of the total energy within the arterial tree. dI is calculated as the product of the change in pressure and the change in velocity during a small interval (sampling period)[151], Equation 7-2, and measures the instantaneous power per unit cross sectional area (Wm^{-2}) that is carried by the wavefront[151 370].

$$dI = dP \,.\, dU$$

Equation 7-2 Wave intensity
dI= wave intensity. dP= change in pressure. dU= change in flow velocity

7.2.2 Wave classifications

7.2.2.1 Forward and backward waves

Waves can be classified by their direction of travel and the rate of change of pressure (dP/dt) that they cause. As WIA is performed from pressure and velocity measurement at one particular point in the artery, the interpretations are relative to this point. Waves that travel forward (away from the heart)[uu] across the point of measurement have a positive dI whereas waves that travel backwards (towards the heart) have a negative dI. As these waves coexist, the net dI will only determine if forwards or backwards waves dominate at any given time and will not fully describe the individual component waves. To do so net dI must be separated into the forward (dI+) and backward (dI-) components[370], Equation 7-3.

[tt] Wave intensity is calculated from the temporal derivatives of pressure and velocity (or surrogate markers), as such the notation dI is used.

[uu] Wave intensity analysis has been utilised in arterial, coronary and venous circulations. The classifications of waves, unless otherwise stated, will be as described in the arterial (systemic and pulmonary) circulations where forwards waves travel away from the heart and backward waves towards the heart.

$$dI = dI_+ + dI_-$$

Equation 7-3 Wave intensity addition
dI= wave intensity. dI+= forward wave intensity. dI- = backward wave intensity.

7.2.2.2 Compression and expansion waves

Waves that increase the rate of change in pressure (dP/dt>0) are called compression waves. Expansion waves (also termed decompression waves by some authors) cause a decrease in the rate of change in pressure (dP/dt<0). Of note, compression waves are caused by compression of fluid but lead to an expansion of the arterial vessel whereas expansion/decompression waves are caused by expansion of fluid volume but lead to a reduction in vessel cross-section[364, 365].

The generation of these waves from contraction and relaxation of the ventricle can be visualised as the pushing of a piston on a fluid filled tube. The relative compression and expansion of the fluid secondary to the piston action generates forward travelling waves, Figure 7-3A. The initial forward compression wave (FCW) travels down the tube increasing pressure and therefore vessel diameter, Figure 7-3B. At the end of compression there is a relative decrease in the pressure and vessel diameter when the piston recoils that generates a forward expansion/decompression wave (FEW). This pair of compression and expansion waves propagate down the tube at a specific wave speed (c) and the wave intensity (dI) can be measured distally for the FCW (unshaded) and FEW (shaded)[365].

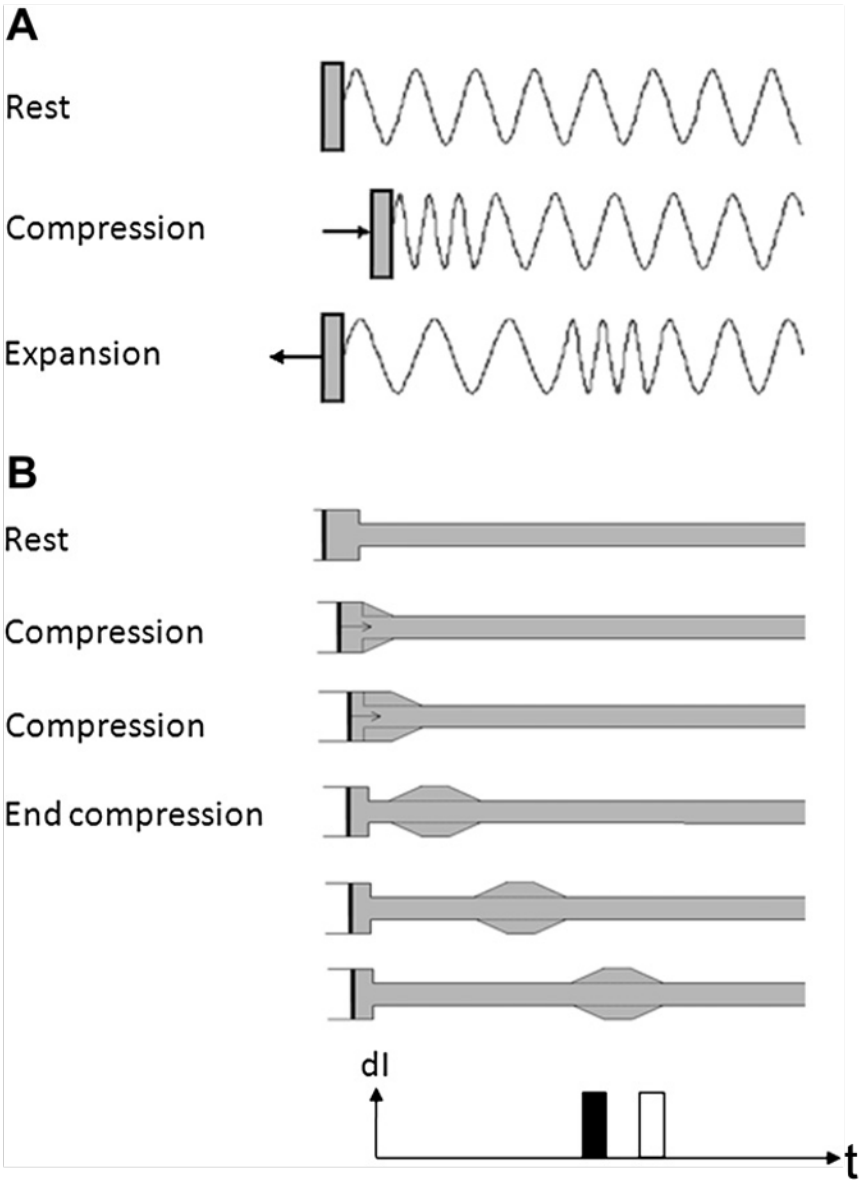

Figure 7-3 Generation and propagation of compression and expansion waves
Generation of compression/expansion waves (A) and propagation of waves down fluid filled column (B). Bottom graph demonstrates the wave intensity (dI) for compression (unshaded) and expansions (shaded) waves over time (t), both are positive as the waves are travelling forward. Image from Hughes et al.[365].

As Hughes states in the definition of a wave there must be, *"an exchange between kinetic and potential energy"*[365], in an artery, kinetic energy (blood flow velocity, U) and potential energy (pressure, P) are therefore linked. The dP that the wave causes must be accompanied by a dU, which is assumed to occur with negligible loss of energy. This can be expressed by the water hammer (Joukowsky) equation, Equation 7-4, where dP is calculated from dU, wave speed (c) and the density of the blood (ρ)[369]. Similar to dI, there are forward and backward wavefronts for pressure (dP+ and dP-) and velocity (dU+ and dU-). Wave speed can be assumed

to be constant (as can blood density) for that particular wave, this assumption and the calculation of wave speed is discussed in detail in 7.2.6.3 page 262.

$$dP_{\pm} = \pm pcdU_{\pm}$$

Equation 7-4 Water hammer equation
dP= change in pressure. *p*= density of blood. c= wave speed. dU= change in flow velocity.

7.2.2.3 Origin of backward waves

In general, a backward wave originates from reflection of a forward travelling wave. Parker describes how this can occur at a "discontinuity of characteristics", i.e. a change in the cross-sectional area of the vessel, a vessel bifurcation or a change in local wave speed. At a bifurcation, the nature of the resultant backward wave is determined by the vasculature distal to this point[364]. The two extremes can be imagined as "open-ended" and "close-ended". In a close-ended system the distal vasculature is completely obstructed and therefore reflects the forward wave as a backward compression wave (BCW) which causes an increase in pressure but a decrease in the forward velocity of blood. An open-ended system, such as a bifurcation to markedly larger daughter vessels, reflects a backward expansion/decompression wave (BEW) which causes a decrease in pressure and an increase in the forward flow of blood[151], Figure 7-4.

Interestingly, the coronary circulation has been shown to generate an early systolic BCW and an early diastolic BEW from the compression and expansions of the distal coronary microvasculature by myocardial contraction[371]. The novel BEW travels towards the aortic origin of the coronary artery and increases the forward velocity of blood flow down the coronary artery[372]. This is an additional component of coronary filling to the pressure gradient driven diastolic filling discussed in 1.2.3.3 page 53.

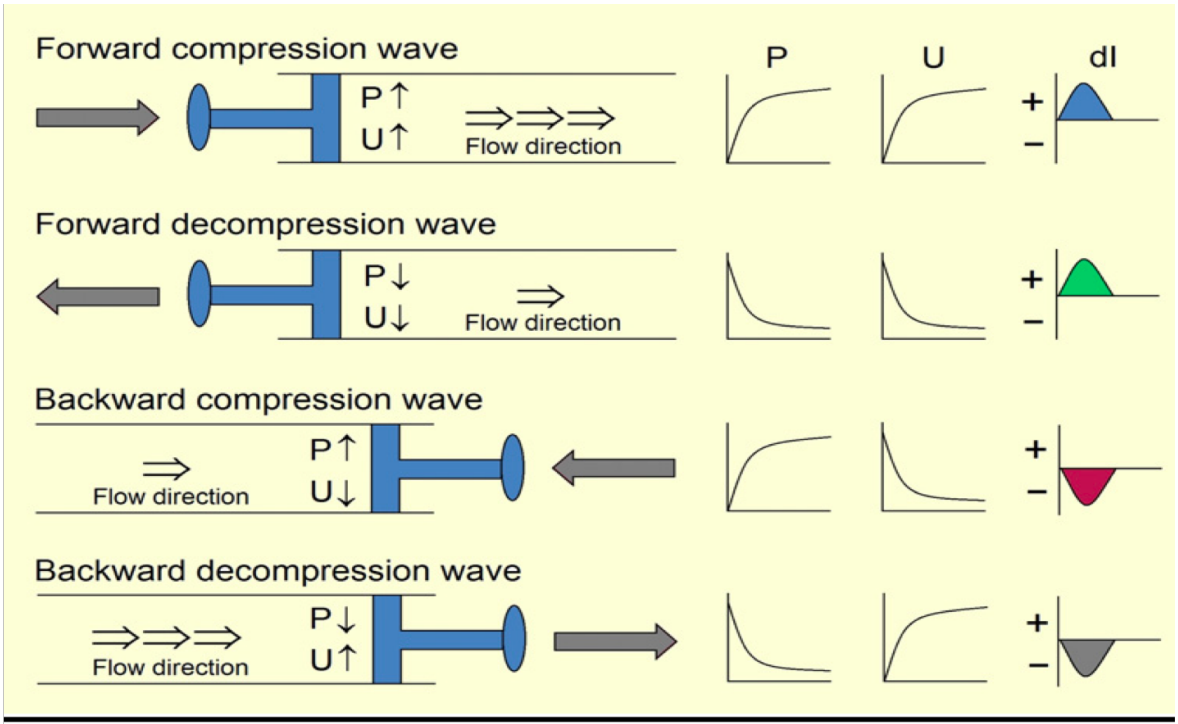

Direction	Character	dP	dU	dI
Forward	Compression	+	+	+
	Expansion/decompression	-	-	+
Backward	Compression	+	-	-
	Expansion/decompression	-	+	-

Figure 7-4 Wave classification
Piston analogy of wave generation with corresponding value of and change in pressure (P and dP), velocity (U and dU) and wave intensity (dI). Note forward waves have positive dI and backward waves negative dI. Compression waves always cause an increase in pressure (dP) but the change in flow velocity (dU) in determined by the direction of travel. As dI is the product of dP and dU forward waves (positive dI) therefore cause an increase or decrease in both dP and dU whereas backward waves cause either an increase in dP and a decrease in dU or vice-versa. Images from Su et al.[151].

7.2.3 Wave separation

If wave speed and blood density are known, the changes in pressure and velocity can be decomposed into the forward and backward components (with the water hammer equation, Equation 7-4) and the components of $dP\pm$ and $dU\pm$ calculated[373], Equation 7-5. $dI+$ and $dI-$ can then be calculated by multiplying the $dP+$ with $dU+$ and $dP-$ with $dU-$ respectively[373], Equation 7-6. This method of separation is based on Parker's original work. Derivations of this have utilised cross-sectional area instead of pressure, allowing non-invasive WIA[374, 375], further methodology is discussed later in 7.2.6.

$$dP_+ = \frac{1}{2}.(dP + pcdU)$$

$$dP_- = \frac{1}{2}.(dP - pcdU)$$

$$dU_+ = \frac{1}{2}.(dU + \frac{dP}{pc})$$

$$dU_- = \frac{1}{2}.(dU - \frac{dP}{pc})$$

Equation 7-5 Separation of change in pressure and velocity
dP= change in pressure. *p*= density of blood. c= wave speed. dU= change in flow velocity.

$$dI_+ = dP_+.dU_+ = \frac{1}{4pc}.(dP + pcdU)^2$$

$$dI_- = dP_-.dU_- = -\frac{1}{4pc}.(dP - pcdU)^2$$

Equation 7-6 Separation of wave intensity
dI= wave intensity. dP= change in pressure. dU= change in flow velocity. *p*= density of blood. c= wave speed.

7.2.4 Interpretation of wave intensity analysis

Parker's initial description and the majority of subsequent investigations relating WIA to pathophysiologic mechanisms have been performed relative to the left ventricle in the systemic circulation and to a lesser extent the coronary arteries[369-371]. As detailed in 7.2.2.3, the coronary circulation is unique for WIA as backward waves are generated de novo. Whilst there are few studies of WIA in the pulmonary circulation, the principles of interpretation are transferable between the circulation and so the evidence in the left ventricle/systemic circulation will also be discussed. The handful of WIAs performed in the pulmonary circulation of human subjects are discussed in detail in 7.2.5. Of note, the studies detailing the changes in wave reflection are primarily of the pulmonary circulation.

7.2.4.1 Wave intensity throughout the cardiac cycle

The temporal relationship of wave intensity to the cardiac cycle is demonstrated in Figure 7-5. It should be noted that, as WIA is performed on a vessel distal to the heart, there will always be a delay between the peak of the R wave on the ECG, ventricular ejection of blood and the onset of increases in pressure, velocity and therefore wave intensity (R – W_1, Figure 7-5) at the site of measurement. The duration of this delay is dependent on the wave speed and the distance between the heart and the point of measurement. In both the pulmonary and systemic circulations, the main waves detected are two positive (forward) waves and an early systolic negative (backward) wave[376]. Separation of the forward and backward pressure components allows identification of the nature of these waves.

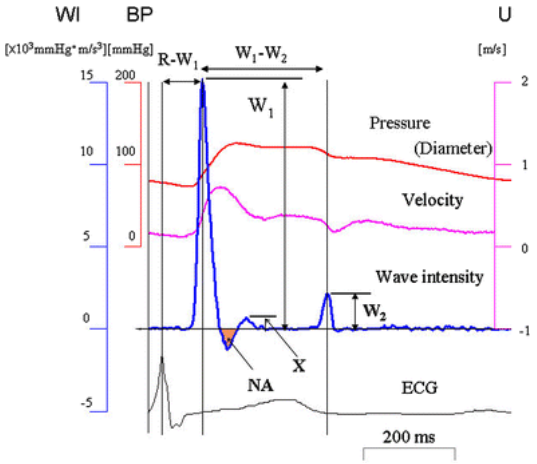

Figure 7-5 Wave intensity throughout cardiac cycle
Wave intensity measured in the carotid artery. Combination of pressure (BP) and velocity (U) profiles to give net wave intensity (WI). Peaks in wave intensity of W_1 and W_2 and time difference between these peaks ($W_1 – W_2$). Note negative WI (NA) immediately following W_1. Also, the onset of pressure, velocity and WI are delayed from the peak of R wave on ECG (R-W_1). Image from Sugawara et al.[376].

7.2.4.2 Separation of waves

An example of WIA in the systemic circulation (carotid artery) is given in Figure 7-6. Of note, vessel diameter is used as a surrogate for pressure. Diameter and area are commonly used in non-invasive assessment of WIA as they have a linear relationship with pressure[351, 377]. In 2002, Vulliémoz et al. detailed the mathematical derivation of the relationship for calculation of wave speed from flow and area (QA method)[378], this method has gained widespread use for wave speed calculation, discussed further in 7.2.6.3, and has been used for non-invasive WIA in the pulmonary circulation[351, 377]. Figure 7-6a and Figure 7-6b demonstrate the measured diameter (D) and velocity (U) in blue (solid line). These waves are

separated in a similar method as Equation 7-5 with the calculated forward components (dD+ and dU+) and backward components (dD- and dU-) then integrated and displayed as D+/P+ (green, dashed line) and D-/P- (red, dotted line).

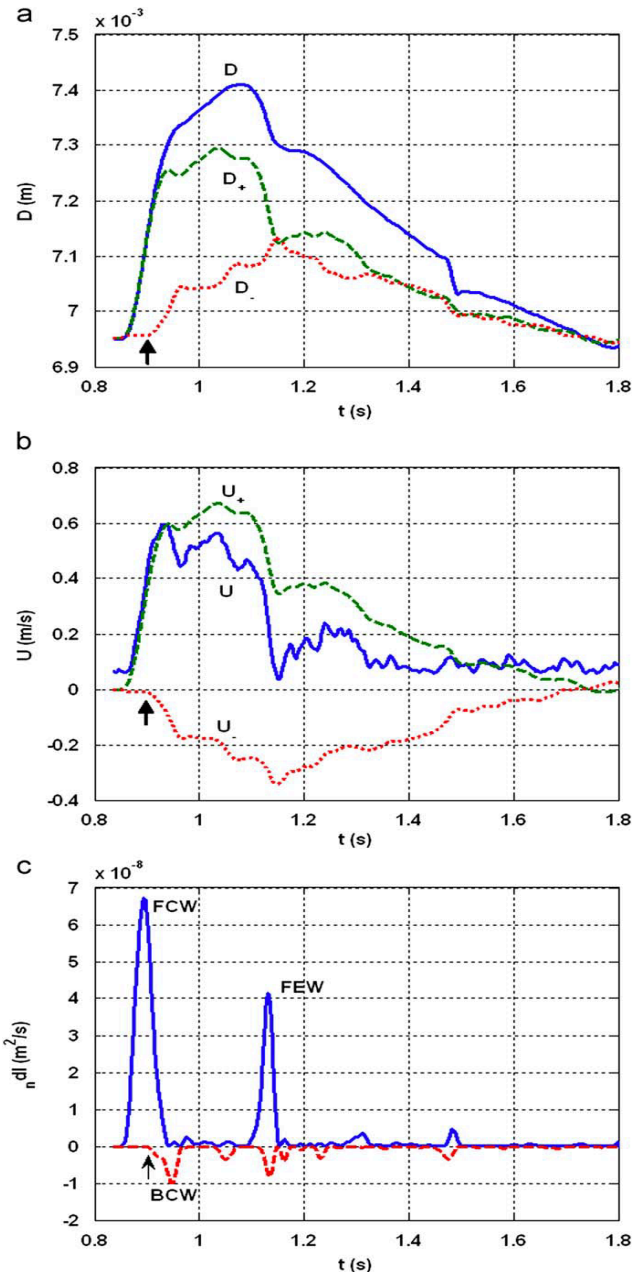

Figure 7-6 Wave separation into positive and negative components
Profiles for carotid artery diameter (D) (a) and velocity (U) (b). Measured values in blue (solid line), separation into forward (+, green, dashed line) and backward (-, red, dotted line) components. Wave intensity (dI) profiles (c) shows forward (blue) and backward (red) waves. Arrows indicate time of onset of backward wave. Note overlap of forward and backward waves that would mask smaller waves without separation. t= time. FCW= forward compression wave. BCW= backward compression wave. FEW= forward expansion wave. Image from Feng et al.[379].

Forward compression wave (FCW). Ventricular contraction causes an initial rapid increase in diameter and velocity, represented by the increases in D+ and U+, which results in a rapid peak in dI+ (calculated by dD+.dU+). This is a forward

(dI>0) compression (dP/dt > 0) wave which is responsible for the forward flow of blood in systole. Note that the FCW is short lived and terminates prior to the peak in diameter (pressure), although the forward flow of blood continues until it is decelerated by a BCW and/or a FEW.

Backward compression wave (BCW). The onset of the backward (reflected) wave is indicated by the arrow. Whilst dI is negative, the direction of D- is positive, i.e. it results in an increase in diameter (dP/dt > 0). As such this is a backward (dI-) compression (dP/dt > 0) wave. As U- is negative, it causes a decrease in forward velocity of blood (dU/dt < 0). Ultimately, a BCW causes an increase in the pressure/ diameter and a decrease in the forward velocity/flow of blood within a vessel. It a sign of increased wave reflection and increased pulsatile afterload, explained further in 7.2.4.4.

Forward expansion wave (FEW). Following peak ventricular contraction there is a rapid decline in D and U, note the changes occur in D+ and U+, therefore it is caused by a forward wave (dI>0). As it causes a decrease in vessel diameter (dP/dt < 0) and velocity (dU/dt <0) it is a forward expansion wave (FEW). This wave travels away from the heart, causes a decrease in blood pressure and a decrease in the forward flow of blood. It offloads the ventricle thus easing ventricular filling and also aids coronary blood flow in the systemic circulation.

7.2.4.3 Interpretation of forward waves

7.2.4.3.1 Forward compression waves

The generation of an FCW is related to the contractile force of the ventricle[vv]. Ohte et al. demonstrated that peak FCW is strongly associated with the maximal rate of LV pressure rise ($r=0.74$, $p<0.001$)[380]. Peak FCW decreases with age and is also independently associated with gender, systolic BP, HR and stroke volume (normalised for body surface area)[381]. Peak FCW is also affected by inotropy;

[vv] The different waves generated by WIA can be quantified by either their maximal value, peak wave intensity (WI), or the total wave energy, calculated by the area under the curve. Both measures are used in literature. Additionally, the timing of the waves can be related to both cardiac function and downstream wave reflection.

dobutamine (increased inotropy) increases FCW, whilst propanolol (decreased inotropy) reduces it[382].

7.2.4.3.2 Forward expansion waves

The description of the FEW, in Parker et al.s' first publication of WIA, challenged the established theory that reflection of arterial blood flow was responsible for the rapid decrease in forward flow of blood in the aorta[369]. Instead, WIA explained that the LV (in this description) generates a forward travelling wave that decreases pressure and forward flow of blood in the aorta, the FEW. The impact of this is that the heart actively stops the forward flow of blood[383].

The rapid decrease in aortic blood flow/pressure cannot be explained purely from the decrease in LV tension. At closure of the aortic valve (AV) the pressure in the LV is always lower than aortic pressure[376]. At this point there remains a forward flow of blood through the aortic valve against a pressure gradient, similar to the *"hangout interval"* of RV ejection described by Dell'italia and Walsh[98], 1.2.2.1 page 40. This continued forward flow of blood and the generation of the FEW are caused by a rapid fall in LV pressure and is influenced by two main factors, the forward momentum of blood leaving the LV (inertia force) and the decrease in LV wall tension[376].

The inertia force of blood is generated by ventricular contraction. As contraction and therefore myocyte shortening stops, the momentum of the blood exiting the ventricle (inertia force) maintains forward flow of blood thus rapidly emptying the ventricle. This leads to a smaller end-systolic volume, greater elastic recoil of the myocytes and a more rapid pressure decline[376, 383]. Ohte et al. have highlighted the active process of the relaxation of the ventricle. High frame rate doppler echocardiography revealed apically directed intra-ventricular blood flow prior to aortic valve closure. This originated at the apex with subsequent flow throughout the entire LV directed towards the apex, except for just below the mitral valve, pulling blood from the aorta towards causing closure of the aortic valve and offloading the ventricle[384].

The generation of a FEW is a product of both mechanisms and as such, reflects the late systolic function and relaxation of the ventricle[376]. This relationship has

been demonstrated by both Ohte et al. and Sugawara et al. in follow-up studies; FEWs have a strong association to LV pressure decay ($r=-0.61$, $p<0.001$) and the time constant of LV relaxation ($r=-0.77$, $p<0.001$)[376, 380].

7.2.4.3.3 Forward waves in disease

The FCWs and FEWs generated by the LV differ depending on the pathophysiologic process affecting it. In dilated cardiomyopathy, the contractile function of the LV is impaired without change in relaxation, therefore there is reduction in the FCW but no change in the FEW[376]. Hypertrophic cardiomyopathy has impaired ventricular relaxation and so has a lower FEW but unchanged FCW[376]. In mitral regurgitation, the LV is distended with impaired relaxation, therefore there is an absence of a FEW. This, however, returns following surgical correction of the valve, whereas FCW is unchanged throughout[385].

7.2.4.4 Backward waves

Backward waves are caused by reflection and so demonstrate the condition of the distal vasculature in the systemic and pulmonary circulations[ww]. As discussed previously in 7.2.2.3, the distal vasculature will determine if the reflected wave is a compression (closed-ended system) or expansion wave (open-ended system). In the pulmonary circulation, BCWs tend to occur in disease as they are a sign increased pulsatile afterload (wave reflection). They cause an increase in pressure and a decrease in the forward flow of blood and therefore add to RV workload. Conversely, BEWs cause a decrease in pressure and an increase in forward flow of blood. They are seen in normal pulmonary vasculature and are beneficial to RV workload[351].

7.2.4.4.1 Wave reflection

Wave reflections occur at a bifurcation, a change in vessel calibre or a change in local wave speed. Between the parent (proximal) and daughter vessel(s) (distal) of an arterial bifurcation there must be constant pressure (conversation of energy) and an equal net volume into and out of the bifurcation (conservation of mass). If

[ww] In the coronary circulation backward waves are generative from the distal end of the coronary arteries secondary to compression and expansion of the micro-circulation during ventricular contraction[372].

the cross-sectional area of the parent (A_0) and daughter vessels (A_1 and A_2) are not matched, there will be a reflection of the incident forward wave. This can be described by the reflection coefficient (Γ), the ratio of pressure changes caused by the reflected wave (δP) to the incident wave (ΔP)[364], Equation 7-7.

$$\Gamma = \frac{\delta P}{\Delta P}$$

Equation 7-7 Reflection coefficient
Γ= reflection coefficient. δP= magnitude of pressure change due to reflected wave. ΔP= pressure change due to incident wave.

The reflection coefficient is determined by the ratio of the parent vessel to daughter vessel(s) (α)[364], Equation 7-8, and the asymmetry[xx] of the diameter of the daughter vessels (γ)[364], Equation 7-9.

$$\alpha = \frac{A_1 + A_2}{A_0}$$

Equation 7-8 Daughter-parent vessel ratio
α= daughter-parent ratio. A_1 and A_2= cross-sectional area of daughter vessels. A_0= cross-sectional area of parent vessel.

$$\gamma = \frac{A_2}{A_1}$$

Equation 7-9 Vessel asymmetry ratio
α= daughter-parent ratio. A_1 and A_2= cross-sectional area of daughter vessels. A_0= cross-sectional area of parent vessel.

Asymmetry (γ) has minimal effect on Γ in fully open or fully closed systems however it influences the α value at which there is no reflection (Γ=0), Figure 7-7. γ can range from 0 (only one daughter vessel, i.e. a dilation or constriction) to 1 (A_1=A_2). In a point in a straight tube α=1 (A_0=A_1) and γ=0 therefore Γ=0 (no wave reflection). In an ideal system with a bifurcation when Γ=0 (no wave reflection) and γ=1 (the daughter vessels are symmetrical) then $\alpha \approx 1.15$ (A_0=(A_1+A_2)/1.15). In

[xx] In this context, assymetry refers to the ratio of vessel area between daughter vessels. The angle between the partner and daughter vessels will however alter the distribution of total flow in that vessel, discussed later in 7.2.4.6, 249.

human arterial systems $\alpha \approx 1.14 \pm 0.03$, evidence that in normal circumstances the arteries are a well-matched system with minimal reflections[364].

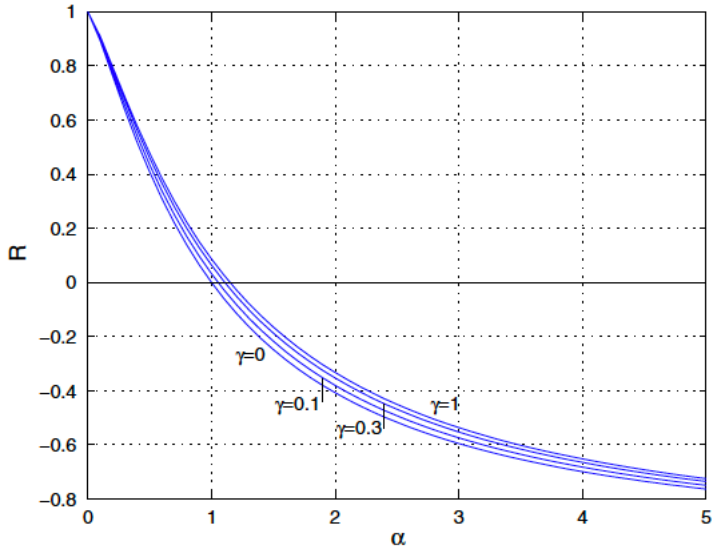

Figure 7-7 Reflection coefficient at a bifurcation
The reflection coefficient (R) is a function of the ratio of daughter to parent vessels (α). γ represent the effect of vessel symmetry of the daughter vessels, γ=0 depicts a straight tube with no bifurcation (purely a dilation of the vessel), γ=1 represents symmetrical bifurcation (daughter vessels equal in size). Image from Parker[364].

The following examples are depicted in Figure 7-8. In a close-ended tube α=0 (A_1 and A_2=0) therefore Γ=1 as the entire incident wave is reflected. In an open-ended tube $\alpha \rightarrow \infty$ and $\Gamma \rightarrow$-1, where the δP approaches the magnitude of the ΔP but as a decrease in pressure, i.e., a BEW increasing the forward velocity of blood.

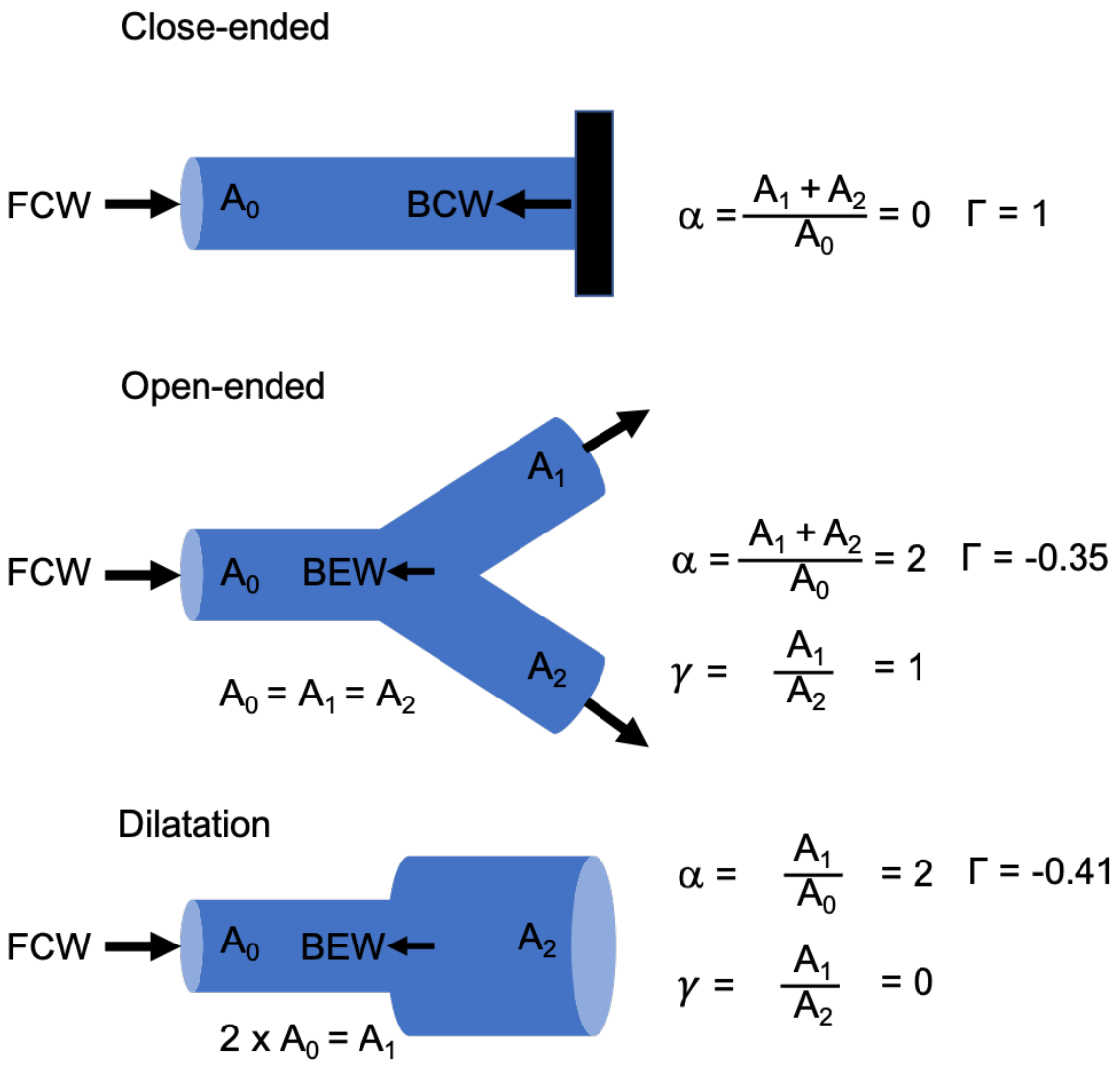

Figure 7-8 Factors influencing reflection coefficient
Three examples of reflection sites and the generation of wave reflection. A0= cross-sectional area of parent vessel. A1 and A2=cross-sectional area of daughter vessels.
Top row, a close-ended parent vessel (A0) that has no daughter vessels (A1 and A2) therefore the ratio of vessel areas (α) is 0. The entire incident forward compression wave (FCW) is reflected and a backward compression wave (BCW).
Middle row, a relatively open-ended vessel. α=2 as the daughter vessels are equal in size to the parent vessel. A1 and A2 are symmetrical (γ) as A1=A2. Reflection coefficient (Γ)=-0.35. The reflected wave is a backward expansion wave (BEW).
Bottom row, dilation of parent vessel. α=2 as the daughter vessel (A2 is twice the size of parent vessel. As A1 does not exist γ =0. Reflection coefficient (Γ) is increased at -0.41. Again, the reflected wave is a BEW.
Image made by author.

The arterial tree contains multiple bifurcations down to the small arteries and arterioles where there is significant wave reflection. These reflections will then be returned through the same vessels they travelled, however at each bifurcation the parent-daughter ratio is altered. Assuming a well-matched forward system (no reflection (Γ=0), α=1.15 and the daughter vessels are equal in size (γ=1)) the reverse of this system would mean the parent-daughter vessels are now arranged

as $(A_2+A_0)/A_1$ and therefore an α>1.15 with Γ<0. As such any wave reflections in the pulmonary vasculature will be reflected for a second time and sent back towards the peripheries[364].

7.2.4.4.2 Wave reflection index

Wave intensity analysis offers an alternative method to calculate wave reflection. Wave reflection index (WRI) is the ratio of the integral of the BCW over the FCW[386], Equation 7-10. Analogous to Γ, WRI calculates the total reflected energy ($\sum$BCW) over the total incident energy ($\sum$FCW). This has two potential benefits over calculation of BCW alone; it removes any numerical differences between methods of calculating WIA and it relates BCW to the incident FCW.

$$\boldsymbol{WRI} = \frac{\sum \boldsymbol{BCW}}{\sum \boldsymbol{FCW}}$$

Equation 7-10 Wave reflection index
WRI= wave reflection index. BCW= backward compression wave. FCW= forward compression wave.

As discussed later in 7.2.6, there are a variety of methods to calculate WIA, this results in values for FCW and BCW that are only directly comparable to studies of the same methodology[151]. WRI describes the ratio of $\sum$BCW to $\sum$FCW and therefore removes any numerical differences between methods. Additionally, it can easily be calculated in studies that only report BCW and FCW areas.

Forward compression wave area is influenced by inotropy, heart rate and loading conditions[381]. As the size of the BCW is dependent on the incident FCW, it will be affected by any factor that changes the FCW and any change in the pulmonary vasculature, WRI minimises the effects of changes in FCW size.

7.2.4.4.3 Distance to site of reflection

Intuitively the distance to the site of wave reflection can be calculated from the wave speed (c) and the time difference between the peaks of the forward and corresponding backward waves[351]. This is an over simplification as it assumes a constant wave speed throughout the vasculature, whereas wave speed actually increases towards the peripheries[387]. It also assumes that there is a single dominant site of reflection.

Davies et al. investigated the relationship between the point of measurement and the distance to reflection site by measuring WIA at progressively distal points in the aorta. They demonstrated that the distance to the reflection site remained constant, irrespective of the point of examination, i.e. as the point of examination moved distally so did the calculated site of reflection. They concluded that there is not a distinct site of reflection and the site of reflection is an amalgamation of all subsequent wave reflection dominated by the proximal reflections, described as the "horizon-effect"[388].

Quail et al. calculated the distance to the site of wave reflection in patients with PAH and healthy controls. In patients with PAH, the distance to wave reflection was markedly reduced at 2-3cm from the point of imaging (midpoint of RPA or LPA), equivalent to the next bifurcation to the lobar PAs. They reference the study by Davies et al. and describe this as evidence of the horizon effect as PAH affects the distal vasculature[351]. It is interesting to note that following lung resection, the point of reflection may actually be the now ligated subsequent bifurcation to the RPA or LPA. As such, a similar finding to Quail et al. following lung resection may represent the true reflection site and not the horizon effect.

7.2.4.5 Reservoir wave hypothesis

Separation of pressure and flow into forward and backward components gives distinct forward and backward components in systole. In order to explain the gradual decline in pressure with no flow during diastole, WIA calculates large simultaneous forward and backward components that cancel each other out[364], left side of Figure 7-9. The pressure decline is caused by a reservoir of pressure in the form of the elastic recoil of the arterial wall, termed the Windkessel effect[389], see 1.2.6.4. Incorporation of a Windkessel reservoir pressure into wave separation removes the diastolic separation between forward and backward waves[364], right side of Figure 7-9.

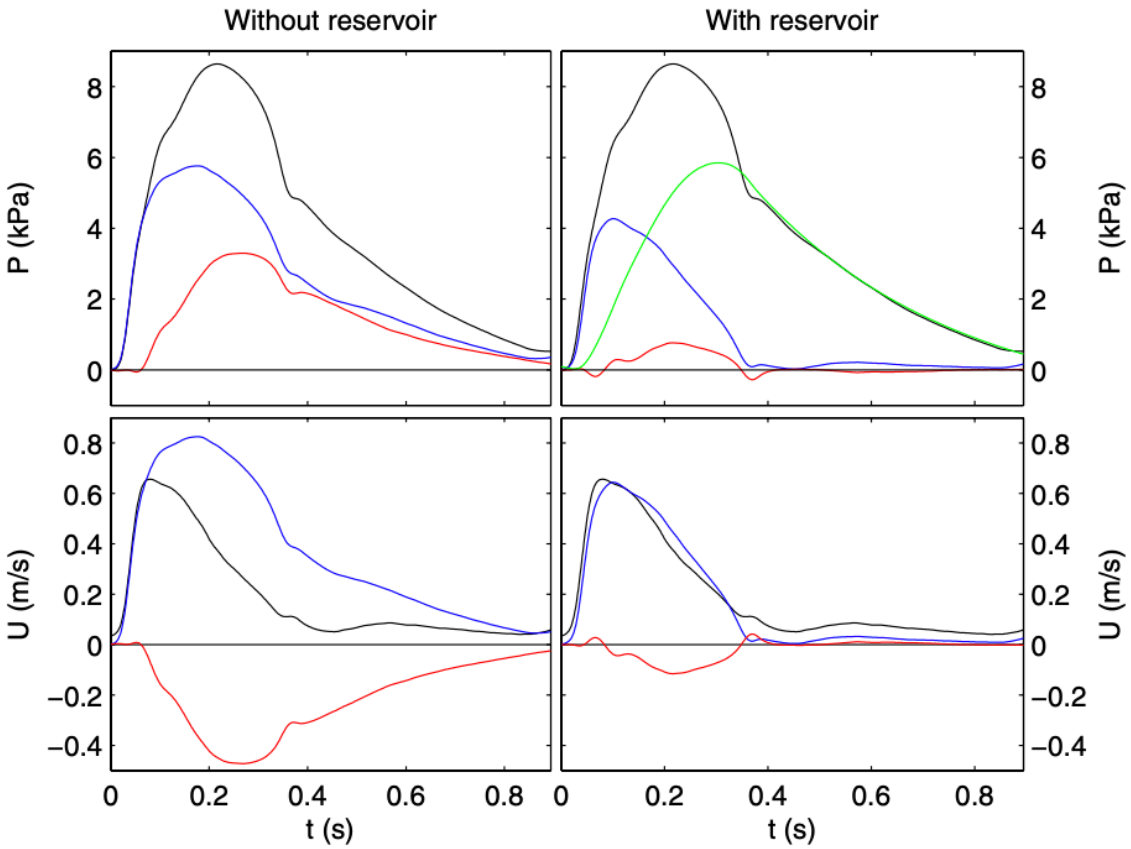

Figure 7-9 Wave intensity analysis with and without pressure reservoir
Separation of pressure (P, top row) and velocity (U, bottom row) into its forward (blue) and backward (red) components. Left column is separation without a pressure reservoir, right column is incorporating a pressure reservoir (green line). Plots are against time (t). Note the cancelling diastolic forward and backwards wave in the plots in the left column are removed by adding the pressure reservoir. Image from Parker et al.[364].

The reservoir wave hypothesis has faced criticism and its use is not universal. Arguments against the mathematical assumptions required for the hypothesis have been made by Westerhof et al. who describe the concept as *"inconsistent"*[390]. Modelling by Alastruey[391] and experimental data by Hametner et al.[392] found that the pressure reservoir calculated is equal to double the backward pressure. Mynard et al. found that the addition of a pressure reservoir to an experimental model of WIA *"markedly underestimates or eliminates"* BCWs, overestimates FEW and BEWs and displayed *"non-physical"* interactions [393, 394].

In summarising the evidence for a pressure reservoir, Parker stated *"preliminary results do not provide conclusive evidence of the utility of reservoir and excess pressures but they do suggest that it is an avenue well worth exploring"*[395].

7.2.4.6 Blood flow distribution across a bifurcation

Whilst cross-sectional area ratios between the parent and daughter vessels influence wave reflection, there are other factors that influence the distribution of the incident blood flow between the daughter vessels[396-398]. This has been elegantly demonstrated in a computer model of variations of PA anatomy in patients with repaired tetralogy of Fallot by Boumpouli et al.[398], Figure 7-10. Whilst the study uses a two-dimensional model of the pulmonary tree, assumes steady flow and non-compliant vessel walls, it highlights the contribution of each factor to the splitting of flow. As detailed in Figure 7-10, the percentage distribution of blood flow in a daughter vessel is reduced when, compared to the other daughter vessel, it has a;

- Smaller vessel diameter
- Longer length
- Increased pressure at its output (afterload)
- Increased angle of vessel at bifurcation (not in figure).

Any decrease in operative vessel diameter may either be secondary to or contributory to a reduction in vessel blood flow. The assumptions described above do not account for the compliance of the PAs and so it cannot be assumed that any change in area alone will determine blood flow distribution without also considering the compliance/distensibility of the vessels.

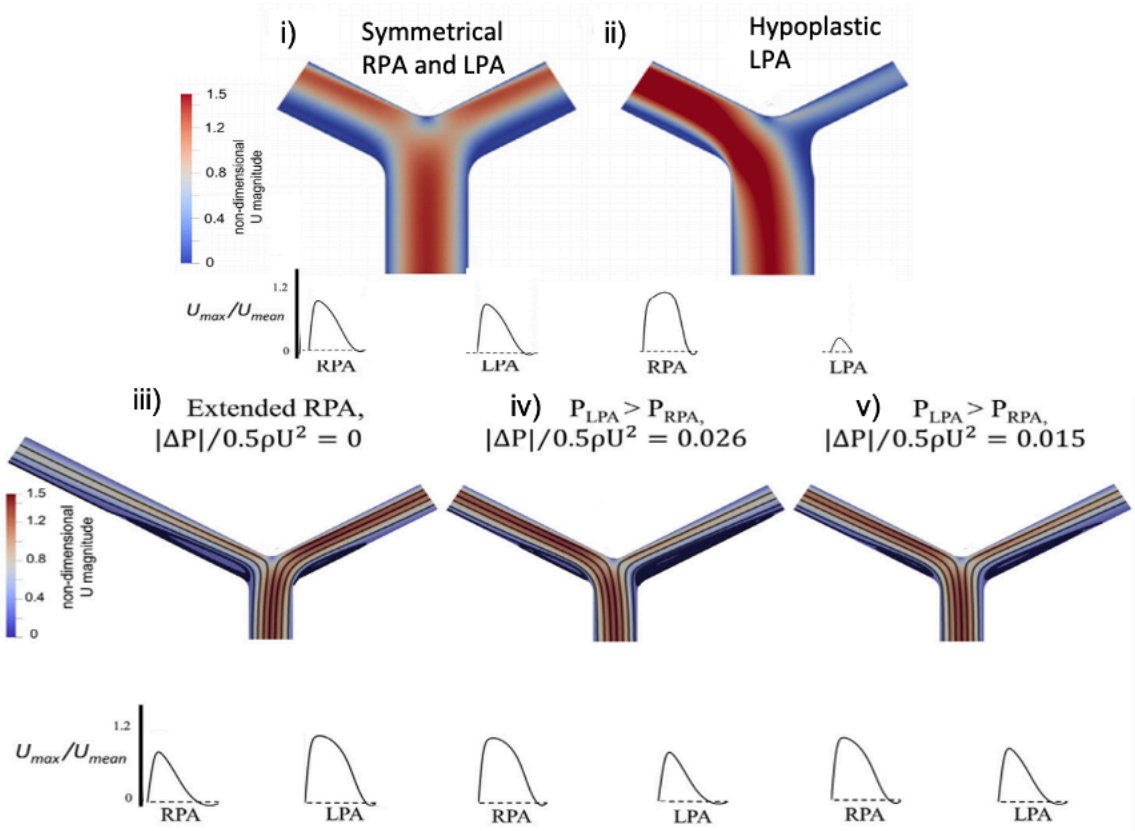

Image	Type of junction	Branch diameter (D.LPA : D.RPA)	Branch length (L.LPA : L.RPA)	Pressure difference $\|\Delta P\| / 0.5\rho U2$	Flow Split (%) (Q.LPA : Q.RPA)
i	Symmetric	1:1	1:1	0	50:50
ii	Hypoplastic LPA	1:2	1:1	0	12:88
iii	Extended RPA	1:1	1:2	0	67:33
iv	Pressure difference =0.026	1:1	1:1	0.026	33:67
v	Pressure difference =0.015	1:1	1:1	0.015	40:60

Figure 7-10 Factors affecting blood flow distribution between right and left pulmonary arteries
Computational presentations of blood flow distribution following repair of tetralogy of Fallot. Velocity (U) of blood flow represented by colour, red= high velocity, blue= low velocity. Corresponding velocity plots displayed for the right pulmonary artery (RPA) and left PA (LPA) beneath each representation of the artery. $|\Delta P|/0.5\rho U^2$= pressure difference normalised for blood density (ρ) and velocity. P= pressure. Table summarises changes flow (Q) split between LPA and RPA for each example of a bifurcation. Adapted from Boumpouli et al.[398]
i) Symmetrical bifurcation with no pressure difference. Equal split of flow 50:50.
ii) Hypoplastic LPA with decreased branch diameter. Decreased LPA flow.
iii) Extended RPA but equal diameters. Decreased RPA flow.
iv) Markedly increased pressure at the LPA output. Markedly reduced LPA flow.
v) Slight increase in LPA output pressure. 40:60 split, similar to normal blood flow distribution.
NB RPA and LPA plots for iii) are swapped from published paper as they are different to results explained in table and text of the paper.

7.2.5 Wave intensity analysis in the pulmonary circulation

There are few studies investigating WIA in the pulmonary circulation in man and no previous studies specifically investigating it following lung resection. Initial work performed in animals demonstrated that the pulmonary circulation has a

similar wave intensity profile to the systemic circulation. In health, the pulmonary vasculature is relatively open-ended generating an early-mid systolic BEW which encourages the forward flow of blood[399-401].

When making comparisons across studies it is important to note that the value of dI is dependent on the sampling time of the data. If the sampling rate is doubled (the time differential is halved) then dP and dU double whilst dI will increase by fourfold (2^2). Direct comparison between studies therefore is only possible when the sampling time is the same[151]. Alternatively, calculation of the time normalised wave intensity (WI) from the time derivatives of pressure (dP/dt) and velocity (dU/dt) can be performed[380]. Calculation of WRI also allows direct comparisons between studies by describing the BCW relative to the FCW.

7.2.5.1 Animal studies

The changes in WIA describing the response of the RV and pulmonary circulation to increased afterload has been neatly demonstrated by Nie et al.[402]. In their concise study, WIA was performed by pulmonary catheter in eight ventilated dogs. Baseline WIA was measured in conditions of normoxia, hypoxia (fraction of inspired O_2 0.08-0.11) and hypoxia with vasodilation (nitric oxide, NO), Figure 7-11. The hypoxic mixtures were both performed in nitrogen and helium to assess if helium increases the diffusion velocity and therefore the effect of NO. FCW and FEW were present at baseline, as described in the systemic circulation. In response to hypoxia the FCW increased as the RV increased contraction to increase cardiac output. The hypoxic vasoconstriction converted the pulmonary vasculature to a relatively closed-ended system, demonstrated by the development of a BCW. This change was partially reversed by pulmonary vasodilation from adding NO to the inspired gas mixture. This reduced the FCW and almost removed the BCW. Helium did not alter the hypoxic response but did increase the effectiveness of NO[402].

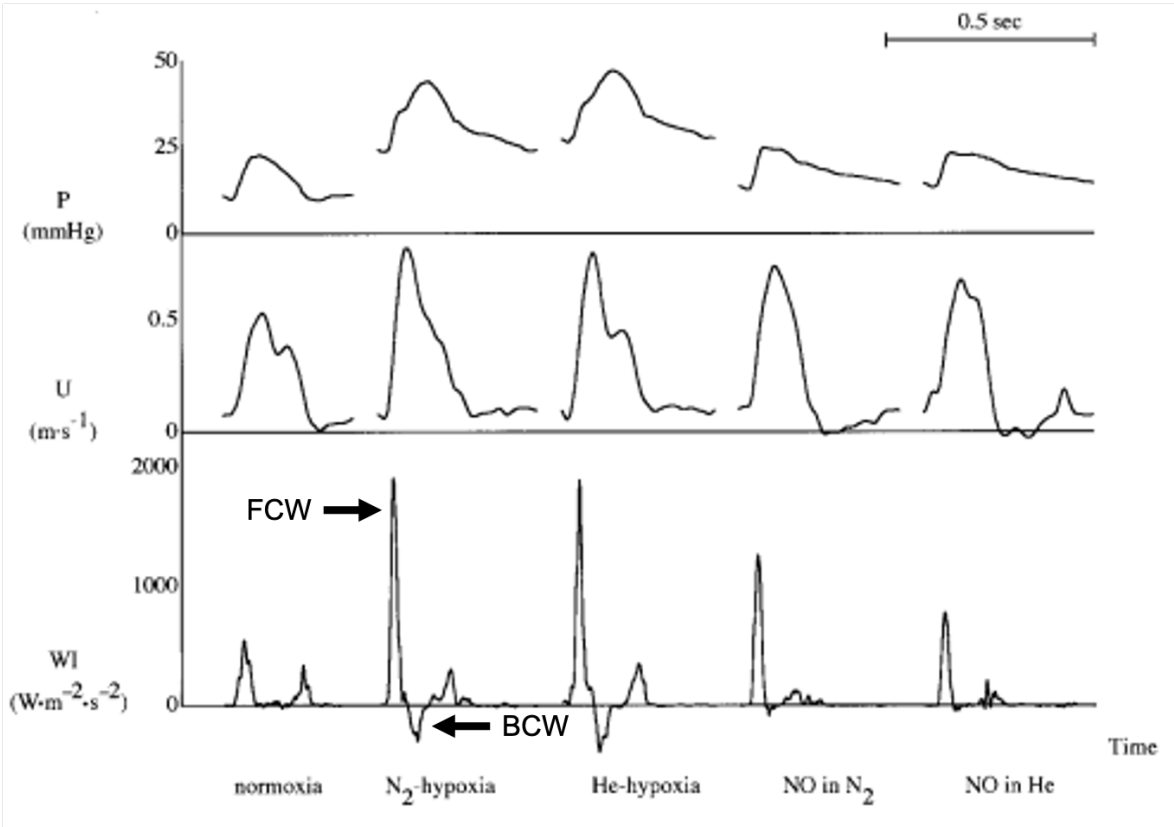

Figure 7-11 Pulmonary wave intensity analysis in hypoxia and vasodilation
Pressure (P), flow velocity (U) and wave intensity (WI) profiles of normoxia, hypoxia and vasodilation. Inhalation of hypoxic gas mixture in nitrogen (N_2) and helium (He) initial increased forward compression wave (FCW, marked on plot) and caused a backward compression wave (BCW). Additional of nitric oxide (NO) to the gas mixtures reduced forward compression wave and backward compression waves. Image from Nie et al.[402]

Further animal models have demonstrated a similar response to hypoxia and have attempted to determine the apparent site of reflection, the results vary between the studies[399-401]. Hollander et al. calculated that in normal conditions BEWs appear to originate from a "proximal site" 3cm from the main PA whereas, in hypoxia, BCWs appear to originate from the pulmonary microcirculation 9cm from the MPA[399]. A similar pattern was demonstrated in sheep by Dwyer et al.[400]. Bouwmeester et al. found the reflection to occur at a constant site for both BEW and BCW, the site corresponds to the junction between the RPA or LPA and the lobar pulmonary arteries[401]. As discussed in 7.2.4.4, the site of wave reflection is unlikely to relate to a single distinct site of reflection in global changes in the pulmonary vasculature and is instead representative of wave reflection distal to the point of measurement. As Quail et al. state,

"This so-called "horizon effect" is due to re-reflection and entrapment of reflected waves and may be even more important in the highly fractal pulmonary circulation."

Quail et al.[351]

7.2.5.2 Human studies

The first study of human pulmonary artery WIA was performed in a 2014 ''proof of principle'' study by Lau et al[403]. WIA measurements were performed invasively by a specialised pulmonary artery catheter (PAC) with a dual-tipped pressure and doppler flow wire in 6 patients with PAH and 7 healthy controls. Patients with established PAH had larger FCW, FEW and BCW compared to controls. The wave reflection index was also increased (0.35±0.05 versus 0.11±0.06; p=0.01) with an apparent reflection site 15±5cm downstream. Wave speed was also increased in PAH (6.9±1.3 $m.s^{-1}$ versus 3.8±1.0 $m.s^{-1}$, p=0.01). These results suggest PAH results in a relatively close-ended pulmonary vasculature with increased wave reflection from the terminal branches and increased RV workload. Although reflection occurs at a more distal site, the increased wave speed resulted in the BCW returning to the RV earlier than in controls[403].

7.2.5.2.1 Pulmonary artery catheter studies

In work from research group of Parker and Hughes, Su et al. have published 3 papers investigating WIA by pulmonary artery catheter in patients referred for cardiac investigations of PAH or CTEPH and controls[404-406]. The three investigations are performed on patients from the same study and assess WIA variation with loading (PAH vs control)[404] and in patients with PAH or chronic thromboembolic pulmonary hypertension (CTEPH) versus controls[405]. Additionally, repeat measurements were performed 3 months following pulmonary endarterectomy for the patients with CTEPH[406]. These studies also offer insight into the potential mechanisms by which the RV responds to PAH and CTEPH, therefore they may help predict and interpret any potential changes following lung resection. An example of the velocity, pressures and WIA profiles generated in the pulmonary circulation of controls and PAH patients are shown in Figure 7-12.

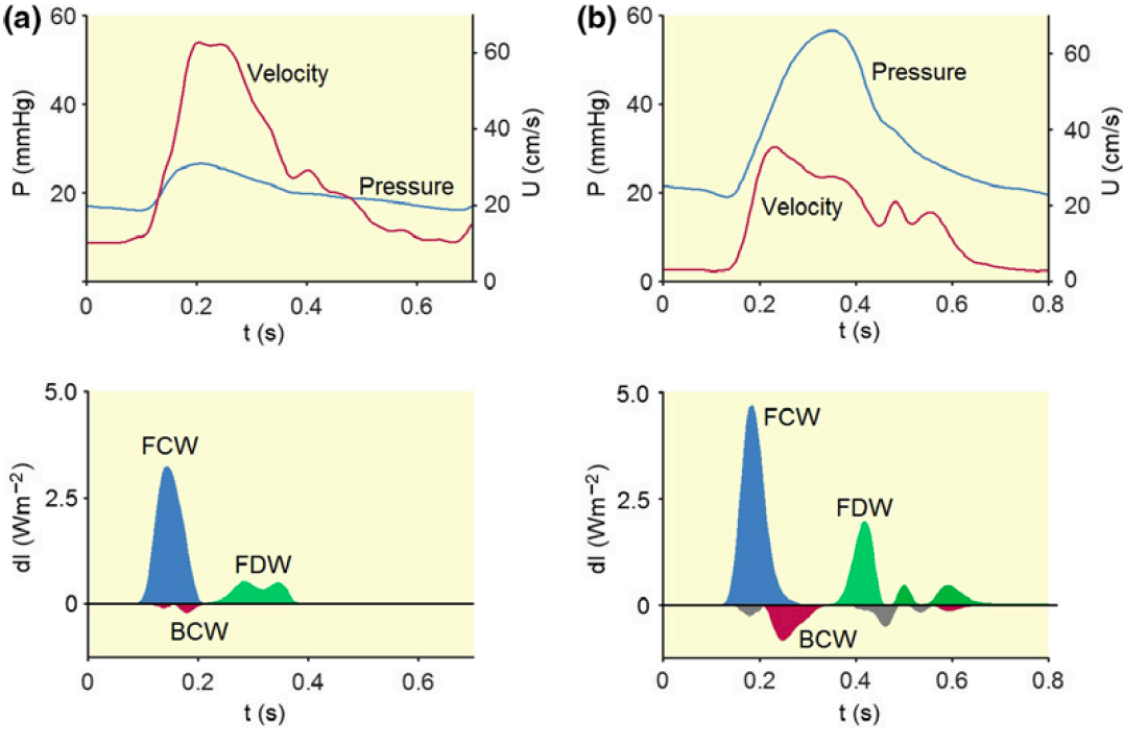

Figure 7-12 Wave intensity analysis in the pulmonary artery
Pressure (P), velocity (U) (top row) and wave intensity (dI) (bottom row) profiles of healthy patient (a) and a patient with pulmonary arterial hypertension (b). Note steeper pressure profile with higher peak and a lower 'notched' velocity profile in b. This is demonstrated as a larger forward compression wave (FCW) and forward expansion (decompression in example) wave (FDW) indicating increased work of the right ventricle. The increased backward compression wave (BCW) indicates increased wave reflection (afterload). Image from Su et al.[151].

The workload of the RV was assessed by calculation of RV energy and power density, defined as the energy and power delivered by the RV to generate the stroke volume per unit cross-sectional area[405], see Equation 7-11, energy density is power density multiplied by the duration of the cardiac cycle. These measures account for the "steady-flow" (hydraulic) portion of RV work as they are averaged over the entire cardiac cycle, similar to PVR. The ratio of oscillatory power/energy to hydraulic power/energy can be estimated by dividing the FCW by the RV power/energy densities[405]. An animal model of PAH demonstrated a slight increase in the hydraulic power of the RV with a decrease in the oscillatory to hydraulic power ratio[407]. This can be interpreted as a change in the nature of energy transfer from the RV to the pulmonary circulation with a greater reliance on hydraulic load, similar to the systemic circulation.

$$Right\ ventricular\ power\ density = (PAPm - RAP).U_{mean}$$

Equation 7-11 Right ventricular power density
PAPm= mean pulmonary artery pressure. RAP= right atrial pressure. U_{mean}=mean flow.

As described by Lau et al.[403], Su et al. also demonstrated greater FCW, FEW, BCW and WRI in patients with PAH and CTEPH compared to control, there were no differences between PAH and CTEPH. Wave speed was $3m.s^{-1}$ in controls, $12m.s^{-1}$ in PAH and $15m.s^{-1}$ in CTEPH ($p<0.001$ for both comparisons vs control). Wave speed was associated with MPAP ($r=0.62$, $p<0.01$), PA pulse pressure ($r=0.78$, $p<0.01$) and TAPSE ($r=-0.58$, $p=0.01$). Peak FCW and FCW area were not associated with any measures of RV function (RV fractional area change and TAPSE). BCW and WRI were not associated with MPAP, PVR or any other parameter. Wave speed increased with severity of pulmonary hypertension whilst WRI was similar at all stages of disease, Figure 7-13. Su et al. interpret this as a sign that an increase in WRI occur early in the development of pulmonary hypertension (increased in all cases irrespective of disease severity) whereas wave speed increases with increasing clinical severity[405].

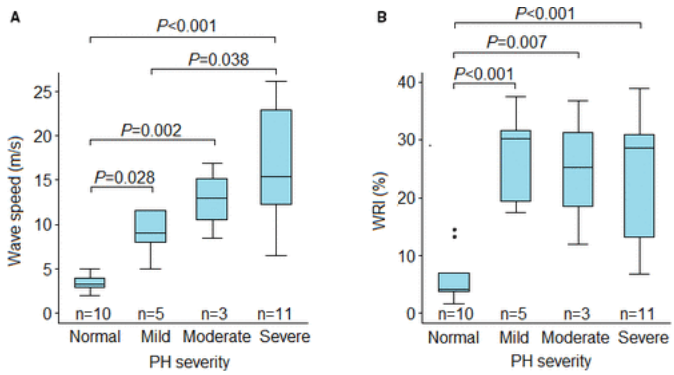

Figure 7-13 Wave speed and reflection index against pulmonary hypertension severity
Note the progressive increase in wave speed with increased pulmonary hypertension (PH) severity whereas wave reflection index (WRI) is greater than normal in PH but it is similar between all stages of PH. Image from Su et al.[405].

RV power and energy density were both increased from control in PAH and CTEPH with no difference between PAH and CTEPH. FCW/RV power density ratio and FCW/RV energy density ratio were similar to control in CTEPH but reduced in PAH, Figure 7-14. Su et al. argue that this may represent differing response of the RV and pulmonary vasculature to afterload between the two disease processes. As discussed in 1.2.3 page 50, the RV has differing responses to gradual and sudden increases in afterload[133]. In PAH there is a gradual change in the PA vasculature increasing afterload whilst in CTEPH the RV is subjected to an episodic stepwise increase in afterload.

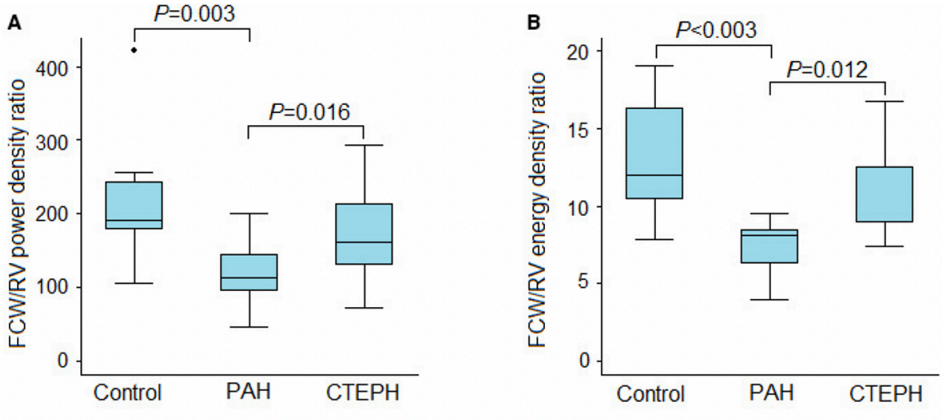

Figure 7-14 Oscillatory to hydraulic power ratios in pulmonary hypertension
Ratio of right ventricular (RV) oscillatory power to hydraulic power calculated by forward compression wave (FCW) divided by RV power density ratio (A) and RV energy density ratio (B). Ratios reduced in pulmonary arterial hypertension (PAH) against control and chronic thromboembolic pulmonary hypertension (CTEPH). Image from Su et al.[405].

Su et al. argue that the reduced oscillatory/hydraulic power ratios in PAH are more likely secondary to differences in pulmonary vasculature adaption than differences in RV adaption. They base this on a higher wave speed, lower PVR and lower MPAP in CTEPH than PAH, although none of these differences is statistically significant. Also, they argue that whilst RV adaption is generally better in diseases such as Eisenmenger syndrome (a chronic increase) the differences may represent a *"more rapid (in most cases) RV adaption to sudden change in pressure load, as it is in CTEPH, versus gradual alteration over time in PAH."* An alternative interpretation of their results is that in PAH there is more marked RV hypertrophy and therefore a greater hydraulic component. RV energy power and density tended to be higher in PAH, although again neither of these differences were statistically significant. Patients with CTEPH may therefore have maintained oscillatory power compared to the stiffer hypertrophied RV adaption of chronic afterload increase. Given that there are only 10 controls, 11 PAH patients and 10 CTEPH patients to compare, the study is likely underpowered to determine such differences.

Su et al. also demonstrated in patients with CTEPH that, although pulmonary artery endarterectomy (PEA) reduced PA pressure, PVR and wave speed; there were no changes in WRI, wave energies or RV energy density. Additionally, the ratio of FCW to RV stroke work was unchanged. This implies that even when PAPs and PVR are reduced, the adapted RV maintains the same oscillatory to hydraulic energy ratio. The preserved WRI demonstrates residual wave reflection and increased afterload which are not evident by simple measurement of PAP and PVR.

This residual afterload may be caused by pulmonary vascular remodelling distal to the sites of the large emboli that are removed and/or secondary to established micro-emboli in other vessels[406]. Again, this highlights the complexities of afterload that PVR and PA pressures overlook.

7.2.5.2.2 Cardiac magnetic resonance studies

Wave intensity analysis can be performed non-invasively by CMR. It allows accurate flow measurement in the MPA, RPA and LPA although as it cannot directly measure pressure, WIA can be calculated with vessel area. Area has been used instead of pressure in ultrasound studies of WIA in the systemic circulation[351, 375]. MPA imaging is subject to through plane motion from contraction of the RV which pulls the MPA inferiorly, shifting the narrower distal MPA into the imaging plane during systole and artificially reducing the increase in area seen in systole[351]. Additionally, the motion of the MPA may bring it in and out of the true cross section of the imaging plane[358], as discussed in 6.6.1 page 220. In comparison, whilst Su et al. were able to perform MPA and RPA WIA, they were unable to perform WIA in the LPA with PACs[405].

Quail et al. utilised CMR to compare WIA in 20 patients (13 PAH and 7 CTEPH) and 10 healthy controls of a similar age[351]. Their methods (discussed below) and results are the most applicable to the investigation performed in this chapter. Similar to Su et al. they demonstrated increased wave speed in disease, although the calculated speeds were much lower in Quail et al. (1.36m.s^{-1} vs 12m.s^{-1} in PAH and 0.72m.s^{-1} vs 3m.s^{-1} in controls). Contrary to Su et al., they demonstrated reduced FCW energy in patients with PAH compared to controls. The main differences between the patients with PAH versus controls can be demonstrated in the backward waves, Figure 7-15. There were BEW in controls (relatively open-ended pulmonary circulation) but BCW (relatively closed-ended pulmonary circulation) in PAH. In this cohort, a BCW area of >0.0006cm^5 had a 100% sensitivity and 91% specificity for detection of a proximal clot (AUROC 0.97). Quail et al. also sought association between haemodynamic variables and WIA parameters. Only FCW was associated with PVR (r=-0.66) and RVEF (r=0.65)[351].

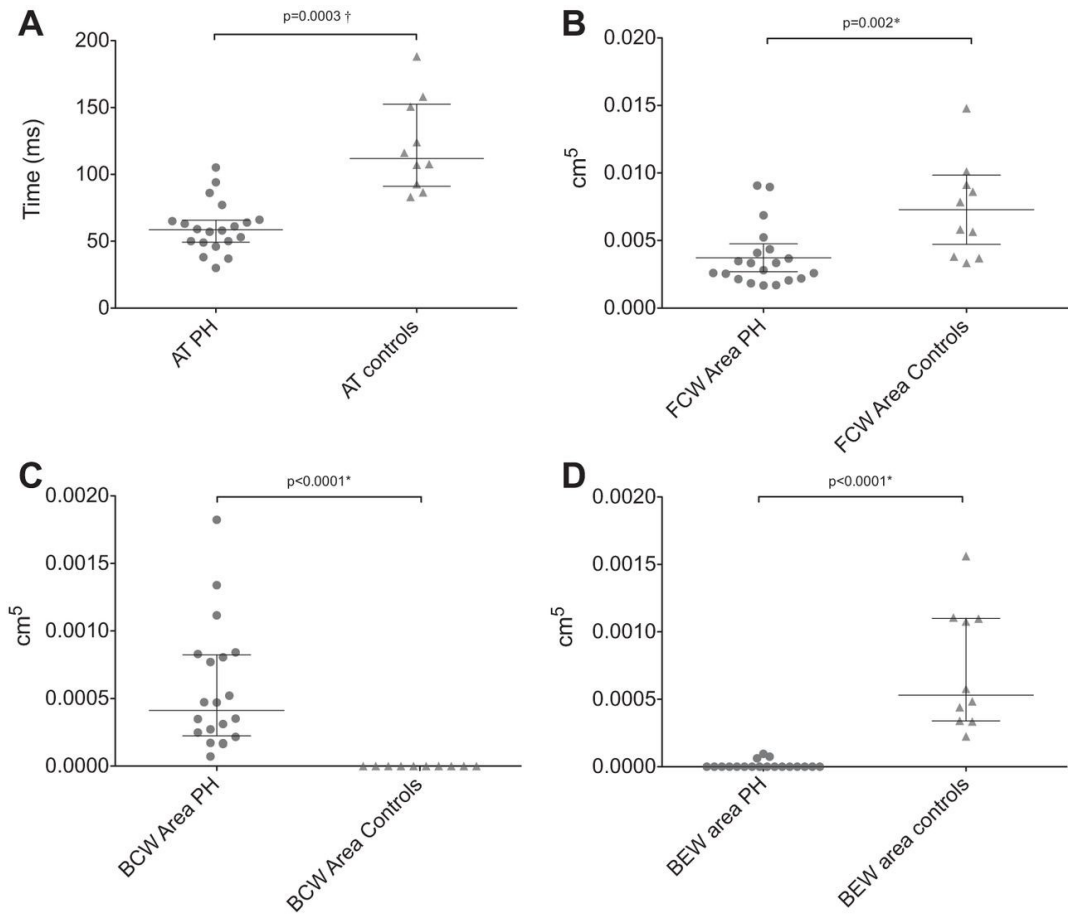

Figure 7-15 Wave intensity analysis in pulmonary hypertension versus control
Acceleration time (AT) (A) and forward compression wave (FCW) (B) were reduced in pulmonary hypertension (PH) against controls. The main difference between the groups was the nature of the wave reflection and therefore the degree of pulsatile afterload. In patients with PH the reflected waves were backward compression waves (BCW) (C) whilst in controls the reflected wave was a backward expansion wave (BEW) (D). Image from Quail et al.[351].

Quail et al. also investigated the relationship between PAAT and WIA. PAAT has been demonstrated to be decreased in PAH with a "notched" flow pattern, demonstrated in panel A of Figure 7-16 and previously[342, 353, 408], Figure 6-4 page 197. The notched flow pattern is a widely recognised indication of PAH[409] and it has been recognised that the notching of the PA flow profile is caused by wave reflection [410], see 6.1.2. This is the first study to demonstrate that the onset of the notching and therefore PAAT occurs when a BCW exceeds the initial FCW. As demonstrated in Figure 7-16 net dI rapidly declines following the initial FCW peak. When dI crosses the x-axis the negative BCW exceeds the remaining positive dI from the FCW, i.e. the BCW is the dominant wave. At this point the effect of the BCW is to reduce forward flow of blood causing the rapid decline in blood flow and the characteristic "notched" flow pattern. In Quail et al.s' study, PAAT was reduced in PAH versus controls and a PAAT of <57.6ms was predictive of the presence of a proximal clot (AUROC 0.84, sensitivity 88%, specificity 81%).

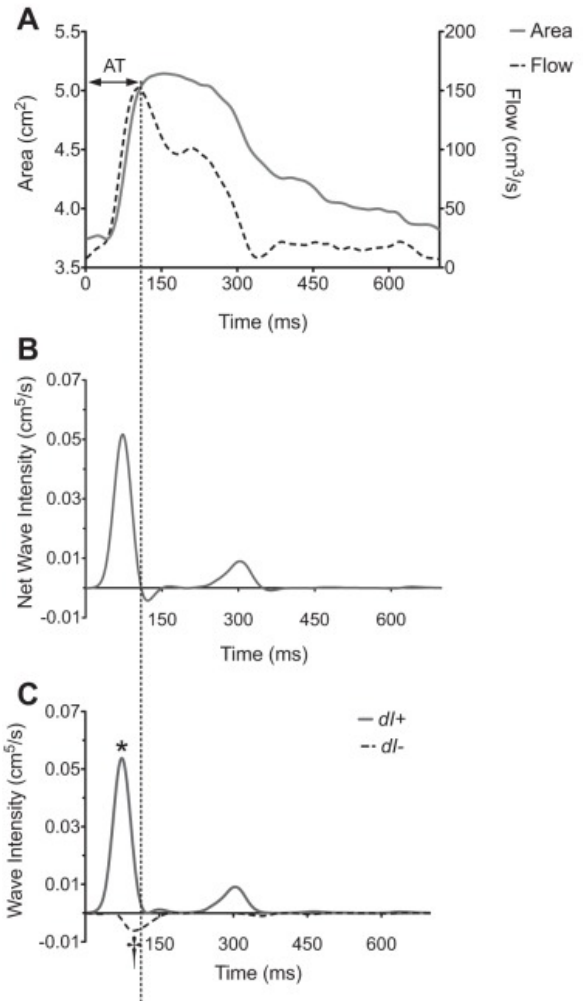

Figure 7-16 Acceleration time and wave intensity analysis
Area and flow plots against time (A) show a "notched" flow profile with a reduced acceleration time (AT) that is temporally related to the onset of negative net wave intensity (B) and the peak of a backward compression wave (†) (C). AT occurs when the negative wave intensity (dI-) is greater than the positive wave intensity (dI+) *= forward compression wave. Image from Quail et al.[351].

Schäfer et al. have performed a retrospective study of children who had required both CMR and right heart catheterisation (RHC) for investigation of PH[377]. Their WIA methodology was based on that of Quail et al.[351], although flow analysis was only performed in the MPA in their departmental protocol. Similar to Quail et al. and Sue et al., they demonstrated increased BCWs and wave speed in PH versus control, although they found no difference in FCW or FEW. Of the WIA parameters they demonstrated; increased wave speed (HR 3.67, [95% CI=1.47-10.20]), increased BCW (HR 2.91, [95% CI=1.18-7.55]) and reduced FEW (HR 0.34, [95% CI=0.11-0.90]) were all prognostic of *"clinical functional worsening"*. Additionally, they showed that increased MPAP, PVR index, end-diastolic pressure and reduced RVEF were also prognostic of clinical deterioration. PA distensibility was also reduced in PH versus controls although it was not predictive of deterioration.

7.2.6 Methods of calculating wave intensity

7.2.6.1 Modality of assessment

Pulmonary WIA was originally performed with PAC in animal models[399-402] and subsequently in man by Lau et al.[403] and Su et al.[404-406]. To date only Quail et al.[351] and Schafer et al.[377] have reported CMR pulmonary WIA in man although feasibility of the technique was originally demonstrated in an abstract by Leimbigler et al. in 2012[411].

As previously discussed, 1.2.5 page 61, analysis of blood flow in the pulmonary arteries can be performed invasively by pulmonary artery catheters or non-invasively by CMR and echocardiography. The main distinction in WIA methodology between techniques, is the measurement of pressure. PAC studies allow direct measurement of pressure and as such calculate WIA as per Equation 7-2, Equation 7-5 and Equation 7-6. Non-invasive techniques measure changes in cross-sectional area instead of changes in pressure. Whilst echocardiography has been used to calculated carotid WIA[379, 383] it has not yet been used to measure pulmonary WIA. An additional benefit of PAC is greater temporal resolution of measurement, 200-1000Hz[403, 405] versus 30-100 Hz with CMR[351, 377].

The other main distinction between PAC and CMR techniques is the ability to perform WIA in the main, left and right PAs. Whilst PAC allows measurement of WIA in the MPA, this is difficult in CMR techniques. The MPA is pulled inferiorly with contraction of the RV causing a distortion the angle of cross section of the curved MPA[358, 412] and pulls the narrower distal MPA into the imaging plane in systole[351]. As cross-sectional area is used as a pressure surrogate, any deviation from the true cross-sectional axis leads to an artefactual increase in area/pressure and therefore WIA. Conversely, compared to CMR, measurement of WIA the RPA or LPA with PAC is challenging. Directing the PAC into the desired artery is difficult and requires live angiographic or x-ray guidance. Su et al. were only included measurements from the RPA as they were unable to obtain satisfactory velocity data from the LPA in “several” patients with CTEPH[405].

7.2.6.2 Data filters

As WIA is calculated as the product of the differences in measured pressure/area and flow/velocity it is very sensitive to noise in these measurements. To minimise this potential source of error, it is necessary to apply a filter to the data. Parker advises use of a Savitzky-Golay filter[364]; this was first described in 1964 and has been described as the *"dawn of the computer-controlled analytical instrument"*[326, 413]. It calculates the central point of a given window size to a polynomial fit of a chosen order to the least sum of square. The window size (n) is the number of data points included in the smoothing calculation ($\frac{n-1}{2}$ points either side of the central point, therefore n is always an odd number), see Figure 7-17. In WIA a second order polynomial is generally used with a symmetrical window size, i.e. a graph of a second order polynomial is given by the equation $f(x)=a_0 + a_1x + a_2x^2$ where $a_2 \neq 0$[326]. The benefit of this filter is that is maintains the peaks and troughs of the original data that are required for detection of the rapid changes in pressure/area and flow/velocity that are essential in WIA.

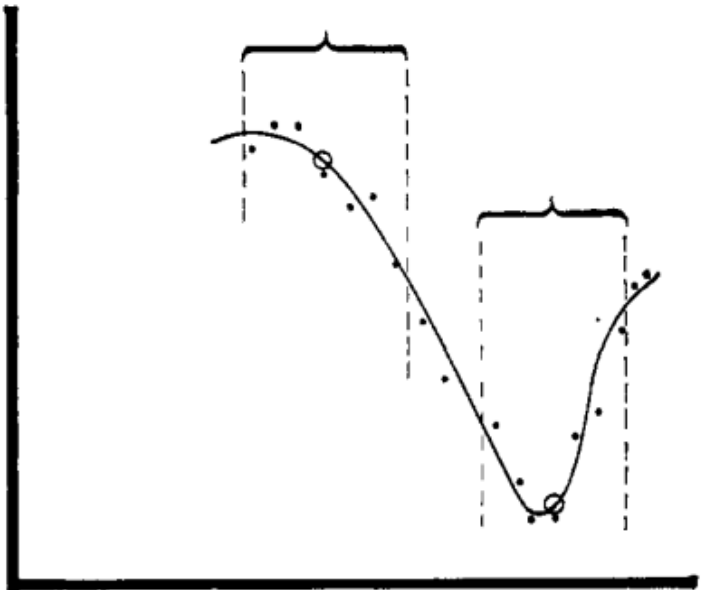

Figure 7-17 Seven-point Savitzky-Golay smoothing filter
Example of a smoothing filter from the original Savitzky and Golay paper. The brackets represent the window size (7) in which the data central data point is replaced by the value in the open circle. Image from Savitzky and Golay[326].

Su et al. (including Parker as an author) used a second order polynomial fit with an 11-point window size in their analysis of data collected with a PAC with a sampling frequency of 200Hz[405]. The width of the window size determines the degree of smoothing, a larger window will result in greater smoothing of the data

and may risk removal of the underlying signal. The most appropriate window size needs to be optimised for the data collected[405]. Quail et al. used a Butterworth filter in their investigation[351]; this removes noise above a set frequency[414] and has been used to a lesser extent in WIA studies[402, 415].

7.2.6.3 Wave speed

There are three broad mechanisms of calculating wave speed (c) in the time domain[yy 416, 417]. The most logical method of wave speed calculation is the time delay (transit time) between the onset of flow/pressure increase between two points a known distance apart. This is called the foot-to-foot method[417], see Figure 7-18(b).

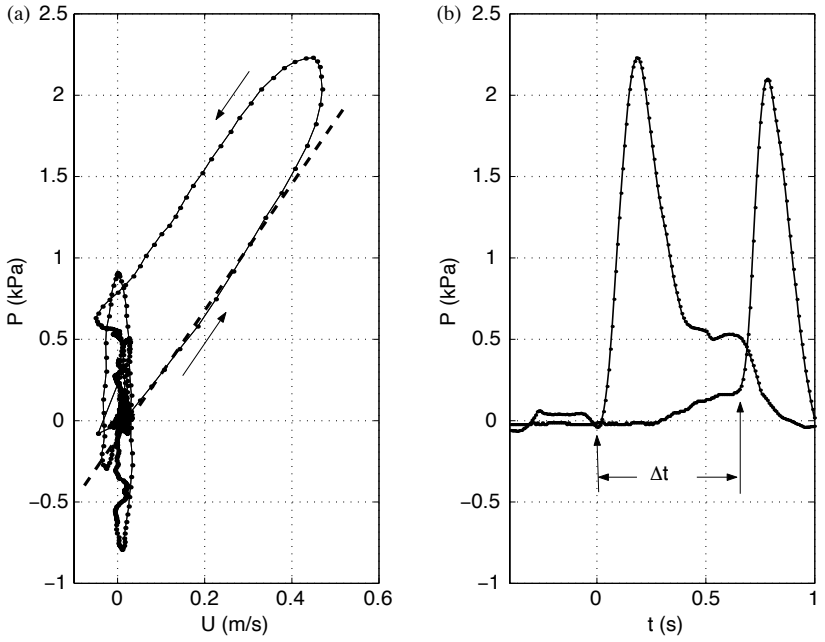

Figure 7-18 Methods of calculation of wave speed
a) Pressure (P) velocity (U) loop over cardiac cycle, arrows demonstrate direction of the loop. Wave speed can be calculated from the gradient of the early systolic linear prior to wave reflection (dashed line in plot).
b) Foot-to-foot method of wave speed calculation. Time difference (Δt) between onset of increase in pressure at two sites of known distance apart. Wave speed calculated as distance/Δt.
Image from Khir and Parker[417]

Rearrangement of the water hammer equation, Equation 7-4, allows calculation of wave speed from the change in pressure and the change in velocity (PU-loop)[418], Equation 7-12. This assumes that in early systole there are no reflected waves and that there is a linear section of the PU-loop, wave speed can therefore be

[yy] Characteristic impedance (Zc) can also be used to calculate wave speed but as detailed above this approach is distinctly separate to the time-domain methods of WIA.

calculated as the gradient of this section, Figure 7-18(a). This method requires a high sampling frequency to have at least three data points (in order to plot an accurate straight line) prior to the influence of wave reflection[351]. Variations of this technique calculate wave speed without direct pressure measurement, instead wave speed is calculated from either the changes in flow (dQ) and change in cross sectional area (dA) (QA-loop)[419] or the change in the natural log of vessel diameter and velocity ((lnD)U-loop)[379]. These methods again rely on detection of a linear early systolic period without wave reflection.

$$c = \frac{dP}{\rho dU}$$

Equation 7-12 PU-loop wave speed calculation
c= wave speed. dP= change in pressure. ρ= density of blood. dU= change in velocity.

Calculation of wave speed in the coronary arteries is not possible with the above methods as there is no stage when wave travel is unidirectional. Davies et al. devised the sum of squares (SOS) method where wave speed is calculated from the changes in P and U[420] or A and Q[351] over the entire cardiac cycle [zz].

$$c = \frac{1}{\rho}\sqrt{\frac{\Sigma\, \mathrm{dP}^2}{\Sigma\, \mathrm{dU}^2}} \cong \sqrt{\frac{\Sigma\, \mathrm{dQ}^2}{\Sigma\, \mathrm{dA}^2}}$$

Equation 7-13 Sum of squares wave speed calculation
c= wave speed. ρ= density of blood. dP= change in pressure. dU= change in velocity. dA= change in cross sectional area. dQ= change in flow.

The influence of wave reflection on calculation of wave speed has been investigated in bench top tube models. All methods show increasing inaccuracy as the site of measurement approaches the site of wave reflection[416, 417, 423]. Compared to the foot-to-foot method (the gold standard), SOS underestimates wave speed whereas loop methods over-estimate wave speed[416]. Interpretation of

[zz] In Quail et al.s' original description of this method the paper states that wave speed was calculated as $\sqrt{\frac{\sum dA^2}{\sum dQ^2}}$. This was highlighted in a letter[421] and Quail replied that the equation in the original paper was a typographical error. They state that the equation displayed Equation 7-13 was used in calculation of their results[422].

wave speed is therefore dependent on both the method used to calculate it and the proximity of measurement site to a site of wave reflection.

In the pulmonary circulation, Su et al. found that in "many" of their participants the PU-loops did not have a linear section from which to calculate wave speed[404-406]. Instead, they use SOS (PU method as they used PACs and therefore measured pressure) to forgo the assumption that there is a reflection free period in systole given that they were investigating hypothesised increased wave reflection in PAH. Quail et al. used the QA-loop for their analysis but also calculated wave speed by the SOS method for comparison (QA method as they used CMR). They show good agreement with minimal bias between the methods but they do not specifically investigate agreement in arteries with and without significant wave reflection[351].

7.2.7 Wave intensity analysis conclusion

Complete assessment of RV afterload is challenging, particularly following lung resection. Cardiac magnetic resonance WIA offers a model to investigate wave reflection and simultaneously measure afterload and assess RV function. Such analysis has not been performed in this population and this investigation allows the first opportunity to track changes in WIA following a defined unilateral anatomical change in the pulmonary vasculature.

7.3 Hypotheses

As detailed in this Chapter, Chapter 3 and throughout this thesis, RV pulsatile afterload is hypothesised to following lung resection. The following are investigated in this chapter (and Chapter 8),

- Pulsatile afterload, measured by WRI,
    a. increases following lung resection
    b. predominately affects operative PA
    c. will originate from a proximal reflection site.

- The magnitude of increase in pulsatile afterload rate will be associated with[aaa]
    a. The altered post-operative distribution of CO between the PAs
    b. reduction in RVEF
    c. impaired strain

7.4 Methods

This investigation was performed on the RPA and LPA flow and area plots described in Chapter 4, where the methodology for the image acquisition, interpretation, initial data processing and reproducibility analysis are explained. The further steps required to perform wave intensity analysis (WIA) are detailed below. Of note, WIA was not performed in the MPA given the potential errors in cross-sectional area measurement demonstrated in the area measurements in this thesis and previously by other authors[351, 358].

7.4.1 Data processing

All data processing was performed in R Studio with original R programmes written by the author[bbb]. The cardiac cycle was divided into 30 frames during CMR scanning and therefore the initial temporal resolution of the data was one thirtieth of the cardiac period. The processes described below were repeated for each individual vessel (RPA or LPA) at each time point for each participant. Statistical analysis was also performed in R Studio.

7.4.1.1 Savitzky-Golay filter

The averaged individual time points of PA flow and area of the dual reported results, detailed in 6.3.1.2 page 200, were uploaded into R. As described by Parker et al.[364] and Su et al.[405], a second order polynomial fit Savitzky-Golay filter was applied to the original data points for flow and area. In order to ensure an accurate fit at the beginning and end of the cardiac cycle the measured data points were repeated three times, giving three cardiac cycles, Figure 7-19. Window sizes (n)

[aaa] This will be explored in Chapter 8.

[bbb] The initial code and training for R was provided by Dr Martin Shaw. Additionally, he was kindly available for ongoing troubleshooting throughout the steep learning curve of R.

of 5, 7, 9 and 11 points were tested for maintenance of signal against removal of noise[ccc]. Visual inspection of the plots generated for filtered data against original data were performed for the entire dataset to select the most appropriate balance between loss of noise and maintenance of signal. The single selected filter width was applied to all vessels for flow and area. The filtered data was then interpolated to a 1ms temporal resolution without further smoothing.

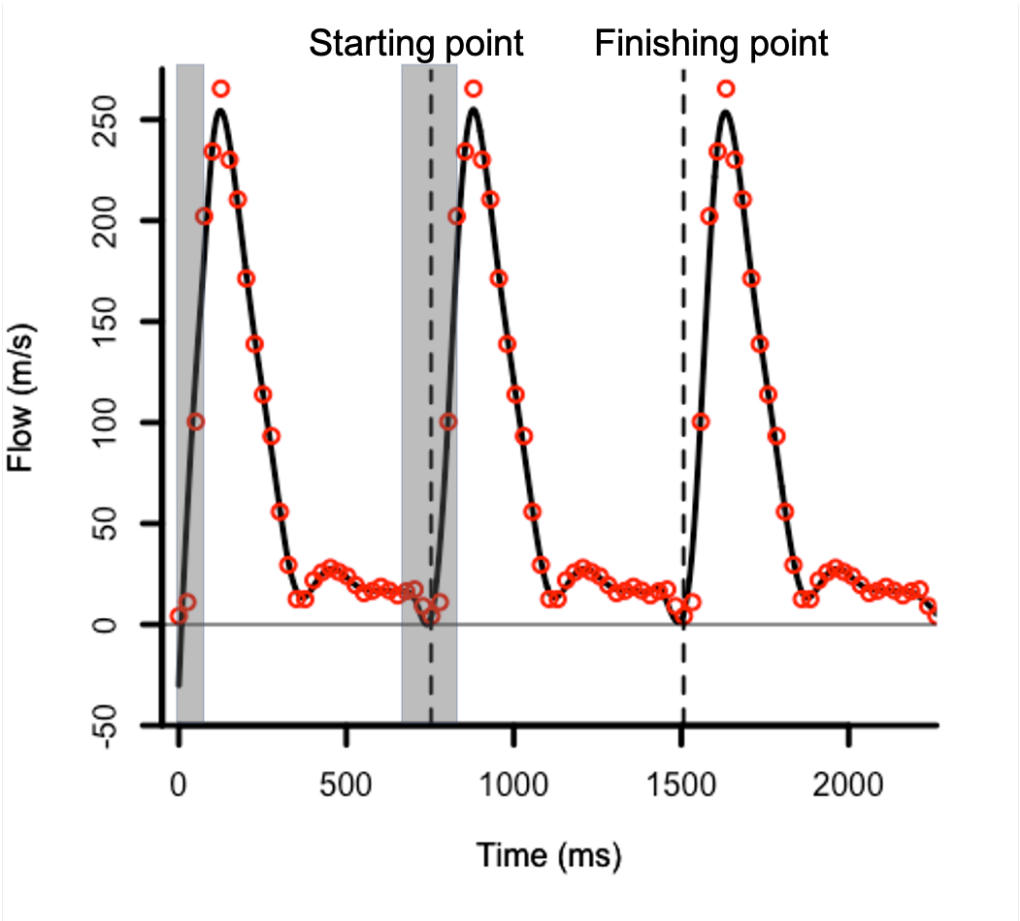

Figure 7-19 Example of Savitzky-Golay filter applied to flow profile
Original data points (red circles) repeated for three cardiac cycles. Black line represents the Savitzky-Golay (second order 7-point window), results interpreted to 1ms temporal resolution. Note the effect of the filter on the first cardiac cycle. The 7-point window only includes the centre (first) data point and the 3 points following (grey shaded area), as such the filtered value is plotted as part of the steep slope of flow increase. In this example the flow calculated is therefore negative. In the second repeated cardiac cycle, when the filter is applied to the "first" data point of the cardiac cycle the 7-point window (second wider grey shaded box) now includes the preceding diastolic plateau in flow. As such the calculated point is more accurately filtered. The same effect occurs, to a lesser extent, at the last point of the cardiac cycle. The filtered data is then extracted for selection of starting point. Flow profile is from patient in this study. Of note, the CMR reported flow profile is an amalgamation of separate cardiac cycles and is only representative a single heartbeat.

[ccc] A window size of 5 will have a closer fit to the original data than a higher size although it will remove the least noise. Noise will have a marked effect on interpretation of the differential of the data.

7.4.2 Wave intensity calculation

The distance between the heart and the site of flow and area measurement may differ not only between LPA and RPA but also differ in the same vessel between different visits. This may be secondary to selection of a more proximal or distal site of analysis or changes in the position of the heart, lungs and pulmonary arteries in the chest following lung resection[227]. In order to minimise the effect of this on comparison between vessels, temporal interpretation of WIA was normalised to the onset of wave intensity in that vessel.

Net wave intensity (dI) was calculated as the product of the change in area (dA) by the change in flow (dQ) as per Quail et al.[351], Equation 7-14. To determine the starting point dI was initially calculated with the filtered and interpolated data of the repeated cardiac cycles, Figure 7-20. The starting point of the flow profile was determined by the time of initiation of the main peak in dI from the central cardiac cycle. This wave was detected by selection of the maximal dI in the central portion of the plot and then the start point was determined as either the preceding time when dI=0 or the preceding turning point when $d^2I=0$ (second temporal derivative). An entire cardiac cycle was extracted from the filtered and smoothed flow and area data from this point. dI was calculated again from this starting point.

$$dI = dA.dQ$$

Equation 7-14 Net wave intensity calculation
dI= net wave intensity. dA= change in area. dQ= change in flow.

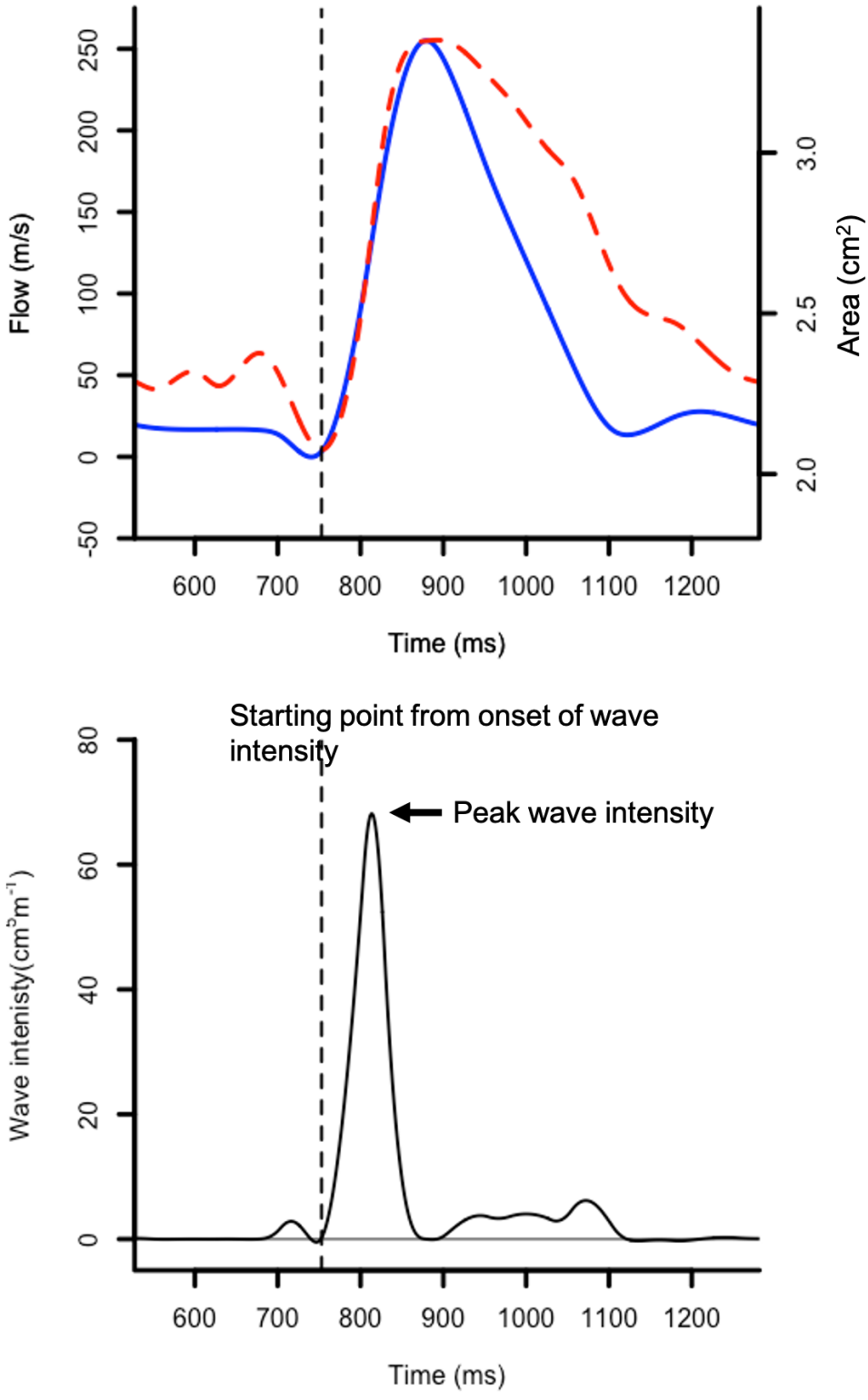

Figure 7-20 Example of net wave intensity calculation and detection of starting point
Top plot, flow (blue solid line) and area (red dashed line) against time from the repeated sample. Starting time point of the plot is after 70% of the preceding cardiac cycle. Bottom plot, net wave intensity (dI) against time. Note rapid increase in dI coincides with the increase in flow and area of top plot. Peak wave intensity measured as the maximal value of dI. The starting point is the latest time preceding this peak at which dI=0 or there is a turning point in dI (measured by the time at which the temporal derivative of dI=0) prior to this peak. Plots from patient in this study.

7.4.2.1 Wave speed calculation

Wave speed (c) was calculated from the sum of squares method (SOS) described by Quail et al.[351], Equation 7-13 page 263. Additionally, wave speed was calculated from the QA-loop method from the filtered and interpolated data, Equation 7-15. A best fit linear regression line was applied to the filtered and smoothed data points corresponding from t=0 until the time of third 3 phase[ddd] of the original CMR imaging (assumed prior to reflection), as per Schafer et al.[377] and Quail et al.[351]. Visual inspection of the QA-loops and gradient (wave speed) generated was performed to determine the presence of a linear period in early systole. SOS and QA-loop results were assessed for agreement and bias with Bland-Altman plots[424]. Following these comparisons, a single method of wave speed calculation was selected for WIA.

$$c = \pm \frac{dQ_{\pm}}{dA_{\pm}}$$

Equation 7-15 Flow-area loop wave speed calculation
c= wave speed. dA= change in area. dQ= change in flow

7.4.2.2 Wave separation

Separation of the flow, area[eee] and wave intensity plots was performed as per Equation 7-16, Equation 7-17 and Equation 7-18. Plots for each separation were generated and visually inspected for anomalies.

$$dQ_{\pm} = \frac{1}{2}(dQ \ \pm cdA)$$

Equation 7-16 Flow wave separation
dQ= change in flow. c= wave speed. dA= change in area.

[ddd] The third phase is a balance between ensuring accuracy of a best fit line (increased data points increase the accuracy) and measuring prior to wave reflection (increased data points increase risk of influence by wave reflection).

[eee] In Quail et al.s' 2015 paper there is an error in the equation for calculation of dA±, it states A rather than dA in the calculation. Equation 7-17 has this error corrected.

$$dA_{\pm} = \frac{1}{2}(dA \pm \frac{1}{c}dQ)$$

Equation 7-17 Area wave separation
dA= change in area. c= wave speed. dQ= change in flow.

$$dI_{\pm} = \pm\frac{c}{4}\left[dA \pm \frac{dQ}{c}\right]^2$$

Equation 7-18 Wave intensity separation
dI= net wave intensity. c= wave speed. dA= change in area. dQ= change in flow.

7.4.2.3 Wave detection

Complete interpretation of the wave intensity plots was performed for all vessels prior to unblinding. The process below describes the initial approach for analysis of all vessels which was successful in the majority of vessels.

An original R programme was written to automatically detect individual forward (dI+) and backward (dI-) waves from the corresponding wave intensity plots and their secondary temporal derivatives (d_2I, d_2I+ and d_2I-). The programme measured the magnitude (value at peak) and the time to the peak (from the start of dI) for each wave. Additionally, it detected the beginning and end of each wave (detailed below) and determined the nature of each wave (expansion or compression). The area under the curve for each wave was calculated using the R package auc::MESS, this calculated the area under the curve between two points defined as the start and end of the wave, see below. Plots for dI+ and dI- were generated as '.pdf' files with the area under each curve marked and shaded accordingly depending on the nature of the wave, example shown in Figure 7-21. Visual inspection of each plot was performed to confirm correct wave identification. Where this approach did not correctly identify the wave forms (usually the beginning or end points of the FEW and BCW) an alternative programme was written for analysis of that wave type with repeat visual inspection performed to ensure accurate wave detection.

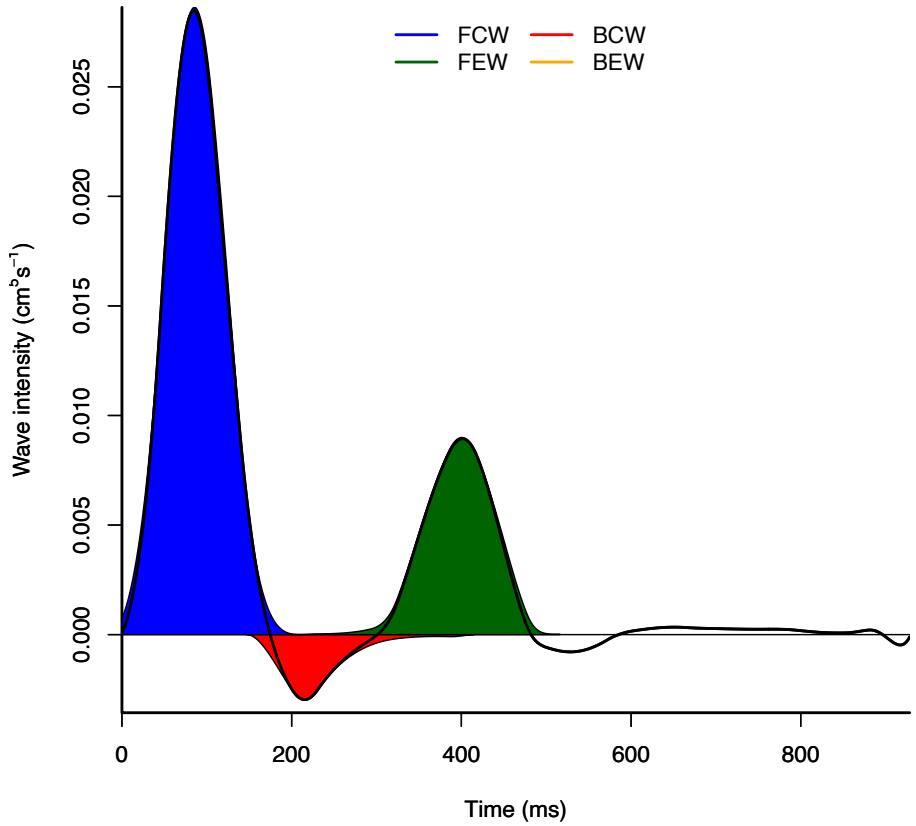

Figure 7-21 Wave intensity plot example
Representative example of wave intensity (WI) plot from patient in this study (MRIRAN31). Black line represents overall WI. Initial peak in WI caused by a forward compression wave (FCW, blue). Secondary positive peak is a forward expansion wave (FEW, green). Most negative point between these peaks in the backward wave which can be a compression wave (BCW, red) or an expansion wave (BEW, orange, not shown in example). Note the areas of the waves were separate to the overall WI measured as they are determined from the forward and backward components of the overall WI.

Forward compression waves and FEWs were detected from the dI+ plots. The magnitude and timing of the FCW was measured from the maximal value for dI+ and the time to this point. The starting point was the beginning of the cardiac cycle and the end of the wave was defined when dI+=0 or d_2I+=0 following that peak dI+. The FEW was detected as the peak in dI+ following the FCW wave. The beginning and end of the wave were detected by the turning point (point at which temporal derivative of dI+= 0) of dI+ immediately preceding or following the FEW peak at which dI+<(0.05 x the magnitude of FEW). This differentiated between small notches in the dI+ plot that create turning points but were not caused by a distinct wave and the boundaries between separate waves.

Backward waves (BW) were detected from the dI- plots. The most negative dI- occurring between the times of the peaks in FCW and FEW was detected as the peak of the backward wave, this approach was taken to ensure the backward wave

measured was a reflection of the FCW and not an earlier artefact, discussed further in 7.6.3. Given that this was either a BCW or BEW, the nature of the wave was determined by analysis of the corresponding contemporaneous dQ and dA. If dA was positive and dQ was negative (measured as dA>dQ) then the wave was classified as a BCW, if dQ>dA then the wave was classified as a BEW. The beginning and end points of this wave were detected as for the FEW although, as dI- was negative it was the turning point at which dI->(0.05 x the magnitude of backward wave). Timing of the backward wave and distance to the reflection site was interpreted together for the backward irrespective if it was a BEW or BCW. Peak WI and area of the BW were expressed as the value of BCW detected. If the wave was a BEW the value was recorded as 0.

Wave reflection index (WRI) was expressed and the sum area of the BCW over the sum of the area of the FCW expressed as a percentage, Equation 7-10 page 246.

7.4.2.4 Distance to reflection site

The distance to reflection site was calculated as per Quail et al. [351], Equation 7-19.

$$Distance\ to\ reflection\ site = \frac{(Time\ to\ peak\ BW - Time\ to\ peak\ FCW)\ x\ wave\ speed}{2}$$

Equation 7-19 Distance to reflection site
BW= backward wave. FCW= forward compression wave.

7.5 Results

As described in Chapter 4, CMR scans were completed in 27 patients pre-operatively, 22 on POD2 and 24 at 2-months. In total flow/area plots were available for WIA in 142 vessels (70 LPAs and 72 RPAs).

7.5.1 Data filtration and inspection

Visual inspection of filtration of the original data by a Savitzky-Golay filter with window widths of 5, 7, 9 and 11 points revealed an optimum window of 7 points for area and flow plots, Figure 7-22. This was deemed the optimum balance between maintenance of original data against reduction of noise.

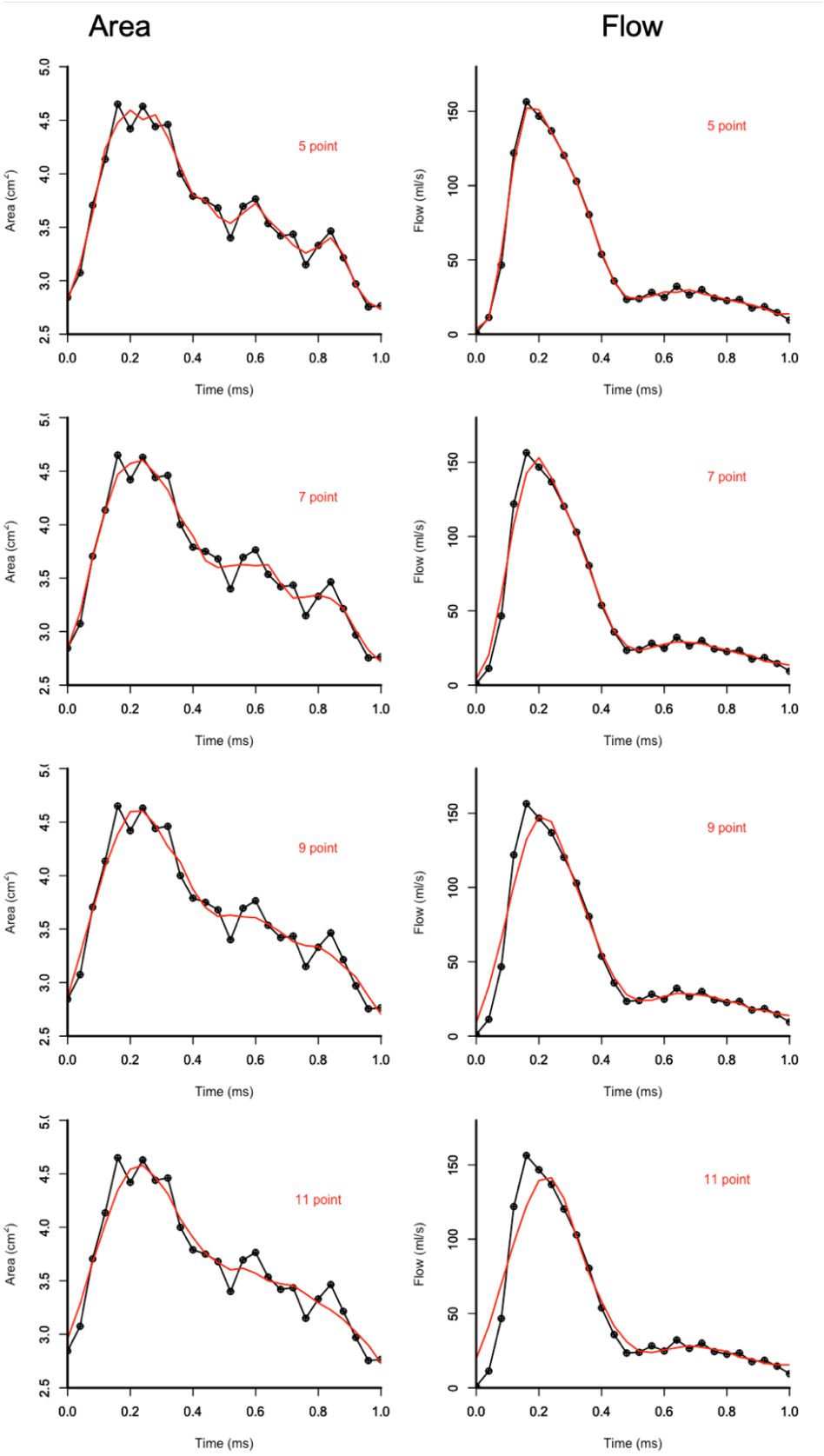

Figure 7-22 Examples of Savitzky-Golay filters of increasing size
Plots of unfiltered measured area (left column) and flow (right column) (black circles and line) with overlapped transformed data from Savitzky-Golay filter of 5 points to 11 points (red line, window size indicted on each plot). Note the effect of increasing window size with progressive loss of the underlying signal, particularly in the area plots. Increasing window size in flow plots results in a delayed representation of the rapid systolic increase in flow. A width of 7 points was selected as the best balance between reduction in noise and maintenance of underlying signal. Images from right pulmonary artery of scan MRIRAN21 in this study.

Visual inspection of WIA plots revealed abnormalities in 6 scans. All 6 scans had marked late diastolic increases in area without corresponding changes in flow, an example is shown in Figure 7-23. Whilst this was not significant enough to be detected in the distensibility results, Chapter 6, the impact on WIA was more pronounced resulting in the calculation of a large wave in late diastole that was non-physiological and would make wave speed calculation by SOS or QA loop inaccurate. Two scans were pre-op, one was on POD2 and three scans were at 2-months post-op. The abnormalities are potentially caused by motion artefact, similar to the MPA scans, discussed further in 6.6.1 page 220. These 6 scans were removed from analysis leaving 68 operative and 68 non-operative PAs (71 RPA and 65 LPAs) for analysis.

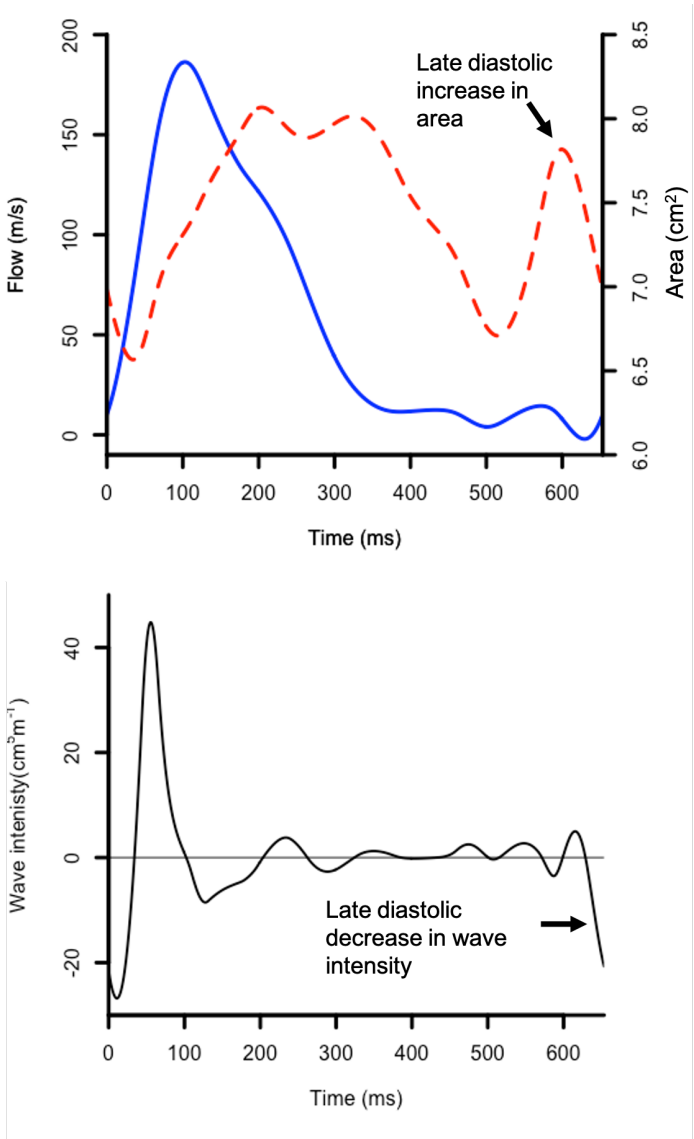

Figure 7-23 Example of abnormal wave intensity plot
Top plot, flow (blue solid line) and area (red dashed line) against time, note the late diastolic increase in area (marked by arrow). Bottom plot, net wave intensity (dI) against time. Note late decrease in wave intensity. Plots from MRIRAN18 in this study.

7.5.2 Wave speed

7.5.2.1 Calculation of wave speed by sum of squares method

Operative PA wave speed decreased post-operatively on POD2 and 2-months ($p<0.001$, paired Wilcoxon for both) whilst non-operative PA wave speed was increased on POD2 before returning to baseline by 2-month, Table 7-1. Operative PA wave speed was similar to non-operative PA pre-operatively ($p=0.856$) but lower on POD2 and at 2-months ($p<0.001$, Wilcoxon rank sum test for both).

Pulmonary artery		Pre-op	POD2	2-months	p-value
Operative	SOS ($m.s^{-1}$)	1.38 (1.28, 1.53)	0.92 (0.73, 1.20) #	0.90 (0.75, 1.06) #	***<0.001***
	n	27	20	21	
Non-operative	SOS ($m.s^{-1}$)	1.29 (1.06, 1.76)	1.60 (1.33, 1.97) #	1.27 (1.10, 1.78) ¥	***0.019***
	n	25	21	22	

Table 7-1 Changes in wave speed over time
Values are median (IQR). SOS= wave speed calculated by the sum of square method. Both Friedman's test. Comparison between time-points Wilcoxon signed rank test. #= significant difference from pre-op. ¥= significant difference from post-operative day 2 (POD2). Significant results ($p<0.05$) highlighted ***bold italics.***

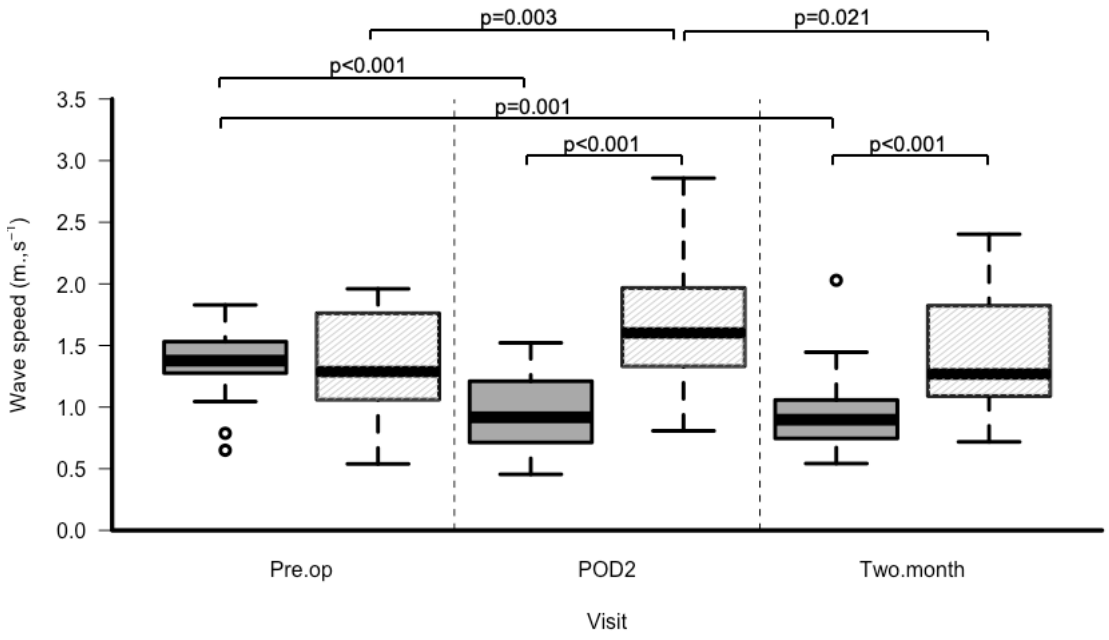

Figure 7-24 Operative and non-operative wave speed
Wave speed calculated from sum of squares technique. Wave speed was reduced post-operatively in the operative pulmonary artery (PA) (dark grey boxes) whilst in the non-operative PA (light grey boxes) wave speed was increased at post-operative day 2 (POD2) compared to pre-op and 2-months, paired Wilcoxon signed rank test for comparisons. Non-operative wave speed was greater than operative at both post-operative time points, Wilcoxon rank sum test.

7.5.2.2 Calculation of wave speed by flow-area loop method

Visual inspection of QA loops for all vessels revealed that 32/136 (23.5%) had marked curvature in early systole, example shown in Figure 7-25. As wave speed was calculated from the best fit line to the linear segment in early systole this prevented wave speed calculation in these scans. The percentage of the vessels scanned that had the curvature (non-linear) did not significantly increase post-operatively; 8/52 (15.3%) pre-operative vessels, 11/41 (26.8%) on POD2 and 13/43 (30.2%) at 2-months (p=0.198, Chi-squared test). There was a similar rate between the right (19/71 (26.7%)) and left PAs (13/65 (20%)) (p=0.353, Chi-squared test) and between operative (19/68 (27.9%)) and non-operative PAs (13/68 (19.2%)) (p=0.225, Chi-squared test). There was a trend to an increase in non-linear scans in the vessels that had undergone resection (POD2 and 2-months operative PA (14/41 (34.1%)) compared to those that had not undergone resection (non-operative PA and pre-op operative PA, (18/95, (18.9%)), (p=0.055, Chi-squared test).

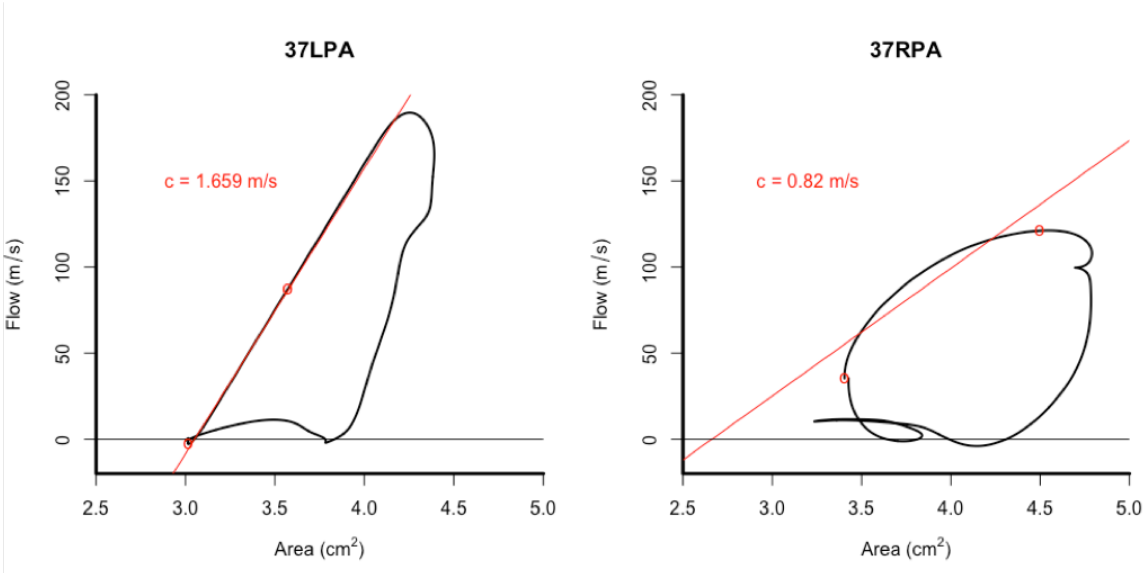

Figure 7-25 Flow-area loop example
Example of flow–area (QA) loop method of wave speed calculation in left and right pulmonary arteries of same scan (MRIRAN 37, patient from study). Flow was plotted against area for the entire cardiac cycle. Wave speed was calculated from the gradient of the plot in early systole. Red circles represent starting time (time= 0ms) and finishing time (time corresponding with third phase of original imaging) from which wave speed was calculated (red gradient line). Note linear segment in early systole in left panel but curved (non-linear) in right.

Table 7-2 depicts the results for wave speed calculated by SOS and QA loop methods. QA loop all (including non-linear scans) and QA loop linear (excluding non-linear scans) did not show a significant change in wave speed over time

although the direction of change in wave speed by the QA loop was similar to the significant changes in the SOS method, i.e. increased non-operative PA wave speed on POD2 only and reduced post-operative wave speed in the operative.PA.

Pulmonary artery	Method	Pre-op	POD2	2-months	p-value
Operative	SOS ($m.s^{-1}$)	1.38 (1.28, 1.53)	0.92 (0.73, 1.20) #	0.90 (0.75, 1.06) #	***<0.001 §***
	n	27	20	21	
	QA All ($m.s^{-1}$)	1.63 (1.29, 1.89)	1.14 (0.85, 1.73)	1.09 (0.93, 1.73)	0.056 *§*
	n	27	20	21	
	QA Linear ($m.s^{-1}$)	1.64 (1.34, 1.90)	1.34 (0.87, 1.78)	1.36 (1.03, 1.78)	0.165 *§*
	n	22	13	14	
Non-operative	SOS ($m.s^{-1}$)	1.29 (1.06, 1.76)	1.60 (1.33, 1.97) #	1.26 (1.11, 1.74) ¥	***0.019 §***
	n	25	21	22	
	QA All ($m.s^{-1}$)	1.45 (1.18, 1.88)	1.74 (1.41, 2.15)	1.47 (1.07, 1.85)	0.101 *§*
	n	25	21	22	
	QA Linear ($m.s^{-1}$)	1.40 (1.13, 1.80)	1.66 (1.35, 2.00)	1.38 (0.97, 1.76)	0.067 *§*
	n	22	17	16	

Table 7-2 Comparison of wave speed by flow-area loop and sum of squares techniques
Values are median (IQR). $SOS^{=}$ sum of square method. QA loop= flow area loop method. *§*= Friedman's test. Comparison between time-points Wilcoxon signed rank test. #= significant difference from pre-op. ¥= significant difference from post-operative day 2 (POD2). Significant results ($p<0.05$) highlighted ***bold italics.***

7.5.2.3 Agreement between methods of calculating wave speed

The agreement between the SOS and the linear QA loop scans showed a median bias of $-0.12 m.s^{-1}$ [95% CI -0.38, $0.07 m.s^{-1}$] for all scans, (SOS-QA). When separated into the resected vessels (operative PA on POD2 and at 2-months) and the non-resected vessels (non-operative PA and pre-op operative PA) there was superior agreement between the SOS and QA in the non-resected vessels. The bias was minimal for the non-resected vessels with good agreement ($-0.06 m.s^{-1}$ [95% CI -0.30,$0.10 m.s^{-1}$] compared to the agreement in the resected vessels ($-0.32 m.s^{-1}$ [95% CI -0.78,$0.10\ m.s^{-1}$], ($p=0.002$, Wilcoxon rank sum test).

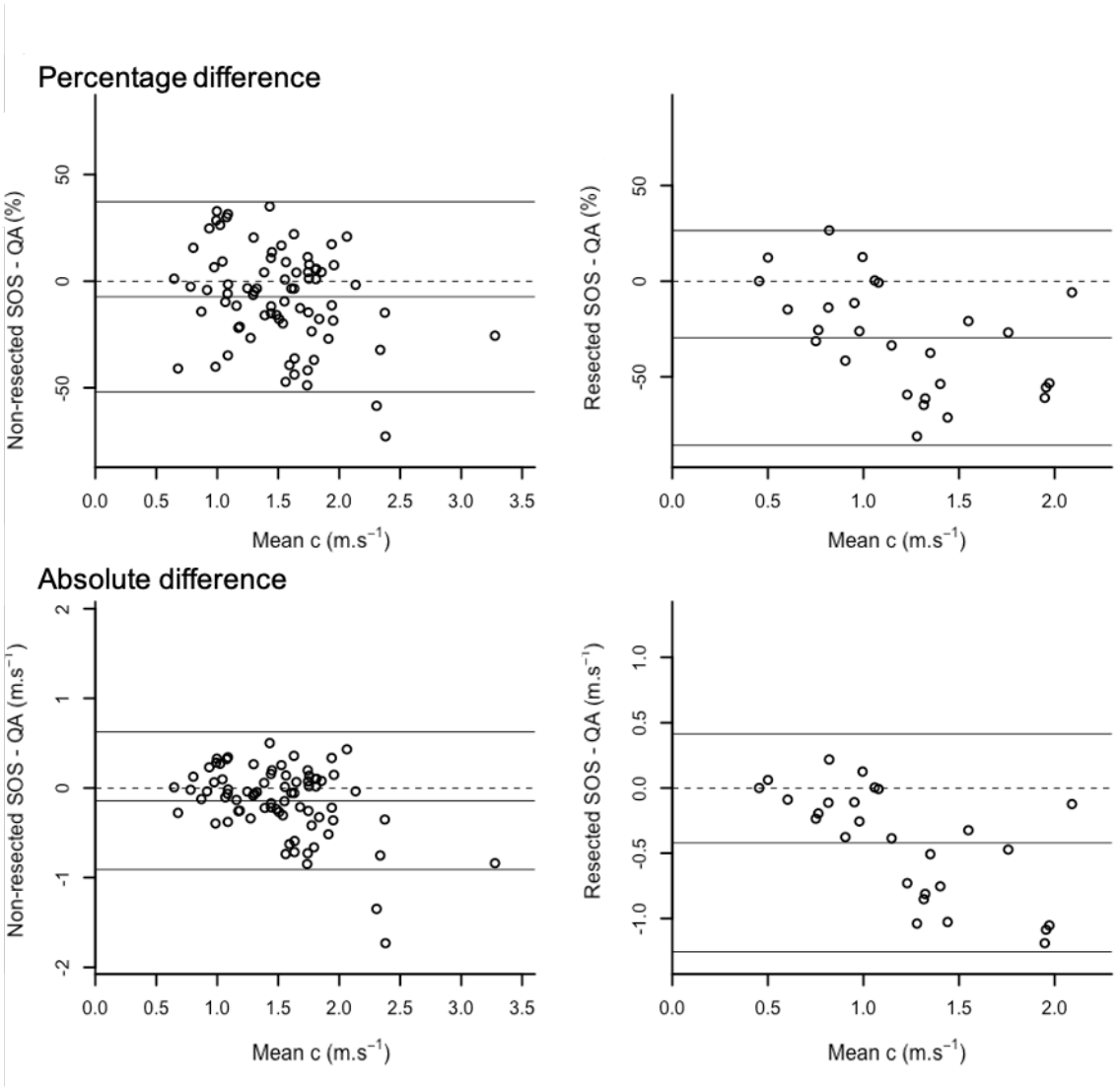

Figure 7-26 Bland-Altmann plots for agreement between methods of wave speed calculations
Top row, percentage difference between wave speed calculation by sum of squares (SOS) and flow – area loop (QA) calculated as (100*(SOS-QA)/SOS) in the PA that had not undergone resection (non-resected, left plot) and that had undergone resection (resected, right plot) against the mean wave speed (c) of the two measures.
Bottom row, absolute difference between SOS and QA in the non-resected (left plot) and resected (right) against the mean wave speed of the two measures.
Note greater bias in the resected PAs and that the absolute and percentage differences are related to mean wave speed.

Given the ability of the SOS method to determine wave speed in every vessel imaged and the overall agreement between methods, the wave speed results from the SOS method were used for wave intensity analysis calculation.

7.5.3 Wave intensity results

Wave intensity analysis calculation and wave detection was possible in all but the six vessels excluded in 7.5.1. In total WIA was performed in 68 operative PAs (27 pre-op, 20 on POD2 and 21 at 2-months) and 68 non-operative PAs (25 pre-op, 21 on POD2 and 22 at 2-months).

7.5.3.1 Forward compression wave

The time to peak FCW was reduced in both vessels on POD2 only ($p<0.008$, paired t-tests), Table 7-3. Non-operative PA FCW peak WI and area were increased on POD2 and 2-months ($p<0.003$, Wilcoxon signed rank) whilst operative PA FCW area was reduced on POD2 and 2-months ($p<0.008$, Wilcoxon signed rank). Operative PA FCW peak WI and FCW area were similar to non-operative PA pre-op ($p>0.583$, Wilcoxon signed rank) but lower on POD2 and at 2months ($p<0.002$, Wilcoxon signed rank) suggesting a differing post-operative distribution between the vessels, Figure 7-27.

Parameter	Pulmonary artery	Pre-op	POD2	2-months	p-value
Time to peak FCW WI (ms)	Non-operative	86.3 (23.7)	72.7 (17.2)#	76.5 (16.9)	***0.017 ****
	Operative	77.6 (19.1)	63.4 (17.4)#	69.7(21.8)¥	***0.022 ****
FCW Peak WI ($x10^{-3}$ $cm^5.s^{-1}$)	Non-operative	18.4 (12.8, 31.4)	39.6 (24.7, 56.2)#	32.2 (18.9, 63.9)#¥	***0.001 §***
	Operative	20.3 (15.4, 33.1)	23.2 (9.7, 27.2)	17.8 (10.5, 22.3)#¥	***0.003 §***
FCW Area ($x10^{-3}$ cm^5)	Non-operative	1.35 (1.01, 2.51)	2.55 (1.94, 3.38)#	2.27 (1.56, 3.73)#¥	***0.001 §***
	Operative	1.54 (1.14, 2.20)	1.38 (0.55, 1.71)#	1.15 (0.72, 1.57)#	***0.001 §***

Table 7-3 Forward compression wave results
Values are mean (SD) or median (IQR). FCW= forward compression wave. WI= wave intensity. *= one-way repeated measures ANOVA. §= Friedman's test. Comparison between time-points paired t-test or Wilcoxon signed rank test. #= significant difference from pre-op. ¥= significant difference from post-operative day 2 (POD2). Significant results ($p<0.05$) highlighted ***bold italics.***

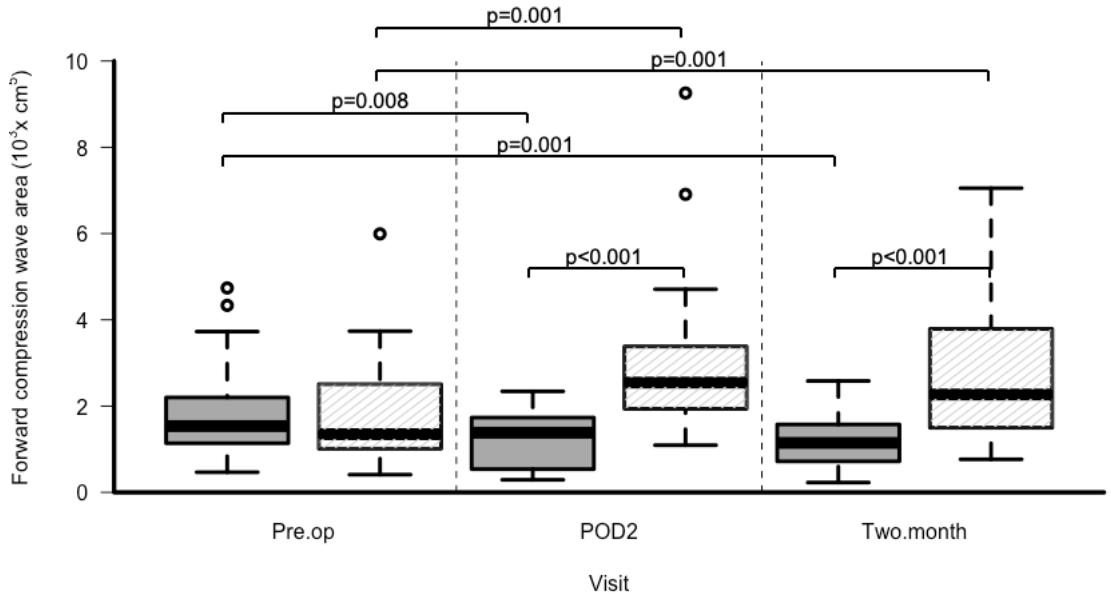

Figure 7-27 Operative and non-operative forward compression wave area
Forward compression wave (FCW) area of the operative pulmonary artery (PA) (dark grey boxes) and non-operative PA (light grey boxes). Operative PA FCW area was decreased on post-operative day 2 (POD2) and at 2-months whereas non-operative PA FCW area was increased at both time points, Wilcoxon signed rank test. Non-operative PA FCW area was not different to operative PA pre-operatively (p=0.583) but was greater at both post-operative time points, Wilcoxon rank sum test.

7.5.3.2 Forward expansion wave

There was no change in the time to peak FEW in the operative PA or non-operative PA, Table 7-4. FEW peak WI and area were increased in the non-operative PA on POD2 and 2-months ($p<0.017$, Wilcoxon signed rank test) whereas operative PA FEW area was reduced from pre-operatively at 2-months only ($p=0.018$, Wilcoxon signed rank). Similar to the FCW results, there was no difference between operative and non-operative PA FEW peak WI and area pre-operatively ($p>0.206$, Wilcoxon) although operative PA WI and area were lower on POD2 and at 2-months ($p<0.002$, all Wilcoxon), Figure 7-28.

Parameter	Pulmonary artery	Pre-op	POD2	2-months	p-value
Time to peak FEW WI (ms)	Non-operative	305.2 (271.1, 342.1)	328.1 (286.1, 359.1)	300.1 (265.4, 338.6)	0.838 ***§***
	Operative	282.4 (58.6)	296.6 (70.8)	286.2 (74.8)	0.566 ***
FEW Peak WI ($x10^{-3}$ $cm^5.s^{-1}$)	Non-operative	3.65 (2.36, 5.86)	7.43 (5.47, 9.33)#	6.79 (4.86, 9.60)#	***0.001 §***
	Operative	4.96 (2.90, 7.37)	4.35 (3.02, 6.87)	3.85 (2.52, 5.88)¥	***0.007 §***
FEW Area ($x10^{-3}$ cm^5)	Non-operative	0.215 (0.127, 0.363)	0.481 (0.278, 0.570)#	0.378 (0.220, 0.562)#	***0.028 §***
	Operative	0.199 (0.134, 0.423)	0.218 (0.107, 0.292)	0.167 (0.134, 0.243)#	***0.025 §***

Table 7-4 Forward expansion wave results
Values are mean (SD) or median (IQR). FEW= forward expansion wave. WI= wave intensity. *= one-way repeated measures ANOVA. §= Friedman's test. Comparison between time-points paired t-test or Wilcoxon signed rank test. #= significant difference from pre-op. ¥= significant difference from post-operative day 2 (POD2). Significant results (p<0.05) highlighted ***bold italics.***

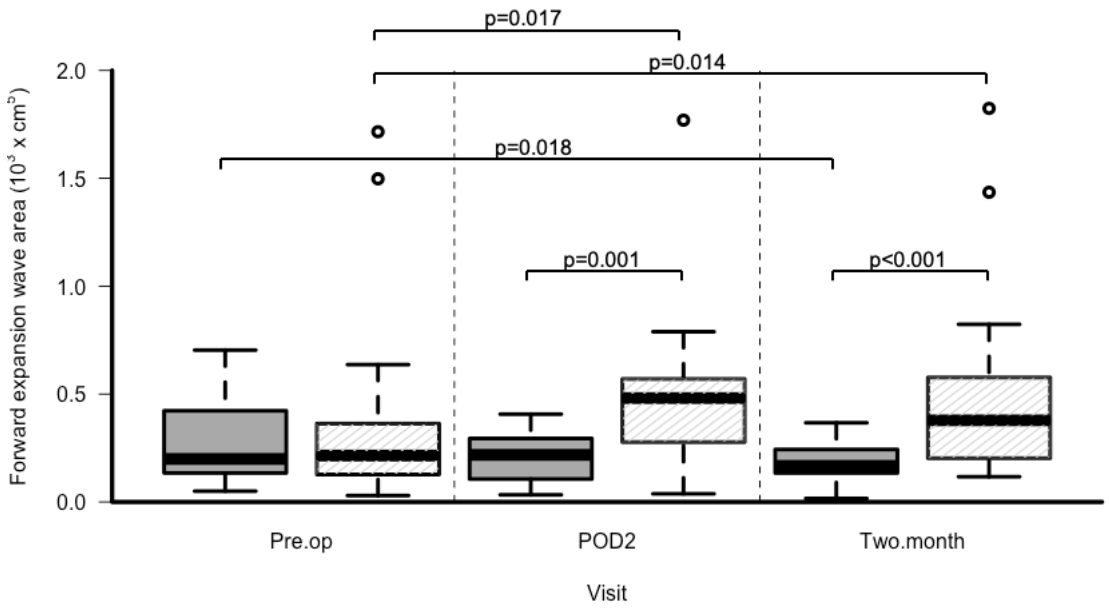

Figure 7-28 Operative and non-operative forward expansion wave area
Forward expansion wave (FEW) area of the operative pulmonary artery (PA) (dark grey boxes) than non-operative (light grey boxes). Operative PA FEW area was decreased at 2-months only whereas non-operative PA FEW area was increased on post-operative day 2 (POD2) and at 2-months, Wilcoxon signed rank test. Non-operative PA FEW area was not different to operative PA pre-operatively (p=0.206) but was greater at both post-operative time points, Wilcoxon rank sum test.

7.5.3.3 Backward waves

The backward waves were predominately compression waves in nature at all time points except for three BEW pre-operatively, one on POD2, and three at 2-months, Table 7-5. There was no difference in the rate of BEW between operative and non-operative PA (p=0.788), RPA or LPA (p=0.244) or time points (p=0.641, all Chi-

squared tests). Also, there was no difference over time in the number of BEWs in the operative PA or non-operative PA (p>0.223, Cochran test).

The time to peak BCW was reduced in operative PA post-operatively on POD2 and 2-months (p<0.005, Wilcoxon signed rank) and was less than the non-operative PA at both post-operative time points (p=0.040 and p=0.003 respectively, both Wilcoxon rank sum). Unlike the opposing change in FCW and FEW between the PAs, non-operative and operative PA BCW peak WI and area were increased on POD2 (p<0.033, all Wilcoxon). Only non-operative PA BCW peak WI and area remained increased at 2-months (p<0.002, both Wilcoxon), Figure 7-29. BCW area in the operative PA was similar in the non-operative PA pre-operatively and on POD2 (p=0.558 and p=0.767 respectively, Wilcoxon rank sum) but operative PA BCW area appeared reduced at 2-months though this did not reach statistical significance (p=0.063 Wilcoxon rank sum).

Parameter	Pulmonary artery	Pre-op	POD2	2-months	p-value
Number of compression waves (n/total)	Non-operative	23/25	20/21	20/22	0.223 †
	Operative	26/27	20/20	20/21	0.607 †
Time to peak BCW WI (ms)	Non-operative	199.0 (44.3)	171.9 (54.0)	192.9 (43.5)	0.113 *
	Operative	182.1 (159.1, 206.1)	139.6 (99.5, 162.3)#	143.1 (119.1, 165.1)#	***0.010 §***
BCW Peak WI ($x10^{-3}$ $cm^5.s^{-1}$)	Non-operative	-0.97 (-1.62, -0.52)	-1.39 (-2.83, -1.17)#	-1.82 (-3.25, -0.81)#	***0.009 §***
	Operative	-0.95 (-1.79, -0.51)	-2.37 (-4.79, -0.91)#	-1.17 (-1.87, -0.48)¥	***0.007 §***
BCW Area ($x10^{-3}$ cm^5)	Non-operative	0.071 (0.032, 0.117)	0.106 (0.060, 0.239)#	0.137 (0.052, 0.269)#	***0.003 §***
	Operative	0.078 (0.038, 0.126)	0.137 (0.0.037, 0.229)#	0.079 (0.019, 0.134)¥	***0.025 §***

Table 7-5 Backward wave results
Values are mean (SD) or median (IQR). BCW= backward compression wave. WI= wave intensity. †= Cochran test. *= one-way repeated measures ANOVA. *§*= Friedman's test. Comparison between time-points paired t-test or Wilcoxon signed rank test. #= significant difference from pre-op. ¥= significant difference from post-operative day 2 (POD2). Significant results (p<0.05) highlighted ***bold italics.***

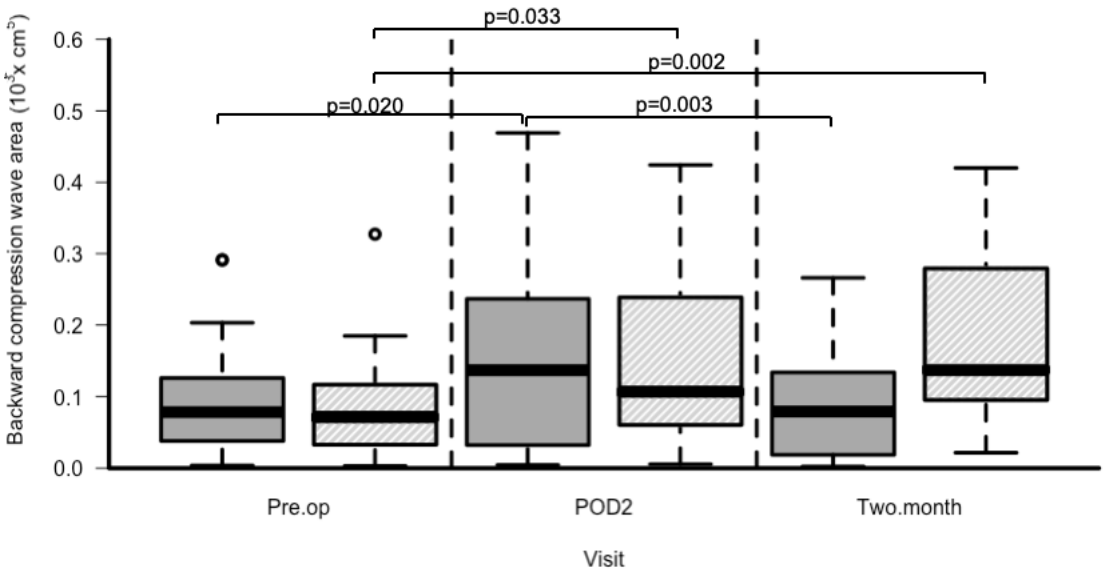

Figure 7-29 Operative and non-operative backward compression wave area
Backward compression wave (BCW) area of the operative pulmonary artery (PA) (dark grey boxes) than non-operative (light grey boxes). Operative and non-operative PA BCW area was increased at post-operative day 2 (POD2) whereas only non-operative PA BCW area remains increased at 2-months. The difference between operative and non-operative PA BCW area approaches significance at 2-months (p=0.063, Wilcoxon rank sum test). Wilcoxon signed rank test for comparisons of the same vessel between time-points.

7.5.3.4 Wave reflection index

Wave reflection index reveals that there was an increase in operative PA WRI on POD2 and at 2-months (p=0.001 and p=0.026 respectively, Wilcoxon), Table 7-6 and Figure 7-30. Non-operative PA WRI was unchanged throughout the study. Operative PA WRI was greater than non-operative PA only on POD2 (p=0.003, Wilcoxon rank sum).

Parameter	Pulmonary artery	Pre-op	POD2	2-months	p-value
WRI (%)	Non-operative	5.09 (2.04, 6.88)	4.26 (2.42, 5.81)	6.07 (3.50, 10.40)	0.197 §
	Operative	4.26 (2.05, 8.65)	9.48 (4.88, 14.89)#	8.01 (2.31, 11.67)#¥	***<0.001 §***

Table 7-6 Wave reflection index results
Values are median (IQR). WRI= wave reflection index. §= Friedman's test. Comparison between time-points Wilcoxon signed rank test. #= significant difference from pre-op. ¥= significant difference from post-operative day 2 (POD2). Significant results (p<0.05) highlighted ***bold italics.***

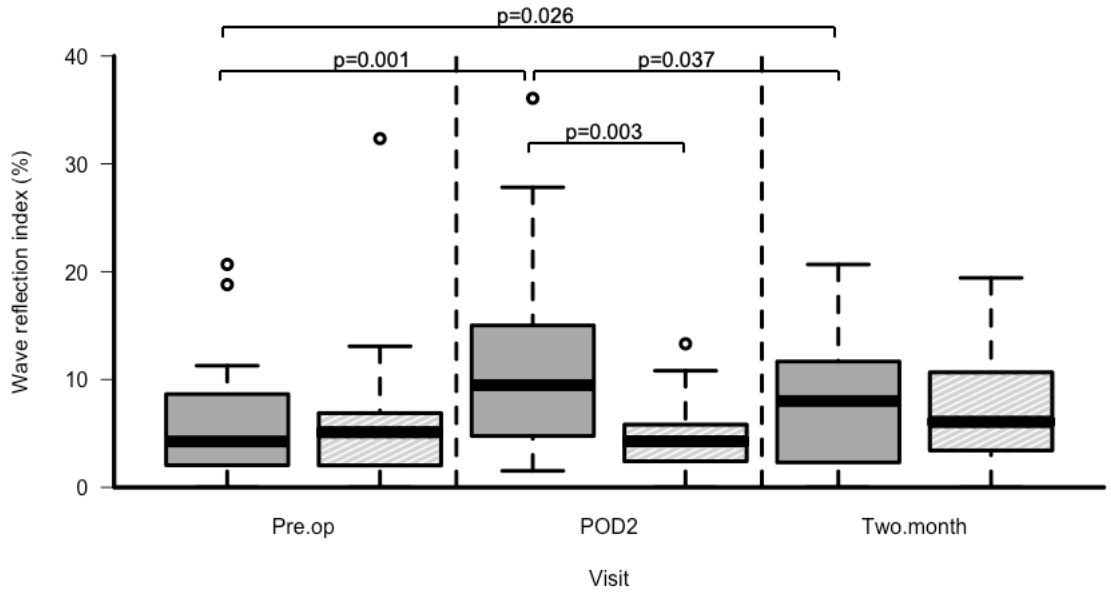

Figure 7-30 Operative and non-operative wave reflection index
Wave reflection index (WRI) of the operative pulmonary artery (PA) (dark grey boxes) and non-operative (light grey boxes). Operative PA WRI was increased at post-operative day 2 (POD2) and at 2-months. No significant non-operative PA changes. Wilcoxon signed rank test for comparisons between time-points and Wilcoxon rank sum test for comparison between vessels at same time-point.

7.5.3.5 Distance to reflection site

The calculated distance to the apparent site of reflection in the operative PA was reduced from pre-op on POD2 and at 2-months ($p<0.001$, Wilcoxon for both). Operative PA distance to reflection site was similar to non-operative PA pre-operatively ($p=0.608$) but less than the non-operative PA on POD2 and at 2-months ($p<0.001$, all Wilcoxon rank sum), Figure 7-31.

Parameter	Pulmonary artery	Pre-op	POD2	2-months	p-value
Distance to reflection site (cm)	Non-operative	6.91 (4.89, 11.2)	8.45 (4.55, 9.96)	7.84 (5.85, 9.98)	0.663
	Operative	6.93 (5.02, 9.25)	2.56 (1.99, 4.70)#	3.23 (2.20, 5.22)#	***0.001***

Table 7-7 Reflection site distance results
Values are median (IQR). Both Friedman's test. Comparison between time-points Wilcoxon signed rank test. #= significant difference from pre-op. ¥= significant difference from post-operative day 2 (POD2). Percentage of flow was calculated from sum of operative and non-operative vessel flow. Significant results ($p<0.05$) highlighted ***bold italics.***

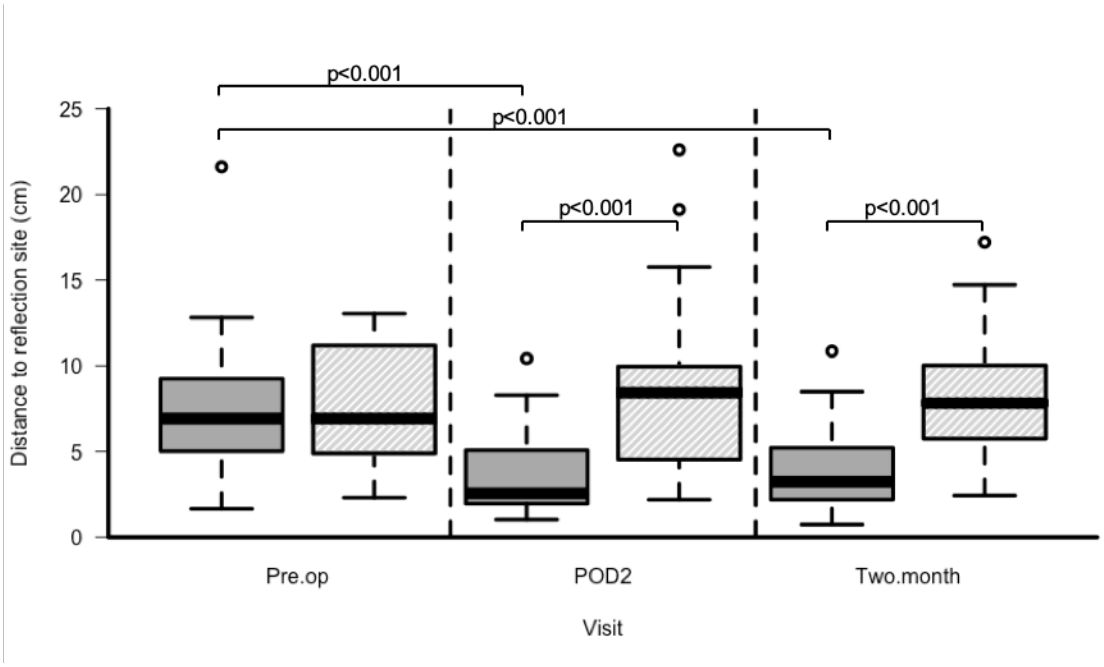

Figure 7-31 Operative and non-operative distance to reflection site
Distance to the reflection site of the operative pulmonary artery (PA) (dark grey boxes) than non-operative (light grey boxes). The site of operative PA reflection was reduced at post-operative day 2 (POD2) and at 2-months. There was no change in the distance to reflection site in the non-operative PA. Note consistent distance to reflection site in pre-operative PAs and post-operative non-operative PAs. Wilcoxon signed rank test for comparisons between time-points and Wilcoxon rank sum test for comparison between vessels at same time-point.

7.5.4 Summary of main results

Wave intensity analysis could be performed in 136/142 (95.8%) vessels imaged. A summary of the main findings are presented in Table 6-11 and in Figure 7-32.

Parameter	Pulmonary artery	Pre-op	POD2	2-months
Wave speed (SOS)	Non-operative		↑	-
	Operative		↓	↓
	Operative vs non-operative	=	↓	↓
FCW area	Non-operative		↑↑	↑
	Operative		↓	↓
	Operative vs non-operative	=	↓	↓
FEW area	Non-operative		↑	↑
	Operative		-	↓
	Operative vs non-operative	=	↓	↓
BCW area	Non-operative		↑	↑
	Operative		↑	-
	Operative vs non-operative	=	=	=
WRI	Non-operative		-	-
	Operative		↑↑	↑
	Operative vs non-operative	=	↑	=
Time to peak BCW	Non-operative		-	-
	Operative		↓	↓
	Operative vs non-operative	=	↓	↓
Distance to reflection site	Non-operative		-	-
	Operative		↓	↓
	Operative vs non-operative	=	↓	↓

Table 7-8 Summary of changes in blood flow and afterload
SOS= sum of squares method. FCW= forward compression wave. FEW= forward compression wave. BCW= backward compression wave. WRI= wave reflection index. POD2= post-operative day 2.
Comparisons are POD2 vs pre-op and 2-months vs pre-op. - = no change. ↓= less than pre-operatively. ↓↓= less than pre-operatively and 2-months. ↑= greater than pre-operatively ↑= greater than pre-operatively and 2-months.
Operative vs non-operative, no difference between measures (=). ↓= operative less than non-operative. ↑= operative greater than non-operative.

A representative example of the WIA changes following lung resection is displayed in Figure 7-32. The WIA plots are displayed for the non-operative (top row) and operative PA (bottom row), pre-operatively (left column), on POD2 (middle column) and at 2-months (right column) for patient RV1. Net wave intensity is plotted by the black line with the forward compression wave area (FCW, blue), forward expansion wave area (FEW, green) and backward compression wave area (BCW, red) highlighted. As net wave intensity is the sum of the forward and backward waves the shaded areas are not bound by the limits of the black line. The results for the FCW, BCW and wave reflection index (WRI) are noted on each plot. Whilst the results may differ between time points in this example, only changes that are significant in analysis of all patients are described below.

Pre-operatively the FCW area, BCW area and WRI are similar between the operative and non-operative PA. The timings of each wave are also similar between the vessels.

On POD2 the FCW area and BCW area in the non-operative PA increases. Both increase by a similar ratio therefore WRI is unchanged. In the operative PA FCW area is reduced both compared to pre-operatively and the non-operative PA. Note the change in the range of the y-axis required in order to visibly display the plot. BCW area is increased from pre-operatively therefore WRI is increased. In spite of the greater BCW area in the non-operative PA, WRI is only increased in the operative PA because of the marked difference in FCW area between the vessels. The time to peak BCW is reduced in the operative PA, compared to pre-operatively and to the non-operative PA, secondary to a more proximal site of wave reflection. Time to peak FCW is marginally reduced whereas time to peak FEW is unchanged.

At 2-months non-operative FCW area and BCW remain increased, again WRI is unchanged as both areas are increased by a similar ratio. Operative FCW area is still reduced although BCW area has returned to pre-operative levels. As the FCW is reduced WRI remains increased, although to a lesser extent. The time to peak BCW remains reduced with an unchanged distance to the site of reflection. Again, the time to peak FCW is marginally reduced whereas time to peak FEW is unchanged.

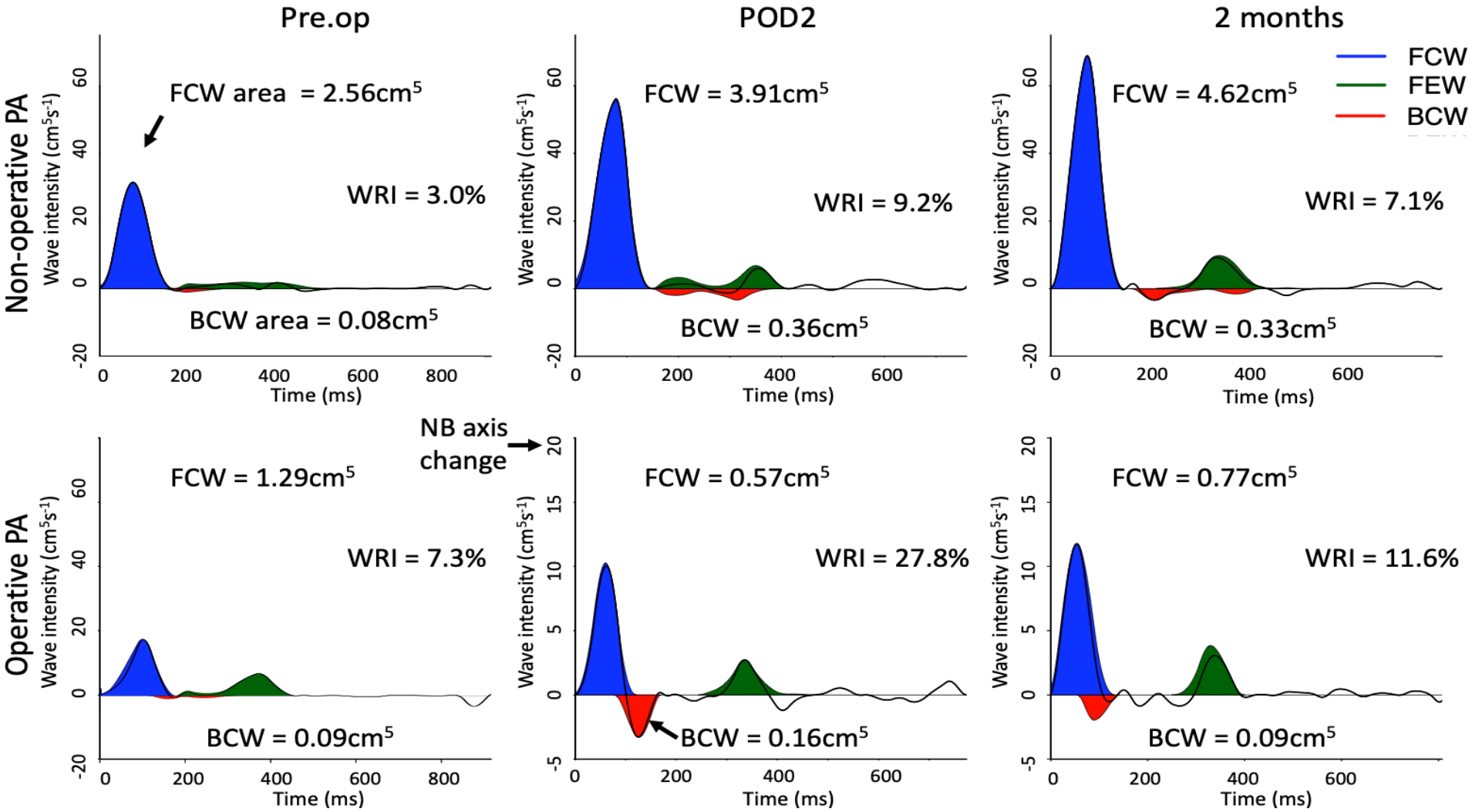

Figure 7-32 Example of change in wave intensity plots following lung resection
Details of plot in text on preceding page

7.6 Discussion

Wave intensity analysis was successfully performed in 95.8% of pulmonary arteries imaged although QA loop wave speed could only be calculated in 76.5% of PAs. Post-operatively there is a decrease in FCW, a decrease in wave speed and an increase in wave reflection in the operative PA. The wave reflection in the operative PA resulted in an earlier BCW potentially from a proximal reflection site. Whilst there is an increase in FCW and BCW in the non-operative PA there is no increase in wave reflection index.

7.6.1 Strengths and limitations

7.6.1.1 Strengths

This is the first human study to measure the sequential change in wave intensity analysis parameters of both pulmonary arteries following lung resection. Whilst previous studies have investigated global changes in the steady components of afterload (PVR and PAP), WIA allows the assessment of pulsatile afterload in each lung. Calculation of WRI allows direct comparison; between each lung in the patient at that time point, between time points, and against results from other pulmonary WIA studies of varying methodology.

As WIA is a developing field there are steps in the methodology that vary between studies. There is no defined and standardised approach to either filtration of the measured data or wave speed calculation. Both may affect the results and therefore both parameters were investigated prior to performing WIA. Whilst a Savitzky-Golay filter is advised by Parker (who originally described WIA) and is used in many studies, its use is not universal and the most appropriate window size is dependent on the data collected. As detailed, 4 window sizes were compared for balance between maintenance of signal and filtration of noise prior to selection of the window size used. Additionally, two differing wave speed calculation methods were compared prior to selection of the method subsequently used for WIA.

7.6.1.2 Limitations

Although CMR has advantages over PAC (it is non-invasive and allows accurate imaging of the LPA and RPA), there are limitations in CMR based WIA compared to a PAC based method. PAC measures pressure directly whereas CMR uses area as a surrogate; whilst this technique is widely used in WIA, it does introduce a potential error secondary to motion artefact[351, 358]. As such, WIA was not performed in the MPA secondary to potential motion artefacts and there were potentially motion artifacts in 6/142 (4.2%) scans.

The spatial and temporal resolution of the CMR data may be limited by the CMR protocol. High CMR spatio-temporal resolution requires long breath holds to limit motion artefact, patients requiring lung resection would likely be unable to complete this even pre-operatively[425]. Flow imaging was performed during free breathing, this can introduce motion artefacts secondary to respiratory movement and limit the spatial resolution of the PA wall and therefore area measurement. Additionally, the effective temporal resolution was limited to one thirtieth of the cardiac cycle, this can fail to detect short lived events such as a BCW or limit the accuracy of wave speed calculation, discussed further in Appendix 1. The CMR protocol was a pragmatic balance between data acquisition and patient experience. An overly long CMR scan time requiring multiple breath holds may have prevented completion of the protocol on post-operative scanning.

7.6.2 Filter selection

Selection of an appropriate window size for the Savitzky-Golay filter is imperative for accurate representation of the underlying data. Too small a window size fails to remove the underlying noise and too large a window size removes too much of the underlying features of the data[426]. Whilst selection of filter size based on user interpretation of the plots generated, as in this study, is common place[427] there are numerous methods to calculate the most appropriate window size[426, 428, 429]. Romo-Cárdenas et al. proposed a method based on the Nyquist-Shannon theorem (a periodic signal must be sampled at least double the highest frequency of the signal). Based on this theorem they state that window size should be calculated based on the 'lobes' present in the underlying signal[426], Equation 7-20. In the flow and area plots to which the filter is applied the underlying profile has four lobes

(systolic and diastolic peaks and the troughs between them) and 30 data points giving a calculated ideal window size of 7, the same as determined by visual inspection of the data.

$$Savitzky - Golay\ window\ size = \frac{data\ points}{lobes\ in\ data\ profile}$$

Equation 7-20 Savitzky-Golay window size calculation
Results rounded to the nearest odd number

7.6.3 Wave speed

The wave speed results in this investigation are similar in magnitude to those seen in the control groups in the previous CMR based pulmonary artery WIA studies by Quail et al.[351] and Schafer et al.[377] although, in common with these studies, they are less than the pulmonary artery catheter work by Su et al.[404-406]. Of note, wave speed decreased post-operatively in the operative PA whereas in all of the above studies wave speed is increased in disease, often by at least double. There are two broad potential explanations for the reduction in wave speed in the operative PA. Either pulmonary vasculature does not stiffen following lung resection during the timeframe of this study (this may occur beyond 2-months) or the wave speed may be artificially reduced secondary to the influence of proximal wave reflection on wave speed calculation. Su et al. demonstrated that increased WRI is present in all grades of PAH whereas wave speed increases with increasing severity. They conclude that the development of increased WRI occurs early in PAH whilst wave speed increases over time with increasing disease severity[405], this may subsequently occur over time in patients from this study.

In a PAH population Su et al. also found that "many" of their patients did not have a linear segment in the PU loop in early systole although they do not quantify the percentage of patients in which this occurs[404]. Within this study 32/136 (23.5%) of scans did not have a distinct linear segment in early systole. There was continuum between the obviously non-linear early systolic segments and the perfectly linear segments therefore any distinction between non-linear and linear segments is subjective. The SOS method eliminates this distinction from interpretation[430].

The lower agreement between QA loop and SOS wave speed calculation and the trend to an increased percentage of non-linear scans in PAs that had undergone resection compared to the non-resected PAs suggest that PA ligation and/or proximal wave reflection limits the utility of the QA loop in this population. The SOS method may however also be influenced by wave reflection and may cause an underestimation of wave speed. It is not possible to conclude which method is most accurate from this study, particularly following resection. Weir-McCall et al. demonstrated that SOS had superior accuracy to QA loop method in a healthy volunteer pulmonary artery catheter study[431]. The primary benefit of the SOS method was its ability to calculate wave speed in all cases and was therefore used for WIA.

The impact of inaccuracy of wave speed calculation on WIA has been investigated by Qureshi et al.[396]. They demonstrated that, compared to modelled and loop methods, SOS wave speed may result in the creation of a small BCW occurring prior to the initial peak in the FCW although it otherwise had minimal effect on WIA interpretation[396]. To mitigate the potential source of error, detection of the peak backward wave was confined to occurring after the peak WI of the FCW in this investigation presented here. Whilst there were small BCWs or BEWs prior to the FCW peak they were not included in the analysis.

Further discussion on the factors affecting the linear segment of the flow-area loop is presented in Appendix 1 page 336.

7.6.4 Wave intensity results

Analysis was possible in 136/142 (95.8%) of all scans performed. The six scans removed had marked diastolic increases in area with no corresponding change in flow within the vessels. These area increases were likely not to be physiological but due to motion artefact which also prevents performing WIA in the MPA[351, 358]. The forward travelling waves are determined by the RV, whereas the backward waves are determined by the vasculature in which the waves travel, as such changes in these waves can respectively be attributed to RV function or to the pulmonary vasculature. The relationship between changes in WIA parameters and RV function are investigated separately in Chapter 8.

Comparison of absolute WI values is only possible between studies which use the same methodology[fff], this limits comparison of absolute values to Quail et al.[351]. Given the marked change in FCW area between the operative and non-operative PAs on POD2 and at 2-months, this further limits comparison to the pre-operative values from this investigation. Median [IQR] FCW area in patients from our study ($1.54x10^{-3}cm^5$ [1.10, 2.49 $x10^{-3}cm^5$] was similar to that seen in patients with PAH or CTEPH in the study by Quail et al. ($2x10^{-3}cm^5$ [$2x10^{-3}cm^5$]) but less than their healthy control group ($5x10^{-3}cm^5$ [$3x10^{-3}cm^5$]). BCWs were present in 129/136 (94.9%) of scans in our study, the BCW area ($0.106x10^{-3}cm^5$ [0.058, $0.163x10^{-3}cm^5$]) was less than the patient group in Quail et al. ($0.4x10^{-3}cm^5$ [$0.6x10^{-3}cm^5$]) who found only BEWs in the control group. The differences between the control group of Quail et al. and the pre-operative values in our study may be explained by the difference in co-morbidity of patients and their age (67 years [IQR 59.0 – 74.0 years] vs 47±3 years in Quail et al.) as FCW decreases with age[381].

7.6.4.1 Relationship between wave intensity parameters and cardiac output

In the systemic circulation, FCW intensity has been shown to increase with increased inotropy whereas FEW is unchanged[432], however, in the pulmonary circulation this relationship has not previously been demonstrated. Total FCW area (operative and non-operative PA combined) increases on POD2 with the increase in cardiac output (CO) and by 2-months total FCW area and CO are similar to pre-operatively. Within-subject testing revealed moderate to strong associations between the increase total FCW area and the increased in CO and heart rate (HR), Table 7-9. Additionally, the average time to peak FCW (average of operative and non-operative PA) is negatively associated with CO and HR. There were only weak associations between the change in total FEW area and CO and between the change in average time to peak FEW and the change in HR. As such, the magnitude and timing of the FCW are greatly augmented by the CO and HR, whereas FEW is affected to a far lesser extent. This suggests that the changes in timing and magnitude of overall FCW on POD2 may reflect the changes in cardiac output and heart rate alone.

[fff] Schafer et al. performed their analysis in a paediatric population and as such indexed the WI results to ejected stroke volume. The indexing and age differences prevent direct comparison of results.

Analysis of covariance, within-subject				
Wave	Measure		Cardiac output	Heart rate
FCW	Total Area	r	***0.611***	***0.521***
		p	***<0.001***	***0.001***
	Average time to peak	r	***-0.398***	***-0.664***
		p	***0.013***	***<0.001***
FEW	Total Area	r	***0.383***	0.250
		p	***0.017***	0.131
	Average time to peak	r	0.044	***-0.334***
		p	0.792	***0.040***

Table 7-9 Pooled association between cardiac output, heart rate and forward compression waves
FCW= forward compression wave. FEW= forward expansion wave. Analysis of covariance with patient as factor. Significant results (p<0.05) highlighted ***bold italics.***

Post-operatively, the percentage of the CO travelling in the non-operative PA increases on POD2 (66.3%±9.52%) and at 2-months (60.9%±11.4%). Similarly, the percentage of total FCW travelling in the non-operative PA increases post-operatively from pre-op (51.4% ±14.2%) to POD2 (69.6%±15.8%) and 2-months (67.1%±15.9%) ($p<0.001$ ANOVA, $p<0.001$ paired t-test for comparisons between pre-op and POD2 and between pre-op and 2-months). The percentage of the total FEW travelling in the non-operative PA also increases post-operatively (46.0%±15.2% pre-op, 61.9%±17.5% on POD2 and 62.4%±17.4% at 2-months, $p<0.001$ ANOVA, $p<0.001$ paired t-tests for comparisons between pre-op and POD2 and between pre-op and 2-months).

7.6.4.2 Wave reflection results

Measurement of the BCW area alone would imply that there is increased pulsatile afterload in both vessels on POD2 and only in the non-operative PA at 2-months. In the pulmonary vasculature the BCW is solely generated by the reflection of the incident FCW, it must therefore be measured relative to the FCW, as a wave reflection index. In the non-operative PA FCW area and BCW area both increase post-operatively although the relative increase is similar and therefore WRI is unchanged. In the operative PA FCW area is decreased at both post-op time points whilst BCW is increased on POD2 and is similar to pre-op at 2-months. When the BCW area is calculated relative to the FCW, it shows increased wave reflection occurs at both POD2 and at 2-months in the operative PA, therefore there is increased pulsatile afterload in the operative PA following lung resection.

Whilst the absolute values of waves calculated in WIA cannot be compared across studies of differing methodologies, this is possible with WRI as the numerical and unit differences between methodologies are cancelled out in WRI and it can be simply calculated from study results. Su et al. calculated median [IQR] WRI for each individual patient in the MPA and a branched PA, they demonstrated increased WRI (values for branched PA therefore similar to the investigation presented) in PAH (24.7% [18.9, 32.6%]) and CTEPH (31.8% [25.8, 36.6%]) vs control (6.36% [3.20, 9.09%]). There was no significant difference between the branched PA and MPA WRI values in any group[405]. Though Schäfer et al. and Quail et al. do not report WRI, indicative figures can be calculated form the averaged results. Schäfer et al. showed an MPA WRI of 36.3% in children with PAH vs 4.6% in control[377] and Quail et al. demonstrated a WRI of 20% in the patient group and 0% in the control group as there were no BCWs[351].

The increase in WRI in our study is comparatively small compared to these results. Contrary to the disease processes in the studies detailed above, lung resection may produce a purely unilateral change in wave reflection. This may contribute to the increased percentage of blood flow through the non-operative PA as blood preferentially flows through the lung with least impedance to flow. If both lungs were affected equally, then WRI may be higher. As discussed in 2.3 page 84, there is evidence of reduced PVreserve on exercise following lung resection[48, 49, 68]. Any increase in the incident FCW in the operative PA with cardiac output increase may cause increased WRI and further disproportionately increase blood flow through the non-operative PA. As the non-operative PA carries a greater percentage of the cardiac output, both at rest and potentially with increases in cardiac output, afterload may rapidly increase even if the non-operative pulmonary vasculature is healthy. As such the unilateral increase in WRI in the operative PA may be an underestimation of the increase in pulsatile afterload.

7.6.4.3 Distance to site of wave reflection

The concept of a distinct physical site of wave reflection has been disputed by Davies et al.[388]. This is based on experimental data in the aorta in which the reflection site remained a constant distance from the point of measurement as it moved distally. If there was a true definitive point of reflection the distance to this point would decrease as the measurement point approaches[388]. Any site of

wave reflection distal to the subsequent bifurcation is affected by re-reflection of the returning wave as crosses the bifurcation in reverse. This concept has been demonstrated by Khir and Parker in a canine study measuring WIA in the ascending aorta. Complete occlusion of descending aorta at the diaphragm generated BCWs in the ascending aorta, whereas occlusion distal to the renal arteries did not generate a discernible BCW. The reflections from a distal site return through a greater number of bifurcations at which the returning BCW is re-reflected towards the peripheries therefore the energy of the returning BCW is progressively diminished[433].

Following lung resection, the site of reflection would logically occur at the bifurcation of the PA to the lobar pulmonary artery that has now been ligated. As such, the reflected wave would not be significantly affected by re-reflection prior to its measurement. In this investigation the apparent site of wave reflection was reduced post-operatively in the operative PA to a median of 2.87cm [2.03-5.22cm], similar to Quail et al. (2-3cm)[351]. This distance is in keeping with the distance from the mid-point of the operative PA (RPA or LPA) to bifurcation to lobar pulmonary artery[351, 396]. Quail et al. do not interpret this reflection site a physical point of reflection but an *"amalgamation of reflections"* as the vascular remodelling of the patients with PAH occurs in the microvasculature[351]. The distance in the investigate presented here may however reflect an actual physical site of wave reflection, similar to that demonstrated by Khir and Parker[433]. As the post-operative reflected BCW in the operative PA is measured without significant (if any) re-reflection this may be the first demonstration of a physical reflection site in the pulmonary vasculature in man.

7.7 Conclusion

The main finding of this investigation is that there is evidence of increased pulsatile afterload in the operative PA following lung resection, measured by an increased wave reflection index. This increase is present on POD2 and persists to 2-months post-op whilst there is no increase in WRI in the non-operative PA. The reflection appears to originate from a proximal site potentially correlating with the resected branch of the pulmonary artery.

Chapter 8 Mechanisms of right ventricular dysfunction following lung resection

In this investigation, association is sought between conventional indices of afterload, wave intensity analysis and the changes in RV function demonstrated earlier in this thesis. Whilst this will result in multiple comparisons, only biologically plausible associations are tested, detailed below with further background throughout this thesis. As described by Hill in his seminal 1965 paper; any association does not imply causation and interpretation must be based on the strength, consistency, temporality and plausibility of the association and ultimately prospective experimentation[434]. Any consistent associations will therefore guide further studies into the mechanisms of RV dysfunction following lung resection, section 9.3 page 333. As Hill concludes,

"All scientific work is incomplete"

Hill 1965[434].

The specific rationale for the association testing performed is discussed below.

8.1 Association testing and hypothesis

The overarching hypothesis of this thesis is that right ventricular dysfunction occurs secondary to an increase in pulsatile afterload following lung resection. In Chapter 6 it is hypothesised that the altered distribution of cardiac output (CO) occurs secondary to an increase in operative PA pulsatile afterload and may therefore be a surrogate marker of afterload. To investigate the relationship between the indices of afterload, the altered distribution of cardiac output and right ventricular function the following comparisons were performed as below.

8.1.1 Association between indices of afterload

Hypotheses,

- There is an association between the change in WRI and the change in PAAT/ET and PA distensibility
- There shortening of PAAT is temporally related to the BCW.

In this thesis three separate indices of afterload are investigated; PAAT (and heart-rate corrected PAAT - PAAT/ET), PA distensibility and WRI[ggg]. Association testing between WRI and conventional afterload indices (PAAT/ET and PA distensibility) are performed to investigate the agreement between different indices of pulsatile afterload. In testing the within-subject association between WRI and PAAT, heart rate must be considered as a potential confounding factor. Sanz et al advise the calculation of PAAT/ET to normalise PAAT to the duration of ejection to adjust for heart rate[342] therefore PAAT/ET is used for all comparisons. *Within-subject* association testing is performed at all time points to assess if a change in WRI is associated with a change in PAAT/ET or PA distensibility. *Between-subject* associations are tested at individual time points to assess the associations between indices in each vessel at each time point, as discussed in 1.2.6.4.2 page 77, the relationship between resistance and compliance may be altered by a proximal PA occlusion.

As a reduction in PAAT is hypothesised to be caused by the arrival of a reflected BCW[351], association testing was performed between the time of peak of the BCW and PAAT. Of note, for results of PAAT described in Chapter 6, the time to peak flow was measured from the start of the cardiac cycle, measured from CMR timing of the ECG, whereas the BCW was measured from the onset of the FCW. In order to remove this potential discrepancy, PAAT timing was calculated form the onset of the FCW for the temporal comparisons alone, whilst the comparisons of PAAT/ET with WRI are performed on the unadjusted values reported in Chapter 6.

[ggg] The association between PAAT, PAAT/ET and distensibility is investigated in Chapter 6. It should be noted that these results are calculated from the same CMR images and therefore the same area and flow results.

Associations between indices of afterload and cardiac output distribution

Hypothesis,

- There is an association between the increase in non-operative PA percentage of CO and,
    a. the increase in pulsatile afterload in the operative PA
    b. the earlier arrival of and reduced distance to wave reflection

The distribution of blood flow across a bifurcation is affected by the outflow pressure difference between the daughter vessels[398]. A unilateral increase in pulsatile afterload may result in an increase in the percentage of cardiac output (percentage.CO) travelling in the contralateral PA. Additionally, the arrival of an early BCW during systole may further decrease the forward flow of blood in that vessel and therefore may also decrease the percentage.CO travelling in that vessel. The *within-subject* associations between the post-operative changes in indices of pulsatile afterload in the operative and non-operative PAs and the post-operative changes in non-operative PA percentage.CO are sought. As there is markedly different CO, heart rate and potentially different mechanisms of dysfunction between POD2 and 2-months, within-subject association testing is performed separately on the changes between pre-op and POD2 and from pre-op and 2-months. The association between the post-operative change in arrival of the BCW (distance to reflection site and time to the peak BCW) and the change in non-operative PA percentage.CO are also tested.

Finally, the relationship between the altered distribution of CO and pulsatile afterload in the MPA is investigated by the association between the increase in non-operative PA percentage.CO and change pulsatile afterload in the MPA (PAAT/ET and PA distensibility).

8.1.2 Associations between indices of afterload and right ventricular function

Hypotheses,

- Right ventricular dysfunction, measured by changes in RVEF and RV strain, is associated with the post-operative increase of,

a. pulsatile afterload in the operative and non-operative PA[hhh]
b. percentage of CO travelling in the non-operative PA.

8.1.2.1 Forward compression wave area

Within-subject testing is performed to assess association between post-operative change in FCW area and the change in RV function (RVEF and strain). As the percentage of total FCW area[iii] travelling in the non-operative PA increased post-operatively, similar to the increase in non-operative PA percentage.CO, the uneven FCW area distribution may also reflect increased operative PA pulsatile afterload.

8.1.2.2 Indices of afterload

Within-subject testing between the change in WRI and the time to BCW and the change in RV function were performed for the operative and non-operative PAs. As demonstrated in Chapter 6, there were associations between the increase in pulsatile afterload (PAAT/ET and PA distensibility) in the non-operative PA and the change in RV function between pre-op and POD2. Although the changes in pulsatile afterload are predominately in the operative PA the redistribution of CO and an inability of the non-operative PA to accommodate the increased blood flow may lead to impaired RV function.

8.1.2.3 Cardiac output distribution

The increase in the non-operative PA percentage.CO may be a sign of increased operative afterload and may also suggest that the indices of afterload in the operative PA are an underestimation of the true increase in pulsatile afterload as blood preferentially flows down the path of least resistance (non-operative PA). It is therefore hypothesised that an increase in the non-operative PA percentage.CO may be associated with impaired RV function.

[hhh] Association testing between RVEF and PAAT, PAAT/ET and distensibility are performed in Chapter 6.

[iii] FCW area was chosen over FCW peak based on the work by Quail et al who demonstrated that the relative difference in FCW peak between healthy controls and patients with PAH was smaller than the relative difference in FCW area[351].

8.2 Results

8.2.1 Association between indices of afterload

8.2.1.1 Association between pulmonary artery acceleration time and wave reflection index

All time point *within-subject* analysis showed a strong negative associations between PAAT/ET and WRI in the operative PA, Table 8-1 and Figure 8-1. There was a weak negative association between PAAT/ET and WRI in the non-operative PA. In each association an increase in WRI (increase in pulsatile afterload) was associated with a decrease in PAAT/ET (increase in pulsatile afterload). Individual time point association showed that on POD2 there was a moderate association between operative PA WRI and PAAT/ET, Figure 8-2, although there were no other significant associations.

Analysis of covariance, within-subject				
Wave reflection index (%)				
			Operative PA	Non-operative PA
PAAT/ET (%)		r	***-0.606***	***-0.354***
		p	***<0.001***	***0.023***
Individual time point analysis				
			Operative PA	Non-operative PA
PAAT/ET (%)	Pre-op	r	0.185	-0.200
		p	0.356 §	0.339 §
	POD2	r	***-0.595***	0.224
		p	***0.005 §***	0.329 *
	2-months	r	-0.179	-0.124
		p	0.436 *	0.592 *

Table 8-1 Associations between pulmonary artery acceleration time and wave reflection index
PAAT/ET= pulmonary artery acceleration time/ejection time. PA= pulmonary artery. POD2= post-operative day 2. Analysis of covariance with patient as factor. *= Pearson's correlation co-efficient. §= Spearman's correlation co-efficient. Significant results (p<0.05) highlighted ***bold italics.***

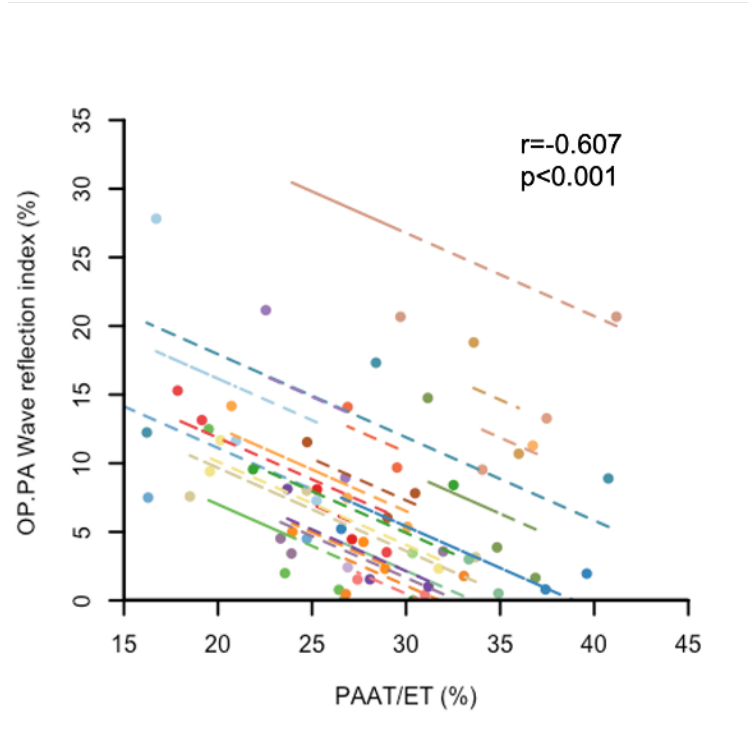

Figure 8-1 All time point within-subject association between operative pulmonary artery acceleration time and wave reflection index
Note strong negative associations between pulmonary artery acceleration time corrected for heart rate (PAAT/ET) and wave reflection index (WRI) in the operative pulmonary artery (OP.PA). A reduction in PAAT/ET is associated with an increase in wave reflection index. Analysis of covariance with patient as factor. Coloured dots represent each patient and lines depict parallel lines of association for each patient.

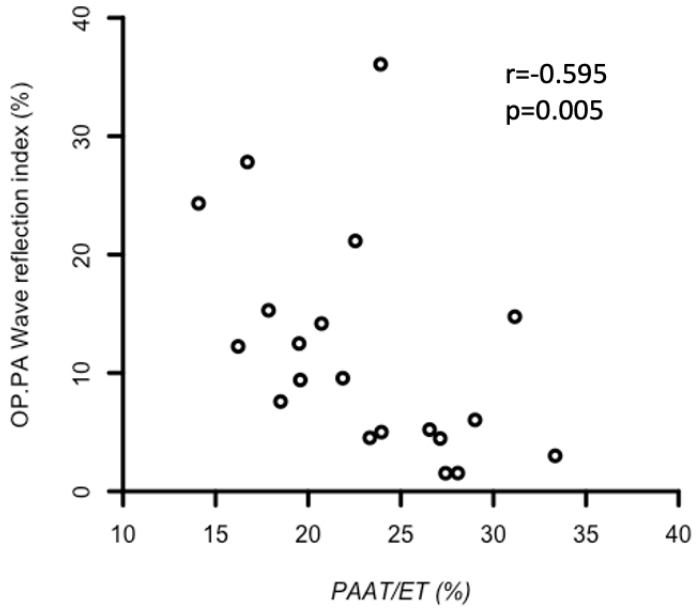

Figure 8-2 Association between operative pulmonary artery acceleration time and wave reflection index on post-operative day two
Note strong negative association between operative pulmonary artery (OP.PA) wave reflection index and pulmonary artery acceleration time corrected for heart rate (PAAT/ET). Spearman's correlation coefficient.

There were consistent moderate to strong positive *within-subject* and individual time point associations between PAAT and the time to the peak backward compression wave in the operative and non-operative PAs except for on POD2 in the non-operative PA which approached significance (p=0.069), Table 8-2.

Analysis of covariance, within-subject				
Time to peak backward compression wave (ms)				
			Operative PA	Non-operative PA
Pulmonary artery acceleration time (ms)		r	***0.571***	***0.592***
		p	***<0.001***	***<0.001***
Individual time point analysis				
			Operative PA	Non-operative PA
Pulmonary artery acceleration time (ms)	Pre-op	r	***0.603***	***0.613***
		p	***0.001 §***	***0.001 ****
	POD2	r	***0.662***	0.414
		p	***0.015 ****	0.069 *
	2-months	r	***0.540***	***0.786***
		p	***0.014 §***	***<0.001 ****

Table 8-2 Associations between pulmonary artery acceleration time and time to peak backward compression wave
PAAT= pulmonary artery acceleration time. PA= pulmonary artery. POD2= post-operative day 2. Analysis of covariance with patient as factor. *= Pearson's correlation co-efficient. §= Spearman's correlation co-efficient. Significant results (p<0.05) highlighted ***bold italics.***

8.2.1.2 Association between pulmonary artery distensibility and wave reflection index

There were no associations between WRI and PA distensibility on within-subject analysis or individual time point analysis in any vessel, Table 8-3.

Analysis of covariance, within-subject				
Wave reflection index (%)				
			Operative PA	Non-operative PA
PA distensibility (%)		r	-0.191	0.020
		p	0.225	0.901
Individual time point analysis				
			Operative PA	Non-operative PA
PA distensibility (%)	Pre-op	r	-0.239	0.058
		p	0.251 §	0.774 §
	POD2	r	0.088	0.429
		p	0.705 *	0.059 §
	2-months	r	-0.151	-0.013
		p	0.513 *	0.956 *

Table 8-3 Association between pulmonary artery distensibility and wave reflection index
PA= pulmonary artery. POD2= post-operative day 2. Analysis of covariance with patient as factor. *= Pearson's correlation co-efficient. §= Spearman's correlation co-efficient. Significant results ($p<0.05$) highlighted ***bold italics.***

8.2.2 Association between indices of afterload and cardiac output distribution

8.2.2.1 Indices of afterload

There were moderate to strong within-subject associations between the change in operative PA indices of afterload and the change in non-operative PA percentage.CO between pre-op and POD2 and between pre-op and 2-months, Table 8-4 and Figure 8-3. All associations consistently showed that an increase in operative pulsatile afterload was associated with an increase in the non-operative PA percentage.CO. The increase in non-operative percentage.CO was associated with a shortening in non-operative PAAT/ET on POD2 and an increased in WRI at 2-months. These two associations suggest that increased non-operative PA percentage.CO was also associated with signs of increased pulsatile afterload (reduced PAAT/ET and increased WRI) in the non-operative PA suggesting that it may be unable to accommodate the increased blood flow without an increase in pulsatile afterload.

Analysis of covariance, within-subject							
Change between pre-op and POD2							
		Operative PA			Non-operative PA		
		WRI (%)	PAAT/ET (%)	Distensi-bility (%)	WRI (%)	PAAT/ET (%)	Distensi-bility (%)
Percentage.CO in non-operative PA(%)	r	***0.728***	***-0.657***	***-0.504***	0.046	***-0.545***	-0.365
	p	***<0.001***	***0.001***	***0.020***	0.851	***0.011***	0.104
Change between pre-op and 2-months							
		Operative PA			Non-operative PA		
		WRI (%)	PAAT/ET (%)	Distensi-bility (%)	WRI (%)	PAAT/ET (%)	Distensi-bility (%)
Percentage.CO in non-operative PA(%)	r	***0.523***	***-0.434***	-0.295	***0.474***	0.225	0.250
	p	***0.010***	***0.038***	0.171	***0.035***	0.303	0.249

Table 8-4 Within-subject association between afterload results and the percentage of cardiac output in the non-operative pulmonary artery
PA= pulmonary artery. Percentage of cardiac output (percentage.CO) calculated as value in non-operative PA divided by the total in operative and non-operative PA, expressed as a percentage. POD2= post-operative day 2. WRI= wave reflection index. PAAT/ET= Pulmonary artery acceleration time/ejection time. Analysis of covariance with patient as factor. Significant results ($p<0.05$) highlighted ***bold italics.***

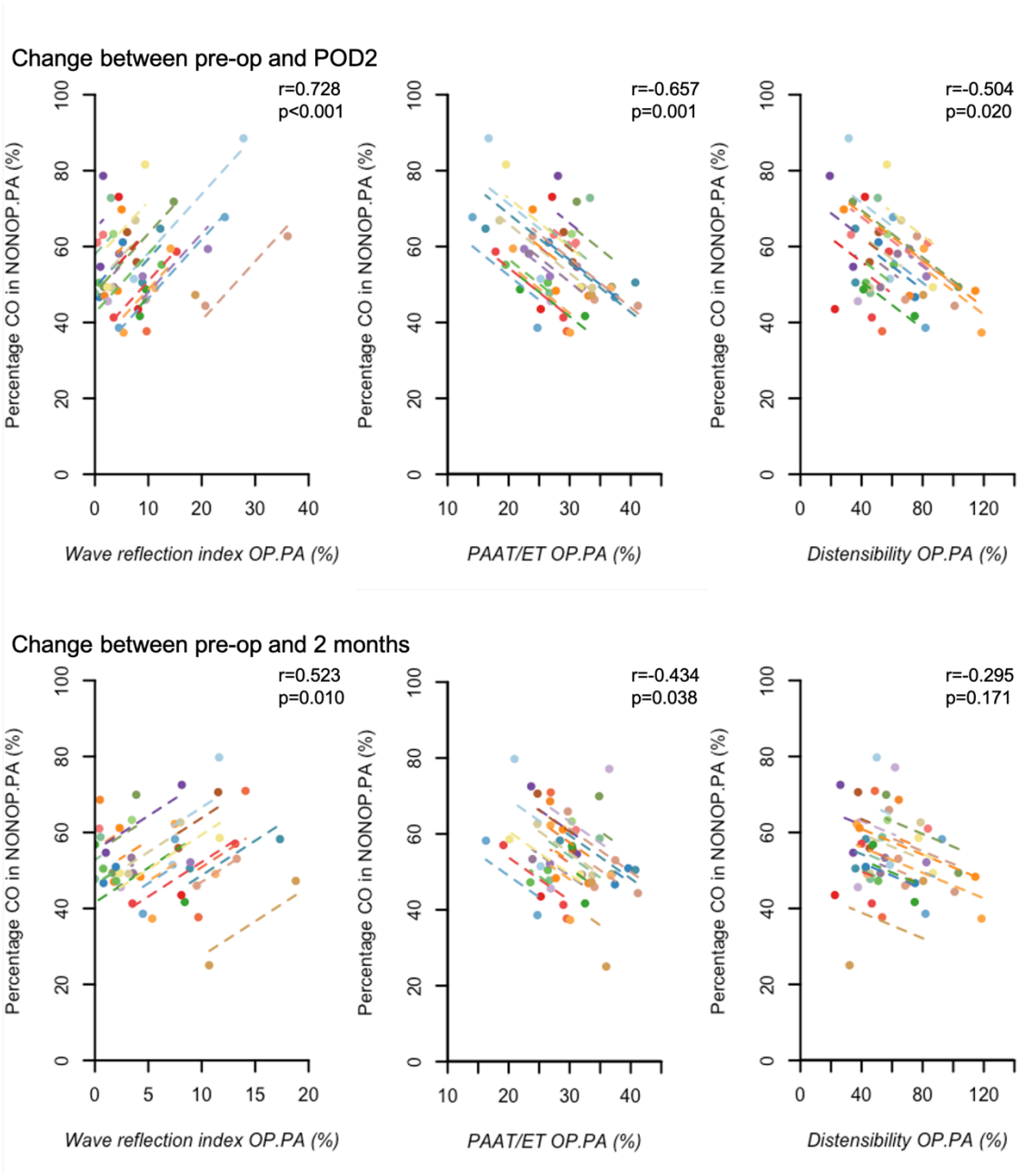

Figure 8-3 Within-subject association between changes in percentage cardiac output in non-operative pulmonary artery and operative pulmonary artery afterload
Within-subject association plots displaying the association between the change in percentage of cardiac output (percentage.CO) in non-operative pulmonary artery (NONOP.PA) with indices of operative pulmonary artery (OP.PA) afterload. Associations shown for wave reflection index (WRI, left column), rate corrected pulmonary artery acceleration time (PAAT/ET, centre column) and PA distensibility (right column). Top row is within-subject associations for change between pre-operative (pre-op) and post-operative day 2 (POD2), bottom row is within-subject associations for change between pre-op and 2-months post-operative. Note increased operative afterload is generally associated with increased non-operative percentage.CO. Analysis of covariance with patient as factor. Coloured dots represent each patient and lines depict parallel lines of association for each patient.

There was a strong *within-subject* association between the change in non-operative percentage.CO and the change in main PAAT/ET between pre-op and POD2, an increase in non-operative percentage.CO was associated with a shortening in PAAT/ET, Table 8-5 and Figure 8-4. This suggests that the increase

in non-operative PA percentage.CO was associated with increase pulsatile afterload in the MPA on POD2. There were no other associations between MPA indices of afterload and non-operative percentage.CO.

Analysis of covariance, within-subject			
Change between pre-op and POD2			
		MPA	
		PAAT/ET (%)	PA distensibility (%)
Percentage.CO in non-operative PA(%)	r	***-0.621***	0.231
	p	***0.003***	0.426
Change between pre-op and 2-months			
		MPA	
		PAAT/ET (%)	PA distensibility (%)
Percentage.CO in non-operative PA(%)	r	-0.035	-0.055
	p	0.874	0.839

Table 8-5 Within-subject association between main pulmonary artery indices of pulsatile afterload and the percentage of cardiac output in the non-operative pulmonary artery
PA= pulmonary artery. MPA= main PA. PAAT/ET= Pulmonary artery acceleration time/ejection time. Percentage of cardiac output (percentage.CO) calculated as value in non-operative PA divided by the total in operative and non-operative PA, expressed as a percentage. POD2= post-operative day 2. Analysis of covariance with patient as factor. Significant results ($p<0.05$) highlighted ***bold italics.***

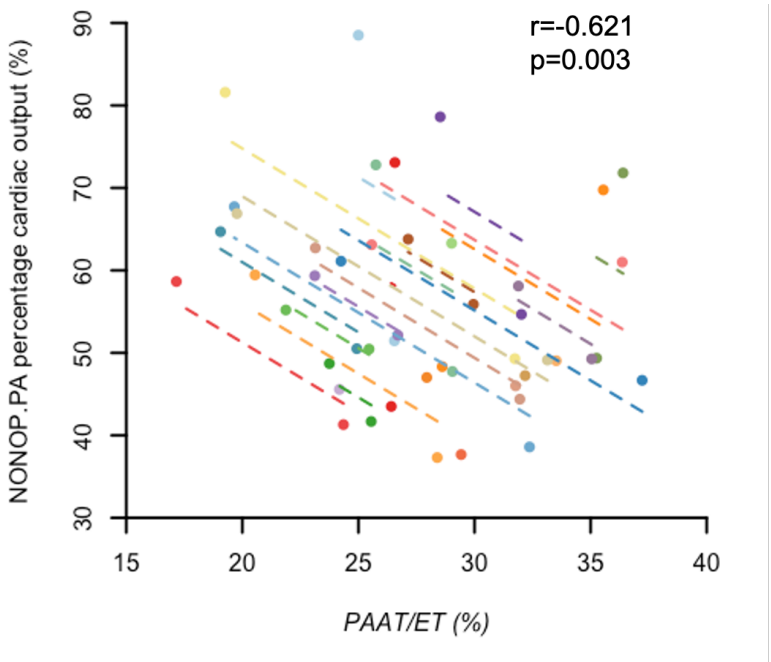

Figure 8-4 Within-subject association between changes in percentage cardiac output in non-operative pulmonary artery and main pulmonary artery acceleration time
Within-subject association plot displaying the association between the change in percentage cardiac output in non-operative pulmonary artery (NONOP.PA) and change in rate corrected pulmonary artery acceleration time (PAAT/ET) in the main pulmonary artery between pre-op and POD2. Note increased non-operative percentage.CO is associated with a reduction in PAAT/ET. Analysis of covariance with patient as factor. Coloured dots represent each patient and lines depict parallel lines of association for each patient.

8.2.2.2 Wave reflection site and timing

There were moderate to strong within-subject associations in the operative PA between the change in distance to reflection site, the time to peak BCW and non-operative PA percentage.CO between pre-op and both post-operative time points. In each comparison more proximal and earlier of wave reflection in the operative PA was associated with an increase in the percentage.CO in the non-operative PA, Figure 8-5. There were no significant associations between the distance to reflection site or time to peak BCW and cardiac output distribution in the non-operative PA.

Analysis of covariance, within-subject					
Change between pre-op and POD2					
		Operative PA		Non-operative PA	
		Distance to reflection site (cm)	Time to peak BCW (ms)	Distance to reflection site (cm)	Time to peak BCW (ms)
Percentage.CO in non-operative PA(%)	r	***-0.560***	***-0.653***	0.463	-0.266
	p	***0.010***	***0.002***	0.061	0.302
Change between pre-op and 2-months					
		Operative PA		Non-operative PA	
		Distance to reflection site (cm)	Time to peak BCW (ms)	Distance to reflection site (cm)	Time to peak BCW (ms)
Percentage.CO in non-operative PA(%)	r	***-0.671***	***-0.594***	0.175	-0.313
	p	***0.001***	***0.006***	0.518	0.238

Table 8-6 Within-subject association between distance to reflection site, time to peak backward compression wave and the percentage of cardiac output in the non-operative pulmonary artery

PA= pulmonary artery. Percentage of cardiac output (percentage.CO) calculated as value in non-operative PA divided by the total in operative and non-operative PA, expressed as a percentage. BCW= backward compression wave. POD2= post-operative day 2. Analysis of covariance with patient as factor. Significant results ($p<0.05$) highlighted ***bold italics.***

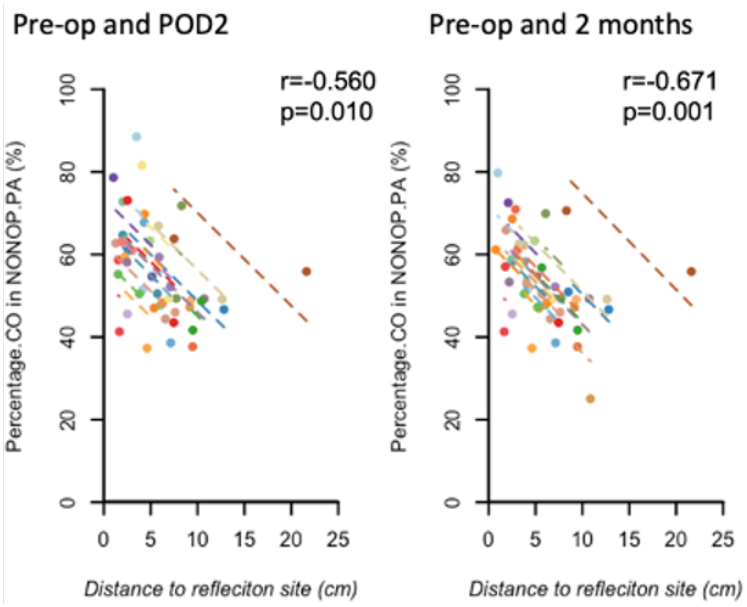

Figure 8-5 Within-subject association between percentage cardiac output in non-operative pulmonary artery and distance to operative pulmonary artery reflection site
Within-subject association plots displaying the association between the change in percentage of cardiac output (percentage.CO) in non-operative pulmonary artery (NONOP.PA) and the distance to the reflection site in the operative pulmonary artery. Change between pre-operative (pre-op) and post-operative day 2 (pre-op and POD2, left plot) and between pre-op and 2-months (right plot). Note increased non-operative percentage.CO is associated with a reduction in the distance to site of reflection. Analysis of covariance with patient as factor. Coloured dots represent each patient and lines depict parallel lines of association for each patient.

8.2.3 Associations between indices of afterload and right ventricular function

8.2.3.1 Forward compression wave

Between pre-op and POD2 there was a moderate negative within-subject association between the change in operative PA FCW area and the change in RVGLS.S (r=-0.545) whilst the association between the change in non-operative FCW area and the change in RVGLS.S also approached significance (r=0.453, p=0.068) although the direction of association was the opposite, Table 7-9. The association between the change in FCW area in the operative PA and the change in RVEF also approached a positive significance (p=0.051) between pre-op and POD2[jjj]. Similarly, between pre-op and 2-months, the association between the change in RVGLS and the change in operative FCW area was negative whereas the association between RVGLS and non-operative PA FCW area was positive, Figure

[jjj] Strain is a negative value, therefore in impaired strain the numerical value of strain increases whereas in impaired RVEF the numerical value decreases, this results in opposing directs of association between a parameter that impairs RV function and strain or RVEF. For example if an increase in an index of afterload results in impaired RV function the association will be positive for strain and negative for RVEF.

8-6. Also, there were opposing directions of associations (or trends to association, p<0.062) for RVEF, RVGLS.FW and RVGLS.S. In each comparison, an increase in non-operative PA FCW area or a decrease in operative PA FCW area were associated with a decrease in RV function.

Analysis of covariance, within-subject						
Change between pre-op and POD2						
			RVEF (%)	RVGLS (%)	RVGLS.FW (%)	RVGLS.S (%)
FCW area (cm^5)	Operative PA	r	0.431	-0.364	-0.178	***-0.545***
		p	0.051	0.137	0.510	***0.019***
	Non-operative PA	r	-0.313	0.413	0.119	0.453
		p	0.179	0.099	0.673	0.068
Change between pre-op and 2-months						
			RVEF (%)	RVGLS (%)	RVGLS.FW (%)	RVGLS.S (%)
FCW area (cm^5)	Operative PA	r	0.416	***-0.504***	-0.450	***-0.460***
		p	0.060	***0.028***	0.053	***0.047***
	Non-operative PA	r	***-0.507***	***0.596***	***0.568***	0.450
		p	***0.019***	***0.009***	***0.014***	0.061

Table 8-7 Within-subject associations between forward compression wave area and indices of right ventricular function
FCW= forward compression wave. PA= pulmonary artery. RVEF= right ventricular ejection fraction. RVGLS= right ventricular global longitudinal strain. RVGLS.FW= free wall RVGLS. RVGLS.S= septal RVGLS. POD2= post-operative day 2. Analysis of covariance with patient as factor. Significant results (p<0.05) highlighted ***bold italics.***

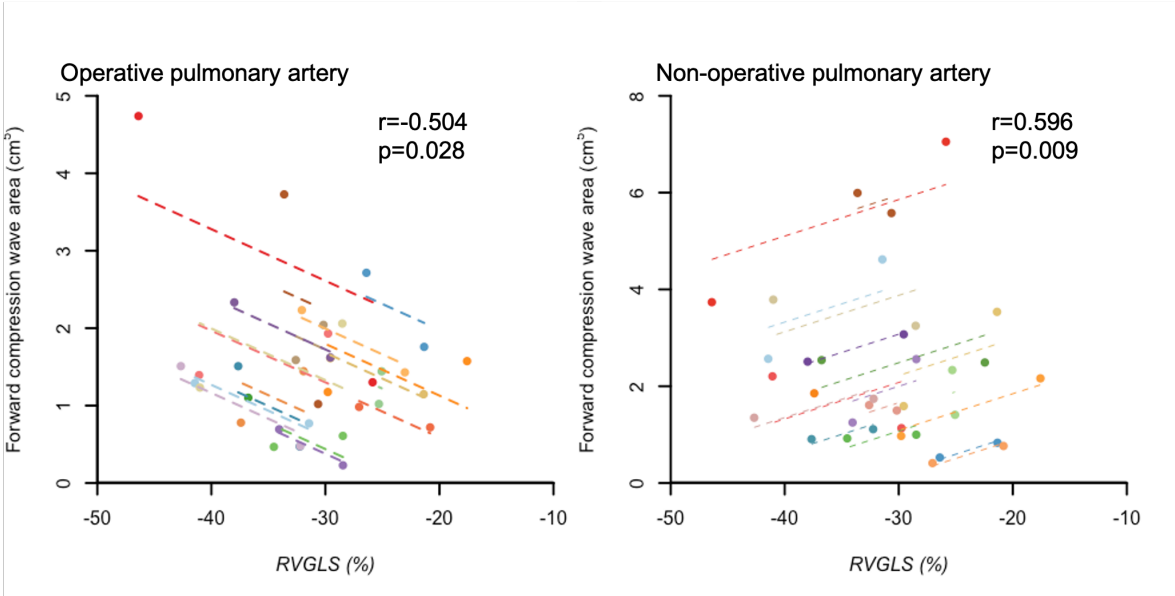

Figure 8-6 Within-subject association between forward compression wave area and right ventricular global longitudinal strain, between pre-operative and 2-months
Within-subject association plots between the change operative pulmonary artery (PA) forward compression wave area (FCW area) (left), the change in non-operative pulmonary artery FCW area (right) against right ventricular global longitudinal strain (RVGLS) between pre-op and 2-months. Note negative association for operative PA and positive association in non-operative PA. Analysis of covariance with patient as factor. Coloured dots represent each patient and lines depict parallel lines of association for each patient.

8.2.3.2 Indices of afterload

8.2.3.2.1 Wave reflection index

There was a moderate negative association between the change in operative PA WRI and the change in RVEF between pre-op and POD2 although there were no other associations between these time points, Table 8-8. Between pre-op and 2-months, there were strong positive within-subject associations between the change in non-operative PA WRI and the changes in RVGLS, RVGLS.S and RVGLS.FW whilst the change in WRI in the operative PA had a moderate positive association with the change in RVGLS.FW and approached significance with the change in RVGLS (p=0.053), Figure 8-7. In each association an increase in WRI was associated with an impairment in RV strain.

Analysis of covariance, within-subject						
Change between pre-op and POD2						
			RVEF (%)	RVGLS (%)	RVGLS.FW (%)	RVGLS.S (%)
WRI (%)	Operative PA	r	***-0.480***	0.015	-0.174	0.224
		p	***0.028***	0.952	0.518	0.329
	Non-operative PA	r	-0.024	0.337	0.311	0.229
		p	0.920	0.186	0.124	0.378
Change between pre-op and 2-months						
			RVEF (%)	RVGLS (%)	RVGLS.FW (%)	RVGLS.S (%)
WRI (%)	Operative PA	r	-0.070	0.450	***0.487***	0.282
		p	0.763	0.053	***0.035***	0.242
	Non-operative PA	r	-0.268	***0.702***	***0.745***	***0.553***
		p	0.240	***0.001***	***<0.001***	***0.017***

Table 8-8 Within-subject associations between wave reflection index and indices of right ventricular function
PA= pulmonary artery. WRI= wave reflection index. RVEF= right ventricular ejection fraction. RVGLS= right ventricular global longitudinal strain. RVGLS.FW= free wall RVGLS. RVGLS.S= septal RVGLS. POD2= post-operative day 2. Analysis of covariance with patient as factor. Significant results ($p<0.05$) highlighted ***bold italics.***

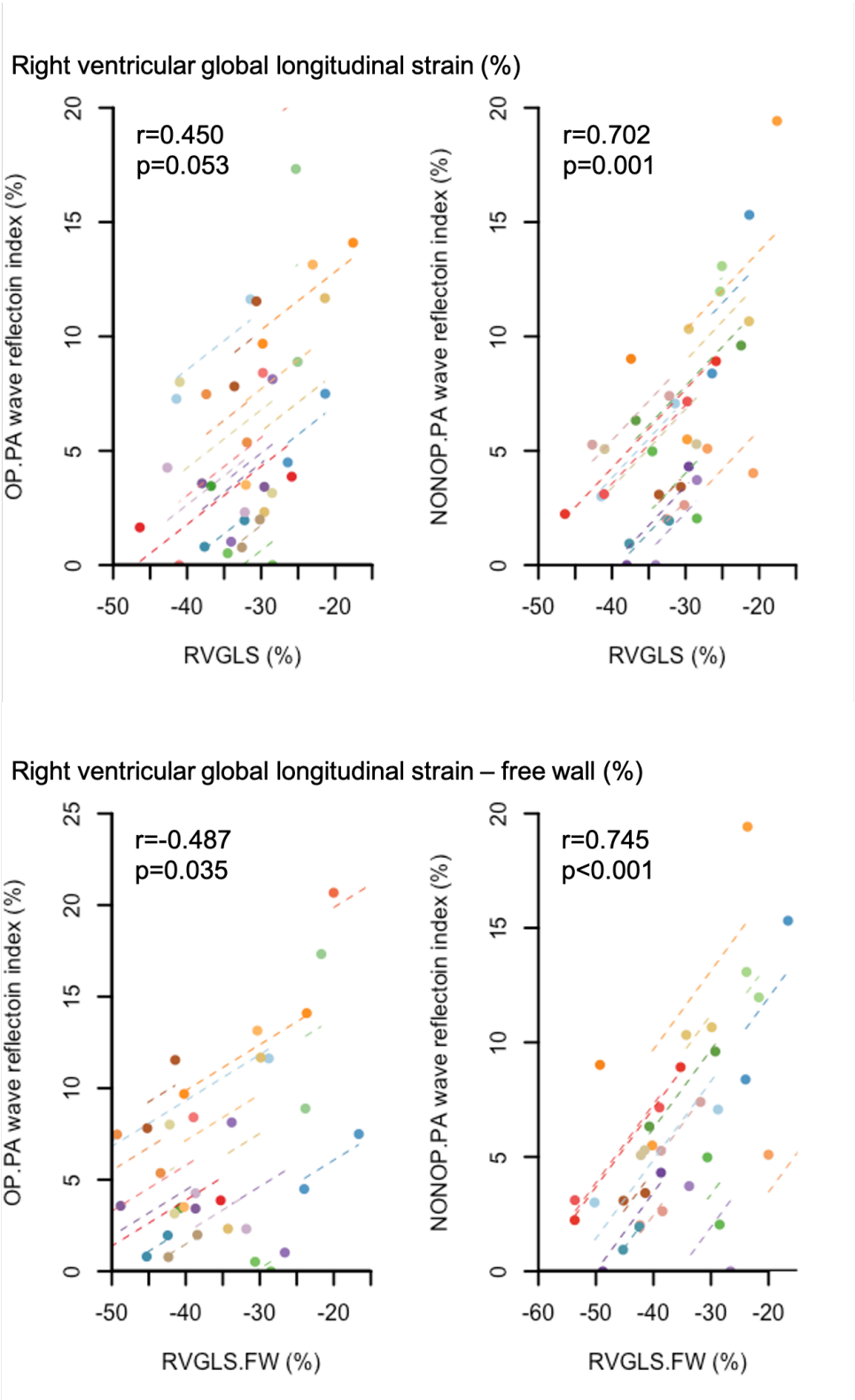

Figure 8-7 Within-subject association between the change in wave reflection index and the change in right ventricular longitudinal strain between pre-operative and 2-months
Within-subject association plots displaying the association between the change in wave reflection index (WRI) and the change right ventricular longitudinal strain (RVGLS, top row) and free wall RVGLS (RVGLS.FW, bottom row) between pre-op and 2-months in the operative pulmonary artery (OP.PA, left column) and non-operative PA (NONOP.PA, right column). Note strong positive associations between the increase in pulsatile afterload (WRI) and impaired RV strain (less negative strain) in the non-operative PA. Analysis of covariance with patient as factor. Coloured dots represent each patient and lines depict parallel lines of association for each patient.

The within-subject associations between the change in PAAT/ET, PA distensibility and the change in RVEF are presented separately in section 6.4.5 page 210.

There were no consistent associations between the change in operative or non-operative PAAT/ET or PA distensibility and the change in RV strain except a moderate negative association between the change in operative PA distensibility and the change in RVGLS.S between pre-op and POD2 (r=-0.508, p=0.031, ANCOVA with patient as factor). In this association an increase in pulsatile afterload (reduction in PA distensibility) was associated with impaired RVGLS.S. There were no with-subject associations between PAAT/ET or PA distensibility in the MPA and RV function (p>0.059).

8.2.3.2.2 Time to peak backward compression wave

There were moderate positive within-subject association between the change in time to peak BCW and change in RVEF in the operative and non-operative PAs between pre-op and POD2, Table 8-9. When corrected for heart rate, (divided by ejection time similar to PAAT/ET) neither of the associations retained significance. There was however a moderate positive association between the change in time to peak BCW in the operative PA between pre-op and 2-months and the corresponding change in RVEF, this retained significance when corrected for heart rate. An early BCW in the operative PA was associated with a reduction in RVEF. There were no within-subject associations between the change in time to peak BCW (p>0.053) or to time to peak BCW/ET (p>0.077) and the change in RV strain.

Analysis of covariance, within-subject							
Change between pre-op and POD2							
			RVEF (%)				RVEF (%)
Time to peak BCW (%)	Operative PA	r	***0.505***	Time to peak BCW/ET(%)	Operative PA	r	0.328
		p	***0.024***			p	0.158
	Non-operative PA	r	***0.553***		Non-operative PA	r	0.430
		p	***0.018***			p	0.097

Change between pre-op and 2-months							
			RVEF (%)				RVEF (%)
Time to peak BCW (%)	Operative PA	r	***0.509***	Time to peak BCW/ET(%)	Operative PA	r	***0.525***
		p	***0.026***			p	***0.021***
	Non-operative PA	r	-0.011		Non-operative PA	r	0.145
		p	0.967			p	0.580

Table 8-9 Within-subject associations between time to peak backward compression wave and indices of right ventricular function
PA= pulmonary artery. BCW= backward compression wave. BCW/ET= BCW normalised for heart rate. RVEF= right ventricular ejection fraction. POD2= post-operative day 2. Analysis of covariance with patient as factor. Significant results (p<0.05) highlighted ***bold italics.***

8.2.3.3 Cardiac output distribution

There were moderate and strong associations between the change in non-operative PA percentage.CO and the change in RVEF between pre-op and both post-operative time points, Table 8-10. In each association, an increased non-operative PA percentage.CO was associated with a decreased RVEF, Figure 8-8.

Analysis of covariance, within-subject					
Change between pre-op and POD2					
		RVEF (%)	RVGLS (%)	RVGLS.FW (%)	RVGLS.S (%)
Percentage.CO in non-operative PA(%)	r	***-0.545***	0.367	-0.087	***0.500***
	p	***0.011***	0.134	0.748	***0.035***

Change between pre-op and 2-months					
		RVEF (%)	RVGLS (%)	RVGLS.FW (%)	RVGLS.S (%)
Percentage.CO in non-operative PA(%)	r	***-0.634***	***0.471***	***0.540***	0.335
	p	***0.002***	***0.042***	***0.017***	0.161

Table 8-10 Within-subject association between right ventricular function and the percentage of cardiac output in the non-operative pulmonary artery
PA= pulmonary artery. Percentage of cardiac output (percentage.CO) calculated as value in non-operative PA divided by the total in operative and non-operative PA, expressed as a percentage. RVEF= right ventricular ejection fraction. RVGLS= right ventricular global longitudinal strain. RVGLS.FW= free wall RVGLS. RVGLS.S= septal RVGLS. POD2= post-operative day 2. Analysis of covariance with patient as factor. Significant results (p<0.05) highlighted ***bold italics.***

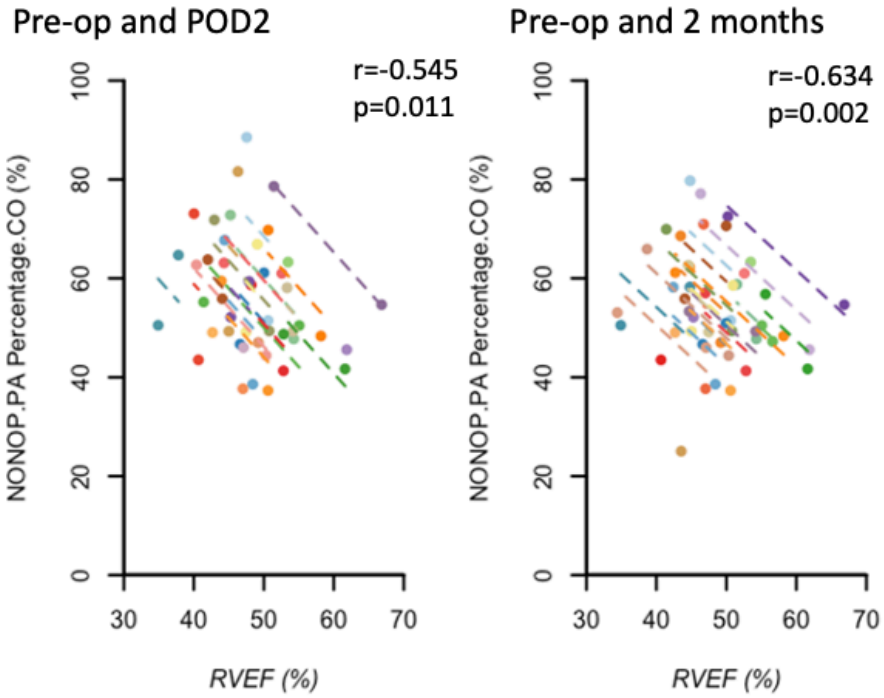

Figure 8-8 Within-subject association between percentage cardiac output in non-operative pulmonary artery and right ventricular ejection fraction
Within-subject association plots displaying the association between the change in percentage of cardiac output (percentage.CO) in non-operative pulmonary artery (NONOP.PA) and the change in right ventricular ejection fraction (RVEF). Comparison demonstrated are between pre-operative and post-operative day 2 (pre-op and POD2, left plot) and pre-op and 2-months (right plot). Note negative association in each comparison, i.e. increased percentage.CO in the non-operative PA is associated with reduced RVEF. Analysis of covariance with patient as factor. Coloured dots represent each patient and lines depict parallel lines of association for each patient.

Within-subject testing showed differing changes in strain between pre.op and POD2 and between pre.op and 2months, Table 8-10 and Figure 8-9. Between pre-op and POD2 there was a moderate positive within-subject association between the change in the non-operative PA percentage.CO and the change in RVGLS.S, an increase in the percentage of cardiac output travelling in the non-operative PA was associated with a reduction in RVGLS.S (less negative i.e. poorer RV function). There was no association between non-operative PA percentage.CO and RVGLS.FW or RVGLS at this point. Conversely, between pre-op and 2-months there was a moderate positive association between the change in non-operative PA percentage.CO and the change in RVGLS.FW and RVGLS with no association between non-operative PA percentage.CO and RVGLS.S at this point.

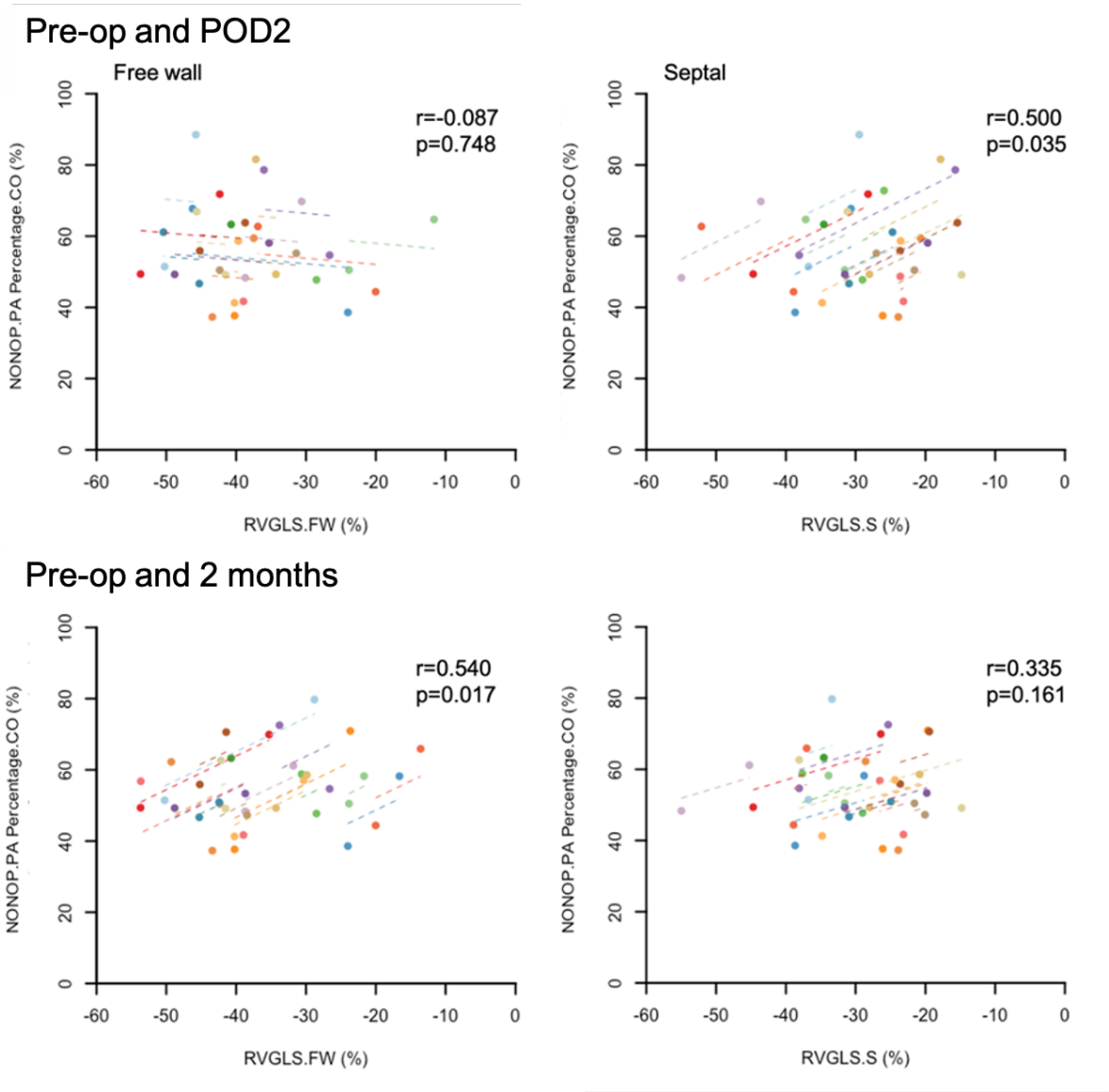

Figure 8-9 Within-subject association between percentage cardiac output in non-operative pulmonary artery and right ventricular longitudinal strain
Within-subject association plots displaying the association between the change in percentage of cardiac output (percentage.CO) in non-operative pulmonary artery (NONOP.PA) and the change in right ventricular longitudinal strain (RVGLS) in the free wall (RVGLS.FW, left side) and septum (RVGSL.S, right side).Top row is within-subject association between pre-operative (pre-op) and post-operative day 2 (POD2), bottom row is between pre-op and 2-months post-operative. Note positive association at pre-op and POD2 in RVGLS.S only whereas between pre-op and 2-months there is a positive association in RVGLS.FW only. Analysis of covariance with patient as factor. Coloured dots represent each patient and lines depict parallel lines of association for each patient.

8.2.4 Summary of main results

Increased indices of pulsatile afterload in the operative PA were associated with an increase in the non-operative PA percentage.CO, i.e. increased operative pulsatile afterload was associated with a diversion of blood towards the non-operative PA, Table 8-11. The increase in non-operative PA percentage.CO was associated with increased non-operative afterload, increased PAAT/ET at POD2

and increased WRI at 2-months, suggesting that non-operative PA may not be able to accommodate the increase in post-operative blood flow.

Summary of within-subject association testing						
Percentage.CO in non-operative PA(%)						
Change between	Pulmonary artery	WRI (%)	PAAT/ET (%)	Distensibility (%)	Distance to reflection site (cm)	Time to peak BCW (ms)
Pre-op and POD2	Operative	+ + +	- - -	- -	- -	- - -
	Non-operative		- -			
Pre-op and 2months	Operative	+ +	- -		- - -	- -
	Non-operative	+ +				

Table 8-11 Summary of associations between the change percentage of cardiac output in the non-operative pulmonary artery and indices of afterload
+/+ +/+ + += weak/moderate/strong positive association. -/- -/- - - = weak/moderate/strong negative association. Blank= no association. Percentage of cardiac output (percentage.CO) calculated as value in non-operative PA divided by the total in operative and non-operative pulmonary artery, expressed as a percentage. POD2= post-operative day 2. WRI= wave reflection index. PAAT/ET= Pulmonary artery acceleration time/ejection time. BCW= backward compression wave.

The within-subject associations between the change in indices of pulsatile afterload, non-operative PA percentage.CO and indices of RV function are summarised in Table 6-11. Between pre-op and POD2 there was a moderate association between increase in operative PA WRI and decrease in RVEF. There were also consistent associations between the increase in non-operative PA WRI and impaired RV strain between pre-op and 2-months, suggesting that if the non-operative PA cannot accommodate the increased blood flow, then impaired RV strain develops. Additionally, between pre-op and 2-months there were consistent associations between non-operative PA percentage.CO and RV strain, in each association increased non-operative PA percentage.CO resulted in impaired RV strain. Finally, there was moderate and strong associations between the increase in non-operative percentage.CO and reduction in RVEF between pre-op and POD2 and between pre-op and 2-months.

Change between	Parameter	Pulmonary artery	RVEF	RVGLS	RVGLS.FW	RVGLS.S
Pre-op and POD2	WRI	Operative	- -			
		Non-operative				
	Time to peak BCW/ET	Operative				
		Non-operative				
	PAAT/ET	Operative				
		Non-operative	+			
	PA distensibility	Operative	+ +			- -
		Non-operative	+ +			
	Percentage.CO	Non-operative	- -			+ +
Pre-op and 2-months	WRI	Operative			+ +	
		Non-operative		+ + +	+ + +	+ +
	Time to peak BCW/ET	Operative	++			
		Non-operative				
	PAAT/ET	Operative				
		Non-operative				
	PA distensibility	Operative				
		Non-operative				
	Percentage.CO	Non-operative	- - -	+ +	+ +	

Table 8-12 Summary of changes in wave intensity analysis parameters, blood flow distribution and indices of right ventricular function
+/+ +/+ + += weak/moderate/strong positive association. -/- -/- - - = weak/moderate/strong negative association. Blank= no association. BCW= Backward compression wave. RVEF= right ventricular ejection fraction. RVGLS= right ventricular global longitudinal strain. RVGLS.FW= free wall RVGLS. RVGLS.S= septal RVGLS. POD2= post-operative day 2. Percentage.CO= percentage of cardiac output. NB Impaired strain results in an increase in value whereas impaired RVEF results in a decrease in its value. The association are therefore in the opposite direction if both RVEF and strain are both impaired by the same factor.

8.3 Discussion

This is the first study to demonstrate the hypothesised association between increased afterload and RV dysfunction following lung resection. Post-operatively the increase in pulsatile afterload in the operative PA diverts blood flow through the non-operative PA resulting in increased non-operative percenage.CO and, if the non-operative PA is unable to accommodate the increased flow, increased non-operative pulsatile afterload. On POD2, reduced RVEF is associated with increased pulsatile afterload in both operative and non-operative PAs and the increase in non-operative PA percentage.CO whereas RVGLS is unchanged. At 2-months, reduced RVEF is again associated with increased non-operative PA percentage.CO and impaired RVGLS has developed secondary to an increase in

non-operative PA WRI and PA percentage.CO. It is argued that these associations are ultimately caused by the increase in operative PA pulsatile afterload.

8.3.1 Strengths and limitations

This is the first study to assess the sequential change in both pulmonary artery wave intensity analysis and perform CMR assessment of RV function following a lung resection. The design of this study allows *within-subject* association testing between the change in WIA parameters and the change in RV function from pre-operative into the immediate and medium term post-operative period following lung resection demonstrating, for the first time, the hypothesised associations between RV function and afterload.

Additionally, this is the first study to perform paired investigations of PA WIA and RV strain in any population. As demonstrated in Chapter 5 there is a delayed reduction in RVGLS and RVGLS.FW by 2-months following lung resection. Within-subject analysis allows association testing between measures of WIA and RV strain to describe the potential mechanisms of this delayed reduction in RVGLS and RVGLS.FW.

Finally, as this study performs assessment of blood flow in the operative and non-operative PAs, it not only allows assessment of unilateral afterload changes but also allows investigation of the distribution of the cardiac output between vessels. A unilateral increase in afterload will divert blood to the contralateral PA and so an increase in non-operative percentage.CO may be a composite measure of increased afterload and may result in impaired RV function, it may also be further influenced by afterload in the non-operative PA.

A limitation of the investigations detailed in this chapter is that the association testing performed results in multiple comparisons. Only biologically plausible association tests are performed in order to limit the number of comparisons, although there remains a significant risk of type 1 error. To limit the impact of this risk the interpretation of the results is based on the strength, consistency, temporality and plausibility of the results as per Hill, detailed in the introduction of this chapter, page 297[434]. Ultimately the results of this investigation (and those detailed in Chapters 5, 6 and 7) are used to guide further investigations detailed

later in section 9.3, Appendix 2 and Appendix 3. As such the interpretation of the results of this thesis will be tested by prospective experimentation.

8.3.2 Association between indices of afterload

Wave intensity analysis predominately assesses the pulsatile components of afterload, in particular wave reflection[151]. All studies that have performed association testing between PVR and BCW or WRI have shown there is no relationship between these measures[351, 377, 406]; therefore WRI is described a measure of the components of afterload that are distinctly separate to PVR[151].

Quail et al demonstrated that the characteristic "notched" flow pattern seen in CTEPH[353], discussed in 6.1.2 page 196, occurs when BCW intensity exceeds FCW intensity[351]. In the investigation presented in this chapter, there were moderate to strong associations between the time to peak BCW and PAAT in the operative and non-operative vessels. In the operative PA, the strong association between PAAT/ET and WRI suggests both indices change with increased wave reflection. The weak association observed in the non-operative PA, however, may be due to lower WRI in that vessel. As PAAT and therefore PAAT/ET are measured from the time to peak flow, they will still be measured even if there is not a significant BCW, as such PAAT/ET may only be reduced and associated with WRI in the presence of a BCW. This is also suggested in the individual time point associations, the only associations between PAAT/ET and WRI occurs on POD2 in the operative PA, when WRI is highest.

There were no associations between WRI and PA distensibility. Similar to PVR, PA distensibility may represent a component of afterload distinctly separate to wave reflection, namely the compliance of vessels. No other study has compared PA distensibility and WRI.

8.3.3 Associations between indices of afterload and cardiac output distribution

As demonstrated in Chapter 6, the non-operative PA percentage.CO increases post-operatively. Whilst there is an obvious physiological requirement for an increase in CO distribution to the now larger (relative to operative) non-operative

lung, the factors that dictate this change in flow highlight the impact of post-operative changes in the pulmonary arterial afterload.

Boumpouli et al performed a computational model study of the factors that affect the distribution of blood flow at the bifurcation of the MPA[398], discussed further in 7.2.4.6 page 249. Although their study is based on modelling patterns of PA flow following surgical repair of tetralogy of Fallot, the factors affecting distribution of CO are potentially universal. In their model, the percentage of cardiac output that travels in a daughter vessel is decreased when that vessel has a higher outflow pressure (unilateral increase in afterload), a smaller cross-sectional area, a longer distance to subsequent bifurcation or a higher angle of take-off from the MPA compared to the other daughter vessel. Following lung resection, increases in indices of pulsatile afterload in the operative PA are consistently associated with the increase of the percentage.CO in the contralateral non-operative PA, similar to the model by Boumpouli et al. Of note, their model only simulates non-pulsatile flow, therefore does not take into account either the magnitude or timing of wave reflection[398]. As demonstrated in Table 8-6, in this current study, there were moderate to strong negative associations between the changes in distance to and timing of wave reflection and non-operative percentage.CO. It is therefore argued that the change in distribution of CO following lung resection is secondary to increased pulsatile afterload, from a proximal reflection site, in the operative PA.

The only prior consistent evidence of increased afterload following lung resection can be found in longer term follow-up (4 years) and exercise studies which reveal increases in PVR and MPAP[49, 67, 68]. Following lung resection, the non-operative PA may be able to accommodate this increase in blood flow at rest and therefore MPAP and PVR do not change. This ability may reduce over time or be insufficient with increased cardiac output during exercise. In the investigation presented here, there is evidence of both situations[kkk]. On POD2 there is an increase in overall CO from pre-op (21%), with a greater relative increase in non-operative PA

[kkk] The association between increased operative PA pulsatile afterload and increased non-operative PA percentage.CO is interpreted as the increased operative PA pulsatile afterload diverts blood flow through the non-operative PA, as per Boumpouli et al. whereas the association between increased non-operative PA pulsatile afterload and increased non-operative PA percentage.CO is interpreted as the increased blood flow results in increased non-operative PA pulsatile afterload, as the non-operative PA is unable to accommodate the increased blood flow.

CO (67%), and there is a reduction in PAAT/ET in the non-operative PA. At 2-months the overall CO is similar to pre-op although non-operative PA WRI is increased with increased non-operative PA percentage.CO. Pulsatile afterload may therefore increase in the non-operative PA over time and on exercise following lung resection.

Although MPA WIA could not be performed, there is evidence of increased wave reflection in the MPA in the setting of increased CO on POD2. The strong negative association between increased non-operative percentage.CO and main PAAT/ET suggests that an increase in operative PA pulsatile afterload results in wave reflection in the MPA (shortened PAAT/ET in the MPA). There are similar within-subject associations between main PAAT/ET and the changes in operative PA; WRI ($r=-0.614$, $p=0.003$), distance to reflection site ($r=0.616$, $p=0.003$) and time to peak BCW ($r=0.582$, $p=0.006$, all ANCOVA with patient as factor) between pre-op and POD2. None of these associations is present between pre-op and 2-months. Similar to the associations between RVEF, BNP and non-operative indices of afterload between pre-op and POD2, 6.6.2 page 222, this may be a purely peri-operative relationship or it may persist post-operatively were the patient challenged by an increase in CO.

8.3.4 Associations between indices of afterload and right ventricular function

8.3.4.1 Forward compression wave

The FCW is generated by RV contraction. Quail et al show that FCW area is associated with RVEF ($r=0.65$, $p=0.002$) although they do not describe if the association is in their control group, patients with pulmonary hypertension or both groups combined[351]. Other studies have failed to replicate this finding. In a paediatric population, Schafer et al found no association between peak FCW and RVEF[377] whilst Su et al did not find any association between FCW (area or peak) and RV fractional area change[405, 406]. Operative and non-operative within-subject associations are in opposing directions, decreased RVEF is associated with increased FCW area in the non-operative PA but it is associated with decreased FCW area in the operative PA. This may be due to the uneven distribution of CO following lung resection, discussed below.

8.3.4.2 Wave reflection index

Previous studies investigating increased afterload following lung resection have measured PA pressures and/or PVR in the MPA, failing to show any increase at rest following resection[48, 49, 58-69]. These indices are incomplete measures of afterload and not only overlook the pulsatile components of afterload[103] but may fail to detect a unilateral increase in afterload[398]. WIA overcomes both of these issues by assessment of pulsatile afterload (WRI) in the operative and non-operative PAs. In all of the WIA studies in the pulmonary system, detailed in 7.2.5 page 250, there is a shared hypothesis that an increase in wave reflection (measured by BCW area or WRI) is responsible for impaired RV function. Only Schafer et al have shown an association between BCW and RVEF ($r=0.41$, $p=0.017$)[377], neither Quail et al[351] or Su et al[405, 406] replicated this finding. In the current study, there was a within-subject association between the change in operative PA WRI and the change in RVEF between pre-op and POD2, suggesting that increased WRI impairs RVEF at this time point, although there was no association between the parameters between pre-op and 2-months.

The consistent positive within-subject associations observed between the change in RV strain and the change in WRI between pre-op and 2-months suggest that increased WRI results in impaired RV strain. Interestingly, the associations are stronger for non-operative PA than for operative PA suggesting that it is an increase in pulsatile afterload in the non-operative PA, rather than the operative PA, that is associated in the development of impaired RV strain by 2-months. This is similar to the within-subject associations between the change in non-operative pulsatile afterload (PAAT/ET and distensibility) and the change in RVEF and BNP between pre-op and POD2, see 6.4.5 page 210.

8.3.4.3 Cardiac output distribution

The opposing within-subject associations between the change in RV function and changes in FCW area in the operative and non-operative PAs seem counter-intuitive, as a decrease in RVEF is associated with both an increase and a decrease in FCW area in the non-operative and operative PA respectively. Additionally, the associations between indices of non-operative pulsatile afterload and RV function initially appear contrary to the hypothesised relationship between an increase in

pulsatile afterload in the operative and a decrease in RV function detailed in 8.1.2. Both of these patterns can be explained by the post-operative change in distribution of CO between the operative and non-operative PAs. Similar to the change in cardiac output distribution, the percentage of the total FCW travelling in the non-operative PA increases post-operatively. The increases in the two indices are strongly associated ($r=0.765$, $p<0.001$, between all-time points, ANCOVA with patient as factor) and are mathematically linked, the FCW is calculated from the change in blood flow. Within-subject association testing reveals that there are moderate to strong associations between an increase in the non-operative PA percentage.CO and impairment of RV function post-operatively.

This comparison reveals the potential mechanisms of reduced RVEF following lung resection demonstrated by McCall et al[232] and detailed in Chapter 4. The consistent within-subject associations between the change in RVEF and the increase in pulsatile afterload in both the operative PA (WRI, distensibility), the non-operative PA (PAAT/ET and distensibility) and the increase in non-operative PA percentage.CO between pre-op and POD2 imply that the POD2 reduction in RVEF is predominately caused by an increase in pulsatile afterload.

The reduction at 2-months is strongly associated with the increase in non-operative PA percentage.CO which in turn is associated with operative PA pulsatile afterload. Whilst, unlike the reduction in RVEF between pre-op and POD2, there are no associations between the change in indices of operative PA pulsatile afterload and the change in RVEF between pre-op and 2-months this may be secondary to the overall decrease in and change in distribution of CO. At 2-months the operative PA shows a relatively modest increase in pulsatile afterload but a reduction in percentage.CO. Compared to POD2, there is lower operative PA wave reflection (increased PAAT/ET and reduced WRI) at 2-months although there is no change in the absolute value of cardiac output travelling in the operative PA. At a lower CO the redistribution of CO through the non-operative PA may mask the true increase in operative PA pulsatile afterload by conventional indices. As described by the concept of reduced PVreserve, detailed in 1.2.6.2 page 71, an increase in CO (similar to POD2) may unmask a further rapid increase in operative PA afterload which may then be associated with a reduction in RVEF.

The reduction in RVGLS at 2months may also contribute to reduced RVEF. As demonstrated in Chapter 5, RVGLS.S decreases on POD2 whereas there is a delayed reduction in RVGLS and RVGLS.FW at 2-months. Between pre-op and 2-months there were moderate to strong positive within-subject associations between the change in non-operative PA WRI and the impairment of RVGLS and RVGLS.FW. There were similar associations between the increase in non-operative PA percentage.CO and impairment of RVGLS, RVGLS.FW and RVGLS.S. These associations suggest that the reduction in RV strain between pre-op and 2-months is caused by a chronic increase in both operative and non-operative pulsatile afterload. Individual time point association testing between RVGLS and WRI reveal a potential mechanism for the lack of change on POD2 and the delayed reduction, Figure 8-10. On POD2 there is a moderate *negative* association between RVGLS and WRI in the operative PA, increased WRI is associated with improved strain. At 2-months, however, there are moderate to strong *positive* associations between WRI and RVGLS in the operative and non-operative PAs, increased WRI is associated with impaired strain. This implies that on POD2, the RV is able to increase RVGLS to compensate for increased pulsatile afterload, i.e. it maintains coupling, however by 2-months this process is exhausted and the RV is no longer able to compensate for the chronic increase in pulsatile afterload, particularly if the non-operative PA is unable to accommodate the increased CO.

The changes in RVGLS secondary to increased pulsatile afterload may also contribute to the reduction in RVEF by 2-months. There is moderate negative within-subject association testing between change in RVEF and change in RVGLS.S ($r=-0.462$, $p=0.040$, ANCOVA with patient as factor) whilst the change in RVGLS approaches significance ($r=-0.425$, $p=0.062$, ANCOVA with patient as factor).

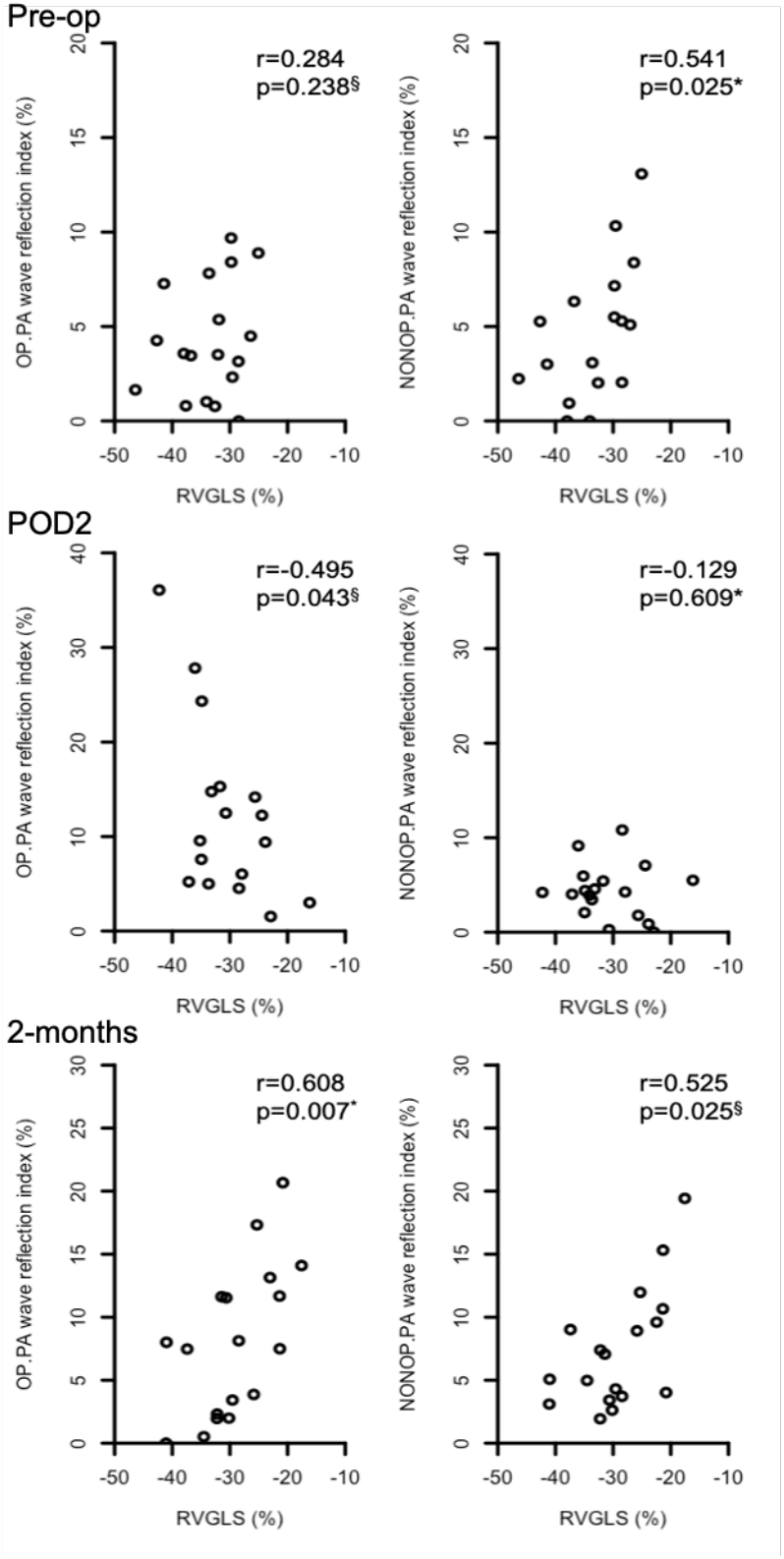

Figure 8-10 Association between right ventricular global longitudinal strain and wave reflection index at individual time points

Pre-operative (top row), post-operative day 2 (POD2, middle row) and 2-months post-operative (bottom row) individual time point association plots between wave reflection index (WRI) and right ventricular global longitudinal strain (RVGLS) in the operative PA (OP.PA, left column) and non-operative PA (NONOP.PA, right column). Note positive associations pre-operatively in the non-operative PA and in both the operative and non-operative PAs at 2-months, however on POD2 there was a moderate negative association between RVGLS and operative PA WRI. WRI is associated with impaired strain pre-operatively and at 2-months post-operatively whereas it is associated with increased strain at POD2. *= Pearson's correlation co-efficient. §= Spearman's correlation co-efficient.

8.4 Conclusion

This investigation demonstrates, for the first time, that an increase in afterload following lung resection is associated with impaired RV function. A post-operative increase in pulsatile afterload in the operative PA results in an increased percentage.CO being diverted through the non-operative PA. This increase is associated with reduced RVEF and impaired RVGLS/RVGLS.FW. Additionally, by 2-months an increase in non-operative pulsatile afterload secondary to the increased percentage.CO appears to lead to the development of impaired RVGLS.

Chapter 9 Major Findings, Conclusions and Future Directions

This thesis investigates the mechanisms of RV dysfunction following lung resection by assessing RV strain and afterload. The major findings of each chapter are detailed below.

9.1 Chapter summaries and major findings

9.1.1 Chapter 5

This chapter details the methodology of strain assessment of RV function and its investigation following lung resection. Global RV longitudinal strain (RVGLS) is unchanged at POD2 but reduced at 2-months following lung resection. Septal RVGLS is reduced at post-operative day 2 (POD2) whereas free wall RVGLS has a delayed reduction at 2-months. At both post-operative time points impaired free wall RVGLS was associated with reduced RVEF.

9.1.2 Chapter 6

This investigation demonstrates, for the first time, an increase in pulsatile afterload following lung resection. Rate corrected pulmonary artery acceleration time (PAAT/ET) and PA distensibility are both increased in the pulmonary artery (PA) supplying the resected lung (operative PA). The distribution of cardiac output (CO) between the PAs is altered post-operatively with an increase in the percentage travelling in the non-operative PA. Whilst there is only a modest shortening of PAAT/ET in the non-operative PA it is the indices of afterload in the non-operative PA that are associated with the reduction in RVEF and increase in BNP on POD2. The altered distribution of cardiac output is hypothesised as a potential mechanism for the decrease in pulmonary vascular reserve (PVreserve) following lung resection, demonstrated in previous studies and explored further in Chapter 8.

9.1.3 Chapter 7

The first use of wave intensity analysis in a lung resection population is described in this chapter. It is a method of combining the changes in PA flow and cross-

sectional area to measure the rate of transport of wave energy in the PAs allowing assessment of the magnitude, timing and direction of wave travel in the PAs. These waves can be classified by the direction of travel as either forwards (away from the heart) or backwards (reflected towards the heart) and by the effect of blood flow as either compression (increase flow of blood in direction of travel) or expansion (decreases flow of blood in direction of travel). An increase in the percentage of the forward compression wave that is reflected as a backward compression wave (wave reflection index) is a marker of increased pulsatile afterload. Similar to the distribution of CO, there was a post-operative increase in the forward compression wave energy in the non-operative PA and a decrease in the operative PA. Further evidence of a post-operative increase in pulsatile afterload was provided by the increase in operative PA wave reflection index on POD2 and at 2-months. The time to peak backward compression wave was reduced in the operative PA post-operatively, suggesting the presence of early wave reflection.

9.1.4 Chapter 8

Comparisons between the conventional measures of pulsatile afterload (PAAT/ET and PA distensibility), findings of wave intensity analysis and RV function (RVEF and RV strain) demonstrate, for the first time, consistent associations between a post-operative increase in afterload and impaired RV function following lung resection.

Post-operatively the increase in pulsatile afterload and the reduction in time to peak wave reflection in the operative PA are consistently associated with the increase in the percentage of cardiac output travelling in the non-operative PA. On POD2, the reduction in RVEF is consistently associated with the altered distribution of cardiac output and the increased afterload in both the operative and non-operative PAs. At 2-months, the reduction in RVEF is strongly associated with the altered distribution of cardiac output and the reduction in time to peak wave reflection in the operative PA. The delayed reduction in RVGLS is consistently associated with the increase in wave reflection (particularly in the non-operative PA) and the altered distribution of cardiac output.

A summary of the main findings in this thesis are presented in Figure 9-1.

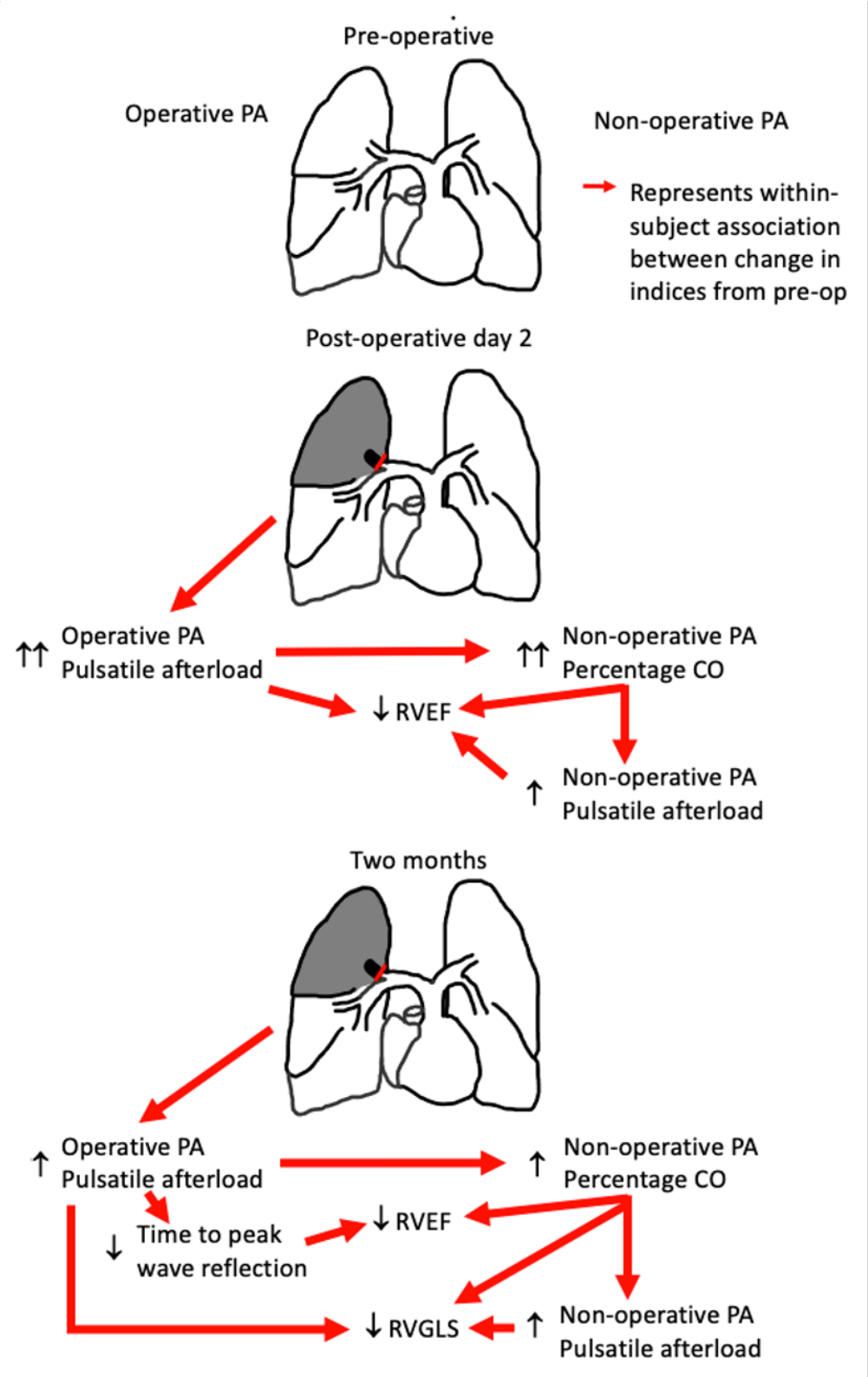

Figure 9-1 Summary of the changes in and within-subject associations between indices of right ventricular afterload and function following lung resection.
Representative example of the changes in right ventricular (RV) afterload and function following lung resection, right upper lobectomy in this example (shaded area) and ligation corresponding pulmonary artery (PA, red line) in the operative PA (left side) with the anatomy of the non-operative PA unchanged (right side). Red arrows represent the within-subject associations between the change in indices between pre-op and the time-point of testing ($p<0.05$). Change in percentage cardiac output (CO) in the non-operative PA displayed on left side. ↑= increase compared to pre-operative, ↑↑= increase compared to pre-operative and 2-months. ↓= decrease compared to pre-operative, ↓↓= decrease compared to pre-operative and 2-months. RVEF= RV ejection fraction. RVGLS= RV global longitudinal strain. Images created by the author.

9.2 Interpretation

Lung resection is a relatively unique insult to the pulmonary vasculature as it is a predominately unilateral insult, as such the conventional approaches to measure RV afterload do not detect the significant changes in afterload that occur. As multiple previous studies have shown, there is no change in PAP or PVR in the immediate post-operative period although they increase over time and on exercise. These measures assess the resistance of the distal pulmonary vasculature and therefore overlook the marked changes in the proximal pulmonary arteries. Assessment of the pulsatile components of afterload reveals the widely hypothesised link between increase afterload and impaired RV function following lung resection. These results must however be interpreted relative to both the overall cardiac output and the distribution of cardiac output at that time.

It is hypothesised that the increase in operative pulsatile afterload and reduction in time to peak wave reflection diverts cardiac output through the non-operative PA, overwhelming the non-operative PA ultimately impairing RV function. This is supported by the consistent associations; between operative PA pulsatile afterload and the time to peak wave reflection and non-operative PA cardiac output, between altered distribution of cardiac output and impaired RV function (RVEF and RVGLS) and between non-operative PA pulsatile afterload and impaired RVGLS.

On POD2 the overall cardiac output is increased from pre-op and the distribution of cardiac output is also altered with 66% of the overall cardiac output traveling in the non-operative PA. Of note, the absolute value of cardiac output in the operative PA is decreased post-operatively potentially secondary to increased pulsatile afterload. On POD2 the non-operative PA is therefore required to accommodate a 67% relative increase in cardiac output (overall increase is 21%) and there is a modest increase in non-operative PA pulsatile afterload (PAAT/ET). The observed reduction in RVEF on POD2 is associated with increased pulsatile afterload in both the operative and non-operative PAs, and the altered distribution of CO. Additionally, the peri-operative increase in BNP observed on POD2 is strongly associated with the increase in non-operative PA pulsatile afterload. The POD2 reduction in RVEF and increase in BNP are therefore hypothesised to be caused by increased pulsatile afterload with the inability of

the non-operative PA to accommodate the increased cardiac output driving the reduction in RV function.

At 2-months overall cardiac output has returned to baseline although the absolute operative PA cardiac output is unchanged from POD2 and there is a 39% to 61% split between the operative and non-operative PAs. There remains an increase in indices of pulsatile afterload in the operative PA compared to pre-op, although to a lesser degree than on POD2, and there is no change in pulsatile afterload in the non-operative PA compared to pre-op. The delayed reduction in RVGLS that occurs at 2-months, demonstrated in Chapter 5, is strongly associated with increased pulsatile afterload in the non-operative PA and moderately associated with the increase in non-operative PA percentage of cardiac output. It is therefore argued that the observed reduction in RVGLS is secondary to a chronic increase in pulsatile afterload, again it appears that it is the inability of the non-operative PA to accommodate the increased cardiac output that drives to the reduction in RV function.

It is notable that there is no association between operative PA pulsatile afterload and RVEF at 2-months. This may, however, be masked by the redistribution of cardiac output to the non-operative PA. The measures of pulsatile afterload in the operative PA may be an underestimation as blood preferentially travels in the non-operative PA and they may rapidly increase with an increase in cardiac output, similar to on POD2. As hypothesised in Chapter 6 the altered distribution of cardiac output may be the underlying mechanism of the decrease in pulmonary vascular reserve seen following lung resection. Ultimately, the altered distribution of cardiac output that contributes to the reduction in RVEF is deemed secondary to increase in operative PA pulsatile afterload and the earlier wave reflection.

9.3 Future work

The design and successful funding of two studies further investigating the mechanism of RV dysfunction following lung resection are detailed below.

9.3.1 Right ventricular contractile reserve following lung resection

As detailed in 1.2.6.2 page 71, the rate of increase MPAP on exercise is greater following lung resection than pre-operatively, i.e. there is decreased pulmonary vascular reserve (PVreserve). A potential pathophysiological mechanism, proposed in 6.6.2.1 page 223, is suggested by the post-operative increase in pulsatile afterload and reduction of the percentage of the cardiac output in the operative PA. Whilst the non-operative pulmonary vasculature is anatomically unchanged the blood flow through it is greatly increased. On exercise both the operative and non-operative PA may be unable to accommodate the increase in cardiac output, as such RV function may be further impaired.

Similar to PVreserve, RV contractile reserve (RVCreserve) can be assessed by the change in RVEF on exercise. Claessen et al demonstrated that in healthy subjects RVEF will increase on exercise (a normal RVCreserve) whereas in CTEPH the RV is unable to increase RVEF in response to exercise[120]. As detailed in 2.3.1.2 page 87, there is evidence for a reduction in RVCreserve following lung resection demonstrated in the studies by Okada et al[48, 49] although the reliability of this results must be questioned as RVEF is estimated by a volumetric pulmonary artery catheter.

The design of a pilot feasibility study to echocardiographically assess RVCreserve and PVreserve following lung resection is detailed in Appendix 2. The funding application (Appendix 2a), a letter confirming success in funding (2b), the study protocol (2c) and confirmation of ethical approval (2d) are all provided, this is all original work devised and written by the author of this thesis. This study has finished recruitment and data collection, completion of data analysis is awaited.

9.3.2 Right ventricular inflammation after lung resection

In this thesis evidence is presented that, following lung resection, an increase in afterload is associated with reduction in RVEF, RV strain and an increase in BNP. These associations have subtly different timings and associations between POD2 and 2-months suggesting subtly different pathophysiological mechanisms. On POD2 there are strong associations between the increase in BNP and indices of

pulsatile afterload, particularly in the non-operative PA. This suggests that the acute increase in pulsatile afterload leads to BNP release secondary to myocardial stretch. Additionally, the transient increase in RVGLS strain (reflecting increased contractility) to compensate for increased pulsatile afterload seen on POD2 and the delayed reduction in RVGLS by 2-months, secondary to chronic afterload, suggests that initial compensatory mechanisms become exhausted.

Rat models of pulmonary embolism (analogous lung resection) results in myocardial oedema and scarring in the RV[134, 135, 321], discussed 1.2.3.4 page 55. The study design and results are comparable to lung resection as there is an acute increase in afterload secondary to PA occlusion that results in impaired RV contractility. The myocardial mechanisms of RV dysfunction may therefore be similar following lung resection. BNP and other biomarkers only give a signal that myocardial damage occurs, but it cannot relate it to a specific region of the heart, nor can it explain what happens to the myocardium following the insult. Cardiac magnetic resonance is a rapidly developing field, with intravenous contrast and specific weighting of imaging it is possible to determine the myocardial water content (oedema) and extra-cellular volume (scarring) of regions of the heart. This has predominately been performed in the larger, more muscular LV but collaborators within the University of Glasgow have developed techniques to perform this in the RV[435]. Such imaging could potentially be able to relate RV function, afterload and contractility to oedema and scarring within the RV itself.

The design of the first CMR study to investigation peri-operative RV oedema and scarring is detailed in the successful grant application, included in the Appendix 3, again this is all original work devised and written by the author of this thesis. Finally, the design of the study includes repeating the analysis performed within this thesis in the new cohort, thus the changes in pulsatile afterload, RV strain and RVEF can be compared to the changes in myocardial oedema and scarring. Recruitment is complete and the initial results demonstrate, for the first time, acute oedema (on POD2) with resultant scarring (at 2-months) in the right ventricle following lung resection, further analysis is currently underway to explore the associations between these results and RV function and afterload.

Appendices

Further investigation:

1. Factors affecting the linear segment of the flow-area loop

Future work:

2. Right ventricular contractile reserve following lung resection
    1. Funding application
    2. Confirmation of funding
    3. Study protocol
    4. Ethical approval
3. Right ventricular inflammation after lung resection.
    1. Funding application
    2. Confirmation of funding

Appendix 1 Factors affecting the linear segment of the flow-area loop

This section provides further discussion on the comparison of the two methods of wave speed calculation used in Chapter 7. Discussion focuses on potential causes of the non-linear segments.

Appendix 1.1 Summary of results

The sum of squares (SOS) and flow-area (QA) loop methods results are summarised in Table 7-2 page 277 and repeated in Table Appendix 1 1. It was not possible to perform the QA loop method in 32/136 (23.5%) scans as they had a marked curvature (non-linear segment) in early systole, example shown in Figure 7-25 page 276, repeated here as Figure Appendix 1 1. There was a trend to an increase in non-linear scans in the PAs that had undergone surgical resection (POD2 and 2-months operative PA (14/41 (34.1%)) compared to those that had not undergone resection (non-resected) (18/95, (18.9%)), (p=0.055, Chi-squared test).

Pulmonary artery	Method	Pre-op	POD2	2-months	p-value
Operative	SOS ($m.s^{-1}$)	1.38 (1.28, 1.53)	0.92 (0.73, 1.20) #	0.90 (0.75, 1.06) #	***<0.001 §***
	n	27	20	21	
	QA All ($m.s^{-1}$)	1.63 (1.29, 1.89)	1.14 (0.85, 1.73)	1.09 (0.93, 1.73)	0.056 *§*
	n	27	20	21	
	QA Linear ($m.s^{-1}$)	1.64 (1.34, 1.90)	1.34 (0.87, 1.78)	1.36 (1.03, 1.78)	0.165 *§*
	n	22	13	14	
Non-operative	SOS ($m.s^{-1}$)	1.29 (1.06, 1.76)	1.60 (1.33, 1.97) #	1.26 (1.11, 1.74) ¥	***0.019 §***
	n	25	21	22	
	QA All ($m.s^{-1}$)	1.45 (1.18, 1.88)	1.74 (1.41, 2.15)	1.47 (1.07, 1.85)	0.101 *§*
	n	25	21	22	
	QA Linear ($m.s^{-1}$)	1.40 (1.13, 1.80)	1.66 (1.35, 2.00)	1.38 (0.97, 1.76)	0.067 *§*
	n	22	17	16	

Table Appendix 1 1 Comparison of wave speed by flow-area loop and sum of squares techniques
Values are median (IQR). c= wave speed. $SOS^{=}$ sum of square method. QA loop= flow area loop method. QA Al= all scans including non-linear (n=136). QA linear= QA scans only with linear segment (n=104). All Friedman's test. Comparison between time-points Wilcoxon signed rank test. #= significant difference from pre-op. ¥= significant difference from post-operative day 2 (POD2). Significant results (p<0.05) highlighted ***bold italics.***

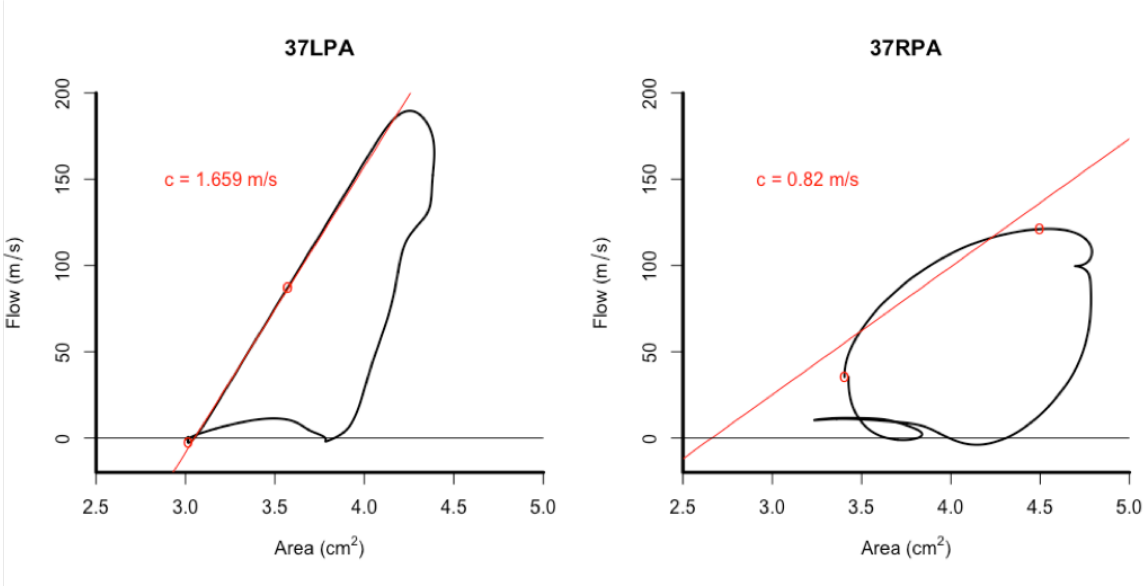

Figure Appendix 1 1 Flow-area loop example
Example of flow – area (QA) loop method of wave speed calculation in left and right pulmonary arteries of same scan (MRIRAN 37, patient from study). Flow was plotted against area for the entire cardiac cycle. Wave speed was calculated from the gradient of the plot in early systole. Red circles represent starting time (time= 0ms) and finishing time (time corresponding with third phase of original imaging) from which wave speed was calculated (red gradient line). Note linear segment in early systole in left panel but curved (non-linear) in right.

Appendix 1.2 Discussion

There is no agreed method to calculate wave speed, particularly in the pulmonary circulation[351]. Three different methods have previously been used; loop methods[351, 377, 431], the sum of squares (SOS)[404-406, 431] and the foot-to-foot method[431]. Within each method, calculation is dependent on the modality used; pulmonary artery catheter (PAC) studies measure pressure and velocity/flow whereas CMR studies measure flow (Q) and area (A). Comparison between the QA methods have been performed in the pulmonary circulation by Quail et al[351] and Weir McCall et al[431]. Quail et al first described the SOS method from QA data and advocated for confining measurement of the QA loop to the first three phases of CMR imaging. They compared the SOS method to the QA loop method and demonstrated minimal bias and good agreement between the measures[351]. Weir-McCall et al performed a more comprehensive comparison between different QA based wave speed calculation (SOS, QA loop from either the entire linear segment or from the first 3 points as per Quail et al[351]) in a healthy volunteer study. They found that the SOS method had improved accuracy and precision compared to the QA loop methods. Of note, the accuracy of all methods were improved with higher temporal resolution[431].

Appendix 1 – Factors affecting the linear segment of the flow-area loop

Wave reflection has been shown to impact wave speed calculation. In the presence of wave reflection, QA based methods tends to underestimate wave speed whereas pressure (P) and velocity (U) based calculations tend to overestimate wave speed[351, 430, 436]. Proximal reflection sites either reduce the duration of, or completely remove the early systolic linear section of the QA or PU loop, from which wave speed is calculated[418]. This may be of particular importance in the pulmonary circulation as the vessels are comparatively short and there are multiple proximal sites of bifurcation compared to the systemic arterial system[404].

Borlotti et al investigated the effect of proximity to a reflection site on the percentage difference between methods of wave speed calculation and the foot-to-foot method (the gold standard) in a bench top simulation using silicone tubing and a piston pump. Compared to the foot-to-foot method, in the setting of a proximal wave reflection, they demonstrated a greater percentage difference in measures using the QA loop than when using the SOS method[lll416]. In the results from this study a similar comparison between the percentage difference between SOS and QA loop methods (100*(SOS-QA)/SOS) demonstrates that the percentage error between the measures increases with increasing proximity of the site of reflection[mmm], but only in the linear scans of the non-resected PAs, Figure Appendix 1 2.

[lll] SOS was calculated from pressure and velocity measurements in this example.

[mmm] Note that the distance to reflection is calculated from the time difference between the FCW and BCW and the wave speed calculated by the SOS method. This measure does not use the QA loop results in its calculation.

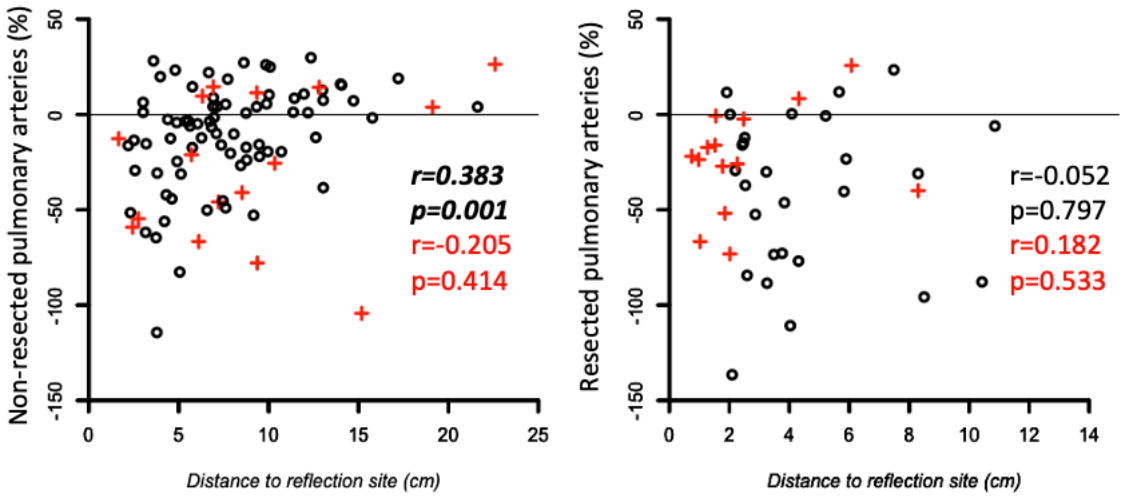

Figure Appendix 1 2 Percentage difference between wave speed calculation methods and distance to reflection site
Percentage difference between wave speed calculation by sum of squares (SOS) and flow – area (QA) loop (100*(SOS-QA)/SOS) plotted against distance to apparent reflection site. Circles represent scans with linear early systolic segments for QA calculation, red + represent the scans with non-linear early systolic segments. All tests Spearman's correlation co-efficient with linear results in black (upper result) and non-linear result in red (lower result). Significant result highlighted in ***bold italics.***
Left plot represents non-resected pulmonary arteries (operative pulmonary artery before surgery (22 linear and 5 non-linear scans) and non-operative pulmonary artery at all time points (55 linear and 13 non-linear scans). Note the increasing percentage difference (QA>SOS) between methods with reducing distance to site of reflection in the linear non-resected scans.
Right plot represents resected pulmonary arteries (post-operative operative PA scans (27 linear and 14 non-linear scans)). No association between distance to reflection site and percentage difference.
Non-linear scans are similar to the linear scans in non-resected pulmonary arteries (left plot). In the resected pulmonary arteries, the non-linear scans predominately have a shorter distance to reflection site than the linear scans (right plot).

If the proximity to the apparent site of reflection site is the major driver of curvature in the early systolic segment then it would be expected to predominately occur in the scans with a proximal reflection. Although a reduced distance to reflection site decreases the agreement between the SOS and QA loop methods in the non-resected PAs it does not seem to influence the linearity of the early systolic segment. In the resected PAs, however, the majority of the non-linear scans occurred in PAs with a shorter distance to the reflection site, Figure Appendix 1 2 and Table Appendix 1 2.

In the resected PAs, the vessels with a non-linear segment have a shorter distance to reflection site, pulmonary artery acceleration time (PAAT), time to peak BCW and time to onset BCW, Table Appendix 1 2. There is no difference in any of these factors between the linear and the non-linear scans in the non-resected PAs although the non-linear vessels have a larger WRI compared to the linear vessels.

Similar to Figure Appendix 1 2, this suggests that separate mechanisms are responsible for the non-linear QA loops in the resected and non-resected PAs.

Measure	Pulmonary arteries	Linear	Non-linear	p-value (linear vs non-linear)
WRI (%)	Resected n=41	7.5 (3.2, 11.3) n=27	12.4 (6.6, 15.0) n=14	0.081
	Non-resected n=95	4.3 (2.3, 7.2) n=77	7.8 (3.9, 12. 3) n=18	***0.045***
Distance to reflection site (cm)	Resected	3.76 (2.53, 5.74)	1.81 (1.34, 2.43)	***0.002***
	Non-resected	7.09 (4.89, 9.89) ‡	7.87 (5.82, 10.97) ‡	0.540
PAAT (ms)	Resected	135.1 (118.1, 158.6)	102.0 (86.0, 116.5)	***0.001***
	Non-resected	152.1 (27.9) ‡	146.1 (26.9) ‡	0.073
Time to peak BCW (ms)	Resected	158.0 (142.1, 171.6)	91.5 (85.5, 113.1)	***<0.001***
	Non-resected	189.2 (48.2) ‡	180.7 (57.6) ‡	0.571
Onset of BCW (ms)	Resected	94.0 (79.0, 105.0)	53.5 (44.3, 61.8)	***0.003***
	Non-resected	111.8 (90.0, 130.1) ‡	110.9 (75.3, 140.8) ‡	0.936
Time of 3rd phase (ms)	Resected	80.9 (13.4)	77.2 (8.8)	0.288
	Non-resected	85.8 (15.7)	83.6 (13.0)	0.555
PAAT - 3rd phase (ms)	Resected	52.0 (42.8, 67.3)	23.3 (16.8, 28.9)	***0.001***
	Non-resected	68.4 (17.8) ‡	57.9 (24.2) ‡	0.107
Time to peak BCW - 3rd phase (ms)	Resected	73.8 (61.1, 95.6)	14.1 (7.8, 30.7)	***<0.001***
	Non-resected	103.4 (44.2) ‡	100.2 (57.6) ‡	0.834
Onset of BCW - 3rd phase (ms)	Resected	12.8 (-2.1, 23.3)	-26.6 (-36.6, -13.8)	***0.002***
	Non-resected	27.7 (4.9, 48.5)	40.7 (-13.9, 58.4) ‡	0.498

Table Appendix 1 2 Comparison of the difference in afterload and timing parameters for flow – area loop with and without a linear segment
WRI= wave reflection index. PAAT= pulmonary artery acceleration time. BCW= backward compression wave. Time of 3rd phase= the final time that wave speed was calculated from, NB it is one tenth of the duration of the cardiac cycle and so is also representative of difference in heart rate between groups. ‡= significantly different to resected pulmonary artery**.** Significant results ($p<0.05$) highlighted in ***bold italics.***

Calculation of wave speed from the QA loop must be performed prior to wave reflection[351, 431]. In the study presented, the QA loop method was performed on the data from the first 3 time points of the cardiac cycle, similar to Quail et al[351].

Appendix 1 – Factors affecting the linear segment of the flow-area loop

The time to the 3rd phase (and therefore heart rate[nnn]) is similar between the linear and non-linear scans and between the resected and non-resected PAs. The time difference from the time of the 3rd phase to PAAT, to the time to peak BCW and to the time to onset BCW are all lower in the non-linear resected PAs than all other vessels. Additionally, the median difference between the time of the 3rd phase to the onset of the BCW is negative. This demonstrates that the onset of the BCW and therefore wave reflection occurs prior to the 3rd phase thus the non-linear section of the QA loop contains wave reflection in the resected PAs.

Quail et al were able to calculate wave speed by the QA loop method from all scans. This is potentially due to the difference in temporal resolution of the CMR imaging between studies. They achieved a temporal resolution of 10.5ms and the QA loop was measured during the first 31.5ms of the cardiac cycle, prior to the time to peak BCW (76ms) and PAAT (67ms)[351]. Similarly, Weir-McCall et al achieved a temporal resolution of 7-12ms in their study comparing methods of wave speed calculation during a 4-minute free breathing sequence[431]. Whilst the accuracy of all methods improved with a higher temporal resolution the SOS method had superior intra- and inter-observer reproducibility than QA loop methods throughout[431]. A greater temporal resolution may detect the presence of a linear segment of the QA loop in a greater percentage of the resected PAs.

In the non-resected PAs, the only significant difference between the linear and non-linear QA loops is an increase in WRI in the non-linear vessels. The timing of the reflected wave is not different between groups and as such a greater temporal resolution may be of limited benefit. An alternative explanation for the non-linear QA loops in the non-resected PAs may be subtle motion or reporting artefacts. As discussed in Chapters 6 and 7 there appears to be a continuum between marked to minor diastolic motion artefacts. This has also been reported by other authors in pulmonary artery CMR studies[351, 358, 431]. WIA studies performed with a PAC measure PA pressure instead of area and therefore do not have the potential motion and reporting artefacts, also they have a greater temporal resolution than CMR (5ms)[404]. In a PAC study, Su et al however found that "many" of the patients

[nnn] On CMR imaging the cardiac cycle is divided into 30 phases irrespective of heart rate. The 3rd phase is therefore equal to 1/10th of the duration of the cardiac cycle and heart rate is equitable to 6/(time to 3rd phase (in seconds)).

in their pulmonary WIA study did not have a linear segment[404-406]. Instead, they relied on the SOS method (with pressure and velocity) to calculate wave speed. A non-linear segment may therefore be present irrespective of modality.

Finally, the foot-to-foot method has be utilised in the pulmonary circulation to measure wave speed between the MPA and RPA/LPA. This approach assumes a constant wave speed from the measurement point in the MPA to the measurement point in the RPA and LPA however, the calculated wave speed was lower in the RPA than the LPA[431]. Whilst it is feasible to perform CMR imaging at two separate points in the RPA/LPA, the short distance between the points could introduce significant error in wave speed calculation and would also double the required scan time for that component of analysis.

Appendix 1.3 Conclusion

The cause(s) of a non-linear segment in early systole are likely multifactorial and different in resected and non-resected PAs. In the resected PAs, the non-linear segments are caused by a proximal site of wave reflection that results in the early arrival of a BCW. In the non-resected PAs, the non-linear scans have a greater WRI although there is no difference in the timing of wave reflection between linear and non-linear QA loops. In the pulmonary circulation the presence of non-linear segments in loop-based wave speed calculation may occur irrespective of the method of assessment, therefore the SOS method is potentially superior.

Appendix 2 Right ventricular contractile reserve following lung resection

Appendix 2.1 Funding application

The Royal College of Anaesthetists
Small Grant Awards 2016

RCoA Reference Number (CRN):
Type of grant/fund applied for: **Ernest Leach Research Fund☒ Sargant Fund☐ Belfast Fund☐**
Name of principal applicant: Adam Glass
Correspondence address and contact number: Department of Cardiothoracic Anaesthesia and Critical Care Golden Jubilee National Hospital Agamemnon Street Clydebank G81 4DY Mobile -
Email address:
Title of project: Assessment of RV contractile reserve on exercise following lung resection – a pilot study

The Royal College of Anaesthetists
Small Grant Awards 2016

A description and justification of the proposed project (not more than 500 words):

Explanatory Notes
Please note that applications for research, travel and education grants will be assessed against three criteria:

1. *Appropriateness and importance at local, national and international level*
2. *Methodology*
3. *Timescale and justification of funding*

Please refer to the more detailed breakdown on the NIAA website: Small Grant Assessment Criteria

Introduction

Lung cancer is the leading cause of cancer death in the UK. Surgical resection offers the best chance of cure; rates are increasing with older and sicker patients now undergoing resection. Unfortunately, morbidity following lung resection remains high. Many patients experience long term dyspnoea and decreased functional capacity, this is poorly associated with the change in lung function[1] and may be influenced by cardiac limitation[2].

Background

Our group has previously investigated changes in cardiac function at rest following lobectomy with echocardiography and cardiac magnetic resonance (CMR) imaging, demonstrating decreased right ventricular ejection fraction (RVEF) but unchanged left ventricular ejection fraction following surgery[3] (Figure 1). Delta RVEF (POD2 from pre-op) was associated with potential cardiac inflammation (delta BNP, r=0.47, p=0.03).

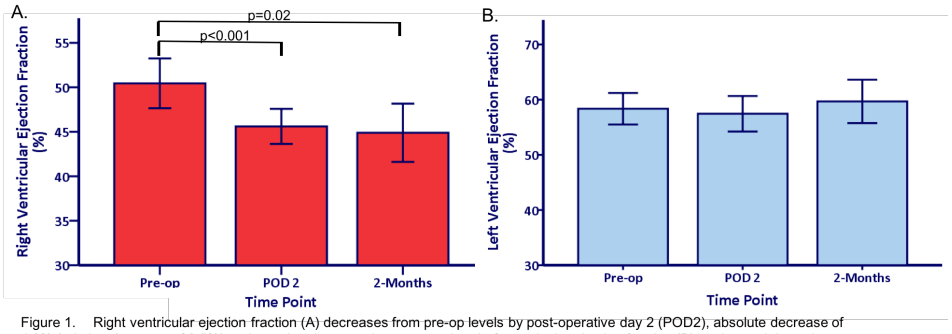

Figure 1. Right ventricular ejection fraction (A) decreases from pre-op levels by post-operative day 2 (POD2), absolute decrease of 4.2% (relative decrease of 8.5%) and remains decreased at two months. Left ventricular ejection fraction (B) unchanged throughout study. Error bars 95% confidence intervals. All paired t-tests.

Although long recognised as a potential cause of decreased exercise capacity following lung resection, RV function on exercise has undergone very little investigation. Using volumetric pulmonary artery catheters to measure RVEF (a technique the accuracy of which has since been challenged[4]), Okada et al showed that three weeks following lobectomy RVEF was decreased at rest and further decreased on exercise in parallel with a marked increase in pulmonary artery pressure and pulmonary vascular resistance. Echocardiographic assessment of RV function is challenging due to its complex shape and retrosternal position but surrogate markers of tricuspid annular plane systolic excursion (TAPSE), tricuspid S wave velocity and RV longitudinal strain (RVLS) have all been shown to associate with RVEF measured by CMR[6]. In our previous study TAPSE correlated best with RVEF (r=0.35, p<0.01) but showed no significant change between time points.

In pulmonary hypertension, the concept of RV contractile reserve is increasingly recognised as an important determinant of exercise capacity and outcome[6]. We hypothesise that following lung resection patients may exhibit similar physiology. The subtle changes in RVEF we have previously observed at rest may manifest as reduced RV contractile reserve on exercise in the face of well documented afterload increase.

Methodology

Appendix 2.1 - Right ventricular contractile reserve following lung resection, Funding application

The Royal College of Anaesthetists
Small Grant Awards 2016

Aims
Primary endpoint

- RV contractile reserve measured as the change in RV function (delta TAPSE) on exercise relative to rest determined pre and 2-months post-operatively.

Secondary endpoints

- Change in contractility (delta RVLS) on exercise.
- Change in afterload (est. pulmonary artery pressure and acceleration time) on exercise.
- Change in markers of cardiac inflammation (BNP, CK-MB, troponin and myoglobin).

Study design
Pilot observational cohort study of patients undergoing video-assisted thoracoscopic lobectomy. With informed consent and ethical approval, five patients will undergo exercise echocardiography pre-operatively and two months post-operatively. The echocardiography protocol will assess RV and LV function, afterload and contractility at rest and on a fixed workload at submaximal exercise.

Timescale and funding justification

Grant funds will cover the echocardiography scanning and blood samples analysis costs. A draft protocol has been prepared and we aim to complete the study in nine months from funding decision.

This study will help inform a larger clinical study examining the functional impact of post-operative RV dysfunction. Ameliorating perioperative RV injury may be a novel therapeutic target and lead to improved patient outcomes following lung resection.

References

1. Pelletier, C., L. Lapointe, and P. LeBlanc, *Effects of lung resection on pulmonary function and exercise capacity.* Thorax, 1990. **45**(7): p. 497-502.
2. Nugent, A.M., et al., *Effect of thoracotomy and lung resection on exercise capacity in patients with lung cancer.* Thorax, 1999. **54**(4): p. 334-8.
3. McCall, P., et al., *The right ventricular response to lung resection.* J Cardiothorac Vasc Anesth, 2016. **30**(supp 1): p. S23-S24.
4. Okada, M., et al., *Right ventricular dysfunction after major pulmonary resection.* J Thorac Cardiovasc Surg, 1994. **108**(3): p. 503-11.
5. 5.Leibowitz, A.B., *Pulmonary artery catheter determined right ventricular ejection fraction and right ventricular end-diastolic volume: another case of "The Emperor Has No Clothes".* Crit Care Med, 2009. **37**(11): p. 2992.
6. Focardi, M., et al., *Traditional and innovative echocardiographic parameters for the analysis of right ventricular performance in comparison with cardiac magnetic resonance.* Eur Heart J Cardiovasc Imaging, 2015. **16**(1): p. 47-52.
7. Sharma, T., et al., *Dobutamine stress for evaluation of right ventricular reserve in pulmonary arterial hypertension.* Eur Respir J, 2015. **45**(3): p. 700-8.

The Royal College of Anaesthetists
Small Grant Awards 2016

Detailed breakdown of costs:

Exercise echocardiography (£150) x 2 visits x 5 patients = £1500

Exercise echocardiography will be performed by band 7, British Society of Echocardiography accredited cardiac physiologists according to a standardised protocol and will be dual reported post processing by blinded observers using *EchoPAC* software.

Cardiac biomarkers (£470 for 25 tests), 5 tests x 5 patients = £470

Alere Triage ProfilER SOB Panel – Testing pre-operatively, post-operatively, POD1, POD2 and 2 months.

Total = £1970

Patient recruitment, sampling, data collection and analysis will be performed by a full time Clinical Anaesthetics Research Fellow (applicant), salaried by the University of Glasgow until August 2017.

Details of other funding that has been applied for or received from other sources:

Nil

Proposed starting date and duration of project: Commencement of study on award with duration of 9 months.

Applicant signature:

Date:

How to apply

Please attach an electronic copy of your curriculum vitae to this form and submit both documents as a SINGLE pdf file using the document upload box on the NIAA website here.

A signed copy should also be sent to: Pamela Hines, NIAA Coordinator, Royal College of Anaesthetists, Churchill House, 35 Red Lion Square, London, WC1R 4SG.

The deadline for all applications is 5.00 pm on Friday, 2 September 2016.

Appendix 2.2 Confirmation of funding

NIAA
National Institute of Academic Anaesthesia

Chairman
Professor Monty Mython

Churchill House
35 Red Lion Square
London WC1R 4SG
tel 020 7092 1680 **fax** 020 7092 1730
email info@niaa.org.uk

Dr Adam Glass

SENT BY EMAIL TO:

22 December 2016

Dear Dr Glass,

RE: Application for RCoA Research, Education & Travel Grants

Thank you for your application for a RCoA Research, Education & Travel grant. I am pleased to inform you that the National Institute of Academic Anaesthesia has agreed to offer funding of **£1,970** from the **Ernest Leach Research Fund** for your project entitled, **Assessment of RV contractile reserve on exercise following lung resection – a pilot study**.

Reimbursement will be made with a direct payment, on submission of receipts and invoices from you.

The College will expect you to complete a short report on the project and its findings. The report should acknowledge RCoA support and will be considered by the National Institute of Academic Anaesthesia for publication on the NIAA website.

The NIAA is keen to build a resource to help future grant applicants and, with your permission, would like to publish an extract of your application on the NIAA website. We would draw on your 500 word project description and no financial or personal details would be included. Please could you confirm whether you are happy for me to do this and whether you would like the extract to be anonymised, or any other details removed, at your earliest convenience.

Please direct any queries to me at the email address below.

Many thanks and congratulations on your award.

Yours sincerely,

Pamela Hines
NIAA Coordinator
phines@rcoa.ac.uk

The Association of Anaesthetists of Great Britain & Ireland
Anaesthesia Journal of the Association of Anaesthetists of Great Britain and Ireland
BJA British Journal of Anaesthesia
RCoA Royal College of Anaesthetists

Appendix 2.3 Study protocol

STUDY PROTOCOL

Version: 1

Date: 07/03/2017

Short title:

Right ventricular contractile reserve following lung resection

Full title:

Assessment of right ventricular contractile reserve on exercise following lung resection – a pilot study

Funding:

Ernest Leech Research Fund 2016,

National Institute of Academic Anaesthesia

Names and appointments of any collaborators:

Chief Investigator:
Dr Ben Shelley
Consultant in Cardiothoracic Anaesthesia and Intensive Care
Golden Jubilee National Hospital
Beardmore Street
Clydebank G81 4HX
Tel: 0141 9515000
E-mail: b.shelley@clinmed.gla.ac.uk

Principal Investigator:
Dr Adam Glass
Clinical Research Fellow
Golden Jubilee National Hospital
Beardmore Street
Clydebank G81 4HX
Tel: 0141 9515000
E-mail: aglass01@doctors.org.uk

Co-Investigator:
Dr Philip McCall
Postgraduate Research Student
Academic Unit of Anaesthesia
Level 4, Walton Building
Glasgow Royal Infirmary
84 Castle Street
Glasgow G4 OSF
Tel: 0141 2114625
E-mail: philipmccall@nhs.net

Co-Investigator:
Professor John Kinsella
Professor and Head of Academic Unit of Anaesthesia
Level 4, Walton Building
Glasgow Royal Infirmary
84 Castle Street
Glasgow G4 OSF
Tel: 0141 2114625
E-Mail: john.kinsella@glasgow.ac.uk

Co-investigator:
Dr Mark Stevens
Consultant in Cardiothoracic Anaesthesia and Intensive Care
Golden Jubilee National Hospital
Beardmore Street
Clydebank G81 4HX
Tel: 0141 9515000
E-mail: Mark.stevens@gjnh.scot.nhs.uk

Co-investigator & Lead Surgeon:
Mr Alan Kirk
Consultant Cardiothoracic Surgeon
Golden Jubilee National Hospital
Beardmore Street
Clydebank G81 4HX
Tel: 0141 9515000
E-mail: Alan.Kirk@gjnh.scot.nhs.uk

Co-investigator & Lead Cardiologist:
Dr Piotr Sonecki
Consultant Cardiologist
Golden Jubilee National Hospital
Beardmore Street
Clydebank G81 4HX
Tel: 0141 9515000
E-mail: piotr.sonecki@nhs.net

Assessment of right ventricular contractile reserve on exercise following lung resection – a pilot study

1. Lay abstract (300)

Introduction

Lung cancer is the second most common cancer in the UK and is the leading cause of cancer related death. Where appropriate, surgery (lung resection) to remove the tumour and the surrounding lung provides the best chance of cure. Post-operatively patients may however suffer long-term shortness of breath greatly limiting their day-to-day function. This shortness of breath is not solely caused by the decrease in lung function but also from a decrease in the performance of the heart. Although the surgery does not directly involve the heart it is thought that it is indirectly damaged by the surgery.

Background

In a previous study our research group showed that the function of the right side of the heart (the part of the heart that pumps blood to the lungs) is decreased following lung resection. There is also evidence that patients with poor right heart function before surgery have more complications after surgery. Investigation of its ability to increase its function on exercise (contractile reserve) can detect decreased right heart function when not apparent at rest. Assessment of the contractile reserve of the right heart has not been reliably performed following lung resection.

Methods

We will perform ultrasound scans of the heart (echocardiography) before and two months after lung resection of seven patients. During the scans we will assess the function of the right heart at rest and on exercise (cycling). Will we perform various methods of assessing right heart function to determine which is most reliably performed.

Aims

The aim of the research is to assess the ability of exercise echocardiography as a method of assessing contractile reserve following lung resection. This will guide further studies investigating both right heart function following surgery and whether poor right heart function on exercise before surgery can detect patients at risk of complications.

2. Background

2.1 Introduction

Lung cancer is the leading cause of cancer death in the UK and has the highest regional incidence within Greater Glasgow and Clyde[1, 2]. Where appropriate, surgical resection offers the best chance of cure. Resection rates have risen markedly over the last ten years[3] with a particular increase in elderly patients [4].

Morbidity following lung resection remains high with many patients experiencing long term dyspnoea resulting in decreased functional/exercise capacity[5-7]. This decrease in capacity is poorly associated with the change in lung function[8] although it may be influenced by cardiac limitation[7, 9]. Guidelines published in 2013 regarding the selection of patients for lung resection concluded that the causes of long term dyspnoea, "remain largely unknown."[10] Nonetheless, The British Thoracic Society now advocate:

"Offer[ing] surgical resection to patients at moderate to high risk of post-operative shortness of breath if they are aware of and accept the risks of dyspnoea and associated complications."[11]

Patients prioritise exercise capacity following lung cancer surgery; patient and public involvement between the (Glasgow) Victoria Infirmary Lung Cancer Support Group and our research group highlighted the challenges faced following 'successful' lung resection. Second only to *"being alive and cancer free"* exercise capacity was the main priority of post-operative patients although they experienced significant impairment of functional capacity. Our research also shows that post-operative patients experience a marked increase in problems with 'mobility' and 'self-care' as evidenced by changes in these domains of the EQ-5D quality of life score[12].

2.2 Right ventricular and pulmonary vascular response to lung resection

Right ventricular function at rest has been shown to decrease following lung resection. Our research group has conducted the only sequential cardiac magnetic resonance (CMR) study assessing RV function following lung resection[a]. We demonstrated a decrease in right ventricular ejection fraction (RVEF)[b] following lobectomy at day two (POD2) and two months post-op (Figure 1)[13]. In our cohort, RVEF on POD2 was associated with length of high dependency stay ($p<0.05$, $r=-0.61$). Others have shown that peri-operative decrease in RV function is associated with both early and late post-operative complications[14, 15]. In another study impaired RV function intra-operatively identified patients in whom late cardio-respiratory symptoms would develop[16], suggesting peri-operative RV dysfunction may have an impact long into the post-operative period.

---

a 'The Pulmonary Vascular / Right Ventricular Response to Lung Resection'. ClinicalTrials.gov identifier - NCT01892800. https://clinicaltrials.gov/show/NCT01892800

b We recognise that assessment of RV function is more complex than measurement of RVEF alone, which is dependent on loading conditions. During analysis we also plan to investigate other parameters of RV function and interpret changes in RVEF in the context of indices of preload, contractility and afterload.

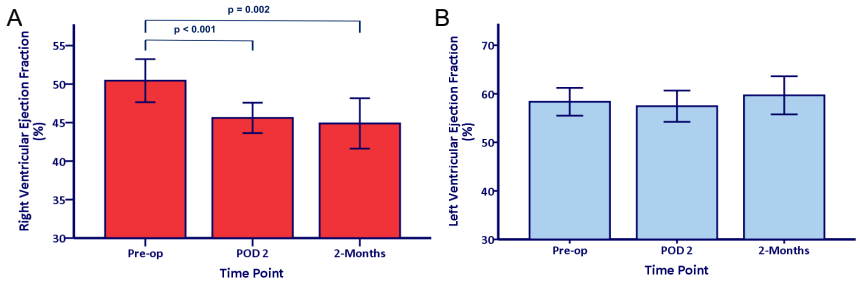

Figure 1 Right ventricular ejection fraction (A) decreases from pre-op levels by post-operative day 2 (POD2), (absolute decrease of 4.9%, relative decrease of 9.7%) and remains low two months. Left ventricular ejection fraction (B) was unchanged throughout study. Error bars 95% confidence intervals. All paired t-tests. McCall et al[13].

Right ventricular function on exercise following lung resection has only been investigated by one research group[17, 18]. In the two studies patients performed submaximal exercise with RVEF calculated from volumetric pulmonary artery catheters (PAC). RVEF did not change from rest on exercise pre-operatively but decreased on exercise at three weeks post-op[18]. In a follow-up study Okada et al. demonstrated that patients with a decrease in RVEF on exercise pre-op experienced more complications, a greater post-operative drop in RVEF and a longer hospital stay[17]. The reliability of derived values of RV volumes and RVEF by PACs has subsequently been shown to be poor, thus limiting the validity of these results[19][20]. Although questions exist of their validity these results imply that not only does RV dysfunction on exercise occur following lung resection but also that its presence pre-operatively may identify patients at risk of complications.

Increased afterload is the most intuitive explanation for reduced RVEF. Intra-operatively afterload, measured by pulmonary vascular resistance (PVR), increases on institution of one-lung ventilation and again on pulmonary artery (PA) clamping[21, 22]. This acute increase returns to baseline however by 24-48 hours post-operatively [18, 22-24] yet RVEF remains depressed at 2 months post-op[13]. We suggest this discord between hypothesis and evidence may exist because PVR fails to assess the full complexity of RV afterload. PVR only assesses resistance to steady flow ignoring the resistance to pulsatile flow that is responsible for up to half the hydraulic work of the RV[25]. In our previous study we demonstrated increases in pulsatile components of afterload at rest with; increased wave reflection, decreased pulmonary artery acceleration time and distensibility. Increased afterload on exercise however has been demonstrated following lung resection; Okada et al observed that as RVEF fell on exercise there was a marked increase in PVR and PA pressure (Figure 2)[18].

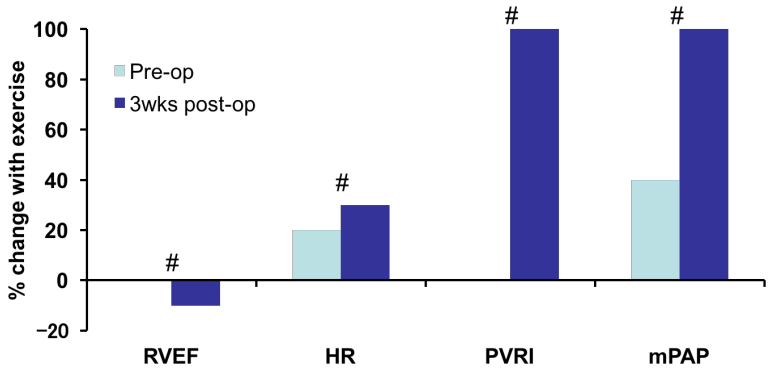

Figure 2 Relative change of cardiovascular parameters on exercise before and after lung resection. RVEF, heart rate (HR), PVR index (PVRI) and mean pulmonary artery pressure (mPAP) on exercise all worsen by three weeks post-op. # p<0.05 paired t-test. Adapted from Okada et al 1994[18].

Biomarker evidence of myocardial injury has also been demonstrated following lung resection by our group. Patients with a decreased functional capacity post-operatively have elevated peri-operative B-type natriuretic peptide (BNP) levels, a marker of myocardial stretch, further relating post-operative functional limitation to cardiac dysfunction[26].

2.3 Right ventricular and pulmonary vascular response to exercise

There is growing appreciation of the importance of assessing the ability of the RV and pulmonary vascular system to maintain/augment its' function in response to exercise[27]. This ability to accommodate changes occurring on exercise is termed 'reserve'. Decrease in both right ventricular contractile reserve (RVCreserve) and pulmonary vascular reserve (PVreserve) have been demonstrated in patients with pulmonary hypertension (PAH).

Right ventricular contractile reserve is defined by Haddad et al as;

"the extent of increase or change in ventricular function that occurs during exercise or pharmacological stress"[28]

Patients with decreased RVCreserve are not able to increase RV function on exercise/stress (Figure 3)[29]. Assessment of RVCreserve can identify RV dysfunction which is not apparent at rest, is associated with a decrease in functional ability and is predictive of survival in this patients with PAH[30-33].

Pulmonary vascular reserve describes the ability of the pulmonary vascular system to cope with an increase in cardiac output. As cardiac output increases there is a linear increase in PA pressure (Figure 3)[29]. The slope of this linear relationship is the PVreserve[29, 34]. Healthy patients have a gradient of 1-2mmHg/l/min whilst >3mmHg/l/min is suggestive of decreased PVreserve[34].

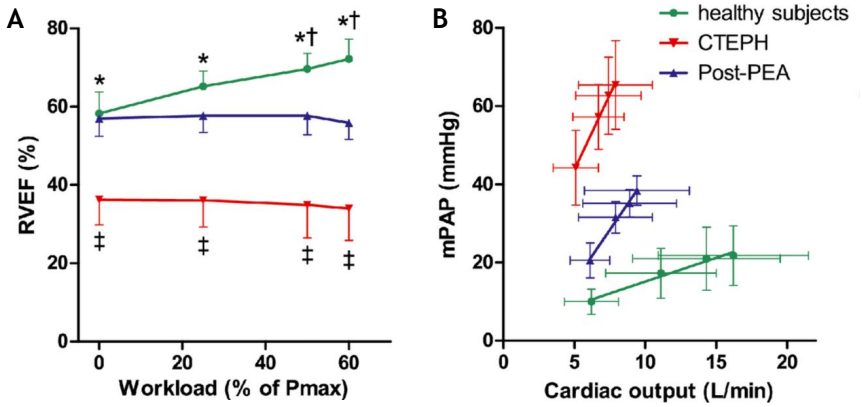

Figure 3. RVCreserve (A) and PVreserve (B) in healthy subjects, patients with chronic thrombo-embolic pulmonary hypertension (CTEPH) and CTEPH patients who have undergone pulmonary endarterectomy (post-PEA). A, healthy subjects and post-PEA have similar RVEF at rest but on exercise post-PEA are unable to increase RVEF. B, gradient of mPAP vs cardiac output increasing from control (1mmHg/L/min) to post-PEA (4.7mmHg/L/min) and CTEPH (6.7mmHg/L/min) with decreasing pulmonary vascular reserve. Adapted from Claessen et al[29].

2.3.1 Methods of assessing reserve

Assessment of the RV is challenging, even at rest, due to its retrosternal position, complex irregular shape and marked load dependence[35]. Assessment RVCreserve relies on accurate and reproducible assessment of regional or global RV function whilst PVreserve requires repeated measurement of pulmonary artery pressure[36].

Cardiac MRI is the gold standard for assessing RV volume/function[35] although cannot measure PA pressures thus preventing conventional PVreserve measurement.

Pulmonary artery catheters reliably assess pressures and flow although volumetric measurements have never reliably been validated against other measures[19] preventing RVCreserve measurement.

Echocardiographic imaging of the entire RV is challenging and is further complicated following lung resection by a potential shift in the position of the heart and hyperinflation[37]. Regional RV assessment and estimated systolic PAP have however been shown to agree with CMR and PAC measurements in pulmonary hypertension by Claessen et al[36].

2.4 Hypothesis and research question

In this pilot study we aim to assess the feasibility of echocardiographic assessment of RVC/PV-reserve pre- and post-operatively in patients undergoing lung resection.

Echocardiographic assessment of the RV is challenging at rest and potentially further complicated by both lung resection and exercise. Not only will we assess the technical feasibility of exercise echocardiography but also the patients' experiences of it with patient satisfaction questionnaires.

We hypothesise that the subtle decrease in RVEF and increase in afterload observed we have observed at rest will manifest as markedly decreased right ventricular contractile and pulmonary vascular reserve on exercise. Additionally, the detection of subtle RV dysfunction pre-op could allow identification of patients at high risk of severe post-op RV dysfunction.

We aim to answer the following questions:

1) Is exercise echocardiographic assessment of RVC/PV-reserve following lung resection
   a) feasible?
   b) acceptable to patients?
2) Does RVC/PV-reserve change following lung resection?
3) Are any observed changes related to the changes in markers of cardiac inflammation (BNP, CK-MB, troponin I, D-dimer and myoglobin)?
4) Are any observed changes related to self-reported functional status?

If the technique proves feasible in this patient group, the results of this pilot study will be used to enable power analysis in the design of a larger observational study to investigate our hypotheses further.

3. Study plan

3.1 Study design

Feasibility pilot study to assess the utility of exercise echocardiography following lung resection. Prospective observational cohort study of 7 patients presenting for video-assisted thoracoscopic surgery (VATS) lobectomy of primary lung cancer.

3.2 Setting

Golden Jubilee National Hospital / West of Scotland Heart and Lung Centre – a NHS tertiary referral cardiothoracic surgical centre (single centre).

3.3 Study summary

The purpose of the study is to assess both the feasibility and patient satisfaction of exercise echocardiography in measurement of RVC/PV-reserve following lung resection.

Patients presenting for VATS lobectomy for suspected lung cancer will undergo exercise echocardiographic assessment pre-operatively and two months post-operatively. Echocardiography will assess RV/LV function and flow/pressure in the main pulmonary artery. This will be performed both at rest and on two-stage cycle-ergometric exercise at set workloads. Contemporaneous blood testing of cardiac biomarkers will also be tested (Table 1).

Recruitment will be limited to patients undergoing anatomical lobectomy with VATS. Surgical technique will be standardised to a single surgeon. Anaesthetic technique will be standardised for analgesia provision, use of vasopressors/inotropes, blood transfusion and peri-operative fluid management (Appendix 1). Such standardisation reflects the normal practice of the surgeon/anaesthetist involved.

	Pre-operatively			Early post-operative period					Follow up
	Recruitment	On admission		Immediately post-op	POD 1	POD 2	POD 3	POD 4	2 Months
Consent	X		Lung Resection						
Baseline demographics	X								
Self-reported functional status • METS, MRC dyspnoea score, NYHA grade and EQ-5D	X								X
Exercise echocardiography • Standardised protocol (appendix 2) • Patient satisfaction questionnaires (appendix 5)		X							X
Biomarkers: • Myocardial dysfunction (BNP, CK-MB, troponin I, D-dimer and myoglobin)		X		X	X	X	X	X	X

Table 1 Timescale of proposed observations. Post-operative day (POD)

4. Objectives and outcome measures

4.1 Primary outcome measures

The primary outcome of the study is to determine if exercise echocardiographic assessment of RVC/PV-reserve is feasible following lung resection and if so which parameter is most reliably imaged. We will assess both image acquisition and patient satisfaction of the procedure. Image acquisition will be assessed by the quality of imaging achieved at rest, on light and on moderate exercise in patients pre-operatively and two months post-operatively (appendix 2). Image quality will be graded at time of scanning by echocardiography technician and then by two blinded observers during post-processing echo analysis.

Patient satisfaction questionnaires will examine the patients' experience of exercise echocardiography (appendix 5), allowing us to assess whether this technique would be acceptable to patients in a subsequent larger observational study.

4.2 Rationale for primary outcome

4.2.1 Methods of assessing reserve

Echocardiographic imaging of the entire RV is challenging and therefore relies upon the use of regional assessment as a surrogate of global RV function, summarised below (Figure 4). We will assess the feasibility of obtaining each of the following measures.

- **Systolic (S') wave velocity** is a load dependent measure of RV contractility derived from tissue doppler imaging of the RV free wall[38].
- **Tricuspid annular plane systolic excursion** (TAPSE) measures the longitudinal shortening of the RV on contraction. TAPSE is highly load dependent[38] although it is frequently used in PAH and RVCreserve assessment[33, 39].
- **RV fractional area change (RVFAC)** is obtained from a long axis of the RV following measurement of the cross-sectional area of the RV at end systole (RVESA) and end diastole (RVEDA)[39]. Its accuracy is limited by the assumption that the RV is concentric although Claessen et al. showed a strong correlation with RVEF on exercise[36]. RVFAC (%) = (RVEDA-RVESA)/RVEDA.
- **Eccentricity index** is a measure of concentricity of the LV that can detect pressure/volume overload of the RV[40]. As RV pressure/volume increases it flattens the interventricular septum causing deformation of the LV thus increasing its eccentricity.
- **Systolic pulmonary artery pressure** can be estimated from the maximal velocity of the tricuspid regurgitant jet[32]. Significant improvement in the ability to detect the jet can be obtained with the administration of agitated colloid[36].

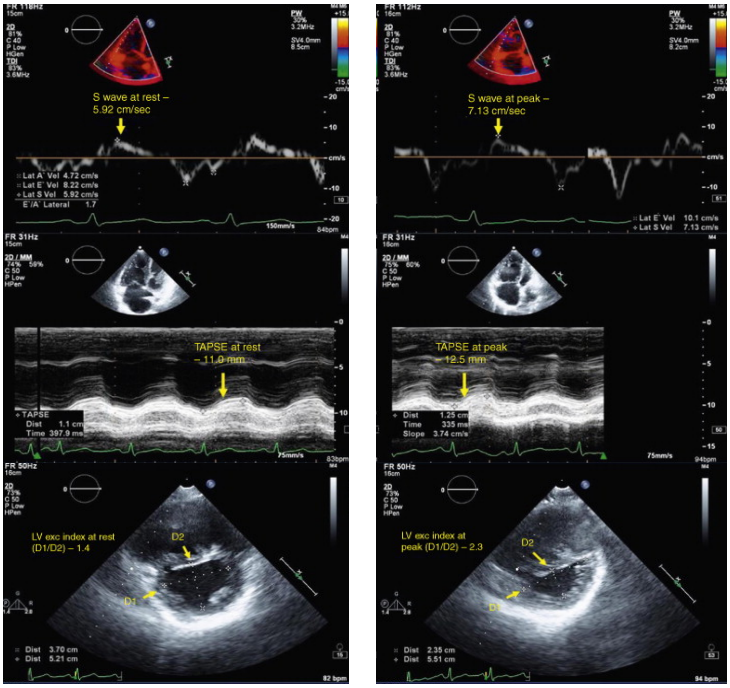

Figure 4. Echocardiographic assessment of RVCreserve of a pulmonary hypertension patient at rest (left) and on exercise (right). i) S wave velocity, ii) TAPSE, and iii) LV eccentricity index (EI). Note increases in S' wave velocity and TAPSE on exercise with a deterioration in EI with flattening of the interventricular septum indicating RV pressure/volume overload. Adapted from Aleida et al.[39]

Exercise capacity assessment following lobectomy by other authors have demonstrated a maximal workload achievable of 67-99 Watts[6, 8, 41-43]. A fixed two stage exercise protocol of 25W and 50W, as per Blumberg et al, will negate the need for maximal exercise capacity assessment and allow comparison of similar workloads pre- and post-operative[31].

4.2.2 Method of assessing patient satisfaction

Lung resection rates are increasing, especially in older patients[4]. These patients tend to have more comorbidities, including cardiac, respiratory and musculoskeletal disorders. The physical ability of patients to complete the exercise component of the study is essential for the test. We will assess patients' experience of the procedure and of the exercise programme and their ability to complete the planned exercises (Appendix 5).

Patients' feedback of the technique will guide further work and potentially pre-operative testing. If the technique of exercise echocardiography is useful in this setting and can detect patients at risk of RV dysfunction post-operatively the procedure may be incorporated into pre-operative testing. It is imperative that we develop a protocol that is acceptable to patients.

4.3 Secondary outcomes

4.3.1 Outcome measures

1) Does RVC/PV-reserve change following lung resection?
2) Are any observed changes related to the changes in markers of cardiac inflammation (BNP, CK-MB, troponin I, D-dimer and myoglobin)?
3) Are any observed changes related to self-reported functional status?

4.3.2 Rationale for secondary outcomes

The study is not powered to detect changes in the secondary outcomes described. The following analysis will be used to power a larger observational cohort study to investigate the hypotheses described.

1) Does RVC/PV-reserve change following lung resection?

Right ventricular contractile reserve will be assessed by the change in measures of RV function from rest to exercise (Δ) pre-operatively to post-operatively. Due to pilot nature of this study we will assess changes in TAPSE, S' and RVFAC.

Pulmonary vascular reserve will be assessed by gradient of systolic/mean PAP against CO pre-operatively vs post-operatively[29]

2) Are any observed changes in RV/PV Reserve related to the changes in markers of cardiac inflammation (BNP, CK-MB, troponin I, D-dimer and myoglobin)?

B-type natriuretic peptide (BNP): is a hormone secreted by cardiac myocytes in response to mechanical stretch. In our previous study patients with elevated pre-operative BNP had lower functional capacity post-operatively [26]. In this previous study BNP was highest on POD2 (the last day of testing) and so, in the proposed study BNP will be assayed at further time-points in order to delineate the timing of the post-operative peak in plasma BNP (Table 1). Plasma BNP may have value as a peri-operative marker of RV dysfunction and may be related to RVCreserve in this patient population.

3) Are any observed changes related to self-reported functional status?

Functional status will be assessed subjectively by written questionnaires pre-operatively and two months post-operatively (Table 1). Scoring will be performed with the New York Heart Association (NYHA) classification[44], WHO performance

status classification[45], MRC Breathlessness Scale[46] and health related quality of life scoring by EQ-5D questionnaire[12].

5. Selection and withdrawal of study subjects

5.1 Inclusion criteria

1) Provision of informed consent
2) Age >16 years
3) Planned elective lung resection by VATS lobectomy

5.2 Exclusion criteria

Subjects fulfilling any of the criteria below will be excluded from the study:

1) Pregnancy
2) On-going participation in any investigational research which could undermine the scientific basis of the study
3) Wedge, segmental or sub-lobar lung resection
4) Pneumonectomy
5) Isolated right middle lobectomy
6) Contraindication to exercise echocardiography, as per British Society of Echocardiography guidelines[47]
   a) Acute coronary syndrome
   b) Left ventricular failure with symptoms at rest
   c) Recent history (within the last week) of life threatening arrhythmias
   d) Severe dynamic or fixed left ventricular outflow tract obstruction
   e) Severe systemic hypertension (systolic blood pressure >220mmHg and/or diastolic blood pressure >120mmHg)
   f) Recent pulmonary embolism or infarction
   g) Thrombophlebitis or active deep vein thrombosis
   h) Known hypokalaemia
   i) Active endocarditis, myocarditis, or pericarditis.

5.3 Rationale for inclusion/exclusion criteria

Lobectomy is the most common lung resection performed[2]. Although pneumonectomy will cause greater physiological disruption they represent less than 6% of lung resections nationally potentially limiting the application of study results. VATS resection rates have rapidly increased in recent years and now account for 70% of resections within the Golden Jubilee National Hospital (the largest thoracic surgical unit in the UK). Lesser resections (including isolated right middle lobectomy) have been excluded as the lesser physiological disruption may be hypothesised to be inadequate to significantly influence RV function and/or impair imaging.

Many of the contraindications for exercise echocardiography are contraindications for surgery, and as such we don't anticipate exclusion of many patients based on these criteria.

5.4 Withdrawal and exclusions

A patient may request withdrawal from the study at any time without it affecting their clinical care. The patient will not have to give a reason for their decision to withdraw.

6. Study conduct

6.1 Recruitment

Patients will be identified from the waiting list of patients presenting to GJNH for lung resection by consultation between Dr Shelley (chief investigator), Dr Glass (principal investigator) and Mr Kirk (lead surgeon). Potentially eligible patients will be approached by either Mr Kirk (lead surgeon) or Dr Stevens (anaesthetist), provided with a patient information leaflet and given a verbal outline of the study when attending the combined anaesthetic and surgical pre-assessment clinic (generally occurring 3 days prior to admission). Mr Kirk and Dr Stevens are part of the patients direct clinical care team. It is hoped Dr Glass or a designated member of the research team will be able to attend this clinic on the majority of occasions for the purpose of an introduction.

Patients will then be advised that Dr Glass or a designated member of the research team will come to see them once admitted prior to their operation, to discuss the study further, to answer any questions that they may have about the study and if appropriate obtain informed consent.

6.2 Consent

Written informed consent will be obtained, following a face-to-face discussion about the study (where patients are given the opportunity to ask questions) by a member of the study team.

6.3 Data collection

Data collection involves:

- Baseline demographic data
- Self-report of exercise tolerance
- Exercise echocardiography
- Laboratory sampling
- Intra-operative data
- Post-operative clinical data

6.3.1 Baseline demographic data

Case note review and routine pre-operative investigations:

- Indication for resection, tumour staging (if applicable)
- Chemo- / Radio- therapy received (if any)

- Alcohol consumption – units per week
- Smoking history – current and pack years, time since abstinence if applicable
- Pulmonary function test results:
  - Forced expiratory volume in 1 second (FEV1)
  - Forced vital capacity (FVC)
  - FEV1/FVC ratio (%)
  - Diffusing lung capacity for carbon monoxide (DLCO)
- Co morbidities
  - As defined by the definitions of Thoracoscore (The Thoracic Surgery Scoring System)
  - Smoking addiction
  - History of cancer
  - COPD
  - Arterial hypertension
  - Heart disease
  - Diabetes mellitus
  - Peripheral vascular disease
  - Obesity
  - Alcoholism
- American Society of Anesthesiologists (ASA) grade
- Medication history (including over the counter medication)
- Height and body weight

6.3.2 Self-report of functional status

Self-report of functional status will be by completion of a written questionnaire (Appendix 6) encompassing the New York Heart Association (NYHA) classification[44], WHO performance status classification[45], MRC Breathlessness Scale[46] and health related quality of life scoring by EQ-5D questionnaire[12].

6.3.3 Echocardiographic imaging

Exercise testing will be performed on a GE eBike EL Ergometer (Freiburg, Germany) at rest and on two fixed workloads. Echocardiography image acquisition will be undertaken on a Vivid E9 cardiovascular ultrasound (GE Healthcare, Freiburg, Germany) by band 7, British Society of Echocardiography accredited cardiac physiologists according to a standardised protocol (Appendix 2). Post processing will be dual reported by blinded observers using *EchoPAC* software (GE Healthcare) and *4D RV-Function analysis* software (TomTec Imaging Systems) according to a standardised protocol (Appendix 3). Echo image quality will be graded at time of scanning and then by the two blinded observers on post-processing analysis (Appendix 4).

6.3.4 Laboratory sampling

Blood sampling: Just prior to induction of anaesthesia a baseline 3ml EDTA blood sample will be collected. A further 3 ml sample will be taken on immediately post-operatively, on post-operative days 1, 2, 3, 4 and on follow up at 2 months. Where

possible blood samples will be taken from a radial arterial cannula (routine for surgeries such as this) or collected along with any bloods required for their normal clinical care to avoid unnecessary venepuncture.

Biomarkers of myocardial dysfunction (BNP, CK-MB, troponin I, D-dimer and myoglobin) will be analysed using the Alere Triage® ProfilER SOB™ Panel system (Alere Ltd. Stockport, UK). Quality control measures will be undertaken as per the manufacture's guidelines. All samples taken for the study will be analysed within 6hours of collection (as per manufacture guidelines) and subsequently disposed of.

6.3.5 Intra- / Peri-operative data

- Anaesthetic techniques / drugs administered
- Regional anaesthetic technique utilised (and success of technique)
- Duration of surgery / anaesthetic
- During the period of one lung ventilation (OLV)
  - Duration of OLV
  - Tidal volume, minute volume, PEEP, inspiratory plateau and peak airway pressure
  - Fraction of inspired oxygen (FiO_2),
  - Need for continuous positive airway pressure (CPAP) / insufflation of operative lung to avoid hypoxia
- Surgery performed (lobectomy / pneumonectomy, operative side)
- Estimated blood loss
- Intravenous fluids and volume delivered

6.3.6 Post-operative clinical data

- Routinely sampled arterial blood gas analyses (ABGs) – (PaO2, PaCO2, [H+], [HCO3-], lactate, base excess) immediately postoperatively and at approximately 6 hourly intervals until HDU discharge postoperatively
- Intravenous fluids administered in first 24 hours
- Duration of HDU / hospital stay
- Formal chest radiology reports
- Incidence of new-onset atrial fibrillation
- Need for vasopressor / inotrope administration
- Need for high flow nasal continuous positive airways pressure / non-invasive ventilation
- Need for ICU admission / positive pressure ventilation
- In-hospital mortality

7. Data Management

7.1 Data collection

Patient data will be collected manually on case report forms (CRFs) by one of the investigators, or an appropriately trained research nurse.

7.2 Database

Anonymised patient data will be stored on a password protected university computer. A patient identifier list will be kept in a locked cabinet within the Anaesthetic Department at Golden Jubilee National Hospital.

7.3 Archiving

Study data will be archived for five years after the completion of the trial. It will be stored within locked filing cabinets within the Department of Anaesthesia, Golden Jubilee National Hospital.

8. Statistical Analysis

8.1 Statistical Methods

8.1.1 Primary outcome

Feasibility of exercise echocardiography will be assessed by the quality of images achieved and patient satisfaction of procedure at each stage of exercise and visit (Appendices 4 & 5). No formal statistical testing will be performed on this information.

8.2.2 Secondary outcomes[c]

- Paired secondary outcomes. Data will be assessed for normality and comparison will be made using a paired *t*-test or Wilcoxon signed ranks test as appropriate.
- Association between secondary outcomes. Exploratory analyses seeking to examine the mechanism of decreased reserve will be undertaken. Association between RVC/PV-reserve, self-reported functional status and cardiac biomarkers will be assessed with Pearson correlation coefficient or its nonparametric alternative, Spearman's rank correlation coefficient, as appropriate.

[c]It is acknowledged that our study lacks power to detect changes in RVC/PV-reserve and its potential association with cardiac biomarkers and functional status. Such comparisons must be reviewed as exploratory analyses and will require further confirmation.

9. Study Organisation

9.1 Sponsor

This study will be sponsored by the National Waiting Times Centre Board (Golden Jubilee National Hospital).

9.2 Administration

All routine clinical and non-clinical co-ordination of the study will be the responsibility of the principal investigator (AG). The chief investigator (BS) will assume responsibility for the overall management and conduct of the trial.

9.3 Indemnity

The NHS research indemnity scheme will apply.

9.4 Monitoring

This study will be sponsored by the National Waiting Times Centre Board (Golden Jubilee National Hospital). As such, the Research and Development department undertake to monitor this research in line with the Research Governance Framework for Health and Community Care (Scotland).

10. Ethics and regulatory approval

The study will be conducted in accordance with the ethical principles that have their origin in the Declaration of Helsinki. The study will be submitted to the West of Scotland Research Ethics Committee for approval.

11. Projected study timetable

We aim to commence recruitment in April 2017, and recruit one patient a week. Factoring time for patient refusal, holidays and unforeseen issues we propose to have completed this study by the end of September 2017.

12. Protocol amendments

Any substantial amendments to the final protocol will be clearly documented and forwarded to the Research Ethics Committee for approval prior to implementation via the IRAS process of Notification of Substantial Amendment.

13. Publication

The results of the study will be reported first to study collaborators.

Subsequently, we plan to communicate our results by reporting them to the funder and presentation at national meetings with publication in appropriate peer reviewed journals.

At the end of the study, all subjects will be thanked in writing for their participation in the study and provided with a short summary of the trial findings. Further details about the trial results and final report will be available on request.

14. Ethics and regulatory approval

The study will be conducted in accordance with the ethical principles that have their origin in the Declaration of Helsinki. The study will be submitted to the West of Scotland Research Ethics Committee for approval.

APPENDIX ONE: Protocol for peri-operative management of study subjects

It is not the intention of this study to alter patient management. This protocol is intended to document and establish uniformity in the intra-operative and post-operative anaesthetic and surgical management of study patients and reflects the standard practice of the clinicians involved.

Intra-operative anaesthetic management

Premedication: Benzodiazepine or none

Intravenous access + arterial line under local anaesthetic.

Thoracic epidural pre-induction or paravertebral catheters intra-operatively.

Induction: Propofol.

Muscle relaxation: any.

Lung isolation: Double-lumen endo-tracheal tube.

Ventilation: Lung protective protocol. Target parameters: TV <8mls/kg, PEEP 0-10cmH2O, Pmax limited to <30cmH2O, FiO2 titrated to maintain SaO2 92%-98%. Generally permissive approach to hypercapnia.

Central venous cannulation (internal-jugular or subclavian) once anaesthetised.

Maintenance: Inhalational anaesthetic agent ± Remifentanil

Fluid management: Generally restrictive approach. Target <1000ml intra-operative fluid unless exceptional losses.

Intra-operative hypotension: Colloid boluses as appropriate. Ephedrine / metaraminol boluses. Rarely metaraminol / noradrenaline by infusion. Use of dobutamine in exceptional circumstances (must be recorded on CRF).

Surgical management:

Video-assisted thoracoscopic surgery (VATS) lobectomy with standard approach with anatomically appropriate lymph node clearance.

Post-operative care:

Analgesia: Regular Paracetamol, NSAID if tolerated.

Paravertebral catheter: Bupivicaine 0.125%, initial rate 15ml/hr. 20ml 0.25% top-up as required.

Fluid management: Maintenance fluid at 1ml/kg/hr up to 70 mls/hr until adequate oral intake. Fluid restriction to less than 2000ml/24 hours unless exceptional drain losses.

Atrial fibrillation: ECG to confirm. Mg+ & K+ replacement in first instance. IV Amiodarone as first line therapy in cases of new-onset atrial fibrillation unless contraindicated. (Patients not in sinus rhythm pre-operatively will be excluded from the study).

Blood transfusion: Concentrated red cell replacement if Hb<8.0g/dL.

APPENDIX TWO: Protocol for Echocardiographic image acquisition

Recorded views:

Imaging will be performed at rest, on constant workload of 25 W and then 50W.

2D

- 4CH (including RA) Required high frame rate– ideally one extra cineloop with reduced sector dimensions (just RV) with high temporal and spatial resolution
- PARASTERNAL SAX
    - AV LEVEL (RVOT, PV, PA)
    - MV level (optional for pure RV assessment)
    - Papillary muscle level
- Subcostal (IVC, RA, RV)

DOPPLER

- Colour
    - PV
    - TV
- PW
    - RVOT
    - TV inflow
- TDI (colour and/or PW)
    - RV FREE WALL
    - TV annulus (inc diastolic)

M MODE (Vivid scans could be obtained off line from 2D scans)

- TV annulus at RV free wall (TAPSE)
- RVOT
- IVC (respirations)

3D – full volume obtained from apical view where possible

APPENDIX THREE: Protocol for Echocardiographic post-processing

Indices of RV preload, contractility, afterload and diastolic dysfunction to be derived from echocardiography during post-processing. This will be collect from images obtained from rest and both stages of exercise. As scientific reviewers often request specific supplementary data, we intend to collect data on all of the indices below. We have **highlighted** those we intend to focus on during our analysis.

Component	Parameter	Technique
Geometric	Chamber dimensions	RV dimensions, RVOT diameters, PA diameter and RV area measured per BSE guidelines.
Preload	Estimated RAP	Derived from IVC collapse.
Contractility	**Fractional area change**	RV end diastolic / systolic areas measured in 4 chamber view per BSE guidelines. RVFAC (%) = (RVEDA – RVESA)/RVEDA
Contractility	**Tricuspid Annular Plane Systolic Excursion (TAPSE)**	Derived from apical 4 chamber view. M mode cursor positioned on lateral portion of the tricuspid annulus.
Contractility	**S' wave velocity**	Derived from TDI of RV free wall at the level of TV annulus.
Contractility	Myocardial performance index (MPI)	Derived from Tissue Doppler Imaging (TDI) of RV free wall at the level of TV annulus. MPI=(IVCT+IVRT)/ET IVCT – isovolumetric contraction time, ET – ejection time.
Contractility	RV outflow tract shortening fraction (RVOT-SF)	M mode, parasternal short axis view at base. RVOT diameters (D) measured at end systole (ES) and diastole (ED) RVOT-SF (%) = (EDRVOTD-ESRVOTD)/EDRVOTD
Contractility	Peak systolic strain and strain rate	Derived from apical 4 chamber view. Peak longitudinal systolic strain assessed globally and in the RV free wall.
Contractility	Myocardial isovolumetric acceleration time (IVA)	Tissue Doppler derived, in basal segment of RV free wall. Ratio between maximal systolic velocity and time to maximum systolic velocity.
Contractility	$RVEF_{3DE}$	Derived from 3D-Echocardiography (3DE).
Afterload	**Estimated PA systolic pressure**	Tricuspid Regurgitant Jet (TRJ) velocity (Bernoulli equation) Where TRJ not obtainable attempt will be made to estimate mean PA pressure from pulmonary regurgitant jet velocity or RV outflow tract acceleration time.

Afterload	**Eccentricity index**	Measure of anterior-posterior : medial-lateral dimension of LV from short axis image at mid papillary level.
Afterload	Pulse wave Doppler of RVOT	Pulmonary artery acceleration time. Shape of flow velocity envelope in RVOT categorised as MSN/LSN/NN
Diastolic dysfunction	Isovolumetric relaxation time (IVRT)	Time from pulmonary valve closure to tricuspid valve opening. Derived from TDI of ventricular free wall.
Diastolic dysfunction	Tricuspid valve E/e'	E/e' ratio measured by tissue Doppler imaging. E – tricuspid flow early diastolic velocity, e' peak early diastolic velocity of lateral tricuspid annulus

APPENDIX FOUR: Echocardiography case report form

Exercise Echo ID number in this study: **EXEC** |__|__|
Reviewer initials: |__|__|

Parameter	Result			Image Quality		
Exercise level	Rest	Low	Mod	Rest	Low	Mod
Fractional area change						
TAPSE						
S' wave velocity						
Estimated PA systolic pressure						
Eccentricity index						

Image Quality	**Score**
Good	**4**
Poor but interpretable	**3**
Poor not interpretable	**2**
Not visualised	**1**

APPENDIX FIVE: Patient satisfaction questionnaire

RV Exercise Echocardiography Questionnaire

Patient ID number in this study: **RVEX** |__|__|

Pre-op ❑ **2 months** ❑

Can you rate how well informed you were about the exercise echocardiography?

- ☐ Very uninformed
- ☐ Somewhat uninformed
- ☐ Well informed
- ☐ Very well informed

How difficult was it for you to undergo the echocardiography at rest?

- ☐ Very difficult
- ☐ Difficult
- ☐ Average
- ☐ Easy
- ☐ Very easy

How difficult was it for you to perform the low intensity exercise?

- ☐ Very difficult
- ☐ Difficult
- ☐ Average
- ☐ Easy
- ☐ Very easy

How difficult was it for you to undergo the echocardiography scanning on low intensity exercise?

- ☐ Very difficult
- ☐ Difficult
- ☐ Average
- ☐ Easy
- ☐ Very easy

How difficult was it for you to perform the moderate intensity exercise?

- ☐ Very difficult
- ☐ Difficult
- ☐ Average
- ☐ Easy
- ☐ Very easy
- ☐

How difficult was it for you to undergo the echocardiography scanning at moderate intensity exercise?

- ☐ Very difficult
- ☐ Difficult
- ☐ Average
- ☐ Easy
- ☐ Very easy

Would you undertake exercise echocardiography again?

- ☐ Yes
- ☐ No

Additional Comments

APPENDIX SIX: Self-reporting functional status questionnaire

Right ventricular contractile reserve following lung resection
CRF 2 – Self-report of functional status / quality of life

Patient ID number in this study:	**RVEX** |__|__|

Pre-op ❑ **2 months** ❑

We would like to ask you some questions about how your health / symptoms effect your day to day life. Please read the instructions and tick the appropriate box. Though, some of the scoring systems overlap it is important that you answer each one individually. This should take no longer than 10 minutes.

Thank you for your time!

World Health Organization Performance status:

Please tick the ONE box that best describes you:

Fully active, able to carry on all pre-disease performance without restriction	❑
Restricted in physically strenuous activity but ambulatory (able to walk) and able to carry out work of a light or sedentary nature, e.g., light house work, office work	❑
Ambulatory (able to walk) and capable of all self-care but unable to carry out any work activities. Up and about more than 50% of waking hours	❑
Capable of only limited self-care, confined to bed or chair more than 50% of waking hours	❑
Completely disabled. Cannot carry on any self-care. Totally confined to bed or chair	❑

MRC Breathlessness Scale:

Please tick the ONE box that best describes you:

No breathlessness except with strenuous exercise	❑
Breathless when walking up an incline or hurrying on the level	❑
Walks slower than most people on the level, or stops after 15 minutes of walking on the level	❑
Stops after a few minutes of walking on the level	❑
Breathless with minimal activity such as getting dressed, to breathless to leave the house	❑

New York Heart Association classification:

Please tick the ONE box that best describes you:

No symptoms and no limitation in ordinary physical activity, e.g. shortness of breath when walking, climbing stairs etc.	❑
Mild symptoms (mild shortness of breath and/or angina) and slight limitation during ordinary activity.	❑
Marked limitation in activity due to symptoms, even during less-than-ordinary activity, e.g. walking short distances (20–100 m).	❑
Severe limitations. Experiences symptoms even while *at rest*. Mostly bedbound.	❑

Quality of Life

Under each heading, please tick the ONE box that best describes your health TODAY

MOBILITY

I have no problems in walking about	❑
I have slight problems in walking about	❑
I have moderate problems in walking about	❑
I have severe problems in walking about	❑
I am unable to walk about	❑

SELF-CARE

I have no problems washing or dressing myself	❑
I have slight problems washing or dressing myself	❑
I have moderate problems washing or dressing myself	❑
I have severe problems washing or dressing myself	❑
I am unable to wash or dress myself	❑

USUAL ACTIVITIES *(e.g. work, study, housework, family or leisure activities)*

I have no problems doing my usual activities	❑
I have slight problems doing my usual activities	❑
I have moderate problems doing my usual activities	❑
I have severe problems doing my usual activities	❑
I am unable to do my usual activities	❑

PAIN / DISCOMFORT

I have no pain or discomfort	❑
I have slight pain or discomfort	❑
I have moderate pain or discomfort	❑
I have severe pain or discomfort	❑
I have extreme pain or discomfort	❑

ANXIETY / DEPRESSION

I am not anxious or depressed	❑
I am slightly anxious or depressed	❑
I am moderately anxious or depressed	❑
I am severely anxious or depressed	❑
I am extremely anxious or depressed	❑

- We would like to know how good or bad your health is TODAY.
- This scale is numbered from 0 to 100.
- 100 means the best health you can imagine.
  0 means the worst health you can imagine.
- Mark an X on the scale to indicate how your health is TODAY.
- Now, please write the number you marked on the scale in the box below.

YOUR HEALTH TODAY = ☐

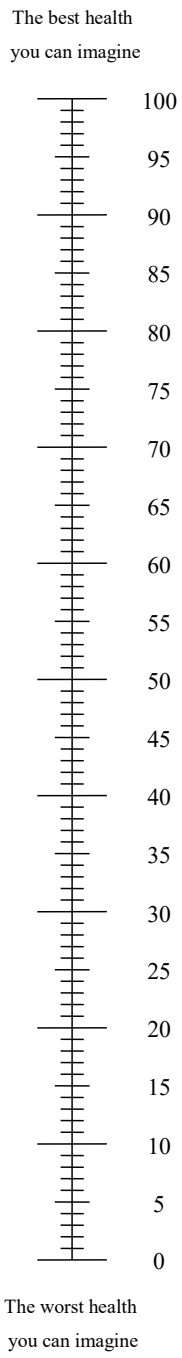

References

1. *Cancer Research UK. Lung Cancer Key Facts*. 2014 12/05/2016].
2. *National Cancer Intelligence Network. Major resections by cancer site, in England; 2006 to 2010.* 12/05/2016].
3. *Second national thoracic surgery activity & outcomes report*. The Society for Cardiothoracic Surgery in Great Britain & Irealnd; 2011 [cited http://www.scts.org/_userfiles/resources/634558869917493937_Thoracic_2011_FINAL.pdf. 12/05/2016].
4. Riaz, S.P., et al., *Recent trends in resection rates among non-small cell lung cancer patients in England.* Thorax, 2012. **67**(9): p. 811-4.
5. Sarna, L., et al., *Impact of respiratory symptoms and pulmonary function on quality of life of long-term survivors of non-small cell lung cancer.* Chest, 2004. **125**(2): p. 439-45.
6. Larsen, K.R., et al., *Cardiopulmonary function at rest and during exercise after resection for bronchial carcinoma.* Ann Thorac Surg, 1997. **64**(4): p. 960-4.
7. Vainshelboim, B., et al., *Limitations in exercise and functional capacity in long-term postpneumonectomy patients.* J Cardiopulm Rehabil Prev, 2015. **35**(1): p. 56-64.
8. Pelletier, C., L. Lapointe, and P. LeBlanc, *Effects of lung resection on pulmonary function and exercise capacity.* Thorax, 1990. **45**(7): p. 497-502.
9. Nugent, A.M., et al., *Effect of thoracotomy and lung resection on exercise capacity in patients with lung cancer.* Thorax, 1999. **54**(4): p. 334-8.
10. Brunelli, A., et al., *Physiologic evaluation of the patient with lung cancer being considered for resectional surgery: Diagnosis and management of lung cancer, 3rd ed: American College of Chest Physicians evidence-based clinical practice guidelines.* Chest, 2013. **143**(5 Suppl): p. e166S-90S.
11. Lim, E., et al., *Guidelines on the radical management of patients with lung cancer.* Thorax, 2010. **65 Suppl 3**: p. iii1-27.
12. Herdman, M., et al., *Development and preliminary testing of the new five-level version of EQ-5D (EQ-5D-5L).* Qual Life Res, 2011. **20**(10): p. 1727-36.
13. McCall, P., et al., *The right ventricular response to lung resection.* Journal of Cardiothoracic and Vascular Anesthesia, 2016. **30**: p. S23-S24.
14. Matyal, R., et al., *Right Ventricular Echocardiographic Predictors of Postoperative Supraventricular Arrhythmias After Thoracic Surgery: A Pilot Study.* Annals of Thoracic Surgery, 2010. **90**: p. 1080-1087.
15. Kowalewski, J., et al., *Right ventricular morphology and function after pulmonary resection.* Eur J Cardiothorac Surg, 1999. **15**(4): p. 444-8.
16. Lewis, J.W., et al., *Right heart function and prediction of respiratory morbidity in patients undergoing pneumonectomy with moderately severe cardiopulmonary dysfunction.* J Thorac Cardiov Sur, 1994. **108**: p. 169-175.
17. Okada, M., et al., *Right ventricular ejection fraction in the preoperative risk evaluation of candidates for pulmonary resection.* J Thorac Cardiovasc Surg, 1996. **112**(2): p. 364-70.
18. Okada, M., et al., *Right ventricular dysfunction after major pulmonary resection.* J Thorac Cardiovasc Surg, 1994. **108**(3): p. 503-11.

19. Leibowitz, A.B., *Pulmonary artery catheter determined right ventricular ejection fraction and right ventricular end-diastolic volume: another case of "The Emperor Has No Clothes".* Crit Care Med, 2009. **37**(11): p. 2992.
20. Hein, M., et al., *Continuous right ventricular volumetry by fast-response thermodilution during right ventricular ischemia: head-to-head comparison with conductance catheter measurements.* Crit Care Med, 2009. **37**(11): p. 2962-7.
21. Waller, D.A., et al., *Pulmonary endothelial permeability changes after major lung resection.* Ann Thorac Surg, 1996. **61**(5): p. 1435-40.
22. Lewis, J.W., et al., *Right heart function and prediction of respiratory morbidity in patients undergoing pneumonectomy with moderately severe cardiopulmonary dysfunction.* J Thorac Cardiovasc Surg, 1994. **108**(1): p. 169-75.
23. Reed, C.E., B.H. Dorman, and F.G. Spinale, *Mechanisms of right ventricular dysfunction after pulmonary resection.* Ann Thorac Surg, 1996. **62**(1): p. 225-31; discussion 231-2.
24. Bäcklund, M., et al., *Effect of oxygen on pulmonary hemodynamics and incidence of atrial fibrillation after noncardiac thoracotomy.* J Cardiothorac Vasc Anesth, 1998. **12**(4): p. 422-8.
25. Champion, H.C., E.D. Michelakis, and P.M. Hassoun, *Comprehensive invasive and noninvasive approach to the right ventricle-pulmonary circulation unit: state of the art and clinical and research implications.* Circulation, 2009. **120**(11): p. 992-1007.
26. McCall, P., et al., *Perioperative BNP changes and functional capacity following lung resection.* Journal of Cardiothoracic and Vascular Anesthesia, 2016. **30**: p. S26-S27.
27. Houston, B.A. and R.J. Tedford, *Putting "at-rest" evaluations of the right ventricle to rest: insights gained from evaluation of the right ventricle during exercise in CTEPH patients with and without pulmonary endarterectomy.* J Am Heart Assoc, 2015. **4**(3): p. e001895.
28. Haddad, F., et al., *The concept of ventricular reserve in heart failure and pulmonary hypertension: an old metric that brings us one step closer in our quest for prediction.* Curr Opin Cardiol, 2011. **26**(2): p. 123-31.
29. Claessen, G., et al., *Pulmonary vascular and right ventricular reserve in patients with normalized resting hemodynamics after pulmonary endarterectomy.* J Am Heart Assoc, 2015. **4**(3): p. e001602.
30. Chaouat, A., et al., *Prognostic value of exercise pulmonary haemodynamics in pulmonary arterial hypertension.* Eur Respir J, 2014. **44**(3): p. 704-13.
31. Blumberg, F.C., et al., *Impact of right ventricular reserve on exercise capacity and survival in patients with pulmonary hypertension.* Eur J Heart Fail, 2013. **15**(7): p. 771-5.
32. Chia, E.M., et al., *Exercise testing can unmask right ventricular dysfunction in systemic sclerosis patients with normal resting pulmonary artery pressure.* Int J Cardiol, 2016. **204**: p. 179-86.
33. Sharma, T., et al., *Dobutamine stress for evaluation of right ventricular reserve in pulmonary arterial hypertension.* Eur Respir J, 2015. **45**(3): p. 700-8.
34. Lewis, G.D., et al., *Pulmonary vascular hemodynamic response to exercise in cardiopulmonary diseases.* Circulation, 2013. **128**(13): p. 1470-9.

35. Haddad, F., et al., *Right ventricular function in cardiovascular disease, part I: Anatomy, physiology, aging, and functional assessment of the right ventricle*. Circulation, 2008. **117**(11): p. 1436-48.
36. Claessen, G., et al., *Accuracy of Echocardiography to Evaluate Pulmonary Vascular and RV Function During Exercise*. JACC Cardiovasc Imaging, 2016. **9**(5): p. 532-43.
37. Smulders, S.A., et al., *Cardiac function and position more than 5 years after pneumonectomy*. Ann Thorac Surg, 2007. **83**(6): p. 1986-92.
38. Howard, L.S., et al., *Echocardiographic assessment of pulmonary hypertension: standard operating procedure*. Eur Respir Rev, 2012. **21**(125): p. 239-48.
39. Almeida, A.R., et al., *Echocardiographic assessment of right ventricular contractile reserve in patients with pulmonary hypertension*. Rev Port Cardiol, 2014. **33**(3): p. 155-63.
40. Ryan, T., et al., *An echocardiographic index for separation of right ventricular volume and pressure overload*. J Am Coll Cardiol, 1985. **5**(4): p. 918-27.
41. Bobbio, A., et al., *Changes in pulmonary function test and cardio-pulmonary exercise capacity in COPD patients after lobar pulmonary resection*. Eur J Cardiothorac Surg, 2005. **28**(5): p. 754-8.
42. Van Mieghem, W. and M. Demedts, *Cardiopulmonary function after lobectomy or pneumonectomy for pulmonary neoplasm*. Respir Med, 1989. **83**(3): p. 199-206.
43. Wang, J.S., R.T. Abboud, and L.M. Wang, *Effect of lung resection on exercise capacity and on carbon monoxide diffusing capacity during exercise*. Chest, 2006. **129**(4): p. 863-72.
44. *The Criteria Committee of the New York Heart Association*. Nomenclature and Criteria for Diagnosis of Diseases of the Heart and Great Vessels. 9th ed. Boston, Mass: Little, Brown & Co, 1994: p. 253-256.
45. Oken, M.M., et al., *Toxicity and response criteria of the Eastern Cooperative Oncology Group*. Am J Clin Oncol, 1982. **5**(6): p. 649-55.
46. Stenton, C., *The MRC breathlessness scale*. Occup Med (Lond), 2008. **58**(3): p. 226-7.
47. Becher, H., et al., *BSE procedure guidelines for the clinical application of stress echocardiography, recommendations for performance and interpretation of stress echocardiography: a report of the British Society of Echocardiography Policy Committee*. Heart, 2004. **90 Suppl 6**: p. vi23-30.

Appendix 2.4 Ethical approval

NHS
Health Research Authority
East of England - Cambridge Central Research Ethics Committee
Royal Standard Place
Nottingham
NG1 6FS

11 April 2017

Dr Ben Shelley
Golden Jubilee National Hospital
Beardmore Street
Clydebank
G81 4HX

Dear Dr Shelley

Study title:	**Assessment of right ventricular contractile reserve on exercise following lung resection – a pilot study**
REC reference:	**17/EE/0134**
IRAS project ID:	**218001**

Thank you for your letter of 31/03/2017 responding to the Proportionate Review Sub-Committee's request for changes to the documentation for the above study.

The revised documentation has been reviewed and approved by the sub-committee.

We plan to publish your research summary wording for the above study on the HRA website, together with your contact details. Publication will be no earlier than three months from the date of this favourable opinion letter. The expectation is that this information will be published for all studies that receive an ethical opinion but should you wish to provide a substitute contact point, wish to make a request to defer, or require further information, please contact please contact hra.studyregistration@nhs.net outlining the reasons for your request.

Under very limited circumstances (e.g. for student research which has received an unfavourable opinion), it may be possible to grant an exemption to the publication of the study.

Confirmation of ethical opinion

On behalf of the Committee, I am pleased to confirm a favourable ethical opinion for the above research on the basis described in the application form, protocol and supporting documentation as revised.

Conditions of the favourable opinion

The REC favourable opinion is subject to the following conditions being met prior to the start of the study.

Management permission must be obtained from each host organisation prior to the start of the study at the site concerned.

Management permission should be sought from all NHS organisations involved in the study in accordance with NHS research governance arrangements. Each NHS organisation must confirm through the signing of agreements and/or other documents that it has given permission for the research to proceed (except where explicitly specified otherwise).

Guidance on applying for HRA Approval (England)/ NHS permission for research is available in the Integrated Research Application System, www.hra.nhs.uk or at http://www.rdforum.nhs.uk.

Where a NHS organisation's role in the study is limited to identifying and referring potential participants to research sites ("participant identification centre"), guidance should be sought from the R&D office on the information it requires to give permission for this activity.

For non-NHS sites, site management permission should be obtained in accordance with the procedures of the relevant host organisation.

Sponsors are not required to notify the Committee of management permissions from host organisations.

Registration of Clinical Trials

All clinical trials (defined as the first four categories on the IRAS filter page) must be registered on a publically accessible database. This should be before the first participant is recruited but no later than 6 weeks after recruitment of the first participant.

There is no requirement to separately notify the REC but you should do so at the earliest opportunity e.g. when submitting an amendment. We will audit the registration details as part of the annual progress reporting process.

To ensure transparency in research, we strongly recommend that all research is registered but for non-clinical trials this is not currently mandatory.

If a sponsor wishes to request a deferral for study registration within the required timeframe, they should contact hra.studyregistration@nhs.net. The expectation is that all clinical trials will be registered, however, in exceptional circumstances non registration may be permissible with prior agreement from the HRA. Guidance on where to register is provided on the HRA website.

It is the responsibility of the sponsor to ensure that all the conditions are complied with before the start of the study or its initiation at a particular site (as applicable).

Ethical review of research sites

The favourable opinion applies to all NHS sites taking part in the study, subject to management permission being obtained from the NHS/HSC R&D office prior to the start of the study (see "Conditions of the favourable opinion" above).

Approved documents

Appendix 2.4 - Right ventricular contractile reserve following lung resection, Ethical approval

The documents reviewed and approved by the Committee are:

Document	*Version*	*Date*
GP/consultant information sheets or letters [GP letter]	1	06 March 2017
Letter from sponsor [Ernest Leech Sponsor Letter]		
Non-validated questionnaire [Pt satisfaction exercise echocardiography]	1	06 March 2017
Participant consent form [Consent Form]	1	06 March 2017
Participant information sheet (PIS) [Patient Info Sheet]	2	28 March 2017
REC Application Form [REC_Form_10032017]		10 March 2017
Research protocol or project proposal [Assessment of RV contractile reserve on exercise following lung resection protocol]	1	07 March 2017
Summary CV for Chief Investigator (CI) [CV Shelley]		13 March 2017
Summary CV for supervisor (student research) [CV - Adam Glass]		22 February 2017
Validated questionnaire [Self reported functional status]		06 March 2017

Statement of compliance

The Committee is constituted in accordance with the Governance Arrangements for Research Ethics Committees and complies fully with the Standard Operating Procedures for Research Ethics Committees in the UK.

After ethical review

Reporting requirements

The attached document "After ethical review – guidance for researchers" gives detailed guidance on reporting requirements for studies with a favourable opinion, including:

- Notifying substantial amendments
- Adding new sites and investigators
- Notification of serious breaches of the protocol
- Progress and safety reports
- Notifying the end of the study

The HRA website also provides guidance on these topics, which is updated in the light of changes in reporting requirements or procedures.

Feedback

You are invited to give your view of the service that you have received from the Research Ethics Service and the application procedure. If you wish to make your views known please use the feedback form available on the HRA website:
http://www.hra.nhs.uk/about-the-hra/governance/quality-assurance

We are pleased to welcome researchers and R & D staff at our RES Committee members' training days – see details at http://www.hra.nhs.uk/hra-training/

Appendix 2.4 - Right ventricular contractile reserve following lung resection, Ethical approval

17/EE/0134	Please quote this number on all correspondence

With the Committee's best wishes for the success of this project.

Yours sincerely

Revd Dr Derek Fraser
Chair

Email: NRESCommittee.EastofEngland-CambridgeCentral@nhs.net

Enclosures: *"After ethical review – guidance for researchers"*

Copy to: *Dr Adam Glass*

Dr Catherine Sinclair, NWTC Board

Appendix 3 Right ventricular inflammation after lung resection

Appendix 3.1 Funding application

NATIONAL INSTITUTE FOR ACADEMIC ANAESTHESIA

ACTACC FUNDED PROJECT GRANT – up to £15,000

Name of Applicant: Dr Ben Shelley .....

Email address: b.shelley@clinmed.gla.ac.uk.....

Position and Department: Consultant in Cardiothoracic Anaesthesia and Intensive Care, Golden Jubilee National Hospital

Department in which the Project will be conducted (if different) .....

Head of Department: Academic - Professor John Kinsella, NHS – Dr Jacqueline Church.....

Names and appointments of any collaborators:

Co-Investigator:

Dr Adam Glass
Clinical Research Fellow
Golden Jubilee National Hospital
Beardmore Street
Clydebank G81 4HX
Tel: 0141 9515000
E-mail: aglass01@doctors.org

Co-Investigator:

Dr Philip McCall
Postgraduate Research Student
Academic Unit of Anaesthesia
Level 4, Walton Building
Glasgow Royal Infirmary
84 Castle Street
Glasgow G4 OSF
Tel: 0141 2114625
E-mail: philipmccall@nhs.net

Co-Investigator:

Professor John Kinsella
Professor and Head of Academic Unit of Anaesthesia
Level 4, Walton Building
Glasgow Royal Infirmary
84 Castle Street
Glasgow G4 OSF
Tel: 0141 2114625
E-Mail: john.kinsella@glasgow.ac.uk

Co-investigator & Lead Surgeon:

Mr Alan Kirk
Consultant Cardiothoracic Surgeon
Golden Jubilee National Hospital
Beardmore Street
Clydebank G81 4HX
Tel: 0141 9515000
E-mail: Alan.Kirk@gjnh.scot.nhs.uk

Appendix 3.1 - Right ventricular inflammation after lung resection Funding application

Dr Ben Shelley - Right ventricular inflammation after lung resection.

Co-investigator & Lead Cardiologist: Prof Colin Berry
Consultant Cardiologist
Golden Jubilee National Hospital
Beardmore Street
Clydebank G81 4HX
Tel: 0141 9515000
E-mail: Colin.berry@glasgow.ac.uk

Co-investigator & MRI Physicist Dr Aleksandra Radjenovic
Senior Lecturer in MRI
Institute of Cardiovascular & Medical Sciences
BHF Glasgow Cardiovascular Research Centre
University of Glasgow
126 University Place
Glasgow, G12 8TA
Tel: +44 (0)141 330 3006
Email: Aleksandra.Radjenovic@Glasgow.ac.uk

Title of proposed research: Right ventricular inflammation after lung resection.
.....
.....

Abstract of proposed research (up to 200 words):

Lung cancer is the leading cause of cancer death within the UK. Surgical resection offers the best chance of cure but is associated with long-term dyspnoea and poor functional capacity. This is poorly associated with changes in respiratory function and maybe influenced by cardiac limitation.

Our research group have demonstrated that right ventricular (RV) function deteriorates following lung resection; a phenomenon widely believed to occur secondarily to increased afterload. In animal models acute increases in RV afterload stimulate neutrophil/macrophage infiltration leading to inflammation and fibrosis. Chronic increases in afterload lead to RV hypertrophy, paradoxical septal movement and RV failure. Our previous study also demonstrated increased afterload and paradoxical septal movement following lung resection.

We hypothesise that abrupt afterload changes occurring intra-operatively and early post-operatively trigger an acute inflammatory RV injury, which is sustained long into the post-operative period by altered flow dynamics within the pulmonary vasculature.

Fifteen patients will undergo sequential cardiac magnetic resonance with T1 mapping, a non-invasive method of assessing myocardial inflammation/fibrosis. We will assess the presence of post-operative RV inflammation and its association to post-operative RV dysfunction. Peri-operative RV protection may provide a therapeutic opportunity, preventing RV dysfunction and ameliorating disabling decreases in functional capacity post-operatively.

Appendix 3.1 - Right ventricular inflammation after lung resection Funding application

Dr Ben Shelley - Right ventricular inflammation after lung resection.

Structured lay abstract (up to 500 words):

Introduction

Lung cancer is the second most common cancer in the UK and is the leading cause of cancer related death. Where appropriate, surgery to remove the tumour and the surrounding lung (lung resection) provides the best chance of cure. Frequently patients are either current or ex-smokers with related lung or heart problems which increase the risks associated with surgery. Following surgery patients may suffer long term shortness of breath, greatly limiting their day-to-day function and lowering quality of life. This shortness of breath is not solely caused by the removal of part of the lung but also from a decrease in the performance of the heart. Although the surgery does not directly involve the heart it is thought that the damage is caused indirectly by the surgery and by the removal of part of the lung.

Function of the heart following lung resection

In a previous study our research group showed that the function of the right side of the heart (the right heart) is decreased following lung resection. The decrease in right heart (the part that supplies blood to the lungs) function was associated with a prolonged stay in the high dependency unit and blood markers indicating damage to the heart. The process by which the damage occurs is poorly understood, but it is thought that an increase in the forces preventing the right heart pumping blood (resistance) is to blame. The decrease in function in the right heart may be caused during surgery by the diminished blood supply to the cancerous lung and, post operatively, as lung resection can cause a long term increase in resistance.

Diseases that cause an increase in resistance to the right heart have been shown to cause damage to different parts of the right heart. An acute increase in resistance can cause inflammation, thinning and scarring whilst a long term increase in resistance causes the right heart to thicken. We believe that the potential damage during the operation will cause permanent damage to the right heart and contribute to shortness of breath and functional limitation.

To investigate the potential inflammation/scarring and the function of the heart we will image the heart with specialised MRI scans. We have used this technique in our previous study with over 80% of patients “easily tolerating the scan” and 84% happy to participate in future research.

Aims

The aim of the research is to determine whether damage occurs in the right heart during and following lung resection and, if so, does it result in scarring. We will compare the function of the right heart before, during and after surgery to determine if the inflammation causes the decrease in right heart function following lung resection. We anticipate that the study will increase our understanding of how the right heart may be damaged by lung resection. We believe this will guide further studies aiming to prevent such damage, ultimately limiting the disabling breathlessness and decrease in heart function that so greatly affects patients’ lives.

Appendix 3.1 - Right ventricular inflammation after lung resection Funding application

4

Dr Ben Shelley - Right ventricular inflammation after lung resection.

Proposed starting date 04/01/17 ..... Estimated duration of research 9 months .....

Signatures: Applicant Date 23/09/16

Head of Department Date. 23/09/16
Prof John Kinsella

Head of Department Date. 23/09/16
Dr Jacqueline Church

Certification by financial officer of proposed institution:

Signature	Position	Date
	R & D Manager GJNH	23/09/16

Appendix 3.1 - Right ventricular inflammation after lung resection Funding application

Dr Ben Shelley - Right ventricular inflammation after lung resection.

TITLE

Right ventricular inflammation after lung resection.

AIMS

1) To assess the feasibility of T1-mapping cardiac magnetic resonance (CMR) investigation of right ventricular (RV) inflammation following lung resection.
2) To determine if inflammation of the RV is present following lung resection.
3) To determine if inflammation observed in the early post-operative period leads to subsequent RV fibrosis.
4) To investigate if inflammation/fibrosis is linked to:
   a) RV function.
   b) Biomarkers of cardiac injury/dysfunction.

BACKGROUND

Introduction

Lung cancer is the leading cause of cancer death in the UK and has the highest regional incidence within Greater Glasgow and Clyde[1, 2]. Where appropriate surgical resection is the first choice treatment; resection rates have risen markedly over the last ten years[3] with a particular increase in elderly patients [4].

Morbidity following lung resection remains high with patients experiencing long term dyspnoea and decreased functional capacity [5, 6]. This decrease in functional capacity is poorly associated with the change in lung function[7] and may be influenced by cardiac limitation[8].

Patients prioritise exercise capacity following lung cancer surgery; patient and public involvement between the (Glasgow) Victoria Infirmary Lung Cancer Support Group and our research group highlighted the challenges faced following 'successful' lung resection. Second only to *"being alive and cancer free"* exercise capacity was the main priority of post-operative patients although they experienced significant impairment of functional capacity. Our research also shows that post-operative patients experience a marked increase in problems with 'mobility' and 'self-care'.

Right ventricular function following lung resection

Right ventricular function has been shown to decrease following lung resection. Our research group has conducted the only sequential CMR study assessing RV function following lung resection[a]. We demonstrated a decrease in right ventricular ejection fraction (RVEF)[b] following lobectomy at day two (POD2) and two months post-op (Figure 1)[9]. A peri-operative decrease in RV function is associated with early and late post-operative complications[10, 11]. In our cohort, RVEF on POD2

[a] 2012 ACTA Project Grant - 'The Pulmonary Vascular / Right Ventricular Response to Lung Resection'. ClinicalTrials.gov identifier - NCT01892800. https://clinicaltrials.gov/show/NCT01892800

[b] We recognise that assessment of RV function is more complex than measurement of RVEF alone, which is dependent on loading conditions. During analysis we also plan to investigate other parameters of RV function and interpret changes in RVEF in the context of indices of preload, contractility (strain) and afterload.

was associated with length of HDU stay ($p<0.05$, $r=-0.61$). In one study impaired RV function intra-operatively identified patients in whom late cardio-respiratory symptoms would develop[12], suggesting peri-operative RV dysfunction may have an impact long into the post-operative period.

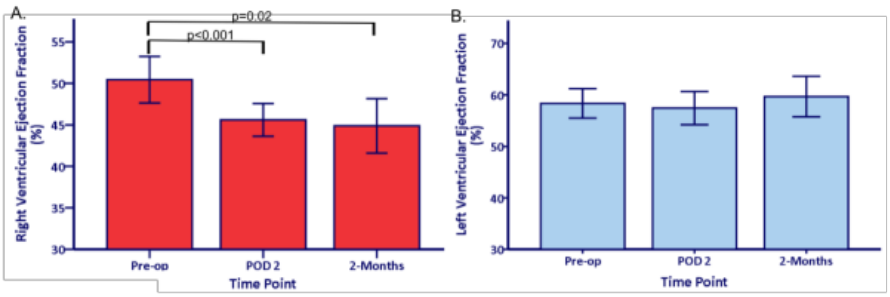

Figure 1. Right ventricular ejection fraction (A) decreases from pre-op levels by post-operative day 2 (POD2), mean absolute decrease of 4.2% (relative decrease of 8.5%) and the decrease remains at two months. Left ventricular ejection fraction (B) was unchanged throughout the study. Error bars 95% confidence intervals. All paired t-tests.

The most intuitive explanation for reduced RVEF is increased afterload. Intra-operatively PVR increases on institution of one-lung ventilation and at PA clamping[13, 14], but this acute increase returns to baseline 24-48 hours post-operatively [14-17] yet RVEF remains depressed at 2 months. Studies using PAP or PVR to assess afterload may not however reflect the full complexity of RV afterload. PVR assesses resistance to steady flow but ignores resistance to pulsatile flow that is responsible for up to half the hydraulic work of the RV[18]. In our previous study we demonstrated increases in pulsatile components of afterload following lobectomy with decreased pulmonary artery acceleration time (PAAT) (Figure 2) and distensibility. Estimated PA systolic pressure was increased at POD2 but not at 2 months ($p<0.05$).

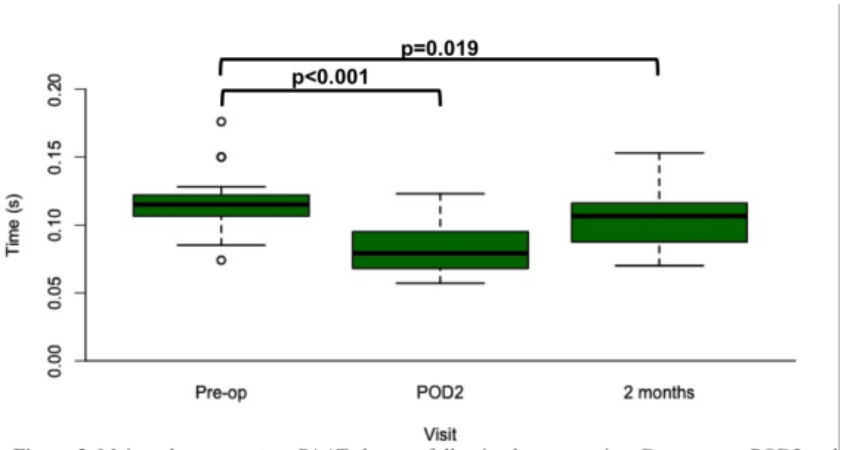

Figure 2. Main pulmonary artery PAAT changes following lung resection. Decrease on POD2 and 2 months post-op in MPA, paired t-tests. PAAT was also decreased at POD2 and 2 months in the operative PA ($p<0.02$).

Appendix 3.1 - Right ventricular inflammation after lung resection

Funding application

Dr Ben Shelley - Right ventricular inflammation after lung resection.

We hypothesise that the well documented abrupt changes in afterload occurring intra-operatively and in the early post-operative period trigger an acute inflammatory RV injury, which is sustained long into the post-operative period by altered flow dynamics and increased 'pulsatile' afterload. Perioperative RV protection may therefore provide a therapeutic opportunity, preventing RV dysfunction and ameliorating disabling decreases in functional capacity post-operatively.

Mechanisms of RV damage secondary to increased afterload

Insights from Pulmonary embolism: RV dysfunction in PE, a syndrome of acutely increased afterload potentially analogous to lung resection, primarily affects the RV free wall and base, sparing the apex. Increased afterload leads to acute RV dilatation, leftward movement of the interventricular septum (IVS), reduced LV filling and LV dysfunction[19-21]. Following PE however the degree of RV dysfunction exhibited is not accounted for by the effects of increased RV afterload or RV ischaemia alone[22].

Evidence from rat models of PE demonstrate an inflammatory response occurring within the RV resulting in decreased contractile function with thinning and scarring of the RV outflow tract[22-25]. Eighteen hours following PE basal segments of the RV show neutrophil/macrophage infiltration[23]. After the initial insult, a secondary macrophage wave occurs which is associated with histological scar formation[24]. Similar RV neutrophil/macrophage infiltration has been seen in human autopsy following fatal PE[26].

Insights from Pulmonary hypertension (PH): In PH the RV is subjected to a gradual increase in afterload leading to RV remodelling and hypertrophy[22]. The RV becomes more concentric with flattening the IVS[27]. Similar to PE, leftward movement of the IVS causes LV dysfunction through reduced diastolic filling and LV end-diastolic volumes[20, 27]. As has been observed following lung resection, in patients with PH exercise causes a further decrease in RVEF with RV dilatation further impairing the LV[15, 28]. This bowing of the IVS can be measured by the eccentricity index (EI), a measure of the deformation of the normally concentric LV[20]. EI is strongly associated with CMR evidence of fibrosis at the ventricular insertion points (VIPs) (Figure 5) which in turn is associated with increased disease severity and RV dysfunction[29-31]. It has been hypothesised that shear stresses from abnormal IVS movement cause fibrosis at VIPs[29].

In our previous study diastolic EI at POD2 and 2 months was significantly associated with RVEF (Figure 3), HDU length of stay and global strain. Decreased RVEF following resection is associated with abnormal septal movement and we hypothesise that fibrosis will be present at the VIPs.

Appendix 3.1 - Right ventricular inflammation after lung resection

Funding application

Dr Ben Shelley - Right ventricular inflammation after lung resection.

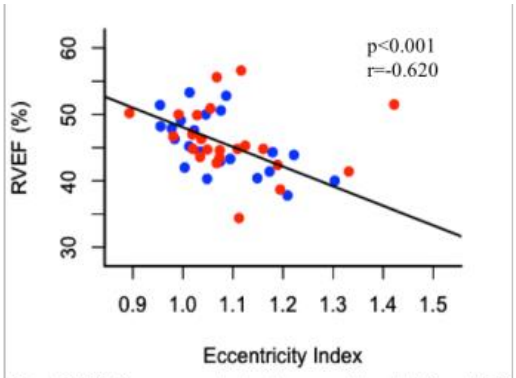

Figure 3. Diastolic EI vs RVEF. Strong association between diastolic EI and POD2 (p<0.005, r=-0.594) (red) and 2 months (p=0.001, r=-0.628) (blue) post-op, Pearson's correlation coefficient.

Assessment of the right ventricle

Cardiac magnetic resonance (CMR) is non-ionising, non-invasive and is the gold standard for RV assessment[32]. In our previous study CMR was well tolerated by patients at all time points with 22/27 patients completing POD2 scanning.

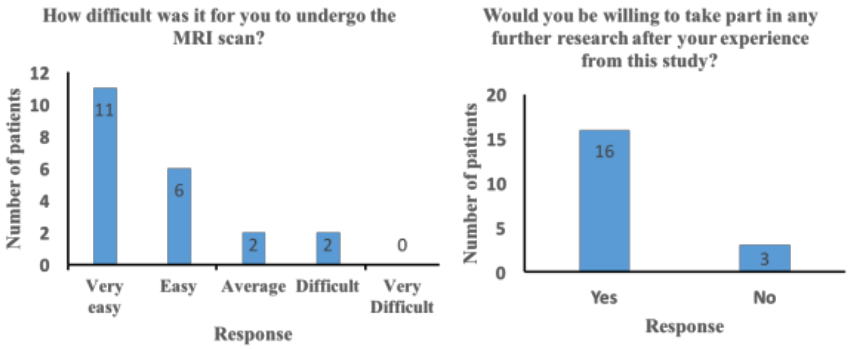

Figure 4. Patient experience of post-operative CMR. Follow-up questionnaire responses from our previous CMR study. 21/27 (78%) patients completed the questionnaire. Neither of the patients who found the MRI scan difficult were unwilling to take part in future studies.

Ventricular function and afterload: CMR can accurately assess ventricular volumes throughout the cardiac cycle allowing ejection fraction calculation. Velocity encoded flow sequences allow measurement of flow, velocity and area changes of the pulmonary arteries[32] and evaluation of afterload[33, 34]. RV contractility can be assessed post-processing with feature tracking strain analysis[35].

Tissue characterisation: T1-mapping is a quantitative method of assessing the magnetic properties of a tissue based on its relaxation time. Taylor et al define T1 relaxation time as "*a measure of how fast the nuclear spin magnetization returns to its equilibrium state after a radiofrequency (RF) pulse"[36]*. Following the RF pulse the magnetisation is measured with sequential imaging

Appendix 3.1 - Right ventricular inflammation after lung resection

Funding application

allowing construction of the T1 recovery curve and therefore T1 from its decay constant (Figure 5)[36-38]. Tissues of different cellular composition and water content will recover at different rates[39]. Native T1 (without contrast) has been shown to increase with oedema and fibrosis[40]. Administration of intravenous contrast (gadolinium) allows calculation of extra-cellular volume (ECV) from T1 values of blood and myocardium pre- and post-contrast. ECV is associated with increased myocardial fibrosis[41] and is predictive of all-cause mortality in cardiomyopathy[42]. In PH, increased T1 and ECV have been demonstrated at the VIP and are associated with both RV function and disease severity[30, 43, 44]. Collaborators in our institution have demonstrated that RV free wall T1 is increased in PH by imaging in systole[45].

Cardiac biomarkers: Troponin and BNP have been shown to increase with acute PE [46-48]. Troponin I is associated with RV dysfunction, adverse outcome and greater segmental obstruction[46, 47] whilst BNP of greater than 100pg/ml is associated with increased mortality[48]. In our study pre-op to POD2 change in BNP was associated with a decrease in RVEF ($p=0.03$, $r=0.47$). Also BNP was higher in patients that had decreased functional capacity post-operatively[49].

Hypothesis

We hypothesise that RV inflammation contributes to the decrement in RV function observed after lung resection and will be revealed by T1 mapping of inflammation/fibrosis.

In exploring this hypothesis we seek to address the following questions:

1) Can RV inflammation be assessed by T1 mapping CMR following lung resection?
2) Is increased T1 (inflammation) present in the RV immediately following lung resection?
3) Does early post-operative inflammation lead to the subsequent development of RV fibrosis?
4) Is oedema/fibrosis associated with changes in
   a) RV function?
   b) Biomarkers of myocardial dysfunction?

Appendix 3.1 - Right ventricular inflammation after lung resection

Funding application

10

Dr Ben Shelley - Right ventricular inflammation after lung resection.

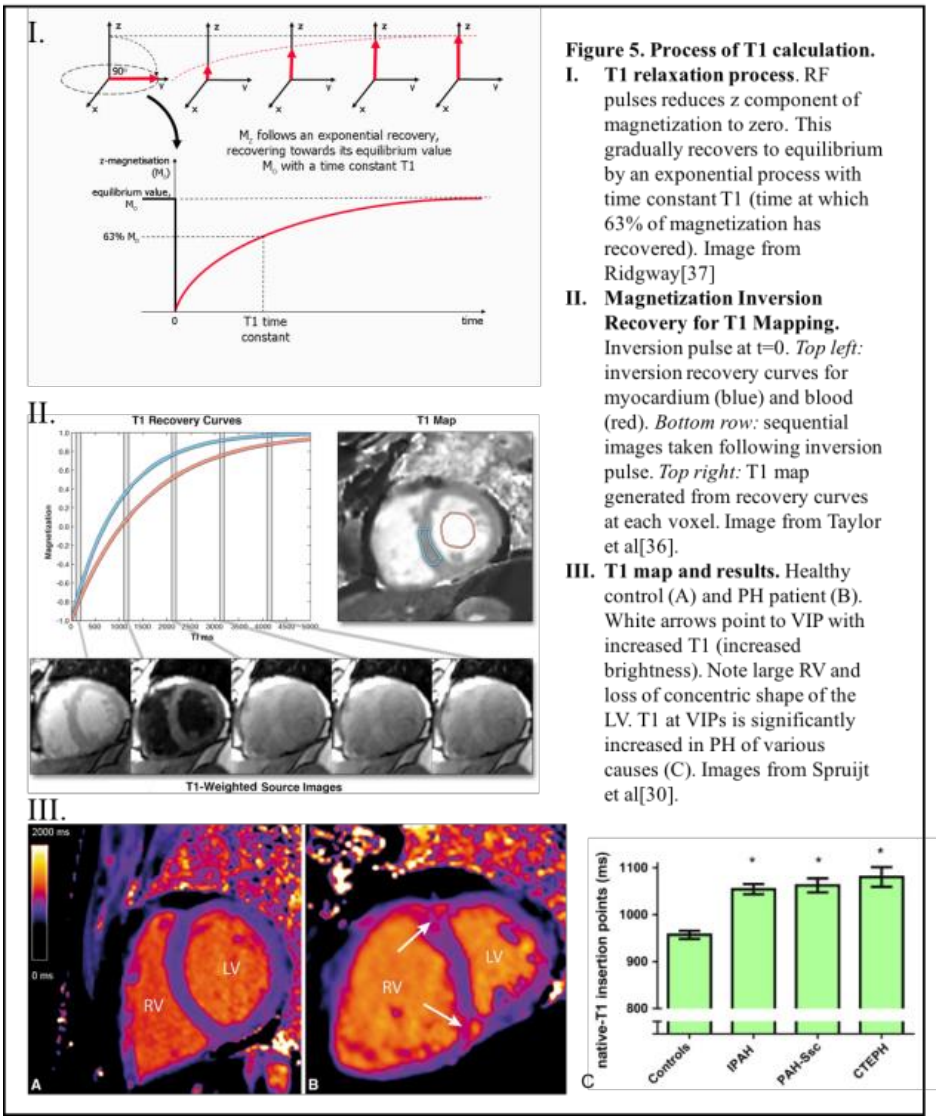

Figure 5. Process of T1 calculation.

I. T1 relaxation process. RF pulses reduces z component of magnetization to zero. This gradually recovers to equilibrium by an exponential process with time constant T1 (time at which 63% of magnetization has recovered). Image from Ridgway[37]

II. Magnetization Inversion Recovery for T1 Mapping. Inversion pulse at t=0. *Top left:* inversion recovery curves for myocardium (blue) and blood (red). *Bottom row:* sequential images taken following inversion pulse. *Top right:* T1 map generated from recovery curves at each voxel. Image from Taylor et al[36].

III. T1 map and results. Healthy control (A) and PH patient (B). White arrows point to VIP with increased T1 (increased brightness). Note large RV and loss of concentric shape of the LV. T1 at VIPs is significantly increased in PH of various causes (C). Images from Spruijt et al[30].

Appendix 3.1 - Right ventricular inflammation after lung resection

Funding application

Dr Ben Shelley - Right ventricular inflammation after lung resection.

EXPERIMENTAL DESIGN

Study design

Prospective observational cohort study of 15 patients presenting for video-assisted thoracoscopic surgery (VATS) lobectomy of primary lung cancer.

Setting

Golden Jubilee National Hospital / West of Scotland Heart and Lung Centre – a NHS tertiary referral cardiothoracic surgical centre (single centre).

Study summary

Patients presenting for VATS lobectomy will undergo CMR assessment of ventricular function, oedema and fibrosis pre-operatively, on POD2 and two months post-operatively. CMR will assess oedema and fibrosis of the ventricles with T1-mapping pre- and post- contrast (gadolinium). RV/LV function, dimensions, strain and flow in the pulmonary arteries (main, left and right) will also be assessed. Contemporaneous blood testing of biomarkers of myocardial dysfunction will be performed (Table 1).

Surgical technique will be standardised to a single surgeon. Anaesthetic technique will be standardised for maintenance, analgesia, vasopressors/inotropes, blood transfusion and fluid management. Such standardisation reflects the normal practice of the individual(s) involved.

Objective and outcome measures

Primary outcome

1) Can RV inflammation be assessed by T1 mapping CMR following lung resection?

Whilst T1 mapping is common practice in the LV its use in the RV is less established. Though all clinical papers investigating RV T1 have been in PH patients with hypertrophied ventricles, T1 in VIPs[30, 44] and in RV free wall have been successfully measured in healthy controls[50]. Whilst we hypothesise we shall observe changes in the RV post-op, these changes are likely to be modest compared to established PH and our pre-op scans will be of relatively healthy hearts. As such, we will focus on the VIPs for our primary end-point as they are most reliably imaged.

Secondary outcomes

1) Is increased T1 (inflammation) present in the RV following lung resection?
2) Does inflammation lead to RV fibrosis?
3) Is oedema/scarring associated with changes in
   a) RV function?
   b) Markers of cardiac inflammation (Table 1)?

Appendix 3.1 - Right ventricular inflammation after lung resection

Funding application

Dr Ben Shelley - Right ventricular inflammation after lung resection.

	Pre-operatively		Lung Resection	Early post-operative period			Follow up
	Recruitment	On admission		Immediately post op	POD 1	POD 2	2 Months
Consent	X						
Baseline demographics	X						
Symptoms / function questionnaires • METS, MRC dyspnoea score, NYHA grade, QoL scoring	X						X
Cardiovascular magnetic resonance • Primary outcome: T1 mapping of VIP • Secondary outcomes: T1 mapping of myocardium, ECV, RVEF, RV strain, afterload and EI.		X				X	X
Biomarkers: • Myocardial dysfunction (Troponin I, BNP, CK-MB, d-Dimer and myoglobin)		X		X	X	X	X
• Renal function (Urea & electrolytes)	X	X			X	X	X
• Haematocrit		X			X	X	X

Table 1 Timescale of proposed observations. Post-operative day (POD).
Haematocrit is required for calculation of ECV.

Appendix 3.1 - Right ventricular inflammation after lung resection

Funding application

Power calculation

Spruijt et al and Reiter et al found similar effect size differences between native T1 at RVIPs in PH vs controls (T1 values differ between studies due to different field strengths):

- Spruijt et al- PH 1060±70ms vs controls 957±27ms, effect size 1.37[30].
- Reiter et al- PH 1298±78ms vs controls 1193±31ms, effect size 1.25[44].

Myocardial infarction (MI) causes a greater difference in native T1 between infarcted myocardium and remote zone (myocardium not directly affected by the infract):

- Carrick et al (collaborators in our institution)- Infarct 1097±52ms vs remote zone 961±25ms effect size 2.36[51].

We hypothesise that the observed difference (effect size) in native T1 observed post-operatively will be modest in comparison to PH or MI. Due to the pilot nature of this study, we have no indicative value from which to calculate power, however as a guide, the effect size for the change in RVEF seen in our previous study was 0.9.

Based on a 2-sided, paired t-test with a significance level of 5% and power of 80%, 12 patients would be required to demonstrate an effect size of 0.9. In our previous study 22/27 (81%) patients completed POD2 scanning. Assuming a minimal sample size of 12 patients, and allowing a margin of 20% for drop outs, 15 patients will be recruited.

Statistical analysis

Primary outcome: Will be assessed through dual reporting of the CMR images and testing intra-/inter-observer variability, previously shown to be exceptionally low ($r_{IC} = 0.96$)[44].

Secondary outcomes: Paired secondary outcomes will be assessed for normality and comparison will be made using a paired *t*-test or Wilcoxon signed ranks test as appropriate. Repeated measures ANOVA or Friedmann's test as appropriate will be used to assess differences between variables repeated over time. Association will be sought between evidence of inflammation/oedema and parameters of RV function and cardiac biomarkers using Pearson correlation coefficient or Spearman's rank correlation coefficient as appropriate.

Appendix 3.1 - Right ventricular inflammation after lung resection Funding application

References

1. *Cancer Research UK. Lung Cancer Key Facts*. 2014 12/05/2016].
2. *National Cancer Intelligence Network. Major resections by cancer site, in England; 2006 to 2010*. 12/05/2016].
3. *Second national thoracic surgery activity & outcomes report*. The Society for Cardiothoracic Surgery in Great Britain & Irealnd; 2011 [cited http://www.scts.org/_userfiles/resources/634558869917493937_Thoracic_2011_FINAL.pdf. 12/05/2016].
4. Riaz, S.P., et al., *Recent trends in resection rates among non-small cell lung cancer patients in England.* Thorax, 2012. **67**(9): p. 811-4.
5. Sarna, L., et al., *Impact of respiratory symptoms and pulmonary function on quality of life of long-term survivors of non-small cell lung cancer.* Chest, 2004. **125**(2): p. 439-45.
6. Larsen, K.R., et al., *Cardiopulmonary function at rest and during exercise after resection for bronchial carcinoma.* Ann Thorac Surg, 1997. **64**(4): p. 960-4.
7. Pelletier, C., L. Lapointe, and P. LeBlanc, *Effects of lung resection on pulmonary function and exercise capacity.* Thorax, 1990. **45**(7): p. 497-502.
8. Nugent, A.M., et al., *Effect of thoracotomy and lung resection on exercise capacity in patients with lung cancer.* Thorax, 1999. **54**(4): p. 334-8.
9. McCall, P., et al., *The right ventricular response to lung resection.* Journal of Cardiothoracic and Vascular Anesthesia, 2016. **30**: p. S23-S24.
10. Matyal, R., et al., *Right Ventricular Echocardiographic Predictors of Postoperative Supraventricular Arrhythmias After Thoracic Surgery: A Pilot Study.* Annals of Thoracic Surgery, 2010. **90**: p. 1080-1087.
11. Kowalewski, J., et al., *Right ventricular morphology and function after pulmonary resection.* Eur J Cardiothorac Surg, 1999. **15**(4): p. 444-8.
12. Lewis, J.W., et al., *Right heart function and prediction of respiratory morbidity in patients undergoing pneumonectomy with moderately severe cardiopulmonary dysfunction.* J Thorac Cardiov Sur, 1994. **108**: p. 169-175.
13. Waller, D.A., et al., *Pulmonary endothelial permeability changes after major lung resection.* Ann Thorac Surg, 1996. **61**(5): p. 1435-40.
14. Lewis, J.W., et al., *Right heart function and prediction of respiratory morbidity in patients undergoing pneumonectomy with moderately severe cardiopulmonary dysfunction.* J Thorac Cardiovasc Surg, 1994. **108**(1): p. 169-75.
15. Okada, M., et al., *Right ventricular dysfunction after major pulmonary resection.* J Thorac Cardiovasc Surg, 1994. **108**(3): p. 503-11.
16. Reed, C.E., B.H. Dorman, and F.G. Spinale, *Mechanisms of right ventricular dysfunction after pulmonary resection.* Ann Thorac Surg, 1996. **62**(1): p. 225-31; discussion 231-2.
17. Bäcklund, M., et al., *Effect of oxygen on pulmonary hemodynamics and incidence of atrial fibrillation after noncardiac thoracotomy.* J Cardiothorac Vasc Anesth, 1998. **12**(4): p. 422-8.
18. Champion, H.C., E.D. Michelakis, and P.M. Hassoun, *Comprehensive invasive and noninvasive approach to the right ventricle-pulmonary circulation unit: state of the art and clinical and research implications.* Circulation, 2009. **120**(11): p. 992-1007.

19. Matthews, J.C. and V. McLaughlin, *Acute right ventricular failure in the setting of acute pulmonary embolism or chronic pulmonary hypertension: a detailed review of the pathophysiology, diagnosis, and management*. Curr Cardiol Rev, 2008. **4**(1): p. 49-59.
20. Ryan, T., et al., *An echocardiographic index for separation of right ventricular volume and pressure overload.* J Am Coll Cardiol, 1985. **5**(4): p. 918-27.
21. Gerges, C., N. Skoro-Sajer, and I.M. Lang, *Right ventricle in acute and chronic pulmonary embolism (2013 Grover Conference series).* Pulm Circ, 2014. **4**(3): p. 378-86.
22. Watts, J.A., M.R. Marchick, and J.A. Kline, *Right ventricular heart failure from pulmonary embolism: key distinctions from chronic pulmonary hypertension.* J Card Fail, 2010. **16**(3): p. 250-9.
23. Watts, J.A., et al., *Cardiac inflammation contributes to right ventricular dysfunction following experimental pulmonary embolism in rats.* J Mol Cell Cardiol, 2006. **41**(2): p. 296-307.
24. Watts, J.A., et al., *Role of inflammation in right ventricular damage and repair following experimental pulmonary embolism in rats.* Int J Exp Pathol, 2008. **89**(5): p. 389-99.
25. Watts, J.A., et al., *Proinflammatory events in right ventricular damage during pulmonary embolism: effects of treatment with ketorolac in rats.* J Cardiovasc Pharmacol, 2009. **54**(3): p. 246-52.
26. Iwadate, K., et al., *Right ventricular damage due to pulmonary embolism: examination of the number of infiltrating macrophages.* Forensic Sci Int, 2003. **134**(2-3): p. 147-53.
27. Chin, K.M., N.H. Kim, and L.J. Rubin, *The right ventricle in pulmonary hypertension.* Coron Artery Dis, 2005. **16**(1): p. 13-8.
28. Holverda, S., et al., *Impaired stroke volume response to exercise in pulmonary arterial hypertension.* J Am Coll Cardiol, 2006. **47**(8): p. 1732-3.
29. Sato, T., et al., *Paradoxical interventricular septal motion as a major determinant of late gadolinium enhancement in ventricular insertion points in pulmonary hypertension.* PLoS One, 2013. **8**(6): p. e66724.
30. Spruijt, O.A., et al., *Increased native T1-values at the interventricular insertion regions in precapillary pulmonary hypertension.* Int J Cardiovasc Imaging, 2016. **32**(3): p. 451-9.
31. Blyth, K.G., et al., *Contrast enhanced-cardiovascular magnetic resonance imaging in patients with pulmonary hypertension.* Eur Heart J, 2005. **26**(19): p. 1993-9.
32. Bradlow, W.M., J.S. Gibbs, and R.H. Mohiaddin, *Cardiovascular magnetic resonance in pulmonary hypertension.* J Cardiovasc Magn Reson, 2012. **14**: p. 6.
33. Quail, M.A., et al., *Noninvasive pulmonary artery wave intensity analysis in pulmonary hypertension.* Am J Physiol Heart Circ Physiol, 2015. **308**(12): p. H1603-11.
34. Sanz, J., et al., *Evaluation of pulmonary artery stiffness in pulmonary hypertension with cardiac magnetic resonance.* JACC Cardiovasc Imaging, 2009. **2**(3): p. 286-95.
35. Prati, G., et al., *Right Ventricular Strain and Dyssynchrony Assessment in Arrhythmogenic Right Ventricular Cardiomyopathy: Cardiac Magnetic Resonance*

Feature-Tracking Study. Circ Cardiovasc Imaging, 2015. **8**(11): p. e003647; discussion e003647.

36. Taylor, A.J., et al., *T1 Mapping: Basic Techniques and Clinical Applications.* JACC Cardiovasc Imaging, 2016. **9**(1): p. 67-81.
37. Ridgway, J.P., *Cardiovascular magnetic resonance physics for clinicians: part I.* J Cardiovasc Magn Reson, 2010. **12**: p. 71.
38. Messroghli, D.R., et al., *Modified Look-Locker inversion recovery (MOLLI) for high-resolution T1 mapping of the heart*. Magn Reson Med, 2004. **52**(1): p. 141-6.
39. Cameron, I.L., V.A. Ord, and G.D. Fullerton, *Characterization of proton NMR relaxation times in normal and pathological tissues by correlation with other tissue parameters*. Magn Reson Imaging, 1984. **2**(2): p. 97-106.
40. Bull, S., et al., *Human non-contrast T1 values and correlation with histology in diffuse fibrosis.* Heart, 2013. **99**(13): p. 932-7.
41. Flett, A.S., et al., *Equilibrium contrast cardiovascular magnetic resonance for the measurement of diffuse myocardial fibrosis: preliminary validation in humans.* Circulation, 2010. **122**(2): p. 138-44.
42. Wong, T.C., et al., *Association between extracellular matrix expansion quantified by cardiovascular magnetic resonance and short-term mortality*. Circulation, 2012. **126**(10): p. 1206-16.
43. García-Álvarez, A., et al., *Association of myocardial T1-mapping CMR with hemodynamics and RV performance in pulmonary hypertension.* JACC Cardiovasc Imaging, 2015. **8**(1): p. 76-82.
44. Reiter, U., et al., *Native myocardial T1 mapping in pulmonary hypertension: correlations with cardiac function and hemodynamics*. Eur Radiol, 2016.
45. Jayasekera, G., et al., *Right Ventricular free wall myocardial tissue characterisation by systolic Cardiac Magnetic Resonance T1 mapping in pulmonary hypertension.* Journal of Cardiovascular Magnetic Resonance, 2016. **18**(1): p. 1-2.
46. Walter, T., et al., *Predictive value of high-sensitivity troponin I and D-dimer assays for adverse outcome in patients with acute pulmonary embolism*. Exp Ther Med, 2013. **5**(2): p. 586-590.
47. Meyer, T., et al., *Cardiac troponin I elevation in acute pulmonary embolism is associated with right ventricular dysfunction.* J Am Coll Cardiol, 2000. **36**(5): p. 1632-6.
48. Kline, J.A., et al., *Comparison of 8 biomarkers for prediction of right ventricular hypokinesis 6 months after submassive pulmonary embolism*. Am Heart J, 2008. **156**(2): p. 308-14.
49. McCall, P., et al., *Perioperative BNP changes and functional capacity following lung resection*. Journal of Cardiothoracic and Vascular Anesthesia, 2016. **30**: p. S26-S27.
50. Kawel-Boehm, N., et al., *In-vivo assessment of normal T1 values of the right-ventricular myocardium by cardiac MRI.* Int J Cardiovasc Imaging, 2014. **30**(2): p. 323-8.
51. Carrick, D., et al., *Pathophysiology of LV Remodeling in Survivors of STEMI: Inflammation, Remote Myocardium, and Prognosis*. JACC Cardiovasc Imaging, 2015. **8**(7): p. 779-89.

Appendix 3.1 - Right ventricular inflammation after lung resection

Funding application

B: A list of the resources which will be required and which will be provided by the Host Institution.

This study is being coordinated by the Academic Unit of Anaesthesia, Pain and Critical Care Medicine at the University of Glasgow who will provide general infrastructure, office space, secretarial support, computing facilities (including statistical software), secure file storage and technical support. BS is a research affiliate, AG is employed by the unit as a clinical research fellow and JK is head of unit.

Clinical studies will take place in the West of Scotland Heart and Lung Centre / Golden Jubilee National Hospital (GJNH), Clydebank. GJNH is a modern tertiary referral cardiothoracic surgical centre equipped to a high standard with appropriate theatre, critical care, laboratory and radiology facilities. Facilities specifically available at GJNH for the conduct of this study include: office space and computing facilities, on-site Research and Development Service, the Beardmore Health Sciences Research Centre (NHS Scotland's new clinical skills and research centre offering consulting rooms and research laboratory facilities) and electronic patient data recording throughout all theatre and critical care areas.

Feasibility: Lung cancer rates in Glasgow are the highest in the UK. Recent audit data has revealed that GJNH is the largest thoracic surgical unit in the UK performing in excess of 500 resections for primary lung cancer each year. Within our last study we recruited 27 lobectomy patients within one year with 27/43 patients approached enrolling. In this study, we propose to recruit just 15 of this population over a period of 6 months. We feel the shorter timeframe is appropriate as 70% of lung resections carried out within the hospital are by VATS. Target recruitment will be one patient per week with sufficient flexibility to allow for refusals, drop outs and holiday periods.

Equipment:

Cardiovascular Magnetic Resonance will be performed within an existing NHS facility (West of Scotland Heart and Lung Centre / Golden Jubilee National Hospital) by NHS staff. Dedicated research time is available at a non-commercial cost per scan. All appropriate software is available for post-processing. Our collaborators and CMR technicians are experienced in performing T1 mapping, have helped developed imaging protocols/methods and have published in this field.

Estimated running costs:

The principal applicant (BS) will be employed for the duration of the project by the National Health Service Scotland. AG will be employed by the University of Glasgow as is JK, CB and AR. Co-investigator AK is employed by the National Health Service Scotland. Support for NHS staff costs (1-2 hours per week for the duration of the project) is covered by NHS Scotland Research and Development under the terms of NHS Scotland's NHS (research) Support Costs policy.

Appendix 3.1 - Right ventricular inflammation after lung resection

Funding application

AG is employed as a clinical research fellow based at the Golden Jubilee National Hospital and will undertake the day-to-day running of the study. It will form the bulk of his research work for its duration. The study and results will be included in his MD entitled "Mechanisms of right ventricular dysfunction following lung resection" which he is currently undertaking with the University of Glasgow.

No additional costs are anticipated over and above those for which application is made.

Ethics Committee approval:

Research Ethics Committees now require evidence of successful peer review. We will therefore seek approval from the West of Scotland REC once we have funding. The applicants are familiar with ethics procedures. We anticipate no problems obtaining approval.

Any resources still to be obtained but not yet funded:

Nil.

Appendix 3.1 - Right ventricular inflammation after lung resection Funding application

Dr Ben Shelley - Right ventricular dysfunction following lung resection, the role of inflammation.

C. Justification for support requested.

Budget justification

Direct costs – staff: Nil

Other direct costs – additional investigations:

(These investigations are research costs over and above direct clinical care costs.)

	Unit cost (£)	**No. / Patient**	**Units required**	**Subtotal / patient (£)**	**Subtotal / study (£) n=15**
Cardiac magnetic resonance imaging CMR scanning will be carried out at GJNH. Dedicated research time is available at a non-commercial cost per scan.	225	3	-	675	10125
Measurement of biomarkers Blood samples for (Troponin I, BNP, CK-MB, d-Dimer and myoglobin) measurement will be analysed using the Alere Triage® PROFILER SOB Panel system (Alere Ltd. Stockport, UK). Hardware is being provided on loan by Alere Ltd - application is made for the cost of consumables only. £470 for 25 tests. (Appendix 2)	18.8	5	-	94	1410

Appendix 3.1 - Right ventricular inflammation after lung resection Funding application

Control panel for biomarkers Alere controls panels required. £191 per 25 tests.	191	-	3	-	573
Subtotal					**12108**

Other direct costs – Misc:

	Unit cost (£)	**No. / Patient**	**Units required**	**Subtotal / patient (£)**	**Subtotal / study (£)**
Photocopying, stationary, printing	250	-	1	-	250
Subtotal					**250**

Total **£12358**

Appendix 3.1 - Right ventricular inflammation after lung resection Funding application

Dr Ben Shelley - Right ventricular dysfunction following lung resection, the role of inflammation.

Appendix 1

Name of Applicant. Dr Ben Shelley……

Details of grant requested

A. STAFF

Staff category: Nil

Grade:

		£
(i)	Salary	
(ii)	Employer's contributions in respect of superannuation and national insurance (where applicable)	
Total staff costs		0

B. EQUIPMENT

£

Continued….

Appendix 3.1 - Right ventricular inflammation after lung resection

Funding application

Dr Ben Shelley - Right ventricular dysfunction following lung resection, the role of inflammation.

Appendix 1 Continued

C. EXPENSES

(a) Materials and consumables	£
Measurement of biomarkers – consumables from Alere	
Blood tests	1410
Controls	573

(b) Animals	£
Purchase	
No application made	
Maintenance	

(c) Other expenses	£
Cardiac magnetic resonance imaging	10125
Miscellaneous – photocopying and printing.	250
TOTAL GRANT REQUESTED	£12358

(Requests for purchase of equipment must be accompanied by three competitive quotations for pricing or where restricted supplier this must be stated.)

Is funding for this project being sought from other bodies? If so, please provide details.

No

Appendix 3.2 Confirmation of funding

09-Dec-2016

YOU MAY BE RECEIVING THIS MAIL IN COPY FOR INFORMATION ONLY

Dear Dr. Glass:

The NIAA grants committee met yesterday to consider your application for ACTACC funding. I am delighted to be able to inform you that your application was recommended for support in full. However ACTACC had insufficient funds to cover the award in full so the difference was made up by AAGBI/Anaesthesia as follows; I hope that you will approve. ACTACC-£7,700; AAGBI/Anaesthesia-£4,658; Total as in application £12,358

This e.mail is a formal notification of funding for which we would request an acceptance e.mail (cc to ACTACC and AAGBI). Please note that if we do not hear from you within two weeks of the date of this award notification then the award will be withdrawn.

For your information I attach a copy of your peer review.

Please find below a copy of the peer review associated with your application and note that the abstracts from your application will posted onto the NIAA (and partner). Please have a look it and let me know if there are any (small) changes that you may wish to make.

In order to claim the funding you (or your finance office) will need to contact ACTACC/AAGBI directly and for your information I copy the relevant details below. There may be some additional conditions (e.g., the need for interim/final reports) that the project funder will provide.

All funding queries (and especially finance office claims) should be directed to ACTACC/AAGBI and NOT NIAA.

Contact for ACTACC: John.Kendall@lhch.nhs.uk
Contact for AAGBI: secretariat@aagbi.org

Successful applicants should contact their CLRN as soon as the award is made and work with them to obtain NIHR portfolio approval and support.

To find out which NIAA grants are recognised for inclusion on the NIHR portfolio click here:
http://www.niaa.org.uk/article.php?newsid=877

To find out more about your local CLRN click here:
http://www.crn.nihr.ac.uk/networks/

On behalf of NIAA and its funding partners I would like to congratulate you on the quality of your application and look forward to seeing your results published.

With kind regards

Sincerely,
Prof. David Lambert
Grants Officer, NIAA e-grants
dgl3@leicester.ac.uk

Reviewer(s)' Comments to Applicant:
Reviewer: 1

Comments to the Applicant
This is a well written and clearly set out pilot project to detect whether inflammation occurs in the the RV following lobectomy/pneumonectomy.

The technique of T1 mapping is well established in assessment of the LV, both for detection of oedema and and quantification of extracellular volume, (a surrogate of interstitial fibrosis).
The major weakness of the application is the sptial resolution of current t1 mapping sequences is low and given that the RV wall is very thin, this inevitably means that partial volume errors (inclusion of blood pool and epicardial fat in quantitative voxels) will significantly affect the results.

Appendix 3.2 - Right ventricular inflammation after lung resection

Confirmation of funding

Reviewer: 2

Comments to the Applicant
MAJOR POINTS:
1. Authors' primary question whether RV inflammation can be assessed by T1 mapping CMR following lung resection is clearly limited by the expectation of only modest information in non-hypertrophied right ventricles. Which strategies will be pursued if T1 mapping does not show anything?
2. Authors need to make clear how T1-mapping can distinguish myocardial fibrosis from myocardial inflammation. Edema may be part of both, therefore a tissue-based analysis would be essential. Have authors EMBs in mind? Unless such data exist, the meaningfulness of MRI is questionable.

MINOR POINTS:
1. Will left heart disease have been sufficiently excluded, e.g. by echo and preoperative coronary catheterization? Some right heart compromise may be the result of increased left ventricular filling pressures after surgical stress.
2. Surgical procedures need to be explained in detail.

Reviewer: 3

Comments to the Applicant
1) The proposal is generally presented. It has a reasonable hypothesis and has clear questions for investigation. However, the units of measurement for the primary outcome (effect size) and the quantifications of multiple sites of measurement of inflammation and fibrosis aren't clear enough. The investigators should explain how they aggregate these data, given that they relate to the main outcomes.

2) The project is simple and deliverable.

3) The applicant has a relevant track record.

4) The costs are mainly for the scans. Other administrative costs are small.
5) The cost effectiveness is reasonable. The results are likely to be useful for £12000 only.

List of References

1. Cancer Research UK. Lung Cancer Key Facts http://www.cancerresearchuk.org/health-professional/cancer-statistics/statistics-by-cancer-type/lung-cancer 2014 [accessed 12/05/2016 http://www.cancerresearchuk.org/health-professional/cancer-statistics/statistics-by-cancer-type/lung-cancer
2. Doll R, Hill AB. The Mortality of Doctors in Relation to Their Smoking Habits. *British Medical Journal* 1954;1(4877):1451-55.
3. Doll R, Hill AB. Smoking and Carcinoma of the Lung. *British Medical Journal* 1950;2(4682):739-48.
4. Treasure T, Russell C, Morton D, et al. Surgical resection of lung cancer England: more operations but no trials to test their effectiveness. *Thorax* 2012;67(9):759-61. doi: 10.1136/thoraxjnl-2012-202006
5. National Institute for Health and Clinical Excellence. Lung Cancer. CG121, 2011.: Available from: https://www.nice.org.uk/guidance/cg121 Date accessed: 12/05/2016; [cited https://www.nice.org.uk/guidance/cg121 12/05/2016].
6. Coleman MP, Forman D, Bryant H, et al. Cancer survival in Australia, Canada, Denmark, Norway, Sweden, and the UK, 1995–2007 (the International Cancer Benchmarking Partnership): an analysis of population-based cancer registry data. *The Lancet* 2011;377(9760):127-38. doi: 10.1016/S0140-6736(10)62231-3
7. Fry WA, Menck HR, Winchester DP. The National Cancer Data Base report on lung cancer. *Cancer* 1996;77(9):1947-55. doi: 10.1002/(sici)1097-0142(19960501)77:9<1947::aid-cncr27>3.0.co;2-z
8. Partridge MR. Thoracic surgery in a crisis. 2002;324(7334):376-77. doi: 10.1136/bmj.324.7334.376
9. Ireland TSfCSiGB. Third National Thoracic Surgery Activity & Outcomes Report https://scts.org/wp-content/uploads/2019/06/Third-thoracic-blue-book-FINAL.pdf2018 [accessed 09/07/2019 2019.
10. Riaz SP, Linklater KM, Page R, et al. Recent trends in resection rates among non-small cell lung cancer patients in England. *Thorax* 2012;67(9):811-4. doi: 10.1136/thoraxjnl-2012-201768
11. Nur U, Quaresma M, De Stavola B, et al. Inequalities in non-small cell lung cancer treatment and mortality. *Journal of Epidemiology and Community Health* 2015;69(10):985-92. doi: 10.1136/jech-2014-205309
12. Riaz SP, Lüchtenborg M, Jack RH, et al. Variation in surgical resection for lung cancer in relation to survival: Population-based study in England 2004–2006. *European Journal of Cancer* 2012;48(1):54-60. doi: 10.1016/j.ejca.2011.07.012
13. Rich AL, Tata LJ, Free CM, et al. Inequalities in outcomes for non-small cell lung cancer: the influence of clinical characteristics and features of the local lung cancer service. *Thorax* 2011;66(12):1078-84. doi: 10.1136/thx.2011.158972
14. Møller H, Coupland VH, Tataru D, et al. Geographical variations in the use of cancer treatments are associated with survival of lung cancer patients. *Thorax* 2018;73(6):530-37. doi: 10.1136/thoraxjnl-2017-210710
15. European Society of Thoracic Surgeons Databse Annual Report 2015 [accessed 23/11/2017

http://www.ests.org/_userfiles/pages/files/ESTS%20201Silver_Book_FULL_PEF.pdf.
16. Young RP, Hopkins RJ, Christmas T, et al. COPD prevalence is increased in lung cancer, independent of age, sex and smoking history. *Eur Respir J* 2009;34(2):380-6. doi: 10.1183/09031936.00144208
17. Salati M, Brunelli A, Decaluwe H, et al. Report from the European Society of Thoracic Surgeons Database 2017: patterns of care and perioperative outcomes of surgery for malignant lung neoplasm. *European Journal of Cardio-Thoracic Surgery* 2017;52(6):1041-48. doi: 10.1093/ejcts/ezx272
18. Shapiro M, Swanson SJ, Wright CD, et al. Predictors of Major Morbidity and Mortality After Pneumonectomy Utilizing The Society for Thoracic Surgeons General Thoracic Surgery Database. *The Annals of Thoracic Surgery* 2010;90(3):927-35. doi: 10.1016/j.athoracsur.2010.05.041
19. O'Dowd C, McRae LA, McMillan DC, et al. Elevated Preoperative C-reactive Protein Predicts Poor Cancer Specific Survival in Patients Undergoing Resection for Non-small Cell Lung Cancer. *Journal of Thoracic Oncology* 2010;5(7):988-92. doi: 10.1097/JTO.0b013e3181da78f9
20. Paul S, Altorki NK, Sheng S, et al. Thoracoscopic lobectomy is associated with lower morbidity than open lobectomy: A propensity-matched analysis from the STS database. *The Journal of Thoracic and Cardiovascular Surgery* 2010;139(2):366-78. doi: 10.1016/j.jtcvs.2009.08.026
21. Cheng D, Downey RJ, Kernstine K, et al. Video-Assisted Thoracic Surgery in Lung Cancer Resection. *Innovations: Technology and Techniques in Cardiothoracic and Vascular Surgery* 2007;2(6):261-92. doi: 10.1097/imi.0b013e3181662c6a
22. Falcoz P-E, Puyraveau M, Thomas P-A, et al. Video-assisted thoracoscopic surgery versus open lobectomy for primary non-small-cell lung cancer: a propensity-matched analysis of outcome from the European Society of Thoracic Surgeon database †. *European Journal of Cardio-Thoracic Surgery* 2016;49(2):602-09. doi: 10.1093/ejcts/ezv154
23. Taioli E, Lee DS, Lesser M, et al. Long-term survival in video-assisted thoracoscopic lobectomy vs open lobectomy in lung-cancer patients: a meta-analysis. 2013;44(4):591-97. doi: 10.1093/ejcts/ezt051
24. Paul S, Isaacs AJ, Treasure T, et al. Long term survival with thoracoscopic versus open lobectomy: propensity matched comparative analysis using SEER-Medicare database. *BMJ : British Medical Journal* 2014;349
25. Lim E, Batchelor T, Shackcloth M, et al. Study protocol for VIdeo assisted thoracoscopic lobectomy versus conventional Open LobEcTomy for lung cancer, a UK multicentre randomised controlled trial with an internal pilot (the VIOLET study). *BMJ Open* 2019;9(10):e029507. doi: 10.1136/bmjopen-2019-029507
26. Jean RA, DeLuzio MR, Kraev AI, et al. Analyzing Risk Factors for Morbidity and Mortality after Lung Resection for Lung Cancer Using the NSQIP Database. *Journal of the American College of Surgeons* 2016;222(6):992-1000.e1. doi: https://doi.org/10.1016/j.jamcollsurg.2016.02.020
27. Pucher PH, Aggarwal R, Qurashi M, et al. Meta-analysis of the effect of postoperative in-hospital morbidity on long-term patient survival. *BJS* 2014;101(12):1499-508. doi: 10.1002/bjs.9615
28. Lugg ST, Agostini PJ, Tikka T, et al. Long-term impact of developing a postoperative pulmonary complication after lung surgery. *Thorax* 2016;71(2):171. doi: 10.1136/thoraxjnl-2015-207697

29. Rueth NM, Parsons HM, Habermann EB, et al. The Long-term Impact of Surgical Complications After Resection of Stage I Nonsmall Cell Lung Cancer: A Population-based Survival Analysis. *Annals of Surgery* 2011;254(2):368-74. doi: 10.1097/SLA.0b013e31822150fe
30. Fernandez FG, Falcoz PE, Kozower BD, et al. The Society of Thoracic Surgeons and The European Society of Thoracic Surgeons General Thoracic Surgery Databases: Joint Standardization of Variable Definitions and Terminology. *The Annals of Thoracic Surgery* 2015;99(1):368-76. doi: 10.1016/j.athoracsur.2014.05.104
31. Shelley BG, McCall PJ, Glass A, et al. Association between anaesthetic technique and unplanned admission to intensive care after thoracic lung resection surgery: the second Association of Cardiothoracic Anaesthesia and Critical Care (ACTACC) National Audit. *Anaesthesia* 2019;74(9):1121-29. doi: 10.1111/anae.14649
32. Kobayashi N, Kobayashi K, Kikuchi S, et al. Long-term pulmonary function after surgery for lung cancer. *Interactive CardioVascular and Thoracic Surgery* 2017;24(5):727-32. doi: 10.1093/icvts/ivw414
33. Kim HK, Lee YJ, Han KN, et al. Pulmonary Function Changes Over 1 Year After Lobectomy in Lung Cancer. *Respiratory Care* 2016;61(3):376. doi: 10.4187/respcare.04284
34. Nezu K, Kushibe K, Tojo T, et al. Recovery and limitation of exercise capacity after lung resection for lung cancer. *Chest* 1998;113(6):1511-6.
35. Funakoshi Y, Takeda S, Sawabata N, et al. Long-term pulmonary function after lobectomy for primary lung cancer. *Asian cardiovascular & thoracic annals* 2005;13(4):311-5. doi: 10.1177/021849230501300404 [published Online First: 2005/11/24]
36. Brunelli A, Xiumé F, Refai M, et al. Evaluation of expiratory volume, diffusion capacity, and exercise tolerance following major lung resection: a prospective follow-up analysis. *Chest* 2007;131(1):141-7. doi: 10.1378/chest.06-1345
37. Brunelli A, Pompili C, Koller M. Changes in Quality of Life After Pulmonary Resection. *Thoracic Surgery Clinics* 2012;22(4):471-85. doi: 10.1016/j.thorsurg.2012.07.006
38. Möller A, Sartipy U. Associations Between Changes in Quality of Life and Survival After Lung Cancer Surgery. *Journal of Thoracic Oncology* 2012;7(1):183-87. doi: 10.1097/JTO.0b013e3182340abb
39. Pompili C, Salati M, Refai M, et al. Preoperative quality of life predicts survival following pulmonary resection in stage I non-small-cell lung cancer†. *European Journal of Cardio-Thoracic Surgery* 2012;43(5):905-10. doi: 10.1093/ejcts/ezs532
40. Poghosyan H, Sheldon LK, Leveille SG, et al. Health-related quality of life after surgical treatment in patients with non-small cell lung cancer: A systematic review. *Lung Cancer* 2013;81(1):11-26. doi: https://doi.org/10.1016/j.lungcan.2013.03.013
41. Vainshelboim B, Fox BD, Saute M, et al. Limitations in exercise and functional capacity in long-term postpneumonectomy patients. *J Cardiopulm Rehabil Prev* 2015;35(1):56-64. doi: 10.1097/HCR.0000000000000085
42. Nugent AM, Steele IC, Carragher AM, et al. Effect of thoracotomy and lung resection on exercise capacity in patients with lung cancer. *Thorax* 1999;54(4):334-8.

43. Wang JS, Abboud RT, Wang LM. Effect of lung resection on exercise capacity and on carbon monoxide diffusing capacity during exercise. *Chest* 2006;129(4):863-72. doi: 10.1378/chest.129.4.863
44. Bobbio A, Chetta A, Carbognani P, et al. Changes in pulmonary function test and cardio-pulmonary exercise capacity in COPD patients after lobar pulmonary resection. *Eur J Cardiothorac Surg* 2005;28(5):754-8. doi: 10.1016/j.ejcts.2005.08.001
45. Bolliger CT, Jordan P, Solèr M, et al. Pulmonary function and exercise capacity after lung resection. *Eur Respir J* 1996;9(3):415-21.
46. Van Mieghem W, Demedts M. Cardiopulmonary function after lobectomy or pneumonectomy for pulmonary neoplasm. *Respir Med* 1989;83(3):199-206.
47. Sarna L, Evangelista L, Tashkin D, et al. Impact of respiratory symptoms and pulmonary function on quality of life of long-term survivors of non-small cell lung cancer. *Chest* 2004;125(2):439-45.
48. Okada M, Ishii N, Yamashita C, et al. Right ventricular ejection fraction in the preoperative risk evaluation of candidates for pulmonary resection. *J Thorac Cardiovasc Surg* 1996;112(2):364-70. doi: 10.1016/S0022-5223(96)70263-5
49. Okada M, Ota T, Matsuda H, et al. Right ventricular dysfunction after major pulmonary resection. *J Thorac Cardiovasc Surg* 1994;108(3):503-11.
50. Larsen KR, Svendsen UG, Milman N, et al. Cardiopulmonary function at rest and during exercise after resection for bronchial carcinoma. *Ann Thorac Surg* 1997;64(4):960-4.
51. Pelletier C, Lapointe L, LeBlanc P. Effects of lung resection on pulmonary function and exercise capacity. *Thorax* 1990;45(7):497-502.
52. Markos J, Mullan BP, Hillman DR, et al. Preoperative assessment as a predictor of mortality and morbidity after lung resection. *Am Rev Respir Dis* 1989;139(4):902-10. doi: 10.1164/ajrccm/139.4.902
53. Corris PA, Ellis DA, Hawkins T, et al. Use of radionuclide scanning in the preoperative estimation of pulmonary function after pneumonectomy. *Thorax* 1987;42(4):285-91.
54. Miyoshi S, Yoshimasu T, Hirai T, et al. Exercise capacity of thoracotomy patients in the early postoperative period. *Chest* 2000;118(2):384-90.
55. Nagamatsu Y, Maeshiro K, Kimura NY, et al. Long-term recovery of exercise capacity and pulmonary function after lobectomy. *J Thorac Cardiovasc Surg* 2007;134(5):1273-8. doi: 10.1016/j.jtcvs.2007.06.025
56. Win T, Groves AM, Ritchie AJ, et al. The effect of lung resection on pulmonary function and exercise capacity in lung cancer patients. *Respir Care* 2007;52(6):720-6.
57. Brunelli A, Kim AW, Berger KI, et al. Physiologic evaluation of the patient with lung cancer being considered for resectional surgery: Diagnosis and management of lung cancer, 3rd ed: American College of Chest Physicians evidence-based clinical practice guidelines. *Chest* 2013;143(5 Suppl):e166S-90S. doi: 10.1378/chest.12-2395
58. Reed CE, Dorman BH, Spinale FG. Mechanisms of right ventricular dysfunction after pulmonary resection. *Ann Thorac Surg* 1996;62(1):225-31; discussion 31-2.
59. Reed CE, Dorman BH, Spinale FG. Assessment of right ventricular contractile performance after pulmonary resection. *Ann Thorac Surg* 1993;56(3):426-31; discussion 31-2.
60. Reed CE, Spinale FG, Crawford FA. Effect of pulmonary resection on right ventricular function. *Ann Thorac Surg* 1992;53(4):578-82.

61. Boldt J, Müller M, Uphus D, et al. Cardiorespiratory changes in patients undergoing pulmonary resection using different anesthetic management techniques. *Journal of cardiothoracic and vascular anesthesia* 1996;10(7):854-59.
62. Elrakhawy H, Alassal M, Shaalan A, et al. Impact of Major Pulmonary Resections on Right Ventricular Function: Early Postoperative Changes2017.
63. Lewis JW, Bastanfar M, Gabriel F, et al. Right heart function and prediction of respiratory morbidity in patients undergoing pneumonectomy with moderately severe cardiopulmonary dysfunction. *J Thorac Cardiovasc Surg* 1994;108(1):169-75.
64. Mageed NA, El-Ghonaimy YAF, Elgamal M-AF, et al. Acute effects of lobectomy on right ventricular ejection fraction and mixed venous oxygen saturation. *Ann Saudi Med* 2005;25(6):481-85. doi: 10.5144/0256-4947.2005.481
65. Bäcklund M, Laasonen L, Lepäntalo M, et al. Effect of oxygen on pulmonary hemodynamics and incidence of atrial fibrillation after noncardiac thoracotomy. *J Cardiothorac Vasc Anesth* 1998;12(4):422-8.
66. Mikami I, Koizumi K, Tanaka S. Changes in right ventricular performance in elderly patients who underwent lobectomy using video-assisted thoracic surgery for primary lung cancer. *The Japanese Journal of Thoracic and Cardiovascular Surgery* 2001;49(3):153-59. doi: 10.1007/BF02913593
67. Nishimura H, Haniuda M, Morimoto M, et al. Cardiopulmonary function after pulmonary lobectomy in patients with lung cancer. *Ann Thorac Surg* 1993;55(6):1477-84.
68. Miyazawa M, Haniuda M, Nishimura H, et al. Longterm effects of pulmonary resection on cardiopulmonary function 1. *Journal of the American College of Surgeons* 1999;189(1):26-33. doi: 10.1016/S1072-7515(99)00071-X
69. Waller DA, Keavey P, Woodfine L, et al. Pulmonary endothelial permeability changes after major lung resection. *Ann Thorac Surg* 1996;61(5):1435-40.
70. Amar D, Burt ME, Roistacher N, et al. Value of perioperative Doppler echocardiography in patients undergoing major lung resection. *The Annals of thoracic surgery* 1996;61(2):516-20.
71. Amar D, Roistacher N, Burt M, et al. Clinical and Echocardiographic Correlates of Symptomatic Tachydysrhythmias After Noncardiac Thoracic Surgery. *CHEST* 1995;108(2):349-54. doi: 10.1378/chest.108.2.349
72. Kowalewski J, Brocki M, Dryjański T, et al. Right ventricular morphology and function after pulmonary resection. *Eur J Cardiothorac Surg* 1999;15(4):444-8.
73. Foroulis CN, Kotoulas CS, Kakouros S, et al. Study on the late effect of pneumonectomy on right heart pressures using Doppler echocardiography. *Eur J Cardiothorac Surg* 2004;26(3):508-14. doi: 10.1016/j.ejcts.2004.05.036
74. Venuta F, Sciomer S, Andreetti C, et al. Long-term Doppler echocardiographic evaluation of the right heart after major lung resections. *Eur J Cardiothorac Surg* 2007;32(5):787-90. doi: 10.1016/j.ejcts.2007.07.033
75. Andaluz-Ojeda D, Gandía F, Duque JL, et al. Biomarkers and Echocardiography in the Postoperative Course of Pulmonary Resection Surgery. 2011;01(01):1-8. doi: 10.4236/ojts.2011.11001
76. Mandal B DV, Kumar B, Kumar A, Ganesan R, Bhat IH. Echocardiographic Evaluation of Right Ventricular Function in the Immediate Postoperative

Period after Major Pulmonary Resections: A Prospective Observational Study. *Journal of Perioperative Echocardiography* 2017;5((2):42-48)
77. Potaris K, Athanasiou A, Konstantinou M, et al. Pulmonary hypertension after pneumonectomy for lung cancer. *Asian Cardiovascular and Thoracic Annals* 2014;22(9):1072-79. doi: 10.1177/0218492314527992
78. Pedoto A, Amar D. Right heart function in thoracic surgery: role of echocardiography. *Curr Opin Anaesthesiol* 2009;22(1):44-9. doi: 10.1097/ACO.0b013e32831d7b72
79. Heerdt P, Malhotra J. The right ventricular response to lung resection. Progress in Thoracic Anesthesia, A Society of Cardiovascular Anesthesiologists Monograph: Lippincott Williams and Wilkins, Philadelphia, PA 2004:221-47.
80. Champion HC, Michelakis ED, Hassoun PM. Comprehensive invasive and noninvasive approach to the right ventricle-pulmonary circulation unit: state of the art and clinical and research implications. *Circulation* 2009;120(11):992-1007. doi: 10.1161/CIRCULATIONAHA.106.674028
81. Voelkel NF, Quaife RA, Leinwand LA, et al. Right Ventricular Function and Failure. *Report of a National Heart, Lung, and Blood Institute Working Group on Cellular and Molecular Mechanisms of Right Heart Failure* 2006;114(17):1883-91. doi: 10.1161/circulationaha.106.632208
82. Lahm T, Douglas IS, Archer SL, et al. Assessment of Right Ventricular Function in the Research Setting: Knowledge Gaps and Pathways Forward. An Official American Thoracic Society Research Statement. *American journal of respiratory and critical care medicine* 2018;198(4):e15-e43. doi: 10.1164/rccm.201806-1160ST
83. Haddad F, Hunt SA, Rosenthal DN, et al. Right ventricular function in cardiovascular disease, part I: Anatomy, physiology, aging, and functional assessment of the right ventricle. *Circulation* 2008;117(11):1436-48. doi: 10.1161/CIRCULATIONAHA.107.653576
84. Haddad F, Doyle R, Murphy DJ, et al. Right ventricular function in cardiovascular disease, part II: pathophysiology, clinical importance, and management of right ventricular failure. *Circulation* 2008;117(13):1717-31. doi: 10.1161/CIRCULATIONAHA.107.653584
85. Ho SY, Nihoyannopoulos P. Anatomy, echocardiography, and normal right ventricular dimensions. *Heart* 2006;92 Suppl 1:i2-13. doi: 10.1136/hrt.2005.077875
86. Sheehan F, Redington A. The right ventricle: anatomy, physiology and clinical imaging. *Heart* 2008;94(11):1510-15. doi: 10.1136/hrt.2007.132779
87. Lorenz CH, Walker ES, Morgan VL, et al. Normal human right and left ventricular mass, systolic function, and gender differences by cine magnetic resonance imaging. *J Cardiovasc Magn Reson* 1999;1(1):7-21. [published Online First: 2001/09/12]
88. Dell'Italia LJ. The right ventricle: anatomy, physiology, and clinical importance. *Current Problems in Cardiology* 1991;16(10):658-720. doi: https://doi.org/10.1016/0146-2806(91)90009-Y
89. Ryan T, Petrovic O, Dillon JC, et al. An echocardiographic index for separation of right ventricular volume and pressure overload. *J Am Coll Cardiol* 1985;5(4):918-27.
90. Kinch JW, Ryan TJ. Right ventricular infarction. *New England Journal of Medicine* 1994;330(17):1211-17.

91. Pinsky MR. The right ventricle: interaction with the pulmonary circulation. *Critical Care* 2016;20(1):266. doi: 10.1186/s13054-016-1440-0
92. Huang W, Yen RT, McLaurine M, et al. Morphometry of the human pulmonary vasculature. *Journal of Applied Physiology* 1996;81(5):2123-33. doi: 10.1152/jappl.1996.81.5.2123
93. Albertine KH. 1 - Anatomy of the Lungs A2 - Broaddus, V. Courtney. In: Mason RJ, Ernst JD, King TE, et al., eds. Murray and Nadel's Textbook of Respiratory Medicine (Sixth Edition). Philadelphia: W.B. Saunders 2016:3-21.e5.
94. Garcia JGN. 6 - Pulmonary Circulation and Regulation of Fluid Balance A2 - Broaddus, V. Courtney. In: Mason RJ, Ernst JD, King TE, et al., eds. Murray and Nadel's Textbook of Respiratory Medicine (Sixth Edition). Philadelphia: W.B. Saunders 2016:92-110.e8.
95. Lumb AB. Chapter 6 - The Pulmonary Circulation. Nunn's Applied Respiratory Physiology (Eighth Edition): Elsevier 2017:89-107.e2.
96. François CJ, Srinivasan S, Schiebler ML, et al. 4D cardiovascular magnetic resonance velocity mapping of alterations of right heart flow patterns and main pulmonary artery hemodynamics in tetralogy of Fallot. *Journal of Cardiovascular Magnetic Resonance* 2012;14(1):16. doi: 10.1186/1532-429x-14-16
97. Carabello BA. Evolution of the study of left ventricular function: everything old is new again: Am Heart Assoc, 2002.
98. Dell'Italia LJ, Walsh RA. Acute determinants of the hangout interval in the pulmonary circulation. *American Heart Journal* 1988;116(5, Part 1):1289-97. doi: https://doi.org/10.1016/0002-8703(88)90454-1
99. Pasipoularides A. Right and left ventricular diastolic pressure-volume relations: a comprehensive review. *J Cardiovasc Transl Res* 2013;6(2):239-52. doi: 10.1007/s12265-012-9424-1 [published Online First: 2012/11/21]
100. Burgess MI, Bright-Thomas RJ, Ray SG. Echocardiographic evaluation of right ventricular function. *Eur J Echocardiogr* 2002;3(4):252-62.
101. Dell'Italia LJ. Mechanism of postextrasystolic potentiation in the right ventricle. *Am J Cardiol* 1990;65(11):736-41. [published Online First: 1990/03/15]
102. Chin KM, Kim NHS, Rubin LJ. The right ventricle in pulmonary hypertension. *Coronary Artery Disease* 2005;16(1):13-18.
103. Tedford RJ. Determinants of right ventricular afterload (2013 Grover Conference series). *Pulm Circ* 2014;4(2):211-9. doi: 10.1086/676020
104. Klabunde R. Cardiovascular physiology concepts: Lippincott Williams & Wilkins 2011.
105. Sonnenblick EH. Force-velocity relations in mammalian heart muscle. *American Journal of Physiology-Legacy Content* 1962;202(5):931-39. doi: 10.1152/ajplegacy.1962.202.5.931
106. Hill AV. The heat of shortening and the dynamic constants of muscle. *Proceedings of the Royal Society of London Series B - Biological Sciences* 1938;126(843):136-95. doi: 10.1098/rspb.1938.0050
107. Chantler PD, Lakatta EG, Najjar SS. Arterial-ventricular coupling: mechanistic insights into cardiovascular performance at rest and during exercise. *Journal of applied physiology* 2008;105(4):1342-51.
108. Yerebakan C, Klopsch C, Prietz S, et al. Pressure-volume loops: feasible for the evaluation of right ventricular function in an experimental model of acute pulmonary regurgitation? *Interact Cardiovasc Thorac Surg* 2009;9(2):163-8. doi: 10.1510/icvts.2008.198275

109. Kuehne T, Yilmaz S, Steendijk P, et al. Magnetic resonance imaging analysis of right ventricular pressure-volume loops: in vivo validation and clinical application in patients with pulmonary hypertension. *Circulation* 2004;110(14):2010-16.
110. Sanz J, Garcia-Alvarez A, Fernandez-Friera L, et al. Right ventriculo-arterial coupling in pulmonary hypertension: a magnetic resonance study. *Heart* 2012;98(3):238-43. doi: 10.1136/heartjnl-2011-300462
111. Vonk-Noordegraaf A, Westerhof N. Describing right ventricular function. *European Respiratory Journal* 2013;41(6):1419.
112. Spruijt OA, de Man FS, Groepenhoff H, et al. The effects of exercise on right ventricular contractility and right ventricular–arterial coupling in pulmonary hypertension. *American journal of respiratory and critical care medicine* 2015;191(9):1050-57.
113. Starling MR, Walsh RA, Dell'Italia LJ, et al. The relationship of various measures of end-systole to left ventricular maximum time-varying elastance in man. *Circulation* 1987;76(1):32-43.
114. Maughan WL, Shoukas AA, Sagawa K, et al. Instantaneous pressure-volume relationship of the canine right ventricle. *Circulation research* 1979;44(3):309-15.
115. Kass DA, Maughan WL. From 'Emax' to pressure-volume relations: a broader view. *Circulation* 1988;77(6):1203-12. doi: 10.1161/01.CIR.77.6.1203
116. Bellofiore A, Chesler NC. Methods for measuring right ventricular function and hemodynamic coupling with the pulmonary vasculature. *Annals of biomedical engineering* 2013;41(7):1384-98.
117. Leeuwenburgh BPJ, Helbing WA, Steendijk P, et al. Biventricular systolic function in young lambs subject to chronic systemic right ventricular pressure overload. *American Journal of Physiology-Heart and Circulatory Physiology* 2001;281(6):H2697-H704. doi: 10.1152/ajpheart.2001.281.6.h2697
118. Pagnamenta A, Fesler P, Vandinivit A, et al. Pulmonary vascular effects of dobutamine in experimental pulmonary hypertension. *Critical Care Medicine* 2003;31(4):1140-46. doi: 10.1097/01.Ccm.0000060126.75746.32
119. Price LC, Wort SJ, Finney SJ, et al. Pulmonary vascular and right ventricular dysfunction in adult critical care: current and emerging options for management: a systematic literature review. *Critical Care* 2010;14(5):R169. doi: 10.1186/cc9264
120. Claessen G, La Gerche A, Dymarkowski S, et al. Pulmonary vascular and right ventricular reserve in patients with normalized resting hemodynamics after pulmonary endarterectomy. *J Am Heart Assoc* 2015;4(3):e001602. doi: 10.1161/JAHA.114.001602
121. Kozian A, Schilling T, Fredén F, et al. One-lung ventilation induces hyperperfusion and alveolar damage in the ventilated lung: an experimental study. *Br J Anaesth* 2008;100(4):549-59. doi: 10.1093/bja/aen021 [published Online First: 2008/03/01]
122. Dorrington KL, Clar C, Young JD, et al. Time course of the human pulmonary vascular response to 8 hours of isocapnic hypoxia. *The American journal of physiology* 1997;273(3 Pt 2):H1126-34. doi: 10.1152/ajpheart.1997.273.3.H1126 [published Online First: 1997/10/10]
123. Lohser J, Slinger P. Lung Injury After One-Lung Ventilation: A Review of the Pathophysiologic Mechanisms Affecting the Ventilated and the Collapsed Lung. *Anesth Analg* 2015;121(2):302-18. doi: 10.1213/ANE.0000000000000808

124. Vieillard-Baron A, Naeije R, Haddad F, et al. Diagnostic workup, etiologies and management of acute right ventricle failure : A state-of-the-art paper. *Intensive Care Med* 2018;44(6):774-90. doi: 10.1007/s00134-018-5172-2 [published Online First: 2018/05/11]
125. Campo A, Mathai SC, Le Pavec J, et al. Outcomes of hospitalisation for right heart failure in pulmonary arterial hypertension. *European Respiratory Journal* 2011;38(2):359. doi: 10.1183/09031936.00148310
126. Vonk Noordegraaf A, Westerhof BE, Westerhof N. The Relationship Between the Right Ventricle and its Load in Pulmonary Hypertension. *Journal of the American College of Cardiology* 2017;69(2):236-43. doi: https://doi.org/10.1016/j.jacc.2016.10.047
127. van Wolferen SA, Marcus JT, Westerhof N, et al. Right coronary artery flow impairment in patients with pulmonary hypertension. *European Heart Journal* 2007;29(1):120-27. doi: 10.1093/eurheartj/ehm567
128. Tji-Joong Gan C, Lankhaar J-W, Marcus JT, et al. Impaired left ventricular filling due to right-to-left ventricular interaction in patients with pulmonary arterial hypertension. *American Journal of Physiology-Heart and Circulatory Physiology* 2006;290(4):H1528-H33. doi: 10.1152/ajpheart.01031.2005
129. Marcus JT, Gan CT, Zwanenburg JJ, et al. Interventricular mechanical asynchrony in pulmonary arterial hypertension: left-to-right delay in peak shortening is related to right ventricular overload and left ventricular underfilling. *J Am Coll Cardiol* 2008;51(7):750-7. doi: 10.1016/j.jacc.2007.10.041
130. Frump AL, Bonnet S, de Jesus Perez VA, et al. Emerging role of angiogenesis in adaptive and maladaptive right ventricular remodeling in pulmonary hypertension. *American Journal of Physiology-Lung Cellular and Molecular Physiology* 2017;314(3):L443-L60. doi: 10.1152/ajplung.00374.2017
131. Rain S, Handoko ML, Trip P, et al. Right Ventricular Diastolic Impairment in Patients With Pulmonary Arterial Hypertension. *Circulation* 2013;128(18):2016-25. doi: 10.1161/CIRCULATIONAHA.113.001873
132. Heerdt PM, Lane P, Pan BY, et al. Nitrosative stress and myocardial sarcoplasmic endoreticular calcium adenosine triphosphatase subtype 2a activity after lung resection in swine. *Anesthesiology* 2007;107(6):954-62. doi: 10.1097/01.anes.0000291446.70921.61
133. Watts JA, Marchick MR, Kline JA. Right ventricular heart failure from pulmonary embolism: key distinctions from chronic pulmonary hypertension. *J Card Fail* 2010;16(3):250-9. doi: 10.1016/j.cardfail.2009.11.008
134. Watts JA, Gellar MA, Obraztsova M, et al. Role of inflammation in right ventricular damage and repair following experimental pulmonary embolism in rats. *Int J Exp Pathol* 2008;89(5):389-99. doi: 10.1111/j.1365-2613.2008.00610.x
135. Watts JA, Zagorski J, Gellar MA, et al. Cardiac inflammation contributes to right ventricular dysfunction following experimental pulmonary embolism in rats. *J Mol Cell Cardiol* 2006;41(2):296-307. doi: 10.1016/j.yjmcc.2006.05.011
136. Sanz J, Dellegrottaglie S, Kariisa M, et al. Prevalence and Correlates of Septal Delayed Contrast Enhancement in Patients With Pulmonary Hypertension[†]. *American Journal of Cardiology* 2007;100(4):731-35. doi: 10.1016/j.amjcard.2007.03.094

137. Gómez A, Bialostozky D, Zajarias A, et al. Right ventricular ischemia in patients with primary pulmonary hypertension. *Journal of the American College of Cardiology* 2001;38(4):1137-42. doi: https://doi.org/10.1016/S0735-1097(01)01496-6
138. Clark JE, Marber MS. Advancements in pressure–volume catheter technology – stress remodelling after infarction. *Experimental Physiology* 2013;98(3):614-21. doi: 10.1113/expphysiol.2012.064733
139. Dell'italia LJ, Walsh RA. Application of a time varying elastance model to right ventricular performance in man. *Cardiovascular research* 1988;22(12):864-74.
140. Wink J, de Wilde RBP, Wouters PF, et al. Thoracic Epidural Anesthesia Reduces Right Ventricular Systolic Function With Maintained Ventricular-Pulmonary Coupling. *Circulation* 2016;134(16):1163.
141. Howard LS, Grapsa J, Dawson D, et al. Echocardiographic assessment of pulmonary hypertension: standard operating procedure. *Eur Respir Rev* 2012;21(125):239-48. doi: 10.1183/09059180.00003912
142. Jategaonkar SR, Scholtz W, Butz T, et al. Two-dimensional strain and strain rate imaging of the right ventricle in adult patients before and after percutaneous closure of atrial septal defects. *European Journal of Echocardiography* 2009;10(4):499-502. doi: 10.1093/ejechocard/jen315
143. Park J-H, Negishi K, Kwon DH, et al. Validation of global longitudinal strain and strain rate as reliable markers of right ventricular dysfunction: comparison with cardiac magnetic resonance and outcome. *Journal of cardiovascular ultrasound* 2014;22(3):113-20.
144. Jamal F, Bergerot C, Argaud L, et al. Longitudinal strain quantitates regional right ventricular contractile function. *American Journal of Physiology-Heart and Circulatory Physiology* 2003;285(6):H2842-H47.
145. Park J-H, Park MM, Farha S, et al. Impaired global right ventricular longitudinal strain predicts long-term adverse outcomes in patients with pulmonary arterial hypertension. *Journal of cardiovascular ultrasound* 2015;23(2):91-99.
146. Saouti N, Westerhof N, Helderman F, et al. RC time constant of single lung equals that of both lungs together: a study in chronic thromboembolic pulmonary hypertension. *American Journal of Physiology-Heart and Circulatory Physiology* 2009;297(6):H2154-H60. doi: 10.1152/ajpheart.00694.2009
147. Lankhaar JW, Westerhof N, Faes TJ, et al. Pulmonary vascular resistance and compliance stay inversely related during treatment of pulmonary hypertension. *Eur Heart J* 2008;29(13):1688-95. doi: 10.1093/eurheartj/ehn103 [published Online First: 2008/03/20]
148. Lankhaar J-W, Westerhof N, Faes TJC, et al. Quantification of right ventricular afterload in patients with and without pulmonary hypertension. *American Journal of Physiology-Heart and Circulatory Physiology* 2006;291(4):H1731-H37. doi: 10.1152/ajpheart.00336.2006
149. Kang KW, Chang HJ, Kim YJ, et al. Cardiac magnetic resonance imaging-derived pulmonary artery distensibility index correlates with pulmonary artery stiffness and predicts functional capacity in patients with pulmonary arterial hypertension. *Circ J* 2011;75(9):2244-51.
150. Benza RL, Miller DP, Gomberg-Maitland M, et al. Predicting Survival in Pulmonary Arterial Hypertension. *Circulation* 2010;122(2):164.
151. Su J, Hilberg O, Howard L, et al. A review of wave mechanics in the pulmonary artery with an emphasis on wave intensity analysis. *Acta*

physiologica (Oxford, England) 2016;218(4):239-49. doi: 10.1111/apha.12803 [published Online First: 2016/09/17]
152. Jiang L, Wiegers S, Weyman A. Right ventricle. *Principle and Practice of Echocardiography Baltimore, Md: Lippincott Williams & Wilkins* 1994:901-21.
153. Knight DS, Kotecha T, Martinez-Naharro A, et al. Cardiovascular magnetic resonance-guided right heart catheterization in a conventional CMR environment – predictors of procedure success and duration in pulmonary artery hypertension. *Journal of Cardiovascular Magnetic Resonance* 2019;21(1) doi: 10.1186/s12968-019-0569-9
154. Rogers T, Ratnayaka K, Khan JM, et al. CMR fluoroscopy right heart catheterization for cardiac output and pulmonary vascular resistance: results in 102 patients. *Journal of Cardiovascular Magnetic Resonance* 2017;19(1):54. doi: 10.1186/s12968-017-0366-2
155. Benza R, Biederman R, Murali S, et al. Role of cardiac magnetic resonance imaging in the management of patients with pulmonary arterial hypertension. *J Am Coll Cardiol* 2008;52(21):1683-92. doi: 10.1016/j.jacc.2008.08.033
156. McCall P, Soosay A, Kinsella J, et al. The utility of transthoracic echocardiographic measures of right ventricular systolic function in a lung resection cohort. *Echo Research and Practice* 2019;6(1):7-15. doi: 10.1530/erp-18-0067
157. Jorstig S, Waldenborg M, Lidén M, et al. Right ventricular ejection fraction measurements using two-dimensional transthoracic echocardiography by applying an ellipsoid model. 2017;15(1) doi: 10.1186/s12947-017-0096-5
158. Fisher MR, Forfia PR, Chamera E, et al. Accuracy of Doppler echocardiography in the hemodynamic assessment of pulmonary hypertension. *American journal of respiratory and critical care medicine* 2009;179(7):615-21.
159. McLure L, Peacock A. Cardiac magnetic resonance imaging for the assessment of the heart and pulmonary circulation in pulmonary hypertension. *European Respiratory Journal* 2009;33(6):1454-66.
160. Prati G, Vitrella G, Allocca G, et al. Right Ventricular Strain and Dyssynchrony Assessment in Arrhythmogenic Right Ventricular Cardiomyopathy: Cardiac Magnetic Resonance Feature-Tracking Study. *Circ Cardiovasc Imaging* 2015;8(11):e003647; discussion e47. doi: 10.1161/CIRCIMAGING.115.003647
161. Morton G, Schuster A, Jogiya R, et al. Inter-study reproducibility of cardiovascular magnetic resonance myocardial feature tracking. *J Cardiovasc Magn Reson* 2012;14:43. doi: 10.1186/1532-429X-14-43
162. Bradlow WM, Gibbs JS, Mohiaddin RH. Cardiovascular magnetic resonance in pulmonary hypertension. *J Cardiovasc Magn Reson* 2012;14:6. doi: 10.1186/1532-429X-14-6
163. Lima JAC, Desai MY. Cardiovascular magnetic resonance imaging: Current and emerging applications. *Journal of the American College of Cardiology* 2004;44(6):1164-71. doi: https://doi.org/10.1016/j.jacc.2004.06.033
164. Addetia K, Bhave Nicole M, Tabit Corey E, et al. Sample Size and Cost Analysis for Pulmonary Arterial Hypertension Drug Trials Using Various Imaging Modalities to Assess Right Ventricular Size and Function End Points. *Circulation: Cardiovascular Imaging* 2014;7(1):115-24. doi: 10.1161/CIRCIMAGING.113.000932

165. D'Alonzo GE, Barst RJ, Ayres SM, et al. Survival in patients with primary pulmonary hypertension: Results from a national prospective registry. *Annals of Internal Medicine* 1991;115(5):343-49. doi: 10.7326/0003-4819-115-5-343
166. Jansen JRC. The thermodilution method for the clinical assessment of cardiac output. *Intensive Care Medicine* 1995;21(8):691-97. doi: 10.1007/BF01711553
167. Hoeper MM, Lee SH, Voswinckel R, et al. Complications of Right Heart Catheterization Procedures in Patients With Pulmonary Hypertension in Experienced Centers. *Journal of the American College of Cardiology* 2006;48(12):2546-52. doi: https://doi.org/10.1016/j.jacc.2006.07.061
168. Hein M, Roehl AB, Baumert JH, et al. Continuous right ventricular volumetry by fast-response thermodilution during right ventricular ischemia: head-to-head comparison with conductance catheter measurements. *Crit Care Med* 2009;37(11):2962-7. doi: 10.1097/CCM.0b013e3181b027a5
169. Steendijk P, Staal E, Jukema JW, et al. Hypertonic saline method accurately determines parallel conductance for dual-field conductance catheter. *American Journal of Physiology-Heart and Circulatory Physiology* 2001;281(2):H755-H63.
170. Steendijk P, Tulner SAF, Wiemer M, et al. Pressure–volume measurements by conductance catheter during cardiac resynchronization therapy. *European Heart Journal Supplements* 2004;6(suppl_D):D35-D42. doi: 10.1016/j.ehjsup.2004.05.012
171. Robin E, Costecalde M, Lebuffe G, et al. Clinical relevance of data from the pulmonary artery catheter. *Critical Care* 2006;10(Suppl 3):S3. doi: 10.1186/cc4830
172. Wiesenack C, Fiegl C, Keyser A, et al. Continuously assessed right ventricular end-diastolic volume as a marker of cardiac preload and fluid responsiveness in mechanically ventilated cardiac surgical patients. *Critical Care* 2005;9(3):R226-R33. doi: 10.1186/cc3503
173. Hoeper MM, Tongers J, Leppert A, et al. Evaluation of Right Ventricular Performance With a Right Ventricular Ejection Fraction Thermodilution Catheter and MRI in Patients With Pulmonary Hypertension. *CHEST* 2001;120(2):502-07. doi: 10.1378/chest.120.2.502
174. Dhainaut JF, Brunet F, Monsallier JF, et al. Bedside evaluation of right ventricular performance using a rapid computerized thermodilution method. *Critical care medicine* 1987;15(2):148-52. doi: 10.1097/00003246-198702000-00014
175. Reuse C, Vincent J-L, Pinsky MR. Measurements of Right Ventricular Volumes during Fluid Challenge. *Chest* 1990;98(6):1450-54. doi: https://doi.org/10.1378/chest.98.6.1450
176. Wagner JG, Leatherman JW. Right Ventricular End-Diastolic Volume as a Predictor of the Hemodynamic Response to a Fluid Challenge. *Chest* 1998;113(4):1048-54. doi: https://doi.org/10.1378/chest.113.4.1048
177. van de Veerdonk MC, Kind T, Marcus JT, et al. Progressive Right Ventricular Dysfunction in Patients With Pulmonary Arterial Hypertension Responding to Therapy. *Journal of the American College of Cardiology* 2011;58(24):2511. doi: 10.1016/j.jacc.2011.06.068
178. Leibowitz AB. Pulmonary artery catheter determined right ventricular ejection fraction and right ventricular end-diastolic volume: another case of "The Emperor Has No Clothes". *Crit Care Med* 2009;37(11):2992. doi: 10.1097/CCM.0b013e3181b01839

179. Kinnunen P, Vuolteenaho O, Ruskoaho H. Mechanisms of atrial and brain natriuretic peptide release from rat ventricular myocardium: effect of stretching. *Endocrinology* 1993;132(5):1961-70. doi: 10.1210/endo.132.5.8477647
180. Beattie WS, Wijeysundera DN. Perioperative cardiac biomarkers: the utility and timing. *Curr Opin Crit Care* 2013;19(4):334-41. doi: 10.1097/MCC.0b013e3283632f07 [published Online First: 2013/07/05]
181. Klok FA, Mos ICM, Huisman MV. Brain-Type Natriuretic Peptide Levels in the Prediction of Adverse Outcome in Patients with Pulmonary Embolism. *American Journal of Respiratory and Critical Care Medicine* 2008;178(4):425-30. doi: 10.1164/rccm.200803-459OC
182. Blyth KG, Groenning BA, Mark PB, et al. NT-proBNP can be used to detect right ventricular systolic dysfunction in pulmonary hypertension. *European Respiratory Journal* 2007;29(4):737. doi: 10.1183/09031936.00095606
183. Nojiri T, Maeda H, Takeuchi Y, et al. Predictive value of B-type natriuretic peptide for postoperative atrial fibrillation following pulmonary resection for lung cancer. *Eur J Cardiothorac Surg* 2010;37(4):787-91. doi: 10.1016/j.ejcts.2009.09.043
184. Gurgo AM, Ciccone AM, D'Andrilli A, et al. Plasma NT-proBNP levels and the risk of atrial fibrillation after major lung resection. *Minerva Cardioangiol* 2008;56(6):581-85.
185. Amar D, Zhang H, Shi W, et al. Brain natriuretic peptide and risk of atrial fibrillation after thoracic surgery. *The Journal of Thoracic and Cardiovascular Surgery* 2012;144(5):1249-53. doi: https://doi.org/10.1016/j.jtcvs.2012.06.051
186. Versprille A. Pulmonary vascular resistance. A meaningless variable. *Intensive Care Med* 1984;10(2):51-3. doi: 10.1007/bf00297557 [published Online First: 1984/01/01]
187. Naeije R. Pulmonary vascular resistance. *Intensive Care Medicine* 2003;29(4):526-29. doi: 10.1007/s00134-003-1693-3
188. Claessen G, La Gerche A, Voigt JU, et al. Accuracy of Echocardiography to Evaluate Pulmonary Vascular and RV Function During Exercise. *JACC Cardiovasc Imaging* 2016;9(5):532-43. doi: 10.1016/j.jcmg.2015.06.018
189. Pagnamenta A, Lador F, Azzola A, et al. Modern Invasive Hemodynamic Assessment of Pulmonary Hypertension. *Respiration* 2018;95(3):201-11. doi: 10.1159/000484942
190. Tousignant C, Van Orman JR. Pulmonary Impedance and Pulmonary Doppler Trace in the Perioperative Period. *Anesthesia & Analgesia* 2015;121(3)
191. Grant BJ, Lieber BB. Clinical significance of pulmonary arterial input impedance. *Eur Respir J* 1996;9(11):2196-9. doi: 10.1183/09031936.96.09112196 [published Online First: 1996/11/01]
192. Milnor WR, Conti CR, Lewis KB, et al. Pulmonary arterial pulse wave velocity and impedance in man. *Circulation research* 1969;25(6):637-49.
193. Murgo JP, Westerhof N. Input impedance of the pulmonary arterial system in normal man. Effects of respiration and comparison to systemic impedance. *Circ Res* 1984;54(6):666-73. doi: 10.1161/01.res.54.6.666 [published Online First: 1984/06/01]
194. Matsuzaki T. Pulmonary vascular input impedance in patients with atrial septal defect. *Acta Medica Nagasakiensia* 1994;39(4):107-13.
195. Haneda T, Nakajima T, Shirato K, et al. Effects of Oxygen Breathing on Pulmonary Vascular Input Impedance in Patients with Pulmonary

Hypertension. *Chest* 1983;83(3):520-27. doi: https://doi.org/10.1378/chest.83.3.520
196. Laskey WK, Ferrari VA, Palevsky HI, et al. Pulmonary artery hemodynamics in primary pulmonary hypertension. *J Am Coll Cardiol* 1993;21(2):406-12. doi: 10.1016/0735-1097(93)90682-q [published Online First: 1993/02/01]
197. Huez S, Brimioulle S, Naeije R, et al. Feasibility of routine pulmonary arterial impedance measurements in pulmonary hypertension. *Chest* 2004;125(6):2121-8. doi: 10.1378/chest.125.6.2121 [published Online First: 2004/06/11]
198. Ravellette K, Kubba S, Airhart S, et al. Increased Pulmonary Vascular Impedance in Patients with Severe Pulmonary Arterial Hypertension. *The FASEB Journal* 2019;33(S1):550.4-50.4. doi: 10.1096/fasebj.2019.33.1_supplement.550.4
199. Hunter KS, Lee PF, Lanning CJ, et al. Pulmonary vascular input impedance is a combined measure of pulmonary vascular resistance and stiffness and predicts clinical outcomes better than pulmonary vascular resistance alone in pediatric patients with pulmonary hypertension. *Am Heart J* 2008;155(1):166-74. doi: 10.1016/j.ahj.2007.08.014 [published Online First: 2007/12/18]
200. Tian L, Hunter KS, Kirby KS, et al. Measurement uncertainty in pulmonary vascular input impedance and characteristic impedance estimated from pulsed-wave Doppler ultrasound and pressure: clinical studies on 57 pediatric patients. *Physiological measurement* 2010;31(6):729-48. doi: 10.1088/0967-3334/31/6/001 [published Online First: 2010/04/22]
201. Weinberg CE, Hertzberg JR, Ivy DD, et al. Extraction of pulmonary vascular compliance, pulmonary vascular resistance, and right ventricular work from single-pressure and Doppler flow measurements in children with pulmonary hypertension: a new method for evaluating reactivity: in vitro and clinical studies. *Circulation* 2004;110(17):2609-17. doi: 10.1161/01.Cir.0000146818.60588.40 [published Online First: 2004/10/20]
202. How to measure pulmonary vascular and right ventricular function. Engineering in Medicine and Biology Society, 2009 EMBC 2009 Annual International Conference of the IEEE; 2009. IEEE.
203. Frank O. Die Grundform des arteriellen Pulses. *Z Biol* 1899;37:483–526.
204. Westerhof N, Elzinga G, Sipkema P. An artificial arterial system for pumping hearts. *J Appl Physiol* 1971;31(5):776-81. doi: 10.1152/jappl.1971.31.5.776 [published Online First: 1971/11/01]
205. Segers P, Brimioulle S, Stergiopulos N, et al. Pulmonary arterial compliance in dogs and pigs: the three-element windkessel model revisited. *The American journal of physiology* 1999;277(2):H725-31. doi: 10.1152/ajpheart.1999.277.2.H725 [published Online First: 1999/08/13]
206. Stergiopulos N, Meister JJ, Westerhof N. Evaluation of methods for estimation of total arterial compliance. *American Journal of Physiology-Heart and Circulatory Physiology* 1995;268(4):H1540-H48. doi: 10.1152/ajpheart.1995.268.4.H1540
207. Pagnamenta A, Vanderpool R, Brimioulle S, et al. Proximal pulmonary arterial obstruction decreases the time constant of the pulmonary circulation and increases right ventricular afterload. *Journal of Applied Physiology* 2013;114(11):1586-92. doi: 10.1152/japplphysiol.00033.2013
208. Tedford RJ, Hassoun PM, Mathai SC, et al. Pulmonary capillary wedge pressure augments right ventricular pulsatile loading. *Circulation*

2012;125(2):289-97. doi: 10.1161/circulationaha.111.051540 [published Online First: 2011/12/02]
209. Tedford RJ, Mudd JO, Girgis RE, et al. Right ventricular dysfunction in systemic sclerosis-associated pulmonary arterial hypertension. *Circ Heart Fail* 2013;6(5):953-63. doi: 10.1161/circheartfailure.112.000008 [published Online First: 2013/06/26]
210. Mahapatra S, Nishimura RA, Sorajja P, et al. Relationship of pulmonary arterial capacitance and mortality in idiopathic pulmonary arterial hypertension. *J Am Coll Cardiol* 2006;47(4):799-803. doi: 10.1016/j.jacc.2005.09.054 [published Online First: 2006/02/21]
211. Gan CT, Lankhaar JW, Westerhof N, et al. Noninvasively assessed pulmonary artery stiffness predicts mortality in pulmonary arterial hypertension. *Chest* 2007;132(6):1906-12. doi: 10.1378/chest.07-1246
212. Sanz J, Kariisa M, Dellegrottaglie S, et al. Evaluation of pulmonary artery stiffness in pulmonary hypertension with cardiac magnetic resonance. *JACC Cardiovasc Imaging* 2009;2(3):286-95. doi: 10.1016/j.jcmg.2008.08.007
213. Tardivon AA, Mousseaux E, Brenot F, et al. Quantification of hemodynamics in primary pulmonary hypertension with magnetic resonance imaging. *American Journal of Respiratory and Critical Care Medicine* 1994;150(4):1075-80. doi: 10.1164/ajrccm.150.4.7921439
214. Heerdt PM. Cardiovascular adaption to lung resection. Thoracic Anesthesia2003.
215. Peacock AJ, Vonk Noordegraaf A. Cardiac magnetic resonance imaging in pulmonary arterial hypertension. *European Respiratory Review* 2013;22(130):526.
216. Diebel LN, Wilson RF, Tagett MG, et al. End-Diastolic Volume: A Better Indicator of Preload in the Critically Ill. *JAMA Surgery* 1992;127(7):817-22. doi: 10.1001/archsurg.1992.01420070081015
217. Fischer GW, Cohen E. An update on anesthesia for thoracoscopic surgery. *Current Opinion in Anaesthesiology* 2010;23(1):7-11. doi: 10.1097/aco.0b013e3283346c6d
218. Wise J. Boldt: the great pretender. *BMJ* 2013;346(mar19 1):f1738-f38. doi: 10.1136/bmj.f1738
219. Kane GC, Sachdev A, Villarraga HR, et al. Impact of age on pulmonary artery systolic pressures at rest and with exercise. *Echo research and practice* 2016;3(2):53-61. doi: 10.1530/ERP-16-0006
220. Evans DC, Doraiswamy VA, Prosciak MP, et al. Complications Associated with Pulmonary Artery Catheters: A Comprehensive Clinical Review. *Scandinavian Journal of Surgery* 2009;98(4):199-208. doi: 10.1177/145749690909800402
221. Amar D, Roistacher N, Burt ME, et al. Effects of diltiazem versus digoxin on dysrhythmias and cardiac function after pneumonectomy. *The Annals of Thoracic Surgery* 1997;63(5):1374-82. doi: 10.1016/s0003-4975(97)80354-2
222. Krowka MJ, Pairolero PC, Trastek VF, et al. Cardiac dysrhythmia following pneumonectomy: clinical correlates and prognostic significance. *Chest* 1987;91(4):490-95.
223. Amar D, Roistacher N, Rusch VW, et al. Effects of diltiazem prophylaxis on the incidence and clinical outcome of atrial arrhythmias after thoracic surgery. *The Journal of Thoracic and Cardiovascular Surgery* 2000;120(4):790-98. doi: 10.1067/mtc.2000.109538

224. Wang Z, Yuan J, Chu W, et al. Evaluation of left and right ventricular myocardial function after lung resection using speckle tracking echocardiography. *Medicine (Baltimore)* 2016;95(31):e4290. doi: 10.1097/MD.0000000000004290
225. Fisher MR, Criner GJ, Fishman AP, et al. Estimating pulmonary artery pressures by echocardiography in patients with emphysema. *Eur Respir J* 2007;30(5):914-21. doi: 10.1183/09031936.00033007
226. Kjaergaard J, Petersen CL, Kjaer A, et al. Evaluation of right ventricular volume and function by 2D and 3D echocardiography compared to MRI. *Eur J Echocardiogr* 2006;7(6):430-8. doi: 10.1016/j.euje.2005.10.009
227. Smulders SA, Holverda S, Vonk-Noordegraaf A, et al. Cardiac function and position more than 5 years after pneumonectomy. *Ann Thorac Surg* 2007;83(6):1986-92. doi: 10.1016/j.athoracsur.2007.01.036
228. Riquet M, Mordant P, Pricopi C, et al. A review of 250 ten-year survivors after pneumonectomy for non-small-cell lung cancer†. *European Journal of Cardio-Thoracic Surgery* 2014;45(5):876-81. doi: 10.1093/ejcts/ezt494
229. Mizushima YMD, Noto HMD, Sugiyama SMD, et al. Survival and Prognosis After Pneumonectomy for Lung Cancer in the Elderly. *The Annals of Thoracic Surgery* 1997;64(1):193-98. doi: 10.1016/S0003-4975(97)82827-5
230. McCall PJ, Arthur A, Glass A, et al. The right ventricular response to lung resection. *The Journal of Thoracic and Cardiovascular Surgery* 2019;158(2):556-65.e5. doi: 10.1016/j.jtcvs.2019.01.067
231. McCall P. The right ventricular response to lung resection. University of Glasgow, 2018.
232. McCall P, Corcoran D, Arthur A, et al. The right ventricular response to lung resection. *Journal of Cardiothoracic and Vascular Anesthesia* 2016;30:S23-S24. doi: 10.1053/j.jvca.2016.03.070
233. McCall P, Sonecki P, Kirk A, et al. Speckle-tracked strain assessment of right
ventricular function after lung resection. *British Journal of Anaesthesia* 2016;116(6):e932-e33. doi: 10.1093/bja/aev406
234. Teng W, McCall P, Kinsella J, et al. Eccentricity index assessment of right ventricular function after lung resection. Abstracts from the BJA Research Forum Glasgow, November 10–11, 2016. *BJA: British Journal of Anaesthesia* 2017;119(2):e13. doi: 10.1093/bja/aew382
235. Young DJ, McCall PJ, Kirk A, et al. B-type natriuretic peptide predicts deterioration in functional capacity following lung resection†. *Interactive CardioVascular and Thoracic Surgery* 2019 doi: 10.1093/icvts/ivz016
236. McCall P, Arthur A, Kirk A, et al. Perioperative BNP changes and functional capacity following lung resection. *Journal of Cardiothoracic and Vascular Anesthesia* 2016;30:S26-S27. doi: 10.1053/j.jvca.2016.03.075
237. Varon AJ, Civetta JM. Of course the emperor has no clothes. *Crit Care Med* 2010;38(4):1228-9. doi: 10.1097/CCM.0b013e3181ce4793
238. Potter E, Marwick TH. Assessment of Left Ventricular Function by Echocardiography: The Case for Routinely Adding Global Longitudinal Strain to Ejection Fraction. *JACC: Cardiovascular Imaging* 2018;11(2, Part 1):260-74. doi: https://doi.org/10.1016/j.jcmg.2017.11.017
239. Reisner SA, Lysyansky P, Agmon Y, et al. Global longitudinal strain: a novel index of left ventricular systolic function. *Journal of the American Society of Echocardiography* 2004;17(6):630-33. doi: 10.1016/j.echo.2004.02.011
240. Tsai S-H, Lin Y-Y, Chu S-J, et al. Interpretation and use of natriuretic peptides in non-congestive heart failure settings. *Yonsei Med J*

2010;51(2):151-63. doi: 10.3349/ymj.2010.51.2.151 [published Online First: 2010/02/12]
241. Lung cancer clinical outcomes publication 2016 2016 [accessed 19/02/2018 https://scts.org/wp-content/uploads/2016/12/LCCOP-2016-report_WEB.pdf.
242. Craig SR, Leaver HA, Yap PL, et al. Acute phase responses following minimal access and conventional thoracic surgery. *European Journal of Cardio-Thoracic Surgery* 2001;20(3):455-63. doi: 10.1016/S1010-7940(01)00841-7
243. Landis JR, Koch GG. The Measurement of Observer Agreement for Categorical Data. *Biometrics* 1977;33(1):159-74. doi: 10.2307/2529310
244. Bland JM, Altman DG. Calculating correlation coefficients with repeated observations: Part 1--Correlation within subjects. *BMJ (Clinical research ed)* 1995;310(6977):446-46. doi: 10.1136/bmj.310.6977.446
245. Bakdash JZ, Marusich LR. Repeated Measures Correlation. *Frontiers in Psychology* 2017;8(456) doi: 10.3389/fpsyg.2017.00456
246. Koo TK, Li MY. A Guideline of Selecting and Reporting Intraclass Correlation Coefficients for Reliability Research. *Journal of Chiropractic Medicine* 2016;15(2):155-63. doi: 10.1016/j.jcm.2016.02.012
247. Reed GF, Lynn F, Meade BD. Use of Coefficient of Variation in Assessing Variability of Quantitative Assays. *Clinical and Vaccine Immunology* 2002;9(6):1235-39. doi: 10.1128/cdli.9.6.1235-1239.2002
248. Holm C, Mayr M, Horbrand F, et al. Reproducibility of transpulmonary thermodilution measurements in patients with burn shock and hypothermia. *The Journal of burn care & rehabilitation* 2005;26(3):260-5. [published Online First: 2005/05/10]
249. Schulz-Menger J, Bluemke DA, Bremerich J, et al. Standardized image interpretation and post processing in cardiovascular magnetic resonance: Society for Cardiovascular Magnetic Resonance (SCMR) board of trustees task force on standardized post processing. *Journal of Cardiovascular Magnetic Resonance* 2013;15(1):35.
250. Yared K, Noseworthy P, Weyman AE, et al. Pulmonary artery acceleration time provides an accurate estimate of systolic pulmonary arterial pressure during transthoracic echocardiography. *J Am Soc Echocardiogr* 2011;24(6):687-92. doi: 10.1016/j.echo.2011.03.008
251. Storaa C, Åberg P, Lind B, et al. Effect of Angular Error on Tissue Doppler Velocities and Strain. *Echocardiography* 2003;20(7):581-87. doi: 10.1046/j.1540-8175.2003.01135.x
252. Sareen N, Ananthasubramaniam K. Strain Imaging: From Physiology to Practical Applications in Daily Practice. *Cardiology in Review* 2016;24(2)
253. McCall P. The right ventricular response to lung resection. University of Glasgow, 2018.
254. McCall P, Steven M, Shelley B. Magnetic resonance imaging safety of Epilong Soft epidural catheters. *Anaesthesia* 2014;69(10):1180. doi: 10.1111/anae.12842 [published Online First: 2014/09/11]
255. Falcoz PE, Conti M, Brouchet L, et al. The Thoracic Surgery Scoring System (Thoracoscore): risk model for in-hospital death in 15,183 patients requiring thoracic surgery. *J Thorac Cardiovasc Surg* 2007;133(2):325-32. doi: 10.1016/j.jtcvs.2006.09.020 [published Online First: 2007/01/30]
256. McCall PJ, Macfie A, Kinsella J, et al. Critical care after lung resection: CALoR 1, a single-centre pilot study. *Anaesthesia* 2015;70(12):1382-9. doi: 10.1111/anae.13267

257. Dandel M, Lehmkuhl H, Knosalla C, et al. Strain and strain rate imaging by echocardiography - basic concepts and clinical applicability. *Current cardiology reviews* 2009;5(2):133-48. doi: 10.2174/157340309788166642
258. Platz E, Hassanein AH, Shah A, et al. Regional right ventricular strain pattern in patients with acute pulmonary embolism. *Echocardiography* 2012;29(4):464-70. doi: 10.1111/j.1540-8175.2011.01617.x
259. Liu B, Dardeer AM, Moody WE, et al. Normal values for myocardial deformation within the right heart measured by feature-tracking cardiovascular magnetic resonance imaging. *International Journal of Cardiology* 2018;252:220-23. doi: 10.1016/j.ijcard.2017.10.106
260. Liu Y, Wang D, Du Q, et al. Evaluation of Right Ventricular Systolic Function in Patients With Chronic Pulmonary Heart Disease by 2-Dimensional Speckle-Tracking Echocardiography. *J Ultrasound Med* 2016;35(11):2333-42. doi: 10.7863/ultra.15.11085
261. Hachulla AL, Lador F, Muller H, et al. P212 MRI derived global right ventricle diastolic strains correlate with mPAP in CTEPH patients. *Chest* 2017;151(5, Supplement):A111. doi: https://doi.org/10.1016/j.chest.2017.04.117
262. Orde S, Behfar A, Stalboerger P, et al. Effect of positive end-expiratory pressure on porcine right ventricle function assessed by speckle tracking echocardiography. *BMC anesthesiology* 2015;15:49. doi: 10.1186/s12871-015-0028-6
263. Mukherjee M, Mercurio V, Tedford RJ, et al. Right ventricular longitudinal strain is diminished in systemic sclerosis compared with idiopathic pulmonary arterial hypertension. *European Respiratory Journal* 2017;50(5):1701436. doi: 10.1183/13993003.01436-2017
264. Meris A, Faletra F, Conca C, et al. Timing and Magnitude of Regional Right Ventricular Function: A Speckle Tracking-Derived Strain Study of Normal Subjects and Patients with Right Ventricular Dysfunction. *Journal of the American Society of Echocardiography* 2010;23(8):823-31. doi: https://doi.org/10.1016/j.echo.2010.05.009
265. Vitarelli A, Mangieri E, Terzano C, et al. Three-Dimensional Echocardiography and 2D-3D Speckle-Tracking Imaging in Chronic Pulmonary Hypertension: Diagnostic Accuracy in Detecting Hemodynamic Signs of Right Ventricular (RV) Failure. *Journal of the American Heart Association*;4(3):e001584. doi: 10.1161/JAHA.114.001584
266. Dahhan T, Siddiqui I, Tapson VF, et al. Clinical and echocardiographic predictors of mortality in acute pulmonary embolism. *Cardiovascular Ultrasound* 2016;14(1):44. doi: 10.1186/s12947-016-0087-y
267. Kanar BG, Şahin A, Göl G, et al. Timing and magnitude of regional right ventricular function and their relationship with early hospital mortality in patients with acute pulmonary embolism. *Anatol J Cardiol* 2019;22(1):26-32. doi: 10.14744/AnatolJCardiol.2019.38906
268. Stergiopoulos K, Bahrainy S, Strachan P, et al. Right ventricular strain rate predicts clinical outcomes in patients with acute pulmonary embolism. *Acute Cardiac Care* 2011;13(3):181-88. doi: 10.3109/17482941.2011.606468
269. Fine NM, Chen L, Bastiansen PM, et al. Outcome prediction by quantitative right ventricular function assessment in 575 subjects evaluated for pulmonary hypertension. *Circ Cardiovasc Imaging* 2013;6(5):711-21. doi: 10.1161/circimaging.113.000640 [published Online First: 2013/07/03]

270. Blessberger H, Binder T. Two dimensional speckle tracking echocardiography: basic principles. *Heart* 2010;96(9):716. doi: 10.1136/hrt.2007.141002
271. Lee J-H, Park J-H. Strain Analysis of the Right Ventricle Using Two-dimensional Echocardiography. *J Cardiovasc Imaging* 2018;26(3):111-24. doi: 10.4250/jcvi.2018.26.e11 [published Online First: 2018/08/29]
272. Freed BH, Tsang W, Bhave NM, et al. Right ventricular strain in pulmonary arterial hypertension: a 2D echocardiography and cardiac magnetic resonance study. *Echocardiography* 2015;32(2):257-63.
273. Kukulski T, Hubbert L, Arnold M, et al. Normal regional right ventricular function and its change with age: a Doppler myocardial imaging study. *J Am Soc Echocardiogr* 2000;13(3):194-204. doi: 10.1067/mje.2000.103106 [published Online First: 2000/03/09]
274. Chang W-T, Liu Y-W, Liu P-Y, et al. The association between right ventricular free wall strain and exercise capacity for health check-up subjects. *PLOS ONE* 2017;12(3):e0173307. doi: 10.1371/journal.pone.0173307
275. Johnson C, Kuyt K, Oxborough D, et al. Practical tips and tricks in measuring strain, strain rate and twist for the left and right ventricles. *Echo research and practice* 2019;6(3):R87-R98. doi: 10.1530/ERP-19-0020
276. Kossaify A. Echocardiographic Assessment of the Right Ventricle, from the Conventional Approach to Speckle Tracking and Three-Dimensional Imaging, and Insights into the "Right Way" to Explore the Forgotten Chamber. *Clin Med Insights Cardiol* 2015;9:65-75. doi: 10.4137/CMC.S27462
277. La Gerche A, Jurcut R, Voigt JU. Right ventricular function by strain echocardiography. *Curr Opin Cardiol* 2010;25(5):430-6. doi: 10.1097/HCO.0b013e32833b5f94 [published Online First: 2010/07/02]
278. Missant C, Rex S, Claus P, et al. Load-sensitivity of regional tissue deformation in the right ventricle: isovolumic versus ejection-phase indices of contractility. *Heart* 2008;94(4):e15. doi: 10.1136/hrt.2006.109520
279. Wright L, Negishi K, Dwyer N, et al. Afterload Dependence of Right Ventricular Myocardial Strain. *Journal of the American Society of Echocardiography* 2017;30(7):676-84.e1. doi: https://doi.org/10.1016/j.echo.2017.03.002
280. Puwanant S, Park M, Popović ZB, et al. Ventricular geometry, strain, and rotational mechanics in pulmonary hypertension. *Circulation* 2010;121(2):259-66. doi: 10.1161/circulationaha.108.844340 [published Online First: 2010/01/06]
281. Hodzic A, Bobin P, Mika D, et al. Standard and Strain Measurements by Echocardiography Detect Early Overloaded Right Ventricular Dysfunction: Validation against Hemodynamic and Myocyte Contractility Changes in a Large Animal Model. *J Am Soc Echocardiogr* 2017;30(11):1138-47.e4. doi: 10.1016/j.echo.2017.07.003 [published Online First: 2017/09/03]
282. Tello K, Dalmer A, Vanderpool R, et al. Cardiac Magnetic Resonance Imaging-Based Right Ventricular Strain Analysis for Assessment of Coupling and Diastolic Function in Pulmonary Hypertension. *JACC Cardiovasc Imaging* 2019;12(11 Pt 1):2155-64. doi: 10.1016/j.jcmg.2018.12.032 [published Online First: 2019/03/18]
283. Murphy E, Glass A, McCall P, et al. Cardiac-magnetic-resonance-derived strain rate: a novel technique for assessing right ventricular diastolic

function post-lung resection. *British Journal of Anaesthesia* 2018;121(2):e29. doi: https://doi.org/10.1016/j.bja.2018.05.038
284. Uyan AP, Uyan C, Ozyurek H. Assessment of right ventricular diastolic filling parameters by Doppler echocardiography. *Pediatrics International* 2003;45(3):263-67. doi: 10.1046/j.1442-200X.2003.01707.x
285. Tee M, Noble JA, Bluemke DA. Imaging techniques for cardiac strain and deformation: comparison of echocardiography, cardiac magnetic resonance and cardiac computed tomography. *Expert Review of Cardiovascular Therapy* 2013;11(2):221-31. doi: 10.1586/erc.12.182
286. Scatteia A, Baritussio A, Bucciarelli-Ducci C. Strain imaging using cardiac magnetic resonance. *Heart Fail Rev* 2017;22(4):465-76. doi: 10.1007/s10741-017-9621-8
287. Kannan A, Poongkunran C, Jayaraj M, et al. Role of strain imaging in right heart disease: a comprehensive review. *Journal of clinical medicine research* 2014;6(5):309-13. doi: 10.14740/jocmr1842w [published Online First: 2014/08/12]
288. Heimdal A, Støylen A, Torp H, et al. Real-Time Strain Rate Imaging of the Left Ventricle by Ultrasound. *Journal of the American Society of Echocardiography* 1998;11(11):1013-19. doi: 10.1016/S0894-7317(98)70151-8
289. Urheim S, Edvardsen T, Torp H, et al. Myocardial Strain by Doppler Echocardiography. *Circulation* 2000;102(10):1158-64. doi: 10.1161/01.CIR.102.10.1158
290. Edvardsen T, Gerber Bernhard L, Garot J, et al. Quantitative Assessment of Intrinsic Regional Myocardial Deformation by Doppler Strain Rate Echocardiography in Humans. *Circulation* 2002;106(1):50-56. doi: 10.1161/01.CIR.0000019907.77526.75
291. Yu CM, Sanderson JE, Marwick TH, et al. Tissue Doppler imaging a new prognosticator for cardiovascular diseases. *J Am Coll Cardiol* 2007;49(19):1903-14. doi: 10.1016/j.jacc.2007.01.078 [published Online First: 2007/05/15]
292. Marwick TH. Measurement of Strain and Strain Rate by Echocardiography: Ready for Prime Time? *Journal of the American College of Cardiology* 2006;47(7):1313-27. doi: https://doi.org/10.1016/j.jacc.2005.11.063
293. Leitman M, Lysyansky P, Sidenko S, et al. Two-dimensional strain–a novel software for real-time quantitative echocardiographic assessment of myocardial function. *Journal of the American Society of Echocardiography* 2004;17(10):1021-29. doi: 10.1016/j.echo.2004.06.019
294. Muraru D, Spadotto V, Cecchetto A, et al. New speckle-tracking algorithm for right ventricular volume analysis from three-dimensional echocardiographic data sets: validation with cardiac magnetic resonance and comparison with the previous analysis tool. *European Heart Journal - Cardiovascular Imaging* 2016;17(11):1279-89. doi: 10.1093/ehjci/jev309
295. Atsumi A, Seo Y, Ishizu T, et al. Right Ventricular Deformation Analyses Using a Three-Dimensional Speckle-Tracking Echocardiographic System Specialized for the Right Ventricle. *J Am Soc Echocardiogr* 2016;29(5):402-11.e2. doi: 10.1016/j.echo.2015.12.014 [published Online First: 2016/02/18]
296. Zerhouni EA, Parish DM, Rogers WJ, et al. Human heart: tagging with MR imaging--a method for noninvasive assessment of myocardial motion. *Radiology* 1988;169(1):59-63. doi: 10.1148/radiology.169.1.3420283

297. Amzulescu MS, De Craene M, Langet H, et al. Myocardial strain imaging: review of general principles, validation, and sources of discrepancies. *European Heart Journal - Cardiovascular Imaging* 2019;20(6):605-19. doi: 10.1093/ehjci/jez041
298. Shehata ML, Cheng S, Osman NF, et al. Myocardial tissue tagging with cardiovascular magnetic resonance. *Journal of Cardiovascular Magnetic Resonance* 2009;11(1):55. doi: 10.1186/1532-429X-11-55
299. Pedrizzetti G, Claus P, Kilner PJ, et al. Principles of cardiovascular magnetic resonance feature tracking and echocardiographic speckle tracking for informed clinical use. *Journal of Cardiovascular Magnetic Resonance* 2016;18(1) doi: 10.1186/s12968-016-0269-7
300. Backhaus SJ, Metschies G, Billing M, et al. Cardiovascular magnetic resonance imaging feature tracking: Impact of training on observer performance and reproducibility. *PloS one* 2019;14(1):e0210127-e27. doi: 10.1371/journal.pone.0210127
301. Pedrizzetti G, Claus P, Kilner PJ, et al. Principles of cardiovascular magnetic resonance feature tracking and echocardiographic speckle tracking for informed clinical use. *Journal of Cardiovascular Magnetic Resonance* 2016;18(1):51. doi: 10.1186/s12968-016-0269-7
302. Chamberlain R, Scalia GM, Wee Y, et al. The Learning Curve for Competency in Right Ventricular Longitudinal Strain Analysis. *Journal of the American Society of Echocardiography* 2020 doi: https://doi.org/10.1016/j.echo.2019.12.011
303. Erley J, Genovese D, Tapaskar N, et al. Echocardiography and cardiovascular magnetic resonance based evaluation of myocardial strain and relationship with late gadolinium enhancement. *Journal of Cardiovascular Magnetic Resonance* 2019;21(1):46. doi: 10.1186/s12968-019-0559-y
304. Belghiti H, Brette S, Lafitte S, et al. Automated function imaging: a new operator-independent strain method for assessing left ventricular function. *Archives of Cardiovascular Diseases* 2008;101(3):163-69. doi: https://doi.org/10.1016/S1875-2136(08)71798-4
305. Il'Giovine ZJ, Mulder H, Chiswell K, et al. Right Ventricular Longitudinal Strain Reproducibility Using Vendor-Dependent and Vendor-Independent Software. *Journal of the American Society of Echocardiography* 2018;31(6):721-32.e5. doi: https://doi.org/10.1016/j.echo.2018.01.008
306. Taha K, Bourfiss M, te Riele ASJM, et al. A head-to-head comparison of speckle tracking echocardiography and feature tracking cardiovascular magnetic resonance imaging in right ventricular deformation. *European Heart Journal - Cardiovascular Imaging* 2020 doi: 10.1093/ehjci/jeaa088
307. Mirea O, Berceanu M, Donoiu I, et al. Variability of right ventricular global and segmental longitudinal strain measurements. *Echocardiography* 2019;36(1):102-09. doi: 10.1111/echo.14218
308. Erley J, Tanacli R, Genovese D, et al. Myocardial strain analysis of the right ventricle: comparison of different cardiovascular magnetic resonance and echocardiographic techniques. *Journal of Cardiovascular Magnetic Resonance* 2020;22(1) doi: 10.1186/s12968-020-00647-7
309. Orde SR, Pulido JN, Masaki M, et al. Outcome prediction in sepsis: speckle tracking echocardiography based assessment of myocardial function. *Critical care (London, England)* 2014;18(4):R149-R49. doi: 10.1186/cc13987

310. de Groote P, Millaire A, Foucher-Hossein C, et al. Right ventricular ejection fraction is an independent predictor of survival in patients with moderate heart failure. *Journal of the American College of Cardiology* 1998;32(4):948-54. doi: https://doi.org/10.1016/S0735-1097(98)00337-4
311. Hamada-Harimura Y, Seo Y, Ishizu T, et al. Incremental Prognostic Value of Right Ventricular Strain in Patients With Acute Decompensated Heart Failure. *Circulation: Cardiovascular Imaging* 2018;11(10):e007249. doi: 10.1161/CIRCIMAGING.117.007249
312. Henein MY, Gronlund C, Tossavainen E, et al. Right and left heart dysfunction predict mortality in pulmonary hypertension. *Clinical physiology and functional imaging* 2017;37(1):45-51. doi: 10.1111/cpf.12266 [published Online First: 2015/06/23]
313. Hardegree EL, Sachdev A, Villarraga HR, et al. Role of Serial Quantitative Assessment of Right Ventricular Function by Strain in Pulmonary Arterial Hypertension. *American Journal of Cardiology* 2013;111(1):143-48. doi: 10.1016/j.amjcard.2012.08.061
314. Sarvari SI, Haugaa KH, Anfinsen O-G, et al. Right ventricular mechanical dispersion is related to malignant arrhythmias: a study of patients with arrhythmogenic right ventricular cardiomyopathy and subclinical right ventricular dysfunction. *European Heart Journal* 2011;32(9):1089-96. doi: 10.1093/eurheartj/ehr069
315. Badagliacca R, Papa S, Valli G, et al. Right ventricular dyssynchrony and exercise capacity in idiopathic pulmonary arterial hypertension. *European Respiratory Journal* 2017;49(6):1601419. doi: 10.1183/13993003.01419-2016
316. Simon MA, Rajagopalan N, Mathier MA, et al. Tissue Doppler imaging of right ventricular decompensation in pulmonary hypertension. *Congest Heart Fail* 2009;15(6):271-76. doi: 10.1111/j.1751-7133.2009.00113.x
317. La Gerche A, Burns AT, D'Hooge J, et al. Exercise Strain Rate Imaging Demonstrates Normal Right Ventricular Contractile Reserve and Clarifies Ambiguous Resting Measures in Endurance Athletes. *Journal of the American Society of Echocardiography* 2012;25(3):253-62.e1. doi: 10.1016/j.echo.2011.11.023
318. McConnell MV, Solomon SD, Rayan ME, et al. Regional right ventricular dysfunction detected by echocardiography in acute pulmonary embolism. *Am J Cardiol* 1996;78(4):469-73. doi: 10.1016/s0002-9149(96)00339-6 [published Online First: 1996/08/15]
319. Mediratta A, Addetia K, Medvedofsky D, et al. Echocardiographic Diagnosis of Acute Pulmonary Embolism in Patients with McConnell's Sign. *Echocardiography* 2016;33(5):696-702. doi: 10.1111/echo.13142
320. Vitarelli A, Barillà F, Capotosto L, et al. Right Ventricular Function in Acute Pulmonary Embolism: A Combined Assessment by Three-Dimensional and Speckle-Tracking Echocardiography. *Journal of the American Society of Echocardiography* 2014;27(3):329-38. doi: https://doi.org/10.1016/j.echo.2013.11.013
321. Watts JA, Gellar MA, Stuart LK, et al. Proinflammatory events in right ventricular damage during pulmonary embolism: effects of treatment with ketorolac in rats. *J Cardiovasc Pharmacol* 2009;54(3):246-52. doi: 10.1097/FJC.0b013e3181b2b699
322. Vitarelli A, Mangieri E, Terzano C, et al. Three-dimensional echocardiography and 2D-3D speckle-tracking imaging in chronic pulmonary hypertension: diagnostic accuracy in detecting hemodynamic

signs of right ventricular (RV) failure. *Journal of the American Heart Association* 2015;4(3):e001584-e84. doi: 10.1161/JAHA.114.001584
323. Smith BCF, Dobson G, Dawson D, et al. Three-Dimensional Speckle Tracking of the Right Ventricle: Toward Optimal Quantification of Right Ventricular Dysfunction in Pulmonary Hypertension. *Journal of the American College of Cardiology* 2014;64(1):41-51. doi: https://doi.org/10.1016/j.jacc.2014.01.084
324. Lord RN, George K, Jones H, et al. Reproducibility and feasibility of right ventricular strain and strain rate (SR) as determined by myocardial speckle tracking during high-intensity upright exercise: a comparison with tissue Doppler-derived strain and SR in healthy human hearts. *Echo research and practice* 2014;1(1):31-41. doi: 10.1530/ERP-14-0011 [published Online First: 2014/07/28]
325. Padervinskienė L, Krivickienė A, Hoppenot D, et al. Prognostic Value of Left Ventricular Function and Mechanics in Pulmonary Hypertension: A Pilot Cardiovascular Magnetic Resonance Feature Tracking Study. *Medicina (Kaunas)* 2019;55(3):73. doi: 10.3390/medicina55030073
326. Savitzky A, Golay MJE. Smoothing and Differentiation of Data by Simplified Least Squares Procedures. *Analytical Chemistry* 1964;36(8):1627-39. doi: 10.1021/ac60214a047
327. Schmidt B, Dick A, Treutlein M, et al. Intra- and inter-observer reproducibility of global and regional magnetic resonance feature tracking derived strain parameters of the left and right ventricle. *European Journal of Radiology* 2017;89:97-105. doi: 10.1016/j.ejrad.2017.01.025
328. Gertz RJ, Lange T, Kowallick JT, et al. Inter-vendor reproducibility of left and right ventricular cardiovascular magnetic resonance myocardial feature-tracking. *PLOS ONE* 2018;13(3):e0193746. doi: 10.1371/journal.pone.0193746
329. Shang Q, Patel S, Steinmetz M, et al. Myocardial deformation assessed by longitudinal strain: Chamber specific normative data for CMR-feature tracking from the German competence network for congenital heart defects. *European Radiology* 2018;28(3):1257-66. doi: 10.1007/s00330-017-5034-2
330. Feisst A, Kuetting DLR, Dabir D, et al. Influence of observer experience on cardiac magnetic resonance strain measurements using feature tracking and conventional tagging. *IJC Heart & Vasculature* 2018;18:46-51. doi: https://doi.org/10.1016/j.ijcha.2018.02.007
331. Bourfiss M, Vigneault DM, Aliyari Ghasebeh M, et al. Feature tracking CMR reveals abnormal strain in preclinical arrhythmogenic right ventricular dysplasia/ cardiomyopathy: a multisoftware feasibility and clinical implementation study. *Journal of cardiovascular magnetic resonance : official journal of the Society for Cardiovascular Magnetic Resonance* 2017;19(1):66-66. doi: 10.1186/s12968-017-0380-4
332. Leng S, Dong Y, Wu Y, et al. Impaired Cardiovascular Magnetic Resonance–Derived Rapid Semiautomated Right Atrial Longitudinal Strain Is Associated With Decompensated Hemodynamics in Pulmonary Arterial Hypertension. *Circulation: Cardiovascular Imaging* 2019;12(5):e008582. doi: 10.1161/CIRCIMAGING.118.008582
333. Chia E-M, Hsieh CHC, Boyd A, et al. Effects of Age and Gender on Right Ventricular Systolic and Diastolic Function Using Two-Dimensional Speckle-Tracking Strain. *Journal of the American Society of*

Echocardiography 2014;27(10):1079-86.e1. doi: https://doi.org/10.1016/j.echo.2014.06.007
334. Park JH, Choi JO, Park SW, et al. Normal references of right ventricular strain values by two-dimensional strain echocardiography according to the age and gender. *Int J Cardiovasc Imaging* 2018;34(2):177-83. doi: 10.1007/s10554-017-1217-9 [published Online First: 2017/07/29]
335. Jayasekera G, Mangion K, Crowe T, et al. Left ventricular strain and dyssynchrony by CMR Feature tracking in Idiopathic Pulmonary Arterial Hypertension(IPAH). *European Respiratory Journal* 2017;50(suppl 61):OA1503. doi: 10.1183/1393003.congress-2017.OA1503
336. Rana M, Yusuff H, Zochios V. The Right Ventricle During Selective Lung Ventilation for Thoracic Surgery. *Journal of Cardiothoracic and Vascular Anesthesia* 2019;33(7):2007-16. doi: https://doi.org/10.1053/j.jvca.2018.11.030
337. Aldo C, Michele E, Claudio P. Cardiac biomarkers and risk assessment in patients undergoing major non-cardiac surgery: time to revise the guidelines? *Clinical Chemistry and Laboratory Medicine (CCLM)* 2014;52(7):959-63. doi: https://doi.org/10.1515/cclm-2013-0900
338. Matyal R, Mahmood F, Hess P, et al. Right Ventricular Echocardiographic Predictors of Postoperative Supraventricular Arrhythmias After Thoracic Surgery: A Pilot Study. *The Annals of Thoracic Surgery* 2010;90(4):1080-86. doi: 10.1016/j.athoracsur.2010.05.019
339. Kiely DG, Levin DL, Hassoun PM, et al. Statement on imaging and pulmonary hypertension from the Pulmonary Vascular Research Institute (PVRI). *Pulmonary Circulation* 2019;9(3):2045894019841990. doi: 10.1177/2045894019841990
340. Swift AJ, Rajaram S, Condliffe R, et al. Pulmonary artery relative area change detects mild elevations in pulmonary vascular resistance and predicts adverse outcome in pulmonary hypertension. *Investigative radiology* 2012;47(10):571-77.
341. Agoston-Coldea L, Lupu S, Mocan T. Pulmonary Artery Stiffness by Cardiac Magnetic Resonance Imaging Predicts Major Adverse Cardiovascular Events in patients with Chronic Obstructive Pulmonary Disease. *Scientific reports* 2018;8(1):14447-47. doi: 10.1038/s41598-018-32784-6
342. Sanz J, Kuschnir P, Rius T, et al. Pulmonary arterial hypertension: noninvasive detection with phase-contrast MR imaging. *Radiology* 2007;243(1):70-9. doi: 10.1148/radiol.2431060477
343. Jardim C, Rochitte CE, Humbert M, et al. Pulmonary artery distensibility in pulmonary arterial hypertension: an MRI pilot study. *Eur Respir J* 2007;29(3):476-81. doi: 10.1183/09031936.00016806
344. Swift AJ, Capener D, Johns C, et al. Magnetic Resonance Imaging in the Prognostic Evaluation of Patients with Pulmonary Arterial Hypertension. *American Journal of Respiratory and Critical Care Medicine* 2017;196(2):228-39. doi: 10.1164/rccm.201611-2365OC
345. Klok FA, Romeih S, Westenberg JJ, et al. Pulmonary flow profile and distensibility following acute pulmonary embolism. *J Cardiovasc Magn Reson* 2011;13:14. doi: 10.1186/1532-429X-13-14
346. Rolf A, Rixe J, Kim WK, et al. Pulmonary vascular remodeling before and after pulmonary endarterectomy in patients with chronic thromboembolic pulmonary hypertension: a cardiac magnetic resonance study. *Int J Cardiovasc Imaging* 2015;31(3):613-9. doi: 10.1007/s10554-014-0580-z

347. Casalino E, Laissy JP, Soyer P, et al. Assessment of right ventricle function and pulmonary artery circulation by cine-MRI in patients with AIDS. *Chest* 1996;110(5):1243-7.
348. Stevens GR, Garcia-Alvarez A, Sahni S, et al. RV dysfunction in pulmonary hypertension is independently related to pulmonary artery stiffness. *JACC Cardiovasc Imaging* 2012;5(4):378-87. doi: 10.1016/j.jcmg.2011.11.020
349. Moral S, Fernández-Friera L, Stevens G, et al. New index α improves detection of pulmonary hypertension in comparison with other cardiac magnetic resonance indices. *Int J Cardiol* 2012;161(1):25-30. doi: 10.1016/j.ijcard.2011.04.024 [published Online First: 2011/05/21]
350. Ray JC, Burger C, Mergo P, et al. Pulmonary arterial stiffness assessed by cardiovascular magnetic resonance imaging is a predictor of mild pulmonary arterial hypertension. *Int J Cardiovasc Imaging* 2019;35(10):1881-92. doi: 10.1007/s10554-018-1397-y [published Online First: 2018/06/24]
351. Quail MA, Knight DS, Steeden JA, et al. Noninvasive pulmonary artery wave intensity analysis in pulmonary hypertension. *Am J Physiol Heart Circ Physiol* 2015;308(12):H1603-11. doi: 10.1152/ajpheart.00480.2014
352. Ali ER, Mohamad AM. Diagnostic accuracy of cardiovascular magnetic resonance imaging for assessment of right ventricular morphology and function in pulmonary artery hypertension. *Egyptian Journal of Chest Diseases and Tuberculosis* 2017;66(3):477-86. doi: https://doi.org/10.1016/j.ejcdt.2016.09.004
353. Hardziyenka M, Reesink HJ, Bouma BJ, et al. A novel echocardiographic predictor of in-hospital mortality and mid-term haemodynamic improvement after pulmonary endarterectomy for chronic thrombo-embolic pulmonary hypertension. *Eur Heart J* 2007;28(7):842-9. doi: 10.1093/eurheartj/ehl534
354. Ibrahim E-SH, White RD. Cardiovascular magnetic resonance for the assessment of pulmonary arterial hypertension: toward a comprehensive CMR exam. *Magnetic Resonance Imaging* 2012;30(8):1047-58. doi: https://doi.org/10.1016/j.mri.2012.03.001
355. Gulsin GS, Singh A, McCann GP. Cardiovascular magnetic resonance in the evaluation of heart valve disease. *BMC Medical Imaging* 2017;17(1):67. doi: 10.1186/s12880-017-0238-0
356. Lotz J, Meier C, Leppert A, et al. Cardiovascular flow measurement with phase-contrast MR imaging: basic facts and implementation. *Radiographics* 2002;22(3):651-71. doi: 10.1148/radiographics.22.3.g02ma11651
357. Wehrum T, Kams M, Schroeder L, et al. Accelerated analysis of three-dimensional blood flow of the thoracic aorta in stroke patients. *The International Journal of Cardiovascular Imaging* 2014;30(8):1571-77. doi: 10.1007/s10554-014-0511-z
358. Laffon E, Bernard V, Montaudon M, et al. Tuning of pulmonary arterial circulation evidenced by MR phase mapping in healthy volunteers. *J Appl Physiol (1985)* 2001;90(2):469-74.
359. Burman ED, Keegan J, Kilner PJ. Pulmonary artery diameters, cross sectional areas and area changes measured by cine cardiovascular magnetic resonance in healthy volunteers. *Journal of Cardiovascular Magnetic Resonance* 2016;18(1):12. doi: 10.1186/s12968-016-0230-9
360. Forouzan O, Warczytowa J, Wieben O, et al. Non-invasive measurement using cardiovascular magnetic resonance of changes in pulmonary artery

stiffness with exercise. *Journal of Cardiovascular Magnetic Resonance* 2015;17(1):109. doi: 10.1186/s12968-015-0213-2
361. Ertan C, Tarakci N, Ozeke O, et al. Pulmonary artery distensibility in chronic obstructive pulmonary disease. *Echocardiography* 2013;30(8):940-4. doi: 10.1111/echo.12170 [published Online First: 2013/03/16]
362. Lewis Gregory D, Bossone E, Naeije R, et al. Pulmonary Vascular Hemodynamic Response to Exercise in Cardiopulmonary Diseases. *Circulation* 2013;128(13):1470-79. doi: 10.1161/CIRCULATIONAHA.112.000667
363. Parker KH. A brief history of arterial wave mechanics. *Medical & biological engineering & computing* 2009;47(2):111-18. doi: 10.1007/s11517-009-0440-5 [published Online First: 2009/02/07]
364. Parker KH. An introduction to wave intensity analysis. *Med Biol Eng Comput* 2009;47(2):175-88. doi: 10.1007/s11517-009-0439-y
365. Hughes AD, Parker KH, Davies JE. Waves in arteries: A review of wave intensity analysis in the systemic and coronary circulations. *Artery Research* 2008;2(2):51-59. doi: https://doi.org/10.1016/j.artres.2008.02.002
366. Avolio A, Westerhof BE, Siebes M, et al. Arterial hemodynamics and wave analysis in the frequency and time domains: an evaluation of the paradigms. *Medical & Biological Engineering & Computing* 2009;47(2):107-10. doi: 10.1007/s11517-009-0455-y
367. Remington JW, O'Brien LJ. Construction of aortic flow pulse from pressure pulse. *The American journal of physiology* 1970;218(2):437-47. doi: 10.1152/ajplegacy.1970.218.2.437 [published Online First: 1970/02/01]
368. Parker KH, Jones CJ. Forward and backward running waves in the arteries: analysis using the method of characteristics. *J Biomech Eng* 1990;112(3):322-6.
369. Parker KH, Jones CJH, Dawson JR, et al. What stops the flow of blood from the heart? *Heart and Vessels* 1988;4(4):241-45. doi: 10.1007/BF02058593
370. Kolyva C, Khir A. Wave intensity analysis in the great arteries – What has been learnt during the last 25 years? Part 1. *International Cardiovascular Forum Journal; Vol 1, No 2 (2013)DO - 1017987/icfjv1i223* 2013
371. Kolyva C, Khir AW. Wave intensity analysis in the ventricles, carotid and coronary arteries – What has been learnt during the last 25 years?: Part 2. *International Cardiovascular Forum Journal; Vol 1, No 3 (2014)DO - 1017987/icfjv1i336* 2014
372. Davies Justin E, Whinnett Zachary I, Francis Darrel P, et al. Evidence of a Dominant Backward-Propagating "Suction" Wave Responsible for Diastolic Coronary Filling in Humans, Attenuated in Left Ventricular Hypertrophy. *Circulation* 2006;113(14):1768-78. doi: 10.1161/CIRCULATIONAHA.105.603050
373. van den Wijngaard JPHM, Siebes M, Westerhof BE. Comparison of arterial waves derived by classical wave separation and wave intensity analysis in a model of aortic coarctation. *Medical & Biological Engineering & Computing* 2009;47(2):211-20. doi: 10.1007/s11517-008-0387-y
374. Quail MA, Steeden JA, Knight D, et al. Development and validation of a novel method to derive central aortic systolic pressure from the MR aortic distension curve. *J Magn Reson Imaging* 2014;40(5):1064-70. doi: 10.1002/jmri.24471

375. Sugawara M, Uchida K, Kondoh Y, et al. Aortic blood momentum – the more the better for the ejecting heart in vivo? *Cardiovascular Research* 1997;33(2):433-46. doi: 10.1016/S0008-6363(96)00241-6
376. Sugawara M, Niki K, Ohte N, et al. Clinical usefulness of wave intensity analysis. *Med Biol Eng Comput* 2009;47(2):197-206. doi: 10.1007/s11517-008-0388-x
377. Schäfer M, Wilson N, Ivy DD, et al. Noninvasive wave intensity analysis predicts functional worsening in children with pulmonary arterial hypertension. *American Journal of Physiology-Heart and Circulatory Physiology* 2018;315(4):H968-H77. doi: 10.1152/ajpheart.00227.2018
378. Vulliémoz S, Stergiopulos N, Meuli R. Estimation of local aortic elastic properties with MRI. *Magn Reson Med* 2002;47(4):649-54.
379. Feng J, Khir AW. Determination of wave speed and wave separation in the arteries using diameter and velocity. *J Biomech* 2010;43(3):455-62. doi: 10.1016/j.jbiomech.2009.09.046
380. Ohte N, Narita H, Sugawara M, et al. Clinical usefulness of carotid arterial wave intensity in assessing left ventricular systolic and early diastolic performance. *Heart Vessels* 2003;18(3):107-11. doi: 10.1007/s00380-003-0700-5 [published Online First: 2003/09/05]
381. Vriz O, Zito C, di Bello V, et al. Non-invasive one-point carotid wave intensity in a large group of healthy subjects. *Heart and Vessels* 2016;31(3):360-69. doi: 10.1007/s00380-014-0600-x
382. Jones CJH, Sugawara M, Kondoh Y, et al. Compression and expansion wavefront travel in canine ascending aortic flow: wave intensity analysis. *Heart and Vessels* 2002;16(3):91-98. doi: 10.1007/s003800200002
383. Ohte N, Narita H, Sugawara M, et al. Clinical usefulness of carotid arterial wave intensity in assessing left ventricular systolic and early diastolic performance. *Heart and Vessels* 2003;18(3):107-11. doi: 10.1007/s00380-003-0700-5
384. Ohte N, Narita H, Akita S, et al. The mechanism of emergence and clinical significance of apically directed intraventricular flow during isovolumic relaxation. *Journal of the American Society of Echocardiography* 2002;15(7):715-22. doi: 10.1067/mje.2002.119113
385. Niki K, Sugawara M, Uchida K, et al. A noninvasive method of measuring wave intensity, a new hemodynamic index: application to the carotid artery in patients with mitral regurgitation before and after surgery. *Heart and Vessels* 1999;14(6):263-71. doi: 10.1007/BF03257237
386. Manisty CH, Zambanini A, Parker KH, et al. Differences in the magnitude of wave reflection account for differential effects of amlodipine- versus atenolol-based regimens on central blood pressure: an Anglo-Scandinavian Cardiac Outcome Trial substudy. *Hypertension* 2009;54(4):724-30. doi: 10.1161/HYPERTENSIONAHA.108.125740
387. Attinger EO. Pressure transmission in pulmonary arteries related to frequency and geometry. *Circ Res* 1963;12:623-41. doi: 10.1161/01.res.12.6.623 [published Online First: 1963/06/01]
388. Davies Justin E, Alastruey J, Francis Darrel P, et al. Attenuation of Wave Reflection by Wave Entrapment Creates a “Horizon Effect” in the Human Aorta. *Hypertension* 2012;60(3):778-85. doi: 10.1161/HYPERTENSIONAHA.111.180604
389. Westerhof N, Bosman F, De Vries CJ, et al. Analog studies of the human systemic arterial tree. *J Biomech* 1969;2(2):121-43.

390. Westerhof N, Segers P, Westerhof BE. Wave separation, wave intensity, the reservoir-wave concept, and the instantaneous wave-free ratio: presumptions and principles. *Hypertension* 2015;66(1):93-98.
391. Alastruey J. On the mechanics underlying the reservoir-excess separation in systemic arteries and their implications for pulse wave analysis. *Cardiovascular Engineering* 2010;10(4):176-89.
392. Hametner B, Wassertheurer S, Hughes AD, et al. Reservoir and excess pressures predict cardiovascular events in high-risk patients. *International journal of cardiology* 2014;171(1):31-36.
393. Mynard JP, Davidson MR, Penny DJ, et al. Non-linear separation of pressure, velocity and wave intensity into forward and backward components. *Medical & biological engineering & computing* 2012;50(6):641-48.
394. Mynard JP, Smolich JJ. Wave reflection and central pressure augmentation. *Journal of Hypertension* 2013;31(4):841-43.
395. Parker KH. Arterial reservoir pressure, subservient to the McDonald lecture, Artery 13. *Artery Research* 2013;7(3-4):171-85.
396. Qureshi MU, Hill NA. A computational study of pressure wave reflections in the pulmonary arteries. *Journal of Mathematical Biology* 2015;71(6):1525-49. doi: 10.1007/s00285-015-0867-2
397. Qureshi MU, Vaughan GDA, Sainsbury C, et al. Numerical simulation of blood flow and pressure drop in the pulmonary arterial and venous circulation. *Biomechanics and Modeling in Mechanobiology* 2014;13(5):1137-54. doi: 10.1007/s10237-014-0563-y
398. Boumpouli M, Danton MHD, Gourlay T, et al. Blood flow simulations in the pulmonary bifurcation in relation to adult patients with repaired tetralogy of Fallot. *Medical Engineering & Physics* 2020;85:123-38. doi: https://doi.org/10.1016/j.medengphy.2020.09.014
399. Hollander EH, Wang JJ, Dobson GM, et al. Negative wave reflections in pulmonary arteries. *Am J Physiol Heart Circ Physiol* 2001;281(2):H895-902.
400. Dwyer N, Yong AC, Kilpatrick D. Variable open-end wave reflection in the pulmonary arteries of anesthetized sheep. *The Journal of Physiological Sciences* 2012;62(1):21-28. doi: 10.1007/s12576-011-0182-7
401. Bouwmeester JC, Belenkie I, Shrive NG, et al. Wave reflections in the pulmonary arteries analysed with the reservoir–wave model. *The Journal of Physiology* 2014;592(14):3053-62. doi: 10.1113/jphysiol.2014.273094
402. Nie M, Kobayashi H, Sugawara M, et al. Helium inhalation enhances vasodilator effect of inhaled nitric oxide on pulmonary vessels in hypoxic dogs. *American Journal of Physiology-Heart and Circulatory Physiology* 2001;280(4):H1875-H81. doi: 10.1152/ajpheart.2001.280.4.H1875
403. Lau EM, Abelson D, Dwyer N, et al. Assessment of ventriculo-arterial interaction in pulmonary arterial hypertension using wave intensity analysis. *Eur Respir J* 2014;43(6):1804-7. doi: 10.1183/09031936.00148313 [published Online First: 2014/01/18]
404. Su J, Manisty C, Simonsen U, et al. Pulmonary artery wave propagation and reservoir function in conscious man: impact of pulmonary vascular disease, respiration and dynamic stress tests. *The Journal of Physiology* 2017;595(20):6463-76. doi: 10.1113/JP274385
405. Su J, Manisty C, Parker Kim H, et al. Wave Intensity Analysis Provides Novel Insights Into Pulmonary Arterial Hypertension and Chronic Thromboembolic Pulmonary Hypertension. *Journal of the American Heart Association*;6(11):e006679. doi: 10.1161/JAHA.117.006679

406. Su J, Hughes AD, Simonsen U, et al. Impact of pulmonary endarterectomy on pulmonary arterial wave propagation and reservoir function. *American journal of physiology Heart and circulatory physiology* 2019;317(3):H505-H16. doi: 10.1152/ajpheart.00181.2019 [published Online First: 2019/06/21]
407. Grignola JC, Ginés F, Bia D, et al. Improved right ventricular-vascular coupling during active pulmonary hypertension. *Int J Cardiol* 2007;115(2):171-82. doi: 10.1016/j.ijcard.2006.03.007 [published Online First: 2006/06/27]
408. Torbicki A, Kurzyna M, Ciurzynski M, et al. Proximal pulmonary emboli modify right ventricular ejection pattern. *European Respiratory Journal* 1999;13(3):616-21.
409. Augustine DX, Coates-Bradshaw LD, Willis J, et al. Echocardiographic assessment of pulmonary hypertension: a guideline protocol from the British Society of Echocardiography. *Echo research and practice* 2018;5(3):G11-G24.
410. Naeije R, Huez S. Reflections on wave reflections in chronic thromboembolic pulmonary hypertensionThe opinions expressed in this article are not necessarily those of the Editors of the European Heart Journal or of the European Society Cardiology. *European Heart Journal* 2007;28(7):785-87. doi: 10.1093/eurheartj/ehm040
411. Leimbigler P, van Amerom J, Grosse-Wortmann L, et al. Measurement of pulmonary arterial pulse wave reflection from single-slice phase-contrast and steady-state free precession MRI. *Journal of Cardiovascular Magnetic Resonance* 2012;14(Suppl 1):W35-W35. doi: 10.1186/1532-429X-14-S1-W35
412. Ibrahim e-S, Shaffer JM, White RD. Assessment of pulmonary artery stiffness using velocity-encoding magnetic resonance imaging: evaluation of techniques. *Magn Reson Imaging* 2011;29(7):966-74. doi: 10.1016/j.mri.2011.04.012
413. Top 10 Articles. *Analytical Chemistry* 2000;72(9):324 A-29 A. doi: 10.1021/ac002801q
414. Butterworth S. On the theory of filter amplifiers. *Wireless Engineer* 1930;7(6):536-41.
415. Flewitt JA, Hobson TN, Wang J, et al. Wave intensity analysis of left ventricular filling: application of windkessel theory. *American Journal of Physiology-Heart and Circulatory Physiology* 2007;292(6):H2817-H23. doi: 10.1152/ajpheart.00936.2006
416. Borlotti A, Li Y, Parker KH, et al. Experimental evaluation of local wave speed in the presence of reflected waves. *J Biomech* 2014;47(1):87-95. doi: 10.1016/j.jbiomech.2013.10.007
417. Khir AW, Parker KH. Measurements of wave speed and reflected waves in elastic tubes and bifurcations. *J Biomech* 2002;35(6):775-83.
418. Khir AW, O'Brien A, Gibbs JS, et al. Determination of wave speed and wave separation in the arteries. *J Biomech* 2001;34(9):1145-55.
419. Rabben SI, Stergiopulos N, Hellevik LR, et al. An ultrasound-based method for determining pulse wave velocity in superficial arteries. *J Biomech* 2004;37(10):1615-22. doi: 10.1016/j.jbiomech.2003.12.031
420. Davies JE, Whinnett ZI, Francis DP, et al. Use of simultaneous pressure and velocity measurements to estimate arterial wave speed at a single site in humans. *Am J Physiol Heart Circ Physiol* 2006;290(2):H878-85. doi: 10.1152/ajpheart.00751.2005

421. Weir-McCall JR, Struthers AD, Lipworth BJ, et al. Letter to the editor: Comparing pace and speed in the pulmonary circulation? *American Journal of Physiology-Heart and Circulatory Physiology* 2016;310(7):H949-H49. doi: 10.1152/ajpheart.00065.2016
422. Quail MA, Segers P, Muthurangu V. Reply to: "Letter to the editor: Comparing pace and speed in the pulmonary circulation?". *American Journal of Physiology-Heart and Circulatory Physiology* 2016;310(7):H950-H50. doi: 10.1152/ajpheart.00120.2016
423. Alastruey J. Numerical assessment of time-domain methods for the estimation of local arterial pulse wave speed. *J Biomech* 2011;44(5):885-91. doi: 10.1016/j.jbiomech.2010.12.002
424. Bland JM, Altman DG. Statistical methods for assessing agreement between two methods of clinical measurement. *Lancet* 1986;1(8476):307-10. [published Online First: 1986/02/08]
425. Biglino G, Steeden JA, Baker C, et al. A non-invasive clinical application of wave intensity analysis based on ultrahigh temporal resolution phase-contrast cardiovascular magnetic resonance. *J Cardiovasc Magn Reson* 2012;14:57. doi: 10.1186/1532-429X-14-57
426. Romo-Cárdenas G, Avilés-Rodríguez GJ, Sánchez-López JdD, et al. Nyquist-Shannon theorem application for Savitzky-Golay smoothing window size parameter determination in bio-optical signals. *Results in Physics* 2018;11:17-22. doi: https://doi.org/10.1016/j.rinp.2018.08.033
427. Gander W, Hřebíček Ji. Solving problems in scientific computing using Maple and MATLAB. 4th, expanded and rev. ed. Berlin ; New York ;: Springer 2004.
428. Krishnan SR, Seelamantula CS. On the Selection of Optimum Savitzky-Golay Filters. *IEEE Transactions on Signal Processing* 2013;61(2):380-91. doi: 10.1109/TSP.2012.2225055
429. Rivolo S, Nagel E, Smith NP, et al. Automatic selection of optimal Savitzky-Golay filter parameters for Coronary Wave Intensity Analysis. *Annu Int Conf IEEE Eng Med Biol Soc* 2014;2014:5056-9. doi: 10.1109/embc.2014.6944761 [published Online First: 2015/01/09]
430. Mynard JP, Kondiboyina A, Kowalski R, et al. Measurement, Analysis and Interpretation of Pressure/Flow Waves in Blood Vessels. *Front Physiol* 2020;11:1085-85. doi: 10.3389/fphys.2020.01085
431. Weir-McCall JR, Kamalasanan A, Cassidy DB, et al. Assessment of proximal pulmonary arterial stiffness using magnetic resonance imaging: effects of technique, age and exercise. *BMJ Open Respir Res* 2016;3(1):e000149. doi: 10.1136/bmjresp-2016-000149 [published Online First: 2016/11/16]
432. Fok H, Guilcher A, Brett S, et al. Dominance of the Forward Compression Wave in Determining Pulsatile Components of Blood Pressure. *Hypertension* 2014;64(5):1116-23. doi: 10.1161/HYPERTENSIONAHA.114.04050
433. Khir AW, Parker KH. Wave intensity in the ascending aorta: effects of arterial occlusion. *Journal of Biomechanics* 2005;38(4):647-55. doi: https://doi.org/10.1016/j.jbiomech.2004.05.039
434. Hill AB. The environment and disease: association or causation?: Sage Publications, 1965.
435. Jayasekera G, Church C, Johnson M, et al. Right Ventricular free wall myocardial tissue characterisation by systolic Cardiac Magnetic Resonance T1 mapping in pulmonary hypertension. *Journal of Cardiovascular Magnetic Resonance* 2016;18(1):1-2. doi: 10.1186/1532-429x-18-s1-p147

436. Segers P, Rietzschel Ernst R, Chirinos Julio A. How to Measure Arterial Stiffness in Humans. *Arteriosclerosis, Thrombosis, and Vascular Biology* 2020;40(5):1034-43. doi: 10.1161/ATVBAHA.119.313132

List of presentations and publications

Presentations

International

2017: Oral presentation, "Pulmonary artery wave intensity analysis following lung resection". EACTA Annual Congress Berlin

2017: Poster and oral presentation (shortlisted for best poster), "Non-invasive indices of right ventricular afterload following lung resection" EACTA Annual Congress Berlin. Second prize for poster presentation.

National

2017: Oral presentation, "Right ventricular strain imaging with cardiac magnetic resonance following lung resection" at ACTACC meeting.

2016: Oral presentation on "Pulmonary artery wave intensity analysis following lung resection" at British Journal of Anaesthesia Autumn Research Forum.

2016: Oral presentation on "Right ventricular afterload following lung resection" at ACTA Spring meeting.

Regional

2016: Oral presentation, "Pulmonary artery wave intensity analysis following lung resection", at Glasgow and West of Scotland School of Anaesthesia Research Club Meeting.

Publications

Full papers

McCall, P. J., A. Arthur, **A. Glass**, D. S. Corcoran, A. Kirk, A. Macfie, J. Payne, M. Johnson, J. Kinsella and B. G. Shelley (2019). "The right ventricular response to lung resection." The Journal of Thoracic and Cardiovascular Surgery 158(2): 556-565.e555.

Abstracts

Glass, A., P. McCall, A. Arthur, J. Kinsella and B. Shelley (2017). "Non-invasive indices of right ventricular afterload following lung resection." Journal of Cardiothoracic and Vascular Anesthesia 31: S73-S74.

Glass, A., P. McCall, A. Arthur, J. Kinsella and B. Shelley (2017). "Pulmonary artery wave intensity analysis following lung resection." Journal of Cardiothoracic and Vascular Anesthesia 31: S5-S6.

Murphy, E., **A. Glass**, P. McCall, J. Kinsella and B. Shelley (2018). "Cardiac-magnetic-resonance-derived strain rate: a novel technique for assessing right ventricular diastolic function post-lung resection." British Journal of Anaesthesia 121(2): e29.

Murphy, E., **A. Glass**, P. McCall and B. Shelley (2019). "Relative kinetics of B-type natriuretic peptide and N-terminal pro B-type natriuretic peptide after lung resection." British Journal of Anaesthesia 123(4): e503-e504.